AD_____

Award Number: DAMD17-98-1-8620

TITLE: Bioenergetic Defects and Oxidative Damage in Transgenic Mouse Models of Neurodegenerative Disorders

PRINCIPAL INVESTIGATOR: Susan E. Browne, M.D.

CONTRACTING ORGANIZATION: Weill Medical College of Cornell University
New York, NY 10021

REPORT DATE: June 2005

TYPE OF REPORT: Final

PREPARED FOR: U.S. Army Medical Research and Materiel Command
Fort Detrick, Maryland 21702-5012

DISTRIBUTION STATEMENT: Approved for Public Release;
Distribution Unlimited

REPORT DOCUMENTATION PAGE

Form Approved
OMB No. 0704-0188

1. REPORT DATE *(DD-MM-YYYY)*	2. REPORT TYPE	3. DATES COVERED *(From - To)*
01-06-2005	Final	1 May 98 – 31 May 05

4. TITLE AND SUBTITLE
Bioenergetic Defects and Oxidative Damage in Transgenic Mouse Models of Neurodegenerative Disorders

5a. CONTRACT NUMBER

5b. GRANT NUMBER
DAMD17-98-1-8620

5c. PROGRAM ELEMENT NUMBER

6. AUTHOR(S)
Susan E. Browne, M.D.

E-Mail: sub2001@med.cornell.edu

5d. PROJECT NUMBER

5e. TASK NUMBER

5f. WORK UNIT NUMBER

7. PERFORMING ORGANIZATION NAME(S) AND ADDRESS(ES)
Weill Medical College of Cornell University
New York, NY 10021

8. PERFORMING ORGANIZATION REPORT NUMBER

9. SPONSORING / MONITORING AGENCY NAME(S) AND ADDRESS(ES)
U.S. Army Medical Research and Materiel Command
Fort Detrick, Maryland 21702-5012

10. SPONSOR/MONITOR'S ACRONYM(S)

11. SPONSOR/MONITOR'S REPORT NUMBER(S)

12. DISTRIBUTION / AVAILABILITY STATEMENT
Approved for Public Release; Distribution Unlimited

13. SUPPLEMENTARY NOTES
Original contains color plates: All DTIC reproductions will be in black and white.

14. ABSTRACT

Abstract is attached at following page.

15. SUBJECT TERMS
Neurotoxin

16. SECURITY CLASSIFICATION OF:			17. LIMITATION OF ABSTRACT	18. NUMBER OF PAGES	19a. NAME OF RESPONSIBLE PERSON
a. REPORT	b. ABSTRACT	c. THIS PAGE			USAMRMC
U	U	U	UU	297	19b. TELEPHONE NUMBER *(include area code)*

ABSTRACT

The initial three years of this project determined the contributions of bioenergetic defects and oxidative stress to neurodegeneration in Huntington's disease (HD) and amyotrophic lateral sclerosis (ALS). A Consortium project, "Mitochondrial Free Radical Generation in Parkinson's Disease", was then incorporated into the grant award (2 years), to assess *in vivo* whether mitochondria are the source of free radical generation in animal models of Parkinson's disease (PD).

Studies in the original grant period generated several novel observations of presymptomatic energetic abnormalities in mouse genetic models of both HD (R6/2, N171-82Q, *Hdh* $^{Q50, 92, 111}$ mice) and ALS (G93A mice). Specifically, *in vivo* studies showed that glucose uptake is non-specifically elevated throughout the forebrain in two HD mouse models (N171-82Q and *HdhQ111 and Q92)* before symptom onset, and that ATP defects and oxidative damage precede symptom onset in some models. In ALS mice, in contrast glucose use is reduced in discrete motor pathways in brain, preceding changes in spinal cord. Studies examining the relationship between mitochondrial complex I inhibition and free radical-mediated oxidative damage in rat neurotoxin models (rotenone and pyridaben) demonstrate increased oxidative damage rapidly after complex I inhibition (including lipid peroxidation and induction of the stress-response marker heme oxygenase-1).

3. TABLE OF CONTENTS

4. INTRODUCTION

OVERVIEW OF ENTIRE GRANT PERIOD:

The goal of the original (Neurotoxin Exposure Program) three-year grant proposal was to gain insight into the roles of mitochondrial energy metabolism and oxidative stress in the etiology of neuronal degeneration in degenerative diseases, specifically Huntington's disease (HD) and amyotrophic lateral sclerosis (ALS), using *in vivo* genetic models of these diseases. In 2002 this proposal was extended by the addition of a second project, entitled "Mitochondrial Free Radical Generation In Parkinson's Disease", which is a constituent (Project III) of a Research Consortium made up of four investigators. This project continues the theme of determining the interactions between energy metabolism and oxidative stress in the etiology of neurodegenerative disorders.

Since the two constitutive projects are ostensibly separate entities, in this report the Introduction and Body (Results) for each are presented separately. Results are presented in order of SOW Aim number. This is followed by a summary of key research accomplishments for both, reportable outcomes from both, and overall conclusions.

INTRODUCTION -1: Neurotoxin Exposure Program Grant "Bioenergetic Defects and Oxidative Damage in Transgenic Mouse Models of Neurodegenerative Disorders"

The goal of this project was to gain insight into the roles of mitochondrial energy metabolism and oxidative stress in the etiology of neuronal degeneration in Huntington's disease (HD) and amyotrophic lateral sclerosis (ALS). The experiments described in the original proposal aimed to determine the relative contributions and sequential order of bioenergetic dysfunction and oxidative damage to the process of cell death in two different transgenic (Tg) mouse models of HD (*Hdh* knock-in mice; R6/2 mice) and one Tg mouse model of familial ALS (G93A SOD1 over-expressors) (White et al, 1997; Mangiarini et al., 1996; Gurney et al., 1994). Over the course of the project, we determined that one of these mouse lines (R6/2 HD mice) develop a diabetic profile that interferes with *in vivo* measurement of cerebral glucose use (Ferrante et al., 2000). Hence, another transgenic mouse line that also expresses a fragment of mutant human huntingtin (N171-82Q mice; Schilling et al., 1999), was substituted for R6/2 mice in some of the experiments. N171-82Q mice develop a phenotype similar to R6/2 mice, but their lifespan is 1-2 months longer. The development of genetically modified mice expressing mutant human transgenes, or mutations in mouse homologues,

and that mimic aspects of the human disease phenotype, provide novel opportunities to assess the temporal progression of pathological changes over the course of disease development in an *in vivo* animal model. In addition, the use of mitochondrial toxins allows us to model in animals the cerebral pathogenic sequelae of cell death induced by naturally occurring agents which are potentially extremely hazardous to humans. In this project we used 3-nitropropionic acid (3-NP), a neurotoxin that produces brain lesions and symptoms in humans resembling those seen in HD.

The studies described in this report utilized both *in vivo* and *in vitro* experimental approaches in mutant mice and in rats, to investigate parameters of cerebral energy metabolism (*in vivo* cerebral glucose use measurement by [^{14}C]-2-deoxyglucose autoradiography; NMR lactate imaging; *in vitro* spectrophotometric oxidative phosphorylation enzyme assays; HPLC detection of metabolites), and to investigate the generation of free radicals and oxidative damage products (HPLC detection; immunohistochemistry).

5. BODY – 1

"Bioenergetic Defects and Oxidative Damage in Transgenic Mouse Models of Neurodegenerative Disorders"

The pathogenetic mechanisms in both Huntington's disease (HD) and amyotrophic lateral sclerosis (ALS) are still unclear, however, in both cases *in vivo* and *in vitro* studies implicate the involvement of bioenergetic defects in the disease process (for review, see Browne and Beal, 2000; Menzies et al., 2002). Attempts to ascertain the role of energetic dysfunction in pathogenesis have been greatly enhanced by the development of several different transgenic mouse lines replicating aspects of each disorder. HD models express the huntingtin gene mutation underlying HD, an abnormal expansion of the polyglutamine (Q) domain in huntingtin protein, encoded by an expanded triplet (CAG) repeat in exon 1 of the huntingtin gene. Familial ALS (FALS) models express some of the multiple Cu/Zn superoxide dismutase (SOD1) mutations that occur in approximately 25% of familial ALS patients. These models allow novel determinations of metabolic parameters over the life-span of the animals, before, during and after onset of pathological changes and disease symptoms. HD mouse lines differ in terms of the site of mutant gene incorporation, CAG repeat length, copy number, and promoter used, and these differences are reflected in the phenotypes of the mice generated. Studies in this project utilize *Hdh* CAG knock-in mice (White et al., 1997), R6/2 transgenic mice overexpressing an N-terminal fragment of human mutant huntingtin, including a 145

polyglutamine repeat stretch (Mangiarini et al., 1996), and N171-82Q mice also expressing an N-terminal fragment of human mutant huntingtin, but with a shorter (82Q) polyglutamine repeat stretch (Schilling et al., 1999). The ALS mouse model employed is the G93A model (Gurney et al., 1994), overexpressing a human SOD1 glycine to alanine mutation. In the thrid year of this project we also utilized a neurotoxin model of HD, using 3-nitropropionic acid (3-NP) to induce striatal-specific brain lesions with a concomitant movement disorder in rats. Model characteristics are discussed in detail in the relevant section below. Summaries of the outcomes of each of the research objectives of this project follow, in chronological order of the annual Aims.

Objective #1: To investigate the effect of expressing 48 CAG repeats – a CAG repeat length consistent with the generation of mutant huntingtin HD patients – on local rates of cerebral glucose use (lCMRglc) in the Hdh mouse model of HD; and to assess any gene dosage effect.

Hdh CAG "knock-in" mice were developed by inserting CAG repeats into exon 1 of the murine huntingtin homologue (*Hdh)* to generate a set of precise genetic HD mouse models which accurately express mutant huntingtin protein (White et al., 1997). Mice expressing 50 or 92 glutamines (encoded by the CAG repeat domains), Hdh^{Q50} and Hdh^{Q92} respectively, do not develop any overt behavioral phenotype over their lifespan. However, they do show cellular changes involving translocation of mutant huntingtin from the cytosol to the nucleus, and formation of intranuclear aggregates or inclusions (NII) containing ubiquitinated mutant huntingtin. The time at which these events occur is CAG repeat length-dependent, occurring earlier in Hdh^{Q92} mice (nuclear huntingin is evident by ~4 months of age; aggregates form by 15 months; Wheeler et al., 2000). Hdh^{Q111} mice expressing a longer polyglutamine stretch have recently been reported (Wheeler et al., 2002). These mice show expedited aggregate formation (by about 6 months of age), and also display a mild behavioral phenotype and striatal-specific cell degeneration by approximately 19 months of age. All mice have normal life-spans.

In this study we used [^{14}C]-2-deoxyglucose *in vivo* autoradiography in four month-old $\boldsymbol{Hdh^{Q50}}$ knock-in mice (time-point chosen to precede pathological changes), expressing a CAG repeat that causes HD in humans (48 CAGs), to determine:

- if cerebral glucose utilization is altered by this HD mutation, and
- the effect of gene dosage on glucose use (homozygous versus heterozygote mice).

We used a modification of the [^{14}C]-2-deoxyglucose *in vivo* autoradiography technique developed by Sokoloff and colleagues (Sokoloff 1977) to measure local rates of cerebral glucose use ($lCMR_{glc}$) in *Hdh* "knock-in" mice (Browne et al., 1999). The [^{14}C]-2-deoxyglucose (2-DG) procedure facilitates localization and quantitation of $lCMR_{glc}$ in discrete anatomical regions throughout the CNS of conscious animals. It's utility is based on the premise that glucose is the primary energy source for cerebral cells, but brain tissue has a minimal capacity to store carbohydrates and therefore relies on glucose extraction from the circulation to fulfill energy demands. Thus, changes in glucose use generally reflect alterations in functional activity within CNS regions. Regional measurement of the rate of uptake of a radiolabelled glucose analog, ^{14}C-2-deoxyglucose, from the blood allows *in vivo* estimation of local rates of energy metabolism. Briefly, the procedure involves surgical implantation of femoral arterial and venous catheters; i.v. administration of [^{14}C]-2-deoxyglucose to the conscious mice; repeated arterial blood sampling for ^{14}C and plasma glucose measures; blood gas analysis; decapitation and brain harvest; cryostat processing of brain into 20μm-thick coronal sections throughout brain; exposure to film with pre-calibrated standards; densitometric measurement of regional ^{14}C levels from autoradiograms and estimation of regional glucose utilization rates.

Animals: Experiments employed 18 mice in three groups: *Hdh* mice both homozygous and heterozygous for the transgene, expressing 50 (Hdh^{Q50}) glutamines (48/48 and 48/7 CAG repeats, respectively) and in normal wild-type littermates (Hdh^{Q7}, 7/7 CAGs). Three mice were excluded from the 2-DG procedure analysis due to abnormal glucose or blood gas levels, indicating non-physiologically normal mice, and one mouse died during surgery.

Physiological variables: Arterial plasma glucose concentration, *p*O2, *p*CO2 and *p*H were measured 35 minutes into the procedure (10 minutes before animal decapitation) to determine the physiological status of the animals (Table 1). There were no significant differences in the levels of any of these measured parameters between 7/7, 48/7 and 48/48 mice ($p > 0.05$, ANOVA, followed by Fisher's PLSD). All measured parameters were within accepted normal ranges, indicating that there are no physiological effects associated with the *Hdh* mutation which might impact on the interpretation of glucose use results. In separate studies we have assessed glucose tolerance in *Hdh* mutant mice, in light of reports that R6/2 mice develop diabetes. We found that neither $Hdh^{Q7, Q50, Q92}$ or ^{Q111} showed any evidence of hyperglycemia or abnormal glucose handling (data not shown).

Table 1: Physiological variables in *Hdh* ^{Q50} CAG Knock-in Mice

Variable	7/7	48/7	48/48
Arterial Glucose (mg/dL)	133.2 ± 6.0	154.3 ± 10.1	134.8 ± 6.6
pO_2 (mmHg)	92.6 ± 2.4	91.8 ± 4.2	85.5 ± 2.7
pCO_2 (mmHg)	39.7 ± 1.8	40.3 ± 1.7	39.6 ± 1.2
*p*H	7.4 ± 0.0	7.4 ± 0.0	7.4 ± 0.0

Data are mean ± SEM, variables measured 35 min after initiation of the [^{14}C]-2-deoxyglucose procedure in *Hdh*^{Q7} (7/7) and *Hdh*^{Q50} (48/7 and 48/48) knock-in mice (n=4-6 per group). There were no statistically significant differences between 48/7, 48/48 and 7/7 mice in any of the parameters measured (p>0.05, ANOVA).

Local Cerebral Glucose Use, lCMR$_{glc}$: We measured cerebral metabolic rates for glucose in 21 brain regions. Glucose use values in each of the brain regions examined are presented in Table 2. Glucose use rates did not significantly differ between *Hdh*^{Q50} and *Hdh*^{Q7} mice in any of the brain regions examined ($p > 0.05$; ANOVA, followed by Fisher's PLSD), and there was no effect of gene dosage in *Hdh*^{Q50} mice (48/48 vs 48/7).

Discussion: Results suggest that cerebral glucose use rates do not differ between *Hdh*^{Q50} and *Hdh*^{Q7} mice in any of the brain regions examined in four month-old mice. Consequently, there was also no observable gene dosage effect in *Hdh*^{Q50} mice (48/48 vs 48/7). This contrasts with the pilot results presented in the original grant proposal, which suggested that glucose use showed a slight elevation in 48/48 mice relative to levels in wild type (7/7, 7/0) mice. This difference in outcome most likely reflects increased variance associated with larger group sizes for investigation. Observations by Wheeler et al. (2000) suggest that both translocation of huntingtin protein from cytosol to the nucleus, and NII formation, are CAG repeat length-dependent processes. Therefore, there is reason to suppose that energetic changes in *Hdh* mice may also vary in time of onset depending on CAG repeat length. Subsequently, studies were extended to mice expressing longer CAG repeats (*Hdh*^{Q92}) in Year 2 of this project (see "Objective # 5").

Table 2: Local Cerebral Glucose Utilization ($lCMR_{glc}$) in *Hdh* ^{Q50} CAG Knock-in Mice

Region	7/7	48/7	48/48
Frontal Cortex	43.3 ± 2.8	45.7 ± 3.3	41.3 ± 4.7
Parietal Cortex	41.3 ± 2.5	43.8 ± 4.1	40.8 ± 4.0
Anterior Cingulate Cortex	55.0 ± 2.0	61.5 ± 6.1	56.9 ± 6.7
Auditory Cortex	50.3 ± 6.2	49.9 ± 3.8	48.7 ± 4.2
Striatum: Dorsolateral	47.5 ± 5.4	51.7 ± 5.3	46.1 ± 4.2
Ventromedial	46.0 ± 5.2	48.4 ± 4.6	45.3 ± 4.7
Globus Pallidus	29.2 ± 2.1	28.7 ± 2.5	29.2 ± 2.1
Hippocampus: CA1	27.8 ± 2.2	28.8 ± 2.6	25.7 ± 2.9
CA3	34.9 ± 2.2	37.7 ± 3.0	33.8 ± 3.9
Dentate Gyrus: Molecular Layer	45.2 ± 3.5	40.2 ± 2.8	41.7 ± 4.0
Dorsolateral Geniculate Body	42.6 ± 3.1	44.3 ± 2.9	42.7 ± 6.4
Medial Geniculate Body	46.1 ± 3.7	57.7 ± 5.3	48.7 ± 7.0
Superior Colliculus: Superficial Layer	38.2 ± 2.9	37.8 ± 2.9	36.2 ± 4.5
Deep Layer	38.5 ± 2.0	37.1 ± 2.6	37.1 ± 4.8
Internal Capsule	14.4 ± 2.0	15.5 ± 2.5	12.4 ± 2.2
Thalamus: Dorsomedial	46.1 ± 2.9	45.4 ± 4.8	44.8 ± 5.4
Ventromedial	34.9 ± 2.2	37.7 ± 3.0	33.8 ± 3.9
Substantia Nigra: *pars reticulata*	24.7 ± 1.8	27.9 ± 2.3	25.0 ± 3.6
pars compacta	44.6 ± 3.5	43.9 ± 3.1	40.1 ± 5.4
Cerebellum: Grey matter	28.4 ± 1.5	29.7 ± 2.6	26.8 ± 3.2
White matter	18.6 ± 1.6	19.8 ± 3.1	17.3 ± 2.0

Local cerebral metabolic rates for glucose (nmol/100g/min) in homozygous (48/48) and heterozygous (48/7) *Hdh*^{Q50} knock-in mice, compared with rates in wild-type (7/7; *Hdh*^{Q7}) littermate controls (n=4-6 per group).
Data presented as mean ± SEM. There were no statistically significant differences between glucose use in 48/48 and 48/7 *Hdh*^{Q50} mice and littermate wild-type controls ($p > 0.05$, ANOVA).

Objective #2: **Measurement of electron transport chain activities in *Hdh* knock-in mice with disease-length and normal-length CAG repeats.**

We used spectrophotometric assays to measure the activities of the mitochondrial electron transport chain enzyme complexes I, II-III and IV, in homogenate preparations of *Hdh* mouse cerebral forebrain and cerebellum (according to the methods outlined in the proposal). We also extended spectrophotometric studies from the original SOW, to measure activity of the tri-carboxylic acid (TCA) cycle enzyme aconitase in the same animal population. Aconitase is of particular interest as its' activity has been shown to be markedly reduced in post-mortem tissue from late stage

HD patients (Tabrizi et al., 1999), and the same group have also reported reduced levels of activity in HD skeletal muscle (Lodi et al., 2000). Enzyme activities per mg protein were corrected by citrate synthase activity per mg protein, to account for the possibility of neuronal or mitochondrial loss.

Animals: Enzyme activities were measured in forebrain and cerebellum (control region) homogenates from 4 month old Hdh^{Q7} (7/7 CAG repeats), Hdh^{Q50} (48/7 and 48/48 CAG repeats), and Hdh^{Q92} (90/7 and 90/90 CAG repeats). This time-point was chosen to precede any pathologic changes in these mice, and to correlate with glucose utilization studies conducted in same age mice. We later went on to measure enzyme activities in mitochondrial preparations from homozygote Hdh^{20} (control) and Hdh^{Q111} (HD) mice, at the same time-point.

Enzyme Activities: We measured activities of the TCA cycle enzymes citrate synthase and aconitase, and of the respiratory chain enzyme complexes I, II-III and IV in brain homogenate preparations from the above mice (Hdh^{Q7} (7/7), Hdh^{Q50} (48/7 and 48/48), and Hdh^{Q92} (90/7 and 90/90). There were no significant alterations in citrate synthase activities in any of the mouse genotypes examined, in forebrain or cerebellum. This indicates no significant loss of neurons and/or mitochondria at this time point. Complex activities were unaltered in Hdh^{Q92} *and* Hdh^{Q50} mice in forebrain homogenates ($p > 0.05$; ANOVA, followed by Fisher's PLSD), although there was evidence of a trend towards reduced complex II-III and IV activities with increasing CAG repeat number. In cerebellum homogenates, however, complex II-III was reduced in 48/7 mice (-38%, $p<0.05$) and showed a trend to decrease in 90/7 and 90/90 mice (-36% and –24%, respectively). Complex IV activity was also significantly reduced in 48/7 and 90/90 mouse cerebellum (-35% and -42%, respectively; $p<0.01$), whilst non-statistically significant trends towards reduced activity were evident in 48/48 and 90/90 mice (-18 and –31%, respectively). Complex I activity in cerebellum also showed a small, significant reduction in activity in 48/7 mice, relative to levels in wild type mice (-19%; $p<0.05$), but was unaltered in other genotypes. Aconitase activity was unaltered in forebrain, but showed a slight increase in 48/48 mice in cerebellum, although 90/7 and 90/90 levels did not differ from wildtype levels. The reason for this small magnitude alteration is currently unclear.

We then used fluorimetric and spectrophotometric assays to determine the activities of several mitochondrial matrix and respiratory chain enzymes (complex I, SDH, cytochrome c oxidase (COX), cytochorome c reductase, α-KGDHC, and PDH), in mitochondria isolated from 4 month-old

homozygous Hdh^{Q111} and Hdh^{Q20} mouse brains (Table 3). PDH and COX activities were significantly elevated in Hdh^{Q111} mitochondria (+36% and +21%, respectively), suggesting that at this age mitochondrial components are upregulated, putatively to compensate for a defect in energy generation.

We also measured oxygen consumption in whole brain mitochondria freshly isolated from 4 month-old homozygous Hdh^{Q111} and Hdh^{Q20} mice, using a Clark-type oxygraph electrode (Table 3). The rates of oxygen consumption supported by both pyruvate + malate, or succinate, did not differ between Hdh^{Q111} and Hdh^{Q20} mitochondria. Hdh^{Q111} mitochondria exerted slightly reduced respiratory control, reflected by the acceptor control ratio (ACR), chiefly due to an elevated State 4 respiration rate. The difference did not reach statistical significance.

Table 3: Mitochondrial oxygen consumption and enzyme activities in Hdh^{Q111} mice.

O_2 Consumption (Substrate/Metabolic State)	***Hdh^{Q20}***	***Hdh^{Q111}***
Pyruvate + Malate		
State 3	230.1 ± 19.9	229.1 ± 10.4
State 4	32.9 ± 2.4	36.3 ± 1.9
ACR	7.2 ± 0.7	6.4 ± 0.5
Succinate		
State 3	171.0 ± 9.3	160.2 ± 14.7
State 4	115.7 ± 6.0	111.2 ± 4.3
ACR	1.5 ± 0.1	1.5 ± 0.2
Enzyme Activities		
Complex I	175 ± 24	179 ± 24
SDH	61 ± 2	63 ± 3
PDH	9.1 ± 0.5	12.4 ± 0.8**
α-KGDHC	14.6 ± 1.1	15.9 ± 1.5
SDH-Cyt.C	51 ± 4	53 ± 3
α–GP-Cyt.C	145 ± 6	149 ± 7
COX	647 ± 46	783 ± 27*

Data are mean ± SEM, in 4 month-old Hdh^{Q111}. mice and age and sex-matched Hdh^{Q20} controls. O_2 consumption rates are nmol O_2/min/mg mitochondrial protein (n=6 per group). Mitochondrial enzyme activities are: nmol NADH/min/mg protein (Complex I, PDH, α-KGDHC; n=8, 6, 6 per group, respectively); nmol DCIP/min/mg protein (SDH; n=6 per group); and nmol cytochrome c/min/mg protein (SDH-Cyt.C, αGP-Cyt.C., COX; n=6, 6, 5 per group, respectively). *p<0.02, ** p=0.002 (Student's t-test). *Abbreviations: ACR*, acceptor control ratio; *Complex I*, NADH:CoQ1 reductase; *COX*, cytochrome c oxidase; *Cyt.C*, cytochrome c reductase; *DCIP:* 2,6-dichlorophenolindophenol; *α-KGDHC*, α-ketoglutarate:NAD^+ reductase; *α–GP*, α-glycerophosphate; *PDH*, pyruvate:NAD^+ reductase; *SDH*, succinate:CoQ1:DCIP reductase.

Discussion: These results suggest that any defects in oxidative phosphoylation enzyme activities detectable in brain homogenates of Hdh^{Qn} mice are of small magnitude, and not necessarily restricted to brain regions susceptible to damage in HD. It is possible that region-specific changes occurring in forebrain structures may be masked since we measured enzyme activities in homogenates of the whole forebrain. Therefore we revisited this question in mitochondria isolated from forebrain of HD (Hdh^{Q111}) and control (Hdh^{Q20}) mice. PDH and COX activities were significantly elevated in Hdh^{Q111} mitochondria, whilst oxidative phosphorylation enzyme activities were unaltered. Taken with findings of unaltered O_2 consumption in HD mouse mitochondria, overall findings suggest that metabolic capacity of mitochondria is largely unaltered by the Hdh^{Qn} gene mutation, but subtle changes in mitochondrial function may occur.

Objective #3: **Measurement of $lCMR_{glc}$ in the G93A human mutant SOD1 overexpression Tg mouse model of ALS. Analysis of the temporal progression of any glucose use changes by measurement at 60, 90 and 120d of age.**

Transgenic mice overexpressing a human mutant form of SOD1 (a glycine to alanine substitution in exon 4, G93A) develop a disease syndrome whose neuropathology and neurological symptoms closely resemble human ALS (Gurney et al, 1994; Dal Canto and Gurney, 1995). Animals show signs of hind limb weakness at approximately 90-110 days of age, and gradually become paralyzed before dying at 150-180d. Numerous Lewy Body-like inclusions are seen at late stages of the disease. Neuropathological changes including microvesiculation are evident prior to the development of neurological symptoms (≈70 days). The involvement of mitochondrial energy metabolism dysfunction in the pathogenesis of this motor disorder is supported by observations that the first pathological events identified in these mice are membrane blebbing and vesiculation of the mitochondria (Dal Canto and Gurney, 1995). The hypothesis of a gain of function mutant SOD1 is supported by findings that animals expressing high levels of human wild type SOD do not develop the clinical disease, and a recent report that transgene expression levels correspond with the degree of neurotoxicity in mice. The aim of our study was to determine whether there is evidence in this mouse model of FALS of any alterations in energy metabolism prior to the onset of symptoms and mitochondrial morphological changes. We also endeavored to determine the pattern of glucose use changes over the lifespan of these animals.

Animals: Experiments employed 46 G93A and wildtype littermate mice, at 60, 90 and 120 days of age. Fourteen mice were excluded prior to the 2-DG procedure, due to death during surgery (n=4), poor blood flow in the femoral catheters (n=7), or abnormally high pre-glucose levels (n=3). Thirty-two mice underwent the 2-DG procedure at 60 days of age (n=9), 90 days (n=12), and 120 days (n=11). Of these, several were excluded from the final glucose use analysis due to poor blood gases, death during the procedure (due to mice pulling out their arterial catheters), abnormal arterial glucose levels, or poor radionuclide perfusion. We encountered many difficulties in achieving optimal physiological conditions and isotope delivery in this strain of mice. Consequently, we have not included 90 day glucose use values in the results below as the group sizes were too small to analyze statistically. Since submission of the last annual report for this project we have analyzed data from additional animals, in more brain regions. We also extended studies to 120 day-old N1029 mice that overexpress a transgene of human non-mutant SOD-1, and therefore serve as a transgenic control for the G93A mice.

Physiological Variables: Multiple physiological parameters in G93A and wild-type were assessed during the 2-DG experimental period, to determine whether any experimental group displayed physiologic changes which might impact on glucose utilization (Table 4). All measured parameters were within normal physiological limits for all experimental groups, at all ages. There were no significant differences in any of the measured parameters between G93A and wild-type littermate mice (ANOVA, $p>0.05$). Arterial plasma glucose levels within groups did not significantly alter over the course of the experiments (Student's paired t-test, $p>0.05$), indicating that mice are not abnormally stressed as a direct result of the experimental procedure.

Rates of Cerebral Glucose Use: Local cerebral metabolic rates for glucose ($lCMR_{glc}$) were calculated in 49 brain regions and 9 spinal cord regions in transgenic G93A mice (n=6 per group) and age-matched littermate controls (n=8-9 per group). Major findings are presented in Figure 1.

Brain: Glucose utilization rates were impaired in multiple brain components of the motor system as early as 60 days of age in G93A mice (the earliest time-point examined). Marked reductions in glucose use were evident in frontal cortex, motor cortex and striatum of G93A SOD1, relative to levels in wild type littermates. This pattern of glucose use reduction was still evident in 120 day-old mice relative to levels in wild-type mice, although non-transgenic wild type glucose use levels were also decreased at this time point, relative to levels at 60 days.

Table 4: Physiological Variables in G93A FALS Mice (Mean ± SEM).

	G93A SOD1 60 Days	
	Wt	**G93A**
Glucose -Pre (mg/dL)	141 ± 8	179 ± 12*
Glucose +45 min (mg/dL)	160 ± 12	183 ± 9
p_aO_2 (mmHg)	110 ± 4	107 ± 4
p_aCO_2 (mmHg)	34 ± 2	39 ± 3
*p*H	7.34 ± 0.02	7.31 ± 0.01
	120 Days	
	Wt	**G93A**
Glucose -Pre (mg/dL)	138 ± 9	143 ± 10
Glucose +45 min (mg/dL)	134 ± 16	179 ± 34
p_aO_2 (mmHg)	100 ± 3	93 ± 10
p_aCO_2 (mmHg)	32 ± 2	40 ± 3
*p*H	7.38 ± 0.01	7.32 ± 0.02*
	N1029 SOD1	
	Wt	**G93A**
Glucose -Pre (mg/dL)	187 ± 8	144 ± 6*
Glucose +45 min (mg/dL)	170 ± 16	147 ± 6
p_aO_2 (mmHg)	117 ± 18	109 ± 8
p_aCO_2 (mmHg)	49 ± 4	42 ± 4
*p*H	7.30 ± 0.03	7.32 ± 0.01

Variables in 60 day (n = 6) and 120 day old (n = 5-6) G93A mice, 21 month old N1029 mice (n = 4-5), and age-matched littermate wildtypes (Wt) (n = 9, 7-8 and 3, respectively). Data are mean ± SEM for arterial plasma glucose concentrations at the start (Glucose-Pre) and end of the 2-DG procedure (Glucose +45 min), and terminal blood gas levels. *$p<0.05$, significant difference relative to age-matched Wt (Student's unpaired t-test). Plasma glucose levels did not alter over the 45 min experiment in any group ($p> 0.05$, Student's paired t-test).

Motor regions of cerebral cortex: Significant glucose use reductions (-19%) were evident in primary motor cortex (Fr1) at 60 days (Figure 1). In contrast, sensorimotor cortical regions, including the hindlimb region, showed no significant glucose use alterations over the life-span of the G93A mice. Sensorimotor cortical regions process overlapping motor and sensory inputs, and send projections both to other motor cortical regions and to the spinal cord via the corticospinal tract (Zilles and Wree , 1995; Gu et al., 1999).

Figure 1: Glucose Use Alterations in G93A Corticospinal Tract and Collaterals.
Major afferent and efferent connections of the primary motor cortex are shown schematically. Bar charts are mean ± SEM local cerebral metabolic rates for glucose ($lCMR_{glc}$, μmol/100g/min) at 60 days and 120 days of age, in G93A mice (open bars) and age-matched wildtype (Wt) littermates. *$p< 0.05$, significantly different from levels in age-matched wildtypes (Student's unpaired t-test).

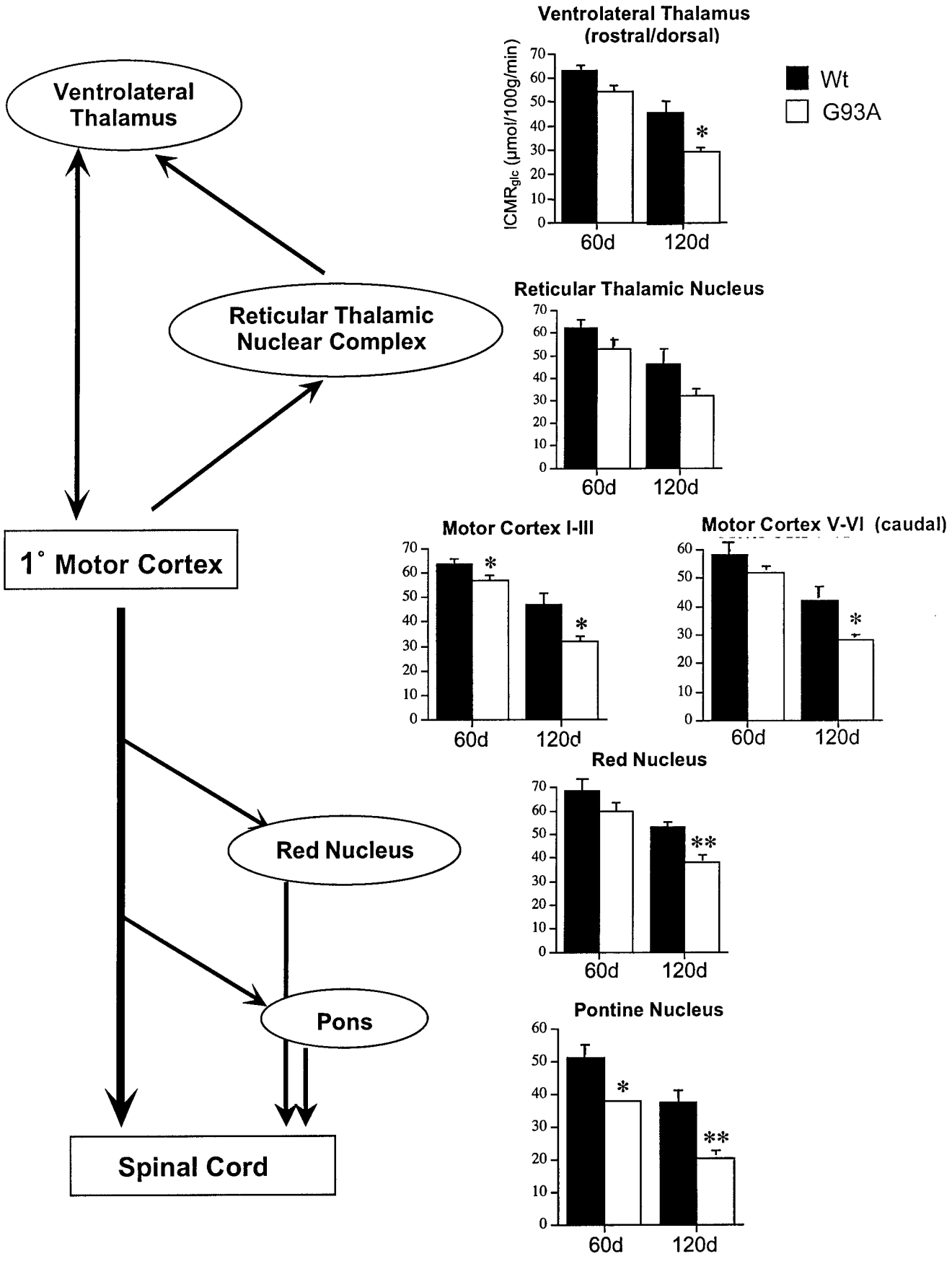
Ventrolateral Thalamus
Reticular Thalamic Nuclear Complex
1° Motor Cortex
Red Nucleus
Pons
Spinal Cord
Ventrolateral Thalamus (rostral/dorsal)
ICMRglc (µmol/100g/min)
Wt
G93A
60d
120d
Reticular Thalamic Nucleus
Motor Cortex I-III
Motor Cortex V-VI (caudal)
Red Nucleus
Pontine Nucleus

Motor cortex efferent projections: The principal projection targets of Fr1 comprise the spinal cord via the corticospinal tract, the striatum, reciprocal connections with other cerebral cortical regions including sensorimotor cortex, and projections to the brainstem pontine nuclei, red nucleus and cranial motor nuclei via collaterals from the corticospinal tract. We found hypometabolism in several of these areas synaptically associated with Fr1 (Figure 1), which differed between regions in age of onset. At 60 days, marked reductions in glucose use in G93A mice were evident in the pontine nuclei (-25%) and the pontine reticular formation (-17%), which contribute to the bulbospinal pathway innervating axial and proximal musculature. Within the rubrospinal pathway, involved in modulating movement in the distal limbs, a trend towards reduced glucose use was apparent in the red nucleus at 60 days, and was statistically significant at 120 days of age.

Thalamic relay nuclei: It is therefore of great interest that glucose use was decreased in multiple thalamic nuclei at 60 days of age, since these nuclei regulate Fr1 activity via reciprocal synaptic connections.

Spinal Cord: In contrast to findings in cerebral motor cortex projection zones, no alterations in glucose use were detected in cervical, thoracic or lumbar regions of the spinal cord in 60 day-old G93A mice (Table 5). This observation suggests that despite abnormalities in projection pathways arising from motor control brain regions at 60 days, functional activity in corticospinal projection zones is maintained at normal levels. By end-stage of the disorder (120 days), glucose use was significantly reduced in the gray matter of all three spinal cord regions in the transgenic mutant mice, relative to levels in non-transgenic wildtype controls (Table 5).

TABLE 5: Local Rates of Glucose Use in Spinal Cord of FALS Mice

	60 Days		120 Days	
	Wt	**G93A**	**Wt**	**G93A**
Spinal Cord				
Cervical - Dorsal	31 ± 9	36 ± 4	21 ± 3	9 ± 3*
Ventral	29 ± 7	36 ± 5	22 ± 4	8 ± 4*
White	15 ± 3	16 ± 2	13 ± 3	9 ± 3*
Thoracic - Dorsal	34 ± 4	36 ± 3	20 ± 3	8 ± 4*
Ventral	34 ± 4	36 ± 3	21 ± 4	4 ± 3
White	17 ± 2	18 ± 1	11 ± 3	11 ± 3*
Lumbar - Dorsal	33 ± 3	36 ± 3	25 ± 4	10 ± 3
Ventral	32 ± 3	37 ± 3	24 ± 4	6 ± 2
White	16 ± 2	19 ± 1	13 ± 3	9 ± 3*

Data are mean ± SEM $lCMR_{glc}$ (μmol/100g/min) in G93A and age-matched littermate wildtype (Wt) mice. *$p<0.05$, **$p<0.005$ significant differences relative to age-matched Wt mice (Student's unpaired t-test). G93A and Wt mice, n = 6 and 9 (60d), and n = 6 and 8 (120d), respectively.

Overexpression of human wildtype SOD1 (N1029 mice) did not alter CNS glucose use rates

It has been reported that overexpression of purely wildtype human SOD1 in N1029 mice eventually induces a motor degeneration phenotype (Jaarsma et al., 2000). We measured energy parameters in these mice at a mature age (21 months) which greatly exceeds that at which glucose use changes were detected in G93A mice (2 months), and was therefore deemed likely to show any SOD1-related glucose use changes. Mice did not exhibit any overt symptoms of motor defects. No significant differences in glucose use values between 21 month-old N1029 and age-matched wildtype littermate mice were detected in any of the five representative brain regions or the 9 spinal cord regions examined (Table 6). These observations suggest that the glucose use changes detected in G93A mice result from expression of the G93A SOD1 mutation, rather than increased SOD1 activity due to the transgene overexpression.

TABLE 6: Glucose Use Rates in Brain and Spinal Cord of Wildtype SOD1 Transgenic Mice

		Wt	**N1029**
Brain			
Frontal Cortex		43 ± 9	49 ± 2
Motor Cortex		38 ± 5	42 ± 3
Striatum		45 ± 9	51 ± 1
Hippocampus CA3		30 ± 12	39 ± 3
Cerebellar Gray Matter		22 ± 3	26 ± 1
Spinal Cord			
Cervical -	Dorsal	27 ± 2	24 ± 2
	Ventral	26 ± 3	24 ± 1
	White	14 ± 2	14 ± 2
Thoracic -	Dorsal	24 ± 1	26 ± 3
	Ventral	22 ± 3	27 ± 3
	White	11 ± 2	14 ± 1
Lumbar -	Dorsal	27 ± 7	25 ± 3
	Ventral	26 ± 6	26 ± 4
	White	14 ± 2	14 ± 2

Data are Mean ± SEM $lCMR_{glc}$ (μmol/100g/min) in 21 month old N1029 mice over-expressing wildtype SOD1, and age-matched littermate wildtype (Wt) mice. $lCMR_{glc}$ in N1029 mice did not differ from rates in wildtypes ($p > 0.05$, Student's unpaired t-test).

Discussion: In summary, the pattern of alterations in glucose use rates in 60 day old G93A mice suggest that functional impairments occur primarily in cerebral motor regions in this model, largely in primary motor cortex and its collaterals, preceding functional dysregulation in corticospinal projection targets. In particular, components of the bulbospinal projection pathway are compromised by 60 days of age, whereas rubrospinal projections become significantly involved later in the disorder, suggesting that axial and proximal components of motor regulation may be affected early in the disease process in this FALS model.

Objective #4. **Measurement of the temporal profiles of electron transport chain activities in the G93A FALS Tg mouse model of FALS**

We augmented the glucose use studies of energy metabolism by investigating mitochondrial respiratory transport chain activities and SOD1 levels using spectrophotometric assays.

Animals: Metabolic enzyme activities were measured in pre-symptomatic (60 day old) G93A SOD1 mice, in homogenate preparations of whole forebrain, brainstem and spinal cord, and cerebellum. We compared enzyme activities with levels in N1029 transgenic wild type controls (Tg-Wt) and non-transgenic wild type littermate controls (Wt). We also measured electron transport enzyme activities in 100-104 day-old G93A mice. Experiments used 53 mice.

Enzyme Activities: a) Results in 60 day-old mice are presented in Table 7. Complex I activity was significantly increased in G93A SOD1 mouse forebrain, relative to levels in Tg-Wt mice at this time-point. In contrast, in G93A spinal cord/brainstem, complex I activity was decreased compared with Wt levels (but not Tg-Wt). In addition, complex IV activity was reduced in the spinal cord/brainstem and cerebellum of G93A mice. Both Tg-Wt and G93A SOD1 mice expressed equivalent levels of cytosolic SOD1 activity (9.4 ± 0.3 vs. 11.4 ± 0.4 Units/mg protein, respectively), which were significantly higher than SOD1 levels in non-Tg Wt mice ($p<0.05$). b) We also measured respiratory chain enzyme activities in the forebrain of 100-104 day-old G93A mice (Table 8). The pattern of elevated complex I activity with no changes in complexes II-III and IV, seen in 60 day mice, is conserved in the forebrain at 100 days of age.

Table 7: Metabolic enzyme activities in 60 day-old G93A and control mice

		Forebrain	Spinal Cord/ Brainstem	Cerebellum
Complex I	Wt	145 ± 11	111 ± 7	88 ± 7
(nmol/min/mg protein/CS)	Tg Wt	130 ± 7	104 ± 6	84 ± 5
	G93A	162 ± 6 **	91 ± 5 †	74 ± 7
Complex II-III	Wt	3.06 ± 0.1	1.40 ± 0.1	1.66 ± 0.1
(nmol/min/mg protein/CS)	Tg Wt	3.15 ± 0.3	1.38 ± 0.1	1.75 ± 0.1
	G93A	3.99 ± 0.2	1.48 ± 0.1	1.54 ± 0.2
Complex IV	Wt	3.77 ± 0.2	1.62 ± 0.1	1.81 ± 0.1
(nmol/min/mg protein/CS)	Tg Wt	3.22 ± 0.3	1.40 ± 0.1	1.52 ± 0.1 †
	G93A	4.41 ± 0.5	1.36 ± 0.1 †	1.19 ± 0.1*†
Cu/Zn SOD	Wt	5.3 ± 0.6		
(U/mg protein)	Tg Wt	9.4 ± 0.3 †		
	G93A	11.4 ± 0.4 **†		

Data are mean ± SEM citrate synthase (CS)-corrected complex activities (nmol/min/mg protein/CS) and Cu/Zn SOD activity (U/mg protein). Activities measured in forebrain, spinal cord/brainstem, and cerebellum of G93A mice, and age-matched N1029 transgenic wildtype mice (TgWt) and littermate wildtype controls (Wt). N = 6-16/group.* $p<0.05$, ** $p<0.05$ significant increase vs Wt Tg (N1029). † $p<0.05$ Change vs Wt (ANOVA, and post-hoc Fisher PLSD).

Table 8: Mitochondrial Respiratory Enzyme and SOD1 Activities in G93A Mice:100-104 days.

	n	Complex I	Complex II-III	Complex IV	Cu/Zn SOD
Wild Type	7	293 ± 22	1.04 ± 0.04	1.14 ± 0.15	4.2 ± 0.1
Tg-Wild Type	7	354 ± 28	1.08 ± 0.09	1.38 ± 0.14	12.4 ± 0.8
G93A	7	386 ± 6 *	1.18 ± 0.12	1.48 ± 0.19	13.4 ± 0.49

Data presented as mean ± SEM citrate synthase (CS)-corrected complex activities (nmol/min/mg protein/CS) and Cu/Zn SOD activity (U activity/mg protein) in cortical mitochondrial fractions and cytosol, respectively. Subjects were G93A mice Tg-wildtype (N1029), and wild type control mice (age range: 100-104d). * $p <$ 0.05, significant difference relative relative to wild type control mice (ANOVA, and post-hoc Fisher PLSD).

Discussion: These findings suggest that the gene defect in G93A mice induces alterations in electron transport chain enzyme activities in forebrain and spinal cord/brainstem regions of the CNS. These alterations are not attributable simply to overexpression of human SOD1, since similar changes do not occur in Tg-Wt (N1029) mice overexpressing normal human SOD1. The observation of elevated

complex I activity in G93A SOD1 mice is consistent with our previous findings of increased complex I activity in cortical regions of FALS patients with the A4V SOD1 mutation (Browne et al., 1998). Results support the suggestion arising from cerebral glucose use observations in "Objective #3", that that metabolic defects may exist before signs of motor impairment (about 90 days) and pathological abnormalities (about 70 days). Further evidence supporting this hypothesis comes from recent findings in this laboratory that levels of the energy metabolite ATP are markedly reduced in G93A mice as early as 30 days in forebrain and spinal cord (data not shown; Browne et al., 2001). Overall, data suggest an important role for metabolic dysfunction in the etiology of the motor neuron disease in this mouse model of ALS.

Objective #5: **To investigate the effects of increasing CAG repeat number on local rates of cerebral glucose use ($lCMR_{glc}$) in a mouse model of HD expressing expanded CAG repeats in murine *HD*: *Hdh* knock-in mice (7, 48 and 90 CAG repeats).**

Complimentary to the cerebral metabolic rates for glucose in *Hdh* mice expressing 50 glutamines, both homozygous and heterozygous for the transgene (Hdh^{Q50}, 48/48 and 48/7 CAG repeats, respectively) reported previously, we also measured [^{14}C]-2-deoxyglucose *in vivo* autoradiography in four month-old Hdh^{Q92} knock-in mice expressing 90 CAG repeats (equivalent to 92 glutamines, 92Q; 90/90 and 90/7 CAG repeats) to determine:

- if energy metabolism is altered by expression of expanded polyglutamines in huntingtin protein,
- the effect of increased CAG repeat number (90 versus 48, assessed in year 1); and
- the effect of gene dosage on glucose use (heterozygous 90/7 versus homozygous 90/90 mice), at a time point preceding the onset of any behavioral changes and neuronal intranuclear inclusion (NII) formation in these mice.

Animals: Experiments employed 21 mice in three groups: *Hdh* mice both homozygous and heterozygous for the transgene, expressing 92 (Hdh^{Q92}) glutamines (90/90 and 90/7 CAG repeats, respectively) and in normal wild-type littermates (Hdh^{Q7}, 7/7 CAGs). Two mice were excluded from the 2-DG procedure analysis due to abnormal glucose or blood gas levels.

Physiological Variables: Arterial plasma glucose concentration, *p*O2, *p*CO2 and *p*H were measured 35 minutes into the procedure (10 minutes before animal decapitation) to determine the physiological status of the animals. There were no significant differences in the levels of any of these measured parameters between 7/7 wild type mice and levels in 90/7 and 90/90 mice ($p > 0.05$, ANOVA, followed by Fisher's PLSD). All measured parameters were within accepted normal ranges,

indicating that there are no physiological effects associated with the *Hdh* mutation that might alter the interpretation of glucose use results.

Glucose Utilization: Glucose use values in 21 brain regions examined are presented in Table 9. A comparison of glucose use values between Hdh^{Q92} and Hdh^{Q50} mice is shown in Figure 2. Glucose use values were markedly increased throughout the brains of 90/90 Hdh^{Q92} mice. Increases reached statistical significance in 15 of the 21 regions examined, and were not restricted to brain regions susceptible to degeneration in HD (ie. striatum, cortex). Furthermore, glucose use levels in 90/90 mice were significantly elevated over levels in 90/7 mice in 3 regions, suggesting a potential gene dosage effect, as well as a CAG length-dependent effect (see Figure 3).

Table 9: Local Cerebral Glucose Utilization ($lCMR_{glc}$) in Hdh^{Q92} CAG Knock-in Mice

REGION	7/7	90/7	90/90
Frontal Cortex	52.3 ± 6.6	60.1 ± 3.6	78.2 ± 6.7 ** †
Parietal Cortex	50.0 ± 7.0	58.5 ± 4.0	75.3 ± 7.6 *
Anterior Cingulate Cortex	74.2 ± 11.8	78.4 ± 7.3	99.2 ± 8.7
Auditory Cortex	51.0 ± 6.0	64.9 ± 5.4	81.5 ± 8.7 *
Striatum: Dorsolateral	57.8 ± 7.1	61.5 ± 5.9	81.1 ± 6.2 * †
Ventromedial	55.8 ± 7.3	58.1 ± 6.1	76.0 ± 6.7
Globus Pallidus	32.3 ± 4.1	38.3 ± 2.5	50.3 ± 7.8 *
Hippocampus: CA1	30.0 ± 4.1	41.3 ± 3.6	50.3 ± 6.9 *
CA3	41.2 ± 5.4	52.7 ± 3.4	66.3 ± 9.6 *
Dentate Gyrus: Molecular Layer	47.7 ± 6.1	55.8 ± 4.6	73.2 ± 6.0 ** †
Dorsolateral Geniculate Body	49.0 ± 6.6	56.9 ± 4.8	71.5 ± 10.1
Medial Geniculate Body	56.8 ± 7.2	67.2 ± 3.7	75.0 ± 9.2
Superior Colliculus: Superficial	46.8 ± 6.1	54.9 ± 4.5	68.2 ± 6.8 *
Layer	46.2 ± 6.1	55.1 ± 3.3	68.1 ± 6.3 *
Deep Layer	12.4 ± 1.7	18.6 ± 1.2	24.2 ± 6.6 *
Internal Capsule	54.7 ± 8.0	65.6 ± 4.4	84.3 ± 10.2*
Thalamus: Dorsomedial	39.6 ± 5.9	47.3 ± 4.0	58.3 ± 7.9 *
Ventromedial	28.6 ± 4.0	37.4 ± 2.0	44.1 ± 6.5 *
Substantia Nigra: *pars reticulata*	48.5 ± 7.7	58.5 ± 4.3	69.7 ± 11.2
pars compacta	31.0 ± 4.2	37.0 ± 2.4	47.5 ± 7.5 *
Cerebellum: Grey matter	21.2 ± 2.3	27.7 ± 1.8	29.8 ± 4.6
White matter			

$lCMR_{glc}$ (nmol/100g/min) in homozygous (90/90) and heterozygous (90/7) Hdh^{Q92} knock-in mice; and wild-type (7/7; Hdh^{Q7}) littermate controls. Data presented as mean ± SEM, (n=4-6 per group).
* $P < 0.05$, ** $P < 0.01$ relative to levels in 7/7 mice; † $P < 0.05$ relative to 90/7 mice (ANOVA, followed by Fisher's PLSD).

Discussion: We previously found that glucose use rates did not significantly differ between Hdh^{Q50} and Hdh^{Q7} mice in any of the brain regions examined ($p > 0.05$; ANOVA, followed by Fisher's

PLSD), and there was no effect of gene dosage in Hdh^{Q50} mice (48/48 vs 48/7). In this study, we found marked increases in glucose use throughout the brains of 90/90 Hdh^{Q92} mice. Increases were significant in 15 of the 21 regions examined. Furthermore, glucose use levels in 90/90 mice were significantly elevated over levels in 90/7 mice in 3 regions, suggesting a potential gene dosage effect, as well as a CAG length-dependent effect (see Figure 2). It has been reported that the rate and extent of huntingtin protein translocation from cytosol to the nucleus, and the formation of nuclear huntingtin aggregates, increase with higher CAG repeat lengths (Wheeler et al., 2000, 2002). Therefore, there is reason to suppose that any energetic changes associated with the huntingtin mutation may also vary in time of onset and extent according to the length of the CAG repeat. We are currently investigating this hypothesis further in Hdh^{Q111} mice.

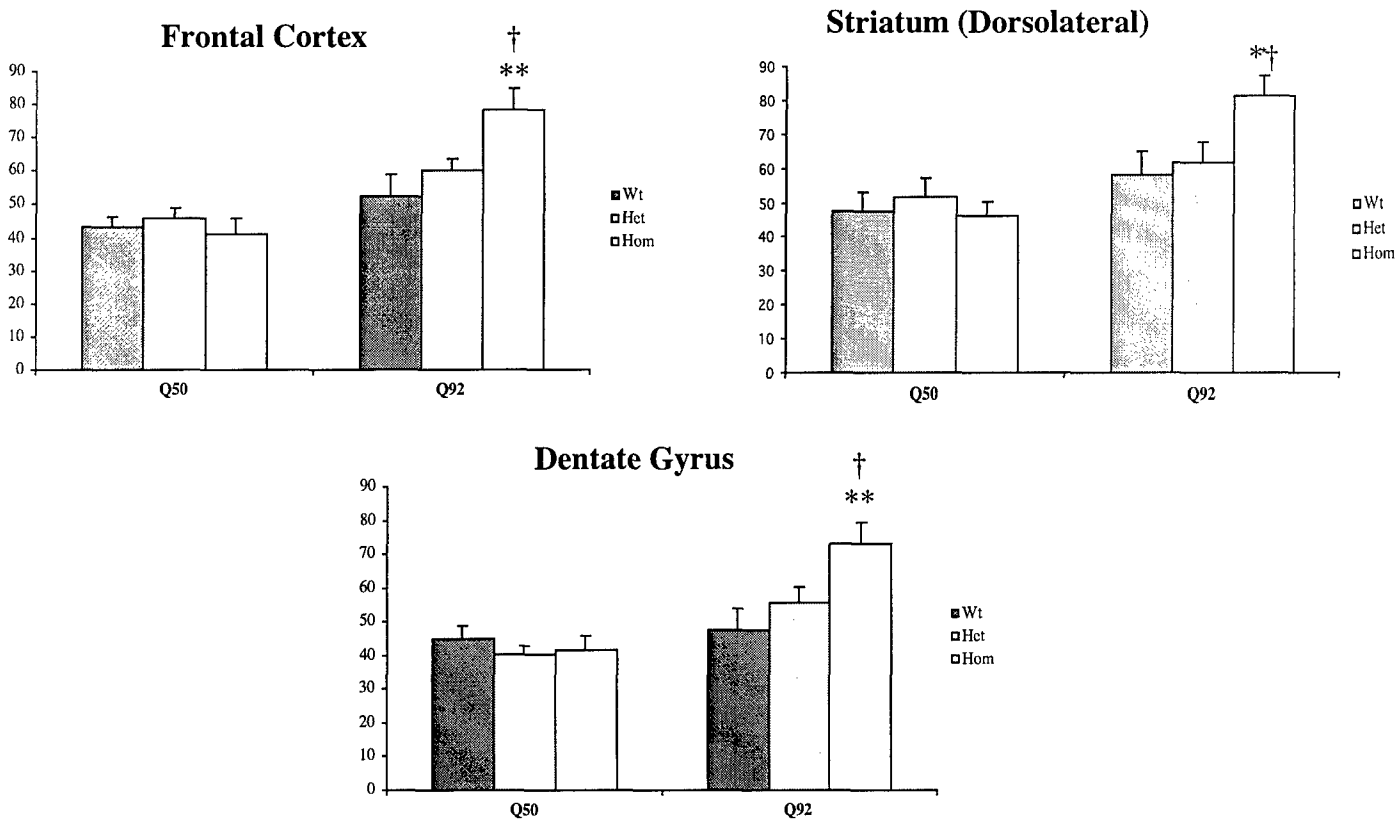

Figure 2: Cerebral Glucose Use in Representative Regions From Hdh^{Q50} and Hdh^{Q92} Mice

$lCMR_{glc}$ (nmol/100g/min) in 4 month-old Hdh^{Q50} and Hdh^{Q92} homozygous (Hom) and heterozygote (Het) mice, and wild-type (Wt, 7/7) littermate controls. Data presented as mean ± SEM, (n=6 per group).* $P < 0.05$, ** $P < 0.01$ relative to levels in 7/7 mice; † $P < 0.05$ relative to 90/7 mice (ANOVA, followed by Fisher's PLSD).

The observation that glucose uptake is increased in multiple forebrain regions as a consequence of the gene mutation in *Hdh*^{Q92} mice may at first seem counter-intuitive. We hypothesize that this reflects increased glucose uptake in an attempt to drive metabolism and overcome a metabolic stress in these animals. The fact that *Hdh*^{Q92} mice do not develop overt signs of motor dysfunction or cell loss in their lifetime suggests that in this case the enhanced glucose uptake is sufficient to maintain required ATP production (however, *Hdh*^{Q92} mice do develop nuclear huntingtin aggregates by 15 months of age, Wheeler et al., 2000). The exact nature of any metabolic stress (eg. glycolytic or mitochondrial) has yet to be elucidated. In contrast, *Hdh*^{Q111} mice develop motor abnormalities by approximately 19 months of age. It will be of interest to compare the time course and magnitude of metabolic abnormalities between *Hdh*^{Q92} and *Hdh*^{Q111} mice.

Objective #6: **To determine if glucose use is altered over the life-span of a transgenic HD mouse model expressing a human mutant HD fragment: R6/2 HD mice.**

In the original grant protocol we proposed measuring cerebral glucose utilization throughout the brains of HD transgenic R6/2 mice, both prior and after symptom onset (at around 8 weeks), to determine if energetic defects play a causative role in disease pathogenesis. Subsequent to award of this grant, we found that R6/2 mutant mice develop a diabetic profile from approximately 7 weeks of age (Ferrante et al., 2000). Mice show elevated basal blood plasma glucose levels (>> 300mg/dL, relative to 150 mg/dL in physiologically normal mice), and reduced glucose tolerance. Elevated baseline plasma levels, outside of a range considered physiologically "normal" (5-16mM / 91-290mg/dL in rodents), confounds use of the [^{14}C]-2-deoxyglucose technique (Sokoloff et al., 1977). This *in vivo* imaging procedure utilizes an 'operational equation' to extrapolate rates of glucose utilization in a given brain region from measured parameters, which include levels of circulating arterial plasma glucose, rate of uptake of injected tracer [^{14}C]-2-deoxyglucose from the circulating blood, and detected levels of [^{14}C] in the brain region of interest at the end of the experiment. The equation also relies on assumed kinetic rate constants for blood-brain transfer of glucose and 2-deoxyglucose, which are based on levels measured in rodents under physiologically "normal" conditions. Outside of these conditions, the kinetic constants used in the operational equation no longer apply and any extrapolated results become unreliable (Sokoloff et al., 1977). Consequently, we have been unable to perform glucose use studies in R6/2 mice due to their basal and stress-induced hyperglycemia. We explored measuring glucose use levels in mice before they develop the

diabetic profile (4-6 weeks of age), but studies in mice this young are confounded by their small size, which makes surgical preparation of the animals extremely difficult and increases stress in the mice.

In lieu of studies in R6/2 mice, we employed another mutant mouse model of HD expressing an N-terminal fragment of human mutant huntingtin, N171-82Q mice with an 82-polyglutamine expansion (Schilling et al., 1999). N171-82Q mice develop a relatively rapid disease phenotype characterized by onset of motor abnormalities, nuclear huntingtin aggregate (NII) deposition, and striatal-specific neuronal loss by 3-4 months of age. Mice generally live 4-5 months, and develop a diabetic profile by 3.5-4 months of age. We carried out studies to identify whether metabolic abnormalities are present in mutant N171-82Q mice at 2 months of age, prior to huntingtin aggregate formation, striatal cell loss, behavioral and diabetic phenotype in this model. This time point was chosen to determine if energetic changes play an early role in the disease. Results were compared with levels in wildtype (Wt) littermates, and in control mice expressing the human transgene with a non-mutant length polyglutamine expansion, N171-18Q. Results are discussed below.

[^{14}C]-2-Deoxyglucose Measures of Cerebral Glucose Use in N171-82Q HD Mice.

Animals: We measured cerebral glucose use rates in conscious N171-82Q mutant mice, N171-18Q transgenic control mice, and non-transgenic wild-type littermate mice at 2 months of age.

***Physiological Variables*:** Mice require 1.5-2h for anesthetic clearance from the brain after surgery. Wild type control and N171-18Q mouse basal arterial glucose levels were normal by 2h after surgery (~150 mg/dL). In contrast, N171-82Q mice required 4-5 hours recovery after anesthesia for their basal glucose levels to return from elevated to approaching normal levels. This is likely due to an inability to buffer anesthesia stress-induced glucose upregulation, although mice are not overtly diabetic at this time point. At the time of the experiment, glucose values in N171-82Q mice were elevated relative to control levels (183 ± 22 vs 155 ± 8 mg/dL), but were within the physiologic "normal" constraints of the procedure. Arterial plasma levels did not alter over the time course of the procedure, indicating that mice were not stressed by the technique. Arterial pO_2, pCO_2 and pH values measured at the end of the 45min 2-DG procedure did not differ between groups and were well within "normal" physiologic ranges for mice. Data are presented in Table 10.

	Wildtype	N171-18Q	N171-82Q
Pre-Glucose (mg/dL)	155.0 ± 8.0	168.7 ± 14.4	182.8 ± 21.9
Glucose + 45 min. (mg/dL)	150.5 ± 5.5	201.3 ± 19.7	174.4 ± 10.7
p_aO_2 (mm Hg)	110.0 ± 9.0	38.7 ± 7.8	121.4 ± 8.6
p_aCO_2 (mm Hg)	40.5 ± 1.7	37.5 ± 3.4	38.8 ± 2.4
pH	7.32 ± 0.03	7.31 ± 0.01	7.36 ± 0.01*
Number of animals	4	7_a	5

TABLE 10: Data presented as mean ± SEM for: arterial plasma glucose concentrations measured immediately before [^{14}C]-2-deoxyglucose isotope injection (Pre-Glucose) and at the end of the 2-DG procedure (Glucose + 45 min); and arterial blood gas levels at the end of the procedure. * $p<0.05$, significant difference relative to N171-18Q mice (ANOVA, followed by Fisher's PLSD post-hoc unpaired t-test). a: p_aCO_2 data only available for 6 N171-18Q mice. Arterial plasma glucose levels did not alter significantly over the 45 min duration of the experiment in any group ($p> 0.05$, Student's paired t-test).

Cerebral Glucose Use ($lCMR_{glc}$): Local cerebral rates of glucose use in N171-82Q mutant mice were significantly elevated in 20 of the 32 forebrain regions examined, relative to levels in wildtype and N171-18Q transgenic control mice,. Rates were unaltered in all five cerebellar regions investigated. Results are presented in Tables 11-13. Figure 3 demonstrates the nature of glucose use changes in 10 representative regions. Glucose use changes were not restricted to regions vulnerable to cell loss in HD (ie. striatum), but occurred in multiple forebrain regions including striatum, all eleven cortex regions examined, auditory, visual and extrapyramidal regions.

Table 11: CORTICAL REGIONS

Region	Wildtype	N171-18Q	N171-82Q
Pre-Frontal: Layers I-III	55.7 ± 8.8	57.1 ± 4.0	72.0 ± 1.5 * †
Pre-Frontal: Layer IV	59.3 ± 10.0	62.4 ± 5.1	78.5 ± 1.1 *
Pre-Frontal: Layers V-VI	49.7 ± 5.0	51.7 ± 3.9	64.7 ± 2.4 *
Frontal: Layers I-III	59.9 ± 7.7	55.1 ± 3.7	68.8 ± 3.9 *
Frontal: Layer IV	59.5 ± 6.3	61.2 ± 3.9	85.2 ± 2.6 ** †
Frontal: Layers V-VI	50.9 ± 4.4	49.5 ± 3.4	65.3 ± 3.0 **
Parietal: Layers I-III	56.5 ± 7.6	47.9 ± 3.9	69.0 ± 3.8 **
Parietal: Layer IV	59.4 ± 9.7	55.1 ± 4.5	80.0 ± 2.5 ** †
Parietal: Layers V-VI	52.5 ± 7.1	50.5 ± 3.7	68.8 ± 2.3 ** †
Anterior cingulate	65.6 ± 10.9	61.2 ± 5.5	85.2 ± 4.2 **
Posterior cingulate	74.0 ± 5.6	74.9 ± 7.5	96.5 ± 4.4 *

Table 12: LIMBIC AND EXTRAPYRAMIDAL REGIONS

Region	Wildtype	N171-18Q	N171-82Q
Striatum:			
Dorsomedial	61.3 ± 7.2	63.9 ± 5.3	72.9 ± 4.0
Dorsolateral	68.8 ± 7.3	73.1 ± 4.0	80.4 ± 2.4
Ventromedial	64.3 ± 5.4	60.4 ± 4.6	77.5 ± 3.3 *
Globus Pallidus	37.2 ± 3.5	39.7 ± 4.0	49.1 ± 2.0
Hippocampus:			
CA1	31.9 ± 5.6	32.4 ± 2.7	42.1 ± 3.5 *
CA3	40.4 ± 6.2	40.9 ± 4.2	50.7 ± 2.6
Dentate gyrus	50.8 ± 7.4	47.1 ± 3.3	61.8 ± 3.1 *
Lateral habenular nucleus	48.7 ± 9.4	67.4 ± 9.5	67.3 ± 7.0
Subthalamic nucleus	63.6 ± 11.1	60.0 ± 5.5	69.3 ± 2.0
Mammilary body	94.0 ± 22.8	88.0 ± 4.0	101.1 ± 6.2
Substantia nigra:			
pars compacta	59.0 ± 6.6	52.3 ± 1.9	64.7 ± 3.6 **
pars reticulata	37.4 ± 7.3	34.1 ± 2.7	42.9 ± 2.5
Cerebellar nucleus	87.0 ± 4.5	91.1 ± 3.6	117.4 ± 9.0 ** †
Cerebellar hemisphere			
granular layer	29.9 ± 3.1	34.5 ± 2.1	37.0 ± 2.1
molecular layer	41.5 ± 4.6	47.5 ± 2.2	52.8 ± 2.4 †
Inferior olive	75.3 ± 12.8	65.2 ± 1.6	73.2 ± 2.9
Cerebellar white matter	24.8 ± 4.3	22.8 ± 1.5	26.8 ± 2.6

Table 13: AUDITORY AND VISUAL REGIONS

Region	Wildtype	N171-18Q	N171-82Q
Visual Regions -			
Visual Cortex: Layer IV	57.1 ± 3.5	62.2 ± 2.1	66.3 ± 5.5
Lateral geniculate body	57.0 ± 7.5	53.7 ± 2.7	62.1 ± 2.4
Superior colliculus:			
Superficial layer	54.2 ± 7.9	54.7 ± 4.5	57.3 ± 2.4
Deep layer	54.9 ± 6.9	53.1 ± 3.2	61.4 ± 2.1
Auditory Regions -			
Auditory Cortex: Layer IV	102.5 ± 4.1	84.5 ± 5.3	105.5 ± 9.1 *
Inferior colliculus	145.3 ± 13.6	125.1 ± 3.0	144.6 ± 18.4
Superior olive	90.0 ± 6.6	85.6 ± 4.0	103.3 ± 8.0 *
Medial geniculate body	81.3 ± 6.5	75.4 ± 3.1	89.4 ± 3.2 *
Cochlear nucleus	87.8 ± 11.1	83.6 ± 3.6	109.1 ± 7.7 **

Local cerebral metabolic rates for glucose (nmol/100g/min) in heterozygous N171-82Q mutant mice (n=5), compared with rates in wild-type littermate controls (n=4), and in heterozygous N171-18Q transgenic controls (n = 7). *$p < 0.05$, relative to levels in wt mice; † $p < 0.05$ relative to levels in 18Q mice (ANOVA & Fischer's PLSD).

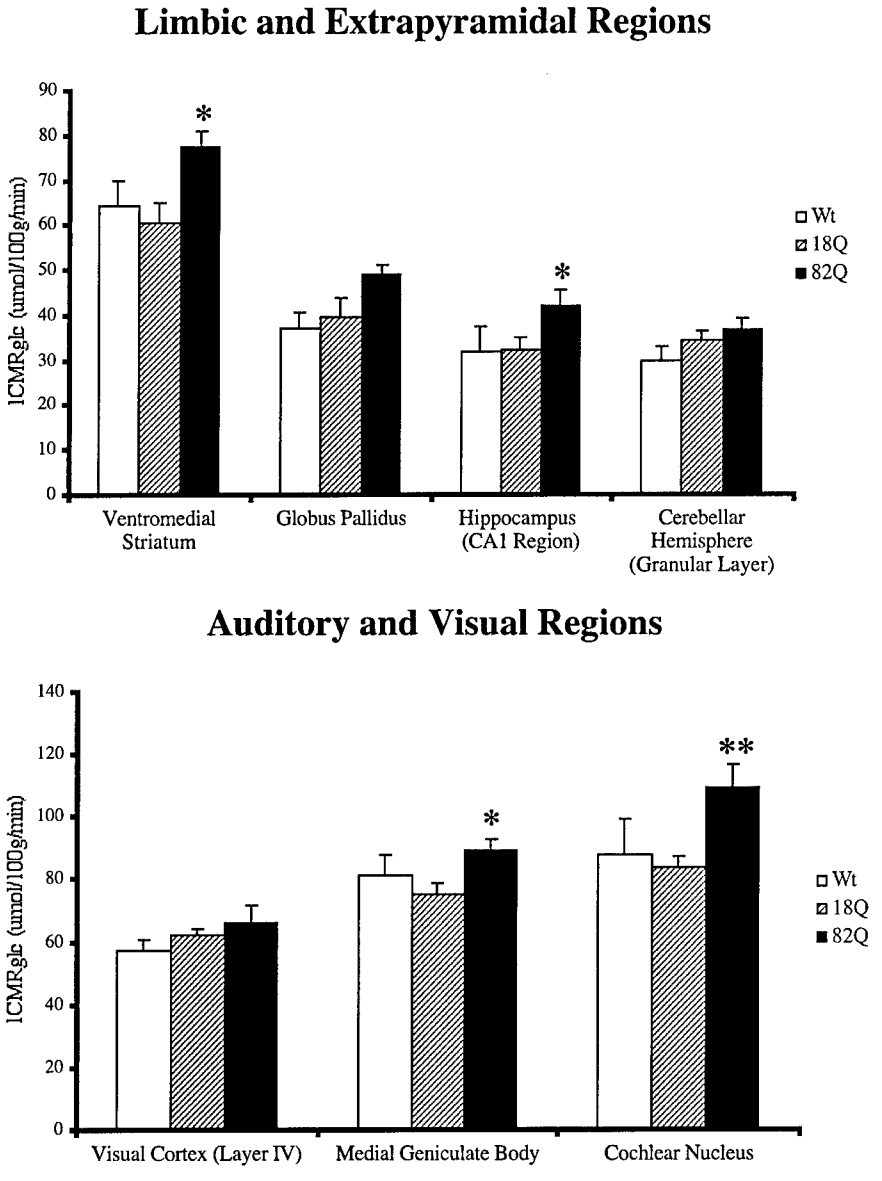

Figure 3: Local cerebral metabolic rates for glucose (nmol/100g/min, mean ± SEM) in heterozygous N171-82Q mutant mice, compared with rates in wildtype littermate controls (Wt), and in heterozygous N171-18Q transgenic controls. *$p < 0.05$, relative to levels in Wt mice; † $p < 0.05$ relative to levels in N171-18Q mice (ANOVA & Fischer's PLSD). N = 4-7 per group.

We hypothesize that up-regulation of glucose uptake by neurons may occur early in the lifespan of HD mouse models, to compensate for impairments in other constituents of metabolic pathways. The increased glucose uptake observed in *Hdh*^{Q92} mice (discussed previously) may be sufficient to prevent cell degeneration in these animals (at least during their 2-year lifespan), but may not be sufficient to prevent neuronal dysfunction in N171-82Q mice. Increases in glucose use appear in multiple forebrain regions in these models. This does not explain the regional selectivity of cell death seen in HD. One potential explanation is that striatal neurons exhibit an increased vulnerability

to metabolic impairments relative to other neuronal populations. This suggestion is supported by observations that striatal cells are particularly vulnerable to mitochondrial toxins (eg. 3-NP, azide), metabolic insults (eg. ischemia), and excitotoxins (eg. quinolinic acid), in addition to the substantial glutamatergic input to the striatum from the cortex.

Objective #7: **Measurement of electron transport chain enzyme activities in R6/2 HD mice, before and after symptom onset and pathological changes.**

There are multiple reports of metabolic enzyme dysfunction in HD post-mortem brain, notably reduced complex II-III, IV, and aconitase activities localized to caudate and putamen (Browne et al., 1997; Gu et al., 1996). We used spectrophotometric assays to measure mitochondrial metabolic enzyme activities in brains from R6/2 HD mice.

Animals: Whole forebrain and cerebellum homogenates were prepared from frozen brain tissue taken from R6/2 mice at 3.5, 8 and 12 weeks of age. Enzyme activities measured were glyceraldehyde-3-phosphate dehydrogenase (GAPDH; glycolytic enzyme); aconitase and citrate synthase (Kreb's cycle enzymes); complexes I, II-III and IV of the mitochondrial electron transport chain. Complex enzyme activities (per mg protein) were corrected by the citrate synthase activity (per mg protein; a mitochondrial matrix enzyme) as a correction for differential mitochondrial number between preparations (data not shown). No alterations in activities of any of the enzymes measured were detected in whole brain homogenates from 3.5 and 8 week-old mice. Increased complex I and II-III activities were detected in R6/2 forebrain at 12 weeks of age. GAPDH activity was significantly elevated in the cerebellum of 12 week-old R6/2 mice relative to wild type littermate control levels. Aconitase activity was unaltered in all regions at all time-points.

Discussion: We found no enzymatic abnormalities in mice at 3 or 8 weeks of age, suggesting that any alterations in these metabolic enzymes occur only after symptom onset. Our findings differ from one previous report which shows reduced complex II-III activity and markedly decreased aconitase activity in forebrain from 12 week-old R6/2 mice (Tabrizi et al., 2000). However, another report found no difference in oxidative phoshorylation enzyme activities in R6/2 striatum and cerebral cortex (Guidetti et al., 2001). Reasons for these discrepancies are not obvious, however the bulk of evidence seems to suggest that mitochondrial enzyme activities are not significantly impaired up to 12 weeks of age in R6/2 mouse forebrain. Our results also suggest that reductions in complex II-III and IV, and aconitase activities in affected brain regions (caudate and putamen) of symptomatic, end-

stage (grade 3 and 4) HD patients are not replicated in the R6/2 model (Browne et al., 1997; Gu et al., 1997; Tabrizi et al., 1999). This latter observation may indicate that the pathophysiology of the R6/2 model differs from HD pathogenesis in humans. Alternatively, the rapid time-course of the disorder in mouse models may preclude the development of metabolic enzyme alterations. In light of the lack of enzymatic changes in cortex and striatum of R6/2 mice we chose not to pursue further studies in this model. We did, however, measure oxidative phopshorylation enzyme activities in three different brain regions of N171-82Q HD mice (data not shown). Results in three month-old symptomatic N171-82Q mice showed no significant alterations in complex II-III, complex IV, or citrate synthase activities in striatum, cerebral cortex, or cerebellum, relative to levels in N171-18Q controls and wildtype littermates (n=20-30 per group) (Browne et al., unpublished observations). This finding further supports the suggestion that alterations in oxidative phosphorylation enzyme activities that are implicated in HD in humans, do not play a causative role in the disease phenotype in mutant mouse models of HD.

Objective #8. **NMR assessment of cerebral lactate levels in *Hdh* and R6/2 mice.**

Increased lactate production is a marker for metabolic dysfunction, putatively indicating elevated glycolytic activity, or pyruvate shunt to form lactate rather than entering mitochondrial metabolic pathways. Lactate levels in brain can be measured non-invasively *in vivo* by NMR spectroscopy.

Animals: We carried out NMR spectroscopic measurements of lactate and metabolite levels in the basal ganglia of anesthetized R6/2 and wildtype littermate mice at 12 weeks of age (n = 5 per group).

Lactate Levels: Lactate levels were calculated as the ratio of lactate to creatine, which we have previously shown to be unaltered in the basal ganglia of R6/2 mice (Ferrante et al., 2000). Results show increased lactate levels in the basal ganglia of R6/2 mice compared with levels in wildtype littermates (Figure 4). The average lactate level in R6/2 mice was 0.14 ± 0.06 (ratio, mean ± SEM), and was unobservable (and hence not quantifiable) in the wildtype mice (evident from Figure 4, which shows the averaged spectra for 5 R6/2 mice and 5 wildtype mice).

Discussion: Results suggest that lactate production in basal ganglia is elevated in symptomatic R6/2 mice, compared with age-matched wildtypes in which basal lactate levels were generally undetectable from background levels. Studies should be expanded to multiple time-points to determine whether

abnormalities in lactate production occur before symptomatic and pathologic changes in this mouse model of HD.

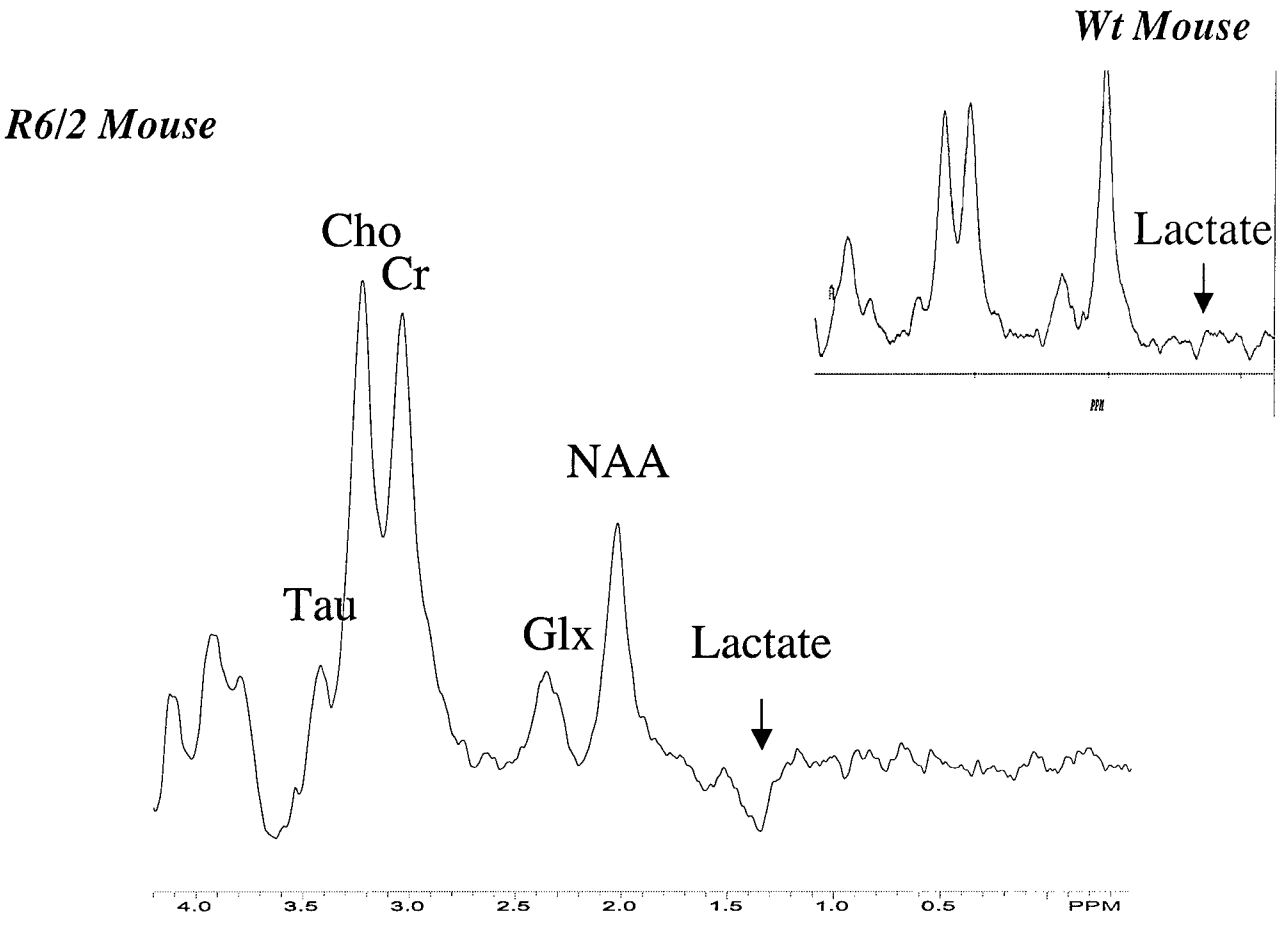

Figure 4: Averaged NMR spectra from basal ganglia of12 week old R6/2 and wildtype (WT) mice (n=5). *Abbreviations:* Cho, choline; Cre, creatine; Glx, glutamine; NAA, N-acetylaspartate; Tau, taurine.

Objective #9. **Assessment of oxidative damage markers in *Hdh* and R6/2 mice.**

In the original specific aims of this project we aimed to use HPLC to measure four different markers of oxidative damage in brain of R6/2 and *Hdh* mouse models of HD. These were protein carbonyls, nDNA OH^8dG; hydroxyl radical production and nitrotyrosine levels. We encountered problems with measurement of two of these markers, nitrotyrosine and protein carbonyls. Despite a great deal of effort to re-instate reliable HPLC detection of nitrotyrosine using Coullarray electro-chemical detection (ESA, Chelmsford MA) following our laboratory's move, we have been unable to reproducibly detect basal nitrotyrosine in mouse brain at levels above background noise. This project consumed several months of work, but unfortunately yielded no results. Similarly, the laborious and

time-consuming protein carbonyl HPLC assay has not generated reproducible data in HD mouse brain.

We have, however, successfully measured levels of the DNA damage product 8-hydroxy-deoxyguanosine (OH^8dG) in nuclear brain extracts of R6/2 mice. We have also developed technology to measure OH^8dG levels in body fluids, including plasma and urine. We have successfully measured levels of hydroxyl radical production in the N171-82Q HD mice (which resemble the R6/2 model). We have also extended studies to examine levels of the lipid oxidative damage markers, malondialdehyde, acrolein, 8-iso-prostaglandin F2 and 4-hydroxynonenal by immuno-histochemical techniques (in lieu of the lack of carbonyl and nitrotyrosine data). Results are presented below.

a) Oxidative Damage Studies: OH^8dG in R6/2 Mouse Urine, Plasma, DNA and Brain Tissue

We examined free OH^8dG levels in urine, plasma and striatal microdialysates and DNA OH^8dG levels in cortex and striatum of the R6/2 mice.

Animals: Thirty R6/2 and 29 littermate wildtype mice at 12 weeks of age were used in experiments.

OH^8dG: We found that urine and plasma concentrations of OH^8dG were significantly increased in the R6/2 mice at 12 weeks of age (Table 14). Furthermore we used *in vivo* microdialysis to demonstrate that there were significant increases in extracellular OH^8dG levels in the striatum of the R6/2 mice as compared to age-matched littermate controls (Table 14). We also found that OH^8dG is increased in genomic DNA isolated from the striatum of R6/2 mice (Figure 5). We utilized OH^8dG immunocytochemistry to show an age-dependent increase in staining, consistent with the biochemical measurements (data not shown).

Discussion: These findings provide direct *in vivo* evidence for increased oxidative stress in the brains of the R6/2 mice. Results are consistent with studies showing progressive increases in staining of other oxidative damage markers for lipid peroxidation, and increased 3-nitrotyrosine staining in the R6/2 mice (Perez-Severiano *et al.*, 2000; Tabrizi *et al.*, 2000). Studies are currently being extended to *Hdh* mice.

Table 14: OH^8dG levels in urine, plasma and microdialysates of R6/2 and control mice.

	R6/2 (n)	Controls (n)
Urine ng/mg creatinine	18.4 ± 4.99 (10)[a]	6.2 ± 0.7 (10)
Plasma pg/ml	24.8 ± 9.49 (30)[b]	51.6 ± 13.6 (29)
Microdialysates pg/ml	2.8 ± 0.26 (10)[c]	2.0 ± 0.2 (9)

Data are mean ± SEM. [a] p=0.02; [b] p=0.006; [c] p= 0.018 vs. controls. (Group sizes in parentheses).

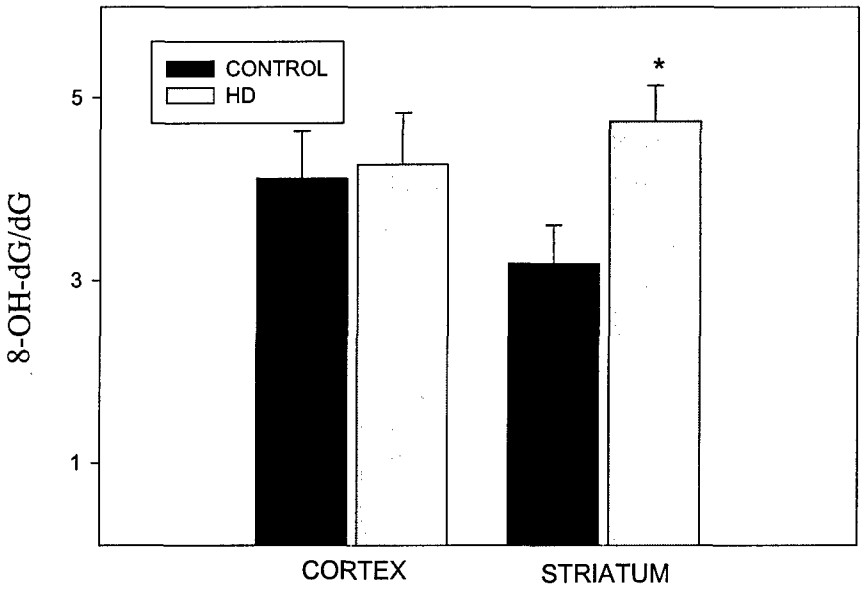

Figure 5: OH^8dG levels in cortex and striatal DNA from R6/2 (HD) and littermate wild-type control mice. Data are mean ± SEM OH^8dG/dG ratios. * $p< 0.05$ (Student's unpaired t-test).

b) Oxidative Damage Studies: Hydroxyl Radical Generation in N171-82Q Mouse Striatum

In another approach to investigate whether oxidative damage to cellular elements is increased as a result of the HD mutation, we used microdialysis with HPLC to compare the rates of hydroxyl (OH^-) radical formation in striatum from N171-82Q and wild-type mice, both at baseline and following cell stress by exposure to a neurotoxin (3-nitropropionic acid, 3-NP). This technique measures the conversion of 4-hydroxybenzoic acid (4-HBA) to 3,4-dihydroxybenzoic acid (3,4-DHBA) by reaction with endogenous OH^-, as a measure of "hydroxyl radical-like" production.

Animals: Experiments were performed in symptomatic N171-82Q mice (n=4), N171-18Q "non-HD" mice (n=6) and wild-type littermate control mice (n=6) at 3 months of age (symptomatic). 4-HBA (400 mg/kg i.p. in saline) was administered to mice, and microdialysate samples were collected from the striatum at 20 minute intervals for the subsequent 3 hours. Mice then received 3-NP (100 mg/kg i.p.), and microdialysates were collected every 20 minutes for a further 3 hours. Levels of 3,4-DHBA in the dialysate, formed by the reaction of hydroxyl radicals with 4-HBA, were measured by HPLC detection.

OH^- Generation: Results are presented as the ratio of 3,4-DHBA to 4-HBA accumulated over the 3 hour periods before and after 3-NP administration (Figure 7). Basal levels of hydroxyl radical generation (3,4-DHBA/4-HBA ratio) are higher in N171-82Q mice than in either N171-18Q

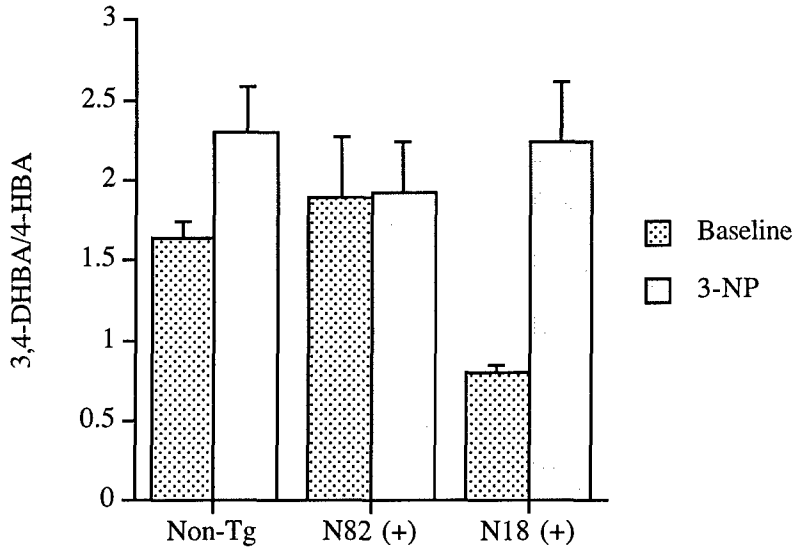

Figure 6: Free Radical Production in N171 HD Mice.

Data are mean ± SD 3,4-DHBA/4-HBA ratios, representative of OH^- radical levels, in 12 week-old mice (baseline), and following stress induced by 3-NP administration (100mg/kg i,p,). Subjects were N171-82Q mutant HD mice (N82+), N171-18Q transgenic controls (N18+), and wildtype littermates (Non-Tg).

transgenic controls, or in wildtype littermate mice. Both control groups showed elevated OH^- production in response to 3-NP, whereas N171-82Q mice did not. The reason for this observation is unclear.

Discussion: Results suggest that HD mice exhibit elevated free radical production in the striatum, a brain region vulnerable to cell loss in HD, around the time of symptom onset (3 months of age in N171-82Q mice). This observation adds support to the hypothesis that free radical damage is involved in disease etiology in this mouse model, but further studies of the temporal pattern of radical generation are needed to verify results and to determine if this is a causative event in pathogenesis. We also require studies in other brain regions to determine if this effect is restricted to vulnerable regions in HD (ie. striatum), or is a widespread, non-specific phenomenon. Studies are being extended to *Hdh* mice.

c) Oxidative Damage Studies: Immunohistochemical Studies in R6/2 Brain

We have initiated immunohistochemical studies in R6/2 mice to qualitatively assess expression levels of other markers of oxidative damage to lipid, namely malondialdehyde, acrolein, 8-iso-prostaglandin F2 and 4-hydroxynonenal. Preliminary findings in 12 week-old R6/2 striatum did not reveal any alterations in levels of malondialdehyde amd acrolein, compared with staining levels in wildtype

littermates (data not shown). However, 8-iso-prostaglandin F2 and 4-hydroxynonenal staining were both found to be increased in R6/2 mice, relative to wild-type levels, in 12 week-old mice (Figure 7).

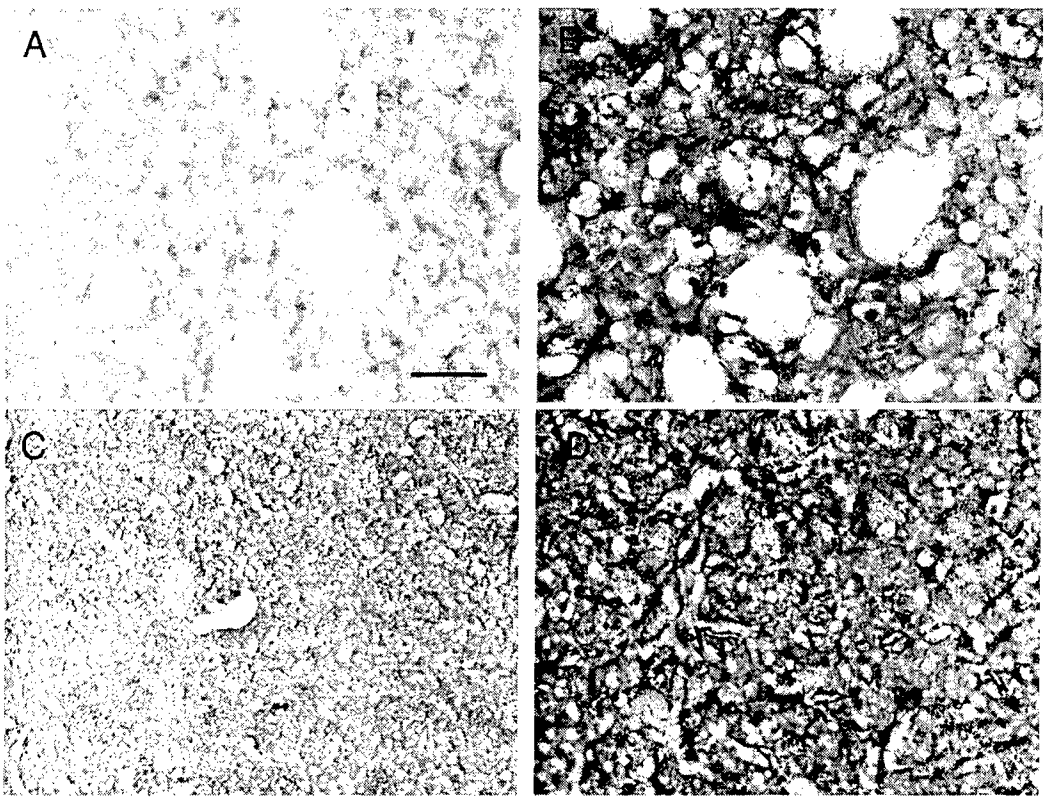

Figure 7: 8-iso-prostaglandin F2 (A, B) and 4-hydroxynonenal (C, D) immunoreactivity in the striatum of wild type (A, C) and R6/2 mice (B, D) showing increased staining in neurons, neuropil and vascular profiles in R6/2 mice. Scale bar = 50 m (A, B), 100 m (C, D).

Objective #10. **Assessment of oxidative damage markers in *G93A ALS Mice*.**

In the original specific aims of this project we aimed to use HPLC to measure four different markers of oxidative damage in G93A mouse CNS: protein carbonyls, nDNA OH^8dG, hydroxyl radical production and nitrotyrosine levels. As discussed in "Objective # 9', we have encountered problems measuring nitrotyrosine levels reproducibly using HPLC techniques. However, elevated nitrotyrosine staining has previously been demonstrated in G93A brain (Ferrante et al., 1997). Therefore, in Year 3 of this project we concentrated on measurements of oxidative damage to protein (protein carbonyl levels) and lipid (malondialdehyde levels).

a) Protein Carbonyl Measures in G93A Mice

Animals: Experiments were carried out in G93A mice and wildtype littermate controls at 90 days of age (immediately prior to symptom onset), 110 days (at symptom onset), and at 130 days (symptomatic, end-stage. (n = 6-8 per group). Measurements were made in tissue from four CNS areas: cerebral cortex, brainstem, cerebellum and spinal cord.

***Results*:** Protein carbonyl levels are presented in Table 15. No differences between G93A and wildtype mice were detected in 90 day-old mice, in any of the regions examined. By 110 days, carbonyl levels were significantly elevated in the spinal cord (+47%) and cerebral cortex (+14%). By 130 days of age, carbonyl levels were further increased in these regions (+80% in spinal cord; +59% in cerebral cortex), but remained unaltered in brainstem and cerebellum.

Table 15: Protein Carbonyl Levels in G93A FALS Mice

	90 Days	**110 Days**	**130 Days**
Spinal Cord			
Control	1.05 ± 0.34	0.99 ± 0.06	0.87 ± 0.17
G93A	1.11 ± 0.34	1.46 ± 0.15 *	1.57 ± 0.17 *
Cerebral Cortex			
Control	0.75 ± 0.08	0.71 ± 0.06	0.81 ± 0.05
G93A	0.86 ± 0.13	0.88 ± 0.05 *	1.29 ± 0.12 *
Brainstem			
Control	1.15 ± 0.12	1.14 ± 0.10	1.21 ± 0.11
G93A	1.13 ± 0.30	1.23 ± 0.09	1.19 ± 0.27
Cerebellum			
Control	0.52 ± 0.10	0.70 ± 0.11	0.87 ± 0.07
G93A	0.53 ± 0.10	0.69 ± 0.06	0.97 ± 0.17

Data are mean ± SEM, carbonyls (U/mg protein), n = 6-8 per group.
* $p < 0.01$, relative to wildtype control values (Student's unpaired t-test).

Discussion: Marked elevations in protein carbonyl levels in both spinal cord and cerebral cortex, with sparing in brainstem and cerebellum, suggest that regions vulnerable to degeneration undergo abnormal levels of oxidative damage to proteins in this ALS model. Trends towards increased oxidation are present in pre-symptomatic 90 day old G93A mice, but do not reach statistical significance until the 110 day time-point, around the onset of symptoms. Mice begin to show pathologic changes at approximately 70 days of age (mitochondrial perturbations, Gurney et al., 1995). It is also noteworthy that the extent of carbonyl elevation is greatest in the spinal cord, which

is the principal site of neuronal degeneration in the ALS phenotype. However, motor neuron cell bodies and motor association areas in the cortex are also affected in the disease, and also show carbonyl increases in this mouse model of ALS. Results indicate that increased oxidative damage occurs in vulnerable regions during a period between the first pathologic changes and the onset of motor symptoms in the G93A model.

b) Malondialdehyde Levels in G93A Mouse Spinal Cord

Mice: Experiments were carried out in G93A mice and wildtype littermate controls at 30 and 50 days of age (prior to pathologic changes), 70 days (around time of first pathological changes), and 110 days (at symptom onset), 8-19 mice per group. Levels were also measured in transgenic N1029 mice that overexpress human normal SOD1, as controls for the transgene manipulation in the G93A mice, at 70 and 110 days of age (n = 9-10 per group). Measurements were made in spinal cord, since this is the major site of degeneration in the ALS model.

***Results*:** Malondialdehyde levels are presented in Table 16. No significant differences between G93A and wildtype mice, or N1029 control mice, were detected at any time-point investigated.

Discussion: Results show no evidence of oxidative damage to lipid detectable using this technique in G93A spinal cord.

Table 16: Malondialdehyde Levels in Mouse Spinal Cord

Mouse Line	30 Days	50 Days	70 Days	110 Days
G93A	12.4 ± 1.8 n=16	8.67 ± 0.67 n=9	8.18 ± 1.53 n=10	10.88 ± 1.63 n=16
N1029			6.17 ± 2.17 n=9	10.42 ± 1.70 n=10
Wt	10.5 ± 2.4 n=16	8.05 ± 1.40 n=12	6.44 ± 1.33 n=8	9.99 ± 2.41 n=19

Data are mean ± SEM, malondialdehyde levels(nM TBA/mg protein), n = 8-19 per group.
$p > 0.05$, relative to both N1029 and wildtype control values (ANOVA).

Objective #11. Measurement of Cerebral Metabolite Levels in HD Mouse Brains

HPLC was used to measure levels of the energy metabolites ATP, ADP, AMP, creatine and phosphocreatine in brain tissue from R6/2 HD mice, according to methods in the original proposal. Studies are currently being carried out in R6/2 mice at younger ages, and in *Hdh* mice.

Animals: Studies in 12 week old mice were performed using brain tissue from R6/2 (n=6) and wildtype littermate mice (n=5).

Results: Metabolite levels in cerebral cortex are presented in Table 17. Results demonstrate that at this time-point, when mice are symptomatic and towards end-stage of their short lifespan, ATP levels in cortex are markedly reduced. In contrast to the approximate 3-fold decrease in ATP levels in R6/2s, relative to wildtype mice, levels of all other metabolites measured were significantly increased.

Table 17: Energy Metabolite Levels in Cerebral Cortex of End-Stage R6/2 mice

	Wildtype n=5	**R6/2** n=6	Unpaired t test
Creatine	49.40 ± 2.66	68.46 ± 1.56	P<0.0001
Phosphocreatine	15.09 ± 0.57	39.30 ± 2.01	P<0.0001
AMP	2.70 ± 1.14	7.99 ± 0.13	P<0.0001
ADP	3.14 ± 0.44	5.78 ± 0.30	P<0.0003
ATP	15.81 ± 1.43	4.65 ± 0.47	P<0.0001

Data are Mean ± SEM (nmol/mg protein).

Discussion: Results suggest that generation of ATP is hindered in symptomatic12 week old mice in this brain region. Elevations in cellular levels of AMP and ADP may reflect an inability to actually generate ATP in cells, leading to a build up of precursors. Increases in levels of other metabolites, phosphocreatine and creatine, may implicate that at this late stage in the disorder, cells are using alternative energy sources. Alternatively, energy demand in this region may be reduced. Further studies are required to determine the significance of these increase in creatine and phosphocreatine. However, the finding of reduced ATP levels is consistent with previous observations using NMR spectroscopy (REF!). We are currently performing studies in another brain region in these mice (cerebellum), and are extending studies to mice at ages preceding symptom onset (4 and 7 weeks) and around symptom onset (9 weeks), to determine the temporal profile of events.

Objective #12. **Measurement of the Effects of 3-NP on Local Cerebral Glucose Use in Rats.**

3-Nitropropionic acid (3-NP) is an inhibitor of complex II of the electron transport chain in mitochondria. Systemic administration in multiple species, including humans, non-human primates, rats and mice, results in selective degeneration of the same populations of basal ganglia neurons that are targeted in Huntington's disease, (ie. spiny projection neurons, with relative sparing of aspiny and cholinergic interneurons). Pathologic changes are accompanied by motor abnormalities and cognitive impairment, again resembling HD. In addition, the enzyme targeted by this agent, complex II (succinate dehydrogenase) has been found to have markedly reduced activity in the caudate and putamen of advanced-stage HD patients (Browne wt al., 1997, Gu et al., 1996). Hence, 3-NP is widely used as a neurotoxin model of HD.

The reason for the selective cell death seen in the brain following 3-NP is unclear, especially since systemic administration of 3-NP results in similar levels of 3-NP throughout the brain, and inhibits complex II activity to the same extent throughout the brain (Browne and colleagues, unpublished observations). Histopathologic investigations suggest that the onset of motor impairment closely correlates witht eh first pathological changes in the striatum I rodent models of 3-NP neurotoxicity. In these studies, we investigated whether bioenergetic changes were evident in the striata of rats treated with 3-NP prior to cell loss and motor impairment in these animals, using [14C]-2-deoxyglucose *in vivo* autoradiography. In the first study we chose a time-point of 3 days post-3-NP treatment commencement, as this time-point preceded histopathologic and motor changes by approximately 1 day. In the same experiment, we also assessed the effects of creatine pre-treatment on glucose use. Creatine has previously been shown to ameliorate cell death induced by 3-NP in rats, possibly by providing an alternative energy supply to cells under energetic stress. The aim of this study was to determine if creatine treatment altered any energetic changes induced by 3-NP treatment at this time-point.

Intraperitoneal injection of 3-NP in rats induces a motor phenotype characterized by initial hindlimb weakness, which rapidly progresses to hindlimb paralysis and death ensues, generally within 24 to 36 hours after the first observations of paralysis. The time-course of this phenotype is dose-dependent, but at doses used in this study (7.5 mg/kg b.i.d.), the first signs of motor impairment occur 4 to 6 days after dosing begins. Rats were fed with diet containing 1% creatine, or normal control diet, for two weeks before 3-NP administration. 3-NP (7.5 mg/kg i.p. b.i.d.,) or vehicle (PBS, Iml/kg i.p. b.i.d.) was administered for 3 days. On the morning of the fourth day (3 days post first injection), rats underwent the 2DG procedure (as described in the original procedure).

Animals: The experiment initially used 44 male Sprague Dawley rats (250-300g at start of experiment). Six animals were excluded from the 3-NP treatment stage due to being over the maximum weight limit (420g) after 2 weeks of creatine treatment. Three rats were excluded on the basis of weight after the 3-NP treatment. Two rats died during the 3-NP administration period. Thirty-three rats (340-420g) underwent the 2-DG procedure. Of these, ten were excluded from the final analysis on the basis of abnormal plasma glucose levels, poor blood gases (indicating non-physiologically normal animals), or poor perfusion of the radionuclide of the animal.

Physiological Vartiables: Arterial plasma glucose, blood gas levels, rectal temperature, and arterial blood pressure were recorded 5 minutes before the commencement of the 2-DG procedure ("Pre" value), and 35 minutes into the procedure ("+35 min" value; 10 minutes prior to rat decapitation at the end of the procedure). Data are presented in Table 18. Glucose levels and temperature were also monitored throughout the procedure. Circulating plasma glucose levels, arterial pO2 and pCO2 tensions, and blood pressure values did not significantly differ between creatine / control or 3-NP/vehicle groups at either test time. Arterial pH and body temperature did show small magnitude reductions in 3-NP treated rats that received creatine, compared with non-creatine fed rats, however levels in these animals were still well within normal physiological ranges, and should not impact upon measured glucose use rates. There were no significant alterations in any parameters within animals over the time course of the experiments (paired t-test, $p>0.05$), indicating that animals did not undergo adverse stress during the procedure.

		Con/PBS	Con/3-NP	Cre / Veh	Cre / 3-NP
Glucose	Pre	156.0 ± 6.8	200.6 ± 23.1	160.3 ± 5.9	195.7 ± 27.2
Glucose	+ 35 min.	154.6 ± 7.6	209.0 ± 17.1	171.2 ± 6.9	188.6 ± 28.7
p_aO_2	Pre	82.7 ± 1.0	87.0 ± 2.0	88.3 ± 4.5	87.5 ± 3.3
p_aO_2	+ 35 min.	84.3 ± 1.9	94.6 ± 2.5 †	87.2 ± 3.5	92.8 ± 1.8
p_aCO_2	Pre	39.4 (1.1	39.8 (0.8	39.6 (1.0	38.1 (1.1
p_aCO_2	+ 35 min.	37.3 (0.6	35.7 (1.6	39.7 (1.2	35.3 (1.2
pH	Pre	7.5 (0.0	7.4 (0.0	7.5 (0.0	7.4 (0.0 **
pH	+ 35 min.	7.5 (0.0	7.4 (0.0	7.5 (0.0	7.4 (0.0 *

TABLE 18: Physiological variables in 3-NP-treated rats. Data presented as mean (SEM for: arterial plasma glucose concentrations measured immediately before [^{14}C]-2-deoxyglucose isotope injection (Pre-Glucose) and at the end of the 2-DG procedure (Glucose + 45 min); and arterial blood gas levels at the end of the procedure. *$p<0.05$, significant difference relative to N171-18Q mice (ANOVA, followed by Fisher's PLSD post-hoc unpaired t-test). a: p_aCO_2 data only available for 6 N171-18Q mice. Arterial plasma glucose levels did not alter significantly over the 45 min duration of the experiment in any group ($p>0.05$, Student's paired t-test).

Glucose Use: Local cerebral glucose use values were measured in twenty brain regions, chosen to include multiple regions throughout the striatum (where 3-NP eventually induces cell loss), regions anatomically connecte with or structurally close to the striatum, and internal control regions (cerebellum grey, and white matter). We found no statistically significant alterations I glucose use between 3-NP-injected and vehicle-injected rats, or between creatine and control-treated rats (with or without 3-NP administration) (Table 19). Values in Control diet fed / Vehicle rats were generally higher than in other groups, but differences did not reach statistical significance.

REGION	Con/PBS	Con/3-NP	Cre / PBS	Cre / 3-NP
Frontal Cortex I-III	102 ± 7	85 ± 10	87 ± 5	89 ± 11
Frontal Cortex IV	117 ± 7	102 ± 11	103 ± 5	108 ± 12
Frontal Cortex V-VI	87 ± 6	76 ± 8	77 ± 3	79 ± 9
Rostral Striatum: Dorsolateral	98 ± 8	88 ± 11	83 ± 4	88 ± 10
Ventromedial	88 ± 6	77 ± 10	78 ± 3	78 ± 11
Dorsomedial	84 ± 8	75 ± 11	74 ± 3	76 ± 10
Striatum: Dorsolateral	93 ± 5	84 ± 10	83 ± 5	82 ± 11
Dorsolateral Rim	99 ± 5	90 ± 12	86 ± 5	86 ± 9
Ventromedial	91 ± 7	77 ± 10	75 ± 3	74 ± 9
Dorsomedial	94 ± 8	80 ± 11	83 ± 6	78 ± 9
Caudal Striatum	91 ± 5	80 ± 11	74 ± 3	80 ± 9
Globus Pallidus	55 ± 4	49 ± 8	45 ± 2	49 ± 7
Hippocampus: CA1	61 ± 4	48 ± 8	48 ± 3	49 ± 6
CA3	77 ± 4	65 ± 9	61 ± 4	63 ± 7
Dentate Gyrus: Molecular Layer	84 ± 8	86 ± 10	75 ± 3	81 ± 10
Nucleus Accumbens	87 ± 7	76 ± 11	71 ± 4	75 ± 8
Substantia Nigra: *pars reticulata*	51 ± 7	57 ± 10	44 ± 2	49 ± 7
pars compacta	81 ± 8	88 ± 8	69 ± 3	80 ± 14
Cerebellum: Grey matter	60 ± 4	57 ± 7	52 ± 3	50 ± 6
White matter	29 ± 4	32 ± 4	27 ± 2	26 ± 4
Number of Animals	6	5	6	6

Table 19: Local Cerebral Glucose Utilization ($lCMR_{glc}$) in rats following 3-NP administration, in animals fed with 1% creatine or control diet. $lCMR_{glc}$ (nmol/100g/min) in homozygous (90/90) and heterozygous (90/7) Hdh^{Q92} knock-in mice; and wild-type (7/7; Hdh^{Q7}) CHANGE ! littermate controls. Data presented as mean ± SEM, (n=4-6 per group). * $P < 0.05$, ** $P < 0.01$ relative to levels in 7/7 mice; † $P < 0.05$ relative to 90/7 mice (ANOVA, followed by Fisher's PLSD).

Discussion: Results suggest that no abnormal alterations in glucose utilization occur in the striatum at this time-point post-3-NP injection, prior to cell degeneration in this region. Observations appear to be consistent with an "all or nothing" effect of 3-NP, suggesting that perhaps cell dysfunction occurs extremely rapidly after critical levels of complex II inhibition are reached following 3-NP

treatment. However, this is not proven by our data, since using this experimental approach it is not possible to determine exactly when motor impairment and cell degeneration *would have* occurred in these animals. A major problem with 3-NP toxicity studies is that there is a large inter-animal variability in time of symptom onset after dosing. Rat strains also vary in vulnerability. Hence, it is difficult to predict when an animal is close to developing striatal defects. However, our data do suggest that if energetic changes occur in this model, they do not occur until later than 3 days in the course of lesion generation (using this dose and rat strain). The original proposal aimed to measure glucose levels at multiple time-points prior to lesion formation, however we will not measure levels at times preceding 3-days, on the basis of the current data. We have conducted pilot studies to try to identify a useful time-point to detect presymptomatic glucose use changes (if any exist). Studies in rats showing the first signs of motor impairment show marked reductions in glucose use in striatal regions where cell loss is already evident (data not shown). However, we have not been able to detect any significant alterations in striatal cell loss prior to striatal cell degeneration, to date.

6. INTRODUCTION – 2: Consortium Project

"Mitochondrial free radical generation in Parkinson's disease"

In 2002 this proposal was extended by the addition of a second project, entitled "Mitochondrial Free Radical Generation In Parkinson's Disease", which is a constituent (Project III) of a Research Consortium made up of four investigators. This project continues the theme of determining the interactions between energy metabolism and oxidative stress in the etiology of neurodegenerative disorders. The aims were to ascertain *in vivo*: 1) Whether inhibition of a component of the mitochondrial respiratory chain (complex I), implicated in the pathogenesis of Parkinson's disease (PD), induces pathogenesis via free radical generation; and, 2) Whether mitochondria are the initial source of these free radicals. Findings may give insight into potential drug targets for PD. These questions are more readily addressed by *in vitro* approaches (covered in other projects within the Consortium), given the extreme technical difficulties of discretely measuring purely mitochondrial events *in vivo*. Therefore we are taking an indirect approach, by measuring the time-course and nature of oxidative events caused by toxic insults directed against discrete mitochondrial components. Results for the second year of this consortium project are presented here. *NB:* In the course of this second year the post-doctoral fellow conducting the bulk of these studies left the department. Since it took some time to recruit a replacement, a no-cost extension was requested, and granted.

A: Overview of Consortium Projects

The overall goals of this grant are to gain insight into the roles of mitochondrial energy metabolism and oxidative stress in the etiology of neuronal damage and death in neurodegenerative disorders. ***This study is Project III of a Consortium consisting of four projects*** (Project I, G. Fiskum PI, Grant # 17-99-1-9483; Project II, T. Sick PI; and Project IV, I. Reynolds PI, Grant # 17-98-1-8628). Projects comprising this consortium used different *in vitro*, *ex vivo,* and *in vivo* approaches to elucidate the specific roles of mitochondria and reactive oxygen species (ROS) in the pathogenesis of Parkinson's disease (PD). **Project III** specifically addresses the contribution of mitochondrial complex I to ROS generation *in vivo*, by measuring oxidative damage markers in rat brain after inhibiting activity of specific complex I subunits.

B. Background

Parkinson's Disease, Complex I, and ROS: Oxidative damage and mitochondrial dysfunction, specifically reduced activity of NADH:ubiquinone oxidoreductase (complex I) of the electron transport chain, are well characterized components of Parkinson's disease (PD) etiology. *In vivo* studies show that complex I inhibition in the brain, by MPTP/MPP^+ or rotenone for example, can result in region-specific neuropathologic changes resembling PD. *In vitro* studies implicate mitochondria as a major source of ROS mediating oxidative damage and pinpoint a number of the >45 complex I subunits identified to date as candidate sites for ROS production.

An important step towards understanding the mechanism of region-specific cell damage in PD is to determine *in vivo* whether there is a direct link between abnormal mitochondrial function and the generation of ROS in the disease. We are approaching this question by manipulating the activities of different mitochondrial complex I subunits, using intracerebral delivery of subunit-specific complex I inhibitors in rats. Markers of ROS generation will then be examnied in post-mortem brain tissue, and *in vivo* by microdialysis, and correlated with measures of complex I activity. We will test inhibitors with different specificities for complex I subunits that are encoded both by mitochondrial (mt) DNA (eg. the ND1 subunit), or by nuclear (n) DNA (eg. the PSST subunit). We will thus determine if selectively altering certain functional components of complex I affects either its activity, and/or ROS generation. By limiting the intervention to a mitochondrial component, and by measuring ROS production shortly after the mitochondrial insult, we will ascertain if generated ROS derive from mitochondria rather than other cellular origins.

Complex I: Structure, Function and ROS Generation: NADH-ubiquinone oxido-reductase (complex I) is the first and largest enzyme complex of the mitochondrial respiratory (or "electron transport") chain. The overall function of complex I is to transfer one pair of electrons from NADH to flavin mono-nucleotide (FMN), and ultimately to ubiquinone (UQ), whilst simultaneously pumping hydrogen ions out of the mitochondrial matrix into the inter-membrane space. Complex I has a molecular mass of approximately 900-1000 kDa and comprises at least 45 subunits (Bourges et al., 2004), 7 of which are encoded by mtDNA (ND1-ND6, ND4L), and the remainder by nDNA. Subunits are organised into an L-shape structure consisting of a hydrophobic membrane arm embedded into the inner mitochondrial membrane (IMM), and a hydrophilic peripheral arm aligned perpendicular to the IMM and directed into the mitochondrial matrix. The peripheral arm has two fractions; a flavoprotein (FP) where electron transfer begins, and iron-sulphur (Fe-S) clusters (N)

several of which act as redox groups that facilitate electron transfer. Binding sites for NADH and FMN are found on the peripheral arm. The membrane arm is comprised of at least 24 nDNA-encoded subunits, the 7 mtDNA subunits, and possibly two Fe-S clusters (Okun et al., 1999).

The electron carrier NADH enables entry of electrons into complex I. There are two well defined binding sites for NADH in eukaryotes, the 51kDa and 39kDa subunits. It is believed the 39kDa subunit is required to maintain stability of the redox group "X" , facilitating electron transfer (Schulte et al., 2001). Electron input occurs via the FMN prosthetic group and the Fe-S clusters (Rasmussen et al., 2001). The 'catalytic core' of complex I is comprised of the PSST, TYKY, NUOD, ND1 and ND5 subunits (Schuler et al., 2001). PSST is a 23-kDa subunit containing one binding site for Fe-S cluster N2. It plays a vital role in electron transfer by functionally coupling N2 to CoQ (Schuler et al., 1999). The binding of CoQ is the final stage in electron transfer via complex I and an important function of the membrane arm. The actual quinone binding site has not been equivocally proven, and different studies suggest it is encoded by the ND1 and ND4 proteins (Triepels et al., 2001), or a hydrophilic 49-kDa/NUOD subunit located at the interface of the peripheral and membrane arms (Darrouzet et al., 1998). The TYKY subunit is proposed to bind two tetranuclear Fe-S clusters (N6a and N6b) that form the novel redox groups found in complex I. TYKY is part of a special class of 8Fe-ferredoxins and works as an electrical driving unit for the proton pump (Rasmussen et al., 2001).

7. BODY – 2: Consortium Project RESULTS

"Mitochondrial free radical generation in Parkinson's Disease"

All studies used male Lewis rats, 250-300g at the commencement of studies. For stereotactic drug injection into the brain, rats are anesthetized with a cocktail of ketamine (100mg/kg) and xylazine (10mg/kg). Rats are placed in a Kopf stereotactic frame, and body temperature maintained at 37°C by means of a heating pad.

Aim 1: To characterize the regional and temporal development of complex I inhibition in specific brain regions at time points after administration of subunit-specific complex I inhibitors to rats.

The first requirement of this aim was to find an optimal dosing regime for rotenone.

Rotenone induces selective degeneration in dopaminergic nigro-striatal projections following systemic administration (either intravenous via the jugular veing, sub-cutaneous injection, or intraperitoneal) (Betarbet et al., 2000; Alam and Schmidt et al., 2002, Sherer et al., 2003,

Antkiewicz-Michaluk et al., 2003). These effects are associated with widespread decreases in complex I activity throughout the brain (Hoglinger et al., 2003), but require chronic low dose administration paradigms for generation of these selective lesions (Antkiewicz-Michaluk et al., 2003). In this study we want to identify oxidative damage paradigms as soon after the complex I inhibition is induced as possible, to try to localize these events to the mitochondria, rather than measuring the downstream repercussions of long-term energetic compromise affecting ROS production in other cellular compartments. Therefore we opted for a direct intracerebral injection administration paradigm for the complex I inhibitors.

(i) Dose-response Curve for Rotenone: Complex I Inhibition 1 hour Post-injection

A dose range of 6, 20 and 60 μmol rotenone was selected for the initial experiments, based on reported effective doses in studies using other routes of administration. Rotenone (6, 20, 60 μmol) or vehicle (DMSO/polyethylene glycol cocktail) was injected bilaterally into the striata of rats (3μl volume, injected over 10 min, plus 5 min lag time before needle is removed; n=4-5/group). After one hour animals were sacrificed by Na-pentobarbital overdose. The striata, cortex and cerebellum were dissected from the brain and rapidly frozen on dry ice. Mitochondrial extracts were prepared from brain regions by repeated centrifugation and exposure to a percoll gradient (modification of Lai and Clark, 1979). Complex I activity was measured in cortex and striatal mitochondria by spectrophotometric assay of the rate of oxidation of NADH at 340nm (Hatefi, 1978). Values were corrected for protein content, determined by the method of Bradford (1976), and for variable amounts of mitochondria in the assay preparations, by measuring activity of the mitochondrial matrix enzyme citrate synthase (rate of oxidation of DTNB at 412nm; Shepherd and Garland, 1969). Results for striatal tissue are demonstrated in Figure 8. Doses of 20 and 60 μmol rotenone produced 25% reductions in complex I activity in the striatum (compared with levels in vehicle-treated rats, $p>0.05$).

The level of complex I inhibition induced by rotenone was more pronounced in the cortex, shown in Table 20. It is postulated that this effect (which was greater than that anticipated) may be due to back-flow of rotenone up the needle tract. Alternatively, it may reflect transport back to cortex via cortico-striatal nerve terminals, although this seems unlikely given the relatively short period following rotenone injection (1h).

Figure 8: Complex I activity in Striatum 1h post-rotenone injection.

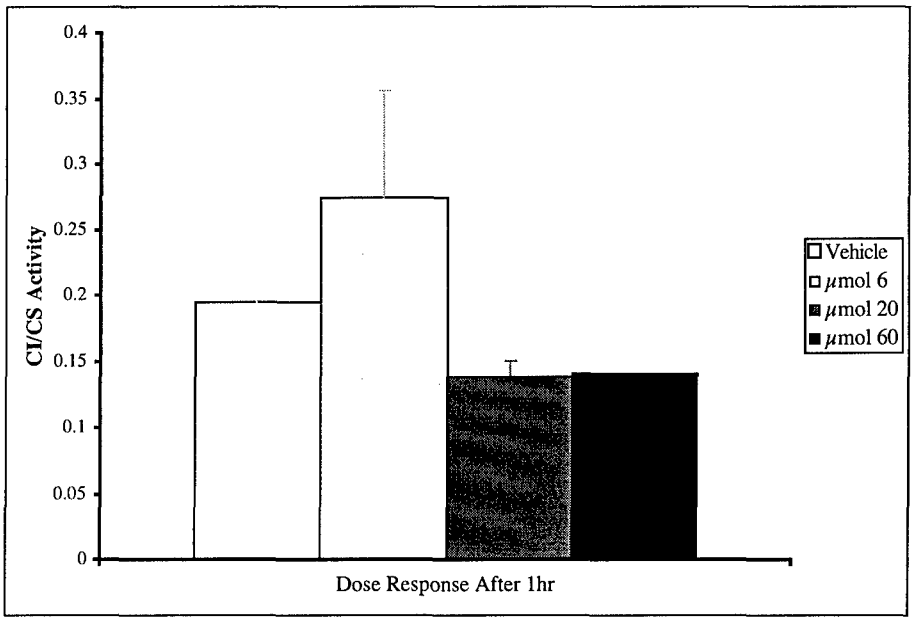

Data presented as mean ± SEM (nmol/min/mg protein/CS) $p > 0.05$, ANOVA. N=4-5/group

Table 20: Complex I Activity in Cortex 1h Post-Intrastriatal Injection.

Rotenone (μmol)	Complex I (nmol/min/mg protein/CS)	% Inhibition
0 (Vehicle)	0.22 ± 0.11	-
6	0.16 ± 0.07	27
20	0.18 ± 0.10	18
60	0.09 ± 0.04 *	59

Data presented as mean ± SEM. * $p < 0.05$, ANOVA followed by Student's unpaired t-test. N=4-5/group.

(ii) **Time Course of Rotenone Effects: Complex I inhibition**

We were dissatisfied with the magnitude of complex I inhibition in the striatum following 60μmol rotenone injection, and therefore conducted pilot experiments with a higher dose, 120μmol. This dose produced an approximate 3 fold reduction in complex I activity in mitochondrial prearations from striatum, in pilot studies assessing effects at 0, 2, 4, 8 and 24h pst-injection. Therefore we chose to use this dose in subsequent experiments. Experiments were expanded to larger group sizes, and results are shown in Figure 9. Complex I activity was not markedly altered up to 4 hours post-injection, but showed a reduction at 8 and 24 hours post-injection.

Figure 9: Time course of Complex I activity in Striatum After Rotenone Injection.

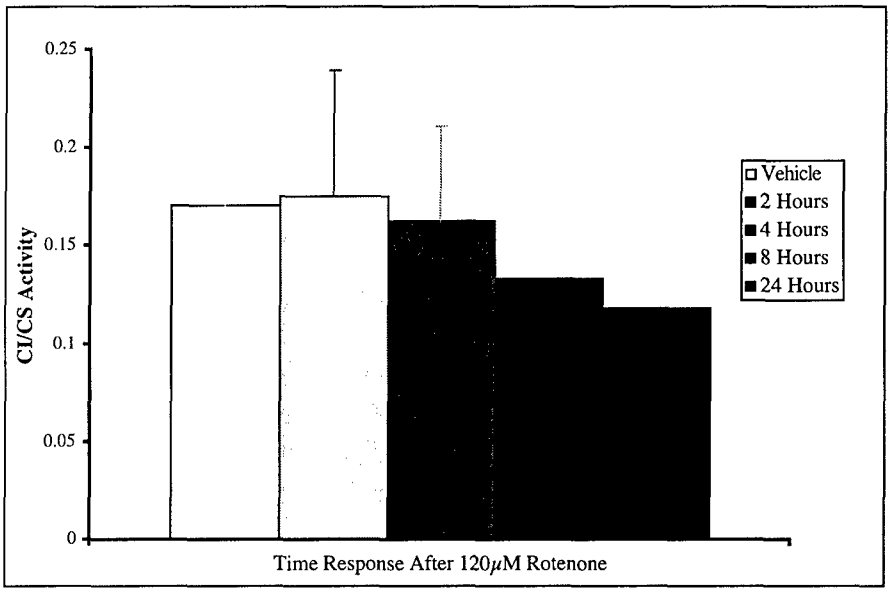

Data presented as mean ± SEM (nmol/min/mg protein/CS) $p > 0.05$, ANOVA. N=4-5/group

Problems encountered:

(a) ***Lesion reproducibility: Attempted to improve by changing rotenone administration route:*** We carried out pilot experiments using an alternative route of rotenone administration, namely intracerebroventricular (i.c.v.) administration, in an attempt to rapidly generate striatal lesions without inducing the mechanical damage inherent to stereotactic injections. Preliminary results using i.c.v. injection of 120μM rotenone were extremely variable in terms of lesion size and complex I inhibition, and therefore this administration route was not pursued.

(b) ***Complex I Activity Reproducibility: Attempted to improve the measurement of Complex I activity changes by inhibitors, using Complex I quantitative histochemistry:***

We encountered many problems with the variability of complex I measurements in brain tissue using the spectrophotometric assay approach. This proved to be extremely time consuming, and tissue consuming. One particular confound is that the inhibitors used likely do not affect complex I activity throughout the entire striatum, and therefore any changes in discrete areas of striatum may be masked in our spectrophotometric assays of complex I activity that use whole striatum. Therefore we performed further time course studies on the effects of rotenone (120μM, intrastriatal injection) on complex I activity, this time using a histochemistry approach with quantitative densitometry to

localize regions of striatum in which complex I was impaired, and to quantify activity changes within these areas (Jung et al. (2002) and Higgins and Greenamyre (1996).

Rats were sacrificed at 1, 4, and 8 hours after unilateral injection of rotenone into one striatum (120μM, 3μl, n=6/gp), and vehicle (3μl DMSA/PEG) into the contralateral striatum. Brains were removed and frozen in isopentane at -43°C, cut into 10μm-thick coronal cryostat sections, and processed for complex I histochemistry with densitometry according to the methods of Jung *et al.* (2002) and Higgins and Greenamyre (1996), respectively. This procedure is a colorimetric assay that measures a change in color of nitro blue tetrazolium (NBT) in response to NADH oxidation by complex I. The amount of complex I activity is extrapolated from the optical density (OD) of the colored product in discrete brain regions, over a given time period. The technique requires comparison of relative enzyme products between sections, and therefore tissue sections must be processed simultaneously under identical conditions.

The areas where NADH oxidation occurred following injections were easily delineated within the striatum, as shown in Figure 10.

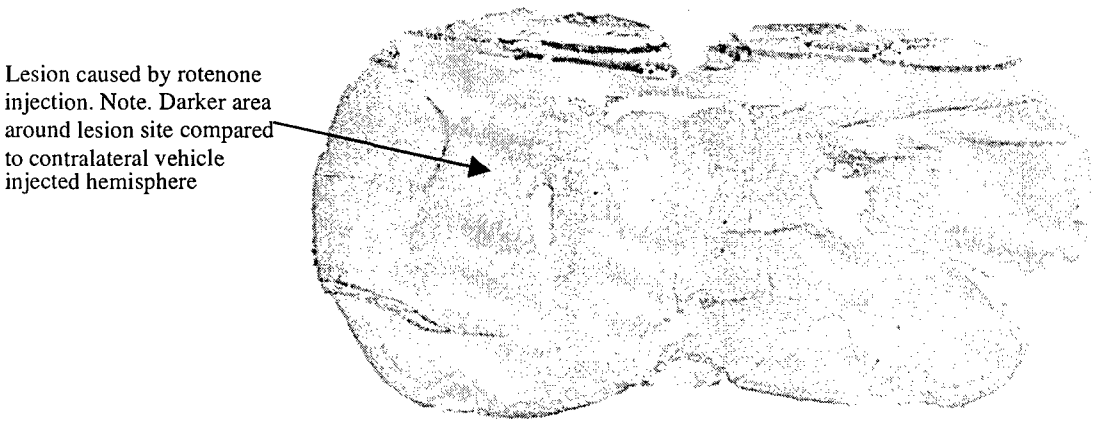

Figure 10: A representative section showing complex I activity histochemistry after injection of 120μM rotenone (left hemisphere) or vehicle (right hemisphere) into the striatum. In this "inverse" phase image a 'ring' of increased intensity appears around the rotenone injected hemisphere, compared to the vehicle-injected hemisphere where a slight increase is evident only in the area of mechanical damage immediately around the needle tract and injection site.

Rotenone produced a decrease in complex I activity (increased density in this inverse exposure) in a larger area of the striatum than vehicle. Relative optical densities in affected regions are shown in Table 20, presented as the difference in optical densities between vehicle-injected and rotenone-injected striata. The extent of rotenone's effect on complex I was minimal 1h post-injection, but increased with time, and was highest 8h post-injection (Table 21). We are still in the process of optimizing incubation conditions to take advantage of this procedure in other experiments.

Table 21: The extent of NADH oxidation following intrastriatal injections. Mean difference values reflect the differences in ODs between vehicle and rotenone-injected hemispheres, measured in the same sections, at each time point (n=4-6/rats gp).

Time post-injection	Mean Difference	*p*-Value
1 hour	0.009	*0.6376*
4 hours	*0.017*	*0.1595*
8 hours	*0.048*	*0.7727*

Aim 2: **To characterize the regional and temporal development of cerebral oxidative damage after complex I inhibition in rats.**

The research goals of this objective were to use HPLC and immunohistochemical approaches to characterize the nature of any oxidative damage arising after intra-striatal inhibitor injections, and to assess the time course of oxidative damage.

(i) ***HPLC Measurement of Tissue MDA Levels After Rotenone Administration:***

We used HPLC to measure tissue levels of malondialdehyde (MDA, lipid peroxidative damage marker) in the striatum, cortex and cerebellum of rats that had received bilateral intrastriatal injections of rotenone (120μM, 3μl), or vehicle (DMSO/PEG, 3μl). Rats were sacrificed at 1, 4, and 8h after rotenone, and 8h after vehicle injection (n=6/gp). Non-injected rats (n=6) were used as baseline controls. Brains were removed, regions dissected out, tissue frozen in isopentane at -43°C and stored at -80°C. For HPLC analysis, tissues were homogenized in 40% ETOH. MDA in the

sample was reacted with thiobarbituric acid (TBA, 42mM), in the presence of butylated hydroxytoluene (BHT, 0.05% in ETOH) and 0.44M phosphoric acid (H_3PO_4), for detection of the MDA-TBA product by the method of Agarwal and Chase (2002). MDA content was extrapolated relative to an MDA standard (Sigma, St. Louis, MO). Results for striatum, cortex and cerebellum are presented in Figure 11. MDA levels were not significantly altered in any of the regions examined up to 8h after rotenone injection.

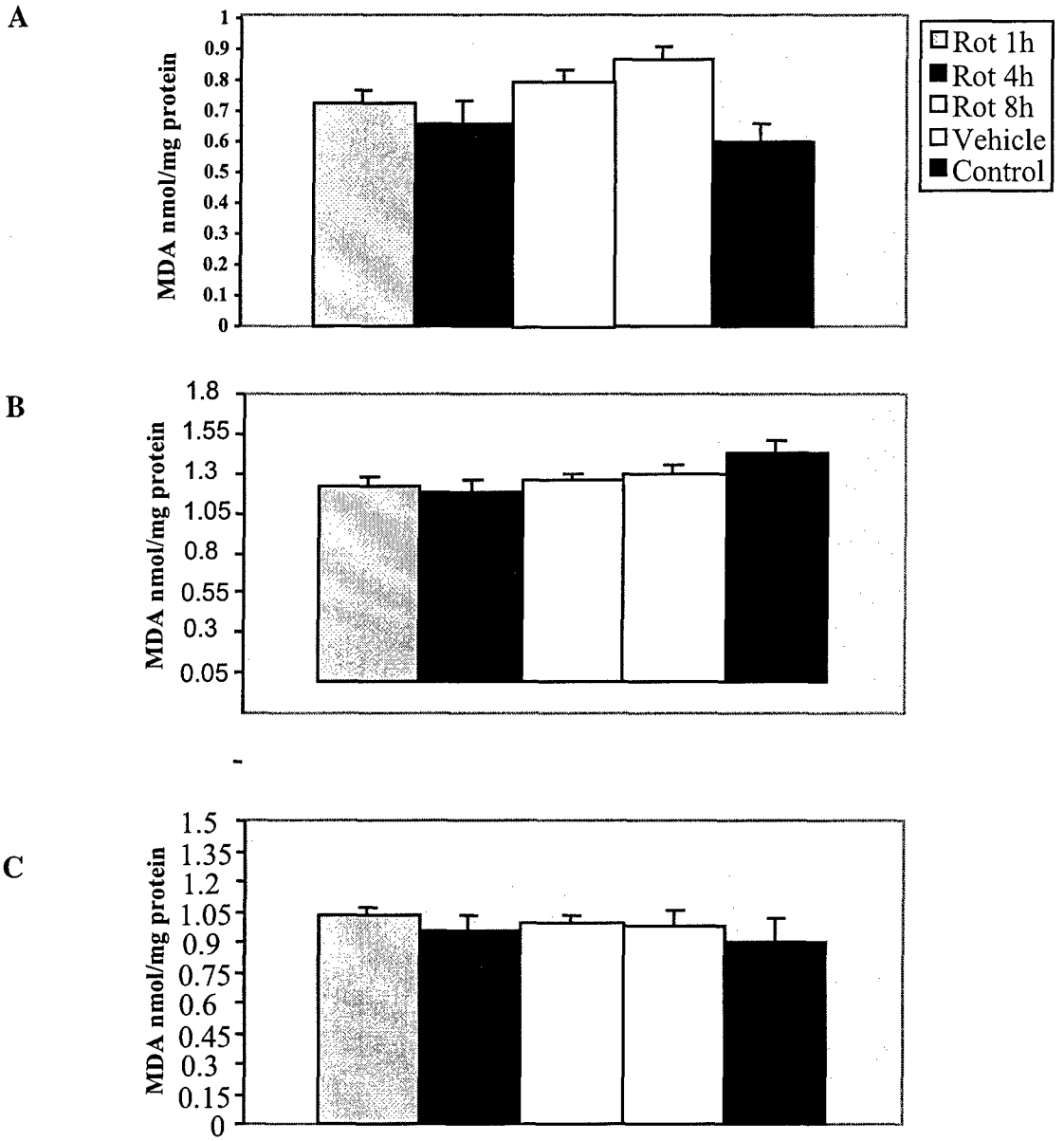

Figure 11: MDA measurements in homogenate preparations from (A) Striatum, (B) cerebral cortex, and (C) cerebellum of rotenone, vehicle and un-injected rats. Data presented as mean +/- SEM (nmol/mg protein), $p>0.05$ (ANOVA, n=6/group).

(ii) ***Immunocytochemical assessment of oxidative damage markers in the striatum immediately after rotenone injection.***

Immunohistochemical Studies: Firstly. we completed assessment of the effects of rotenone insult on levels of the lipid peroxidation markers malondialdehyde and 8-iso-prostaglandin F2, and on the oxidative stress response marker heme oxygenase. Experiments used immunohistochemical approaches at 8h and 24h after rotenone administration. Heme oxygenase-1 is a member of the stress-response protein superfamily that catalyzes the rate-limiting step in heme degradation in brain and other tissues. We used a marker for inducible hemeoxygenase, HO-1. The HO-1 gene contains a heat shock element in its promoter region and is rapidly induced upon exposure to heme, metal ions, sulfhydryl compounds, UV light, and various pro-oxidants. Its metabolic products (carbon monoxide and bilirubin) have been shown to exert potent antioxidant and anti-inflammatory activities, and thus the HO pathway is a fundamental defensive mechanism for neurons exposed to an oxidant challenge. In the brain, astrocytes strongly express HO-1 in response to injury (Gonzales et al., 2002).

Rotenone (120μmol in 3μl) was unilaterally injected into one striatum in rats (as previously described), and vehicle (DMSO/PEG) into the contralateral hemisphere. Rats were euthanized by transcardial perfusion with 4% paraformaldehyde under Na-pentobarbital anesthesia, and fixed brains removed and cut into coronal cryostat sections. Adjacent serial sections through the striatum were then stained for:

a) *Malondialdehyde*, using rabbit antiserum against malondialdehyde-modified protein (kindly provided by Dr. Craig Thomas, Hoechst Marion Roussel) 1:1,000.
b) *8-iso-prostaglandin F2*, using rabbit anti-8-iso-prostaglandin F2 (Assay Designs, Inc., Ann Arbor, MI) 1: 1,000.
c) *Heme oxygenase-1*, using rabbit anti-heme oxygenase-1 (StressGen, British Columbia, Canada) 1: 3,000.

Results are shown in Figure 12. Increased staining for all three markers were evident in rotenone-injected striata, compared with vehicle-injected hemispheres in the same animals, both at 8h post-injection, and at 24h. The pattern and approximate numbers of positively stained cells for each marker did not markedly differ between the two time points, suggesting that the maximal initial effect on oxidation may be achieved by 8 hours. Differences were apparent in the pattern and scope of staining with each of the markers. Malondialdehyde-positive cells were most prominent in the immediate vicinity of the lesion/injection site following rotenone. Cell morphologies suggest that most cells stained were neurons, but this must be verified by colocalizaion studies. Iso-prostaglandin

F2 showed an intermediate level of staining, affecting more cells than malondialdehyde, over a larger area of striatum. Heme oxygenase-1 positive cells were the most abundant of all the markers examined. They were also present in the largest striatal volume. In addition, both glial and neuronal populations appear to stain positively for heme oxygenase-1.

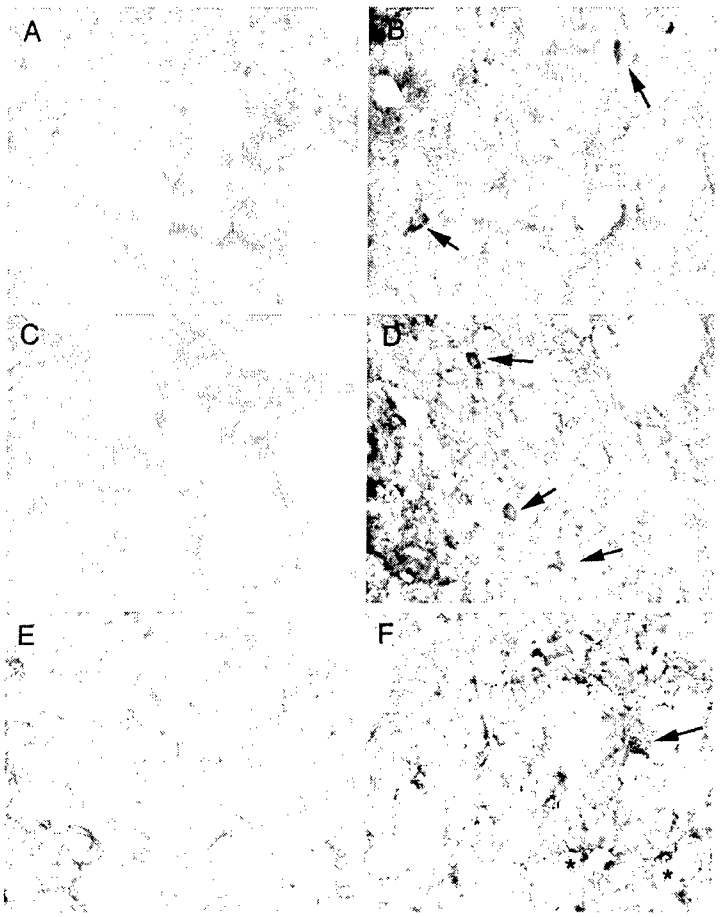

Figure 12
Malondialdehyde (A, B), Isoprostane (C, D) and Heme oxygenase-1 (E, F) immunostaining of the caudate adjacent to the injection site, 8 hours after vehicle (A, C, E) or rotenone (B, D, F) injection. Immunoreactive neurons (arrows) and glia (asterisks) are shown.

We then extended these studies by examining levels of these markers (MDA, F2 isoprostane, and HO-1 immunostaining), in addition to and the DNA oxidation marker 8-hydroxydeoxyguanosine (8-OHdG), in rat striatum 1, 2 and 4h after unilateral stereotaxic intra-striatal injections of rotenone (120μM, 3μl), and vehicle (DMSO/PEG) into the contralateral striatum. Rats were perfused with 4% paraformaldehyde, their brains removed and post-fixed in paraformaldehyde for 24 hours, transferred to 70% ETOH, and then paraffin embedded. Coronal (30μm) sections were cut with a microtome. Sections were immunostained as follows:

d) *Malondialdehyde (MDA):* Rabbit anti-malondialdehyde-modified protein (kindly provided by Dr. Craig Thomas, Hoechst Marion Roussel), diluted 1:1,000.

e) *8-iso-prostaglandin F2 (PgF2)*: Rabbit anti-Pg F2 (Assay Designs Inc., Ann Arbor, MI), 1: 1,000.

f) *Heme oxygenase-1 (HO-1)*: Rabbit anti-HO-1 (StressGen, British Columbia, Canada), 1: 3,000.

d) *8-OHdG:* Mouse anti-8-OHdG (Vector Laboratories (Burlingame, CA, USA), diluted 1:500.

Haematoxylin and eosin (H&E) staining was used to delineate the extent of the lesion in each animal.

Results are shown in Figure 13. In contrast to the elevations in lipid peroxidation (MDA, PgF2) and oxidative stress (HO-1) markers by 8h post-rotenone, reported previously, these markers were unaltered acutely (1h) after rotenone injection. The DNA damage marker 8-OHdG, however, was markedly upregulated 1h after rotenone injection compared to levels in both vehicle-injected and control (uninjected) rats. The nature of the 8-OHdG effect is examined at higher magnification in Figure 14. Figure 15 demonstrates that increased DNA damage could also be seen distal to the actual injecion site, demonstrating a diffuse response to complex I inhibition. These observations suggest that DNA oxidation is induced extremely rapidly after inhibition of complex I by rotenone, whereas other stress responses are relatively delayed. Results implicate ROS generation as a rapid and therefore potentially pathogenic consequence of rotenone administration.

The findings of elevated MDA immunoreactivity at the site of rotenone injection, evident at 8 and 24h post-injection contrast with our previous HPLC observations of no detectable changes in striatal MDA levels. We hypothesise that this discrepancy results from the fact that increased MDA immunoreactivity was restricted to an area of striatum in close proximity to the needle tract, suggesting that in this time frame MDA generation is restricted to regions close to the core area of complex I inhibition. Hence, we would not expect to detect MDA elevations in either the cortex or cerebellum in the HPLC studies, and any changes in striatum may be masked by the relatively large amount of striatal tissue sampled with respect to the area in which immunoreactivity reveals MDA generation is elevated.

Figure 13: Immunohistochemical staining for oxidative damage markers in serial sections from the striatum of control (uninjected), vehicle, or rotenone injected animals, one hour post-injection. Left panels, a representative control rat; Center panels, Vehicle-treated; Right panels, representative sections from a rotenone-injected rat. **A-C:** Haematoxylin and eosin (H&E) staining. **D-F:** MDA; **G-I: F2-**Isoprostane; **J-L:** HO-1; **M-O:** 8-OHdG. After local administration of rotenone acute formation of 8-OHdG is seen indicating marked DNA oxidation. Local injection of rotenone did not propagate formation of oxidative markers for lipid peroxidation (MDA or F2-Isoprostane), or the stress-response element HO-1. Scale bar = 100μm.

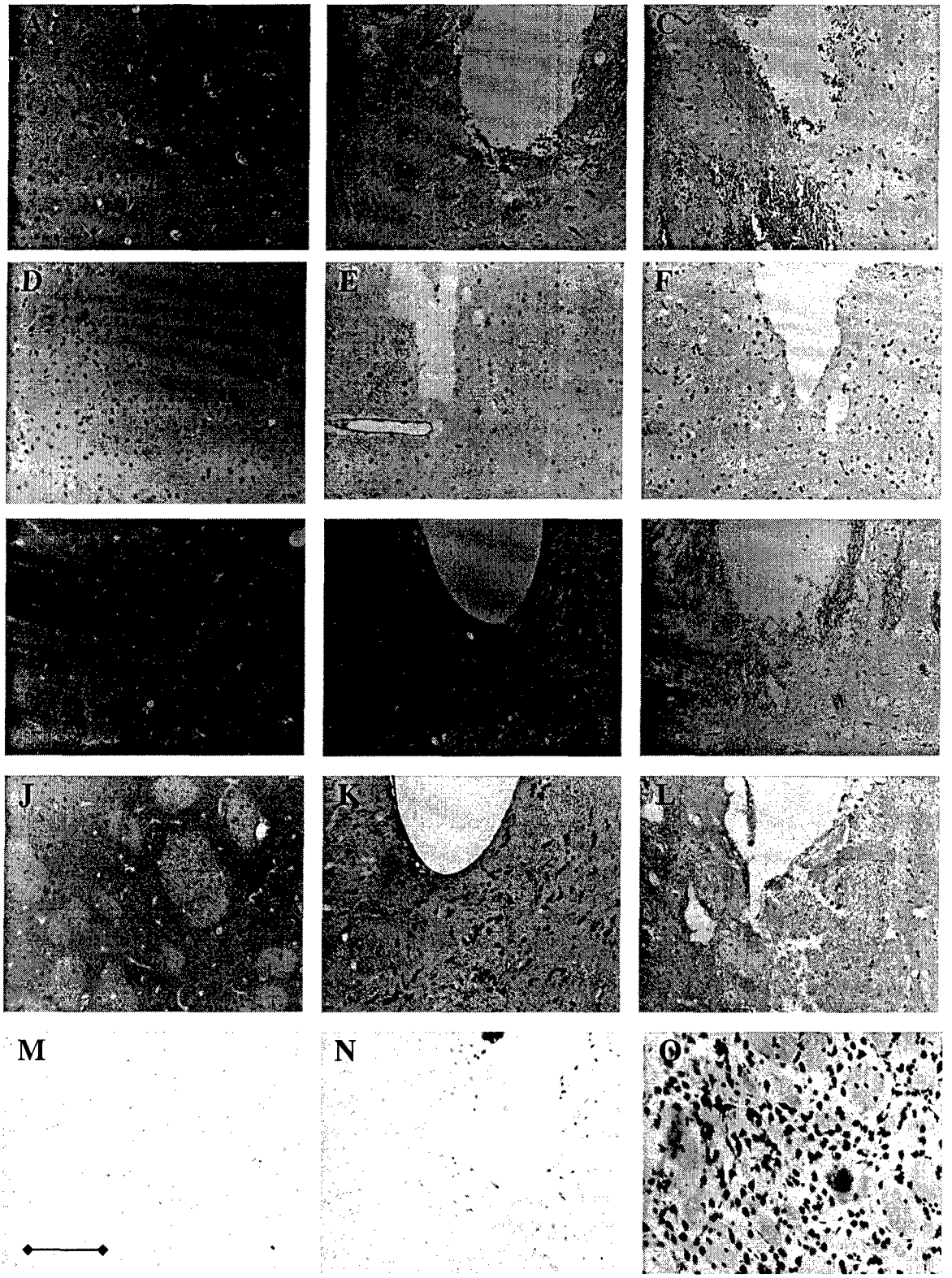
A
C
D
E
F
J
K
L
M
N
O

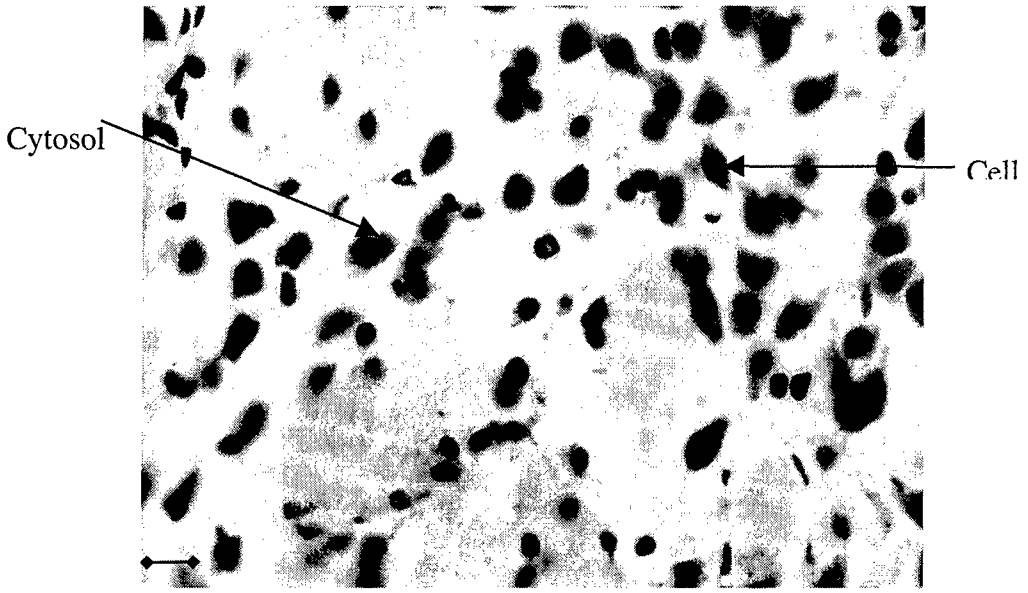

Fig 14: Magnification of plate O above, 8-0HdG in rotenone injected animal, scale bar = 50μm

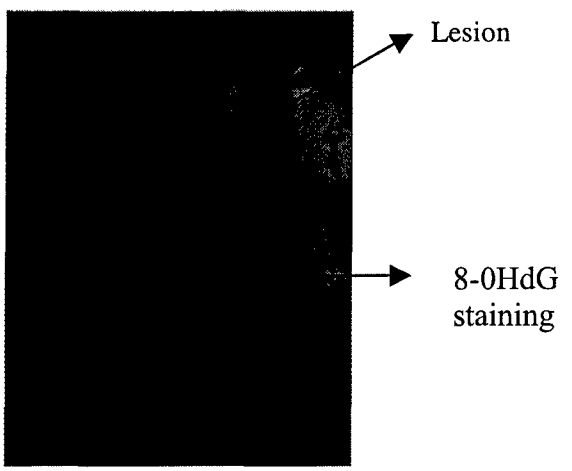

Figure 15: 8-OHdG staining is seen ventral to the lesion site within the striatum.

Discussion: The major finding is that the complex I inhibitor rotenone induces oxidative damage extremely rapidly after introduction into tissue, with elevated levels of the DNA damage marker 8-OHdG evident as soon as 1h after rotenone injection. This time-point appears to precede evidence of complex I enzyme activity inhibition by rotenone (measured by spectrophotometric and histochemical assays in this project). This observation suggests that deleterious effects of rotenone may be independent of its effects on the NADH oxidative activity of complex I, but do not rule out complex I as a source of ROS. Damage to other cellular elements, including lipids, is slower, but is evident by 8h post-injection. We are currently assessing oxidative damage markers at intermediate time points after rotenone.

8. KEY RESEARCH ACCOMPLISHMENTS

(1) Neurotoxin Exposure Program Studies:

a) HD Mouse Studies:

1. The finding that cerebral glucose use is not significantly altered in Hdh^{Q50} CAG knock-in mice at 4 months of age, relative to levels in wild type animals; and that no gene dosage effect is seen in Hdh^{Q50} mice (48/48 vs. 48/7 CAG repeats).
2. The finding of impaired activities of complexes II-III and IV of the electron transport chain in Hdh^{Q50} and Hdh^{Q92} mouse brain cerebellum at 4 months of age (preceding symptom onset and NII formation).
3. The finding that cerebral glucose use is significantly increased in Hdh^{Q92} CAG knock-in mice at 4 months of age, relative to levels in wild type animals, and relative to levels in Hdh^{Q50}mice .
4. The finding that cerebral glucose use in Hdh^{Q92} CAG knock-in mice shows a gene-dosage effect, with homozygote (90/90 CAG repeat) mice showing increased glucose use elevations than heterozygote (90/7) mice. In fact, the magnitude of glucose use increases in 90/90 mice is approximately double levels in 90/7 mice.
5. The finding that alterations in cerebral glucose use in Hdh^{Q92} mice is evident at 4 months of age in these animals (the earliest time-point investigated). These changes precede pathological or behavioral changes in Hdh^{Q92} mice. (NB: Hdh^{Q92} mice do not develop a movement disorder, unlike Hdh^{111} mice and other HD transgenic mouse models). There is evidence that mutant huntingtin protein (*htt*) is translocating to the nucleus at this time-point, but neuronal intranuclear inclusions (NII) are not evident until 15 months of age in this model (Wheeler et al., 2000). Aggregate formation occurs faster in Hdh^{Q111} mice, hence we are currently examining the same parameters of energy metabolism in these animals.
6. The finding that presymptomatic increases in glucose utilization also occur in multiple forebrain regions in another transgenic HD mouse line, N171-82Q mice expressing a mutant human HD fragment with an 82 polyglutamine repeat. Taken together, findings suggest that metabolic compromise may be an early event in the pathophysiology associated with the expression of mutant huntingtin protein. Glucose use elevations suggest that cells may be attempting to increase glycolytic ATP production, or increase substrate feed into mitochondrial energetic pathways to compensate for a metabolic stress or blockade. The exact mechanism has yet to be elucidated.

7. The finding that aconitase activity is increased in the cerebellum of Hdh^{Q50} (48/48) mice at 4 months of age.
8. Assessment of cerebral respiratory rates in the Hdh^{Q111} mutant moue model of HD – no alteration at a timepoint when cerebral glucose uptake is elevated (4 months of age).
9. Assessment of ATP synthesis in the Hdh^{Q111} mutant moue model of HD – trend to increase at a timepoint when cerebral glucose uptake is elevated (4 months of age).
10. The finding that R6/2 transgenic HD mice develop a diabetic profile, with onset at 7-8 weeks of age (around the time of movement disorder symptom onset).
11. Observations that metabolic enzymes which show impaired activity in late-stage HD patients (reduced complex II-III and IV in post-mortem brain) do not show evidence of altered activities in pre-symptomatic R6/2 HD mouse brains (whole tissue homogenate preparations; 3.5 and 8 week-old mice). Some alterations are evident in late-stage (12 week-old) R6/2 mice. However, the nature of the metabolic enzyme activities we detected did not correlate with observations in symptomatic HD patients (Browne et al., 1997), or with previously reported alterations in homogenate samples from 12 week old R6/2 mice (Tabrizi et al., 2000). It is possible that use of whole brain homogenate preparations is masking any subtle region-specific changes occur, for example in the striatum of R6/2 mouse brains. Therefore we are currently repeating these assays in striatal preparations from these mice.
12. The finding of reduced ATP levels in symptomatic HD mice (R6/2 model) forebrain, and to a lesser extent in cerebellum.
13. Demonstration of elevations in other key phosphorylated energy metabolites over the course of phenotype generation in the R6/2 HD mouse model – most notably phosphocreatine.
14. Determination of the time course of alterations in high-energy phosphates, over the life-span of R6/2 HD mice.
15. The observation that cerebral glucose utilization in striatum does not appear to be significantly altered prior to lesion formation induced by 3-NP administration in rats, and acute model of HD-like pathology.
16. The finding of increased lactate production in symptomatic HD mice, suggesting abnormal energy metabolism at this stage of the disorder in R6/2 mice. This is consistent with lactate elevations seen in symptomatic HD patients.

17. Increases in multiple oxidative damage markers (OH8dG, hydroxyl radical, F2 isoprostaglandins, and hydroxynonenol) in symptomatic R6/2 and N171-82Q HD mouse models.

b) ALS Mouse Studies:

18. The finding that cerebral glucose use is reduced in several forebrain regions in the G93A transgenic mouse model of FALS at 60 days of age – a time point preceding the onset of the first pathological changes in these mice.
19. Reduced glucose use rates are first evident in the brain – preceding changes in the spinal cord, although motor neuron degeneration in the spinal cord ultimately occurs – suggesting that cerebral energetic changes may influence neuronal function and integrity in the spinal cord.
20. More profound cerebral glucose use changes are evident in brains of older, symptomatic ALS mice (120 days), when metabolic defects are also evident in the spinal cord.
21. Glucose use alterations in G93A ALS mouse brains occur in discrete anatomically related components of the cerebrospinal motor tract.
22. The finding of increased complex I activity in the forebrain of G93A mice at 60 days of age, indicating impaired mitochondrial energy metabolism consistent with the defect seen in FALS A4V patients with a SOD1 mutation, which precedes onset of symptoms and pathological changes.
23. Profound reductions in cerebral ATP levels as early as 30 days of age (presymptomatic) in G93A ALS mice.
24. Findings of increased oxidative damage to protein (carbonyl detection), but not lipid (malondialdehyde) in the G93A ALS model. Earliest effects occurred in symptomatic mice (110d).

(II) Consortium Project:

25. Elucidation of optimum dosing paradigms and complex I measurements in a rat rotenone intrastriatal-injection model of PD-like neurodegeneration.
26. Elucidation of the time-line of complex I inhibition following rotenone injection.
27. Demonstration of early elevations in lipid peroxidation markers (malondialdehyde and 8-iso-prostaglandin F2) around the site of rotenone insult in rat striatum.

28. Demonstration of early and extensive induction of the cell stress marker heme oxygenase 1, following rotenone insult in rat striatum.
29. Development and characterization of the histochemical/densitometric assay of complex I activity in post-mortem rat brain sections.
30. Demonstration of the area of complex I inactivation by rotenone in rat striatum, using the histochemical procedure.
31. Demonstration of the temporal development of complex I activity impairments after intrastriatal rotenone injection, using the histochemical procedure.
32. Testing of intracerebroventricular adminstration of rotenone to rats as a possible alternative route of inhibitor administration, to improve reproducibility of striatal complex I inhibition; and subsequent dismissal of this approach.
33. Demonstration of extremely early elevations in a marker of oxidative damage to DNA (8-OHdG) in the striatum of rotenone-injected rats (evident by 1h post-injection; earliest time-point examined to date).
34. Demonstration that although lipid peroxidation markers (malondialdehyde and 8-iso-prostaglandin F2) are elevated around the site of rotenone insult in rat striatum by 8h post-injection (previously shown), these markers are induced *after* DNA damage is evident (ie. they are not evident 1h post-injection).
35. Demonstration that induction of the cell stress marker heme oxygenase 1 following rotenone insult in rat striatum (previously reported), follows DNA damage (ie. not evident at 1h post-injection).
36. The finding that increased generation of the lipid peroxidation marker MDA locally around the site of rotenone injection 8h post-injection (reported previously), is not reflected in an overall elevation of striatal MDA levels measured by HPLC. We hypothesize this is most likely due to the discrete localization of any MDA production induced by rotenone, which may be masked in the whole-striatum homogenate preparation used for HPLC studies.

9. REPORTABLE OUTCOMES

Manuscripts (related to these projects)

1. **BROWNE SE***, Yang LY, DiMauro J-PP, Licata SC, Beal MF. (2006) Bioenergetic abnormalities in discrete cerebral motor pathways presage spinal cord pathology in the G93A SOD1 mouse model of ALS. *Neurobiol Dis. In Press.*
2. Gardian G, **BROWNE SE**, Choi DK, Klivenyi P, Gregorio J, Kubilus JK, Ryu H, Langley B, Ratan RR, Ferrante RJ, Beal F. Neuroprotective effects of phenylbutyrate in the N171-82Q transgenic mouse model of Huntington's disease. *J Biol. Chem* (2005) 280:556-563.
3. Kim S-Y, Marekov L, Bubber P, **BROWNE SE**, Stavrovskaya I, Lee J, Steinert PM, Blass JP, Beal MF, Gibson GE, Cooper AJL. Mitochondrial aconitase is a transglutaminase 2 substrate: Transglutamination is a probable mechanism contributing to high-molecular-weight aggregates of aconitase and loss of aconitase activity in Huntington disease brain. *Neurochem. Res.* (2005) *In press.*
4. **BROWNE SE*** and Beal MF. The Energetics of Huntington's Disease. *Neurochem. Res* (2004) 29: 531-46.
5. Klivenyi P, Starkov AA, Calingasan NY, Gardian G, **BROWNE SE,** Yang, L, Bubber P, Gibson GE, Patel MS, Beal MF. Mice deficient in dihydrolipoamide dehydrogenase show increased vulnerability to MPTP, malonate and 3-nitropropionic acid neurotoxicity. *J. Neurochem.* (2004) 88: 1352-60.
6. Klivenyi P, Ferrante RJ, Gardian G, **BROWNE S**, Chabrier P-E, Beal MF. Neuroprotective effects of BN82451 in a transgenic mouse model of Huntington's disease. *J. Neurochem.* (2003) 86: 267-272.
7. Wu AS, Aguirre N, Calingasan NY, **BROWNE SE**, Crow JP, Kiaei M, Beal MF. Iron porphyrin treatment extends survival in a transgenic animal model of amyotrophic lateral sclerosis. *J. Neurochem.* (2003) 85:142-150.
8. **BROWNE SE*,** Beal MF. Toxin-induced mitochondrial dysfunction. *Int Rev Neurobiol.* (2002) 53: 243-79.
9. Andreassen OA, Dedeoglu A, Stanojevic V, Hughes DB, **BROWNE SE**, Leech CA, Ferrante RJ, Habener JF, Beal MF, Thomas MK. Huntington's Disease of the Endocrine Pancreas: Insulin Deficiency and Diabetes Mellitus due to Impaired Insulin Gene Expression. *Neurobiol Dis* (2002) 11:410-424.
10. **BROWNE SE***, Ferrante RJ, Beal MF. Oxidative stress in Huntington's disease. *Brain Pathol.* (1999) 9:147-163.

Submitted Manuscripts:

11. Fuller, SW, DiMauro J-PP, Starkov AA, Burr HN, Wheeler VC, Beal MF, Macdonald ME, **BROWNE SE*.** (2005) Energetic abnormalities precede pathological changes in a mouse model of Huntington's Disease. *J Neurosci. Submitted.*

Book Chapters

1. **BROWNE SE.** Huntington's Disease. In: *Manual of Neuropsychiatric Disorders*. F Tarazi and J Schetz, Eds. *Humana Press*. (2005) 63-86.
2. **BROWNE SE**, Beal MF. Huntington's disease. In: Functional Neurobiology of Ageing. PR Hof, CV Mobbs, Eds. *Academic Press* (2000) 711-725.

Conference Abstracts

1. McConoughey SJ, Cooper AJL, Krasnikov BF, **Browne SE**, Beal MF, Chavez JC, Ratan RR. (2005) Transcriptional dysregulation of genes involved in adaptation to metabolic stress in Huntington's disease. Soc. Neurosci. Abs. 31. Submitted
2. DiMauro J-PP, McConoughey SJ, Burr HN, **Browne SE**. (2005) Mitochondrial and Energetic Dysfunction in Animal Models of Huntington's Disease. Intl. Soc. Neurochem. In press.

3. DiMauro J-PP, Yang LY, Fuller SW, **Browne SE.** (2005) Metabolic Abnormalities Precede Pathologic Changes in the G93A SOD1 Mouse Model of ALS. Brain 05 & Brain/PET 05, J.CBF Metab. In press.
4. **Browne SE** (2004) Huntington's disease pathogenesis – key roles for mitochondria. J. Neurochem. 90 (Supp. 1) S13-02.
5. **Browne SE,** Choi D-K, Gardian G, Howard V, Schomer A, Strout P, Beal MF. (2004) Phenylbutyrate Administration Post-Symptom Onset Improves Survival in a Mouse HD Model. Hereditary Disease Foundation, "HD 2004: Changes, Advances and Good News". F17.
6. McConoughey SJ, Howard V, **Browne SE.** (2004) Glut1 and Glut3 transporters in Huntingtin mutant mice. Forum of European Neurosciences 2004, A020.17.
7. DiMauro J-PP, McConoughey SJ, Burr HN, **Browne SE.** (2004) Cerebral Glucose Utilization Defects precede Pathological Changes in Mouse Models of Huntington's Disease. Gordon Research Conference: Brain Energy Metabolism and Blood Flow. (No abstract published).
8. **Browne SE,** DiMauro J-PP, Albrecht RJ, Burr HN. (2003) The evolution of metabolic defects in a knock-in mutant mouse model of Huntingtons disease. Soc. Neurosci. Abs. 29: 130.12
9. Saydoff JA, Liu LS, Brenneman D, Garcia RAG, Hu ZY, Cardin S, Gonzalez A, von Borstel RW, Beal MF, **Browne SE.** (2003) Uridine prodrug PN401 is neuroprotective in the R6/2 and N171-82Q mouse models of Huntington's disease. Soc. Neurosci. Abs. 29: 130.11
10. Kim S-Y, Marekov L, Bubber P, **Browne S,** Stavrovskaya I, Son JH, Beal MF, Blass JP, Gibson GE, Cooper AJL. (2003) Mitochondrial Aconitase as a Transglutaminase Target: Implication for Mitochondrial Dysfunction in Huntington Brain. Soc. Neurosci. Abs. 29: 130.5
11. Burr H, DiMauro J-PP, Gregorio J, **Browne SE.** (2003) [^{14}C]-2-Deoxyglucose *in vivo* autoradiographic studies reveal alterations in cerebral metabolism precede pathologic changes in two mutant mouse models of Huntingtin's disease. *Brain 03 & Brain/PET 03, J.CBF Metab.* 23 (Supp. 1): 585.
12. **Browne SE,** DiMauro J-PP, Albrecht RJ, Burr HN. (2003) The evolution of metabolic defects in a knock-in mutant mouse model of Huntingtons disease. Soc. Neurosci. Abs. 29: 130.12
13. **Browne SE.** Disruptions of cellular energy metabolism in HD: evidence for treatment effects? Frontiers in Neurodegeneration – Huntington's disease. (2002).
14. Gregorio J, Burr H, Klivenyi P, Gardian G, von Borstel RW, Saydoff JA, Beal MF, **Browne SE.** Manipulating oxidative damage and energy metabolism: Novel neuroprotectants in HD mouse models. HDF: Changes, Advances and Good news $(CAG)_n$. (2002) 18.
15. Gregorio J, DiMauro J-P P, Narr S, Fuller SW, **Browne SE.** Cerebral metabolism defects in HD: Glucose utilization abnormalities in multiple HD mouse models. Soc. Neurosci. Abs. (2002) 28: 195.10
16. Wu AS, Aguirre N, Calingasan NY, Browne SE, Crow JP, Kiaei M, Beal MF. Iron porphyrin treatment extends survival in a transgenic animal model of amyotrophic lateral sclerosis. Soc. Neurosci. Abs. (2002) 28: 789.1
17. **Browne SE.** Disruptions of cellular energy metabolism in HD: evidence for treatment effects? *Frontiers in Neurodegeneration – Huntington's disease.* (2002).
18. **Browne SE,** DiMauro J-P P, Narr S. Metabolic changes precede phenotypic changes in mutant mouse models of HD. *World Federation on Neurology Research Group on Huntington's Disease* (2001)
19. **Browne SE,** Yang L, Fuller SW, Beal MF. Metabolic changes precede pathologic changes in the G93A mouse model of a familial amyotrophic lateral sclerosis. *Soc. Neurosci. Abs.* (2001) 27: 580.6.
J-P P DiMauro, S Narr, MF Beal, **Browne SE.** Cerebral energy metabolism in mutant mouse models of Huntington's disease. *Soc. Neurosci. Abs.* (2001) 27: 432.1.
20. **Browne SE,** Wheeler V, White JK, Fuller SW, MacDonald, M, Beal MF. Dose-dependent alterations in local cerebral glucose use associated with the huntingtin mutation in *Hdh* CAG knock-in transgenic mice. *Soc. Neurosci. Abs.* (1999) 25: 218.11.
21. Hughes DB, Thomas M, Dedeoglu A, **Browne SE,** Ferrante RJ, Andreassen OA, Beal MF. Hyperglycemia in a transgenic animal model of Huntington's disease. *Soc. Neurosci. Abs.* (1999) 25: 237.14.

22. **Browne SE**, Andreassen OA, Hughes DB, Ferrante RJ, Jenkins BG, Beal MF. Cerebral energetic defects in transgenic animal models of Huntington's disease. *World Federation on Neurology Research Group on Huntington's Disease.* (1999) 18: 46.
23. **Browne SE**, Licata SC, Beal MF. Energetic defects in a transgenic mouse model of familial ALS. *J. Neurochem.* (1999) S27B.

☒

Invited Presentations (Since 2002)

May 7th 2002 — Biochemistry Department Seminar Series
University of Maryland, Baltimore, MD, USA.
"Animal Models of Neurodegenerative Disorders: Insights into Pathogenesis"

July 20th –21st 2002 — Hereditary Disease Foundation, Mary Jennifer Selznick Workshop,
Cardiff, WALES, UK.
"Behavioral Assessment in Mouse Models of Huntington's Disease."

October 16th-18th 2002 — Young ALS Investigator's Workshop
Lafayette, PA, USA.
"Cerebral Energy Metabolism in G93A Mice."

April 15th 2003 — American Society for Pharmacology and Experimental Therapeutics,
Symposium: Animal Models of Neuropsychiatric Diseases.
San Diego, CA, USA.
"Modeling Huntington's Disease in the Mouse: Mechanistic and Therapeutic Insights"

June 5th 2003 — University of Edinburgh, SCOTLAND, UK,
Department of Neuroscience Seminar Series.
"The Cerebral Energetics of Huntington's Disease".

November 17th 2003 — Farber Institute for Neuroscience, Research Seminar
Thomas Jefferson University Medical College, Philadelphia, PA, USA.
"CNS Energetics and SOD1 in ALS Pathogenesis".

December 2nd 2003 — McLean Hospital, Neuroscience Seminar.
Harvard Medical School, Belmont, MA, USA.
"CNS Metabolism and the pathogenesis of ALS."

March 19th 2004 — Mayo Clinic Seminar Series,
Mayo Jacksonville, Jacksonville, FL, USA.
"CNS Energy Metabolism and the Pathogenesis of Huntington's Disease".

August 15th 2004 — Hereditary Disease Foundation, "HD 2004: Changes, Advances and Good News"
Boston, MA, USA.
"Phenylbutyrate Administration Post-Symptom Onset Improves Survival in a Mouse HD Model"

August 17th 2004 — American Neurochemistry Society, 35th Annual Meeting.
Symposium: Role of mitochondria in Neurodegeneration"
New York, NY, USA.
"Huntington's disease pathogenesis – key roles for mitochondria."

December 4th 2004	Cold Spring Harbor Conference on Drug Discovery in Neurodegenerative Diseases. Cold Spring Harbor, NY, USA. *" Administration of a histone deacetylase inhibitor post-symptom onset improves outcome in a mouse model of Huntington's disease."*
June 8th 2005	International Society of Cerebral Blood Flow and Metabolism, Brain 05 & Brain/PET 05 Meeting. Amsterdam, NL. *"Metabolic Abnormalities Precede Pathologic Changes in the G93A SOD1 Mouse Model of ALS."*
August 26th 2005	International Society for Neurochemistry, and European Society for Neurochemistry, 20th Biennial Meeting. Innsbruck, Austria. *"Mitochondrial and Energetic Dysfunction in Animal Models of Huntington's Disease."*

10. CONCLUSIONS

The overall goals of this proposal were to gain insight into the roles of defects in CNS energy metabolism and oxidative stress in mechanisms of neuronal death and dysfunction in neurodegenerative disorders. Outcomes may impact therapeutic strategies for treatment of both degenerative disorders and neurotoxin exposure. Previous studies in human and animal models have implicated the involvement of mis-metabolism and oxidative damage in the pathogenesis of several neurodegenerative diseases including Parkinson's disease (PD). This project concentrated largely on using *in vivo* techniques in whole animal models of degenerative disorders, to gain insight into disease mechanisms at all stages of pathogenesis.

In the first three years of this grant we made substantial progress in characterizing the nature of changes in cerebral energy metabolism seen in the R6/2, N171-82Q and *Hdh* mouse models of HD, both *in vivo* and *in vitro*. We have also shown that cerebral glucose metabolism is impaired in the G93A transgenic mouse model of FALS (overexpressing human mutant SOD1) at 60 days of age, and ATP generation is depressed as early as 30 days. Our observations suggest that energetic dysfunction may play an intrinsic role in the pathogenesis of the motor neuron disorder seen in both HD and ALS mouse models, since alterations precede symptomatic and pathological changes in these animals.

Results in mutant mouse models of both ALS and HD clearly demonstrate the early involvement of metabolic changes in the sequence of events initiated by expression of the mutant disease gene, prior to pathologic changes, symptom onset and cell death. The nature of the metabolic

changes seen differs between the HD and ALS models, suggesting that the nature of triggering events set in motion by the gene defect may vary in these disorders. It still remains to elucidate the exact pathway from mutant gene expression to induction of metabolic changes. Overall, outcomes of these studies will have a great impact on the development of therapeutic strategies for these diseases and potentially for other neurodegenerative disorders in which metabolic dysfunction occurs, including PD and mitochondrial neurotoxin exposure. Results support the potential efficacy of pro-energy agents, or metabolism-enhancing agents, in therapeutic strategies for HD and ALS. We have been successful in completing the majority of studies outlined in our specific aims, and have also conducted additional studies to augment findings from the original proposal.

In the consortium project section of this grant report we extended studies to explore the role of mitochondria, and in particular mitochondrial complex I, as a source of reactive oxygen species (ROS) in the context of another degenerative disorder, PD. Studies address the inter-relationship between energetic defects and oxidative damage in neurotoxin models of PD in rats. Again using *in vivo* approaches, we have made progress towards optimizing experimental conditions for assessing the temporal association between inhibiting complex I activity at specific mitochondrial subunit sites, and producing free radicals and hence oxidative damage. We have further characterized the nature of the complex I inhibition induced by rotenone, and have commenced studies with another complex I inhibitor, pyridaben, which shows a different pattern of complex I subunit specificity to rotenone (dosing with this agent still needs fin-tuning, as results to date show substantial variability in lesion size and reproducibility). We have also expanded on our novel observations of increased free radical-mediated damage after rotenone injection into rat striata. We have novel and tantalizing data showing the induction of oxidative damage to lipids and DNA, and the induction of the cell stress-responder heme oxygenase-1, at a time point shortly after complex I inhibition. Notably, we have been able to demonstrate that oxidative damage to DNA is evident as soon as 1h post-rotenone injection (manuscript in preparation).

☒
☒
☒
☒

11. REFERENCES

Agarwal, R. and S. Chase (2002). Rapid, fluorimetric-liquid chromatographic determination of malondialdehyde in biological samples. *J Chromatography_B* 775: 121-6.

Alam M, Schmidt WJ. Rotenone destroys dopaminergic neurons and induces parkinsonian symptoms in rats. Behav Brain Res. 2002 136:317-24.

Andreassen OA, Dedeoglu A, Ferrante RJ, Jenkins BG, Ferrante KL, Thomas M, Friedlich A, Browne SE, Schilling G, Borchelt DR, Hersch SM, Ross CA, Beal MF. Creatine increase survival and delays motor symptoms in a transgenic animal model of Huntington's disease. Neurobiol Dis. 2001 8:479-91.

Antkiewicz-Michaluk L, Karolewicz B, Romanska I, Michaluk J, Bojarski AJ, Vetulani J. 1-Methyl-1,2,3,4-tetrahydroisoquinoline protects against rotenone-induced mortality and biochemical changes in rat brain. Eur J Pharmacol. 2003 466:263-9.

Betarbet, R., Sherer, T.B., MacKenzie, G., Garcia-Osuna, M., Panov, A.V. and Greenamyre, J.T., 2000. Chronic systemic pesticide exposure reproduces features of Parkinson's disease. Nat. Neurosci. 3, pp. 1301–1306.

Bourges I, Ramus C, Mousson De Camaret B, Beugnot R, Remacle C, Cardol P, Hofhaus G, Issartel JP. (2004) Structural organization of mitochondrial human complex I: role of the ND4 and ND5 mitochondria-encoded subunits and interaction with the prohibitin. *Biochem J.* 383:491-9

Bradford MM. (1976) A rapid and sensitive method for the quantitation of microgram quantities of protein utilizing the principle of protein-dye binding. Anal. Biochem. 72: 248-254.

Browne SE, Ayata C, Huang PL, Moskowitz MA, Beal MF. Lack of either endothelial or neuronal nitric oxide synthase isoforms does not differentially affect basal cerebral glucose metabolism in knockout mice. *J. Cereb Blood Flow Metab.* (1999) 19:144-148.

Browne SE, Beal MF. Huntington's disease. In: Funtional Neurobiology of Ageing. PR Hof, CV Mobbs, Eds. *Academic Press* (2000) 711-725

Browne SE, Bowling AC, MacGarvey U, Baik MJ, Berger SC, Muqit MMK, Bird ED and Beal MF. (1997) Oxidative damage and metabolic dysfunction in Huntington's Disease: Selective vulnerability of the basal ganglia. Annals Neurol. 41: 646-653.

Dal Canto, MC and Gurney, ME. (1995) Neuropathological changes in two lines of mice carrying a transgene for mutant human Cu, Zn SOD, and in mice overexpressing wild type SOD: a model of familial amyotrophic lateral sclerosis (FALS). Brain Res. 676: 25-40.

Darrouzet E, I. J., Lunardi J, Dupuis A. (1998). "The 49-kDa subunit of NADH-ubiquinone oxidoreductase (Complex I) is involved in the binding of piericidin and rotenone, two quinone-related inhibitors." Federation of European Biochemical Societies Letters 431: 34-38.

Ferrante RJ, Andreassen OA, Jenkins BG, Dedeoglu A, Kuemmerle S, Kubilus JK, Kaddurah-Daouk R, Hersch SM, Beal MF. (2000) Neuroprotective effects of creatine in a transgenic mouse model of Huntington's disease. J Neurosci 20:4389-97

Gonzales S, Erario MA, Tomaro ML. Heme oxygenase-1 induction and dependent increase in ferritin. A protective antioxidant stratagem in hemin-treated rat brain. Dev Neurosci. 2002 24:161-8.

Gu M, Gash MT, Mann VM, Javoy-Agid F, Cooper JM and Schapira AHV (1996) Mitochondrial defect in Huntington's disease caudate nucleus. Ann Neurol. 39: 385-389.

Guidetti P, Charles V, Chen EY, Reddy PH, Kordower JH, Whetsell WO Jr, Schwarcz R, Tagle DA. (2001) Early degenerative changes in transgenic mice expressing mutant huntingtin involve dendritic abnormalities but no impairment of mitochondrial energy production. Exp Neurol 169:340-50.

Gurney, M.E. *et al.* (1994) Motor neuron degeneration in mice expressing a human Cu, Zn superoxide dismutase mutation. Science 264: 1772-1775.

Hatefi Y. (1978) Preparation and properties of NADH: ubiquinone oxidoreductase (complex I). EC 1.6.5.3. Methods Enzymol. 53: 11-14.

Higgins DS Jr, Greenamyre JT. 3H]dihydrorotenone binding to NADH: ubiquinone reductase (complex I) of the electron transport chain: an autoradiographic study. J Neurosci. 1996 16:3807-16.

Hoglinger GU, Feger J, Prigent A, Michel PP, Parain K, Champy P, Ruberg M, Oertel WH, Hirsch EC. Chronic systemic complex I inhibition induces a hypokinetic multisystem degeneration in rats. J Neurochem. 2003 84:491-502.

Jung C, Higgins CM, Xu Z. A quantitative histochemical assay for activities of mitochondrial electron transport chain complexes in mouse spinal cord sections. J Neurosci Methods. 2002 114:165-72.

Lai JC, Clark JB. Preparation of synaptic and nonsynaptic mitochondria from mammalian brain. Methods Enzymol. 1979 55:51-60.

Lodi R, Schapira AH, Manners D, Styles P, Wood NW, Taylor DJ, Warner TT.(2000) Abnormal in vivo skeletal muscle energy metabolism in Huntington's disease and dentatorubropallidoluysian atrophy. Ann Neurol 48:72-6

Ludolph AC, He F, Spencer PS, Hammerstad J, Sabri M. 3-Nitropropionic acid-exogenous animal neurotoxin and possible human striatal toxin. Can J Neurol Sci. 1991 18:492-8.

MacDonald ME. (2002) Early phenotypes that presage late-onset neurodegenerative disease allow testing of modifiers in Hdh CAG knock-in mice. Hum Mol Genet. 11:633-40.

Magnitsky S, Toulokhonova L, Yano T, Sled VD, Hagerhall C, Grivennikova VG, Burbaev DS, Vinogradov AD, Ohnishi T. EPR characterization of ubisemiquinones and iron-sulfur cluster N2, central components of the energy coupling in the NADH-ubiquinone oxidoreductase (complex I) in situ. J Bioenerg Biomembr. 2002 34:193-208.

Manfredi G, Yang L, Gajewski CD, Mattiazzi M. Measurements of ATP in mammalian cells. Methods. 2002 26:317-26.

Mangiarini L, Sathasivam K, Seller M, Cozens B, Harper A, Hetherington C, Lawton M, Trottier Y, Lehrach H, Davies SW and Bates G. (1996) Exon 1 of the HD gene with an expanded CAG repeat is sufficient to cause a progressive neurological phenotype in transgenic mice. Cell 87: 493-506.

Menzies FM, Ince PG, Shaw PJ.(2002) Mitochondrial involvement in amyotrophic lateral sclerosis Neurochem Int 40:543-51.

Okun JG, L. P., Brandt U (1999). "Three classes of inhibitors share a common binding domain in mitochondrial complex I (NADH:ubiquinone oxidoreductase)." The Journal of Biological Chemistry 274: 2625-30.

Rasmussen TSD, Brors B, Kintscher L, Weiss H, Friedrich T (2001). "Identification of two tetranuclear FeS clusters on the ferredoxin-type subunit of NADH:ubiquinone oxidoreductase (complex I)." Biochemistry 40(20): 6124-31.

Schilling G, Bacher MW, Sharp AH, Jinnah HA, Duyao K, Kotzuk JA, Slunt HH, Ratovitski T, Cooper JA, Jenkins NA, et al., (1999) Intranuclear inclusions and neuritic aggregates intransgenic mice expressing a mutant N-terminal fragment of huntingtin. Hum. Molec. Genet. 8:397-407.

Schuler F, C. J. (2001). "Functional coupling of PSST and ND1 subunits in NADH:ubiquinone oxidoreductase established by photoaffinity labeling." Biochimica et Biophysica Acta 1506(1): 79-87.

Schuler F, Y. T., Di Bernardo S, Yagi T, Yankovskaya V, Singer TP, Casida JE. (1999). "NADH-quinone oxidoreductase: PSST subunit couples electron transfer from iron-sulfur cluster N2 to

quinone." Proceedings of the National Academy of Sciences of the United States of America 96(7): 4149-53.

Schulte, U. (2001). "Biogenesis of Respiratory Complex 1." Journal of Bioenergetics and Biomembranes 33(3): 205-12.

Shepherd D and Garland PB. (1969) Citrate synthase from rat liver. Meth. Enzymol. 13: 11-16.

Sherer TB, Kim JH, Betarbet R, Greenamyre JT. (2003) Subcutaneous rotenone exposure causes highly selective dopaminergic degeneration and alpha-synuclein aggregation. Exp Neurol. 179:9-16.

Sokoloff, L, Reivich, M, Kennedy, C *et al.* (1977) The [^{14}C]2-deoxyglucose method for the measurement local cerebral glucose utilization. Theory, procedure, and normal values in the conscious and anaesthetized rat. J. Neurochem. 28: 897-916.

Tabrizi SJ, Cleeter MWJ, Xuereb J, Taanman JW, Cooper JW, Schapira AHV. (1999) Biochemical abnormalities and excitotoxicity in Huntington's disease brain. Ann. Neurol. 45: 25-32.

Tabrizi SJ, Workman J, Hart PE, Mangiarini L, Mahal A, Bates G, Cooper JM, Schapira AH. (2000) Mitochondrial dysfunction and free radical damage in the Huntington R6/2 transgenic mouse. Ann Neurol. 47: 80-6.

Triepels RH, V. D. H. L., Trijbels JM, Smeitink JA. (2001). "Respiratory chain complex I deficiency." American Journal of Medical Genetics 106: 37-45.

Wheeler VC, Gutekunst CA, Vrbanac V, Lebel LA, Schilling G, Hersch S, Friedlander RM, Gusella JF, Vonsattel JP, Borchelt DR,

Wheeler VC, White JK, Gutekunst CA, Vrbanac V, Weaver M, Li XJ, Li SH, Yi H, Vonsattel JP, Gusella JF, Hersch S, Auerbach W, Joyner AL, MacDonald ME. (2000) Long glutamine tracts cause nuclear localization of a novel form of huntingtin in medium spiny striatal neurons in HdhQ92 and HdhQ111 knock-in mice. Hum Mol Genet. 9: 503-13.

White JK, Auerbach W, Duyao MP, Vonsattel J-P, Gusella JF, Joyner AL and MacDonald ME. (1997) Huntingtin function is required for mouse brain development and is not impaired by the Huntington's disease CAG expansion mutation. Nature Gen. 17: 404-410.

Yu ZX, Li SH, Evans J, Pillarisetti A, Li H, Li XJ. Mutant huntingtin causes context-dependent neurodegeneration in mice with Huntington's disease. J Neurosci. 2003 23:2193-202.

12. APPENDICES

a) C.V. for Dr, Browne (PI) attached

b) 10 Manuscripts and 2 book chapters directly arising from these studies are appended (Listed in manuscripts and book chapter section of 9, Reportable Outcomes).

Personnel Supported by Grant

Susan E. Browne, PhD (Principal investigator)

Sara Fuller, BS — Victor Howard, BS

Jon-Paul DiMauro, BS — Debbie Fried, BMed

Jason Gregorio BS

APPENDIX 1

CURRICULUM VITAE

Name and Title: Susan Elizabeth Browne Ph.D., Assistant Professor.

Date of Birth: 13th December 1966

Academic Address: Neurology and Neuroscience, Weill Medical College of Cornell University, Neurology Dept., A502, 525 E. 68th St., New York NY 10021.

Tel: (212) 746-4672
Fax: (212) 746-8276
E-mail: sub2001@ med. cornell.edu

Education:

1985-1989 B.Sc. (with Honors), Pharmacology. University of Aberdeen, Scotland

1989-1993 Ph.D., Neuroscience. University of Glasgow, Scotland.
Thesis: "Excitatory amino acid receptor-mediated events in the brain: Quantitative autoradiographic studies."
Supervisor: Prof. James McCulloch, Wellcome Surgical Institute.

Professional Experience:

1993-1996 **Post-Doctoral Research Fellow**, Neurology Research, Massachusetts General Hospital (MGH) and Harvard Medical School (HMS), Boston MA.

1996-1999 **Instructor**, Neurology Research, HMS, Boston MA.

1997-1999 **Assistant**, Neurology Service, MGH, Boston MA.

1999 - Present **Assistant Professor** of Neuroscience, Weill Medical College of Cornell University, New York NY.

2001 - Present **Assistant Professor**, Weill Graduate School of Medical Sciences of Cornell University; Program in Neuroscience.

Grant Support:

Principal Investigator:

2005-2007 **High Q Foundation.** ***PI***
"Therapeutic efficacy in mouse models of HD" $ TBA

1999-2005 **Department of Defense USAMRAA: DAMD 7-98-1-8620.** ***PI***
Neurotoxin Exposure Treatment Research Program:
"Bioenergetic defects and oxidative damage in transgenic mouse models of neurodegenerative disorders". $1,010,230

1997-2006 **Huntington's Disease Society of America.** ***Co-PI.***
Coalition for the Cure:
"Metabolic defects and oxidative damage in a transgenic mouse model of Huntington's disease." $100,000 *p.a.*

2000-2002 **Huntington's Disease Society of America.** ***PI***
"The role of energy metabolism in pathogenesis in transgenic mouse models of HD and another CAG repeat disorder". $100,000

Investigator:

1999-2008 **NIH: 1R01 NS39258** (Beal PI)
"Bioenergetics in animal models of Huntington's disease."

2004-2007 **NIH: 1U01 NS04907** (Beal PI)
"Development of new therapies in Huntington's disease."

2005-2010 **NIH: P01** (Gibson, PI).
"Mitochondrial Dysfunction in Transgenic Mice with Neurodegeneration",
Role: Co-Project Leader.

Fellowships Held:

1996-1999 **Amyotrophic Lateral Sclerosis Association:**
"An *in vivo* investigation of the cerebral metabolic consequences of motor neuron disease: Measurement of local cerebral glucose utilization in a transgenic mouse model of familial ALS."

1996-1999	**Muscular Dystrophy Association:** "Cerebral energy metabolism in a transgenic mouse model of ALS."
1995	**Sandoz Foundation for Gerontological Research:** "Effect of impairment of mitochondrial energy metabolism and oxidative damage on cerebral glucose metabolism."
1993-1995	**Huntington's Disease Society of America:** "Mitochondrial energy metabolism and oxidative damage in Huntington's disease."
Prizes/Awards:	
1989	Wellcome Trust Ph.D. Studentship
1997	*HDSA / Astra Merck Scholarship* WFN HD Research Meeting, Sydney, Australia.
2002	*ALS Associaion Invitation:* Young ALS Investigators Workshop
2005	*International Society for Neurochemistry (INS) Young Investigator,* Colloquium speaker and Travel Award. Innsbruck, Austria.
Teaching:	*Weill Graduate School of Medical Sciences of Cornell University*
2000-present	**Course Director:** "The Neurobiology of Degenerative Diseases". Neuroscience Graduate Program. **Lecturer**: "Molecular Neuropharmacology". Neuroscience and Pharmacology Graduate Programs.
2000-2002	**Lecturer, Course Tutor:** "Brain and Mind". Neuroanatomy Department, Weill Medical College.
Students:	Ph.D. Rotation Supervisor: Christina Higgins, Stephen McConoughey 2001- Adriana Galvan, Carl Wonders, Sebastian Schaffer.
2003	B. Med (Australia) Supervisor: Debbie Fried.
Committees and Professional Affiliations:	***Reviewer, NIH:*** NINDS, Translational Research Cooperative Agreement (2003), and CDIN (2004-present). ***Reviewer,*** Italian Telethon Foundation (2005-), Neurological Foundation of New Zealand. (2005-), High Q Foundation, (2004-) Institutional Animal Care and Use Committee (WMC, 2003-present) PhD Committee Chair (Ms. Laura Towart, Weill Med. College) British Neuroscience Association UK (1991-present) Society for Neuroscience (1994-present) International Society of Cerebral Blood Flow and Metabolism (1997-) American Society for Neurochemistry (2002-present)
Local Coordinator:	Society for Neuroscience Greater New York Chapter (2004-)
Journal Reviewer:	Brain Research, Brain Research Reviews, European J. Neuroscience, Experimental Brain Research, Experimental Neurology, J. Cerebral Blood Flow & Metabolism, J. Neurochemistry, J. Neuroscience, Neurobiology of Disease, Stroke.
Techniques: *In Vivo* (rats and mice):	[^{14}C]-2-deoxyglucose autoradiographic measurement of local cerebral metabolic rates for glucose, in conscious rats and mice. [^{14}C]-methylglucose autoradiography. [^{125}I]-MK-801 autoradiography. Stereotactic intracerebral injections: excitotoxin and mitochondrial toxin lesions of discrete brain regions. Mechanical visual pathway lesions by orbital enucleation. Vascular cannulation. Systemic drug administration.

In Vitro: (human and rodent CNS tissue):	Quantitative ligand binding autoradiography, sections and homogenates. Histological lesion analysis. Immunocytochemistry Densitometry. Mitochondrial isolation. Mitochondrial DNA and nuclear DNA extraction. Spectrophotometric metabolic enzyme activity assays. HPLC detection of oxidative damage products. Oxygraph. ATP synthesis luciferin/luciferase assay. PCR. RT-PCR. Molecular biology techniques. Affymetrix gene microarry.

PUBLICATIONS

1. Gardian G, **BROWNE SE**, Choi DK, Klivenyi P, Gregorio J, Kubilus JK, Ryu H, Langley B, Ratan RR, Ferrante RJ, Beal F. Neuroprotective effects of phenylbutyrate in the N171-82Q transgenic mouse model of Huntington's disease. *J Biol. Chem* (2005) 280:556-563.
2. Kim S-Y, Marekov L, Bubber P, **BROWNE SE**, Stavrovskaya I, Lee J, Steinert PM, Blass JP, Beal MF, Gibson GE, Cooper AJL. Mitochondrial aconitase is a transglutaminase 2 substrate: Transglutamination is a probable mechanism contributing to high-molecular-weight aggregates of aconitase and loss of aconitase activity in Huntington disease brain. *Neurochem. Res.* (2005) *In press.*
3. Licata SE, Yang LY, DiMauro J-PP, Fuller SW, Beal MF, **BROWNE SE*.** (2005) Cerebral metabolic defects presage pathological changes in the G93A SOD1 mouse model of ALS. *J. Neurosci. Submitted.*
4. Fuller, SW, DiMauro J-PP, Starkov AA, Burr HN, Wheeler VC, Beal MF, Macdonald ME, **BROWNE SE*.** (2005) Energetic abnormalities precede pathological changes in a mouse model of Huntington's Disease. *Neuron. Submitted.*
5. Choi D-K, Calingasan NY, Chen J, Howard VG, Strout PC, Beal MF, **BROWNE SE*.** (2005) Epigenetic modulation of gene transcription in Huntington's disease. *J. Neurosci. Submitted.*
6. Huntington Study Group. (2005) Safety and tolerability of high dosage Coenzyme Q_{10} in Huntington's disease and in healthy subjects *Neurology. Submitted.*
7. Ferrante RJ, Ryu H, Kubilus J, D'Mello, Sugars KL, Lee J, Lu P, Smith K, **BROWNE S**, Beal MF, Kristal BS, Stavrovskaya IG, Hewett S, Rubinsztein DC, Langley B, Ratan RR. Chemotherapy for the brain: The antitumor antibiotic mithramycin prolongs survival in a mouse model of Huntington's disease. *J Neurosci.* (2004) 24:10335-10342.
8. Starkov AA, Fiskum G, Chinopoulos C, Lorenzo BJ, **BROWNE SE**, Patel MS, Beal MF. Mitochondrial alpha-ketoglutarate dehydrogenase complex generates reactive oxygen species. *J Neurosci.* (2004) 24:7779-88.
9. **BROWNE SE*** and Beal MF. The Energetics of Huntington's Disease. *Neurochem. Res* (2004) 29: 531-46.
10. **BROWNE SE,** Roberts II LJ, Dennery PA, Doctrow SR, Beal MF, Barlow C, Levine RL. Treatment with a catalytic antioxidant corrects the neurobehavioral defect in ataxia-telangiectasia mice. *Free Rad Biol Med.* (2004) 36: 938-942
11. Petrucelli L, Dickson D, Kehoe K, Taylor J, Synder H, Kim J, Grover A, McGowan E, Prihar G, De Lucia M, Lewis J, Dillmann WH, **BROWNE SE**, Hall AE, Voellmy R, Dawson T, Wolozin B, Hardy J and Hutton M. CHIP and Hsp70 Regulate Tau Ubiquitination, Degradation and Aggregation. *Hum Molec Gen.* (2004) 13:703-14
12. Klivenyi P, Starkov AA, Calingasan NY, Gardian G, **BROWNE SE,** Yang, L, Bubber P, Gibson GE, Patel MS, Beal MF. Mice deficient in dihydrolipoamide dehydrogenase show increased vulnerability to MPTP, malonate and 3-nitropropionic acid neurotoxicity. *J. Neurochem.* (2004) 88: 1352-60.
13. Yang LC, Sugama S, Lorenzl S, **BROWNE SE**, Gregorio J, Chirichigno J, Joh TH, Beal MF, Albers DS. Minocycline exacerbates MPTP toxicity in an *in vivo* model of Parkinson's disease. *J. Neurosci. Res* (2003) 74: 278-85.
14. Klivenyi P, Ferrante RJ, Gardian G, **BROWNE S**, Chabrier P-E, Beal MF. Neuroprotective effects of BN82451 in a transgenic mouse model of Huntington's disease. *J. Neurochem.* (2003) 86: 267-272.

15. Wu AS, Aguirre N, Calingasan NY, **BROWNE SE**, Crow JP, Kiaei M, Beal MF. Iron porphyrin treatment extends survival in a transgenic animal model of amyotrophic lateral sclerosis. *J. Neurochem.* (2003) 85:142-150.
16. **BROWNE SE*,** Beal MF. Toxin-induced mitochondrial dysfunction. *Int Rev Neurobiol.* (2002) 53: 243-79.
17. Andreassen OA, Dedeoglu A, Stanojevic V, Hughes DB, **BROWNE SE**, Leech CA, Ferrante RJ, Habener JF, Beal MF, Thomas MK. Huntington's Disease of the Endocrine Pancreas: Insulin Deficiency and Diabetes Mellitus due to Impaired Insulin Gene Expression. *Neurobiol Dis* (2002) 11:410-424.
18. **BROWNE SE**, Lin L, Mattson A, Georgievska B, Isacson O. Cognitive deficits correlate with sustained cerebral hypometabolism after selective degeneration of the basal forebrain cholinergic system in rats. *Expt. Neurol.* (2001) 170: 36-47.
19. Jeitner TM, Bogdanov MB, Mattson WR, Daikhin Y, Yudkoff M, Folk JE, Steinman L, **BROWNE SE,** Beal MF, Blass JP, Cooper AJL. N(epsilon)-(gamma-L-glutamyl)-L-lysine (GGEL) is increased in cerebrospinal fluid of patients with Huntington's disease. *J Neurochem.* (2001) 79:1109-1112.
20. Andreassen OA, Dedeoglu A, Ferrante RJ, Jenkins BG, Ferrante KL, Thomas M, **BROWNE SE**, Friedlich A, Hersch SM, Borchelt DR, Ross CA, Beal MF. Creatine increases survival and delays motor symptoms in a transgenic animal model of Huntington's disease. *Neurobiol. Ageing.* (2001) 8: 479-491.
21. Albers DS, Augood SJ, Park LCH, **BROWNE SE**, Martin DM, Adamson J, Hutton M, Standaert DG, Vonsattel JPG, Gibson GE, Beal MF. Frontal lobe dysfunction in PSP: Evidence for oxidative stress and mitochondrial impairment. *J. Neurochem.* (2000). 74: 878-881.
22. **BROWNE SE***, Ferrante RJ, Beal MF. Oxidative stress in Huntington's disease. *Brain Pathol.* (1999) 9:147-163.
23. **BROWNE SE***, Ayata C, Huang PL, Moskowitz MA, Beal MF. Lack of either endothelial or neuronal nitric oxide synthase isoforms does not differentially affect basal cerebral glucose metabolism in knockout mice. *J. Cereb Blood Flow Metab.* (1999) 19:144-148.
24. **BROWNE SE***. Neurodegenerative disease. *IDrugs* (1999) 2: 4-6.
25. Polidori MC, Mecocci P, **BROWNE SE**, Senin U, Beal MF. Oxidative damage to mitochondrial DNA in Huntington's disease parietal cortex. *Neurosci Lett* (1999) 272:53-6
26. Simon DK, Pulst SM, Sutton JP, **BROWNE SE**, Beal MF, Johns DR. Familial multisystem degeneration with parkinsonism associated with the 11778 mitochondrial DNA mutation. *Neurology* (1999) 53:1787-93.
27. **BROWNE SE**, Bowling AC, Baik MJ, Gurney M,Brown RH Jr., Beal MF. Metabolic dysfunction in familial, but not sporadic, amyotrophic lateral sclerosis. *J. Neurochem.* (1998) 71: 281-287.
28. **BROWNE SE***, Muir J, Robbins TW, Page KJ, Everitt BJ, McCulloch J. The cerebral metabolic effects of manipulating glutamatergic systems within the basal forebrain in conscious rats. *Eur. J. Neurosci.* (1998) 10: 649-663.
29. Matthews RT, Yang L, **BROWNE SE**, Baik MJ, Beal MF. Coenzyme Q_{10} administration increases brain mitochondrial concentrations and exerts neuroprotective effects. *PNAS* (1998) 95: 8892-8897.
30. **BROWNE SE**, Bowling AC, MacGarvey U, Baik MJ, Berger SC, Muqit MMK, Bird ED, Beal MF. Oxidative damage and metabolic dysfunction in Huntington's disease: selective vulnerability of the basal ganglia. *Ann. Neurol.* (1997) 41: 646-653.
31. Ferrante RJ, **BROWNE SE**, Shinobu LA, Bowling AC, Baik MJ, MacGarvey U, Kowall NW, Brown RH Jr, Beal MF. Evidence of increased oxidative damage in both sporadic and familial amyotrophic lateral sclerosis. *J. Neurochem.* (1997) 69: 2064-2074.
32. Beal MF, Ferrante RJ, **BROWNE SE**, Matthews RT, Kowall NW, Brown RH Jr. Increased 3-nitrotyrosine in both sporadic and familial amyotrophic lateral sclerosis. *Ann. Neurol.* (1997) 42: 644-654.
33. Matthews RT, Ferrante RJ, Jenkins BG, **BROWNE SE**, Goetz K, Berger S, Chen IY, Beal MF. Iodoacetate produces striatal excitotoxic lesions. *J. Neurochem.* (1997) 69: 285-289.
34. Schulz JB, Matthews RT, Muqit MMK, **BROWNE SE**, Beal MF. Inhibition of neuronal nitric oxide synthase by 7-nitroindazole protects against MPTP-induced neurotoxicity in mice. *J. Neurochem.* (1995) 64: 936-939.

35. Macrae IM and **BROWNE SE.** Brain structures involved in the hypotensive effects of rilmenidine: evaluation by [^{14}C]2-deoxyglucose autoradiography. *J. Cardiovasc. Pharmacol.* (1995) 26 Suppl 2:S55-58.
36. **BROWNE SE** and Beal MF. Oxidative damage and mitochondrial dysfunction in neurodegenerative diseases. *Biochem. Soc. Trans.* (1994) 22: 1002-1006.
37. **BROWNE SE** and Macrae IM. Differential patterns of local cerebral glucose utilisation associated with rilmenidine- or B-HT 933-induced hypotension. *Brain Res.* (1994) 666: 216-222.
38. **BROWNE SE** and McCulloch J. AMPA receptor antagonists and local cerebral glucose utilization in the rat. *Brain Res.* (1994) 641: 10-20.
39. Fujisawa H, Dawson D, **BROWNE SE**, MacKay KB, Bullock R, McCulloch J. Pharmacological modification of glutamate neurotoxicity *in vivo*. *Brain Res.* (1993) 629: 73-78.
40. **BROWNE SE**, Horsburgh K, Dewar D, McCulloch J. D-[^{3}H]-Aspartate binding does not map glutamate-releasing neurones in the retino-fugal projection: an autoradiographic comparison with [^{3}H]-cyclohexyladenosine binding. *Molec. Neuropharmacol.* (1991) 1: 129-133.
41. Pertwee RG, **BROWNE SE**, Ross TM, Stretton CD. An investigation of the involvement of GABA in certain pharmacological effects of delta-9-tetrahydrocannabinol. *Pharmacol. Biochem. Behav.* (1991) 40: 581-585.

* *Corresponding author*

BOOK CHAPTERS

1. **BROWNE SE.** Huntington's Disease. In: *Manual of Neuropsychiatric Disorders*. F Tarazi and J Schetz, Eds. *Humana Press*. (2005) 63-86.
2. **BROWNE SE**, Beal MF. Toxin Induced Mitochondrial Dysfunction. In: *Mitochondrial Function and Dysfunction*. AHV Schapira, Ed. *Academic Press* (2002) 241-280.
3. **BROWNE SE**, Beal MF. Huntington's disease. In: Functional Neurobiology of Ageing. PR Hof, CV Mobbs, Eds. *Academic Press* (2000) 711-725.
4. **BROWNE SE**. Mitochondrial dysfunction and oxidative damage in Huntington's disease. In: *Neurodegenerative Diseases: Mitochondria and Free Radicals in Pathogenesis*. MF Beal, I Bodis-Wollner, N Howell Eds. *Wiley-Liss Inc.* (1997) 361-374.

ABSTRACTS (Last 2 Years)

1. Choi D-K, Calingasan NY, Chen J, Beal MF, **Browne SE*.** (2005) Epigenetic modulation in Huntington's disease. *Soc. Neurosci. Abs.* 31. *Submitted*
2. McConoughey SJ, Cooper AJL, Krasnikov BF, **Browne SE**, Beal MF, Chavez JC, Ratan RR. (2005) Transcriptional dysregulation of genes involved in adaptation to metabolic stress in Huntington's disease. *Soc. Neurosci. Abs.* 31. *Submitted*
3. Musatov SA, Browne SE, Henning MS, Stavarache MA, Goldfein JA, Kaplitt MG. (2005) Neuroprotective effects of XIAP gene therapy in models of Huntington's disease. *Soc. Neurosci. Abs.* 31. *Submitted*
4. DiMauro J-PP, McConoughey SJ, Burr HN, **Browne SE.** (2005) Mitochondrial and Energetic Dysfunction in Animal Models of Huntington's Disease. *Intl. Soc. Neurochem.* In press.
5. DiMauro J-PP, Yang LY, Fuller SW, **Browne SE.** (2005) Metabolic Abnormalities Precede Pathologic Changes in the G93A SOD1 Mouse Model of ALS. *Brain 05 & Brain/PET 05, J.CBF Metab.* In press.
6. **Browne SE,** Choi D-K, Gardian G, Kubilus J, Ryu H, Ferrante RJ, Beal MF. (2004) Administration of a histone deacetylase inhibitor post-symptom onset improves outcome in a mouse model of Huntington's disease. *Cold Spring Harbor Conference on Drug Discovery in Neurodegenerative Diseases.*
7. **Browne SE,** Choi D-K, Gardian G, Howard V, Schomer A, Strout P, Beal MF. (2004) Beneficial effects of transcriptional modulation by phenylbutyrate in a mouse model of Huntington's disease. *Soc. Neurosci. Abs.* 30: 938.6.

8. **Browne SE** (2004) Huntington's disease pathogenesis – key roles for mitochondria. *J. Neurochem.* 90 (Supp. 1) S13-02.
9. **Browne SE,** Choi D-K, Gardian G, Howard V, Schomer A, Strout P, Beal MF. (2004) Phenylbutyrate Administration Post-Symptom Onset Improves Survival in a Mouse HD Model. *Hereditary Disease Foundation, "HD 2004: Changes, Advances and Good News".* F17.
10. McConoughey SJ, Howard V, **Browne SE.** (2004) Glut1 and Glut3 transporters in Huntingtin mutant mice. *Forum of European Neurosciences 2004,* A020.17.
11. DiMauro J-PP, McConoughey SJ, Burr HN, **Browne SE.** (2004) Cerebral Glucose Utilization Defects precede Pathological Changes in Mouse Models of Huntington's Disease. *Gordon Research Conference: Brain Energy Metabolism and Blood Flow.* (No abstract published).
12. **Browne SE**, DiMauro J-PP, Albrecht RJ, Burr HN. (2003) The evolution of metabolic defects in a knock-in mutant mouse model of Huntingtons disease. *Soc. Neurosci. Abs.* 29: 130.12
13. Saydoff JA, Liu LS, Brenneman D, Garcia RAG, Hu ZY, Cardin S, Gonzalez A, von Borstel RW, Beal MF, **Browne SE.** (2003) Uridine prodrug PN401 is neuroprotective in the R6/2 and N171-82Q mouse models of Huntington's disease. *Soc. Neurosci. Abs.* 29: 130.11
14. Kim S-Y, Marekov L, Bubber P, **Browne S**, Stavrovskaya I, Son JH, Beal MF, Blass JP, Gibson GE, Cooper AJL. (2003) Mitochondrial Aconitase as a Transglutaminase Target: Implication for Mitochondrial Dysfunction in Huntington Brain. *Soc. Neurosci. Abs.* 29: 130.5
15. Choi D, Kim Y, Lorenzl S, Yang L, Sugama S, **Browne SE**, Beal F, Joh T. (2003) Attenuation of MPTP-elicited degeneration of SN DA neurons in MMP-3 null mice. *Soc. Neurosci. Abs.* 29: 409.14
16. Kwong JQ, Begum H, **Browne SE**, Beal MF, Kaplitt MG, Manfredi G. (2003) RNAi-Mediated inhibition of mutated htt in Huntington's disease models. *Soc. Neurosci. Abs.* 29: 208.18
17. Calingasan NY, Klivenyi P, Gardian G, Chen J, **Browne SE**, Beal MF. (2003) Dihydrolipoamide dehydrogenase (DLD) deficiency increases the vulnerability of mouse brain to mitochondrial toxins. *Soc. Neurosci. Abs.* 29: 732.2
18. Burr H, DiMauro J-PP, Gregorio J, **Browne SE.** (2003) [^{14}C]-2-Deoxyglucose *in vivo* autoradiographic studies reveal alterations in cerebral metabolism precede pathologic changes in two mutant mouse models of Huntingtin's disease. *Brain 03 & Brain/PET 03, J.CBF Metab.* 23 (Supp. 1): 585.

INVITED SPEAKER (Last 2 years)

April 15th 2003	American Society for Pharmacology and Experimental Therapeutics, Symposium: Animal Models of Neuropsychiatric Diseases. San Diego, CA, USA. *"Modeling Huntington's Disease in the Mouse: Mechanistic and Therapeutic Insights"*
June 5th 2003	University of Edinburgh, SCOTLAND, UK, Department of Neuroscience Seminar Series. *"The Cerebral Energetics of Huntington's Disease".*
November 17th 2003	Farber Institute for Neuroscience, Research Seminar Thomas Jefferson University Medical College, Philadelphia, PA, USA. *"CNS Energetics and SOD1 in ALS Pathogenesis"*
December 2nd 2003	McLean Hospital, Neuroscience Seminar. Harvard Medical School, Belmont, MA, USA. *"CNS Metabolism and the pathogenesis of ALS."*
March 19th 2004	Mayo Clinic Seminar Series, Mayo Jacksonville, Jacksonville, FL, USA. *"CNS Energy Metabolism and the Pathogenesis of Huntington's Disease".*

August 15th 2004	Hereditary Disease Foundation, "HD 2004: Changes, Advances and Good News" Boston, MA, USA. *"Phenylbutyrate Administration Post-Symptom Onset Improves Survival in a Mouse HD Model"*
August 17th 2004	American Neurochemistry Society, 35th Annual Meeting. Symposium: Role of mitochondria in Neurodegeneration" New York, NY, USA. *"Huntington's disease pathogenesis – key roles for mitochondria."*
December 4th 2004	Cold Spring Harbor Conference on Drug Discovery in Neurodegenerative Diseases. Cold Spring Harbor, NY, USA. *" Administration of a histone deacetylase inhibitor post-symptom onset improves outcome in a mouse model of Huntington's disease."*
June 8th 2005	International Society of Cerebral Blood Flow and Metabolism, Brain 05 & Brain/PET 05 Meeting. Amsterdam, NL. *"Metabolic Abnormalities Precede Pathologic Changes in the G93A SOD1 Mouse Model of ALS."*
August 26th 2005	International Society for Neurochemistry, and European Society for Neurochemistry, 20th Biennial Meeting. Innsbruck, Austria. *"Mitochondrial and Energetic Dysfunction in Animal Models of Huntington's Disease."*

Accepted 1/4/06

APPENDIX 2

Elsevier Editorial System(tm) for Neurobiology of Disease

Manuscript Draft

Manuscript Number:

Title: Bioenergetic abnormalities in discrete cerebral motor pathways presage spinal cord pathology in the G93A SOD1 mouse model of ALS

Article Type: Regular Article

Section/Category:

Keywords: Amyotrophic lateral sclerosis; ATP; brain; cerebral glucose metabolism; corticospinal tract; creatine; 2-deoxyglucose; motor neuron; motor neurone disease; spinal cord.

Corresponding Author: Dr. Susan E Browne, PhD

Corresponding Author's Institution: Weill Medical College of Cornell University

First Author: Susan Browne

Order of Authors: Susan Browne; Lichuan Yang, MD; Jon-Paul P DiMauro, BS; Stephanie E Licata, PhD; M Flint Beal, MD

Manuscript Region of Origin:

Abstract: Multiple cell death pathways are implicated in the etiology of amyotrophic lateral sclerosis (ALS), but the cause of the characteristic motor neuron degeneration remains unknown. To determine whether CNS metabolic defects are critical for ALS pathogenesis, we examined the temporal evolution of energetic defects in the G93A SOD1 mouse model of familial ALS. [14C]-2-deoxyglucose in vivo autoradiography in G93A mice showed that glucose utilization is impaired in components of the corticospinal and bulbospinal motor tracts prior to either pathologic or bioenergetic changes in the spinal cord. This was accompanied by significant depletions in cortical ATP content in presymptomatic mice, which was partially ameliorated by

creatine administration. Findings suggest that bioenergetic defects are involved in the initial stages of mSOD1-induced toxicity in G93A mice, and imply that the selective dysfunction and degeneration of spinal cord motor neurons in this model may be secondary to dysfunction within cerebral motor pathways.

Accepted 1/4/06
Neurobiol. of Dis.
CNS bioenergetic defects in ALS,

Regular Article

Bioenergetic Abnormalities in Discrete Cerebral Motor Pathways Presage Spinal Cord Pathology in the G93A SOD1 Mouse Model of ALS

Susan E Browne[1], Lichuan Yang[1], Jon-Paul DiMauro[1], Stephanie E Berger[2], Sara Fuller[1], M Flint Beal[1].

[1]Department of Neurology and Neuroscience, Weill Medical College of Cornell University, New York, NY USA; [2]Department of Neurology, Massachusetts General Hospital, Boston, MA USA.

Running Title: CNS bioenergetic defects in ALS
Abstract: 148 words
Tables: 5
Figures: 4

Corresponding Author:
Susan E. Browne, Ph.D.
Neurology and Neuroscience,
Weill Medical College of Cornell University,
525 E. 68th Street, A-502,
New York, NY 10021 USA.
sub2001@med.cornell.edu
Tel: (212) 746-4672
Fax: (212) 746-8276

ABSTRACT

Multiple cell death pathways are implicated in the etiology of amyotrophic lateral sclerosis (ALS), but the cause of the characteristic motor neuron degeneration remains unknown. To determine whether CNS metabolic defects are critical for ALS pathogenesis, we examined the temporal evolution of energetic defects in the G93A SOD1 mouse model of familial ALS. [^{14}C]-2-deoxyglucose *in vivo* autoradiography in G93A mice showed that glucose utilization is impaired in components of the corticospinal and bulbospinal motor tracts prior to either pathologic or bioenergetic changes in the spinal cord. This was accompanied by significant depletions in cortical ATP content in presymptomatic mice, which was partially ameliorated by creatine administration. Findings suggest that bioenergetic defects are involved in the initial stages of mSOD1-induced toxicity in G93A mice, and imply that the selective dysfunction and degeneration of spinal cord motor neurons in this model may be secondary to dysfunction within *cerebral* motor pathways.

Key words: Amyotrophic lateral sclerosis; ATP; brain; cerebral glucose metabolism; corticospinal tract; creatine; 2-deoxyglucose; motor neuron; motor neurone disease; spinal cord.

INTRODUCTION

The rapidly progressing phenotype of muscle weakness and wasting, paralysis, and ultimately death in amyotrophic lateral sclerosis (ALS) results from the selective and inexorable loss of CNS motor neurons (Mulder et al., 1986). ALS is distinguished from similar disorders by the involvement of both lower motor neurons in spinal cord and brainstem (innervating skeletal muscle) and of upper motor neurons in cerebral cortex and brainstem constituting the corticospinal and bulbospinal tracts (Tandan and Bradley, 1985). Several different detrimental processes have been identified in the CNS during the disease course in ALS (see Strong, 2003), but the definitive pathogenic mechanism remains unclear. Findings of Cu/Zn superoxide dismutase (SOD1) mutations in 25% of familial ALS (FALS) patients (Ratovitski et al., 1999), and observations that mice expressing mutant SOD1 (mSOD1) recapitulate phenotypic and pathologic features of the disease, suggest that the toxic downstream events induced by mSOD1 may be common to both FALS and sporadic-onset ALS (SALS).

Among the deleterious processes identified in ALS, abnormalities in CNS energy metabolism are well documented. Symptomatic SALS patients display progressive hypometabolism in brain motor regions (Hatezawa et al., 1988). Reports of abnormal structure, number and localization of mitochondria in ALS motor neurons and skeletal muscle led to suggestions of compromised mitochondrial function (Hirano et al. 1984: Sasaki and Iwata, 1996; Siklos et al., 1996), corroborated by findings of altered respiratory chain enzyme activities in ALS spinal cord and motor cortex (Bowling et al., 1993; Fujita et al., 1996; Browne et al.,1998; Borthwick et al., 1999). Mutant mouse models of ALS have subsequently provided evidence that mitochondrial dysfunction may be critically involved in ALS pathogenesis. Morphological changes in mitochondria are the earliest detected pathologic events in mouse lines over-expressing SOD1 with G37R or G93A mutations (Dal-Canto and Gurney, 1995; Wong et al.,1995; Kong and Xu 1998; Sasaki et al., 2004). In G93A mice, decreased mitochondrial respiration and abnormal enzyme activities have been reported (Browne et al.,1998; Kirkinezos et al., 2005), and agents that enhance energy metabolism extend life-span and delay

symptom onset (Matthews et al., 1998; Klivenyi et al., 1999). In addition, studies of mitochondrial toxins in preparations of mixed cells from spinal cord suggest that motor neurons are especially vulnerable to metabolic compromise (Kaal et al., 2000; Van Westerlaak et al, 2001). There is also evidence that mSOD1, recently shown to enter mitochondria (Higgins et al., 2002; Mattiazzi et al., 2002; Liu et al., 2004; Vijayvergiya et al., 2005), can alter mitochondrial function. Expression of human G37R or G93A mSOD1 in a motor neuron cell line induced morphological abnormalities in mitochondria, reduced mitochondrial complex II and IV activities, and increased cell vulnerability to oxidative stress (Menzies et al., 2002).

Despite these numerous reports, it remains unclear whether energy defects underlie neuronal death in ALS. To address whether mSOD1-induced metabolic defects are key factors in cell death processes, we used *in vivo* imaging procedures to map functional alterations in CNS glucose metabolism throughout the brain and spinal cord of the G93A mouse model of FALS, at pre- and post-symptomatic ages. We found that CNS glucose metabolism is defective before the first pathological signs of motor neuron disease occur in G93A mice, and that impairments occur primarily in discrete brain motor regions contributing to corticospinal projections. Decreased glucose utilization in the cerebral motor cortex was accompanied by marked reductions in ATP generation. Glucose utilization in the spinal cord, in contrast, was unaltered at this age, but becomes impaired as mice age. Results suggest that metabolic defects may be principal components of the neurotoxic mechanism in ALS, and provide insight into the temporal involvement of upper and lower motor neurons in this FALS model.

MATERIALS AND METHODS

Animals.

G93A transgenic mice over-expressing human mutant SOD1 ($G93A^{G1H/B6SJLF1}$) and N1029 mice over-expressing human wild type SOD1 (Gurney et al., 1994) were obtained from Jackson Laboratories (Bar Harbor, ME). Lines were maintained by crossing into the B6SJLF1 mice (Jackson Laboratories, Bar Harbor, ME). Non-transgenic wild type littermates served as controls. Mice were housed at room temperature in a 12h light/dark cycle with free access to food and water. All procedures were reviewed and approved by Institutional Animal Care and Use Committees (Massachusetts General Hospital and Weill Medical College) prior to experiment commencement.

In Vivo Measurement of CNS Glucose Utilization Rates.

Fully quantitative [^{14}C]-2-deoxyglucose (2-DG) *in vivo* autoradiography was carried out according to Sokoloff's method (Sokoloff et al., 1977) modified for use in mice (Browne et al., 1999). Briefly, mice were anesthetized with 2.0% isoflurane in O_2, and PE10 polyethylene cannulae inserted into one femoral artery and one femoral vein. Cannulae were fed under the skin to extrude at the nape of the neck. Animals recovered from anesthesia for 2-3h and were allowed free movement throughout the experimental period. The 2-DG procedure was initiated by intravenous injection of 4μCi [^{14}C]-2-deoxy-D-glucose (56.0 mCi/mmol; NEN, Boston MA) in 50μl heparinized saline over 30 sec, followed by a 50μl saline bolus to clear the cannula. Over the subsequent 45min, ten timed arterial blood samples were collected for analysis of blood glucose (Glucose 2 Analyzer, Beckman Coulter, USA) and ^{14}C levels (Liquid Scintillation Counter, Beckman Coulter, USA). Arterial blood gases pCO_2, pO_2 and pH were measured in 80μl of blood withdrawn 44min into the procedure (IL 1725 Blood Gas Analyzer, Instrumentation Laboratory, Lexington, MA). 45min after isotope administration animals were decapitated, their brains and spinal cords removed and rapidly frozen in isopentane at -43°C. Brains and spinal cords were cut into 20μm-thick coronal cryostat sections and triplicate serial sections

collected onto heated coverslips at 140μm intervals. Sections were exposed to ^{14}C-sensitive film (Kodak Biomax MR-1) along with precalibrated ^{14}C standards (Amersham) for 4-6 days. Local tissue isotope concentrations in 58 areas of interest were measured from the resultant autoradiograms by computer-assisted densitometry (MCID 5 Image Analysis System, Imaging Research, Ontario, Canada). Optical densities were measured in discrete structures in three to six serial sections per structure. Mean local rates of glucose use ($lCMR_{glc}$) were then calculated using Sokoloff's operational equation for the procedure employing the lumped constant for the rat (Sokoloff et al., 1977), in the absence of calculated rate constants for mouse CNS. Anatomical regions were localized using the atlas of Paxinos and Franklin (2001).

HPLC Determination of Bioenergetic Markers.

Tissue Preparation: Creatine (Cr), adenosine monophosphate (AMP), adenosine diphosphate (ADP), and adenosine triphosphate (ATP) levels were measured by HPLC using a modification of published procedures (Bernocchi et al., 1994). Metabolites were measured in brain and spinal cord from G93A transgenic mice and age-matched littermate controls at 30, 60, 90 and 120 days of age; in 120 day old G93A and wildtype mice treated from 90 days with creatine (2% in diet; Purina Mills, Richmond, IN); and in N1029 transgenic mice overexpressing human wildtype SOD1 at 180 days of age (n = 5 or 10 per group, per time point). Mice were sacrificed by decapitation into liquid nitrogen. Brain and spinal cord were later removed on a frozen cold plate (-20°C), and the rostral (frontal) area of cerebral cortex, and the cerebellum, were dissected out. Brain and spinal cord samples were then stored at -80°C.

HPLC Protocol: The apparatus consisted of a gradient HPLC pump (Perkin-Elmer, Norwalk, CT), a 490 multiple UV wavelength detector (Waters Associates, Milford, MA) with a WISP 712 autosampler, and a Shimadzu 501 integrator (Shimadzu Scientific Instruments Inc., Columbia, MD). Frozen motor cortex, cerebellum and spinal cord tissue was dissected on a freezing cold plate (-2O°C) and homogenized in 0.4 M perchloric acid (10 ml per mg wet weight). The homogenate was centrifuged

and 200µl of the supernatant neutralized with 10 µl of 4M K_2CO_3 and re-centrifuged. The resultant supernatant was then stored at -80°C until injected. Standards of creatine, AMP, ADP, and ATP were prepared in 0.4 M perchloric acid at concentrations of 10 mM for creatine, cyclocreatine, and PCr, and 5 mM for AMP, ADP, and ATP (based on tissue concentrations), and then neutralized by the same procedure. Samples were separated on a 15 cm x 3 µm C18 Nikko Bioscience HPLC column (ESA, Inc., Chelmsford, MA) at a flow rate of 1 ml/min, using a gradient consisting of buffers A (25 mM Na_2HPO_4,100 mg/L tetrabutylammonium (TBA), pH 5.5) and B (200 mM NaH_2PO_4, 100 mg/L TBA, 10% acetonitrile, pH 4.0). Gradient conditions were 100% buffer A for minutes 0-5, 100% buffer A transitioning to 100% buffer B over minutes 5-20, and 100% buffer B from minute 20 to 31. Samples were monitored at 214 nm over 0-9 min, and at 260 nm over 9-31 min. The retention times were (in min): creatine, 1.8; AMP, 19.5; ADP, 21.7; and ATP, 23.8. All standards were linear over a 100-fold concentration range. Reagents were obtained from Sigma Aldrich (St. Louis, MO).

Statistical Analysis.

2-DG: Systemic physiological variables, and local rates of cerebral glucose use ($lCMR_{glc}$) in brain and spinal cord regions, in G93A, N1029, and wild-type littermate mice are presented as mean ± SEM. Statistical comparisons between G93A mice and littermates, or N1029 mice and littermate controls, were made by Student's unpaired t-test. Arterial plasma glucose concentrations before (-pre) and at the end of the experiment (+45min) within animals were compared using Student's paired t-test.

HPLC: Tissue ATP, ADP, AMP and creatine levels in G93A mice, littermates and N1029 mice are presented as mean ± SEM. Statistical comparisons between SOD1 mice and littermates were made by one-way ANOVA followed by the Tukey-Kramer multiple comparisons test (InStat; GraphPad, San Diego, CA, U.S.A.)

RESULTS

Glucose Utilization in G93A FALS Mice

Rates of glucose utilization were measured in multiple discrete regions throughout the brains and spinal cords of conscious, freely moving $G93A^{G1H}$ SOD1 mice at ages preceding pathological changes (60 days) and at end-stage of the disorder (120 days), in age-matched wildtype littermate mice, and in aged transgenic wildtypes (N1029 mice over-expressing human wildtype SOD1, 21 months). Assays used the fully quantitative *in vivo* [^{14}C]-2-deoxyglucose (2-DG) technique of Sokoloff et al. (1977) adapted for the mouse (Browne et al., 1999).

Physiological Variables

Arterial plasma glucose concentrations were measured before and during the 2-DG procedure, and blood gases (pCO_2, pO_2, and calculated pH) were assayed immediately prior to sacrifice, to determine if any experimental groups displayed physiologic abnormalities that might impact on glucose utilization (Table 1). Slight alterations in initial plasma glucose levels in G93A (60 day) and N1029 mice, and pH levels in 120 day old G93A mice, relative to age-matched wildtypes, were detected (Student's unpaired t-test, $p<0.05$). Levels, however, remained well within normal physiological limits for mice, and therefore are unlikely to impact on glucose use rates. No other statistically significant differences were detected. Arterial plasma glucose levels did not alter over the course of the experiments (Student's paired t-test, $p>0.05$), indicating that mice were not abnormally stressed by the experimental procedure.

Local Rates of Glucose Use in G93A Brain

Local cerebral metabolic rates for glucose ($lCMR_{glc}$) were measured in 49 brain regions in transgenic G93A mice (n=6 per group) and age-matched littermate controls (n=8-9 per group). Results are presented in Table 2. Glucose utilization rates were found to be impaired in multiple brain components of the motor system as early as 60 days of age in G93A mice (the earliest time-point examined).

Motor regions of cerebral cortex: Significant glucose use reductions (-19%) were evident in primary motor cortex at 60 days (Table 2, Figure 1). Hypometabolism was evident in both cortical innervation sites (layers I-III) and in efferent projection zones (layer V) in Fr1 motor cortex (anatomical classification according to Zilles and Wree, 1995). In contrast, sensorimotor cortical regions, including the hindlimb region, showed no significant glucose use alterations over the life-span of the G93A mice. Sensorimotor cortical regions process overlapping motor and sensory inputs, and send projections both to other motor cortical regions and to the spinal cord via the corticospinal tract (Zilles and Wree , 1995; Gu et al., 1999). Within this complex motor circuitry, however, the present results suggest that activity in the spinal cord in G93A mice may be influenced by impaired functional activity in projections from the primary motor cortex and its collaterals, rather than by somatosensory efferents.

Motor cortex efferent projections: The principal projection targets of the primary motor cortex comprise the spinal cord via the corticospinal tract, the striatum, reciprocal connections with other cerebral cortical regions including sensorimotor cortex, and projections to the brainstem pontine nuclei, red nucleus and cranial motor nuclei via collaterals from the corticospinal tract. We found that a pattern of hypometabolism emerged in several of these areas synaptically associated with the primary motor cortex (Figure 2, Table 2), which differed between regions in age of onset. At 60 days, marked reductions in glucose use in G93A mice were evident in the pontine nuclei (-25%) and the pontine reticular formation (-17%), which contribute to the bulbospinal pathway innervating axial and proximal musculature. Within the rubrospinal pathway, involved in modulating movement in the distal limbs, a trend towards reduced glucose use was apparent in the red nucleus at 60 days, and was statistically significant at 120 days of age.

Thalamic relay nuclei: As noted above, significant reductions in glucose use were evident in G93A motor cortex input layers (I-III), as well as projection zones (layer V) at 60 days of age. It is therefore of great interest that glucose use was decreased in multiple thalamic nuclei at this age (Table 2, Figures 1 and 2). The motor system is extremely complex, and Fr1 of primary motor cortex receives afferent innervation from multiple other cortical and sub-cortical regions. Key components of this innervation are thalamic nuclei, in particular ventrolateral (VL) and ventromedial (VM) nuclei (Cicirata et al., 1986; Zilles and Wree, 1995). We found early reductions in glucose use in the rostral VL thalamus which projects to caudal primary motor cortex (hindlimb modulation), in both dorsal and ventral aspects (projecting to proximal and distal hindlimb areas of motor cortex, respectively) (Cicirata et al., 1986). The caudal VL thalamus (projecting to rostral, forelimb, motor cortex) shows early trends to reduced glucose use, significantly decreased by 120 days. Ventromedial and ventroposterior-medial thalamic nuclei also show impaired glucose metabolism at 60 days of age. However, interpretation of these glucose use changes to determine the principal site of functional impairments in the motor cortex is complicated by the fact that there are many reciprocal projections between thalamus and motor cortex. In particular, the ventrolateral thalamus is innervated by both direct and indirect (via the reticular thalamic nuclei complex) projections arising from Fr1 of primary motor cortex (Figure 2) (Cicirata et al., 1990). In addition, reciprocal connections exist between sensorimotor cortex and thalamic nuclei (Killackey and Sherman, 2003; Tracey and Waite, 1995).

Other brain regions; recruitment with increasing age: In pre-symptomatic (60 day-old) G93A mice, glucose use changes were largely restricted to regions involved in motor control. Glucose utilization was unaltered in 36 of the 49 brain regions examined, including non-motor control regions. As G93A mice aged, the magnitude of existing cerebral glucose use reductions were exacerbated (Table 2). By 120 days of age reduced glucose uptake was also evident in multiple other forebrain regions, including cingulate, auditory and visual cortices, dorsolateral geniculate body, mammillary body, sub-thalamic

nucleus, superior colliculus, and some cerebellar regions. Other motor projection targets including the striatum showed trends towards reduced glucose use that did not reach statistical significance.

It should also be noted that wildtype mice showed a trend towards lower glucose use rates as mouse age increased, in multiple brain regions (Table 2). Since glucose use rates were assayed in 60 day-old mice (randomized G93A mice and age-matched wildtype littermates) and in 120 day-old mice in separate experiments, at different times, the effects of age on wildtype (G93A littermate) mouse glucose use rates cannot be statistically compared in this study. It is therefore unclear whether this age-effect on wildtype rates is artifactual. However, despite this caveat, the magnitude of the difference in rates between G93A and wildtypes is generally exacerbated in the majority of affected brain regions in older (120 day) mice.

Temporal pattern of glucose use changes in spinal cord.

Local cerebral metabolic rates for glucose ($lCMR_{glc}$) were also measured in 9 spinal cord regions in the G93A mice and age-matched littermate controls (Table 3). In contrast to findings in cerebral motor cortex projection zones, no alterations in glucose use were detected in cervical, thoracic or lumbar regions of the spinal cord in 60 day-old G93A mice (Table 3, Figure 3). This observation suggests that despite abnormalities in projection pathways arising from motor control brain regions at 60 days, functional activity in corticospinal projection zones is maintained at normal levels. By end-stage of the disorder (120 days), glucose use was significantly reduced in the gray matter of all three spinal cord regions in the transgenic mutant mice, relative to levels in non-transgenic wildtype controls (Table 3, Figure 3). The extremely low glucose use levels in G93A spinal cord at this time point likely reflect loss of corticospinal innervation of motor neurons, and low motor neuron density in the spinal cord at end-stage (Zang and Cheema, 2002).

In summary, the pattern of alterations in glucose use rates in 60 day old G93A mice suggest that functional impairments occur primarily in cerebral motor regions in this model, largely in primary motor cortex and its collaterals, preceding functional dysregulation in corticospinal projection targets. In particular, components of the bulbospinal projection pathway are compromised by 60 days of age, whereas rubrospinal projections become significantly involved later in the disorder, suggesting that axial and proximal components of motor regulation may be affected early in the disease process in this FALS model.

Overexpression of human wildtype SOD1 (N1029 mice) had no effect on CNS glucose use rates

It has been reported that overexpression of purely wildtype human SOD1 in N1029 mice eventually induces a motor degeneration phenotype (Jaarsma et al., 2000). We measured energy parameters in these mice at a mature age (21 months), since this advanced age greatly exceeds that at which glucose use changes were detected in G93A mice (2 months), and is therefore deemed likely to reveal any SOD1-related glucose use changes. Mice did not exhibit any overt signs of motor defects. No significant differences in glucose use values between 21 month-old N1029 and age-matched wildtype littermate mice were detected in any of the five representative brain regions (including primary motor cortex) or the 9 spinal cord regions examined (Table 4). These observations suggest that the glucose use changes detected in G93A mice result from expression of the G93A SOD1 mutation, rather than increased SOD1 activity due to the transgene overexpression.

ATP generation is impaired in G93A mouse CNS at 30 days of age.

Following our observations of decreased cerebral glucose use rates in 60 day-old G93A mice, we examined whether glucose uptake reductions were reflected by alterations in the generation of ATP and other high energy metabolites. Findings suggest that metabolic defects and glucose use changes may be functionally linked in this FALS model.

Basal levels of the energy metabolites ATP, ADP, AMP and creatine were determined in flash-frozen rostral cerebral cortex, cerebellum, and spinal cord from G93A and littermate wildtype mice at 30, 60, 90 and 120 days of age (Table 5). Basal ATP levels in cerebral cortex were 42% lower in G93A mice than in age-matched controls in 30 day-old animals ($p < 0.01$). The extent of impairment in ATP production progressed with age, and was 71% lower than levels in age-matched controls by 120 days of age (Figure 4). ADP levels were also significantly reduced in G93A cortex at 60 days of age, although to a lesser extent than ATP, with a maximum observed reduction of 48% by 120 days. Creatine levels were normal in 30 day old G93A mice, but were depleted maximally in both cerebral cortex and spinal cord by 90 days (by 44% and 47%, respectively). Reductions in ADP and ATP levels in G93A spinal cord were apparent at 60 days of age (the youngest age examined for this region), but alterations were not statistically significant. ATP depletions in spinal cord did, however, show a marked attenuation following 30 days treatment with 2% creatine. AMP levels did not alter over time in any region. No metabolite changes were detected in the cerebellum. Metabolite levels in aged (180 day) N1029 mice overexpressing normal human SOD1 did not significantly differ from levels in wild-type littermate mice, suggesting that metabolite depletion is caused by the SOD1 mutation, as oppose to SOD1 overexpression. ATP, ADP and creatine levels in the cerebral cortex of these mice were significantly higher than in 120 day old G93A mice, whereas no significant changes were found when compared with the 120 day old G93A-littermate wildtype mice.

Creatine rescues ATP depletion.

We have previously reported beneficial effects of creatine treatment in the G93A mouse model of FALS (Klivenyi et al., 1999). Creatine's protective effects purportedly arise from enhancing access to energy stores within cells (Tarnopolsky and Beal, 2001). We examined the effects of creatine administration, from the time of symptom onset, on levels of ATP and other metablites. Treatment of mice with 2% creatine in the diet from 90 days of age markedly attenuated the declines in cerebral

cortical levels of both ATP and ADP seen in G93A mice, increasing concentrations to 72.5% and 75% of wild-type control levels, respectively, at 120 days (Table 5, Figure 4). This was associated with a complete restoration of creatine levels in the spinal cord, and partially restored levels in cerebral cortex by 120 days.

DISCUSSION

Mitochondrial and energetic defects are implicated in the pathogenesis of motor neuron degeneration in ALS, but their precise contribution to the disease mechanism is unclear. Here we demonstrate that expression of the G93A SOD1 mutation induces energy dysfunction in discrete CNS motor regions long before motor neuron degeneration occurs. The marked reduction in cerebral cortex ATP levels detected in 30 day-old G93A mice, well before pathology and symptom onset, represents the earliest deleterious event reported to date in this ALS model. Not only do these studies strongly support the hypothesis that metabolic dysfunction in the CNS plays a critical early role in mSOD1's mechanism of toxicity, but most importantly the glucose utilization studies provide novel neuroanatomic information about the evolution of functional deficits in CNS motor regions. Specifically, we have demonstrated that widespread mSOD1 expression in mice results in impaired functional neuronal activity discretely in CNS motor circuitry. Glucose use impairments were detected first in *brain* motor pathways, including components of the corticospinal tract, while deficits in the spinal cord occurred later. It is therefore postulated that the ultimately damaging events that lead to spinal cord motor neuron dysfunction and degeneration in ALS may result from impaired transynaptic activation in corticospinal projections.

$G93A^{G1H}$ mSOD1 mice were used in this study because they develop a disease syndrome closely resembling ALS neuropathology and symptoms, including hind-limb weakness and tremor at 80-90 days of age, paralysis between 105-115 days, and premature death at 120-150 days (Gurney et al.,

1994; Dal-Canto and Gurney, 1995; Kong and Xu, 1998). The earliest pathologic changes in these animals are swelling and vacuolization of spinal cord motor neuron mitochondria at approximately 70 days of age (Dal-Canto and Gurney, 1995; Higgins et al., 2003). We found that CNS glucose use rates, measured in conscious and freely moving animals, were impaired in several forebrain motor regions of G93A mice prior to both symptom and pathology onset (60 days). Primary motor cortex, brainstem components of the bulbospinal tract, and thalamic nuclei involved in the regulation of motor control were principally affected, while glucose use was unaltered throughout the spinal cord at this age. By 120 days, when the mice were grossly phenotypic, paralyzed and approaching death, glucose use impairments were exacerbated and hypometabolism more widespread, affecting other motor tracts including the rubrospinal pathway, cervical, thoracic and lumbar spinal cord, and non-motor areas. These spinal cord deficits likely reflect the motor neuron loss prevalent at end-stage and concomitant reductions in presynaptic activity.

Under normal physiologic conditions, alterations in rates of glucose uptake into CNS tissue is driven by, and therefore reflects, rates of functional activity within neurons (Sokoloff et al., 1977). Glucose use correlates principally with changes in activity at neuron terminals since these are the primary sites of energy consumption (largely maintaining ionic gradients at the membrane), and hence mitochondrial localization (Ames, 2003). The pre-symptomatic glucose use reductions in G93A mice indicate decreased synaptic activity in the primary motor cortex and associated thalamic and pontine nuclei. In the context of a chronic neurodegenerative disorder, possible causes include the disruption of neurotransmitter pathways innervating these regions, synaptic dysfunction or loss, or effects on glucose transport. In tandem studies we found simultaneous region-specific ATP depletions that exceeded glucose deficits in magnitude (in 30 day-old G93A mouse cerebral cortex ATP is decreased by 43% versus a 19% maximal suppression of glucose use). It is currently unclear whether the detected functional impairment is secondary to metabolic changes, or *vice versa.*

A number of potential scenarios exist. One possibility is that ATP generation is impaired, perhaps as a result of defects in the mitochondrial respiratory chain, leading to reduced activity of ATP-dependent cellular processes, which may eventually translate into a reduced demand for glucose. Whilst there are several reports of respiratory chain enzyme defects in cell lines and yeast expressing mSOD1 (Menzies et al., 2002; Gunther et al., 2004), in G93A mouse CNS measurable defects have thus far only been detected in older mice (Browne et al.,1998; Jung et al., 2002; Mattiazi et al., 2002; Kirkinezos et al., 2005). However, Kirkinezos et al (2005) recently reported reduced respiration of CNS mitochondria from 30-56 day-old G93A mice, under certain substrate conditions, linked with a cytochrome c defect. A detectable complex IV deficiency was not, however, evident until mice were symptomatic. In addition, we previously reported a slight reduction in complex IV activity in brainstem and spinal cord tissue as early as 60 days in G93A mice, although its activity was unaltered in cerebral cortex mitochondria at this age (Browne et al., 1998). It is also plausible that mSOD1 may directly interfere with glucose consumption mechanisms, resulting in less ATP availability and concomitant reduced neuronal activity. Alternatively, it is possible that the G93A SOD1 mutation may induce an uncoupling of ATP generation from glucose uptake. These possibilities have yet to be investigated.

In the scenario that impaired energy metabolism underlies neuronal dysfunction and degeneration, increasing ATP generation may be beneficial. We previously found that creatine administration delayed symptom onset, extended lifespan, and reduced neuronal loss, oxidative damage and cerebrospinal fluid (CSF) glutamate levels in G93A mice (Klivenyi et al., 1999; Andreassen et al., 2001). In this study we found that creatine supplementation in the diet was associated with a partial restoration of the diminished ATP and ADP levels found in G93A cerebral cortex and spinal cord. This effect was significant even though metabolite levels were markedly reduced (>50% reductions in ATP in frontal cerebral cortex) when creatine administration commenced at 90 days of age. It appears that creatine's protective effects are most likely due to improved energy metabolism, since we have previously demonstrated that creatine's beneficial effect in G93A mice is independent of a direct effect on the

mitochondrial creatine kinase (mitoCK, a component of the mitochondrial permeability transition located in the intermembrane space of mitochondria, IMM) (Wendt et al., 2002), and that it is neuroprotective in mice lacking mitoCK (Klivenyi et al., 2004). Creatine is phosphorylated to PCr in the IMM, and is then transported into the cytosol (Walliman et al., 1998). There, the energy pool can be regenerated by transphosphorylation of PCr to ATP, which is catalyzed by cytosolic CK (B-CK in brain) located in close vicinity of cellular ATPases (Wendt et al., 2002). The present data support the hypothesis that increased cellular levels of creatine, following dietary supplementation, can enhance ATP regeneration via elevated PCr levels, and thus improve the cellular energy status of CNS cells.

The exact mechanism whereby mSOD1 expression inhibits neuronal functional activity has yet to be determined. One possibility is that a direct interaction between mSOD1 and mitochondria has detrimental effects on ATP generation. This hypothesis is supported by findings that mSOD1 can penetrate mitochondria (Higgins et al., 2002; Mattiazzi et al, 2002; Liu et al., 2004; Vijayvergiya et al., 2005), and is associated with mitochondrial dysfunction (Carri et al.,1997; Jaarsma et al., 2001; Takeuchi et al., 2002). In addition, the majority of studies in G93A mice cite mitochondrial abnormalities as the earliest pathological changes evident at ~70 days (Dal-Canto and Gurney, 1995; Higgins et al., 2003; Sasaki et al., 2004). Neurodegeneration occurs primarily in spinal cord motor neurons (~90 days), although brain motor regions show cell loss at later stages (Dal-Canto and Gurney, 1995). One recent study, however, reports subtle neuronal loss (~10%) in the corticospinal, bulbospinal and rubrospinal tracts of G93A mice at 60 days of age (Zang and Cheema, 2002). This degree of cell body loss is unlikely to explain the ~20% reductions in energy demand we detected in primary motor cortex, but may contribute to reduced synaptic activity in affected pathways. Overall, these observations highlight the fact that pathologic events in this FALS model are not restricted to the spinal cord, and that cerebral motor neurons are involved relatively early in the disease process.

How then do our novel findings of early upper motor neuron dysfunction correlate with the traditional view of ascending motor neuron loss in ALS, and in the G93A model? Lower motor

neurons degenerate in G93A mice. The present results suggest that this neuronal selectivity may result from reduced activity in transynaptic pathways innervating spinal cord motor neurons, coupled with an increased vulnerability of this neuronal population to metabolic impairments (Menzies et al., 2002). Our observations that mSOD1 induces early metabolic defects outside the spinal cord are in accord with increasing evidence that mSOD1's toxic trigger does not occur in spinal cord motor neurons. Neuronal expression of mSOD1 alone is insufficient to induce motor neuron degeneration (Lino et al., 2002). Furthermore, mSOD1s effects are not restricted to motor neurons, including widespread aggregate deposition and Na,K-ATPase deficits throughout the CNS (Ellis et al., 2003; Strong and Rosenfeld, 2003). It appears that mSOD1 expression in other cell types may initiate widespread metabolic impairments in multiple motor CNS regions to which motor neurons are innately sensitive. Coupled with characteristics peculiar to spinal cord motor neurons, including their length and consequent high energy demand and dependence on efficient axonal transport mechanisms, metabolic defects may increase the susceptibility of motor neurons to excitotoxic damage in ALS.

While the prevailing view is that motor neuron loss in ALS involves retrograde degeneration, an alternative hypothesis is that an anterograde ("dying-forward") transneuronal degeneration occurs in ALS (Eisen and Weber, 2001). Support for this proposal is currently somewhat limited, but includes observations of corticospinal degeneration in patients (Ellis et al., 2001). Further, a report that the initial degeneration in G93A mice involves upper motor neurons (Zang and Cheema, 2002), may be consistent with the present study's observations of early functional impairment in components of the forebrain motor system.

A number of detrimental cellular events are set in motion during ALS pathogenesis. Evidence supports the eventual involvement of apoptotic cascades, inflammatory responses, impaired neurofilament function and axonal trafficking, aberrant protein processing, oxidative damage and excitotoxicity (Julien, 2001; Strong and Rosenfeld, 2003). Energetic defects can induce or exacerbate several of the toxic pathways listed above and thus could provide a unifying link between multiple

detrimental cascades. The most compelling hypothesis for pathogenesis following metabolic defects is secondary excitotoxicity, induced by decreased ATP production. Subsequent impairment of membrane Na,K-ATPases may be sufficient to allow membrane depolarization and render neurons vulnerable to extracellular glutamate (Albin and Greenamyre, 1992). It has been proposed that glutamate excitotoxicity in ALS spinal cord is exacerbated by elevated CSF glutamate levels and alterations in EAAT2 glutamate transporters (Alexander et al., 2000; Howland et al., 2002; Spreux-Varoquax et al., 2002), and the glutamate release inhibitor riluzole affords partial protection in both ALS patients and animal models (Bensimon et al., 2002). Motor neurons are also extremely sensitive to damage by glutamate and mitochondrial toxins (Kaal et al., 2000; Rothstein et al., 1993). Our findings of motor region-specific reductions in glucose uptake and ATP production in G93A mice support the possibility that motor neurons are under metabolic stress that increases their susceptibility to glutamate injury. Furthermore, a recent study demonstrated that G93A mice have an underlying Na,K-ATPase defect (Ellis et al., 2003). Energetic compromise in motor neurons in combination with existing Na,K-ATPase defects may be sufficient to exceed thresholds for cell damage.

In conclusion, these studies provide novel evidence that bioenergetic defects are extremely early consequences of mSOD1 expression *in vivo*, and therefore may be key components of the neurodegenerative mechanism induced by mSOD1 in FALS. However, many different SOD1 mutations occur within the FALS populations, in addition to the fact that FALS patients represent only a small fraction of the ALS population. It is therefore possible that the energetic abnormalities detected here are not universal in FALS, but are restricted to the G93A SOD1 mutation. To determine whether these findings are relevant in the broader context of FALS pathogenesis, we have therefore conducted pilot experiments to determine CNS glucose use rates in G85R mSOD1 mice. This mouse line was chosen because the animals express a different SOD1 mutation that is associated with a similar ALS-like phenotype, but lacking overt mitochondrial pathology. Preliminary results show decreased glucose

use in brain and spinal cord of symptomatic G85R mice (data not shown), suggesting that bioenergetic defects may be common to mSOD1-associated pathogenesis.

The findings of impaired glucose utilization in transynaptic corticospinal motor pathways provide, to our knowledge, the first demonstration of a functional correlate for CNS metabolic impairments in ALS mouse models. Results also imply that mSOD1 toxicity initially induces functional changes in discrete motor processing regions in G93A mouse brain, presaging events in spinal cord execution centers. These observations suggest that the selective vulnerability of spinal cord motor neurons in mouse models of FALS may be influenced by impaired functional activity in corticospinal motor afferents.

REFERENCES

Albin RL and Greenamyre JT. 1992. Alternative excitotoxic hypotheses. Neurology 42, 733-738.

Alexander GM, Deitch JS, Seeburger JL, Del Valle L, Heiman-Patterson TD. 2000. Elevated cortical extracellular fluid glutamate in transgenic mice expressing human mutant (G93A) Cu/Zn superoxide dismutase. J Neurochem 74 1666-1673.

Ames A 3rd. 2000. CNS energy metabolism as related to function. Brain Res. Rev. 34,42-68.

Andreassen OA, Jenkins BG, Dedeoglu A, Ferrante KL, Bogdanov MB, Kaddurah-Daouk R, Beal MF. 2001. Increases in cortical glutamate concentrations in transgenic amyotrophic lateral sclerosis mice are attenuated by creatine supplementation. J. Neurochem. 77, 383-390.

Bensimon G, Lacomblez L, Delumeau JC, Bejuit R, Truffinet P, Meininger V; Riluzole/ALS Study Group II. 2002. A study of riluzole in the treatment of advanced stage or elderly patients with amyotrophic lateral sclerosis. J. Neurol. 249, 609-615.

Bernocchi P, Ceconi C, Cargnoni A, Pedersini P, Curello S, Ferrari R. 1994. Extraction and assay of creatine phosphate, purine, and pyridine nucleotides in cardiac tissue by reversed-phase high-performance liquid chromatograph. Anal. Biochem. 222, 374-379.

Bezzi P, Domercq M, Brambilla L, Galli R, Schols D, De Clercq E, Vescovi A, Bagetta G, Kollias G, Meldolesi J, Volterra A. 2001. CXCR4-activated astrocyte glutamate release via TNFalpha: amplification by microglia triggers neurotoxicity. Nat. Neurosci. 4, 702-710.

Borthwick GM, Johnson MA, Ince PG, Shaw PJ, Turnbull DM. 1999. Mitochondrial enzyme activity in amyotrophic lateral sclerosis: implications for the role of mitochondria in neuronal cell death. Ann. Neurol. 46, 787-790.

Bowling AC, Schulz JB, Brown RH, Beal MF. 1993. Superoxide dismutase activity, oxidative damage, and mitochondrial energy metabolism in familial and sporadic amyotrophic lateral sclerosis. J. Neurochem. 61, 2322-2325.

Browne SE, Ayata C, Huang PL, Moskowitz MA, Beal MF. 1999. The cerebral metabolic consequences of nitric oxide synthase (NOS) deficiency: Glucose utilization in neuronal and endothelial NOS null mice. J. Cereb. Blood Flow Metab. 19, 144-148.

Browne SE, Bowling AC, Baik MJ, Gurney M, Brown RH Jr, Beal MF. 1998. Metabolic dysfunction in familial, but not sporadic, amyotrophic lateral sclerosis. J. Neurochem 71, 281-287.

Carri MT, Ferri A, Battistoni A, Famhy L, Gabbianelli R, Poccia F, Rotilio G. 1997. Expression of a Cu,Zn superoxide dismutase typical of familial amyotrophic lateral sclerosis induces mitochondrial alteration and increase of cytosolic $Ca2^{+}$ concentration in transfected neuroblastoma SH-SY5Y cells. FEBS Lett. 414, 365-368.

Cicirata F, Angaut P, Cioni M, Serapide MF, Papale A. 1986. Functional organization of thalamic projections to the motor cortex. An anatomical and electrophysiological study in the rat. Neuroscience 19, 81-99.

Cicirata F, Angaut P, Serapide MF, Panto MR. 1990. Functional organization of the direct and indirect projection via the reticularis thalami nuclear complex from the motor cortex to the thalamic nucleus ventralis lateralis. Exp. Brain Res. 79,325-337.

Cleveland DW, Rothstein JD. 2001. From Charcot to Lou Gehrig: deciphering selective motor neuron death in ALS. Nat. Rev. Neurosci. 11, 806-819.

Dal Canto MC, Gurney ME. 1995. Neuropathological changes in two lines of mice carrying a transgene for mutant human Cu, Zn SOD, and in mice overexpressing wild type SOD: a model of familial amyotrophic lateral sclerosis (FALS). Brain Res. 676, 25-40.

Eisen A, Weber M. 2001. The motor cortex and amyotrophic lateral sclerosis. Muscle 24, 564-573.

Ellis CM, Suckling J, Amaro E Jr, Bullmore ET, Simmons A, Williams SC, Leigh PN. 2001. Volumetric analysis reveals corticospinal degeneration and extramotor involvement in ALS. Neurology 9, 1571-1578.

Ellis DZ, Rabe J. Sweadner KJ. 2003. Global loss of Na,K-ATPase and its nitric oxide-mediated regulation in a transgenic mouse model of amyotrophic lateral sclerosis. J. Neurosci. 23, 43-51.

Fujita K, Yamauchi M, Shibayama K, Ando M, Honda M, Nagata Y. 1996. Decreased cytochrome c oxidase activity but unchanged superoxide dismutase and glutathione peroxidase activities in the spinal cords of patients with amyotrophic lateral sclerosis. J. Neurosci. Res. 45, 276-281.

Gu X, Staines WA Fortier PA. 1999. Quantitative analyses of neurons projecting to primary motor cortex zones controlling limb movements in the rat. Brain Res. 835, 175-187.

Gunther MR, Vangilder R, Fang J, Beattie DS. 2004. Expression of a familial amyotrophic lateral sclerosis-associated mutant human superoxide dismutase in yeast leads to decreased mitochondrial electron transport. Arch Biochem Biophys. 431, 207-14.

Gurney ME, Pu H, Chiu AY, Dal Canto MC, Polchow CY, Alexander DD, Caliendo J, Hentati A, Kwon YW, Deng HX. 1994. Motor neuron degeneration in mice that express a human Cu, Zn superoxide dismutase mutation. Science 264, 1772-1775.

Hatazawa J, Brooks RA, Dalakas MC, Mansi L, Di Chiro G. 1988. Cortical motor-sensory hypo-metabolism in amyotrophic lateral sclerosis: a PET study. J. Comput. Assist. Tomogr. 12, 630-636.

Higgins CM, Jung C, Ding H, Xu Z. 2002. Mutant Cu, Zn superoxide dismutase that causes motoneuron degeneration is present in mitochondria in the CNS. J. Neurosci. 22, RC215.

Higgins CM, Jung C, Xu Z. 2003. ALS-associated mutant SOD1 G93A causes mitochondrial vacuolation by expansion of the intermembrane space and by involvement of SOD1 aggregation and peroxisomes. BMC Neurosci. 4, 16.

Hirano, A., Nakano, I., Kurland, L.T., Mulder, D.W., Holley, P.W., Saccomanno, G. 1984. Fine structural study of neurofibrillary changes in a family with amyotrophic lateral sclerosis. J. Neuropathol. Exp. Neurol. 43, 471-80.

Howland DS, Liu J, She Y, Goad B, Maragakis NJ, Kim B, Erickson J, Kulik J, DeVito L, Psaltis G, DeGennaro LJ, Cleveland DW, Rothstein JD. 2002. Focal loss of the glutamate transporter EAAT2 in a transgenic rat model of SOD1 mutant-mediated amyotrophic lateral sclerosis (ALS). PNAS 99, 1604-1609.

Jaarsma D, Haasdijk ED, Grashorn JA, Hawkins R, van Duijn W, Verspaget HW, London J, Holstegem JC. 2000. Human Cu/Zn superoxide dismutase (SOD1) overexpression in mice causes mitochondrial vacuolization, axonal degeneration, and premature motoneuron death and accelerates motoneuron disease in mice expressing a familial amyotrophic lateral sclerosis mutant SOD1. Neurobiol Dis 7, 623-643.

Jaarsma D, Rognoni F, van Duijn W, Verspaget HW, Haasdijk ED, Holstege JC (2001) CuZn superoxide dismutase (SOD1) accumulates in vacuolated mitochondria in transgenic mice

expressing amyotrophic lateral sclerosis-linked SOD1 mutations. Acta Neuropathol (Berl) 102:293-305.

Julien JP (2001) Amyotrophic lateral sclerosis. Unfolding the toxicity of the misfolded. Cell 104:581-591.

Jung C, Higgins CM, Xu Z., 2002. Mitochondrial electron transport chain complex dysfunction in a transgenic mouse model for amyotrophic lateral sclerosis. J Neurochem. 83, 535-45.

Kaal EC, Vlug AS, Versleijen MW, Kuilman M, Joosten EA, Bar PR (2000) Chronic mitochondrial inhibition induces selective motoneuron death in vitro: a new model for amyotrophic lateral sclerosis. J Neurochem 74:1158-1165.

Killackey HP, Sherman SM (2003) Corticothalamic projections from the rat primary somatosensory cortex. J Neurosci 23:7381-7384.

Klivenyi P, Ferrante RJ, Matthews RT, Bogdanov MB, Klein AM, Andreassen OA, Meuller G, Wermer M, Kaddurah-Daouk R, Beal MF (1999) Neuroprotective effects of creatine in a transgenic animal model of amyotrophic lateral sclerosis. Nat Med 5:347–350.

Klivenyi P, Calingasan NY, Starkov A, Stavrovskaya IG, Kristal BS, Yang L, Wieringa B, Beal MF., 2004. Neuroprotective mechanisms of creatine occur in the absence of mitochondrial creatine kinase. Neurobiol Dis. 15, 610-7.

Kong J, Xu Z (1998) Massive mitochondrial degeneration in motor neurons triggers the onset of amyotrophic lateral sclerosis in mice expressing a mutant SOD1. J Neurosci 18:3241-3250.

Lino MM, Schneider C, Caroni P (2002) Accumulation of SOD1 mutants in postnatal motoneurons does not cause motoneuron pathology or motoneuron disease. J Neurosci 22:4825-4832.

Liu J, Lillo C, Jonsson PA, Vande Velde C, Ward CM, Miller TM, Subramaniam JR, Rothstein JD, Marklund S, Andersen PM, Brannstrom T, Gredal O, Wong PC, Williams DS, Cleveland DW., 2004. Toxicity of familial ALS-linked SOD1 mutants from selective recruitment to spinal mitochondria. Neuron. 43, 5-17.

Matthews RT, Yang L, Browne SE, Baik JM, Beal MF (1998) Coenzyme Q_{10} administration increases brain mitochondrial concentrations and exerts neuroprotective effects. PNAS 95:8892-8897.

Mattiazzi M, D'Aurelio M, Gajewski CD, Martushova K, Kiaei M, Beal MF, Manfredi G (2002) Mutated human SOD1 causes dysfunction of oxidative phosphorylation in mitochondria of transgenic mice. J Biol Chem 277:29626-29633.

Menzies FM, Cookson MR, Taylor RW, Turnbull DM, Chrzanowska-Lightowlers ZM, Dong L, Figlewicz DA, Shaw PJ (2002) Mitochondrial dysfunction in a cell culture model of familial amyotrophic lateral sclerosis. Brain 125:1522-1533.

Paxinos G, Franklin KBJ (2001) The Mouse Brain in Stereotaxic Coordinates. San Diego CA: Academic Press.

Ratovitski T, Corson LB, Strain J, Wong P, Cleveland DW, Culotta VC, Borchelt DR (1999) Variation in the biochemical/biophysical properties of mutant superoxide dismutase 1 enzymes and the rate of disease progression in familial amyotrophic lateral sclerosis kindreds. Hum Mol Genet 8:1451-1460.

Rothstein JD, Jin L, Dykes-Hoberg M, Kuncl RW (1993) Chronic inhibition of glutamate uptake produces a model of slow neurotoxicity. PNAS 90:6591-6595.

Sasaki S, Iwata M (1996) Ultrastructural study of synapses in the anterior horn neurons of patients with amyotrophic lateral sclerosis. Neurosci Lett 204:53-56.

Sasaki S, Warita H, Murakami T, Abe K, Iwata M.. 2004. Ultrastructural study of mitochondria in the spinal cord of transgenic mice with a G93A mutant SOD1 gene. Acta. Neuropathol. (Berl) 107, 461-74.

Siklos L, Engelhardt J, Harati Y, Smith RG, Joo F, Appel SH (1996) Ultrastructural evidence for altered calcium in motor nerve terminals in amyotropic lateral sclerosis. Ann Neurol 39:203-216.

Sokoloff L, Reivich M, Kennedy C, Des Rosiers MH, Patlak CS, Pettigrew KD, Sakurada O, Shinohara M (1977) The [^{14}C]2-deoxyglucose method for the measurement of local cerebral glucose utilization. Theory, procedure, and normal values in the conscious and anaesthetized rat. J Neurochem 28:897-916.

Spreux-Varoquaux O, Bensimon G, Lacomblez L, Salachas F, Pradat PF, Le Forestier N, Marouan A, Dib M, Meininger V (2002) Glutamate levels in cerebrospinal fluid in amyotrophic lateral sclerosis: a reappraisal using a new HPLC method with coulometric detection in a large cohort of patients. J Neurol Sci 193:73-78.

Strong M, Rosenfeld J (2003) Amyotrophic lateral sclerosis: a review of current concepts. Amyotroph Lateral Scler Other Motor Neuron Disord 4:136-143.

Takeuchi H, Kobayashi Y, Ishigaki S, Doyu M, Sobue G (2002) Mitochondrial localization of mutant superoxide dismutase 1 triggers caspase-dependent cell death in a cellular model of familial amyotrophic lateral sclerosis. J Biol Chem 227:50966-50972.

Tandan R, Bradley WG (1985) Amyotrophic lateral sclerosis Part 1: Clinical features, pathology, and ethical issues in management. Ann Neurol 184:271-280.

Tarnopolsky MA, Beal MF (2001) Potential for creatine and other therapies targeting cellular energy dysfunction in neurological disorders. Ann Neurol 49:561-7.

Tracey J, Waite PME (1995) Somatosensory System. In: The Rat Nervous System (Paxinos G, ed), pp689-704. San Diego CA: Academic Press.

Van Westerlaak MG, Joosten EA, Gribnau AA, Cools AR, Bar PR (2001) Chronic mitochondrial inhibition induces glutamate-mediated corticomotoneuron death in an organotypic culture model. Exp Neurol 167:393-400.

Vijayvergiya C, Beal MF, Buck J, Manfredi G. 2005. Mutant superoxide dismutase 1 forms aggregates in the brain mitochondrial matrix of amyotrophic lateral sclerosis mice. J. Neurosci. 25, 2463-70.

Wendt S, Dedeoglu A, Speer O, Wallimann T, Beal MF, Andreassen OA., 2002. Reduced creatine kinase activity in transgenic amyotrophic lateral sclerosis mice. Free Radic Biol Med. 32, 920-6.

Wong PC, Pardo CA, Borchelt DR, Lee MK, Copeland NG, Jenkins NA, Sisodia SS, Cleveland DW, Price DL (1995) An adverse property of a familial ALS–linked SOD1 mutation causes motor neuron disease characterized by vacuolar degeneration of mitochondria. Neuron 14:1105–1116.

Zang DW, Cheema SS. (2002) Degeneration of corticospinal and bulbospinal systems in the superoxide dismutase $1^{G93A\ G1H}$ transgenic mouse model of familial amyotrophic lateral sclerosis. Neurosci Letts 332:99-102.

Zilles K, Wree A (1995) Cortex: areal and laminar structure. In: The Rat Nervous System (Paxinos G, ed), pp.649-685. San Diego CA: Academic Press.

FIGURE LEGENDS

Figure 1. Reduced glucose utilization in primary motor cortex and thalamic nuclei of pre-symptomatic G93A mice. Representative autoradiograms from a 60 day old G93A mouse (bottom), and an age-matched wild-type littermate (Wt), at the level of the rostral primary motor cortex (left), and the rostral thalamus (right). Images are color-coded for local cerebral metabolic rates for glucose ($lCMR_{glc}$) according to the calibration bar. Glucose use is markedly reduced in G93A motor cortex (Fr1 delineated by arrows in Wt), and in thalamic nuclei including the rostral ventrolateral thalamus. No overt glucose use changes are apparent in the hindlimb column of sensorimotor cortex (arrowhead).

Figure 2. Glucose use alterations in G93A corticospinal tract and collaterals. Major afferent and efferent connections of the primary motor cortex are shown schematically. Bar charts are mean ± SEM local cerebral metabolic rates for glucose ($lCMR_{glc}$, μmol/100g/min) at 60 days and 120 days of age, in G93A mice (open bars) and age-matched wildtype (Wt) littermates. *$p< 0.05$, significantly different from levels in age-matched wildtypes (Student's unpaired t-test).

Figure 3. Hypometabolism in spinal cord is evident in symptomatic G93A mice. Local cerebral metabolic rates for glucose ($lCMR_{glc}$, μmol/100g/min) in gray and white matter of cervical, thoracic and lumbar spinal cord regions at: A, 60 days, and B, 120 days of age. Data are mean ± SEM in G93A mice (open bars) and age-matched wildtype (Wt) littermates. *$p< 0.05$, significantly different from age-matched wildtype levels (Student's unpaired t-test). 60 days, n = 6 Wt, 8 G93A; 120 days, n = 5 Wt, 4 G93A. *Abbrev:* Dors, dorsal gray area; Vent, ventral gray area.

Figure 4. Reduced cortical ATP and ADP levels in G93A mice are partially restored by creatine. Metabolite levels in G93A mice and N1029 mice are presented as percent of levels in age-matched wild-type littermate mice. N1029 levels (180 day old mice) were compared with metabolite levels in the oldest G93A wildtype group assessed (120 days). Data are mean ± SEM in 30, 60, 90 and 120 day old G93A mice, and in 120 day old mice treated with 2% creatine from 90 days of age (120d + Cre). *$p< 0.05$, **$p< 0.01$, significant difference relative to age-matched wild-type levels; † $p< 0.05$, significant difference relative to level in creatine-treated mice (ANOVA followed by post-hoc Tukey-Kramer multiple comparisons test).

Table 1: Physiological Variables in G93A and N1029 Mice.

	G93A SOD1 60 Days	
	Wt	**G93A**
Glucose -Pre (mg/dL)	141 ± 8	179 ± 12*
Glucose +45 min (mg/dL)	160 ± 12	183 ± 9
p_aO_2 (mmHg)	110 ± 4	107 ± 4
p_aCO_2 (mmHg)	34 ± 2	39 ± 3
*p*H	7.34 ± 0.02	7.31 ± 0.01
	120 Days	
	Wt	**G93A**
Glucose -Pre (mg/dL)	138 ± 9	143 ± 10
Glucose +45 min (mg/dL)	134 ± 16	179 ± 34
p_aO_2 (mmHg)	100 ± 3	93 ± 10
p_aCO_2 (mmHg)	32 ± 2	40 ± 3
*p*H	7.38 ± 0.01	7.32 ± 0.02*
	N1029 SOD1	
	Wt	**N1029**
Glucose -Pre (mg/dL)	187 ± 8	144 ± 6*
Glucose +45 min (mg/dL)	170 ± 16	147 ± 6
p_aO_2 (mmHg)	117 ± 18	109 ± 8
p_aCO_2 (mmHg)	49 ± 4	42 ± 4
*p*H	7.30 ± 0.03	7.32 ± 0.01

Variables in 60 day (n = 6) and 120 day old (n = 6) G93A mice, 21 month old N1029 mice (n = 4-5), and age-matched littermate wildtypes (Wt) (n = 9, 7-8 and 3, respectively). Data are mean ± SEM for arterial plasma glucose concentrations at the start (Glucose-Pre) and end of the 2-DG procedure (Glucose +45 min), and terminal blood gas levels. *$p<0.05$, significant difference relative to age-matched Wt (Student's unpaired t-test). Plasma glucose levels did not alter over the 45 min experiment in any group ($p>0.05$, Student's paired t-test).

Table 2: Local Rates of Glucose Use in FALS Mouse Brain

	60 Days		120 Days	
	Wt	**G93A**	**Wt**	**G93A**
Cerebral Cortex				
1° Motor: layer I-III	70 ± 3	57 ± 2**	47 ± 5	32 ± 2*
(Rostral) layer IV	74 ± 3	62 ± 2**	48 ± 5	33 ± 2*
layer V-VI	65 ± 3	53 ± 2**	47 ± 5	32 ± 2*
1° Motor: layer I-III	64 ± 2	57 ± 2*	47 ± 5	32 ± 2*
(Caudal) layer IV	67 ± 3	60 ± 3	50 ± 6	33 ± 2*
layer V-VI	58 ± 3	52 ± 2	42 ± 5	28 ± 2*
Sensorimotor, Hindlimb:				
layer I-III	55 ± 2	51 ± 4	40 ± 6	29 ± 3
layer IV	58 ± 2	53 ± 4	43 ± 6	32 ± 2
layer V-VI	53 ± 2	49 ± 3	38 ± 6	27 ± 2
Sensorimotor, Barrel field:				
layer I-III	67 ± 3	60 ± 4	47 ± 5	33 ± 3
layer IV	75 ± 2	68 ± 5	53 ± 5	37 ± 3
layer V-VI	66 ± 2	58 ± 4	44 ± 5	31 ± 3
Anterior Cingulate	69 ± 3	65 ± 4	53 ± 7	34 ± 2*
Posterior Cingulate	77 ± 2	72 ± 3	61 ± 7	37 ± 2*
Auditory: layer IV	75 ± 4	73 ± 5	59 ± 7	35 ± 3*
Visual: layer IV	57 ± 4	49 ± 3	43 ± 5	29 ± 2*
Motor Tracts				
Striatum	76 ± 5	66 ± 4	58 ± 7	41 ± 3
Thalamic Nuclei:				
Reticular Complex	62 ± 4	53 ± 4	46 ± 7	32 ± 3
Anteromedial	74 ± 5	66 ± 5	59 ± 8	43 ± 2
Anteroventral	74 ± 5	62 ± 4	58 ± 6	39 ± 1*
Ventrolateral - Rostral, dorsal	62 ± 3	53 ± 3*	46 ± 5	29 ± 2*
Ventrolateral - Rostal, ventral	59 ± 2	52 ± 3*	45 ± 5	27 ± 3*

Ventrolateral - Caudal	60 ± 3	52 ± 4	43 ± 5	26 ± 2*
Ventromedial	75 ± 4	62 ± 4*	57 ± 6	38 ± 3*
Ventroposterior - Medial	58 ± 3	50 ± 3*	42 ± 4	28 ± 2*
Red Nucleus	69 ± 4	60 ± 4	53 ± 2	38 ± 3**
Interpeduncular Nucleus	69 ± 5	65 ± 4	57 ± 10	40 ± 3
Pontine Nuclei	51 ± 4	38 ± 1*	37 ± 4	20 ± 2**
Pontine Reticular Formation	48 ± 2	40 ± 3*	37 ± 6	22 ± 2*
Paramedian Raphe Nucleus	63 ± 5	52 ± 3	47 ± 7	29 ± 3
Inferior Olive	62 ± 2	58 ± 6	39 ± 2	30 ± 6
Limbic/Extrapyramidal/Other				
Hippocampus: CA1	38 ± 2	34 ± 2	25 ± 4	19 ± 2
CA3	49 ± 4	43 ± 2	38 ± 6	25 ± 3
Globus Pallidus	45 ± 2	41 ± 2	31 ± 4	23 ± 3
Dentate Gyrus	55 ± 3	47 ± 3	43 ± 6	34 ± 3
Dorsolateral Geniculate Body	58 ± 4	50 ± 3	46 ± 5	32 ± 2*
Subthalamic Nucleus	62 ± 3	53 ± 3*	53 ± 5	34 ± 3*
Mammillary Body	78 ± 4	68 ± 3	71 ± 8	42 ± 3*
Medial Geniculate Body	72 ± 4	61 ± 4	50 ± 7	34 ± 4
Substantia Nigra:				
pars compacta	55 ± 3	47 ± 3*	42 ± 5	29 ± 3
pars reticulata	39 ± 5	33 ± 2	26 ± 5	18 ± 3
Superior colliculus:				
superficialis	56 ± 3	49 ± 3	45 ± 6	30 ± 2*
profundum	56 ± 3	48 ± 3	46 ± 7	30 ± 2
Superior Olivary Nucleus	73 ± 3	61 ± 4*	48 ± 7	36 ± 4
Inferior Colliculus	97 ± 7	85 ± 8	64 ± 10	42 ± 5
Cochlear Nucleus	92 ± 11	74 ± 7	60 ± 10	34 ± 5*
Cerebellar Grey- molecular	48 ± 3	43 ± 2	34 ± 4	24 ± 3*
Cerebellar Grey- granular	35 ± 2	33 ± 2	24 ± 4	17 ± 3

Cerebellar White	24 ± 1	22 ± 1	16 ± 3	15 ± 5

Data are mean ± SEM $lCMR_{glc}$ (μmol/100g/min) in G93A and age-matched littermate wildtype (Wt) mice. *p<0.05, **p<0.005 significant differences relative to age-matched Wt mice (Student's unpaired t-test). G93A and Wt mice, n = 6 and 9 (60d), and n = 6 and 8 (120d), respectively. Cerebral regions are classified according to the nomenclature of Zilles and Wree (1995). Primary (1^o) motor cortex corresponds to Fr1.

Table 3: Local Rates of Glucose Use in FALS Mouse Spinal Cord

	60 Days		120 Days	
	Wt	**G93A**	**Wt**	**G93A**
Spinal Cord				
Cervical - Dorsal	31 ± 9	36 ± 4	21 ± 3	9 ± 3*
Ventral	29 ± 7	36 ± 5	22 ± 4	8 ± 4*
White	15 ± 3	16 ± 2	13 ± 3	9 ± 3*
Thoracic - Dorsal	34 ± 4	36 ± 3	20 ± 3	8 ± 4*
Ventral	34 ± 4	36 ± 3	21 ± 4	4 ± 3
White	17 ± 2	18 ± 1	11 ± 3	11 ± 3*
Lumbar - Dorsal	33 ± 3	36 ± 3	25 ± 4	10 ± 3
Ventral	32 ± 3	37 ± 3	24 ± 4	6 ± 2
White	16 ± 2	19 ± 1	13 ± 3	9 ± 3*

Data are mean ± SEM $lCMR_{glc}$ (μmol/100g/min) in G93A and age-matched littermate wildtype (Wt) mice. *p<0.05, **p<0.005 significant differences relative to age-matched Wt mice (Student's unpaired t-test). G93A and Wt mice, n = 6 and 9 (60d), and n = 6 and 8 (120d), respectively.

Table 4: Glucose Use Rates in Brain and Spinal Cord of Wildtype SOD1 Transgenic Mice

		Wt	N1029
Brain			
Frontal Cortex		43 ± 9	49 ± 2
Motor Cortex		38 ± 5	42 ± 3
Striatum		45 ± 9	51 ± 1
Hippocampus CA3		30 ± 12	39 ± 3
Cerebellar Gray Matter		22 ± 3	26 ± 1
Spinal Cord			
Cervical -	Dorsal	27 ± 2	24 ± 2
	Ventral	26 ± 3	24 ± 1
	White	14 ± 2	14 ± 2
Thoracic -	Dorsal	24 ± 1	26 ± 3
	Ventral	22 ± 3	27 ± 3
	White	11 ± 2	14 ± 1
Lumbar -	Dorsal	27 ± 7	25 ± 3
	Ventral	26 ± 6	26 ± 4
	White	14 ± 2	14 ± 2

Data are Mean ± SEM $lCMR_{glc}$ (μmol/100g/min) in 21 month old N1029 mice over-expressing wildtype SOD1, and age-matched littermate wildtype (Wt) mice. $lCMR_{glc}$ in N1029 mice did not differ from rates in wildtypes ($p > 0.05$, Student's unpaired t-test).

Table 5: CNS Metabolite Levels in SOD1 Transgenic Mice

AGE Days	Mice	n	ATP (nmol/mg protein) Cortex	Cerebellum	Spinal Cord	ADP (nmol/mg protein) Cortex	Cerebellum	Spinal Cord
30	Wt	10	16.0 ± 0.9	17.8 ± 0.7	N/A	7.3 ± 0.3	3.9 ± 0.4	N/A
	G93A	10	9.3 ± 1.1**	15.7 ± 0.9	N/A	3.5 ± 0.3**	3.5 ± 0.3	N/A
60	Wt	5	15.3 ± 0.5	12.6 ± 0.9	8.6 ± 2.1	9.1 ± 1.1	4.6 ± 0.4	5.8 ± 1.1
	G93A	5	8.7 ± 0.6**	12.5 ± 1.9	4.9 ± 1.5	6.1 ± 0.4	4.7 ± 0.5	5.6 ± 1.0
90	Wt	5	14.1 ± 2.4	11.9 ± 1.5	7.8 ± 2.8	9.9 ± 0.7	5.0 ± 0.8	6.0 ± 1.2
	G93A	5	7.0 ± 1.1**	6.1 ± 1.2	4.4 ± 1.2	5.8 ± 0.8**	4.2 ± 0.7	5.3 ± 1.0
120	Wt	5	10.9 ± 1.2	13.7 ± 1.6	9.2 ± 2.6	10.0 ± 0.5	4.6 ± 0.7	5.2 ± 0.9
	G93A	5	3.1 ± 1.1**	13.2 ± 1.2	3.0± 0.8	5.2 ± 0.4**	5.4 ± 0.5	6.2 ± 0.9
120	G93A + Cre	5	7.9 ± 0.9 †	10.7 ± 1.7	8.5 ± 1.4	7.5 ± 0.6	4.1 ± 0.8	5.6 ± 0.7
150	N1029	4	10.5 ± 1.4	13.2 ± 3.3	6.3 ± 1.2	8.7 ± 1.2	5.3 ± 1.4	6.9 ± 0.5

AGE Days	Mice	n	AMP (nmol/mg protein) Cortex	Cerebellum	Spinal Cord	CREATINE (nmol/mg protein) Cortex	Cerebellum	Spinal Cord
30	Wt	10	14.4 ± 0.6	8.8 ± 0.3	N/A	68 ± 2	71 ± 2	N/A
	G93A	10	14.9 ± 0.8	8.7 ± 0.5	N/A	62 ± 2	66 ± 2	N/A
60	Wt	5	13.7 ± 1.0	3.9 ± 0.4	5.9 ± 1.0	84 ± 5	90 ± 4	84 ± 12
	G93A	5	10.2 ± 0.6	4.1 ± 0.4	5.7 ± 0.7	54 ± 4**	87 ± 10	60 ± 8
90	Wt	5	15.6 ± 1.7	4.3 ± 0.8	6.9 ± 0.4	91 ± 5	79 ± 10	100 ± 6
	G93A	5	10.3 ± 0.7	4.1 ± 0.7	5.6 ± 0.8	51 ± 4**	86 ± 18	63 ± 5 **
120	Wt	5	13.8 ± 1.3	4.0 ± 0.6	5.1 ± 0.4	76 ± 7	88 ± 14	73 ± 6
	G93A	5	13.6 ± 0.8	4.9 ± 0.4	6.9 ± 0.7	55 ± 5	104 ± 4	71 ± 3
120	G93A + Cre	5	12.6 ± 1.4	3.7 ± 0.6	4.6 ± 0.3	63 ± 7†	77 ± 9	91 ± 3 ††
180	N1029	4	13.9 ± 1.7	4.4 ± 1.3	6.3 ± 0.3	78 ± 7	89 ± 2	72 ± 1

Data are mean ± SEM ATP, ADP, AMP and creatine levels measured in 30, 60, 90 and 120 day old G93A mice, in 120 day old mice treated with 2% creatine from 90 days (G93A + Cre), and in 180 day old N1029 mice. *$p< 0.05$, **$p< 0.01$, significant differences relative to age-matched wildtype levels;

† $p< 0.05$, †† $p< 0.01$, significant differences relative to age-matched untreated G93A mice (ANOVA followed by post-hoc Tukey-Kramer multiple comparisons test).

Figure 1
Click here to download high resolution image

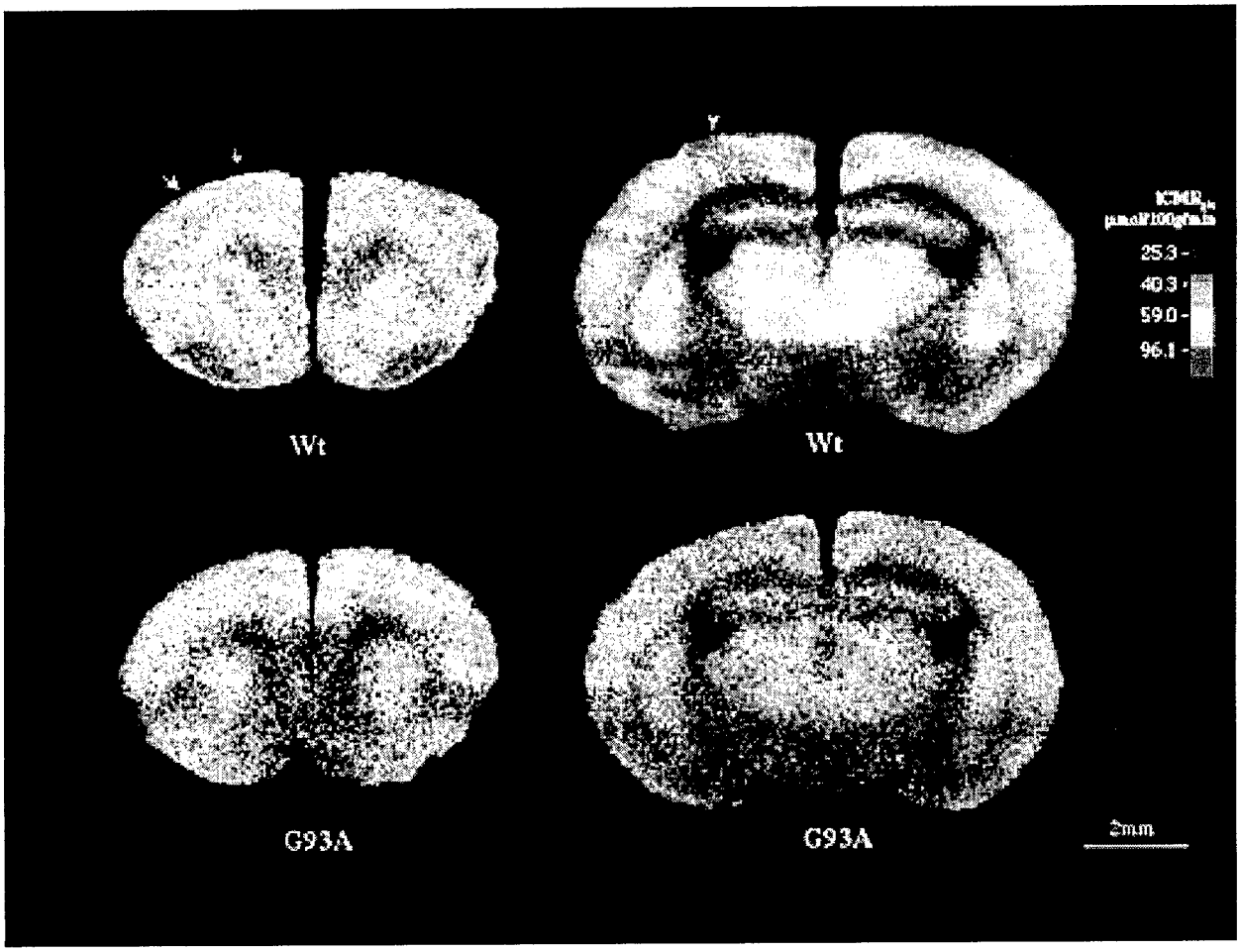

Figure 2

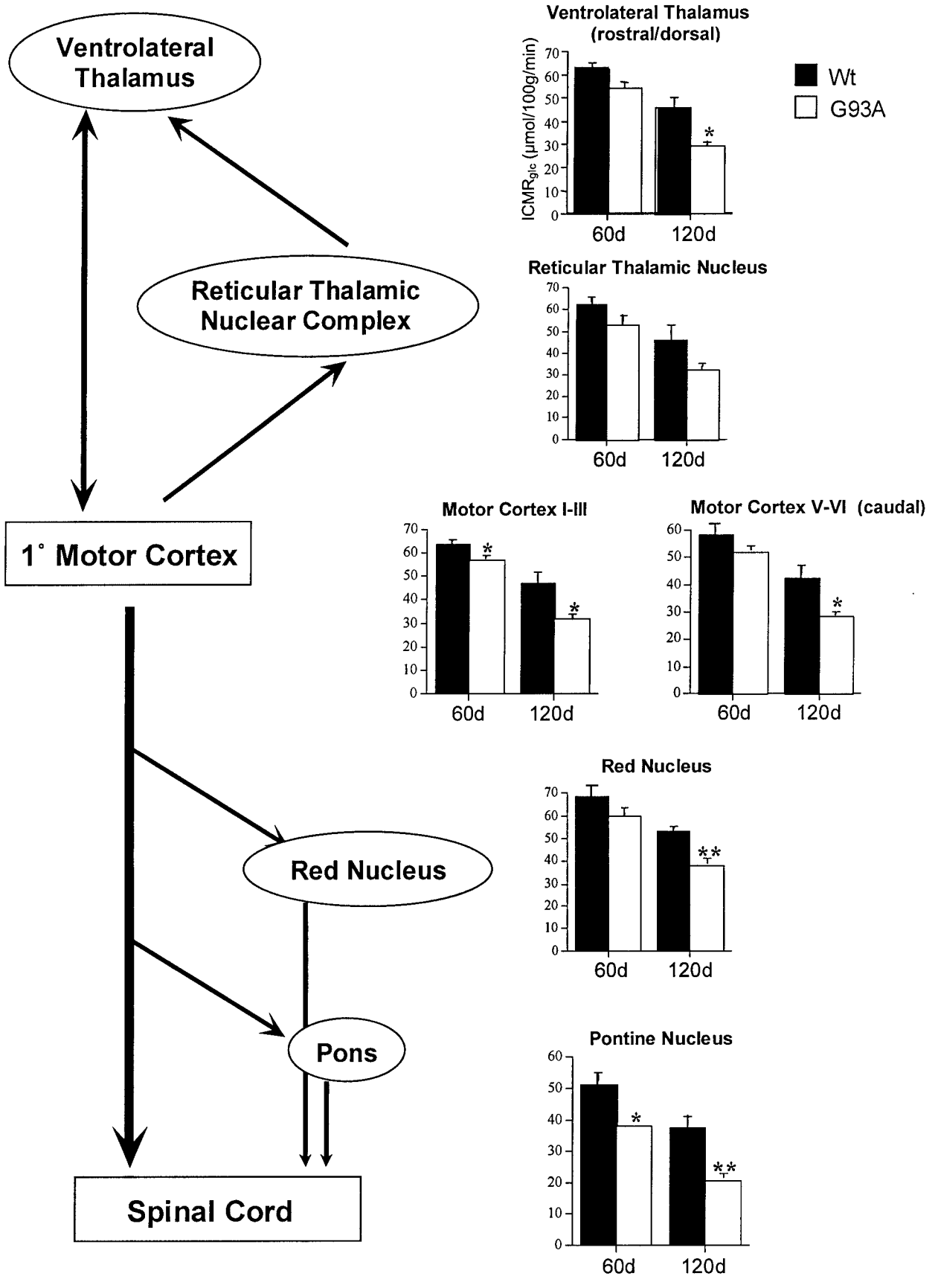
Ventrolateral Thalamus
Reticular Thalamic Nuclear Complex
1° Motor Cortex
Red Nucleus
Pons
Spinal Cord
Ventrolateral Thalamus (rostral/dorsal)
ICMRglc (µmol/100g/min)
Wt
G93A
60d
120d
Reticular Thalamic Nucleus
Motor Cortex I-III
Motor Cortex V-VI (caudal)
Red Nucleus
Pontine Nucleus

Figure 3

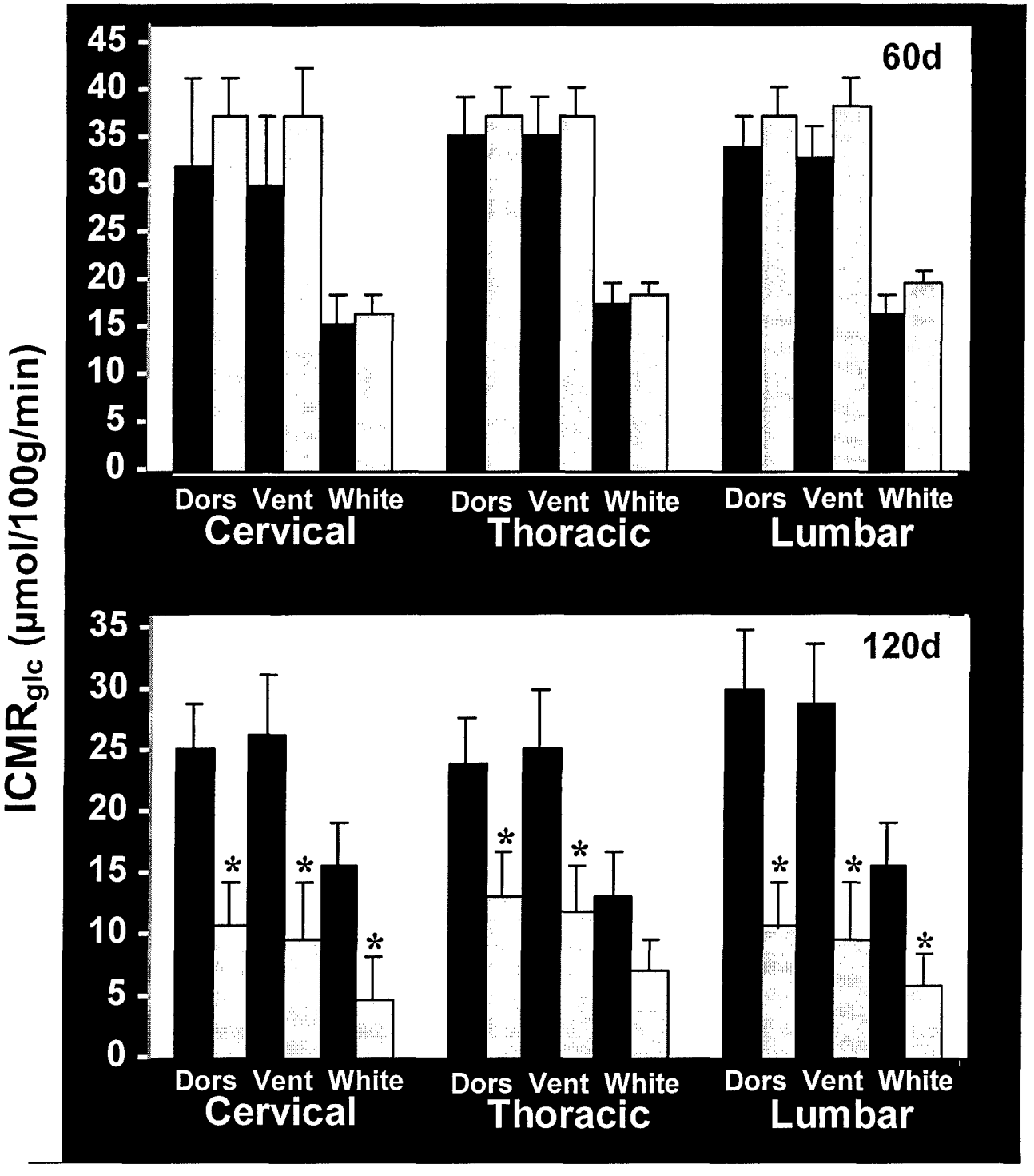
ICMRglc (µmol/100g/min)
60d
120d
Dors Vent White
Cervical
Thoracic
Lumbar
0
5
10
15
20
25
30
35
40
45
*

Figure 4

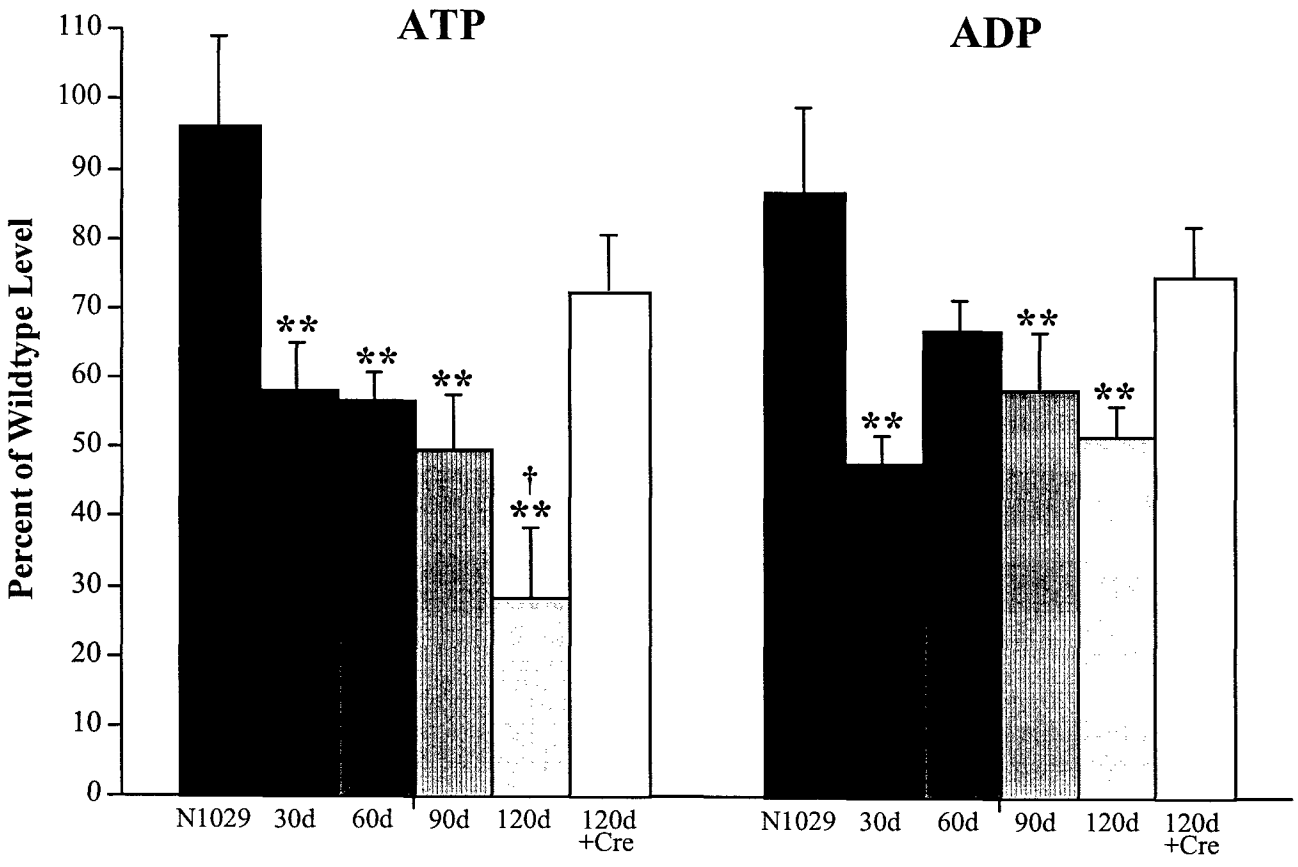
ATP
ADP
Percent of Wildtype Level
110
100
90
80
70
60
50
40
30
20
10
0
**
**
**
†
**
**
**
**
N1029
30d
60d
90d
120d
120d +Cre
N1029
30d
60d
90d
120d
120d +Cre

Supplementary Data

Table 1: Local Cerebral Glucose Utilization ($lCMR_{glc}$) in G85R transgenic mice.

	G85R Mice (10 Months – Endstage)	
	Wildtype	G85R (+)
Frontal Cortex	65 ± 6	44 ± 14
Motor Cortex	60 ± 5	39 ± 16
Striatum	68 ± 9	50 ± 14
Hippocampus CA3	45 ± 4	26 ± 9
Cerebellum Grey	41 ± 4	15 ± 2*

Local cerebral metabolic rates for glucose (nmol/100g/min) in G85R transgenic SOD1 mutant mice (n=5) and G85R wild type littermate controls (Wild Type; n=3 per group). Data presented as mean ± SEM. * $p<0.05$, significant difference between G85R mutant mice and wild type littermate controls (Student's unpaired t-test).

THE JOURNAL OF BIOLOGICAL CHEMISTRY

APPENDIX 3

Vol. 280, No. 1, Issue of January 7, pp. 556–563, 2005
Printed in U.S.A.

Neuroprotective Effects of Phenylbutyrate in the N171-82Q Transgenic Mouse Model of Huntington's Disease*

Received for publication, September 7, 2004, and in revised form, October 12, 2004
Published, JBC Papers in Press, October 19, 2004, DOI 10.1074/jbc.M410210200

Gabriella Gardian‡, Susan E. Browne‡, Dong-Kug Choi‡, Peter Klivenyi‡, Jason Gregorio‡, James K. Kubilus§¶, Hoon Ryu§¶, Brett Langley‖, Rajiv R. Ratan‡‖, Robert J. Ferrante§¶, and M. Flint Beal‡ ‡‡**

*From the ‡Department of Neurology and Neuroscience, Weill Medical College of Cornell University, New York-Presbyterian Hospital, New York, New York 10021, the §Geriatric Research Education and Clinical Center, Bedford Veterans Affairs Medical Center, Bedford, Massachusetts 01730, the ¶Departments of Neurology, Pathology, and Psychiatry, Boston University School of Medicine, Boston, Massachusetts 02118, the ‖Department of Neurology, Harvard Medical School and The Beth Israel Deaconess Medical Center, Boston, Massachusetts 02115, and the **Burke Medical Research Institute, White Plains, New York 10605*

Huntington's disease (HD) is caused by an expansion of exonic CAG triplet repeats in the gene encoding the huntingtin protein (Htt), however, the means by which neurodegeneration occurs remains obscure. There is evidence that mutant Htt interacts with transcription factors leading to reduced histone acetylation. We report that administration of the histone deacetylase inhibitor phenylbutyrate after onset of symptoms in a transgenic mouse model of HD significantly extends survival and attenuates both gross brain and neuronal atrophy. Administration of phenylbutyrate increased brain histone acetylation and decreased histone methylation levels as assessed by both immunocytochemistry and Western blots. Phenylbutyrate increased mRNA for components of the ubiquitin-proteosomal pathway and down-regulated caspases implicated in apoptotic cell death, and active caspase 3 immunoreactivity in the striatum. These results show that administration of phenylbutyrate, at doses that are well tolerated in man, exerts significant neuroprotective effects in a transgenic mouse model of HD, and therefore represents a very promising therapeutic approach for HD.

Huntington's disease (HD)[1] is caused by a mutation that leads to an expansion of a stretch of polyglutamines in the Htt protein. The expanded polyglutamine domains can interact with other polyglutamine containing proteins, including several transcription factors (1). Alterations in gene transcription occur as an early feature of transgenic mouse models of HD and other polyglutamine diseases (2–4). One example is recruitment of CREB-binding protein (CBP) into aggregates of polyglutamine containing proteins in cultured cell lines (5, 6). CBP is depleted from its normal nuclear localization and sequestered into Htt containing aggregates in cell culture, transgenic mice, and human HD postmortem brain tissue (7). CBP functions as a histone acetyltransferase enzyme. Mutant huntingtin directly binds to the acetyltransferase domains of CBP and another protein, P300/CBP associated factor, which results in a reduction of the acetyltransferase activity in cell-free assays as well as a decrease in the level of histone acetylation in mammalian cells (8). There is, however, evidence of increased CRE-mediated transcription in a transgenic mouse model of HD (9).

Histone acetylation helps transcription factors gain access to specific regions of DNA when it is tightly packed in chromatin, and thereby increases gene transcription. In a *Drosophila* model of polyglutamine-dependent neurodegeneration, histone deacetylase (HDAC) inhibitors arrest the ongoing progressive neuronal degeneration (8). The toxic effects of polyglutamines in yeast were mitigated by the HDAC inhibitor trichostatin A (10). Furthermore, histone acetylation is reduced in cell lines that express a mutant androgen receptor with an expanded polyglutamine repeat, and this is reversed by overexpression of CBP or by treatment with HDAC inhibitors, with a concomitant reduction in cell loss (11). The HDAC inhibitor suberoylanilide hydroxamic acid (SAHA) ameliorates motor deficits in the R6/2 transgenic mouse model of HD, although its effects on survival were not assessed. (12). The HDAC inhibitor sodium butyrate improves survival and attenuates striatal atrophy in the R6/2 transgenic mouse model of HD when administered presymptomatically starting at 21 days of age (13). A critical issue, however, is whether HDAC inhibitors exert neuroprotective effects when administered after the onset of symptoms, analogous to the situation in HD patients. We found that the HDAC inhibitor phenylbutyrate exerts significant effects on survival and ameliorates histopathologic degeneration in the N171-82Q transgenic mouse model of HD when administered after the onset of symptoms. Furthermore, we show for the first time that histone methylation is markedly increased in the N171-82Q transgenic mouse model of HD, and that this is ameliorated by phenylbutyrate treatment.

MATERIALS AND METHODS

Animals—Transgenic N171-82Q mice were originally obtained from Drs. Ross and Borchelt (The Johns Hopkins University, Baltimore, MD), and maintained on a B6C3F1 background (Jackson Laboratories, Bar Harbor, ME). The offspring were genotyped using a PCR assay on tail DNA. Mice were housed 4–5 per cage with free access to food and water, under standard conditions with a 12-h light/dark cycle. All

* This work was supported by the Huntington's Disease Society of America Coalition for the Cure program, the Hereditary Disease Foundation, and National Institutes of Health NINDS Grants NS32958 (to M. F. B.), NS35255, and NSO45242 (to R. J. F.), and the Veterans Administration. The costs of publication of this article were defrayed in part by the payment of page charges. This article must therefore be hereby marked "*advertisement*" in accordance with 18 U.S.C. Section 1734 solely to indicate this fact.

‡‡ To whom correspondence should be addressed: Dept. of Neurology and Neuroscience, Weill Medical College of Cornell University, 525 East 68th St., Rm. F610, New York, NY 10021. Tel.: 212-746-6575; Fax: 212-746-8532; E-mail: fbeal@med.cornell.edu.

[1] The abbreviations used are: HD, Huntington's disease; Htt, huntingtin; HDAC, histone deacetylase; CBP, CREB-binding protein; CREB, cAMP-response element-binding protein; PBS, phosphate-buffered saline; RT, reverse transcriptase; SAHA, suberoylanilide hydroxamic acid.

animal experiments were performed in accordance with the NIH Guide for the Care and Use of Laboratory Animals and were approved by the Weill Medical College of Cornell University Institutional Animal Care and Use Committee. Male and female N171-82Q mice, and littermates, were equally distributed between experimental groups.

Treatment—Mice received intraperitoneal injections of 4-phenylbutyric acid sodium salt (100 mg/kg/day, volume 3.33 ml/kg; Triple Crown USA, Inc., Perkasie, PA) or vehicle (PBS, 3.33 ml/kg), 6 days per week from 75 days of age.

Survival—Thirty-six mice (24 in the drug and 12 in the vehicle groups) were used in survival, weight, and behavior studies. Mice were observed daily, and deemed to have reached end-stage of the disorder when they could no longer initiate movement after being gently agitated for 2 min. Death was recorded when animals reached this stage and were euthanized by Na-pentobarbital overdose, or at the time of natural death if this occurred between daily inspections.

Behavioral and Weight Assessment—Motor performance was assessed using an accelerating rotarod apparatus (Columbus Instruments, Columbus, OH). The rotarod was accelerated from 0 rpm at a rate of 5.3 rpm/min over 180 s, then maintained at 16 rpm for a further 120 s (300 s total). The time elapsed on the rotarod measures the motor competency of the mouse in the task. Mice were given two rotarod training sessions to acclimate them to the apparatus, and then tested twice weekly from 75 days of age. Each mouse undertook three 300-s trials per test session, with the best result recorded. Mice were weighed twice a week.

HDAC Inhibition—The HDAC inhibitory action of phenylbutyrate was confirmed by an *in vitro* HDAC fluorescent activity assay (Biomol, Plymouth Meeting, PA), as previously described (14). Phenylbutyrate was incubated with the HeLa extract for 30 min, and then incubated for 25 min with developer.

Histone Acetylation and Methylation Levels in Brain Tissue—Fifteen N171-82Q and littermate wild-type mice (aged 4–5 months) received single intraperitoneal injections of 100 mg/kg Na-phenylbutyrate in PBS or vehicle (PBS). Mice were sacrificed 0, 1, 2, 3, and 4 h post-injection (n = 3 per group), brain and spleen were harvested and immediately frozen in liquid nitrogen. Nuclear fractionation was carried out according to Ref. 15. Levels of acetylated H3 histones were measured by Western blot analysis according to published methods (anti-acetylated H3 dilution 1:3000; anti-acetylated H4 dilution 1:2000) (16). Levels were compared with butyrate-treated and untreated HeLa cell extracts. Histone methylation in both vehicle and Na-phenylbutyrate-treated wild-type and N171-82Q mice at 0, 1, 2, and 3 h was measured by Western blot analysis using an anti-dimethylated H3 (Lys-9) antibody (Upstate Biotechnology, Lake Placid, NY). Anti-acetylated H3 and H4 antibodies as well as butyrate-treated and control HeLa cell extracts were obtained from Upstate Biotechnology (Lake Placid, NY) and anti-rabbit IgG horseradish peroxidase from Amersham Biosciences. The Western blots were quantitated using computer-assisted densitometry.

Histology and Immunohistochemical Localization of Acetylated and Methylated Histones—Mice were treated with 100 mg/kg Na-phenylbutyrate or PBS from 75 days of age. At 100 or 120 days of age, mice were deeply anesthetized and transcardially perfused with 4% paraformaldehyde (n = 5 per group). Brains were removed, post-fixed with the perfusant for 2 h, and then cryoprotected in 20% glycerol, 2% Me_2SO. Brains were then cut into frozen 50-μm thick sections, and serial sections stained for Nissl substance (cresyl violet) or immunostained with an antibody recognizing the first 256 amino acids of human huntingtin (EM48, dilution, 1:1,000). An antibody to ubiquitin (dilution, 1:200, Dako Corp., Carpintena, CA) was also used to confirm the presence of protein aggregates. Immunocytochemical localization of acetylated histone H3 and acetylated histone H4 was conducted in adjacent sections, as previously described (17). Immunocytochemical detection of histone methylation was done using an antibody to anti-dimethyl-histone H3 (Lys-9) (Upstate Biotechnology, Lake Placid, NY). Caspase activation was examined using an affinity purified anti-active caspase 3 antibody (dilution, 1:1000, BD Pharmingen).

Stereology/Quantitation—Serial-cut coronal tissue sections beginning from the most rostral segment of the neostriatum to the level of the anterior commissure were used for huntingtin aggregate analysis. Unbiased stereologic counts of huntingtin-positive aggregates ($\geq$1.0 μm diameter) were obtained from the dorsolateral neostriatum in 5 mice each from phenylbutyrate-treated and PBS-treated N171-82Q mice at 120 days using Neurolucida Stereo Investigator software (Microbrightfield, Colchester, VT). The total areas of the rostral neostriatum were defined in serial sections in which counting frames were randomly sampled. The optical dissector method was employed estimating the

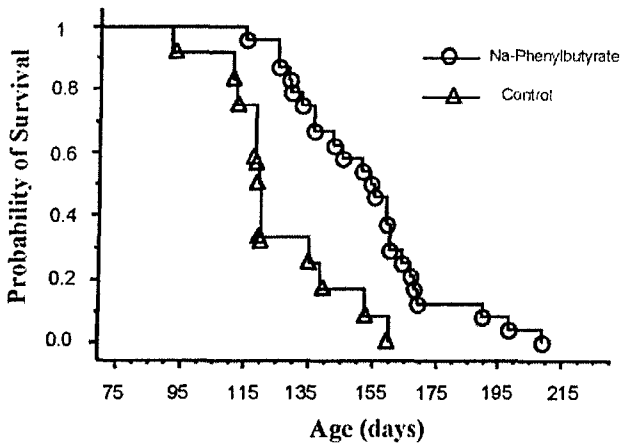

FIG. 1. **Effects of administration of phenylbutyrate starting at 75 days of age on survival in the N171-82Q transgenic mouse model of HD.** Phenylbutyrate significantly improved survival (p < 0.0001, Mantel-Cox log-rank test).

number of huntingtin-positive aggregates. Striatal neuron areas were analyzed by microscopic videocapture using a Windows-based image analysis system for area measurement (Optimas, Bioscan Inc., Edmonds, WA). The software automatically identifies and measures profiles. All computer identified cell profiles were manually verified as neurons and exported to Microsoft Excel. Cross-sectional areas were analyzed using Statview.

RNA Isolation and Microarray Analysis—Striata were dissected from mouse brains and immediately frozen in liquid nitrogen. Total RNA was isolated by extraction with TRIzol (Invitrogen). Labeled cRNA probes were generated from total RNA samples using the MessageAmp™ cRNA kit (Ambion Inc., Austin, TX). Briefly, the procedure consists of reverse transcription of 2 μg of total RNA with a T7 oligo(dT) primer bearing a T7 promoter sequence followed by *in vitro* transcription of the resulting DNA with T7 RNA polymerase to generate antisense RNA copies of each mRNA (Ambion Inc.). The quality of total RNA and labeled cRNA were assessed with Agilent's Lab-on-a-Chip total RNA nano-biosizing assay (Agilent Technologies, Palo Alto, CA). Biotinylated cRNA probes were hybridized to Murine Genome Array U74Av2 chips, containing 6,000 identified genes and 6,000 EST clusters, using the Affymetrix Fluidics Station 400 according to the manufacturer's standard protocol. The image data on each individual microarray chip was scaled to 250 target intensity, using the Microarray Suite software (Affymetrix, Santa Clara, CA). Drug-induced alterations in gene expression were analyzed using the GeneSpring software (Silicon Genetics, Redwood, CA). Data analysis was carried out on 10 microarrays (5 PBS-treated and 5 phenylbutyrate-treated mice). Normalization was carried out using default normalization parameters by GeneSpring software as follows: per sample, by dividing the raw data by the 50th percentile of all measurement, and per gene, by dividing the raw data by the median of the expression level to specific samples. Data from probe sets representing genes that failed the detection criteria (labeled "absent" or "marginal" in all 10 microarrays) were eliminated, and all further analyses were carried out in the remaining 7,116 probe sets. The Welch t test statistical method was used to find differentially expressed genes by two-group comparisons, and genes were assumed to be significantly up-regulated or down-regulated if the calculated p value was <0.05.

Real-time RT-PCR—One-step quantitative real-time RT-PCR using a LightCycler thermal cycler system (Roche Diagnostics) was performed to confirm microarray results. PCR was carried out with the SYBR Green quantitative RT-PCR system (Sigma) and gene-specific primers for 40 cycles according to the manufacturer's protocols. After amplification, a melting curve analysis and length verification by gel electrophoresis were carried out to confirm the specificity of PCR products. As a negative control, template RNA was replaced with PCR-grade water. Calculations of threshold cycle and difference were analyzed with LightCycler analysis software (Roche). Gene-specific primers were designed using LightCycler probe design software (Roche). PCR primer pairs used for each gene were as follows: Gfer, 5′-GCCTGCACAATGAGGT-3′ and 5′-GGCTCAGATGCACTTTAAT-3′; Gstm3, 5′CTCTGCCTACATGAAGAG-3′ and 5′-GGAGAGAGAACCGGGA-3′; Psma3, 5′-CATTAGCAGACATAGCGAG-3′ and 5′-ATCACGGCAAGTCATTT-3′; Casp9, 5′-AGAACGACCTGACTGC-3′ and 5′-CTCCCGTTGAAGATATTCAC-3′; Cflar, 5′-TGGAATACCGTGACAGTC-3′ and 5′-CTTGCAT-

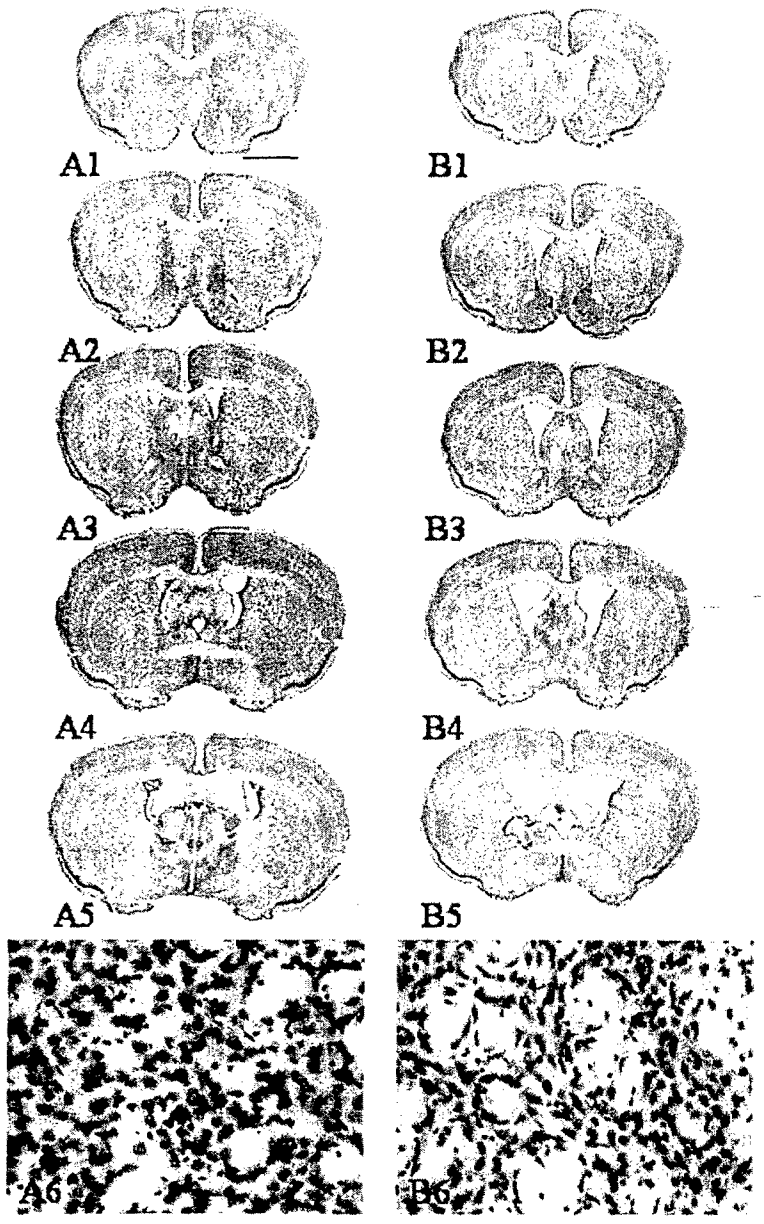

FIG. 2. **Gross brain and histopathological neuroprotection with phenylbutyrate treatment.** Photomicrographs of coronal serial sections through the rostral neostriatum at the level of the anterior commissure in phenylbutyrate-treated (*A1–5*) and PBS-treated (*B1–5*) N171-82Q HD transgenic mice at 120 days. There was gross atrophy of the brain in the PBS-treated N171-82Q mice along with ventricular enlargement. In contrast, the phenylbutyrate-treated N171-82Q mice at 120 days (*A*) show significantly less atrophy and ventricular enlargement than the PBS-treated N171-82Q mice. Corresponding Nissl-stained tissue sections from the dorso-medial aspect of the neostriatum in phenylbutyrate-treated (*A6*) and PBS-treated mice (*B6*) showed marked neuronal atrophy in the PBS-treated N171-82Q mice. *Scale bars* in *A* and *B* equal 2 mm, except A6 and B6 equal 100 μm.

ATCGGCGAAC-3′; Prkce, 5′-AAACACCCTTATCTAACCCA-3′ and 5′-AGATCACTCCGTGCTG-3′; glyceraldehyde-3-phosphate dehydrogenase, 5′-AGAGCTGAACGGGAAG-3′ and 5′-GTTGAAGTCGCAGGAG-3′.

Data Analysis—Data were expressed as the mean ± S.E. Statistical comparisons of rotarod, weight data, bioassay, and histological data were compared by analysis of variance or repeated measures analysis of variance. Survival data were analyzed using Kaplan-Meier survival curves and the Mantel-Cox log-rank test.

RESULTS

Systemic administration of phenylbutyrate at a dose of 100 mg/kg intraperitoneal 6 days per week starting at 75 days of age produced a significant increase in survival of 23% in the N171-82Q transgenic mouse model of HD (Fig. 1) ($p < 0.0001$). Life span was 153.2 ± 4.8 days in the phenylbutyrate-treated mice and 124.5 ± 5.4 days in mice that received vehicle.

Surprisingly, phenylbutyrate treatment had no significant effects on weight loss or on motor performance as assessed by rotarod performance in the N171-82Q mice (data not shown). This contrasts with findings using other therapeutic interventions including creatine and minocycline, in which improved survival is accompanied by improved motor performance and delayed weight loss (18). Treatment with another HDAC inhibitor, SAHA, before onset of symptoms ameliorated rotarod deficits, but had no effect on grip strength (12). Treatment with sodium butyrate starting at 21 days of age improved both rotarod performance and weight loss (13). The lack of beneficial effects on motor symptoms in the present study may reflect the fact that therapy was initiated after symptom onset.

Histopathologic studies in brains of treated and untreated mice were performed at both 100 and 120 days of age. These studies showed a significant attenuation of gross brain atrophy and ventricular enlargement, as well as neuronal atrophy after phenylbutyrate treatment, which was significant at 120 days (Fig. 2). At 120 days the total brain volume in the phenylbutyrate-treated mice was 21.6% greater than in PBS ($p < 0.01$) and the ventricular volume was 82.4% less ($p < 0.001$). Whereas marked striatal neuron atrophy was present in untreated N171-82Q mice at 120 days, phenylbutyrate treatment significantly reduced striatal neuron atrophy in N171-82Q mice (wild-type littermate control: 143.9 ± 11.9 μm^2; phenylbutyrate-treated N171-82Q mice: 116.5 ± 17.5 μm^2; PBS-treated N171-82Q mice: 54.2 ± 25.3 μm^2; $F_{3,15} = 12.85$; phenylbutyrate *versus* PBS, $p < 0.01$). The numbers of Htt and

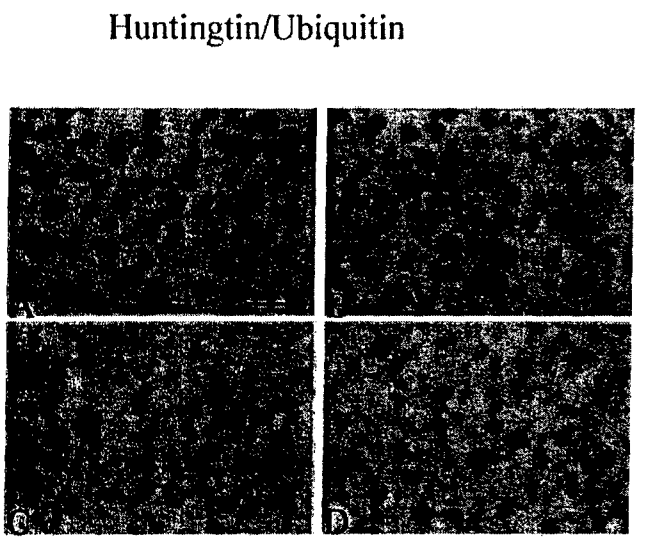

FIG. 3. **Huntingtin and ubiquitin immunoreactivity in phenylbutyrate-treated N171-82Q mice.** Huntingtin-immunostained tissue sections from the neostriatum of PBS-treated (*A*) and phenylbutyrate-treated N171-82Q mice at 120 days (*B*) show no difference in the number and size of huntingtin aggregates and inclusions between treated and untreated mice. Similarly, there were no differences in ubiquitin-positive inclusions between PBS-treated and phenylbutyrate-treated N171-82Q mice (*C* and *D*, respectively). *Scale bar* in *A* equals 50 μm and corresponds to all photomicrographs.

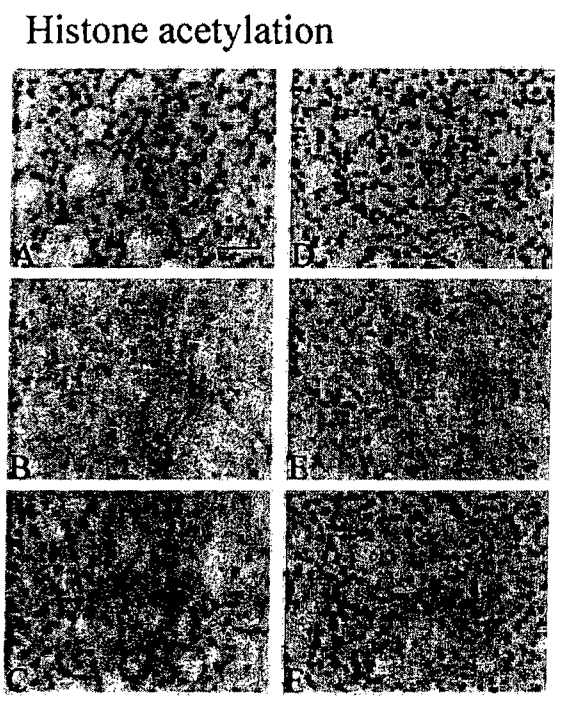

FIG. 4. **Striatal tissue immunohistochemistry of acetylated histone 3 and 4 in phenylbutyrate-treated N171-82Q mice.** Robust acetylated histone 3 and 4 immunohistochemistry was present in wild-type littermate control striatal tissue specimens (*A* and *D*, respectively), with hypoacetylation in the N171-82Q mice (*B* and *E*, respectively). Phenylbutyrate treatment increased acetylation of histone 3 and 4 in N171-82Q mice (*C* and *F*, respectively). *Bar* in *A* equals 100 μm and applies to all figures.

ubiquitin-stained aggregates were unaltered by phenylbutyrate administration (Fig. 3) (Huntingtin aggregates in phenylbutyrate-treated N171-82Q mice: $3.25 \times 10^6 \pm 1.11$; PBS-treated N171–82Q mice: $3.11 \times 10^6 \pm 1.02$, $F_{2,10} = 1.09$; $p < 0.38$). These results are similar to observations with sodium butyrate in the R6/2 transgenic mouse model of HD (13). Treatment with SAHA had no effect on numbers of aggregates and gross morphology, but showed a tendency to reduce neuronal atrophy (12). To verify that the effects we observed were because of an increase in histone acetylation, we performed both immunocytochemistry and Western blots. Administration of phenylbutyrate for 2 weeks increased immunostaining for both acetylated histone H3 and histone H4 in striatal neurons (Fig. 4). Administration of phenylbutyrate at 100 mg/kg increased histone acetylation in the spleen (not shown) and brain at 2 h post-administration (Fig. 5). Another histone modification that can repress gene transcription is methylation of lysine 9 on histone 3. Using immunocytochemistry we found a marked increase in methylation of histone 3 in the striatum at 120 days of age, which was markedly attenuated by phenylbutyrate treatment (Fig. 6). This finding was confirmed by Western blots (Fig. 7). We verified that phenylbutyrate dose dependently inhibited histone deacetylase activity in *vitro* with an IC_{50} of ~10 mM.

We also examined the effects of phenylbutyrate on gene expression levels using Affymetrix gene arrays. Phenylbutyrate was administered for 2 weeks starting at 75 days of age to 5 N171-82Q mice, whereas 5 mice received vehicle. Transcription products in striatum of the two groups were compared (Table I). To validate the alterations of gene expression at the mRNA level, which appeared on the microarray, real-time RT-PCR was performed using a LightCycler thermal cycler system (Fig. 8). Expression of selected genes (*Gfer*, *Gstm3*, and *Psma3*) were significantly up-regulated after phenylbutyrate treatment compared with controls ($p < 0.05$), whereas the other genes (*Casp9*, *Cflar*, and *Prkce*) showed significantly lower expression after phenylbutyrate treatment than in controls ($p < 0.05$). Because caspase 9 is involved in activation of caspase 3, and is increased in HD patients, we examined caspase 3 immunoactivity at 120 days of age (19) (Fig. 9). It was markedly increased in the striatum of the N171-82Q mice as compared with controls, similar to the observations in the R6/2 mice. The increase was markedly attenuated by phenylbutyrate treatment.

DISCUSSION

There is substantial evidence that impaired gene transcription plays a role in the pathogenesis of HD. Prior studies showed that treatment with HDAC inhibitors is effective in attenuating polyglutamine toxicity *in vitro* (10, 11). Treatment with HDAC inhibitors arrests ongoing progressive neuronal degeneration is a *Drosophila* model of polyglutamine neurotoxicity (8). The HDAC inhibitor SAHA was recently shown to improve motor function in the R6/2 transgenic mouse model of HD (12), and sodium butyrate improves motor function and exerts neuroprotective effects in this model when administered presymptomatically (13).

In the present study we administered the HDAC inhibitor phenylbutyrate to the N171-82Q transgenic mouse model of HD. N171-82Q mice express a cDNA encoding a 171-amino acid N-terminal fragment of huntingtin exon 1 containing 82 CAG repeats (20). The mice develop tremors, progressive weight loss, incoordination, and abnormal hind limb clasping by 3 to 4 months of age, and die prematurely at 4–6 months of age (18, 20). Mice appear normal for the first 2 months of life, but the initial phenotypic abnormality is failure to gain weight from 2 months onwards. Striatal *N*-acetylaspartate concentration is reduced as early as 50 days of age (indicating neuronal dysfunction), and abnormal systemic glucose tolerance occurs by 75 days of age (18, 21). Significant reductions in gene expression include reductions in dopamine D2 receptors, adenosine A2a receptors, and adenylyl cyclase (4). Diffuse nuclear accumulation of Htt and rare nuclear aggregates as well as cytoplasmic aggregates occur as early as 4 weeks of age (20). There

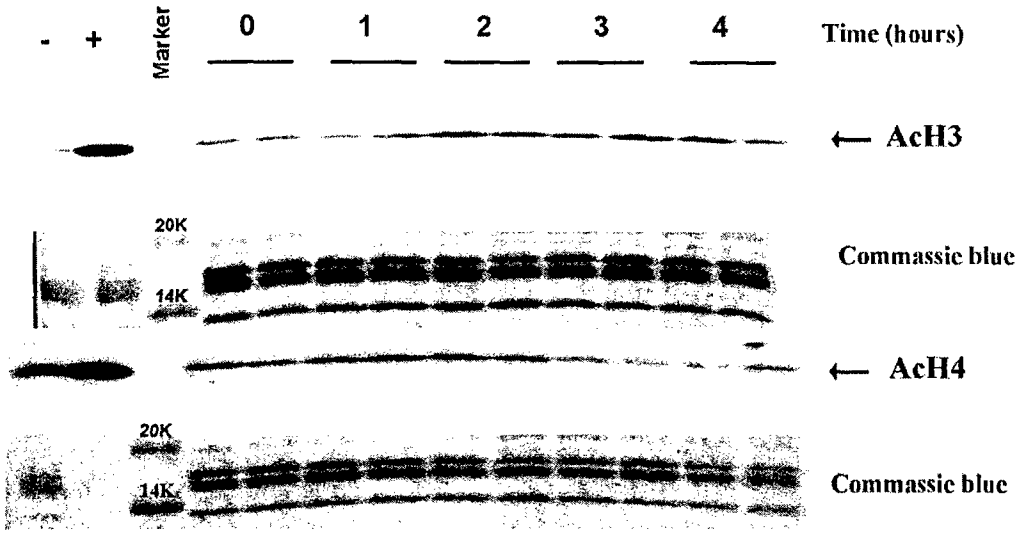

FIG. 5. **Western blots showing the effects of phenylbutyrate treatment (100 mg/kg intraperitoneal) on histone acetylation in the brain of N171-82Q at 0, 1, 2, 3, and 4 h after administration.** There were significant increases in acetylated histones 3 (*AcH3*) and 4 (*AcH4*) at 2 h ($p < 0.05$, analysis of variance followed by Newman-Keuls). Control histones from untreated (−) or sodium butyrate-treated (+) HeLa cells were used as a positive control for histone acetylation detection (lanes − and +, respectively).

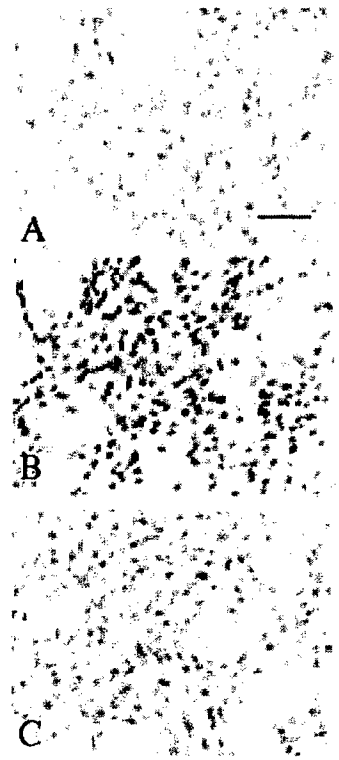

FIG. 6. **Striatal tissue immunohistochemistry for methylation of lysine 9 in histone 3 at 120 days of age.** The immunocytochemical staining for methylation is markedly increased in the N171-82Q mice (*B*) as compared with wild-type controls (*A*). Phenylbutyrate markedly attenuated the increase in methylation (*C*). *Bar* in *A* equals 100 μm and applies to all figures.

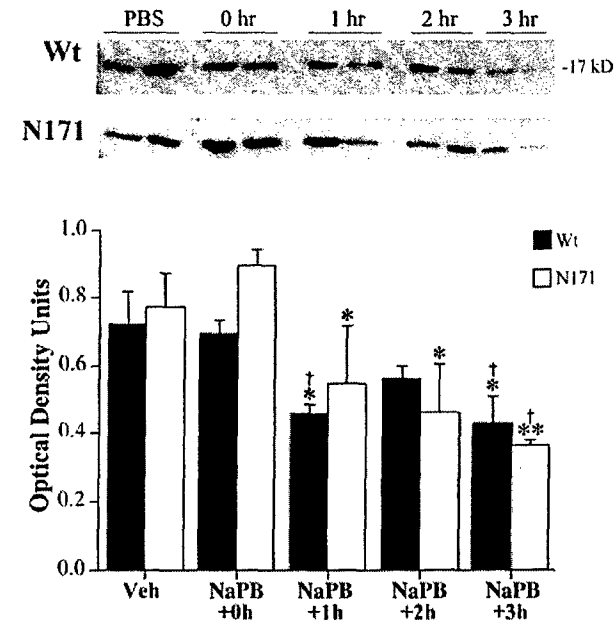

FIG. 7. **Western blots showing the effects of phenylbutyrate treatment on histone methylation in the brain of N171-82Q mice and age-matched wild-type (*Wt*) mice at 0, 1, 2, and 3 h after administration, or 3 h after vehicle (PBS).** There was a significant decrease in histone methylation at 2 and 3 h after phenylbutyrate (*PBA*) administration. *, $p < 0.05$; **, $p < 0.01$, significant difference between phenylbutyrate. PBA-treated mice and control mice were sacrificed immediately after PBA injection (*PBA + 0 h*); † $p < 0.05$, significant difference relevant to vehicle (*Veh*, *PBS*)-injected mice. $n = 4$/group.

are degenerating neurons as assessed by caspase staining, terminal deoxynucleotidyl transferase-mediated UTP nick end labeling, and electron microscopy (22).

We found that administration of phenylbutyrate starting at 75 days of age produced a significant 23% improvement in survival. This is particularly impressive because we started therapy at 75 days, which is a time point after which the N171-82Q mice have shown initial symptoms (20, 23). Administration of other therapies is much less effective when initiated after onset of symptoms. Administration of a combination of coenzyme Q_{10} and remacemide to N171-82Q mice from 21 days of age extended survival by 17% and improved motor performance (24), however, when this dosing regimen was initiated at 56 days of age motor performance deterioration was delayed, but there was no beneficial effect on survival (25). Creatine administration in the N171-82Q mice improved survival by 19% when administered from 28 days of age (18), however, it is much less effective when treatment is initiated after the onset of symptoms in the R6/2 transgenic mouse model of HD (26).

TABLE I
Selected mRNA changes in the striatum of phenylbutyrate-treated N171-82Q mice

Gene	GenBank™ accession number	Expression pattern	*p* value	Description	Chromosome location	Affymetrix probe set ID
Ccl27	AW124975	Induced	0.0088	Chemokine (C-C motif) ligand 27	412.7 cM	100972_s_at
Sybl1	X96737	Induced	0.0157	Synaptobrevin like 1	X 0.5 cM	102885_at
Lypla1	A1875934	Induced	0.0318	Lysophospholipase 1	1 A1	97207_f_at
Gfer	U40494	Induced	0.0342	Growth factor, erv1 (augmenter of liver regeneration)	1710.0 cM	160269_at
Gstm3	J03953	Induced	0.0435	Glutathione *S*-transferase	3	97682_r_at
Strn3	AW124985	Induced	0.0067	sTriatin, calmodulin-binding protein 3	12 C1	100878_at
Cdv3	A1837005	Induced	0.0069	Carnitine deficiency associated gene expressed in ventricle 3	9	160326_at
Usp29	AA673236	Induced	0.0191	Ubiquitin-specific protease 29	76.5 cm	96433_at
Psma3	AF055983	Induced	0.0121	Proteasome (prosome, macropain) subunit, α type 3	3	92544_f_at
Tcerg1	AB023485	Induced	0.0039	Transcription elongation regulator 1 (CA150)	18 B3	101008_at
Psmc3	AA409481	Induced	0.0129	Proteasome (prosome, macropain) 26 S subunit, ATPase 3	247.0 cm	100225_f_at
Casp9	AB019600	Repressed	0.0494	Caspase 9	4 E1	100367_g_at
Ephx1	U89491	Repressed	0.0004	Epoxide hydrolase 1, microsomal	198.5 cm	101587_at
Prkce	AF028009	Repressed	0.0409	Protein kinase C	17 E4	94161_at
Cflar	Y14041	Repressed	0.0190	CASP8 and FADD-like apoptosis regulator	130.1 cm	103217_at
Psmd10	AB022022	Repressed	0.0126	Proteasome (prosome, macropain) 26 S subunit, non-ATPase, 10	X F1	103319_at
Stk10	D89728	Repressed	0.0453	Serine/threonine kinase 10	1116.0 cm	93680_at

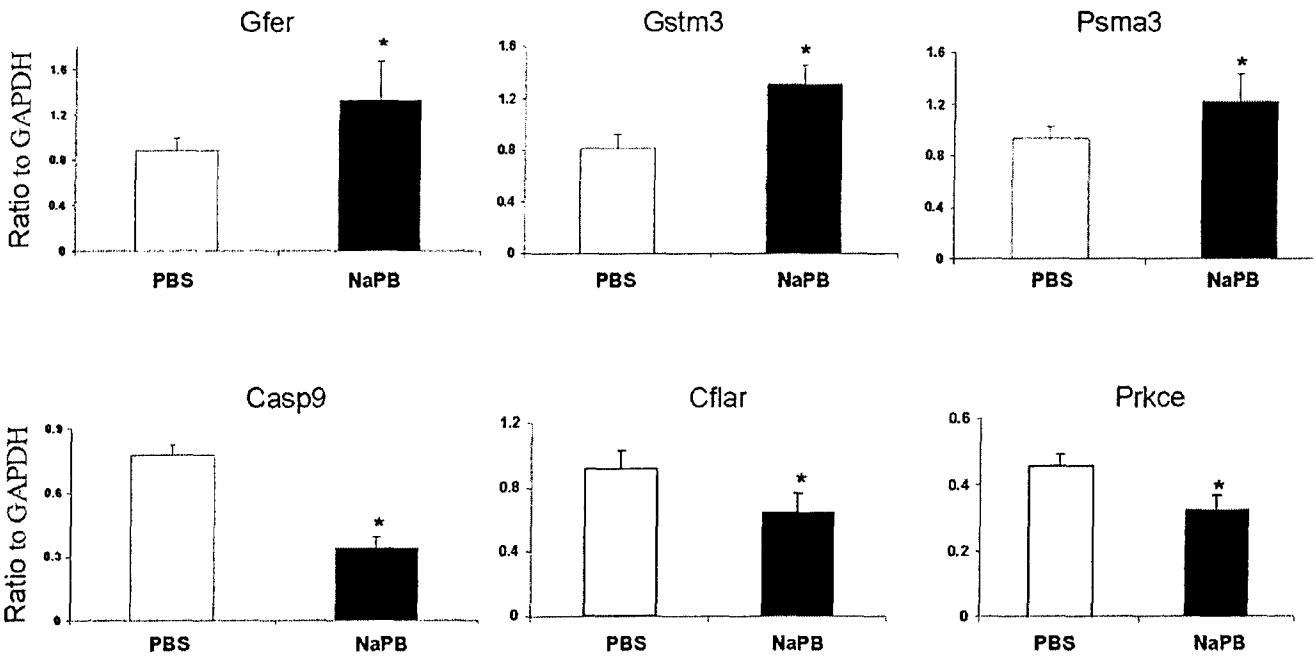

FIG. 8. **Quantitative real-time RT-PCR analysis of genes identified by microarray analysis as differentially expressed.** Total RNA was extracted and real-time RT-PCR was performed with SYBR Green I dye using a LightCycler thermal cycler system. The expression level is shown as the weight ratio of the target gene to glyceraldehyde-3-phosphate dehydrogenase (*GAPDH*); *Gfer* (growth factor), *Gstm3* (glutathione *S*-transferase), *Psma3* (proteasome subunit, α type 3), *Casp9* (caspase 9), *Cflar* (*CASP8* and Fas-activated death domain-like apoptosis regulator), and *Prkce* (protein kinase C). Data are mean ± S.E. for 4–5 samples; calculated by the comparative cycle threshold method. *, $p < 0.05$, compared with PBS-injected mice.

The finding that phenylbutyrate is effective in symptomatic transgenic HD mice is consistent with observations in a *Drosophila* model of polyglutamine toxicity, which showed that HDAC inhibitors were neuroprotective even when administered to animals already exhibiting neurodegeneration (8). In addition, phenylbutyrate extends the lifespan in wild-type *Drosophila* when administered late in life (27). These observations suggest that phenylbutyrate administration may be beneficial to HD patients after onset of symptoms. Surprisingly, there were no significant effects on weight loss or motor deficits, which may reflect the fact that therapy was initiated after symptom onset. Similarly, SAHA did not effect weight loss, although it improved both rotarod performance and grip strength when administered presymptomatically (12).

Histopathologic studies of phenylbutyrate in the N171-82Q mice showed a trend toward reduced atrophy at 100 days of age. At 120 days of age there was a significant reduction in gross brain atrophy, ventricular enlargement, and striatal neuron atrophy. Presymptomatic treatment with sodium butyrate also attenuates brain atrophy, ventricular enlargement, and striatal neuron atrophy (13). Interestingly, phenylbutyrate treatment had no effect on huntingtin and ubiquitin-stained aggregates, which is consistent with observations made with SAHA and sodium butyrate (12, 13). The effects of HDAC

FIG. 9. **Striatal tissue immunocytochemistry for active caspase 3 at 120 days of age.** The immunocytochemical staining for active caspase 3 is markedly increased in the N171-82Q mice (*B*) as compared with wild-type controls (*A*). Phenylbutyrate markedly attenuated the increase in active caspase 3 immunoreactivity (*C*). *Bar* in *A* equals 100 μm and applies to all figures.

inhibitors contrast with the therapeutic effects of agents such as creatine, coenzyme Q_{10} with remacemide, and cystamine, which significantly reduce numbers of Htt immunoreactive aggregates (18, 24, 28). Minocycline and dichloroacetate also increase survival in transgenic HD mice, without altering aggregate load (29, 30). Our findings therefore provide further evidence that therapeutic effects in transgenic mouse models of HD can occur independently of effects on aggregate deposition.

We verified that phenylbutyrate increases acetylation of both histone H3 and histone H4 in the brains of treated mice using both immunocytochemistry and Western blots. We also examined histone methylation. Whereas histone acetylation is thought to relax the chromatic structure leading to increased gene transcription, subsequent histone methylation (particularly on lysine 9 of histone 3) leads to transcriptional repression, assisting termination of gene transcription (31). Prior studies showed an interaction between histone deacetylases and histone methyltransferases that repress transcription (32, 33). DNA methyltransferases that repress transcription also interact with histone deacetylases (34, 35). We show for the first time a marked increase in methylation of lysine 9 of histone H3 in symptomatic N171-82Q mice relative to wild-type levels, which was markedly attenuated by treatment with phenylbutyrate. The finding suggests that phenylbutyrate mediates its effects by both increasing histone acetylation as well as reducing histone methylation, thereby increasing expression of genes critical to cell survival. We also examined the effects of phenylbutyrate on gene expression levels. Genes that showed significant increases in expression following phenylbutyrate administration included glutathione *S*-transferase, striatin calmodulin-binding protein 3, ubiquitin-specific protease 29, proteosome subunit α type 3 and the proteosome 26 S subunit (*ATPase 3*), whereas caspase 9, caspase 8/FADD-like apoptosis regulator, and proteasome 26 S subunit (non-*ATPase 10*) were significantly decreased. Consistent with the up-regulation of caspase 9, active caspase 3 was also increased in the striatum, and this increase was attenuated by phenylbutyrate treatment. Because aberrant protein degradation and apoptosis are implicated in HD pathogenesis, these alterations may contribute to the therapeutic effects of phenylbutyrate (36, 37).

Our findings show that administration of the HDAC inhibitor phenylbutyrate exerts neuroprotective effects and increases survival in symptomatic HD transgenic mice, supporting studies in which HDAC inhibitors were administered presymptomatically (12, 13). The findings are robust and the 23% increase in survival is the best overall therapeutic effect yet reported in the N171-82Q HD model. The effects of this HDAC inhibitor are consistent with findings both in cell culture models and in *Drosophila* models of polyglutamine toxicity (8, 10, 11, 38), and are also consistent with reports that overexpression of several transcription factors including CBP, $TAF_{11}130$, and Sp1 can abrogate cell death produced by proteins containing polyglutamine expansions *in vitro* (7, 39, 40). In addition, a recent study showed that HDAC inhibitors can prevent oxidative neuronal death via an Sp1 dependent pathway (41), which is of particular interest with regard to HD mouse models because we and others found evidence of increased oxidative damage in HD transgenic mice (42–44).

Phenylbutyrate is a particularly promising agent for therapeutic trials in man because of extensive experience with its use in patients for treatment of urea cycle disorders, sickle cell anemia, thalassemia minor, and cystic fibrosis (45–47). Patients with ornithine transcarbamylase deficiency have been treated long-term with doses of phenylbutyrate between 350 and 600 mg/kg/day without significant side effects (48, 49). Phase one trials in cancer patients showed good tolerability at doses of 400–500 mg/kg/day (50, 51). Our effective dose of 100 mg/kg/day in mice is therefore well within the tolerable range. These findings suggest that phenylbutyrate is an extremely promising agent for treatment of HD.

Acknowledgments—The secretarial assistance of Greta Strong, Connie Boyd, and Sharon Melanson is gratefully acknowledged. Holly Burr, Victor Howard, and Patrick Strout are thanked for essential technical assistance. We thank Zhaoying Xiang for advice on microarray data analysis. Chris Ross, David Borchelt, and Gabrielle Schilling are thanked for providing the N171-82Q mice.

REFERENCES

1. Cha, J. H. (2000) *Trends Neurosci.* **23,** 387–392
2. La Spada, A. R., Fu, Y. H., Sopher, B. L., Libby, R. T., Wang, X., Li, L. Y., Einum, D. D., Huang, J., Possin, D. E., Smith, A. C., Martinez, R. A., Koszidin, K. L., Treuting, P. M., Ware, C. M., Hurley, J. B., Ptacek, L. J., and Chen, S. (2001) *Neuron* **31,** 913–927
3. Lin, X., Antalffy, B., Kang, D., Orr, H. T., and Zoghbi, H. Y. (2000) *Nat. Neurosci.* **3,** 157–163
4. Luthi-Carter, R., Strand, A., Peters, N. L., Solano, S. M., Hollingsworth, Z. R., Menon, A. S., Frey, A. S., Spektor, B. S., Penney, E. B., Schilling, G., Ross, C. A., Borchelt, D. R., Tapscott, S. J., Young, A. B., Cha, J. H., and Olson, J. M. (2000) *Hum. Mol. Genet.* **9,** 1259–1271
5. Kazantsev, A., Preisinger, E., Dranovsky, A., Goldgaber, D., and Housman, D. (1999) *Proc. Natl. Acad. Sci. U. S. A.* **96,** 11404–11409
6. Steffan, J. S., Kazantsev, A., Spasic-Boskovic, O., Greenwald, M., Zhu, Y. Z., Gohler, H., Wanker, E. E., Bates, G. P., Housman, D. E., and Thompson, L. M. (2000) *Proc. Natl. Acad. Sci. U. S. A.* **97,** 6763–6768
7. Nucifora, F. C., Jr., Sasaki, M., Peters, M. F., Huang, H., Cooper, J. K., Yamada, M., Takahashi, H., Tsuji, S., Troncoso, J., Dawson, V. L., Dawson, T. M., and Ross, C. A. (2001) *Science* **291,** 2423–2428
8. Steffan, J. S., Bodai, L., Pallos J., Poelman, M., McCampbell, A., Apostol, B. L., Kazanstev, A., Schmidt, E., Zhu, Y. Z., Greenwald, M., Kurokawa, R., Housman, D. E., Jackson G. R., Marsh, J. L., and Thompson, L. M. (2001) *Nature* **413,** 739–743
9. Obrietan, K., and Hoyt, K. R. (2004) *J. Neurosci.* **24,** 791–796
10. Hughes, R. E., Lo, R. S., Davis, C., Strand, A. D., Neal, C. L., Olson, J. M., and Fields, S. (2001) *Proc. Natl. Acad. Sci. U. S. A.* **98,** 13201–13206
11. McCampbell, A., Taye, A. A., Whitty, L., Penney, E., Staffan, J. S., and Fischbeck, K. H. (2001) *Proc. Natl. Acad. Sci. U. S. A.* **98,** 15179–15184
12. Hockly, E. Richon, V. M., Woodman, B., Smith, D. L., Zhou, X., Rosa, E., Sathasivam, K., Ghazi-Noori, S., Mahal, A., Lowden, P. A., Steffan, J. S.,

Marsh, J. L., Thompson, L. M., Lewis, C. M., Marks, P. A., and Bates, G. P. (2003) *Proc. Natl. Acad. Sci. U. S. A.* **100,** 2041–2046
13. Ferrante, R. J., Kubilus, J. K., Lee, J., Ryu, H., Beesen, A., Zucker, B., Smith, K., Kowall, N. W., Ratan, R. R., Luthi-Carter, R., and Hersch, S. M. (2003) *J. Neurosci.* **23,** 9418–9427
14. Richon, V. M., Zhou, X., Rifkind, R. A., and Marks, P. A. (2001) *Blood Cells Mol. Dis.* **27,** 260–264
15. Ausubel, F. M., Brent, R., Kingston, R. E., Moore, D. D., Seidman, J. G., Smith, J. A., and Struhl, K. (eds) (2000) *Current Protocols in Molecular Biology*, pp. 61–111, Wiley, New York
16. Warrell, R. P., Jr., He, L. Z., Richon, V., Calleja, E., and Pandolfi, P. P. (1998) *J. Natl. Cancer Inst.* **90,** 1621–1625
17. Richon, V. M., Sandhoff, T. W., Rifkind, R. A., and Marks, P. A. (2000) *Proc. Natl. Acad. Sci. U. S. A.* **97,** 10014–10019
18. Andreassen, O. A., Dedeoglu, A., Ferrante, R. J., Jenkins, B. G., Ferrante, K. L., Thomas, M., Friedlich, A., Browne, S. E., Schilling, G., Borchelt, D. R., Hersch, S. M., Ross, C. A., and Beal, M. F. (2001) *Neurobiol. Dis.* **8,** 479–491
19. Kiechle, T., Dedeoglu, A., Kubilus, J., Kowall, N. W., Beal, M. F., Friedlander, R. M., Hersch, S. M., and Ferrante, R. J. (2002) *Neuromol. Med.* **1,** 183–195
20. Schilling, G., Becher, M. W., Sharp, A. H., Jinnah, H. A., Duan, K., Kotzuk, J. A., Slunt, H. H., Ratovitski, T., Cooper, J. K., Jenkins, N. A., Copeland, N. G., Price, D. L., Ross, C. A., and Borchelt, D. R. (1999) *Hum. Mol. Genet.* **8,** 397–407
21. Jenkins, B. G., Andreassen, O. A., Dedeoglu, A., Leavitt, B., Hayden, M., Borchelt, D., Ross, C. A., Detloff, P., Ferrante, R. J., and Beal, M. F. (2004) *J. Neurochem.*, in press
22. Yu, Z. X., Li, S. H., Evans, J., Pillarisetti, A., Li, H., and Li, X. J. (2003) *J. Neurosci.* **23,** 2193–2202
23. Schilling, G., Jinnah, H. A., Gonzales, V., Coonfield, M. L., Kim, Y., Wood, J. D., Price, D. L., Li, X. J., Jenkins, N., Copeland, N., Moran, T., Ross, C. A., and Borchelt, D.R. (2001) *Neurobiol. Dis.* **8,** 405–418
24. Ferrante, R. J., Andreassen, O.A., Dedeoglu, A., Ferrante, K. L., Jenkins, B. G., Hersch, S. M., and Beal, M. F. (2002) *J. Neurosci.* **22,** 1592–1599
25. Schilling, G., Coonfield, M. L., Ross, C. A., and Borchelt, D. R. (2001) *Neurosci. Lett.* **315,** 149–153
26. Dedeoglu, A., Kubilus, J. K., Ferrante, K. L., Hersch, S. M., Beal, M. F., and Ferrante, R.J. (2003) *J. Neurochem.* **85,** 1459–1471
27. Kang, H.-L., Benzer, S., and Min, K.-T. (2002) *Proc. Natl. Acad. Sci. U. S. A.* **99,** 839–843
28. Dedeoglu, A., Kubilus, J. K., Jeitner, T. M., Matson, S. A., Bogdanov, M., Kowall, N. W., Matson, W. R., Cooper, A. J., Ratan, R. R., Beal, M. F., Hersch, S. M., and Ferrante, R. J., (2002) *J. Neurosci.* **22,** 8942–8950
29. Chen, M., Ona, V. O., Li, M., Ferrante, R. J., Fink, K. B., Zhu, S., Bian, J., Guo, L., Farrell, L. A., Hersch, S. M., Hobbs, W., Vonsattel, J.-P., Cha, J.-H. J., and Friedlander, R. M. (2000) *Nat. Med.* **6,** 797–801
30. Andreassen, O. A., Ferrante, R. J., Huang, H. M., Dedeoglu, A., Park, L., Ferrante, K. L., Kwon, J., Borchelt, D. R., Ross, C. A., Gibson, G. E., and Beal, M. F. (2001) *Ann. Neurol.* **50,** 112–117
31. Zhang, Y., and Reinberg, D. (2001) *Genes Dev.* **15,** 2343–2360
32. Pal, S., Yun, R., Datta, A., Lacomis, L., Erdjument-Bromage, H., Kumar, J., Tempst, P., and Sif, S. (2003) *Mol. Cell. Biol.* **23,** 7475–7487
33. Gui, C. Y., Ngo, L., Xu, W. S., Richon, V. M., and Marks, P. A. (2004) *Proc. Natl. Acad. Sci. U. S. A.* **101,** 1241–1246
34. Deplus, R., Brenner, C., Burgers, W. A., Putmans, P., Kouzarides, T., de Launoit, Y., and Fuks, F. (2002) *Nucleic Acids Res.* **30,** 3831–3838
35. Sekimata, M., Takahashi, A., Murakami-Sekimata, A., and Homma, Y. (2001) *J. Biol. Chem.* **276,** 42632–42638
36. Friedlander, R. M. (2003) *N. Engl. J. Med.* **348,** 1365–1375
37. Jana, N. R., Zemskov, E. A., Wang, G. H., and Nukina, N. (2001) *Hum. Mol. Genet.* **10,** 1049–1059
38. Taylor, J. P., Taye, A. A., Campbell, C., Kazemi-Esfarjani, P., Fischbeck, K. H., and Min, K-T. (2003) *Genes Dev.* **17,** 1463–1468
39. Dunah, A. W., Jeong, H., Griffin, A., Kim, Y. M., Standaert, D. G., Hersch, S. M., Mouradian, M. M., Young, A. B., Tanese, N., and Krainc, D. (2002) *Science* **296,** 2238–2243
40. Shimohata, T., Nakajima, T., Yamada, M., Uchida, C., Onodera, O., Naruse, S., Kimura, T., Koide, R., Nozaki, K., Sano, Y., Ishiguro, H., Sakoe, K., Ooshima, T., Sato, A., Ikeuchi, T., Oyake, M, Sato, T., Aoyagi, Y., Hozumi, I., Nagatsu, T., Takiyama, Y., Nishizawa, M., Goto, J., Kanazawa, I., Davidson, I., Ranese, N., Takahashi, H., and Tsuji, S. (2000) *Nat. Genet.* **26,** 29–36
41. Ryu, H., Lee, J., Olofsson, B. A., Mwidau, A., Dedeoglu, A., Escudero, M., Flemington, E., Azizkhan-Clifford, J., Ferrante, R. J., and Ratan, R. R. (2003) *Proc. Natl. Acad. Sci. U. S. A.* **100,** 4281–4286
42. Bogdanov, M. B., Andreassen, O. A., Dedeoglu, A., Ferrante, R. J., and Beal, M. F. (2001) *J. Neurochem.* **79,** 1246–1249
43. Perez-Serviano, F., Rios, C., and Segovia, J. (2000) *Brain Res.* **862,** 234–237
44. Tabrizi, S. J., Workman, J., Hart, P. E., Mangiarini, L., Mahal, A., Bates, G., Cooper, J. M., and Schapira, A. H. (2000) *Ann. Neurol.* **47,** 80–86
45. Dover, G. J., Brusilow, S., and Charache, S. (1994) *Blood* **84,** 339–343
46. Hoppe, C., Vichinsky, E., Lewis, B., Foote, D., and Styles, L. (1999) *Am. J. Hematol.* **62,** 221–227
47. Rubenstein, R. C., and Zeitlin, P. L. (1998) *Am. J. Respir. Crit. Care Med.* **157,** 484–490
48. Burlina, A. B., Ogier, H., Korall, H., and Trefz, F. K. (2001) *Mol. Genet. Metab.* **72,** 351–355
49. Maestri, N. E., Brusilow, S. W., Clissold, D. B., and Bassett, S. S. (1996) *N. Engl. J. Med.* **335,** 855–859
50. Carducci, M. A., Gilbert, J., Bowling, M. K., Noe, D., Eisenberger, M. A., Sinibaldi, V., Zabelina, Y., Chen, T. L., Grochow, L. B., and Donehower, R. C. (2001) *Clin. Cancer Res.* **7,** 3047–3055
51. Gilbert, J., Baker, S. D., Bowling, M. K., Grochow, L., Figg, W. D., Zabelina, Y., Donehower, R. C., and Carducci, M. A. (2001) *Clin. Cancer Res.* **7,** 2292–2300

APPENDIX 4

Neurochemical Research, Vol. 30, No. 10, October 2005 (© 2005), pp. 1245–1255
DOI: 10.1007/s11064-005-8796-x

Mitochondrial Aconitase is a Transglutaminase 2 Substrate: Transglutamination is a Probable Mechanism Contributing to High-Molecular-Weight Aggregates of Aconitase and Loss of Aconitase Activity in Huntington Disease Brain*

Soo-Youl Kim,[1,4,7] Lyuben Marekov,[5] Parvesh Bubber,[4] Susan E. Browne,[1] Irina Stavrovskaya,[4] Jongmin Lee,[1] Peter M. Steinert,[5,6] John P. Blass,[1,2,4] M. Flint Beal,[1] Gary E. Gibson,[1,4] and Arthur J. L. Cooper[1,3,4]

(Accepted May 10, 2005)

Transglutaminase activity was found to be present in highly purified non-synaptosomal rat brain mitochondria. A 78-kDa protein in these organelles was shown to be a transglutaminase 2 substrate, and incubation of a non-synaptosomal mitochondrial lysate with transglutaminase 2 yielded high-M_r proteins. The 78-kDa protein was identified as mitochondrial aconitase by MALDI-TOF analysis. Aconitase activity was decreased in a dose-dependent manner when non-synaptosomal rat brain mitochondria were incubated with transglutaminase 2. Transglutaminase activity is increased about 2-fold in the mitochondrial fraction of HD caudate. Moreover, Western blotting of the mitochondrial fraction revealed that most of the mitochondrial aconitase in HD caudate is present as high-M_r aggregates. Aconitase activity was previously shown to be decreased in Huntington disease (HD) caudate (a region severely damaged by the disease). The present findings suggest that an increase of transglutaminase activity in HD caudate may contribute to mitochondrial dysfunction by incorporating aconitase into inactive polymers.

KEY WORDS: Huntington disease; mitochondrial aconitase; non-synaptosomal mitochondria; transglutaminase.

* Special issue dedicated to Dr. Bernd Hamprecht.

[1] Department of Neurology and Neuroscience, Weill Medical College of Cornell University, New York, NY 10021, USA.
[2] Department of Medicine, Weill Medical College of Cornell University, New York, NY 10021, USA.
[3] Department of Biochemistry, Weill Medical College of Cornell University, New York, NY 10021, USA.
[4] Burke Medical Research Institute, White Plains, NY 10605, USA.
[5] Laboratory of Skin Biology, National Institute of Arthritis and Musculoskeletal and Skin Diseases, National Institutes of Health, Bethesda, MD 20892, USA.
[6] Deceased.
[7] Address reprints request to: Dr. S.-Y. Kim, Division of Basic Sciences, National Cancer Center, 809 Madu-dong, Ilsandong-gu, Goyang, Kyonggi-do 410-351, Republic of Korea. Tel: 82-31-920-2290 Fax: 82-31-920-2006.

INTRODUCTION

Transglutaminases (TGases) belong to a family of enzymes that catalyzes the Ca^{2+}-dependent nucleophilic addition of the ε-amino group of a lysyl residue (K) in a protein/polypeptide (acyl acceptor)

Abbreviations: Aco 1, cytosolic aconitase; Aco 2, mitochondrial aconitase; AD, Alzheimer disease; APP, amyloid precursor protein; DTT, dithiothreitol; GDH, glutamate dehydrogenase; GGEL, N^{ε}-(γ-L-glutamyl)-L- lysine; HD, Huntington disease; htt, huntingtin; KGDHC, α-ketoglutarate dehydrogenase complex; LDH, lactate dehydrogenase; PD, Parkinson disease; Q_n, polyglutamine domain; TCA, trichloroacetic acid; TFA, trifluoroacetic acid; TGase 2, transglutaminase type 2 also known as tissue transglutaminase.

to the carboxamide moiety of a glutaminyl (Q) residue of a protein/polypeptide substrate (acyl donor) to form an N^{ε}-(γ-L-glutamyl)-L-lysine (GGEL) isopeptide bond (cross-link) and ammonia (1). The GGEL linkage is a marker for TGase activity, and has been used for that purpose in the studies described below. Polyamines may also act as acyl acceptors (1).

Several lines of evidence suggest that aberrant TGase activity, although not causative, may contribute to the inexorable decline associated with several neurodegenerative diseases. For example, inherent TGase activity is increased in affected brain regions in several neurodegenerative diseases, including Huntington disease (HD) (2–4), Alzheimer disease (AD) (5–7), Parkinson disease (PD) (8) and supranuclear palsy (9). GGEL linkages have been detected in protein aggregates in AD- and HD brain (6,10,11), and free GGEL isodipeptide is increased in HD brain (10), HD CSF (12) and AD CSF (13). GGEL cross-links have also been detected in paired-helical filaments in AD brain (14). In a model system, Junn et al. (15) showed that protein deposits are formed when COS-7 cells and human embryonic kidney (HEK) 293T cells overexpressing α-synuclein (a component of protein aggregates in PD brain) are co-transfected with TGase 2. Overexpression of α-synuclein alone in COS-7 cells was not sufficient to induce formation of protein deposits (15). In addition, the formation of α-synuclein protein aggregates was increased by the Ca^{2+} ionophore A23187 and prevented by cystamine, an *in vitro* TGase inhibitor/alternative substrate (15). Previous studies have shown that cystamine treatment prolongs the lifespan and reduces associated tremor and abnormal movements in HD transgenic mice, possibly in part due to inhibition of TGase activity (3,10). Recently, Mandrusiak et al. (16) showed that the N terminus of the androgen receptor containing a Q_n repeat is an excellent Q and K substrate for TGase 2, forming cross-linked polymers. Mutation of the androgen receptor through elongation of a Q_n repeat causes spinobulbar muscular dystrophy. HEK GFP^u-1 cells expressing TGase 2 and mutated androgen receptor exhibited proteasome dysfunction (16). Moreover, GGEL cross-links were detected immunohistochemically in protein aggregates in the brains of spinobulbar muscular dystrophy transgenic mice, but not in the controls (16). Perhaps the most compelling evidence for a role of TGases in neurodegenerative disease is provided by the work of Mastroberardino et al. (17). These authors reported a reduction in neuronal cell death, improved behavior and prolonged survival in R6/1 (an HD-like model) × TGase $2^{-/-}$ (knockout) mice compared to R6/1 × TGase $2^{+/+}$ mice with intact TGase 2.

Several mechanisms have been suggested to explain how TGase activity might contribute to the pathogenesis of neurodegenerative diseases. One possibility is that TGase assists in the generation of insoluble protein deposits such as senile plaques, nuclear and cytosolic inclusions, and Lewy bodies (4,6,15,18,19) that may trigger a cytotoxic cascade. It has also been proposed that increased expression of TGase may escalate apoptosis (e.g., 20). Some evidence suggests that aberrant TGase 2 activity leads to mitochondrial dysfunction. For example, Piacentini et al. (20) showed that neuroblastoma (SK-N-BE(2)) and 3T3 fibroblast cells transfected with TGase 2 contain constitutively hyperpolarized mitochondria and increased reactive oxygen intermediates. When subjected to oxidative stress, these cells showed increased apoptosis. Piacentini et al. (20) suggested that TGase 2 may act as a 'sensitizer' to apoptosis.

A defect in mitochondrial energy metabolism leading to increased susceptibility to excitotoxic injury has been suggested as a potential mechanism contributing to the pathogenesis of HD (21–23). Activities of mitochondrial enzymes involved in oxidative phosphorylation (complex II–III and IV) are significantly reduced in the vulnerable regions of HD brain by the end-stage of the disease (22,23). Aconitase (Aco) activity is also reduced in the HD caudate and putamen (24). Administration of 3-nitropropionic acid (3-NPA), a mitochondrial toxicant that inhibits succinate dehydrogenase, causes a selective loss of medium spiny neurons in the striatum of rats and primates that is similar to HD neuropathology (25,26). Recent work shows that the mutant protein in HD (huntingtin, htt) which contains an expanded Q_n domain – or htt fragments containing the mutation – localizes with mitochondria in models of HD, and may contribute to abnormalities of Ca^{2+} influx and susceptibility of the mitochondria to a Ca^{2+}-induced permeability transition and cytochrome *c* release (27–29). However, the mechanism by which the mutated htt causes bioenergetic dysfunction remains unknown.

We have recently shown that mouse brain mitochondria contain TGase activity (30). In the present work we tested the possibility that mitochondrial proteins may be TGase substrates, thereby contributing to mitochondrial dysfunction in HD.

EXPERIMENTAL PROCEDURES

Reagents

NAD^+, $NADP^+$, dithiothreitol (DTT), thiamine pyrophosphate, sodium α-ketoglutarate, sodium pyruvate, leupeptin, succinylated casein, succinylated casein, sodium thiomalate, EDTA, EGTA, HEPES, ferrous ammonium sulfate, α-cyano-4-hydroxycinammic acid, trifluoroacetic acid (TFA), trichloroacetic acid (TCA), Tris, Tricine, Triton X-100, bovine serum albumin (BSA; fatty acid free), magnesium chloride, sodium citrate, bovine fibrinogen (plasma faction 1), semi-purified guinea pig liver TGase 2 (specific activity ~2 U/mg, where 1 U is 1 μmol of hydroxamate formed per min in a reaction mixture containing 100 mM hydroxylamine and 50 mM carbobenzoxy L-glutaminylglycine; 37°C), porcine heart isocitrate dehydrogenase ($NADP^+$) (20 U/mg), and lubrol PX were from Sigma (St. Louis, MO).

Preparation of Non-Synaptosomal Rat Brain Mitochondria

Non-synaptosomal rat brain mitochondria were prepared by the method of Lai et al. (31,32) with minor modifications. Briefly, 6 rats were decapitated and the forebrains were removed and rapidly placed in ice-cold isolation medium containing 320 mM sucrose, 0.5 mM EGTA, 10 mM HEPES, pH 7.4. The brain samples were minced, washed in isolation medium and homogenized in a loose fitting Dounce homogenizer with 90 ml of isolation medium. The brain homogenate was centrifuged for 3 min at 1300 *g* in a Beckman JA-17 rotor and the pellet was discarded. The supernatant was then centrifuged for 3 min at 1300 *g*. The supernatant from this step was then centrifuged at 17,000 *g* for 8 min. The resulting pellet, containing a crude mixture of mitochondria and synaptosomes, was re-suspended in 10 ml of isolation medium and layered onto a preformed Ficoll gradient (bottom layer, 7 ml 10% Ficoll; top layer 7 ml 7.5% Ficoll). The crude mitochondrial fraction was centrifuged at 99,000 *g* for 30 min in a swinging bucket rotor (Beckman SW-28). The pellet containing non-synaptosomal mitochondria was re-suspended in 15 ml of isolation media. The mitochondrial suspension was centrifuged at 17,000 *g* for 8 min. The resultant brown pellet was washed once with 7.5 ml of isolation buffer supplemented with 500 μg/ml BSA and centrifuged at 17,000 *g* for 8 min. The final pellet, the purified non-synaptosomal brain mitochondrial fraction, was re-suspended by gentle homogenization in 250 μl of buffer containing 320 mM sucrose, 20 μM EGTA, 10 mM HEPES, pH 7.4. The mitochondrial suspension was frozen at −20°C. Aco 2 (mitochondrial isozyme of aconitase) activity in this mitochondrial preparation is stable following at least one freeze-thaw cycle.

Preparation of a Mitochondrial Fraction from HD Brains

Tissue was obtained at post-mortem from caudate and frontal cortex (FCX) of eight HD patients (Vonsattel Grade 3 or 4) and eight age- and sex-matched non-diseased control patients. The tissues were obtained from the Harvard Brain Bank, and were from a subgroup we employed previously in studies that demonstrated oxidative damage and changes in metabolic enzyme in end-stage HD brain (23) [HD: 5 M, 3 F; age, 65.1 ± 0.9 y; post-mortem interval, 16.8 ± 2.3 h. Controls: 5 M, 3 F; age, 72.8 ± 6.7 y; post-mortem interval, 14.5 ± 3.8 h. There were no significant differences between the two groups with $P > 0.05$]. Tissue was stored at −80°C. Mitochondria were extracted from this tissue according to the method of Lai et al. (31,32). Briefly, brain tissue was homogenized on ice in isolation buffer containing 1 mM Tris HCl, 1 mM EDTA, 0.25 M sucrose, pH 7.4 (5 vol: 1 g tissue). Mitochondria were extracted by serial differential centrifugations, with application of the sub-cellular pellet to a Ficoll gradient. The resultant mitochondrial pellets were diluted to the appropriate protein concentration in isolation buffer and stored at −80°C. The freeze-thawing process might be expected to compromise the integrity of the mitochondria purified from the previously frozen human brain tissue. However, in separate experiments the specific activity of LDH (a cytosolic marker) in non-synaptosomal mitochondria isolated from previously frozen mouse brain was ~3% that in the cytosolic fraction (30). This finding indicates that if human brain tissue behaves similarly to mouse brain tissue, then a single-freeze thawing of human brain tissue should result in very little rupturing and resealing in the isolated human brain mitochondria.

Western Blotting

Samples were applied to the wells of 10–20% gradient SDS gels using Tricine buffer (Invitrogen, Carlsbad, CA), and then transferred to polyvinylidene difluoride (PVDF) membranes (Invitrogen, Carlsbad, CA). Western blotting was performed as described previously (33). For Western blotting using monoclonal anti-isopeptide (GGEL) (anti-mouse, 814-MAM, CovalAb, Lyon, France), polyclonal anti-Aco 2 (anti-rabbit, from the late Dr. Paul Srere's laboratory at the University of Texas, Austin) (34), anti-TGase 2 (anti-human) (6), and monoclonal anti-α-complex I-NADH reductase (Oxph I, oxidative phosphorylation complex I) (Molecular Probes, Eugene, OR), the concentration of primary antibody was 5 μg/ml and that of secondary antibody was 0.1 μg/ml. The blot was developed by enhanced chemiluminescence (Pierce, Milwaukee, WI).

Positive Control for 814-MAM Antibody Recognition of GGEL Linkages

In vitro cross-linked fibrinogen was used as a positive control for GGEL cross-linked protein. Purified fibrinogen (2 μg) was incubated with either 10^{-4} U or 10^{-3} U of guinea pig liver TGase 2 for 1 h at 37°C in 20 μl of Tris–HCl, pH 7.5, containing 10 mM $CaCl_2$. After incubation, one half of the sample (10 μl) was analyzed by Western blotting for GGEL cross-links and the other half (10 μl) was analyzed by SDS-PAGE and Coomassie Blue staining for protein bands. BSA (2 μg) was used as a negative control.

Identification of a Major Target of TGase 2 in Rat Brain Non-Synaptosomal Mitochondria

The rat brain non-synaptosomal mitochondria prepared as described above (30 μg) were incubated for 30 or 60 min at 37°C with 10^{-2} U of TGase 2 in a buffer consisting of 30 μl of 10 mM Tris–acetate (pH 7.5), 1 mM EDTA and 10 mM $CaCl_2$. For controls, fractions were incubated in the same buffer without Ca^{2+} or TGase 2. The reaction was stopped by addition of an

equal volume of SDS-Tricine sample buffer, boiled, and a 30-µl aliquot analyzed by SDS-PAGE (10–20% polyacrylamide gels). After staining with Coomassie Blue, a protein with a molecular mass of ~78 kDa was noted to disappear with time (See the results). This protein from a time zero lane was excised from the gel for mass spectral analyses.

Mass Spectral Analysis

The gel containing the excised band was crushed and extracted with 200 µl of 50% (w/v) acetonitrile in 25 mM Tris–HCl (pH 8.1), followed by 200 µl of 100% acetonitrile, and dried *in vacuo*. The gel pieces were re-hydrated in 40 µl of 20 µg/ml modified trypsin (Promega) in 25 mM Tris–HCl (pH 8.1) and digested overnight at 37°C. Peptides were extracted with 150 µl of 60% (v/v) acetonitrile containing 0.1% (w/v) trifluoroacetic acid (TFA), and concentrated under vacuum to 10–12 µl. The extracts were freed from salts with zip-tip pipette tips (Millipore), eluted with 2–3 µl of 50 mM α-cyano-4-hydroxycinammic acid in 50% (v/v) acetonitrile and 0.1% (w/v) TFA and spotted directly onto a mass-spectrometer sample plate. Mass spectra were acquired using a Voyager DE-PRO MALDI-TOF mass spectrometer at an accelerating voltage of 20 kV, a delay time of 100 ns, and a reflector voltage of 75% of maximum; 64–128 scans from a nitrogen laser (337 nm) were averaged in each recorded spectrum. Identification of proteins was accomplished through an online database search (ProFound http://129.85.19.192/profound_bin/WebProFound.exe) (35).

Enzyme Assays

TGase was assayed by a modification of the method of Folk (1), in which covalent binding of [1,4-^{14}C]putrescine to succinylated casein was determined. The reaction mixture (0.5 ml) contained 0.1 M Tris–acetate pH 7.5, 1% (w/v) succinylated casein, 1 mM EDTA, 10 mM $CaCl_2$, 0.5% (v/v) lubrol PX, 5 mM DTT, 0.15 M NaCl, 0.5 µCi of [1,4-^{14}C]putrescine (Dupont-New England Nuclear; 118 Ci/mole) and enzyme. Following incubation at 37°C for 1 h, the reaction was terminated by addition of 4.5 ml of cold (4°C) 7.5% (w/v) TCA. The TCA-insoluble precipitate was collected onto GF/A glass fiber filters, washed with cold 5% (w/v) TCA, dried and counted.

Aco 2 activity was measured by adapting the spectrophotometric procedure of Morton et al. (36) to a 96-well plate fluorometer. The reaction mixture (250 µl) contained isocitrate dehydrogenase (200 mU), 50 mM Tris–HCl buffer (pH 7.4), 0.6 mM magnesium chloride, 5 mM sodium citrate and 0.5 mM $NADP^+$. The linear increase in fluorescence (excitation 340 nm; emission 430 nm) due to formation of NADPH was monitored for 30 min at 30°C in a 96-well fluorometric plate reader (Molecular Devices, Sunnyvale, California). To activate Aco 2 in the mitochondrial pellet, the organelles were incubated with 20 mM sodium thiomalate and 4 mM ferrous ammonium sulfate for 30 min at 37°C prior to the fluorometric analysis.

LDH and glutamate dehydrogenase (GDH) activities were measured in a 96-well plate spectrophotometer (Molecular Devices, Sunnyvale, California) as described (37), except that the incubation temperature was 37°C. Proteins were measured by the micro-Biuret method using the Sigma Bradford Protein Assay Kit and BSA as a standard.

Determination of Aco 2 Activity in Purified Rat Brain Non-Synaptosomal Mitochondria Exposed to TGase 2

The previously frozen mitochondrial pellet (30 µg of protein) was suspended in 500 µl of lysis buffer (50 mM Tris–HCl (pH 7.0), 1 mM DTT, 0.2 mM EGTA, 0.08 % (v/v) Triton X-100 and 50 µM leupeptin). An aliquot (37.5 µl) of this suspension was added to 30 µl of a solution containing 0.5 mM Ca^{2+} and 10^{-3} or 10^{-2} U TGase 2, and incubated at 37°C for 1 h. Aco 2 in the 67.5-µl suspension was activated by addition of an equal volume of activation solution (20 mM sodium thiomalate and 4 mM ammonium sulfate). After incubation at 37°C for 30 min, an aliquot (25 µl) was withdrawn and aconitase activity was measured relative to controls containing the mitochondrial suspension, but lacking either TGase 2 or Ca^{2+}.

Determination of Aco 2 Polymerization in Purified Non-Synaptosomal Rat Brain Mitochondria Exposed to TGase 2

The previously frozen mitochondria were suspended in 320 mM sucrose, 20 µM EGTA, 10 mM HEPES, pH 7.4, and centrifuged. The reaction mixture was 20 µl of 10 mM Tris–acetate, pH 7.5, containing 10 µg of mitochondrial pellet, 10^{-2} U TGase 2 with/without 20 mM Ca^{2+}, and with/without 50 mM EDTA. After 0, 30, and 60 min incubation, each sample was subjected to SDS-PAGE and transferred to a PVDF membrane for Western blotting against Aco 2 or GGEL.

Statistical Analysis

Data are presented as mean ± SEM. *P* values were determined by the Student's unpaired *t*-test. A *P* value of ≤ 0.05 was considered statistically significant.

RESULTS

TGase Expression and GGEL Cross-links in the Non-Synaptosomal Mitochondrial Fraction of Rat Brain

TGase activity was detected in the highly purified non-synaptosomal mitochondrial fraction of rat brain (Fig. 1a). TGase activities in the cytosolic and non-synaptosomal mitochondrial fractions were 139 ± 19 and 18 ± 4 pmol/h/mg of protein, respectively. Thus, the specific activity of TGase in the non-synaptosomal mitochondrial fraction is about 14% that in the cytosolic fraction. Since the specific activity of TGase in the mitochondria is lower than that in the cytosol the possibility existed that the TGase in the non-synaptosomal mitochondrial fraction resulted from contamination with cytosol. To confirm that the mitochondrial fraction contained little cytosolic contamination, the activities of LDH (a predominantly cytosolic enzyme) and GDH

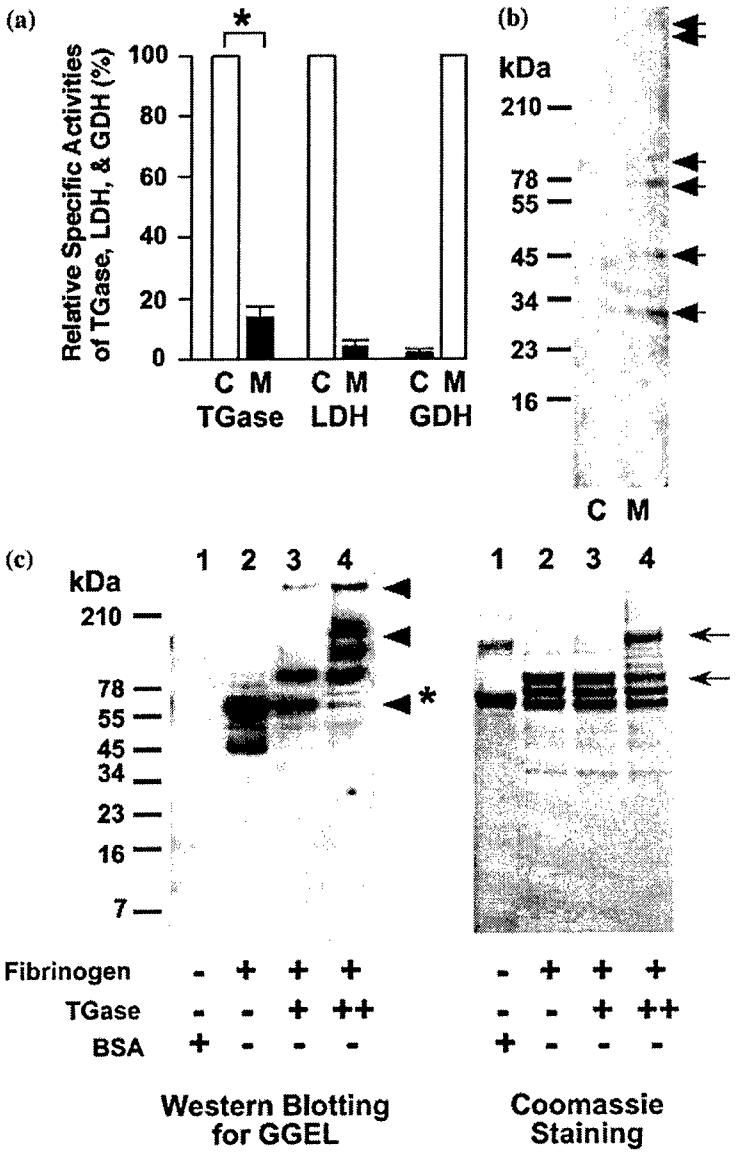

Fig. 1. TGase activity in the cytosol and non-synaptosomal mitochondria of rat brain and the presence of N^{ε}-(γ-L-glutamyl)-L-lysine (GGEL) in the mitochondrial fraction. **a**, Relative specific activities of TGase, lactate dehydrogenase (LDH; cytosolic marker) and glutamate dehydrogenase (GDH, mitochondrial marker) in cytosolic (C) and mitochondrial fractions (M). *The difference in TGase specific activity between C and M is significant with $P < 0.001$ ($n = 6$ different preparations). The differences in GDH and LDH specific activities between the C and M fractions were also highly significant ($P < 0.001$). The specific activities of LDH in the cytosol and GDH in the mitochondria were 520 ± 20 and 105 ± 5 μmol/min/mg of protein, respectively. **b**, Western blots of cytosolic (C) and mitochondrial (M) rat brain fractions. Anti-GGEL antibody was used in the Western blots; 30 μg of protein was added to each lane. **c**, Positive controls and negative controls for the antibody used in (b). Lane 1 contained 2 μg of BSA as a negative control. Notice the strong Coomassie Blue staining for BSA but complete lack of staining on Western blots. Lane 2 contained 2 μg of fibrinogen incubated in the absence of TGase 2. Lane 3 contained fibrinogen incubated with 10^{-4} U of TGase 2 (positive control). Lane 4 contained fibrinogen incubated with 10^{-3} U of TGase 2 (positive control). The band denoted by the asterisk represents fibrinogen that was already dimerized by the action of Factor XIIIa during purification before addition of TGase 2/Ca^{2+}. Two additional major and several minor bands are also recognized by the antibody in lane 4. Coomassie Blue staining also indicates the presence of additional bands in lane 4.

(a predominantly mitochondrial enzyme) were measured in the preparation. Fig. 1a shows that LDH activity is present in the mitochondrial fraction. However, the specific activity of LDH in the mitochondrial fraction (0.028 ± 0.003 μmol/min/mg of protein) is very low relative to that in the cytosolic fraction (0.824 ± 0.032 μmol/min/mg of protein). The ratio of LDH specific activity in mitochondria versus that in cytosol (0.034) is considerably lower than the specific activity of TGase in the mitochondria relative to the cytosol (0.14), indicating that the mitochondrial TGase activity is unlikely to be due primarily to contamination with cytosol.

To determine whether the rat brain non-synaptosomal mitochondrial fraction possesses a "signature" of TGase catalysis, we subjected aliquots of the purified organelles to Western blotting using antibody (814-MAM, CovalAb) directed against the isopeptide GGEL linkage. Six distinct positive bands (arrowheads) were detected in the non-synaptosomal mitochondrial fraction, but not in the cytosolic fraction (Fig. 1b). The specificity of some commercially available antibodies to GGEL linkages has been questioned (38). We therefore tested in our own laboratory whether the antibody recognizes "authentic" GGEL linkages. As a positive control we used fibrinogen as a TGase substrate. Fibrinogen contains three main components (Aα, Aβ, and γ). Murthy et al. (39) showed that TGase 2 catalyzes the covalent intermolecular cross-linking of Aα to γ yielding a heterodimer and higher-M_r polymers. Factor XIIIa (but not TGase 2) catalyzes the covalent linkage of two γ chains (39). The purified plasma fibrinogen obtained from Sigma has some GGEL cross-linked γ–γ dimers (denoted by an asterisk in Fig. 1c, lane 2), presumably formed by the action of endogenous Factor XIIIa. However, Western blotting shows additional GGEL-linked species after incubation with TGase 2 (Fig. 1c, lanes 3 and 4). The GGEL-positive bands are more prominent at the higher concentration of TGase 2 (compare lanes 3 and 4 in Fig. 1c).

Aco 2 is a TGase 2 Target in Non-Synaptosomal Rat Brain Mitochondria *In Vitro*

To determine possible targets of TGase 2 in the rat brain non-synaptosomal mitochondrial fraction, extracts were incubated with TGase 2 for 30 and 60 min and subjected to SDS PAGE. Coomassie Blue staining revealed that a protein with a mass of about 78 kDa disappeared over the 1-h incubation period (Fig. 2a and b). This disappearance was

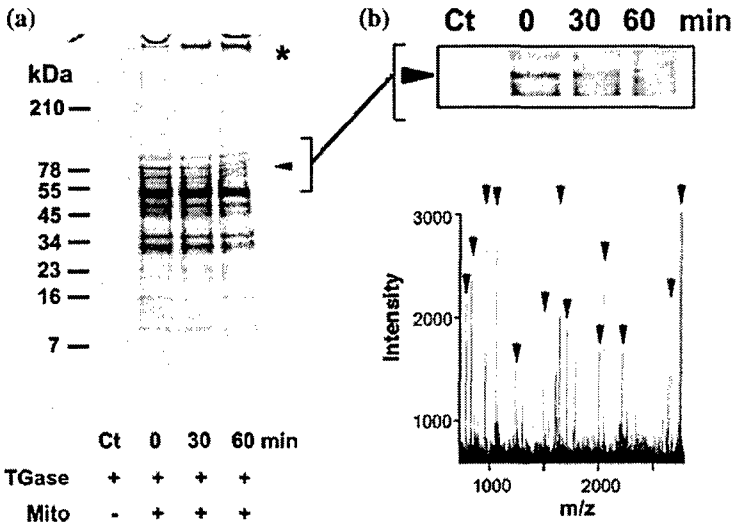

Fig. 2. Identification of mitochondrial aconitase (Aco 2) as a mitochondrial target of TGase 2 *in vitro*. (a) The lane marked + TGase – Mito contained 10^{-2} U of purified guinea pig TGase 2 only (control). The lanes to the right of this lane contained 30 μg of protein from purified rat brain non-synaptosomal mitochondria + 10^{-2} U TGase 2. At the times indicated, the reaction was stopped with SDS Tricine sample buffer. (See the Experimental Procedures section). Aliquots from each time point were then subjected to 10–20% SDS-Tricine gel electrophoresis and stained with Coomassie Blue. A ~78 kDa protein at time zero was reduced in intensity after 60 min of incubation (small arrowhead). High-M_r material (at the top of the gel) increased with time (denoted by an asterisk). (b) Top: Enlargement of the area of the gel containing proteins centered around the M_r value of ~80,000. (b) Bottom: Mass spectrum of a tryptic digest of material excised from the gel centered at M_r 78,000 at the time zero point. The arrowheads in the mass spectrum indicate exact matches to Aco 2 sequences.

accompanied by the time-dependent appearance of large protein aggregates at the top of the gel (denoted by an asterisk in Fig. 2a). MALDI-TOF analysis of a tryptic digest of the 78-kDa protein showed an exact match (i.e., 100% probability) to those predicted for Aco 2 (Fig. 2b). Database searching using ProFound was performed on line (see the Experimental Procedures section). A total of 29 unique monoisotopic ions were obtained as compared to the negative control from the digest and used for peptide mass fingerprinting in the rat NCBInr database. MALDI-TOF analysis also showed that the large M_r complex contained Aco 2 (data not shown).

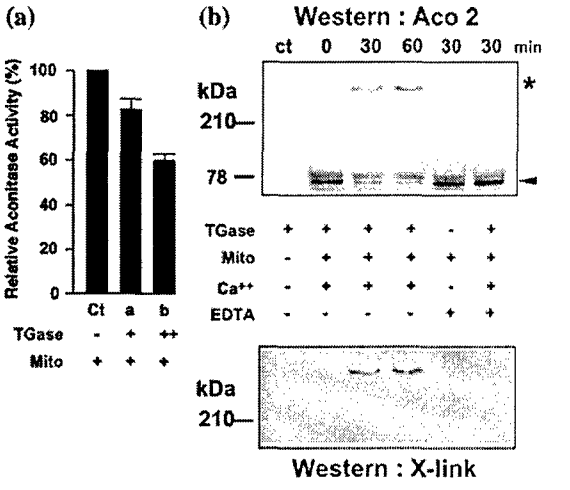

Fig. 3. Effect of TGase 2 on Aco 2 activity and polymerization. **a**: Rat brain mitochondria (30 μg) were incubated for 1 h at 37 °C with 10^{-3} U of TGase 2 (a), 10^{-2} U of TGase 2 (b), or without TGase 2 (Ct; control). Aco 2 activity in the whole mitochondrial suspension was then measured (see the Experimental Procedures section). $N=3$ separate preparations. The relative Aco 2 activities of (a) and (b) are significantly different from that of the control (Ct) with $P<0.05$. The absolute value in the control was 0.256 nmol/min/mg. **b**: Rat brain mitochondria (30 μg) were incubated with or without 10^{-2} U of TGase 2 for 0, 30, and 60 min. One half of the reaction mixture was subjected to Western blotting for Aco 2 (upper blot) and the other half was subjected to Western blotting for GGEL linkages (lower blot; X-link = GGEL). In the presence of active TGase 2, Western blotting showed a decrease of Aco 2 (arrowhead) and an increase of high-M_r polymers at the top of the gel (denoted by an asterisk) (3rd and 4th lanes). Western blotting of GGEL cross-links detected polymerized Aco 2 on the top of the gel.

Inhibitory Effect of TGase 2 on Aco 2 Activity

To determine whether TGase 2 affects Aco 2 activity, we measured the enzyme activity before and after incubation of rat brain non-synaptosomal mitochondria with TGase 2. The rat brain non-synaptosomal mitochondrial fraction was reconstituted in Aco 2 activation buffer. The mitochondria were then incubated with 10^{-3} U of TGase 2 or with 10^{-2} U of TGase 2 for 1 h at 37°C (see the Experimental Procedures section). After the incubation, Aco 2 activity was measured. Fig. 3a shows that there is a TGase 2-dependent loss of Aco 2 activity. The specific activities of Aco 2 in control, TGase treated (10^{-3} U) and TGase treated (10^{-2} U) brain mitochondrial samples were 0.36, 0.24 and 0.20 mU/μg of protein, respectively. Western blotting for Aco 2 showed that the decrease of intact Aco 2 (arrowhead) is accompanied by the appearance of immunopositive high-M_r polymers at the top of the gel (denoted by an asterisk) in a time-dependent manner (Fig. 3b). This high-M_r material also cross reacts with antibody to GGEL cross links (Fig. 3b).

Human HD Brain Mitochondria: Increased TGase Activity and Increased High-M_r Aco 2

TGase activity was measured in the mitochondrial fractions obtained from caudate and frontal cortex (FCX) of human HD and control brains (Fig. 4a). The TGase specific activity in the HD caudate and frontal cortex is increased about 100% and 30%, respectively, compared to that in sex and age-matched controls (Fig. 4a). In a separate experiment, Western blotting of the mitochondrial fraction from human HD and control brains was carried out against Aco 2 and GGEL cross links (Fig. 4b,c,d). The intensity of the ~78 kDa Aco 2 band is diminished in HD caudate specimens relative to most of the control caudate specimens (Fig. 4b,d). In every HD caudate specimen, this diminished ~78-kDa band is associated with the appearance of high-M_r material at the bottom of the respective well. This high-M_r material is immunopositive for Aco 2 and GGEL cross-links by Western blotting (Fig. 4b). In contrast, in only one control caudate specimen is there appreciable high-M_r material immunopositive for Aco 2. Loss of 78-kDa Aco 2 is not apparent in HD frontal cortex, and high-M_r material immunopositive for Aco 2 and GGEL cross-links is not present in the wells (Fig. 4b). The presence of a strong OxPh I signal in the HD samples indicates that the lack of Aco 2 immunoreactivity in these HD samples cannot be due to a general loss of mitochondrial protein.

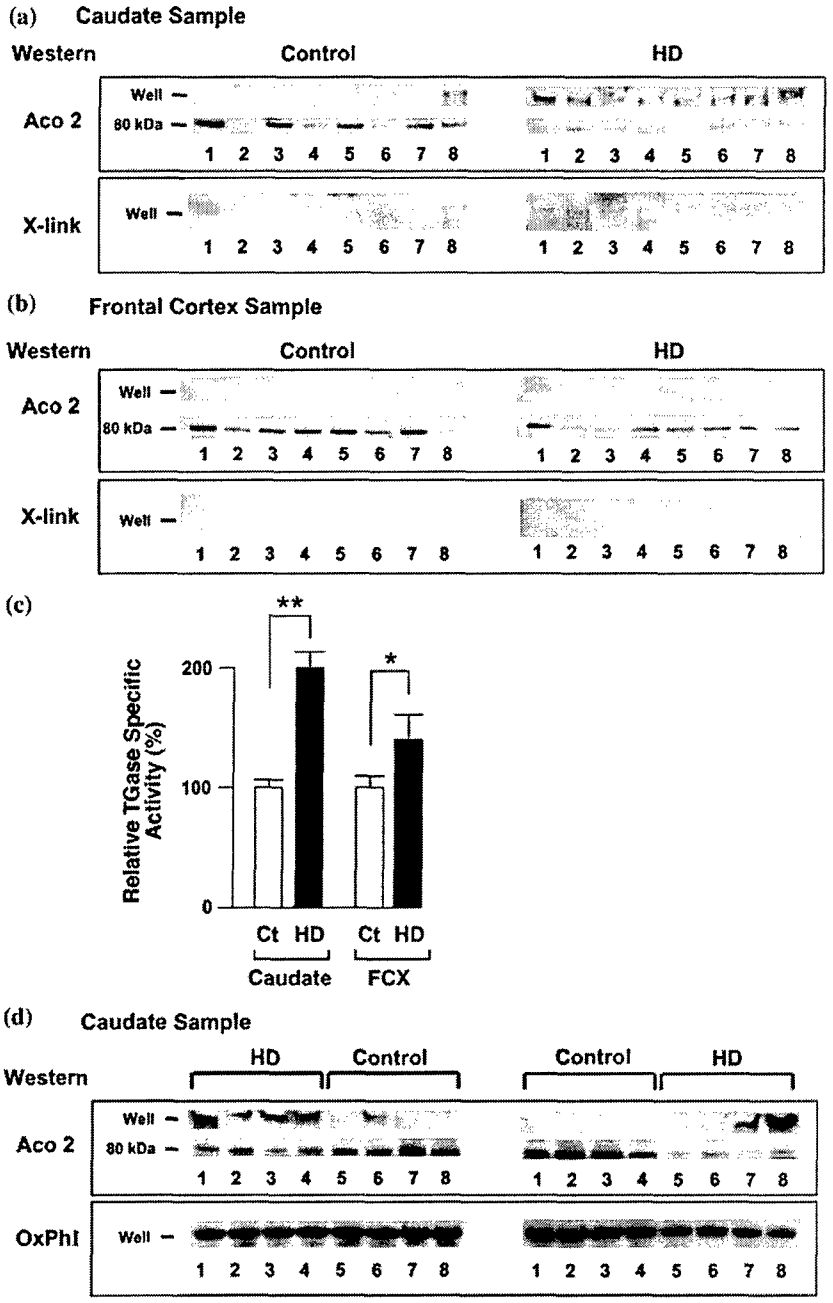

Fig. 4. Huntington Disease (HD) mitochondria: TGase activity, Western blots of Aco 2, and Western blots of GGEL cross links in mitochondria from eight control and eight HD brains. (a) Relative TGase specific activities in mitochondria prepared from the caudate and frontal cortex (FCX) of normal control (Ct) and HD brains. $*P < 0.04$ and $**P < 0.001$, respectively; $n = 3$. (b) Western blots of Aco 2 and GGEL cross links (X-link) in caudate specimens. (c) Western blots of Aco 2 and GGEL cross links (X-link) in frontal cortex specimens. Twenty μg of mitochondrial protein was added to each lane. Note that in (b) and (c) although the control and HD specimens were added to separate gels, the gels were run simultaneously and blotted simultaneously. (d) Additional Western blots of Aco 2 in human brain. The blot is the same as that shown in blot (b) except that controls and HD samples were analyzed on the *same* gel. The intensity of the Aco 2 band relative to that of the mitochondrial marker (OxPh I) is considerably reduced in all HD samples relative to controls. Baseline values of TGase specific activities in mitochondria prepared from caudate and frontal cortex in normal brain were 1.48 and 6.30 pmol/h/mg of protein, respectively. Although (b) and (d) contain similar information, both are shown to demonstrate that the loss of the Aco 2 immunopositive band in the caudate of HD brain is reproducible.

DISCUSSION

Presence of TGase in Non-Synaptosomal Rat Brain Mitochondria

We recently reported that TGase activity is present in non-synaptosomal mouse brain mitochondria (30). The present work shows that TGase activity is also present in highly purified non-synaptosomal rat brain mitochondria (Fig. 1). However, because the specific activity in the rat brain non-synaptosomal mitochondria is relatively low compared to that of the homogenate, it was important to verify (1) that the low amount of TGase activity in the purified rat brain non-synaptosomal mitochondria was not due to damage and leakage of contents during purification, and (2) conversely, that the presence of low TGase activity in the purified non-synaptosomal mitochondria was not due to contamination with TGase 2 (the major cytosolic TGase of brain). The very high specific activity of GDH (mitochondrial marker) in the non-synaptosomal mitochondrial fraction relative to that of the cytosol (Fig. 1) suggests that there was very little damage to the non-synaptosomal mitochondria (leakage of mitochondrial contents to the cytosol) during homogenization of the rat brain. Moreover, the low specific activity of LDH (cytosolic marker) in the rat brain non-synaptosomal mitochondria (Fig. 1) suggests that there is relatively little contamination of cytosolic elements in the purified organelles, and certainly too little to account for all the mitochondrial TGase activity. Data in the literature indicate that about 1% of LDH activity in rat liver and heart is truly associated with mitochondria (40, and references quoted therein). No such data are available for rat brain, but if a similar situation exists in that organ, then this would strengthen the evidence that TGase activity is inherently present in rat brain non-synaptosomal mitochondria, because the ratio of TGase specific activity in mitochondria to cytosol (~0.14) is already considerably greater than the ratio of LDH specific activity in mitochondria to cytosol (~0.034).

Presence of GGEL Cross-Links in Rat Brain Non-Synaptosomal Mitochondrial Proteins

At least six proteins in the mitochondrial fraction were detected by Western blotting using isodipeptide (GGEL)-specific antibody (Fig. 1). Four of the cross-linked proteins found here are of relatively small size. Possibly, the bands may represent proteins that contain an internal cross-link or represent proteins attached to small peptides. Precedence exists for internal cross-linking. For example, TGase 2 can catalyze internal cross-links in tau protein (14). The finding of GGEL-containing protein bands in the mitochondrial fraction is further evidence that TGase is present (and active) in rat brain mitochondria. Work on identifying these GGEL-containing proteins is ongoing in our laboratory. Fig. 1a shows that there is ~20-fold enrichment of GDH in the non-synaptosomal mitochondria relative to cytosol. Thus, since we applied the same amount of protein in the lanes containing cytosol and mitochondria (Fig. 1b), the latter lane contained a considerably enriched preparation, which may account for the more readily detectable cross links in the non-synaptosomal mitochondria than in the cytosol. The commercial GGEL antibodies we used possessed satisfactory specificity under the conditions in which we used them (Fig. 1c), although, as noted above, their specificity has been questioned (38). In future work we will identify the immunopositive proteins and verify the presence of cross-links.

Aco 2 is a Substrate of TGase 2

Aconitase activity is present in mitochondria (Aco 2) and cytosolic (Aco 1) compartments in most tissues, but in human brain it is mostly mitochondrial (41). Therefore, aconitase measurements in human brain homogenates are a reflection of Aco 2 activity. Aco 2 is known to be especially sensitive to oxidative stress (42). Brain aconitase activity is decreased in Friedreich's ataxia (43) and HD (24). We identified a potential major TGase 2 target in rat brain mitochondria as Aco 2 by MALDI-TOF analysis (Fig. 2). We also showed that incubation of rat brain mitochondria with TGase 2 results in loss of Aco-2 activity, which is accompanied by the appearance of high-M_r Aco 2 polymers (Fig. 3a,b). At present we do not know whether Aco 2 is an acyl acceptor, acyl donor, or both, or whether the high-M_r polymers formed in the experiments depicted in Fig. 3 contain only Aco-2 or Aco-2 bound to other mitochondrial proteins. We also have not yet identified the enzyme(s) responsible for the TGase activity present in rat brain mitochondria. We have used TGase 2 as a surrogate for the mitochondrial TGase. This is a reasonable approach because TGases generally have overlapping specificities. For example, it was recently shown that TGases 1, 2 and 3 are each capable of cross-linking mutant htt in a cell model (44).

Understanding how Aco 2 is polymerized may be of relevance in understanding the profound loss of aconitase activity in affected regions of HD brain.

The amount of 78-kDa Aco 2 (non-polymerized) in the severely affected caudate region of HD brain is greatly diminished compared to that in control caudate. This loss of the ~78 kDa band is associated with the appearance of high-M_r material (in the wells) which cannot penetrate the gel, and which is immunopositive for Aco 2 on Western blotting (Fig. 4). Loss of 78-kDa Aco 2 was not apparent in the relatively less affected HD frontal cortex, and high-M_r material immunopositive for Aco 2 was not present in the wells (Fig. 4). The mechanism of loss of Aco 2 in affected HD brain is not yet clear. Possibly, an increase of TGase activity in the mitochondria or the availability of an abnormal, pathologically long Q_n substrate may be responsible, at least in part, for the loss of Aco 2 activity.

CONCLUSIONS

TGase activity is present in rat brain non-synaptosomal mitochondria, where it appears to be responsible for cross-linking several proteins. TGase activity is increased 2-fold in mitochondria prepared from damaged areas of human HD brain. Under pathological conditions, increased TGase activity in the mitochondrial fraction may contribute to the loss of Aco 2 activity in HD brain, and possibly in neural tissue in other neurodegenerative diseases, including AD. It is also conceivable that damaged mitochondria may expose some Aco 2 to cytosolic TGase 2. Increased cross-linking of Aco 2 may contribute to loss of this key TCA cycle enzyme in neurodegenerative diseases. Such a loss of Aco 2 activity may contribute to the well-documented mitochondrial dysfunction associated with neurodegenerative diseases.

ACKNOWLEDGMENTS

This work was supported in part by NIH Grant, PO1 AG14930, AG19589. We thank Virginia Poffenberger for the kind donation of Aco 2 antibodies, and the Harvard Brain Tissue Resource Center (supported by NIH grant R24-MH 068855), McLean Hospital, Belmont, MA, for the donation of HD brain tissue.

REFERENCES

1. Folk, J. E. 1980. Transglutaminases. Annu. Rev. Biochem. 49:517–531.
2. Karpuj, M. V., Garren, H., Slunt, H., Price, D. L., Gusella, J., Becher, M. W., and Steinman, L. 1999. Transglutaminase aggregates huntingtin into nonamyloidogenic polymers, and its enzymatic activity increases in Huntington's disease. Proc. Natl. Acad. Sci. USA 96:7388–7393.
3. Karpuj, M. V., Becher, M. W., Springer, J. E., Chabas, D., Youssef, S., Pedotti, R., Mitchell, D., and Steinman, L. 2002. Prolonged survival and decreased abnormal movements in transgenic model of Huntington disease, with administration of the transglutaminase inhibitor cystamine. Nat. Med. 8:143–149.
4. Lesort, M., Chun, W., Johnson, G. V. W., and Ferrante, R. J. 1999. Tissue transglutaminase is increased in Huntington's disease brain. J. Neurochem. 73:2018–2027.
5. Johnson, G. V. W., Cox, T. M., Lockhart, J. P., Zinnerman, M. D., Miller, M. L., and Powers, R. E. 1997. Transglutaminase activity is increased in Alzheimer's disease brain. Brain Res. 751:323–329.
6. Kim, S-Y., Grant, P., Lee, J. H., Pant, H. C., and Steinert, P. M. 1999. Differential expression of multiple transglutaminases in human brain. Increased expression and cross-linking by transglutaminases 1 and 2 in Alzheimer's disease. J. Biol. Chem. 274:30715–30721.
7. Citron, B. A., SantaCruz, K. S., Davies, P. J. A., and Festoff, B. W. 2001. Intron-exon swapping of transglutaminase mRNA and neuronal Tau aggregation in Alzheimer's disease. J. Biol. Chem. 276:3295–3301.
8. Citron, B. A., Suo, Z., SantaCruz, K., Davies, P. J. A., Qin, F., and Festoff, B. W. 2002. Protein cross linking, tissue transglutaminase, alternative splicing and neurodegeneration. Neurochem. Int. 40:69–78.
9. Zemaitaitis, M. O., Kim, S-Y, Halverson, R. A., Troncoso, J. C., Lee, J. M., and Muma, N. A. 2003. Transglutaminase activity, protein, and mRNA expression are increased in progressive supranuclear palsy. J. Neuropathol. Exp. Neurol. 62:173–184.
10. Dedeoglu, A., Kubilus, J. K., Jeitner, T. M., Matson, S. A., Bogdanov, M., Kowall, N. W., Matson, W. R., Cooper, A. J. L., Ratan, R. R., Beal, M. F., Hersch, S. M., and Ferrante, R. J. 2002. Therapeutic effects of cystamine in a murine model of Huntington's disease. J. Neurosci. 22:8942–8950.
11. Zainelli, G. M., Ross, C. A., Troncoso, J. C., and Muma, N. A. 2003. Transglutaminase cross-links in intranuclear inclusions in Huntington disease. J. Neuropathol. Exp. Neurol. 62:14–24.
12. Jeitner, T. M., Bogdanov, M. B., Matson, W. R., Daikhin, Y., Yudkoff, M., Folk, J. E., Steinman, L., Browne, S. E., Beal, M. F., Blass, J. P., and Cooper, A. J. L. 2001. N^{ε}-(γ-L-Glutamyl)-L-lysine (GGEL) is increased in the cerebrospinal fluid of patients with Huntington's disease. J. Neurochem. 79:1109–1112.
13. Nemes, Z., Fésüs, L., Égerházi, A., Keszthelyi, A., and Degrell, I. M. 2001. N^{ε}(γ-Glutamyl)lysine in cerebrospinal fluid marks Alzheimer type and vascular dementia. Neurobiol. Aging 22:403–406.
14. Singer, S. M., Zainelli, G. M., Norlund, M. A., and Muma, N. A. 2002. Transglutaminase bonds in neurofibrillary tangles and paired helical filament tau early in Alzheimer's disease. Neurochem. Int. 40:17–30.
15. Junn, E., Ronchetti, R. D., Quezado, M. M., Kim, S.-Y., and Mouradian, M. M. 2003. Tissue transglutaminase-induced aggregation of α-synuclein: Implications for Lewy body formation in Parkinson's disease and dementia with Lewy bodies. Proc. Natl. Acad. Sci. USA 100:2047–2052Huntington's disease. J. Neurosci. 22:8942–8950.

16. Mandrusiak, L. M., Beitel, L. K., Wang, X., Scanlon, T. C., Chevalier-Larsen, E., Merry, D. E., and Trifiro, M. A. 2003. Transglutaminase potentiates ligand-dependent proteasome dysfunction induced by polyglutamine-expanded androgen receptor. Hum. Mol. Genet. 12:1497–1506.
17. Mastroberardino, P. G., Iannocola, C., Nardacci, R., Bernassola, F., Lurenzi, V.De, Melino, G., Pavone, F., Oliverio, S., Fesus, L., and Piacentini, M. 2002. 'Tissue' transglutaminase ablation reduces neuronal death and prolongs survival in a mouse model of Huntington's disease. Cell Death Differ. 9:873–880.
18. Selkoe, D. J., Abraham, C., and Ihara, Y. 1982. Brain transglutaminase: *in vitro* cross linking of human neurofilament proteins into insoluble polymers. Proc. Natl. Acad. Sci. USA 79:6070–6074.
19. Cariello, L., Cristofaro, T.de, Zanetti, L., Cuomo, T., Di Maio, L., Campanella, G., Rinaldi, S., Zanetti, P., Di Lauro, R., and Varrone, S. 1996. Transglutaminase activity is related to CAG repeat length in patients with Huntington's disease. Hum. Genet. 98:633–635.
20. Piacentini, M., Farrace, M. G., Piredda, L., Matarrese, P., Ciccosanti, F., Falasca, L., Rodolfo, C., Giammarioli, A. M., Verderio, E., Griffin, M., and Malorni, W. 2002. Transglutaminase overexpression sensitizes neuronal cell lines to apoptosis by increasing mitochondrial membrane potential and cellular oxidative stress. J. Neurochem. 81:1061–1072.
21. Gu, M., Gash, M. T., Mann, V. M., Javoy-Agid, F., Cooper, J. M., and Schapira, A. H. V. 1996. Mitochondrial defects in Huntington's disease. Ann. Neurol. 39:385–389.
22. Browne, S. E. and Beal, M. F. 2004. The energetics of Huntington's disease. Neurochem. Res. 29:531–546.
23. Browne, S. E, Bowling, A. C., MacGarvey, U., Baik, M. J., Berger, S. C., Muqit, M. M., Bird, E. D., and Beal, M. F. 1997. Oxidative damage and metabolic dysfunction in Huntington's disease: Selective vulnerability of the basal ganglia. Ann. Neurol. 41:646–653.
24. Tabrizi, S. J., Cleeter, M. W., Xuereb, J., Taanman, J. W., Cooper, J. M., and Schapira, A. H. 1999. Biochemical abnormalities and excitotoxicity in Huntington's disease brain. Ann. Neurol. 45:25–32.
25. Beal, M. F., Brouillet, E., Jenkins, B. G., Ferrante, R. J., Kowall, N. W., Miller, J. M., Storey, E., Srivastava, R., Rosen, B. R., and Hyman, B. T. 1993. Neurochemical and histologic characterization of striatal excitotoxic lesions produced by the mitochondrial toxin 3-nitropropionic acid. J. Neurosci. 13:4181–4192.
26. Brouillet, E., Hantraye, P., Ferrante, R. J., Dolan, R., Leroy-Willig, A., Kowall, N. W., and Beal, M. F. 1995. Chronic mitochondrial energy impairment produces selective striatal degeneration and abnormal choreiform movements in primates. Proc. Natl. Acad. Sci. USA 92:7105–7109.
27. Panov, A. V., Gutekunst, C. A., Leavitt, B. R., Hayden, M. R., Burke, J. R., Strittmatter, W. J., and Greenamyre, J. T. 2002. Early mitochondrial calcium defects in Huntington's disease are a direct effect of polyglutamines. Nat. Neurosci. 5:731–736.
28. Yu, Z. X., Li, S. H., Evans, J., Pillarisetti, A., Li, H., and Li, X. J. 2003. Mutant huntingtin causes context-dependent neurodegeneration in mice with Huntington's disease. J. Neurosci. 23:2193–2202.
29. Choo, Y. S., Johnson, G. V. W., Macdonald, M., Detloff, P. J., and Lesort, M. 2004. Mutant huntingtin directly increases susceptibility of mitochondria to the calcium-induced permeability transition and cytochrome *c* release. Hum. Mol. Gen. 13:1407–1420.
30. Krasnikov B. F., Kim, S.-Y, Ryu, H., Xu, H., Stavrovskaya, I., Iismaa, S., Ratan, R. R., Blass, J. P., Gibson, G. E. and Cooper, A. J. L. 2005. Transglutaminase activity is present in highly purified non-synaptosomal mouse brain and liver mitochondria. Biochemistry 44: 7830–7843.
31. Lai, J. C. K., Walsh, J. M., Dennis, S. C., and Clark, J. B. 1977. Synaptic and non-synaptic mitochondria from rat brain: Isolation and characterization. J. Neurochem. 28:625–631.
32. Lai, J. C. K. and Clark, J. B. 1979. Preparation of synaptic and nonsynaptic mitochondria from mammalian brain. Methods Enzymol. 55:51–60.
33. Kim, S.-Y., Chung, S.-I., Yoneda, K., and Steinert, P. M. 1995. Expression of transglutaminase 1 in human epidermis. J. Invest. Dermatol. 104:211–217.
34. Melnick, J. Z., Preisig, P. A., Moe, O. W., Srere, P., and Alpern, R. J. 1998. Renal cortical mitochondrial aconitase is regulated in hypo- and hypercitraturia. Kidney Int. 54:160–165.
35. Zhang, W. and Chait, B. T. 2000. ProFound-An expert system for protein identification using mass spectrometric peptide mapping information. Anal. Chem. 72:2482–2489.
36. Morton, R. L., Iklé, D., and White, C. W. 1998. Loss of lung mitochondrial aconitase activity due to hyperoxia in bronchopulmonary dysplasia in primates. Am. J. Physiol. 274:L127–L133.
37. Park, L. C. H., Gibson, G. E., Bunik, V., and Cooper, A. J. L. 1999. Inhibition of select mitochondrial enzymes in PC12 cells exposed to *S*-(1,1,2,2-tetrafhluoroethyl)-L-cysteine. Biochem. Pharmacol. 58:1557–1565.
38. Johnson, G. V. W. and LeShoure, R. 2004. Immunoblot analysis reveals the isopeptide antibodies do not specifically recognize the ε(γ-glutamyl)lysine bonds formed by transglutaminase activity. J. Neurosci. Methods 134:151–158.
39. Murthy, S. N. P., Wilson, J., Guy, S. L., and Lorand, L. 1991. Intramolecular cross linking of monomeric fibrinogen by tissue transglutaminase. Proc. Natl. Acad. Sci. USA 88:10601–10604.
40. Brooks, G. A., Dubouchard, H., Brown, M., Sicurello, J. P., and Butz, C. E. 1999. Role of mitochondrial lactate dehydrogenase and lactate oxidation in the intracellular lactate shuttle. Proc. Natl. Acad. Sci. USA 96:1129–1134.
41. Slaughter, C. A., Hopkinson, D. A., and Harris, H. 1977. The distribution and properties of aconitase isozymes in man. Ann. Hum Genet. 40:385–401.
42. Melov, S., Coskum, P., Patel, M., Tuinstra, R., Cottrell, B., Jun, A. S., Zastawny, T. H., Dizdaroglu, M., Goodman, S. I., Huang, T. T., Miziorko, H., Epstein, C. J., and Wallace, D. C. 1999. Mitochondrial disease in superoxide dismutase 2 mutant mice. Proc. Natl. Acad Sci. USA 96:846–851.
43. Schapira, A. H. 1999. Mitochondrial involvement in Parkinson's disease, Huntington's disease, hereditary spastic paraplegia and Friedreich's ataxia. Biochim. Biophys. Acta 1410:159–170.
44. Zainelli, G. M., Dudeck, N. L., Ross, C. A., Kim, S.-Y., and Muma, N. A. 2005. Mutant huntingtin protein. A substrate for transglutaminase 1, 2, and 3. J. Neuropath. Exp. Neurol. 64:58–65.

Neurochemical Research, Vol. 29, No. 3, March 2004 (© 2004), pp. 531–546

APPENDIX 5

The Energetics of Huntington's Disease*

Susan E. Browne[1,2] and M. Flint Beal[1]

(Accepted August 20, 2003)

Huntington's disease (HD) is a hereditary neurodegenerative disorder that gradually robs sufferers of the ability to control movements and induces psychological and cognitive impairments. This devastating, lethal disease is one of several neurological disorders caused by trinucleotide expansions in affected genes, including spinocerebellar ataxias, dentatorubral-pallidoluysian atrophy, and spinal bulbar muscular atrophy. HD symptoms are associated with region-specific neuronal loss within the central nervous system, but to date the mechanism of this selective cell death remains unknown. Strong evidence from studies in humans and animal models suggests the involvement of energy metabolism defects, which may contribute to excitotoxic processes, oxidative dmage, and altered gene regulation. The development of transgenic mouse models expressing the human HD mutation has provided novel opportunities to explore events underlying selective neuronal death in HD, which has hitherto been impossible in humans. Here we discuss how animal models are redefining the role of energy metabolism in HD etiology.

KEY WORDS: Huntington's disease; Huntingtin; mitochondria; energy metabolism; glucose utilization; genetic models.

INTRODUCTION

Huntington's disease (HD) is an autosomal dominantly inherited neurodegenerative disorder that is characterized by the insidious progressive development of mood disturbances, behavioral changes, involuntary choreiform movements, and cognitive impairments. Onset is most commonly in adulthood, with a typical duration of 15–20 years before premature death.

* Special issue dedicated to Professor John B. Clark.

[1] Departments of Neurology and Neuroscience, Weill Medical College of Cornell University, New York, New York.

[2] Address reprint requests to: Susan E. Browne, Department of Neurology and Neuroscience, A-502, Weill Medical College of Cornell University, 525 East 68th Street, New York, New York, 10021. Tel: 212-746-4672; Fax: (212) 746-8276; E-mail: sub2001@med.cornell.edu

DISCUSSION

The Neuropathologic and Genetic Basis of Huntington's Disease

The motor and behavioral disturbances in HD reflect the selective pattern of cell loss in the brain and the specific neurotransmitter pathways affected. Although it is often regarded as a basal ganglia disease, because the predominant neuropathological feature is progressive caudal to rostral degeneration of the caudate putamen (1), HD is in fact a multisystem disorder. By end stage, when more than 90% of caudate putamen neurons are lost and the striatum is severely atrophic and gliotic, degeneration is also evident in several other brain regions, including the cerebral cortex, globus pallidus (GP), and to a lesser extent thalamus, subthalamic nucleus, nucleus accumbens, substantia nigra, cerebellum, and white matter (1).

GABA-ergic (γ-aminobutyric acid) medium spiny projection neurons, which constitute 80% of striatal neurons, are most vulnerable in HD. The first clinical symptoms of the disease correlate with loss of 30%–40% of striatal dopamine D1 and D2 receptors localized on the medium spiny neurons (2). Within these neurons, GABA co-localizes with enkephalin (ENK), substance-P (SP), dynorphin, or calbindin. Aspiny interneurons containing nicotinamide adenine dinucleotide phosphate diaphorase (NADPH-d), neuropeptide Y (NPY), somatostatin (SS), and nitric oxide synthase (NOS) are relatively spared in HD. ENK-positive spiny neurons projecting to the external segment of the globus pallidus (GPe) degenerate earliest in the disease, preceding SP-containing neurons projecting to the internal segment (GPi) (3). Hence the spontaneous, uncontrolled movements typical of HD appear to result from the disruption of basal ganglia–thalamocortical pathways that regulate movement control (4). The pathological basis of the mood disturbances and personality changes that are often the earliest and most debilitating of the symptoms for patients, are less clear. However, it is likely that cortical neuronal dysfunction before overt cell loss, particularly in prefrontal regions, underlies these traits (5).

The genetic defect in HD is an expansion of an unstable CAG repeat encoding glutamines (Q), close to the 5′ end of the chromosome 4 gene for huntingtin protein (6). Expansion of this trinucleotide stretch to 34–39 CAG repeats in one allele confers risk of developing HD, but above 39 repeats the disease is completely penetrant. Several features of the disease phenotype are influenced by CAG repeat length, including age of onset (7) and the extent of DNA fragmentation in striatal neurons (8). HD also shows the trait of "anticipation" resulting from instability of the repeat size during transmission (9).

Despite knowledge of the HD gene defect, mutant huntingtin's toxic action has not yet been identified. In fact, the function of wildtype huntingtin is not clear either, although it is implicated in developmental apoptosis, neurogenesis, and intracellular trafficking mechanisms (10–13). Evidence points to the mutation inducing a toxic gain of function, rather than causing loss of wildtype huntingtin function, because mice lacking one allele of wildtype huntingtin show little or no pathology (14). Huntingtin is, however, essential for development, as evidenced by the fact that *HD* homologue–null mice die *in utero*. Findings that this phenotype can be completely rescued by crossing into knock-in mice that express a mutant polyglutamine expansion (Hdh^{Q50} mice) imply that huntingtin's normal function persists despite the presence of a pathogenic glutamine repeat (11). Expression levels for huntingtin are also critical, and mice expressing abnormally low levels of murine huntingtin exhibit developmental abnormalities (15).

The preferential vulnerability of striatal neurons in HD is enigmatic and cannot be simply explained in terms of the distribution of abnormal huntingtin, because the gene mutation is expressed throughout the body and does not show a marked selectivity for cerebral regions targeted by the disease process (16,17).

Within the striatum there is some evidence suggesting differential distribution between distinct neuronal populations (18–20), but it appears more likely that vulnerability to degeneration is conferred by another property of striatal neurons. At the neuronal level, huntingtin protein is widely expressed throughout cells, with a largely cytoplasmic distribution in perikarya, axons, dendrites, and some nerve terminals. Mutant huntingtin contains several cleavage sites for caspases and proteases (21), and as the disease progresses, N-terminal fragments of huntingtin form ubiquitinated protein aggregates in neuronal nuclei (neuronal intranuclear inclusions [NII]) and in dystrophic neurites (cytoplasmic inclusions [CI]). These aggregates have been identified in both HD brain and in the brains of multiple mouse lines expressing mutant huntingtin (22–26). The question of whether huntingtin aggregates are directly toxic is still a matter of debate, although the current weight of opinion favors a lack of involvement or even a neuroprotective role (27,28). Nuclear localization of mutant htt, however, does seem to be necessary for cell damage. One study demonstrated that transfecting mouse clonal cells with either full-length or truncated huntingtin containing mutant CAG repeat lengths induced toxicity along with the formation of both nuclear and cytosolic inclusions, whereas huntingtin with wild-type CAG repeats remained within the cytoplasm and was inert (29). Inhibiting caspase activity with Z-VAD-FMK increased cell survival but had no effect on either NII or CI number, implying that neuronal death is independent of aggregate formation in this model. In addition, introducing a nuclear export signal to mutant huntingtin abrogates toxicity *in vitro* (30). A provokative corollary to this issue is a recent report suggesting that nuclear localization of mutant huntingtin only occurs in nondividing cells, perhaps contributing to the neuronal selectivity of huntingtin toxicity (31).

Although mutant huntingtin's initial toxic trigger remains elusive, experimental evidence supports roles for several different detrimental cell pathways at some stage of the degenerative process within targeted neurons. These include apoptotic cascades, excitotoxicity, the possibility of huntingtin aggregate toxicity, and pernicious effects of huntingtin protein–protein interactions, putatively via

transglutaminase-catalyzed polyglutamine interactions with glutamines, lysines, and polyamines in other proteins (32–34). The latter is a particularly intriguing hypothesis, because huntingtin has been shown to have an affinity for many proteins critically involved in cell survival, including BDNF, glyceraldehyde 3-phosphate dehydrogenase (GAPDH), calmodulin, caspase-3, α-adaptin, and a number of transcription factors, including Sp1, CBP, and p53 (32,35–38).

Another prominent component of HD pathogenesis is altered energy metabolism. Energetic defects in the HD population have been chronicled for many years; however, the specific role of impaired metabolism and mitochondrial defects in cell death pathways is still unclear. Are metabolic defects a primary event inducing cell death cascades, or are they secondary to another cellular defect? And if they are causative, how does mutant huntingtin trigger this effect? Can huntingtin directly influence mitochondrial function, or are mitochondrial defects the result of intranuclear events? The purpose of this review is to address the current status of knowledge on the role of energetic defects in cell death processes in HD, and how metabolic compromise can influence other detrimental cellular processes that are implicated in the disease. A brief review of historical evidence for metabolic defects in HD patients is presented, and the remainder of this review will concentrate more on the groundbreaking evidence gained in recent years from genetic models of the disease.

Bioenergetic Defects Are a Profound Feature of Huntington's Disease

The first hypotheses of energetic impairments in HD arose from observations of pronounced weight loss in patients, despite sustained caloric intake (39). Weight loss does not correlate with chorea, suggesting it is an insidious event resulting from the disease mutation rather than secondary to hyperactivity (40). Then positron emission tomography (PET) studies revealed that glucose metabolism in the basal ganglia and cerebral cortex is markedly reduced in symptomatic HD patients (5,41,42). Furthermore, the extent of caudate hypometabolism correlates well with declines in clinical test scores for bradykinesia, rigidity, dementia, and functional capacity. Similarly, putaminal hypometabolism predicts the extent of chorea and defects in eye movements, whilst hypometabolism in the thalamus correlates with the degree of dystonia in patients (5,43). Reduced cerebral functional activity in symptomatic patients may simply reflect neuronal loss, but more compelling evidence for a potential causative role of energetic defects comes from findings that striatal hypometabolism precedes the bulk of tissue loss and occurs in asymptomatic at-risk subjects (44–46). Approximately 50% of gene-positive mutation carriers exhibit metabolic defects years before the onset of clinical symptoms (46,47). In addition, patients suffering psychological disturbances and mood changes often exhibit cortical hypometabolism before the onset of motor symptoms (5). The involvement of a defect in glycolysis has also been suggested by findings that symptomatic HD patients have elevated lactate production in the basal ganglia and occipital cortex, detected by proton nuclear magnetic resonance (^{1}H-NMR) imaging (48,49). Interestingly, this abnormal lactate generation can be ameliorated by treatment with the metabolic cofactor coenzyme Q_{10} (50). NMR spectroscopy has also revealed marked increases in cerebrospinal fluid (CSF) pyruvate content and reductions in muscle phosphocreatine (PCr)/creatine and ATP/phosphocreatine ratios in symptomatic patients (50–52).

Consequently, biochemical studies in HD postmortem tissue have revealed alterations in the activity of several key components of oxidative phosphorylation and the tricarboxylic acid (TCA) cycle in brain regions targeted in HD. Pyruvate dehydrogenase activity is decreased in basal ganglia and hippocampus, and striatal oxygen consumption is reduced in HD patients (53). Activities of complexes II, III, and IV of the electron transport chain are markedly and selectively reduced in caudate and putamen of advanced grade (3 and 4) HD patients (54,55). Impaired complex I activity has been reported in muscle from HD patients but appears to be unaffected in brain (54,56,57). However, findings that respiratory chain enzyme activities are unchanged in presymptomatic and early-stage HD patients suggests that these enzymatic changes are secondary to the pathogenic process (58), a hypothesis largely supported by observations in mutant mouse models of HD (discussed below). The most profound enzyme defect detected in HD to date is the dramatic reduction in activity of the TCA cycle enzyme aconitase in affected brain regions and muscle ($>-70\%$; 59). Sites of metabolic abnormalities in HD are summarized in Figure 1. Interestingly, mitochondrial abnormalities and metabolic defects are also features of other trinucleotide repeat diseases including SCA1, SCA2, and SCA3, adding fuel to speculation that energetic defects play common roles in these disorders and may be directly linked to the polyglutamine defect (60,61).

GAPDH is another metabolic enzyme that has been implicated in HD pathogenesis, on the basis of the propensity for polyglutamines to bind the enzyme (35). Glycolytic activity of GAPDH, however, was

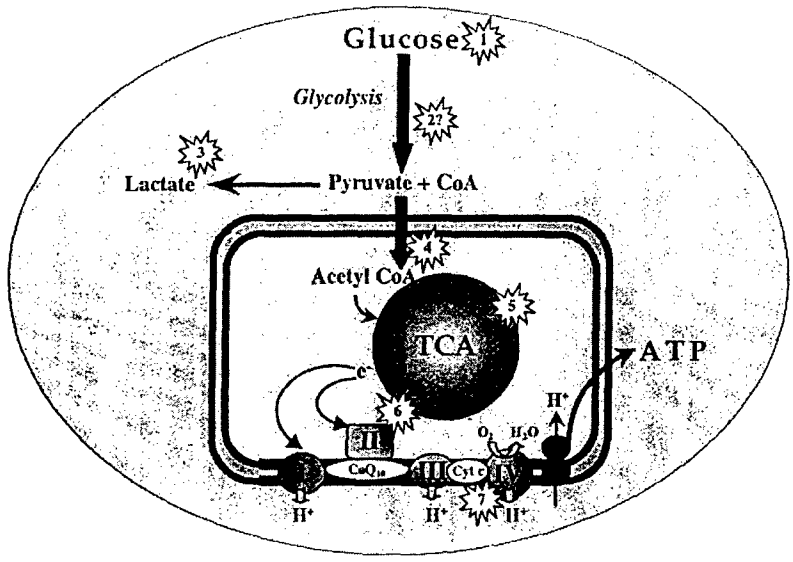

Fig. 1. A schematic representation of the sites of impairments in the glucose metabolic pathway identified to date in neurons of HD patients, and, in some cases, in mutant mouse models. *Sites:* 1, Glucose uptake; 2, glyceraldehyde-3-phosphate dehydrogenase, GAPDH (glycolytic dysfunction not proven); 3, lactate production increased; 4, pyruvate dehydrogenase; 5, aconitase; 6, succinate dehyrogenase; 7, cytochrome oxidase.

found to be conserved throughout the brain in late stage HD (54). This does not rule out the possibility that other actions of this promiscuous molecule are affected in the disease, including effects on microtubule-mediated intracellular trafficking or apoptosis. Recent reports have subsequently shown that the subcellular localization of GAPDH is altered by mutant huntingtin expression, with increased nuclear localization in both human fibroblasts and in neurons from a transgenic mouse model (62–64). The appearance of an abnormal high molecular weight form of GAPDH in fibroblast nuclei has also been associated with decreased glycolytic activity (62).

Mitochondrial Toxins Mimic Huntington's Disease

The relevance of succinate dehydrogenase (SDH) defects to the HD phenotype is underscored by the fact that mitochondrial toxins that selectively inhibit succinate dehydrogenase in the TCA cycle and complex II, namely 3-nitropropionic acid (3-NP) and malonate, induce striatal-selective lesions in humans, rodents, and primates that closely resemble those seen in HD (65,66). Systemic 3-NP intoxication in humans induces basal ganglia lesions visible by CT-scans, localized principally to the putamen but sometimes extending to the caudate, that are associated with multiple cognitive symptoms, including acute encephalopathies and coma, and motor abnormalities (65). Systemic administration of 3-NP to both rodents and primates produces age-dependent striatal lesions that are strikingly similar to those seen in HD (67,68). In primates, chronic 3-NP administration produces selective striatal lesions characterized by a depletion of calbindin neurons with sparing of NADPH-d neurons, and proliferative changes in the dendrites of spiny neurons. Animals also show both spontaneous and apomorphine-inducible choreiform movement disorders resembling those in HD (66). 3-NP basal ganglia lesions in rats are associated with elevated lactate levels, similar to the increased lactate production seen in HD patients (69). Inhibition of cerebral SDH activity by 3-NP has been demonstrated *in vivo* in a number of studies. 3-NP markedly inhibits SDH activity within 2 h of intraperitoneal administration in rodents, producing 50%–70% reductions in SDH activity throughout the brain (68; Browne and Beal, unpublished observations), consistent with the degree of complex II-III deficiency reported in HD striatum in postmortem studies (54). Interestingly, the neurodegenerative sequelae of systemic administration of the toxin are largely restricted to the striatum, despite its relatively homogeneous distribution and uniform reduction in SDH activity throughout the brain (68; Browne and Beal, unpublished observations). This observation appears to once again underscore the vulnerability of striatal neurons to metabolic stress.

Genetic Models of Huntington's Disease: How Do Energetic Defects Evolve?

The discovery of the gene mutation in HD and the subsequent generation of animal models expressing this mutation has transformed studies into HD etiology, by conferring the ability to map early events in the disease and track the development of pathologic processes relative to disease symptoms. The mutant HD gene has now been expressed in a number of different organisms, including *Caenorhabditis elegans,* drosophila, mice, and rats (28,37,70,71). Although lower organisms may provide reasonable models for rapid screening of potential therapeutic agents, rodent models are proving most useful for examining the contributions of different cellular mechanisms of disease and for testing the efficacy of putative therapeutics.

Multiple mouse models of HD now exist, falling into three broad categories: (i) Mice expressing exon-1 fragments of human huntingtin gene (*HD*) containing polyglutamine mutations (in addition to both alleles of murine wildtype huntingtin [*hdh*]). (ii) Mice expressing the full-length human *HD* gene (plus murine *hdh*). and (iii) Mice with pathogenic CAG repeats inserted into the existing CAG expansion in murine *hdh.* These models vary in terms of the site of transgene incorporation, promoter used, gene expression levels, CAG repeat length, copy number, and background mouse strain used. As a result, mouse phenotypes vary greatly between lines, as demonstrated in Table I (10,24,25,72–79). Most notably, although all models exhibit some features typical of HD (invariably including huntingtin protein aggregate formation at some stage), not all models develop striatal neuronal death. This phenomenon seems to depend ultimately on the context in which the huntingtin mutation is expressed (as demonstrated elegantly in [80]). However, some generalities can be drawn from surveying the available mouse lines. Firstly, mice require longer CAG repeats than humans to elicit pathogenic events, putatively because of their relatively short life spans. Second, age of onset of disease phenotype is accelerated by expressing gene fragments and is faster with shorter fragments. Similarly, mouse life span is more rapidly curtailed by expressing shorter fragments. In contrast, expression of longer fragments or full-length huntingtin seems to be associated with the development of neuronal death patterns more closely resembling human HD pathology. However, age of phenotype onset, aggregate formation, and cell death are all slower in full-length models (including knock-in mice) compared with fragment models. Within each of these subsets, longer CAG repeats accelerate all phenotypes.

Do Energetic Defects Contribute to Pathogenesis in Mouse Huntington's Disease Models?

The most prominent metabolic alterations in HD patients are weight loss and region-specific alterations in cerebral glucose use, cerebral lactate levels, and the activities of mitochondrial enzymes involved in glucose metabolism. These parameters are gradually being systematically investigated in different mouse HD models, and a temporal profile of pathogenic events is slowly emerging.

Reduced body weight and brain weight are features of mice expressing fragments of human huntingtin (e.g., R6/2 and N171-82Q) but are not so typical of full-length htt models (25,72). Alterations in cerebral glucose utilization, however, are early events in different HD mouse lines (81,82). Using quantitative 2-deoxyglucose densitometry in awake, freely moving mice, we found that glucose use changes occur presymptomatically in HD mouse brains. In contrast to most reports in humans, the first detected alterations in mouse lines are marked elevations in glucose use in multiple forebrain regions. Most interestingly, this hypermetabolism occurs before any evidence of pathological changes, aggregate formation, or symptoms in these animals. This observation has now been recapitulated in two distinctly different HD mutant mouse models, Hdh^{Q92} and Hdh^{Q111} knock-in mice expressing mutant CAG expansions in the murine homologue *HD* gene (11) and N171-82Q mice expressing a fragment of human huntingtin gene containing 82 CAGs (25). Hdh^{Q50} and Hdh^{Q92} mice do not develop an overt behavioral phenotype, but Hdh^{Q111} mice show striatal-specific cell loss around 24 months of age (83). Further, nuclear retention of full-length htt is seen long before cell death (~12 weeks) and occurs selectively in striatal medium spiny neurons. Increased CAG repeat length in this line is associated with acceleration of neuronal intranuclear inclusion (NII) formation, evident by 10 months of age in Hdh^{Q111} mice and by 15 months in Hdh^{Q92}, but NII are not seen in Hdh^{Q50} mice (26,83). In contrast, N171-82Q mice that express a fragment of human huntingtin develop a behavioral phenotype more closely reminiscent of HD, developing weight loss, gait abnormalities, impaired motor performance on a rotarod apparatus, systemic glucose intolerance, and NII formation by 3–4 months of age, before premature death at around 4.5–6 months (25).

Glucose use studies were performed in HD mice before the onset of symptoms or NII formation (4-month-old Hdh^{Q50}, Hdh^{Q92}, and Hdh^{Q111} mice, and 2-month-old N171-82Q mice), and in Hdh^{Q92} mice post-NII formation (15 months). Widespread increases in forebrain glucose

Table 1. Transgenic and Knock-in Mouse Models of Huntington's Disease

Mouse Lines	Q	Tremor, rotarod, clasping	Symptom onset (age/wk)	Weight loss	Energy defects	NII formation (age/wk)	Neuronal loss (age/wk)	Comments	Life span (age/wk)
HD Exon 1 Fragment									
R6/2[72,22]	144	✓	8	✓	✓	3.5	Atrophy	*R6/2:* Diabetes,	13–21
R6/1	115	✓	15–20	X	N/D	20	(Stri, CTX)	seizures, "dark"	32–40
Constitutive promoter, 1.9 kb C57B16/CBA								neurons, htt in mitochondria, mitochondria degeneration	
N171[25]									
Mouse prion promoter	82	✓	12	✓	✓	12–16	Stri, CTX	*82Q:* Glucose intolerance,	18–24
171aa	44	X	–	X	X	None	–	apoptosis	Normal
C57B1/6J × C3H/HEJ	18	X	–	X	X	None	–		Normal
HD100, HD46[73]									
Rat NSE promoter	100	✓	12–16	X	N/D	CTX, Stri	Stri-few (32)	Dysmorphic dendrites,	N/D
3 kb SJL/B6	46	X	–	X	N/D		–	increased $[Ca^{2+}]_i$ after NMDA	N/D
Tet-Off[74]									
CamKIIa-tTA Tet-Off promoter C57B1/6J × CBA	94	✓	10 *p.e.* (in 50%)	X	N/D	4 *p.e.*	Atrophy (Stri)	Reversible aggregate appearance, gliosis and receptor changes.	N/D
Full-Length Transgenic									
YAC[24]	72	✓	12	✓	N/D*	60	Stri (52)	Impaired Ca^{2+} handling	N/D
1–2 copies	48	X	42	X	N/D*	None	None	by mitochondria	N/D
FVB/N	18	X	–	X	N/D*	None	None		Normal
HD89[75]									
CMV promoter	89	✓	16	X	N/D*	12 (Few, Stri, CTX)	Stri, CTX-few	Striatal glisosis, apoptosis,	52–60 (+/+)
2–22 copies	48	X	16	X	N/D*		None	dendritic changes	72–80 (+/−)
FVB/N	16	X	–	X	N/D*				Normal
Murine Trageted									
Hdh Knockin[11, 26]	111	X	None	X	✓	40	Stri (80–96)	cAMP impairments	96 (+/+)
Constitutive promoter	92	X	None	X	✓	60	None		Normal
CD1 × 129Sv	50	X	None	X	X	None	None		Normal
CAG Knock-in[76]									
Constitutive promoter	94	X	X	N/D	N/D	None	None	NMDA sensitivity,	N/D
C57B16/J × 129Sv	71	X	X	N/D	N/D	None	None	hypokinesia (16 wk)	N/D
Hdh 150Q[77]									
Constitutive promoter	150	✓	25 (+/+)	✓	N/D	40 (Stri, Nuc Accum)	N/D	Gliosis in striatum,	N/D
C57B1/6J × 129/O1a			60 (+/−)		N/D			some seizures	
Hdh4/6 Knockin[78]									
Constitutive promoter	80	X	None	N/D	N/D	>46	None	Aggression (12 wk)	N/D
C57B1/6J × FVB/N	72	X	None	N/D	N/D	None	None		N/D
HD/Hdh Chimera[79]									
Constitutive promoter Exon 1/intron 1 fragments C57B1/6J × ICR	80	X	N/D	N/D	N/D	None	None	Gliosis, CAG instability	N/D

Note: The models listed reflect those reported by 5/2003.

*ND**, no changes found in respiratory chain enzyme activities in symptomatic mice; other metabolic parameters have not yet been determined.

aa, Amino acid; CTX, cortex; htt, huntingtin protein; N/D, not determined to date; Nuc. accum, nucleus accumbens; *p.e.*, post-expression; Q, glutamine; Stri, striatum; Tet, tetracycline.

use levels were evident in 4-month-old Hdh^{Q92} and Hdh^{Q111} mice (but not Hdh^{Q50}), and in 2-month-old N171-82Q mice. Notably, glucose use changes in *Hdh* mice were exacerbated in mice with longer CAG repeats and in homozygote versus heterozygote mice, suggesting the extent of increased cerebral glucose demand in CAG length-dependent and gene dosage–dependent (81,82). In older Hdh^{Q111} mice, striatal glucose use was depressed, suggestive of neuronal dysfunction before cell loss. Increases in glucose uptake before any pathological changes suggest that cells have increased their glucose demand to fulfill functional requirements, perhaps as a result of impaired activity of specific metabolic enzymes, uncoupling of mitochondria, or increased dependence on glycolysis. Notably, there is one report in humans of elevated cortical glucose use in presymptomatic HD gene-carriers (47). Limited observations in humans perhaps reflect a lack of studies involving early enough imaging to detect subtle, region-specific presymptomatic hypermetabolism. Another point of interest is that glucose use changes are not restricted to brain regions especially susceptible to degeneration (i.e., the cortex and striatum). This observation supports suggestions that selective loss of striatal neurons may be associated with their apparent vulnerability to metabolic stress.

To determine the principal sites at which metabolism is impaired, studies are in progress to examine the functional capacities of multiple components of the glucose metabolic pathway in these and other HD mice. Additional models include R6/2 mice expressing a human *HD* N-terminal fragment and transgenics expressing full-length human mutant *HD* with its constitutive regulatory elements in a YAC construct (see Table I). R6/2 mice (with 144–170 CAGs) were the first mutant HD mice developed and therefore are the best characterized to date (22,72). Mice have an extremely short life span (generally 13–17 weeks) and develop (in chronological order) NII (~3–4 weeks), gait abnormalities, rotarod impairments, glucose intolerance, body weight loss, brain weight loss, diabetes, striatal atrophy (6–10 weeks), and cerebral neurotransmitter receptor alterations (notably metabotropic glutamate and dopamine alterations around 12 weeks of age) (22,72,76). YAC72Q transgenics show a more slowly progressing phenotype, the earliest abnormality reported to date being impaired calcium handling by 4–5 months of age (24,84). Mice go on to develop NII, and some striatal and cortical cell loss, but live a normal life span. Initial metabolic findings in these models suggest that ATP synthesis may be impaired in N171-82Q and R6/2 mice (Browne, Beal, and Yang, unpublished observations). Interestingly, we found that activities of mitochondrial enzyme complexes II and IV (known to be defective in late-stage HD) are normal in both *Hdh* and N171-82Q mice (82). This finding seems to be typical of multiple HD mouse models (58), with only one exception to date, a report of reduced aconitase and complex II activities in late-stage R6/2 mice (85).

Does Mutant Huntingtin Directly Interact with Mitochondria? Evidence from Genetic Models

The studies described thus far are suggestive of an early role for mitochondrial defects in HD etiology, but until recently a direct link between the huntingtin mutation and mitochondrial function has been lacking. However, evidence is gradually emerging that the mutant protein may directly interact with neuronal mitochondria. One study has systematically examined histological parameters in four different mouse lines (R6/2, R6/1, N171-82Q, and Hdh150CAG mice) and found evidence of degenerated mitochondria in striata in late-stage symptomatic mice (80). These degenerating mitochondria were most prominent in the R6/2 line and notably could be detected before other marked pathological changes within neurons (at about 8–10 weeks of age) and concomitant with symptom onset in these animals. The degeneration is typified by mitochondrial swelling, disruption of the cristae and mitochondrial membranes, and eventual condensation and lysosomal engulfment. Moreover, this report provides the first evidence of a direct interaction of huntingtin protein with mitochondria, by demonstrating the localization of huntingtin N-terminal antibody EM48 immunogold particles both within degenerating mitochondria, and on their surfaces, in R6/2 mouse brain (80). Although R6/2 mice show evidence of striatal atrophy and neuronal shrinkage, there is little detectable striatal cell loss by the time of their premature death at 13–17 weeks of age (22). In contrast, N171-82Q mice show much more marked striatal and cortical-specific neuronal degeneration by end stage. This cell death appears to be largely via apoptotic mechanisms, and there is evidence that mitochondrial cytochrome *c* release is involved, triggering caspase-9 activation (34,80). Another study has reported the association of full-length mutant huntingtin with the surface of mitochondria in YAC-72Q transgenic mice (84).

Functional changes in mitochondria caused by mutant huntingtin have also recently been shown by the demonstration that polyglutamines can influence mitochondrial calcium handling. Panov et al. (86) exposed

mitochondria isolated from rat liver and human lymphoblasts to glutathione *S*-transferase fusion proteins containing polyglutamine tracts of different lengths. Pathogenic polyglutamine constructs (62Q) slightly decreased mitochondrial membrane potential and rendered mitochondria more vulnerable to Ca^{2+}-induced depolarization than mitochondria incubated with wild-type polyglutamine residues (19Q and 0Q). This impairment in calcium handling in the presence of only pathological-length polyglutamines implies that the polyglutamine stretch in mutant huntingtin may alter membrane depolarization, making cells more vulnerable to excitotoxic injury and the consequences of permeability transition. However, results to date give little insight into the regional vulnerability of striatal and cortical CNS neurons in HD. One potential explanation is that a combined effect of huntingtin-mediated increased vulnerability and region-specific alterations in ATP generation underlie regional susceptibility.

Enhancing Metabolism is Protective in Huntington's Disease: Indirect Evidence of Energetic Defects

Circumstantial evidence that energetic defects contribute to neurodegenerative processes in HD is provided by findings that agents that enhance energy production in the brain exert beneficial effects. NMR measurements of lactate production in humans and in rodent mitochondrial toxin models suggest that coenzyme Q_{10} and creatine are neuroprotective, putatively via enhancing cerebral energy metabolism (50,69). Oral administration of CoQ_{10} ameliorated elevated lactate levels seen in the cortex of HD patients, an effect that was reversible on withdrawal of the agent (50). CoQ_{10}, which also has antioxidant effects, also improves symptoms in some other mitochondria-associated disorders, including MELAS and Kearns Sayre syndrome, reducing CSF and serum lactate and pyruvate levels, and enhancing mitochondrial enzyme activities in platelets (87,88). Furthermore, CoQ_{10} attenuates neurotoxicity induced by the mitochondrial toxins MPTP and malonate in animal models (89,90), and was found to increase survival and delay symptom onset in two genetic mouse models of HD (R6/2 and N171–82Q) (91,92). These findings led to CoQ_{10} being tested in a 30-month clinical trial in early-stage HD patients, both in combination with the weak NMDA receptor antagonist remacemide, and alone (93). Although this multiarm trial did not detect a significant ameliorative effect of CoQ_{10}, it did demonstrate a trend toward a protective effect, with treatment slowing the decline in "total functional capacity" of HD patients by 13%. Although findings were not immediately conclusive, results are encouraging and further studies of different doses are planned.

An alternative strategy to enhance cerebral energy metabolism is to increase brain energy stores of the high-energy compound phosphocreatine (PCr) via systemic creatine administration (94,95). Oral creatine treatment successfully attenuated neurotoxicity induced by 3-NP in rats, ameliorating increases in striatal lactate levels and decreases in levels of high-energy phosphate compounds (including ATP) induced by the toxin (69). Furthermore, oral creatine administration has been found to delay disease onset in two HD mouse models, and protect against purkinje cell loss in a transgenic mouse model of another polyglutamine repeat disease, SCA1 (96–98). As a result of these promising effects, creatine's efficacy in HD is currently being assessed in clinical trials. A third approach to modulate energy metabolism therapeutically that has proved efficacious in HD mutant mice, is stimulation of pyruvate dehydrogenase activity by treatment with dichloroacetate (99). Pyruvate dehydrogenase complex activity is impaired in symptomatic R6/2 trangenic mice, but this defect can be reversed with dichloroacetate (DCA) treatment (99). DCA also significantly increased survival, improved motor function, delayed loss of body weight, attenuated the development of striatal neuron atrophy, and prevented diabetes in both the R6/2 and N171–82Q mouse models of HD.

How Are Energetic Changes Deleterious to Neurons in Huntington's Disease?

Excitotoxicity. Impaired energy metabolism, resulting from a toxic action of mutant huntingtin, may be detrimental to cells by inducing excitotoxic damage (100,101). Reduced ATP production can result in cell death directly via disrupting energy-dependent processes. ATP is essential to fuel ionic pumps that generate and maintain ionic and voltage gradients across neuronal membranes, including Na^+/K^+-ATPase pumps that control resting membrane potential and ATPases that regulate intracellular Ca^{2+} levels. Impaired Na^+/K^+-ATPase pump activity may prevent membrane repolarization, resulting in prolonged or inappropriate opening of voltage-dependent ion channels. If severe enough, this partial membrane depolarization can facilitate activation of NMDA receptors by endogenous, normally inert levels of glutamate. In this scenario a concomitant Ca^{2+} influx will occur, triggering nitric oxide synthase (NOS) activation and free radical production. This hypothesis is supported by findings that normally

ambient levels of excitatory amino acids become toxic in the presence of oxidative phosphorylation inhibitors, sodium-potassium pump inhibitors, glucose deprivation, or potassium-induced partial cell membrane depolarization (102–104).

Evidence for excitotoxic processes in HD patients comes primarily from studies of NMDA receptors in HD postmortem tissue. Selective depletion of NMDA receptors has been found in HD striatum, suggesting that neurons bearing NMDA receptors are preferentially vulnerable to degeneration (105). Findings of similar reductions in the striatum of an asymptomatic at-risk patient imply that excitotoxic stress may occur early in the disease process (106). Animal models provide the bulk of evidence for excitotoxicity in HD pathogenesis. Excitotoxic striatal lesions in rats and primates closely resemble those seen in HD brain, with NMDA agonists such as quinolinic acid producing neuronal-specific lesions that show relative sparing of NADPH-diaphorase and parvalbumin-positive neurons typical of HD (89). In primates, quinolinic acid produces striking sparing of NADPH diaphorase neurons, as well as an apomorphine inducible movement disorder (107). In contrast, although AMPA/kainate receptor agonists also produce striatal lesions, they do not replicate the pattern of selective cell loss characteristic of HD.

Excitotoxic processes are also implicated in cell death mediated by mitochondrial toxins that deplete ATP production, including 3-nitropropionic acid (3-NP), 3-acetylpyridine (3-AP), aminooxyacetic acid (AOAA), 1-methyl-4-phenylpyridinium (MPP^+), and malonate (66,90). Systemic administration of 3-NP results in increased binding of tritiated MK-801 (an NMDA receptor channel ligand), consistent with activation of NMDA receptors as a secondary consequence of energy depletion in this model (108). Consequently, 3-NP and malonate lesions can be prevented by prior removal of glutamatergic excitatory corticostriatal inputs by decortication, by glutamate release inhibitors such as riluzole, and by NMDA receptor antagonists including MK-801 (90). Taken together these observations imply that 3-NP toxicity is mediated by secondary excitotoxic mechanisms.

Genetic models of HD also provide evidence of a role for excitotoxic mechanisms in the development of neuronal damage, but findings to date suggest differences between mouse models dependent on the context in which the gene defect is expressed. In YAC-72Q mice, striatal quinolinic acid lesions were exacerbated relative to lesion volumes in wildtype mice, at ages preceding motor symptom onset (109). Cultured neonatal medium spiny neurons expressing the YAC72Q transgene also showed susceptibility to excitotoxic damage induced by NMDA, but not AMPA, which could be abolished by the NMDA receptor NR2B subunit–specific antagonist ifenprodil. NMDA toxicity was also found to be abrogated in cerebellar cells, putatively as a result of their lower levels of NR2B expression (109). The authors therefore hypothesized that regional expression of NR2B subunits may correlate with the severity of neuronal degeneration in HD.

In contrast, another transgenic mouse model that expresses an N-terminal fragment of huntingtin and 46 or 100 CAGs (73) shows no preferential susceptibility to quinolinic acid excitotoxic lesions (110). However, expression of the HD mutation in the context of a shorter gene fragment and longer CAG repeats in R6/2 (145 CAG) and R6/1 (115 CAG) mice conferred resistance to quinolinic acid, malonate, NMDA, and 3-NP toxicity (111,112). One hypothesis to explain the resistance of neurons in these mice is reduced synaptic activity. Dopamine levels in R6/1 mice show 70% depletions in extracellular dopamine relative to wildtype littermate levels (112,113). However, intrastriatal malonate administration in R6/1 mice resulted in a temporary increase in local dopamine release, although lesion volume was reduced by 80% in these animals. In contrast, increased susceptibility to NMDA of R6/2 striatal and cortical neurons has been demonstrated *ex vivo* (76), an observation recapitulated in an *HD* knockin model (76). In another study measuring EPSCs in R6/2 mouse striatal medium spiny neurons, reductions in spontaneous activity were detected at the time of symptom onset in these mice (114). Transmission depression was overt by the time mice become severely impaired (~11–12 weeks of age). The authors demonstrated this to be due to reduced presynaptic events in glutamateric input neurons, implicating defects in the corticostriatal projection pathway in this HD model. The fact that the glutamate release inhibitor riluzole prolongs survival in R6/2 mice (115) reinforces suggestions of an excitotoxic component in this mouse model.

Oxidative Damage. There is evidence that oxidative damage occurs in HD brain and in models of the disorder (54,81,116). Findings in HD patients include increased incidence of DNA strand breaks, exacerbated lipofuscin accumulation (a marker of lipid peroxidation), elevated DNA oxidative damage products such as 8-hydroxydeoxyguanosine (OH^8dG), and increased immunohistochemical staining of oxidative damage products in HD striatum and cortex, including 3-nitrotyrosine (a marker for peroxynitrite-mediated protein nitration), malondialdehyde (marker for oxidative damage to lipids), heme oxygenase (formed during oxidative stress), and OH^8dG (81). Oxidative stress may be a direct mechanism of

huntingtin-linked cellular damage; however, findings that increased oxidative damage to DNA and lipids occurs after symptom onset in the R6/2 transgenic mouse model of HD (117) suggest that it is a downstream event in neuronal dysfunction. It is therefore possible that oxidative damage is induced by energetic defects or secondary excitotoxicity.

Ca^{2+} influx into neurons after activation of excitatory amino acid receptors may trigger increased free radical production via NO-mediated mechanisms, and associated oxidative damage to cellular elements including proteases, lipases, and endonucleases, ultimately leading to cell death (118,119). Direct evidence linking excitotoxicty to free radical generation comes from studies using electron paramagnetic resonance that show that NMDA dose-dependently increases superoxide formation in cultured cerebellar neurons (120). The effects are blocked by NMDA antagonists or removing extracellular Ca^{2+}. This is consistent with findings that exposure of isolated cortical mitochondria to 2.5 μM Ca^{2+}, which is similar to intracellular concentrations induced by excitotoxic stimuli, leads to free radical generation (121). NMDA, kainic acid, and AMPA all stimulate free radical generation in synaptosomes and electron paramagnetic resonance have shown generation of free radicals *in vivo* following systemic kainic acid administration. Further evidence supporting a role for oxidative damage in HD is that the energetic defects seen in HD brain are similar to those induced in cell culture by peroxynitrite, which preferentially inhibits complexes II and III and (to a lesser extent) complex IV activity in the electron transport chain (122).

3-NP toxicity in animals is also associated with increased oxidative damage in the CNS. Hydroxyl (OH^-) free radical production is elevated in the striatum following systemic 3-NP administration, as are levels of the DNA damage marker 8-hydroxy-deoxyguanosine (OH^8dG) and 3-nitrotyrosine (123). Findings that 3-NP-induced lesions and concomitant increases in oxidative damage markers are markedly attenuated in mice overexpressing the superoxide free radical scavenger Cu/Zn superoxide dismutase (SOD1), imply that oxidative free radicals contribute to lesion formation (66). Furthermore, 3-NP striatal lesions are attenuated by free radical spin traps and nitric oxide synthase (NOS) inhibitors (124). In addition, lack of the free radical scavenging enzyme glutathione peroxidase (GSHPx) in knockout mice exacerbates striatal damage and 3-nitrotyrosine elevations caused by systemic administration of 3-NP (66).

Energy Metabolism and Transcriptional Regulation. One potential role for early metabolic alterations in huntingtin-mediated toxicity involves cyclic adenosine 3′,5′-monophosphate (cAMP) signaling. Decreased transcription of genes regulated by cAMP responsive element (CRE) binding protein (CREB) have been implicated in several polyglutamine disorders, including HD. It has been proposed that this decreased transcriptional activity may be due to sequestration of transcriptional coactivators such as CREB binding protein (CBP) and $TAF_{II}130$ into protein aggregates as the disease progresses. This seems unlikely to be the primary step in HD pathogenesis, because evidence shows that NII formation can occur relatively late in the disease process. Also, CBP sequestration cannot explain the dominant reduction in BDNF transcription observed in a *STHdhQ111* striatal cell line, because these cells do not develop inclusions (125). An alternative hypothesis is that a deficiency in cAMP underlies abrogated CRE-mediated gene transcription. cAMP generation is an energy-dependent process, requiring ATP as a precursor, that is reduced in CSF, parietal cortex, and lymphoblastoid cell lines from HD patients (125,126). Furthermore, the adenylate cyclase stimulator forskolin abrogates toxicity induced by expression of mutant huntingtin fragments in PC12 cells (127). In a recent study, Gines et al. (125) used Hdh^{Q111} mice and striatal cell lines to test whether reductions in cAMP link energetic defects with altered CRE signaling in this HD model. cAMP levels were significantly reduced in cortex and striata of these mice by 10 weeks of age, far preceding the formation of nuclear huntingtin aggregates and neuronal death. Further, associated reductions in levels of transcriptionally active phospho-CREB, concomitant with reduced expression of BDNF, were also evident in the cortex of these mice by 5 months of age, indicative of reduced PKA/CREB signaling. These authors went on to suggest that this defect is a result of impaired ATP synthesis induced by the mutant full-length huntingtin, based on observations in a transfected striatal cell line. Notably, mutant huntingtin transfected cells also display elevations in free radical generation and an increased vulnerability to the respiratory chain inhibitor 3-NP.

Changes in cAMP-mediated transcription will have downstream effects on many cell components. One in particular that has gained much interest in HD is brain-derived neurotrophic factor (BDNF). Reduced cAMP-dependent transcription of BDNF is a robust feature of HD pathophysiology. By grades II and III of the disease, BDNF protein and mRNA levels in frontoparietal cortex are halved, and this effect can be mimicked by expressing full-length human mutant huntingtin in a rat CNS parental cell line (128,129). Reduced levels of cortical and striatal BDNF have subsequently been demonstrated in multiple mouse models of HD expressing mutant huntingtin (including R6/2, N171-82Q, *Hdh,* and YAC-72

lines) and are associated with robust alterations in BDNF gene transcription across several different HD mouse lines (125,129–131). In contrast, mice expressing human wild-type huntingtin show increased levels of BDNF. Taken with observations that the striatal pool of BDNF arises from cortical projection neurons, in which huntingtin is widely expressed, it has been suggested that the selective vulnerability of striatal neurons may result from loss of neurotrophic support by BDNF. BDNF also protects neurons against metabolic and excitotoxic insults (132,133) and has been shown to be a promising substrate for cell replacement therapy approaches (134,135). Intrigueingly, a dietary restriction regimen that has been shown to increase BDNF levels in the cerebral cortex, striatum, and hippocampus of mice and rats, was found to increase survival, improve motor performance, ameliorate weight loss, and delay huntingtin aggegate formation and systemic glucose intolerance in R6/2 HD mice (136). The direct protective effect of downregulating metabolic substrates in this manner has yet to be elucidated, but dietary restriction has previously been found to extend life span and is neuroprotective against a number of cell stresses.

Gene profiling studies in HD mouse models also indicate that regulation of several genes involved in mitochondrial function and energy metabolism may be abnormally affected by mutant huntingtin expression. These include creatine kinase, ATP synthase, and subunits of cytochrome *c* oxidase, as well as genes modulating calcium handling and multiple cAMP-regulated genes (130,131,137–139). Although it is tempting to speculate that transcriptional changes in metabolic genes may contribute to HD pathogenesis, caution is warranted in interpreting these observations, because transcriptional changes in a multitude of genes affecting a plethora of different cellular pathways are detected in HD models, of which metabolic components are only a small subset.

Mutant Huntingtin Influences Glucose's Activity as a Signaling Molecule. Another proposed mechanism of cellular damage by mutant huntingtin is disruption of proteosome clearance of ubiquitinated proteins, including mutant huntingtin aggregates. However, clearance of huntingtin may also occur by autophagy. Ravikumar et al. (140) have recently demonstrated that increased intracellular glucose levels are neuroprotective in cultured kidney cells transfected with a mutant huntingtin construct containing 74Q. Reduced huntingtin exon 1 aggregation was also observed. Their results suggest that this is due to increased autophagy as a consequence of dephosphorylation of the authophagy regulator rapamycin (mTOR), concomitant with phosphorylation of glucose to glucose-6-phosphate (140,141). Glucose-mediated regulation of mTOR activity has other implications for cell survival, because it is involved in multible crucial cell processes, including growth and translation of protein transcripts. Further, glucose is also a possible regulator of Akt, which influences cell growth and survival. Cell death in this model is abrogated by overexpression of the GLUT1 astrocytic glucose transporter. This may have direct consequences in HD, as mutant huntingtin exon 1 expression in PC12 cell lines downregulates GLUT1 expression (142), suggesting an intrinsic mechanism of reduced clearance of proteins including huntingtin in HD. This group detected altered expression levels of four genes involved in glucose metabolism in huntingtin transfected PC12 cells (Glut1, Pfkm, Aldolase A, and Enolase), and also demonstrated that augmented expression of Glut1 and Pfkm (another key regulatory protein for glycolysis) rescued both COS7 and SK-N-SH cells from polyglutamine-induced death. These observations raise interesting questions regarding the possible consequences of the initial increases in cerebral glucose uptake detected in mutant mouse models of HD, suggesting that perhaps a feedback loop to remove intracellular mutant huntingtin is set in motion.

CONCLUSION

Studies in human postmortem tissue and *in vivo* imaging techniques have indicated that defects in energy metabolism contribute to neuronal decline at some stage in the HD pathogenesis, but are insufficient to characterize their exact roles. The availability of genetic animal models of the disease is now making it possible to accurately elucidate the nature of this contribution and its importance in modulating mutant huntingtin's toxicity. It is apparent from initial studies that the nature of the genetic model itself affects the pathogenic profile associated with expression of mutant huntingtin, and effects on cerebral energy metabolism vary accordingly. Thus an overview of effects in multiple models is gradually building a picture of how huntingtin's effects on energy metabolism influences pathogenesis of the disease. It is still too early to identify the initial action of mutant huntingtin that triggers selective neuronal dysfunction and cell death pathways, but evidence from both mitochondrial toxin and genetic mouse models suggests that energetic defects occur early in the pathogenic process, and precede overt pathological and symptomatic markers of disease onset. Further, there are tantalizing reports that mutant huntingtin may itself have a direct

interaction with mitochondria and that modulating energy metabolism can affect gene transcription.

ACKNOWLEDGMENT

Studies into glucose metabolism and oxidative metabolism in HD mouse models were supported by grants from the Department of Defense (Browne PI, DAMD17-98-1-8620) and the Huntington's Disease Society of America Coalition for the Cure (Beal and Browne PIs).

REFERENCES

1. Vonsattel, J. P. G. and DiFiglia, M. 1998. Huntington disease. J. Neuropathol. Exp. Neurol. 57:369–384.
2. Andrews, T. C., Weeks, R. A., Turjanski, N., Gunn, R. N., Watkins, L. H., Sahakian, B., Hodges, J. R., Rosser, A. E., Wood, N. W., and Brooks, D. J. 1999. Huntington's disease progression: PET and clinical observations. Brain 122:2353–2363.
3. Beal, M. F., Ellison, D. W., Mazurek, M. F., Swartz, K. J., Malloy, J. R., Bird, E. D., and Martin, J. B. 1988. A detailed examination of substance P in pathologically graded cases of Huntington's disease. J. Neurol. Sci. 84:51–61.
4. Albin, R. L., Reiner, A., Anderson, K. D., Penney, J. B., and Young, A. B. 1990. Striatal and nigral neuron subpopulations in rigid Huntington's disease: Implications for the functional anatomy of chorea and rigidity-akinesia. Ann. Neurol. 27:357–365.
5. Kuwert, T., Lange, H. W., Langer, K.-J., Herzog, H., Aulich, A., and Feinendegen, L. E. 1990. Cortical and subcortical glucose consumption measured by PET in patients with Huntington's disease. Brain 113:1405–1423.
6. The Huntington's Disease Collaborative Research Group. 1993. A novel gene containing a trinucleotide repeat that is expanded and unstable on Huntington's disease chromosome. Cell 72:971–983.
7. MacDonald, M. E., Vonsattel, J.-P., Shrinidhi, J., Couropmitree, N. N., Cupples, L. A., Bird, E. D., Gusella, J. F., Myers, R. H. 1999. Evidence for the GluR6 gene associated with younger onset age of Huntington's disease. Neurology 53:1330–1332.
8. Butterworth, N. J., Williams, L., Bullock, J. Y., Love, D. R., Faull, R. L., and Dragunow, M. 1998. Trinucleotide (CAG) repeat length is positively correlated with the degree of DNA fragmentation in Huntington's disease striatum. Neuroscience 87:49–53.
9. Ross, C. A. 1995. When less is more: Pathogenesis in glutamine repeat neurodegenerative diseases. Neuron 15:493–496.
10. DiFiglia, M., Sapp, E., Chase, K., Schwarz, C., Meloni, A., Young, C., Martin, E., Vonsattel, J.-P., Carraway, R., Reeves, S. A., Boyce, F. M., and Aronin, N. 1995. Huntingtin is a cytoplasmic protein associated with vesicles in human and rat brain neurons. Neuron 14:1075–1081.
11. White, J. K., Auerbach, W., Duyao, M. P., Vonsattel, J.-P., Gusella, J. F., Joyner, A. L., and MacDonald, M. E. 1997. Huntingtin function is required for mouse brain development and is not impaired by the Huntington's disease CAG expansion mutation. Nat. Genet. 17:404–410.
12. Rigamonti, D., Bauer, J. H., De-Fraja, C., Conti, L., Sipione, S., Sciorati, C., Clementi, E., Hackam, A., Hayden, M. R., Li, Y., Cooper, J. K., Ross, C. A., Govoni, S., Vincenz, C., and Cattaneo, E. 2000. Wild-type huntingtin protects from apoptosis upstream of caspase-3. J. Neurosci. 20:3705–3713.
13. Hoffner, G., Kahlem, P., and Dijan, P. 2002. Perinuclear localization of huntingtin as a consequence of its binding to microtubules through an interaction with beta-tubulin: Relevance to Huntington's disease. J. Cell Sci. 115:941–948.
14. Duyao, M. P., Auerbach, A. B., Persichetti, F., Barnes, G. T., McNeil, S. M., Ge, P., Vonsattel, J.-P., Gusella, J. F., Joyner, A. L., and MacDonald, M. E. 1995. Inactivation of the mouse Huntington's disease gene homolog Hdh. Science 269:407–410.
15. Auerbach, W., Hurlbert, M. S., Hilditch-Maguire, P., Wadghiri, Y. Z., Wheeler, V. C., Cohen, S. I., Joyner, A. L., MacDonald, M. E., and Turnbull, D. H. 2001. The HD mutation causes progressive lethal neurological disease in mice expressing reduced levels of huntingtin. Hum. Mol. Genet. 10:2515–2523.
16. Sharp, N. H., Love, S. J., Schilling, G., Li, S.-H., Li, X.-J., Bao, J., Wagster, M. V., Kotzuk, J. A., Steiner, J. P., Lo, A., Hedreen, J., Sisodia, S., Snyder, S. H., Dawson, T. M., Ryugo, D. K., and Ross, C. A. 1995. Widespread expression of the Huntington's disease gene (IT-15) protein product. Neuron 14:1065–1074.
17. Sapp, E., Schwarz, C., Chase, K., Bhide, P. G., Young, A. B., Penney, J., Vonsattel, J. P., Aronin, N., and DiFiglia, M. 1997. Huntingtin localization in brains of normal and Huntington's disease patients. Ann. Neurol. 42:604–612.
18. Ferrante, R. J., Gutekunst, C. A., Persichetti, F., McNeil, S. M., Kowall, N. W., Gusella, J. F., MacDonald, M. E., Beal, M. F., and Hersch, S. M. 1997. Heterogeneous topographic and cellular distribution of huntingtin expression in the normal human neostriatum. J. Neurosci. 17:3052–3063.
19. Fusco, F. R., Chen, Q., Lamoreaux, W. J., Figueredo-Cardenas, G., Jiao, Y., Coffman, J. A., Surmeier, D. J., Honig, M. G., Carlock, L. R., and Reiner, A. 1999. Cellular localization of huntingtin in striatal and cortical neurons in rats: Lack of correlation with neuronal vulnerability in Huntington's disease. J. Neurosci. 19: 1189–1202.
20. Meade, C. A., Deng, Y. P., Fusco, F. R., Del Mar, N., Hersch, S., Goldowitz, D., and Reiner, A. 2002. Cellular localization and development of neuronal intranuclear inclusions in striatal and cortical neurons in R6/2 transgenic mice. J. Comp. Neurol. 449:241–269.
21. Lunkes, A., Lindenberg, K. S., Ben-Haiem, L., Weber, C., Devys, D., Landwehrmeyer, G. B., Mandel, J.-L., and Trottier, Y. 2002. Proteases acting on mutant huntingtin generate cleaved products that differentially build up cytoplasmic and nuclear inclusions. Mol. Cell 10:259–269.
22. Davies, S. W., Turmaine, M., Cozens, B., DiFiglia, M., Sharp, A., Ross, C. A., Scherzinger, E., Wanker, E. E., Mangiarini, L., and Bates, G. 1997. Formation of neuronal intranuclear inclusions (NII) underlies the neurological dysfunction in mice transgenic for the HD mutation. Cell 90:537–548.
23. DiFiglia, M., Sapp, E., Chase, K. O., Davies, S. W., Bates, G. P., Vonsattel, J.-P., and Aronin, N. 1997. Aggregation of huntingtin in neuronal intranuclear inclusions and dystrophic neurites in brain. Science 277:1990–1993.
24. Hodgson, J. G., Agopyan, N., Gutekunst, C.-A., Leavitt, B. R., LePiane, F., Singaraja, R., Smith, D. J., Bissada, N., McCutchoon, K., Nasir, J., Jamot, L., Li, X.-J., Rosemond, E., Roder, J. C., Phillips, A. G., Rubin, E. M., Hersch, S. M., and Hayden, M. R. 1999. A YAC mouse model for Huntington's disease with full-length mutant huntingtin, cytoplasmic toxicity, and selective striatal neurodegeneration. Neuron 23:1–20.
25. Schilling, G., Bacher, M. W., Sharp, A. H., Jinnah, H. A., Duyao, K., Kotzuk, J. A., Slunt, H. H., Ratovitski, T., Cooper, J. A., Jenkins, N. A., et al. 1999. Intranuclear inclusions and neuritic aggregates in transgenic mice expressing a mutant N-terminal fragment of huntingtin. Hum. Mol. Genet. 8:397–407.
26. Wheeler, V. C., White, J. K., Gutekunst, C. A., Vrbanac, V., Weaver, M., Li, X. J., Li, S. H., Yi, H., Vonsattel, J. P., Gusella, J. F., Hersch, S., Auerbach, W., Joyner, A. L., and MacDonald, M. E. 2000. Long glutamine tracts cause nuclear localization of a novel form of huntingtin in medium spiny striatal neurons in HdhQ92 and HdhQ111 knock-in mice. Hum. Mol. Genet. 9:503–513.
27. Saudou, F., Finkbeiner, S., Devys, D., and Greenberg, M. E. 1998. Huntingtin acts in the nucleus to induce apoptosis but death does not correlate with the formation of intranuclear inclusions. Cell 95:55–66.

28. Rubinsztein, D. C. 2002. Lessons from animal models of Huntington's disease. Trends Gen. 18:202–209.
29. Kim, M., Lee, H. S., LaForet, G., McIntyre, C., Martin, E. J., Chang, P., Kim, T. W., Williams, M., Reddy, P. H., Tagle, D., Boyee, F. M., Won, L., Heller, A., Aronin, N., and DiFiglia, M. 1999. Mutant huntingtin expression in clonal striatal cells: Dissociation of inclusion formation and neuronal survival by caspase inhibition. J. Neurosci. 19:964–73.
30. Peters, M. F., Nucifora, F. C. Jr., Kushi, J., Seaman, H. C., Cooper, J. K., Herring, W. J., Dawson, V. L., Dawson, T. M., and Ross, C. A. 1999. Nuclear targeting of mutant Huntingtin increases toxicity. Mol. Cell Neurosci. 14:121–128.
31. Martin-Aparicio, E., Avila, J., and Lucas, J. J. 2002. Nuclear localization of N-terminal mutant huntingtin is cell cycle dependent. Eur. J. Neurosci. 16:355–359.
32. Cooper, A. J. L., Sheu, K.-F. R., Burke, J. R., Onodera, O., Strittmatter, W. J., Roses, A. D., and Blass, J. P. 1997. Transglutaminase-catalyzed inactivation of glyceraldehyde 3-phosphate dehydrogenase and α-ketoglutarate dehydrogenase complex by polyglutamine domains of pathological length. Proc. Natl. Acad. Sci. USA 94:12604–12609.
33. Cooper, A. J., Sheu, K. F., Burke, J. R., Strittmatter, W. J., Gentile, V., Peluso, G., and Blass, J. P. 1999. Pathogenesis of inclusion bodies in (CAG)n/Qn-expansion diseases with special reference to the role of tissue transglutaminase and to selective vulnerability. J. Neurochem. 72:889–899.
34. Hickey, M. A. and Chesselet, M. F. 2003. Apoptosis in Huntington's disease. Prog. Neuropsychopharmacol. Biol. Psychiatry 27:255–265.
35. Burke, J. R., Enghild, J. J., Martin, M. E., Jou, Y.-S., Myers, R. M., Roses, A. D., Vance, V. M., and Strittmatter, W. J. 1996. Huntingtin and DRPLA proteins selectively interact with the enzyme GAPDH. Nat. Med. 2:347–350.
36. Aronin, N., Kim, M., Laforet, G., and DiFiglia, M. 1999. Are there multiple pathways in the pathogenesis of Huntington's disease? Phil. Trans. R. Soc. Lond. 354:995–1003.
37. Steffan, J. S., Bodai, L., Pallos, J., Poelman, M., McCampbell, A., Apostol, B. L., Kazantsev, A., Schmidt, E., Zhu, Y. Z., Greenwald, M., Kurokawa, R., Housman, D. E., Jackson, C. R., Marsh, J. L., and Thompson, L. M. 2001. Histone deacetylase inhibitors arrest polyglutamine-dependent neurodegeneration in Drosophila. Nature 413:739–743.
38. Dunah, A. W., Jeong, H., Griffin, A., Kim, Y. M., Standaert, D. G., Hersch, S. M., Mouradian, M. M., Young, A. B., Tanese, N., and Krainc, D. 2002. Sp1 and TAFII130 transcriptional activity disrupted in early Huntington's disease. Science 296:2238–2243.
39. O'Brien, C. F., Miller, C., Goldblatt, D., Welle, S., Forbes, G., Lipinski, B., Panzik, J., Peck, R., Plumb, S., Oakes, D., Kurlan, R., and Shoulson, I. 1990. Extraneural metabolism in early Huntington's disease. Ann. Neurol. 28:300–301.
40. Djousse, L., Knowlton, B., Cupples, L. A., Marder, K., Shoulson, I., and Myers, R. H. 2002. Weight loss in early stage of Huntington's disease. Neurology 59:1325–1330.
41. Andrews, T. C. and Brooks, D. J. 1998. Advances in the understanding of early Huntington's disease using the functional imaging techniques of PET and SPET. Mol. Med. Today 4:532–539.
42. Kuhl, D. E., Markham, C. H., Metter, E. J., Riege, W. H., Phelps, M. E., and Mazziotta, J. C. 1985. Local cerebral glucose utilization in symptomatic and presymptomatic Huntington's disease. Res. Publ. Assoc. Res. Nerv. Men. Dis. 63:199–209.
43. Berent, S., Giordani, B., Lehtinen, S., Markel, D., Penney, J. B., Buchtel, H. A., Starosta Rubinstein, S., Hichwa, R., and Young, A. B. 1988. Positron emission tomographic scan investigations of Huntington's disease: Cerebral metabolic correlates. Ann. Neurol. 23:541–546.
44. Grafton, S. T., Mazziotta, J. C., Pahl, J. J., St George-Hyslop, P., Haines, J. L., Gusella, J., Hoffman, J. M., Baxter, L. R., and Phelps, M. E. 1992. Serial changes of cerebral glucose metabolism and caudate size in persons at risk for Huntington's disease. Arch. Neurol. 49:1161–1167.
45. Kuwert, T., Lange, H. W., Boecker, H., Titz, H., Herzog, H., Aulich, A., Wang, B. C., Nayak, U., and Feinendegen, L. E. 1993. Striatal glucose consumption in chorea-free subjects at risk of Huntington's disease. J. Neurol. 241:31–36.
46. Antonini, A., Leenders, K. L., Spiegel, R., Meier, D., Vontobel, P., Weigell-Weber, M., Sanchez-Pernaute, R., de Yebenez, J. G., Boesiger, P., Weindl, A., and Maguire, R. P. 1996. Striatal glucose metabolism and dopamine D2 receptor binding in asymptomatic gene carriers and patients. Brain 119:2085–2095.
47. Feigin, A., Leenders, K. L., Moeller, J. R., Missimer, J., Kuenig, G., Spetsieris, P., Antonini, A., and Eidelberg, D. 2001. Metabolic network abnormalities in early Huntington's disease: An [(18)F] FDG PET study. J. Nucl. Med. 42:1591–1595.
48. Jenkins, B. G., Koroshetz, W., Beal, M. F., and Rosen, B. 1993. Evidence for an energy metabolism defect in Huntington's disease using localized proton spectroscopy. Neurology 43:2689–2695.
49. Jenkins, B. G., Rosas, H. D., Chen, Y. C., Makabe, T., Myers, R., MacDonald, M., Rosen, B. R., Beal, M. F., and Koroshetz, W. J. 1998. ^{1}H NMR spectroscopy studies of Huntington's disease: Correlations with CAG repeat numbers. Neurology 50:1357–1365.
50. Koroshetz, W. J., Jenkins, B. G., Rosen, B. R., and Beal, M. F. 1997. Energy metabolism defects in Huntington's disease and possible therapy with coenzyme Q_{10}. Ann. Neurol. 41:160–165.
51. Nicoli, F., Vion-Dury, J., Maloteaux, J. M., Delwaide, C., Confort-Gouny, S., Sciaky, M., and Cozzone, P. J. 1993. CSF and serum metabolic profile of patients with Huntington's chorea: A study by high resolution proton NMR spectroscopy and HPLC. Neurosci. Lett. 154:47–51.
52. Lodi, R., Schapira, A. H., Manners, D., Styles, P., Wood, N. W., Taylor, D. J., and Warner, T. T. 2000. Abnormal *in vivo* skeletal muscle energy metabolism in Huntington's disease and dentatorubropallidoluysian atrophy. Ann. Neurol. 48:72–76.
53. Butterworth, J., Yates, C. M., and Reynolds, G. P. 1985. Distribution of phosphate-activated glutaminase, succinic dehydrogenase, pyruvate dehydrogenase, and γ-glutamyl transpeptidase in post-mortem brain from Huntington's disease and agonal cases. J. Neurol. Sci. 67:161–171.
54. Browne, S. E., Bowling, A. C., MacGarvey, U., Baik, M. J., Berger, S. C., Muqit, M. M. K., Bird, E. D., and Beal, M. F. 1997. Oxidative damage and metabolic dysfunction in Huntington's disease: Selective vulnerability of the basal ganglia. Ann. Neurol. 41:646–653.
55. Gu, M., Gash, M. T., Mann, V. M., Javoy-Agid, F., Cooper, J. M., and Schapira, A. H. V. 1996. Mitochondrial defect in Huntington's disease caudate nucleus. Ann. Neurol. 39:385–389.
56. Parker, W. D. Jr., Boyson, S. J., Luder, A. S., and Parks, J. K. 1990. Evidence for a defect in NADH:ubiquinone oxidoreductase (complex I) in Huntington's disease. Neurology 40:1231–1234.
57. Arenas, J., Campos, Y., Ribacoba, R., Martin, M. A., Rubio, J. C., Ablanedo, P., and Cabello, A. 1998. Complex I defect in muscle from patients with Huntington's disease. Ann. Neurol. 43: 397–400.
58. Guidetti, P., Charles, V., Chen, E. Y., Reddy, P. H., Kordower, J. H., Whetsell, W. O. Jr., Schwarcz, R., and Tagle, D. A. 2001. Early degenerative changes in transgenic mice expressing mutant huntingtin involve dendritic abnormalities but no impairment of mitochondrial energy production. Exp. Neurol. 169:340–50.
59. Tabrizi, S. J., Cleeter, M. W., Xuereb, J., Taanman, J. W., Cooper, J. M., and Schapira, A. H. 1999. Biochemical abnormalities and excitotoxicity in Huntington's disease brain. Ann. Neurol. 45:25–32.
60. Mastrogiacomo, F., LaMarche, J., Dozic, S., Lindsay, G., Bettendorff, L., Robitaille, Y., Schut, L., and Kish, S. J. 1996. Immunoreactive levels of alpha-ketoglutarate dehydrogenase subunits in Friedreich's ataxia and spinocerebellar ataxia type 1. Neurodegen. 5:27–33.
61. Matsuishi, T., Sakai, T., Naito, E., Nagamitsu, S., Kuroda, Y., Iwashita, H., and Kato, H. 1996. Elevated cerebrospinal fluid lactate/pyruvate ratio in Machado-Joseph disease. Acta Neurol. Scand. 93:72–75.

62. Mazzola, J. L. and Sirover, M. A. 2001. Reduction of glyceraldehyde-3-phosphate dehydrogenase activity in Alzheimer's disease and in Huntington's disease fibroblasts. J. Neurochem. 76:442–449.
63. Mazzola, J. L. and Sirover, M. A. 2002. Alteration of nuclear glyceraldehyde-3-phosphate dehydrogenase structure in Huntington's disease fibroblasts. Brain Res. Mol. Brain Res. 100:95–101.
64. Senatorov, V. V., Charles, V., Reddy, P. H., Tagle, D. A., and Chuang, D. M. 2003. Overexpression and nuclear accumulation of glyceraldehyde-3-phosphate dehydrogenase in a transgenic mouse model of Huntington's disease. Mol. Cell Neurosci. 22:285–297.
65. Ludolph, A. C., He, F., Spencer, P. S., Hammerstad, J., and Sabri, M. 1990. 3-Nitropropionic acid: Exogenous animal neurotoxin and possible human striatal toxin. Can. J. Neurol. Sci. 18:492–498.
66. Browne, S. E. and Beal, M. F. 2002. Toxin-induced mitochondrial dysfunction. Int. Rev. Neurobiol. 53:243–279.
67. Brouillet, E., Hantraye, P., Ferrante, R. J., Dolan, R., Leroy-Willig, A., Kowall, N. W., and Beal, M. F. 1995. Chronic mitochondrial energy impairment produces selective striatal degeneration and abnormal choreiform movements in primates. Proc. Natl. Acad. Sci. USA 92:7105–7109.
68. Brouillet, E., Guyot, M. C., Mittoux, V., Altairac, S., Conde, F., Palfi, S., and Hantraye, P. 1998. Partial inhibition of brain succinate dehydrogenase by 3-nitropropionic acid is sufficient to initiate striatal degeneration in rat. J. Neurochem. 70:794–805.
69. Matthews, R. T., Yang, L., Jenkins, B. J., Ferrante, R. J., Rosen, B. R., Kaddurah-Daouk, R., and Beal, M. F. 1998. Neuroprotective effects of creatine and cyclocreatine in animal models of Huntington's disease. J. Neurosci. 18:156–163.
70. Faber, P. W., Alter, J. R., MacDonald, M. E., and Hart, A. C. 1999. Polyglutamine-mediated dysfunction and apoptotic death of a Caenorhabditis elegans sensory neuron. Proc. Natl. Acad. Sci. USA 96:179–184.
71. von Horsten, S., Schmitt, I., Nguyen, H. P., Holzmann, C., Schmidt, T., et al. 2003. Transgenic rat model of Huntington's disease. Hum. Mol. Genet. 12:617–24.
72. Mangiarini, L., Sathasivam, K., Seller, M., Cozens, B., Harper, A., Hetherington, C., Lawton, M., Trottier, Y., Lehrach, H., Davies, S. W., and Bates, G. 1996. Exon 1 of the HD gene with an expanded CAG repeat is sufficient to cause a progressive neurological phenotype in transgenic mice. Cell 87:493–506.
73. Laforet, G. A., Sapp, E., Chase, K., McIntyre, C., Boyce, F. M., Campbell, M., Cadigan, B. A., Warzecki, L., Tagle, D. A., Reddy, P. H., Cepeda, C., Calvert, C. R., Jokel, E. S., Klapstein, G. J., Ariano, M. A., Levine, M. S., DiFiglia, M., and Aronin, N. 2001. Changes in cortical and striatal neurons predict behavioral and electrophysiological abnormalities in a transgenic murine model of Huntington's disease. J. Neurosci. 21: 9112–9123.
74. Yamamoto, A., Lucas, J. J., and Hen, R. 2000. Reversal of neuropathy and motor dysfunction in a conditional model of Huntington's disease. Cell 101:57–66.
75. Reddy, P. H., Williams, M., Charles, V., Garrett, L., Pike-Buchanan, L., Whetsell, W. O. Jr., Miller, G., and Tagle, D. A. 1998. Behavioural abnormalities and selective neuonal loss in HD transgenic mice expressing mutated full-length HD cDNA. Nat. Genet. 20:198–202.
76. Levine, M. S., Klapstein, G. J., Koppel, A., Gruen, E., Cepeda, C., Vargas, M. E., Jokel, E. S., Carpenter, E. M., Zanjani, H., Hurst, R. S., Efstratiadis, A., Zeitlin, S., and Chesselet, M. F. 1999. Enhanced sensitivity to N-methyl-D-aspartate receptor activation in transgenic and knockin mouse models of Huntington's disease. J. Neurosci. Res. 58:515–532.
77. Lin, C. H., Tallaksen-Greene, S., Chien, W. M., Cearley, J. A., Jackson, W. S., Crouse, A. B., Ren, S., Li, X. J., Albin, R. L., and Detloff, P. J. 2001. Neurological abnormalities in a knock-in mouse model of Huntington's disease. Hum. Mol. Genet. 10: 137–144.
78. Shelbourne, P. F., Killeen, N., Hevner, R. F., Johnston, H. M., Tecott, L., Lewandoski, M., Ennis, M., Ramirez, L., Li, Z., Iannicola, C., Littman, D. R., and Myers, R. M. 1999. A Huntington's disease CAG expansion at the murine Hdh locus is unstable and associated with behavioural abnormalities in mice. Hum. Mol. Genet. 8: 763–774.
79. Ishiguru, H., Yamada, K., Sawada, H., Nishii, K., Ichino, N., Sawada, M., Kurosawa, Y., Matsushita, N., Kobayashi, K., Goto, J., Hashida, H., Masuda, N., Kanazawa, I., and Nagatsu, T. 2001. Age-dependent and tissue-specific CAG repeat instability occurs in mouse knock-in for a mutant Huntington's disease gene. J. Neurosci. Res. 65:289–297.
80. Yu, Z.-X., Li, S.-H., Evans, J., Pillarisetti, A., Li, H., and Li, X.-J. 2003. Mutant huntingtin causes context-dependent neurodegeneration in mice with Huntington's disease. J. Neurosci. 23:2193–2202.
81. Browne, S. E., Wheeler, V., White, J. K., Fuller, S. W., MacDonald, M., and Beal, M. F. 1999. Dose-dependent alterations in local cerebral glucose use associated with the huntingtin mutation in Hdh CAG knock-in transgenic mice. Soc. Neurosci. Abstr. 25:218.11.
82. Gregorio, J., DiMauro, J.-P. P., Narr, S., Fuller, S. W., and Browne, S. E. 2002. Cerebral metabolism defects in HD: Glucose utilization abnormalities in multiple HD mouse models. Soc. Neurosci. Abstr. 28:195.10
83. Wheeler, V. C., Gutekunst, C. A., Vrbanac, V., Lebel, L. A., Schilling, G., Hersch, S., Friedlander, R. M., Gusella, J. F., Vonsattel, J. P., Borchelt, D. R., MacDonald, M. E. 2002. Early phenotypes that presage late-onset neurodegenerative disease allow testing of modifiers in Hdh CAG knock-in mice. Hum. Mol. Genet. 11:633–640.
84. Panov, A. V., Gutekunst, C. A., Lelavitt, B. R., Hayden, M. R., Burke, J. R., Strittmatter, W. J., and Greenamyre, J. T. 2002. Early mitochonrial calcium defects in Huntington's disease are a direct effect of polyglutamines. Nat. Neurosci. 5:731–736.
85. Tabrizi, S. J., Workman, J., Hart, P. E., Mangiarini, L., Mahal, A., Bates, G., Cooper, J. M., and Schapira, A. H. 2000. Mitochondrial dysfunction and free radical damage in the Huntington R6/2 transgenic mouse. Ann. Neurol. 47:80–86.
86. Panov, A. V., Burke, J. R., Strittmatter, W. J., and Greenamyre, J. T. 2003. In vitro effects of polyglutamine tracts on Ca^{2+}-dependent depolarization of rat and human mitochondria: Relevance to Huntington's disease. Arch. Biochem. Biophys. 410:1–6.
87. Bresolin, N., Bet, L., Binda, A., Moggio, M., Comi, G., Nador, F., Ferrante, C., Carenzi, A., and Searlato, G. 1988. Clinical and biochemical correlations in mitochondrial myopathies treated with coenzyme Q_{10}. Neurology 38:892–899.
88. Ihara, Y., Namba, R., Kuroda, S., Sato, T., and Shirabe, T. 1989. Mitochondrial encephalomyopathy (MELAS): Pathological study and successful therapy with coenzyme Q_{10} and idebenone. J. Neurol. Sci. 90:263–271.
89. Beal, M. F., Henshaw, D. R., Jenkins, B. G., Rosen, B. R., and Schulz, J. B. 1994. Coenzyme Q_{10} and nicotinamide block striatal lesions produced by the mitochondrial toxin malonate. Ann. Neurol. 36:882–888.
90. Schulz, J. B., Matthews, R. T., Henshaw, D. R., and Beal, M. F. 1996. Neuroprotective strategies for treatment of lesions produced by mitochondrial toxins: Implications for neurodegenerative diseases. Neurosci. 71:1043–1048.
91. Schilling, G., Coonfield, M. L., Ross, C. A., and Borchelt, D. R. 2001. Coenzyme Q10 and remacemide hydrochloride ameliorate motor deficits in a Huntington's disease transgenic mouse model. Neurosci. Lett. 315:149–153.
92. Ferrante, R. J., Andreassen, O. A., Dedeoglu, A., Ferrante, K. L., Jenkins, B. G., Hersch, S. M., and Beal, M. F. 2002. Therapeutic effects of coenzyme Q10 and remacemide in transgenic mouse models of Huntington's disease. J. Neurosci. 22:1592–1599.
93. Huntington Study Group. 2001. A randomized, placebo-controlled trial of coenzyme Q10 and remacemide in Huntington's disease. Neurology 57:375–376.
94. Wyss, M. and Schulze, A. 2002. Health implications of creatine: Can oral creatine supplementation protect against neurological and atherosclerotic disease? Neuroscience 112:243–260.

95. Tarnopolsky, M. A. and Beal, M. F. 2001. Potential for creatine and other therapies targeting cellular energy dysfunction in neurological disorders. Ann. Neurol. 49:561–574.
96. Ferrante, R. J., Andreassen, O. A., Dedeoglu, A., Kuemmerle, S., Kubilus, J. K., Kaddurah-Daouk, R., Hersch, S. M., and Beal, M. F. 2000. Neuroprotective effects of creatine in a transgenic mouse model of Huntington's disease. J. Neurosci. 20: 4389–4397.
97. Andreassen, O. A., Dedeoglu, A., Ferrante, R. J., Jenkins, B. J., Ferrante, K. L., Thomas, M., Friedlich, A., Browne, S. E., Schilling, G., Borchelt, D. R., Hersch, S. M., Ross, C. A., Beal, M. F. 2001. Creatine increase survival and delays motor symptoms in a transgenic animal model of Huntington's disease. Neurobiol. Dis. 8: 479–491.
98. Kaemmerer, W. F., Rodrigues, C. M., Steer, C. J., and Low, W. C. 2001. Creatine-supplemented diet extends Purkinje cell survival in spinocerebellar ataxia type 1 transgenic mice but does not prevent the ataxic phenotype. Neuroscience 103:713–724.
99. Andreassen, O. A., Ferrante, R. J., Huang, H. M., Dedeoglu, A., Park, L., Ferrante, K. L., Kwon, J., Borchelt, D. R., Ross, C. A., Gibson, G. E., and Beal, M. F. 2001. Dichloroacetate exerts therapeutic effects in transgenic mouse models of Huntington's disease. Ann. Neurol. 50:112–117.
100. Albin, R. L. and Greenamyre, J. T. 1992. Alternative excitotoxic hypotheses. Neurology 42:733–738.
101. Browne, S. E., Ferrante, R. J., and Beal, M. F. 1999. Oxidative stress in Huntington's disease. Brain Pathol. 9:147–163.
102. Novelli, A., Reilly, J. A., Lysko, P. G., and Henneberry, R. C. 1988. Glutamate becomes neurotoxic via the N-methyl-D-aspartate receptor when intracellular energy levels are reduced. Brain Res. 451: 205–212.
103. Henneberry, R. L., Novelli, A., Cox, J. A., and Lysko, P. G. 1989. Neurotoxicity at the N-methyl-D-aspartate receptor in energy-compromised neurons: An hypothesis for cell death in aging and disease. Ann. NY Acad. Sci. 568:225–233.
104. Zeevalk, G. D. and Nicklas, W. J. 1991. Mechanisms underlying initiation of excitotoxicity associated with metabolic inhibition. J. Pharm. Exp. Ther. 257:870–878.
105. Dure, L. S. 4th, Young A. B., and Penney, J. B. 1991. Excitatory amino acid binding sites in the caudate nucleus and frontal cortex of Huntington's disease. Ann. Neurol. 30:785–793.
106. Albin, R. L., Young, A. B., Penney, J. B., Handelin, B., Balfour, R., Anderson, K. D., Markel, D. S., Tourtellotte, W. W., and Reiner, A. 1990. Abnormalities of striatal projection neurons and N-methyl-D-aspartate receptors in presymptomatic Huntington's disease. N. Engl. J. Med. 322:1293–1298.
107. Ferrante, R. J., Kowall, N. W., Cipolloni, P. B., Storey, E., and Beal, M. F. 1993. Excitotoxin lesions in primates as a model for Huntington's disease: Histopathologic and neurochemical characterization. Exp. Neurol. 119:46–71.
108. Wullner, U., Young, A. B., Penney, J. B., and Beal, M. F. 1994. 3-Nitropropionic acid toxicity in the striatum. J. Neurochem. 63: 1772–1781.
109. Zeron, M. M., Hansson, O., Chen, N., Wellington, C. L., Leavitt, B. R., Brundin, P., Hayden, M. R., and Raymond, L. A. 2002. Increased sensitivity to N-methyl-D-aspartate receptor-mediated excitotoxicity in a mouse model of Huntington's disease. Neuron 33:849–860.
110. Petersen, A., Chase, K., Puschban, Z., DiFiglia, M., Brundin, P., and Aronin, N. 2002. Maintenance of susceptibility to neurodegeneration following intrastriatal injections of quinolinic acid in a new transgenic mouse model of Huntington's disease. Exp. Neurol. 175:297–300.
111. Hansson, O., Castilho, R. F., Korhonen, L., Lindholm, D., Bates, G. P., and Brundin, P. 2001. Partial resistance to malonate-induced striatal cell death in transgenic mouse models of Huntington's disease is dependent on age and CAG repeat length. J. Neurochem. 78:694–703.
112. Hickey, M. A. and Morton, A. J. 2000. Mice transgenic for the Huntington's disease mutation are resistant to chronic 3-nitopropionic acid-induced striatal toxicity. J. Neurochem. 75:2163–2171.
113. Petersen, A., Hansson, O., Puschban, Z., Sapp, E., Romero, N., Castilho, R. F., Sulzer, D., Rice, M., DiFiglia, M., Przedborski, S., and Brundin, P. 2001. Mice transgenic for exon 1 of the Huntington's disease gene display reduced striatal sensitivity to neurotoxicity induced by dopamine and 6-hydroxydopamine. Eur. J. Neurosci. 14:1425–1435.
114. Cepeda, C., Hurst, R. S., Calvert, C. R., Hernandez-Echeagaray, E., Nguyen, O. K., Jocoy, E., Christian, L. J., Ariano, M. A., and Levine, M. S. 2003. Transient and progressive electrophysiological alterations in the corticostriatal pathway in a mouse model of Huntington's disease. J. Neurosci. 23:961–996.
115. Schiefer, J., Landwehrmeyer, G. B., Luesse, H. G., Sprunken, A., Puls, C., Milkereit, A., Milkereit, E., and Kosinski, C. M. 2002. Riluzole prolongs survival time and alters nuclear inclusion formation in a transgenic mouse model of Huntington's disease. Mov. Disord. 17:748–757.
116. Polidori, M. C., Mecocci, P., Browne, S. E., Senin, U., and Beal, M. F. 1999. Oxidative damage to mitochondrial DNA in Huntington's disease parietal cortex. Neurosci. Lett. 272:53–56.
117. Bogdanov, M. B., Andreassen, O. A., Dedeoglu, A., Ferrante, R. J., Beal, M. F. 2001. Increased oxidative damage to DNA in a transgenic mouse model of Huntington's disease. J. Neurochem. 79:1246–1249.
118. Calabrese, V., Scapagnini, G., Giuffrida-Stella, A. M., Bates, T. E., and Clark, J. B. 2001. Mitochondrial involvement in brain function and dysfunction: Relevance to aging, neurodegenerative disorders and longevity. Neurochem. Res. 26:739–764.
119. Brown, G. C. and Borutaite, V. 2001. Nitric oxide, mitochondria, and cell death. IUBMB Life 52:189–195.
120. Lafon-Cazal, M., Culcasi, M., Gaven, F., Pietri, S., and Bockaert, J. 1993. Nitric oxide, superoxide and peroxynitrite: Putative mediators of NMDA-induced cell death in cerebellar granule cells. Neuropharmacology 32:1259–1266.
121. Dykens, J. A. 1994. Isolated cerebral and cerebellar mitochondria produce free radicals when exposed to elevated Ca^{2+} and Na^{+}: Implications for neurodegeneration. J. Neurochem. 63:584–591.
122. Bolanos, J. P., Heales, S. J. R., Land, J. M., and Clark, J. B. 1995. Effect of peroxynitrite on the mitochondrial respiratory chain: Differential susceptibility of neurones and astrocytes in primary culture. J. Neurochem. 64:1965–1972.
123. Schulz, J. B., Henshaw, D. R., MacGarvey, U., and Beal, M. F. 1996. Involvement of oxidative stress in 3-nitropropionic acid neurotoxicity. Neurochem. Intl. 29:167–171.
124. Schulz, J. B., Henshaw, D. R., Siweck, D., Jenkins, B. G., Ferrante, R. J., Cipolloni, P. B., Kowall, N. W., Rosen, B. R., Beal, M. F. 1995. Involvement of free radicals in excitotoxicity *in vivo*. J. Neurochem. 64:2239–2247.
125. Gines, S., Seong, I. S., Fossale, E., Ivanova, E., Trettel, F., Gusella, J. F., Wheeler, V. C., Persichetti, F., and MacDonald, M. E. 2003. Specific progressive cAMP reduction implicates energy deficit in presymptomatic Huntington's disease knock-in mice. Hum. Mol. Genet. 12:497–508.
126. Cramer, H., Warter, J. M., and Renaud, B. 1984. Analysis of neurotransmitter metabolites and adenosine 3′ 5′-monophosphate in the CSF of patients with extrapyramidal motor disorders. Adv. Neurol. 40:431–435.
127. Wyttenbach, A., Swartz, J., Kita, H., Thykjaer, T., Carmichael, J., Bradley, J., Brown, R., Maxwell, M., Schapira, A., Orntoft, T. F., et al. 2001. Polyglutamine expansions cause decreased CRE-mediated transcription and early gene expression changes prior to cell death in an inducible cell model of Huntington's disease. Hum. Mol. Genet. 10:1829–1845.
128. Ferrer, I., Goutan, E., Marin, C., Rey, M. J., and Ribalta, T. 2000. Brain-derived neurotrophic factor in Huntington disease. Brain Res. 866:257–261.

129. Zuccato, C., Ciammola, A., Rigamonti, D., Leavitt, B. R., Goffredo, D., Conti, L., MacDonald, M. E., Friedlander, R. M., Silani, V., Hayden, M. R. et al. 2001. Loss of huntingtin-mediated BDNF gene transcription in Huntington's disease. Science 293:493–498.
130. Luthi-Carter, R., Strand, A., Peters, N. L., Solano, S. M., Hollingsworth, Z. R., Menon, A. S., Frey, A. S., Spektor, B. S., Penney, E. B., Schilling, G., Ross, C. A., Borchelt, D. R., Tapscott, S. J., Young, A. B., Cha, J. H., Olson, J. M. 2000. Decreased expression of striatal signaling genes in a mouse model of Huntington's disease. Hum. Mol. Genet. 9:1259–1271.
131. Luthi-Carter, R., Hanson, S. A., Strand, A. D., Bergstrom, D. A., Chun, W., Peters, N. L., Woods, A. M., Chan, E. Y., Kooperberg, C., Krainc, D., Young A. B., Tapscott, S. J., and Olson, J. M. 2002. Dysregulation of gene expression in the R6/2 model of polyglutamine disease: Parallel changes in muscle and brain. Hum. Mol. Genet. 11:1911–1926.
132. Cheng, B. and Mattson, M. P. 1994. NT-3 and BDNF protect CNS neurons against metabolic excitotoxic insults. Brain Res. 640:56–67.
133. Duan, W. and Guo, Z. 2001. Brain-derived neurotrophic factor mediates an excitoprotective effect of dietary restriction in mice. J. Neurochem. 76:619–626.
134. Bemelmans, A. P., Horellou, P., Pradier, L., Brunet, I., Colin, P., and Mallet, J. 1999. Brain derived neurotrophic factor-mediated protection of striatal neurons in an excitotoxic rat model of Huntington's disease, as demonstrated by adenoviral gene transfer. Hum. Gene Ther. 10:2987–2997.
135. Perez-Navarro, E., Canudas, A. M., Akerund, P., Alberch, J., and Arenas, E. 2000. Brain-derived neurotrophic factor, neurotrophin-3 and neurotrophin-4/5 prevent the death of striatal projection neurons in a rodent model of Huntington's disease. J. Neurochem. 75:2190–2199.
136. Duan, W., Guo, Z., Jiang, H., Ware, M., Li, X. J., and Mattson, M. P. 2003. Dietary restriction normalizes glucose metabolism and BDNF levels, slows disease progression, and increases survival in huntingtin mutant mice. Proc. Natl. Acad. Sci. USA 100:2911–2916.
137. Luthi-Carter, R., Strand, A. D., Hanson, S. A., Kooperberg, C., Schilling, G., LaSpada, A. R., Merry, D. E., Young, A. B., Ross, C. A., Borchelt, D. R., Olson, J. M. 2002. Polyglutamine and transcription: Gene expression changes shared by DRPLA and Huntington's disease mouse models reveal context-independent effects. Hum. Mol. Genet. 11:1927–1937.
138. Chan, E. Y., Luthi-Carter, R., Strand, A., Solano, S. M., Hanson, S. A., DeJohn, M. M., Kooperberg, C., Chase, K. O., DiFigliia, M., Young, A. B., Leavitt, B. R., Cha, J. H., Aronin, N., Hayden, M. R., and Olson, J. M. 2002. Increased huntingtin protein length reduces the number of polyglutamine-induced gene expression changes in mouse models of Huntington's disease. Hum. Mol. Genet. 11:1939–1951.
139. Sipione, S., Rigamonti, D., Valenza, M., Zuccato, C., Conti, L., Pritchard, J., Kooperberg, C., Olson, J. M., and Cattaneo, E. 2002. Early transcriptional profiles in huntingtin-inducible striatal cells by microarray analyses. Hum. Mol. Genet. 11:1953–1965.
140. Ravikumar, B., Stewart, A., Kita, H., Kato, K., Duden, R., and Rubinsztein, D. C. 2003. Raised intracellular glucose concentrations reduce aggregation and cell death caused by mutant huntingtin exon 1 by decreasing mTOR phosphorylation and inducing autophagy. Hum. Mol. Genet. 12:985–994.
141. Ravikumar, B., Duden, R., and Rubinsztein, D. C. 2002. Aggregate-prone proteins with polyglutamine and polyalanine expansions are degraded by autophagy. Hum. Mol. Genet. 11:1107–1117.
142. Kita, H., Carmichael, J., Swartz, J., Muro, S., Wyttenbach, A., Matsubara, K., Rubinsztein, D. C., and Kato, K. 2002. Modulation of polyglutamine-induced cell death by genes identified by expression profiling. Hum. Mol. Genet. 11:2279–2287.

APPENDIX 6

Journal of Neurochemistry, 2004, **88**, 1352–1360 doi:10.1046/j.1471-4159.2003.02263.x

Mice deficient in dihydrolipoamide dehydrogenase show increased vulnerability to MPTP, malonate and 3-nitropropionic acid neurotoxicity

Peter Klivenyi,* Anatoly A. Starkov,* Noel Y. Calingasan,* Gabrielle Gardian,* Susan E. Browne,* Lichuan Yang,* Parvesh Bubber,*† Gary E. Gibson,*† Mulchand S. Patel‡ and M. Flint Beal*

**Department of Neurology and Neuroscience, Weill Medical College of Cornell University, New York Presbyterian Hospital, New York, New York, USA*

†Burke Medical Research Institute, White Plains, New York, USA

‡Department of Biochemistry, School of Medicine and Biomedical Sciences, State University of New York at Buffalo, Buffalo, New York, USA

Abstract

Altered energy metabolism, including reductions in activities of the key mitochondrial enzymes α-ketoglutarate dehydrogenase complex (KGDHC) and pyruvate dehydrogenase complex (PDHC), are characteristic of many neurodegenerative disorders including Alzheimer's Disease (AD), Parkinson's disease (PD) and Huntington's disease (HD). Dihydrolipoamide dehydrogenase is a critical subunit of KGDHC and PDHC. We tested whether mice that are deficient in dihydrolipoamide dehydrogenase ($Dld^{+/-}$) show increased vulnerability to 1-methyl-4-phenyl-1,2,3,6-tetrahydropyridine (MPTP), malonate and 3-nitropropionic acid (3-NP), which have been proposed for use in models of PD and HD. Administration of MPTP resulted in significantly greater depletion of tyrosine hydroxylase-positive neurons in the substantia nigra of $Dld^{+/-}$ mice than that seen in wild-type littermate controls. Striatal lesion volumes produced by malonate and 3-NP were significantly increased in $Dld^{+/-}$ mice. Studies of isolated brain mitochondria treated with 3-NP showed that both succinate-supported respiration and membrane potential were suppressed to a greater extent in $Dld^{+/-}$ mice. KGDHC activity was also found to be reduced in putamen from patients with HD. These findings provide further evidence that mitochondrial defects may contribute to the pathogenesis of neurodegenerative diseases.

Keywords: Alzheimer, Huntington, mitochondria, neurodegenerative diseases, Parkinson, oxidative damage.

J. Neurochem. (2004) **88**, 1352–1360.

There is accumulating evidence that the α-ketoglutarate dehydrogenase complex (KGDHC) is involved in neurodegenerative disorders. KGDHC activities are reduced in postmortem brain tissue of patients with Parkinson's disease (PD) (Mizuno *et al.* 1990; Gibson *et al.* 2003), and in both postmortem brain tissue and fibroblasts of patients with Alzheimer's disease (AD) (Gibson *et al.* 1988; Butterworth and Besnard 1990; Mizuno *et al.* 1990; Sheu *et al.* 1994; Kish *et al.* 1999). Interestingly, the KGDHC defect is found in postmortem brain tissue of patients with the Swedish amyloid precursor protein 670/671 mutation, which causes familial AD (Gibson *et al.* 1998). The enzyme is inactivated by oxidative stress induced by 4-hydroxynonenal, H_2O_2 and peroxynitrite (Chinopoulos *et al.* 1999; Park *et al.* 1999; Gibson *et al.* 2002).

Received October 6, 2003; revised manuscript received November 2, 2003; accepted November 5, 2003.

Address correspondence and reprint requests to M. Flint Beal, MD, Department of Neurology and Neuroscience, Weill Medical College of Cornell University, New York Presbyterian Hospital, 525 E 68th Street, New York, NY 10021, USA. E-mail: fbeal@med.cornell.edu

Abbreviations used: AD, Alzheimer's disease; BSA, bovine serum albumin; HD, Huntingdon's disease; KGDHC, α-ketoglutarate dehydrogenase complex; KPBS, potassium phosphate-buffered saline; MDA, malondialdehyde; MPP^+, 1-methyl-4-phenylpyridinium; MPTP, 1-methyl-4-phenyl-1,2,3,6-tetrahydropyridine; NeuN, neuron-specific nuclear protein; 3-NP, 3-nitropropionic acid; PBS, sodium phosphate-buffered saline; PD, Parkinson's disease; PDHC, pyruvate dehydrogenase complex; SDH, succinate dehydrogenase; TCA, tricarboxylic acid; TH, tyrosine hydroxylase.

KGDHC is a member of the α-ketoacid dehydrogenase complex family (Gibson *et al.* 2000a). This family also includes the pyruvate dehydrogenase complex (PDHC) and branched chain α-ketoacid dehydrogenase complex. Dihydrolipoamide dehydrogenase (EC 1.6.4.3) (encoded by *Dld* gene), which is also known as E3, is a critical subunit shared by all three dehydrogenases. It is a flavin-containing protein that transfers reducing equivalents from a dihydrolyl moiety to NAD^+, to form NADH and complete the catalytic process of the complex. The product of the *Dld* gene catalyzes the oxidation of dihydrolipoyl moities of four mitochondrial multienzyme complexes: PDHC, KGDHC, branched-chain α-ketoacid dehydrogenase and the glycine cleavage system.

Mice with a deficiency of dihydrolipoamide dehydrogenase have been developed (Johnson *et al.* 1997). Homozygous mice with disruption of the gene die *in utero* at a very early gastrulation stage. The heterozygous mice develop normally but have approximately half of wild-type activity for E3, for all affected multienzyme complexes, and the glycine cleavage system in liver and kidney (Johnson *et al.* 1997). In the present experiments we examined whether these mice show altered vulnerability to the dopaminergic neurotoxin 1-methyl-4-phenyl-1,2,3,6-tetrahydropyridine (MPTP), which has been used to model PD, and to malonate and 3-nitropropionic acid (3-NP), which have been used in models of Huntington's disease (HD) (Beal *et al.* 1993a, 1993b; Brouillet *et al.* 1995; Beal 2001).

Materials and methods

MPTP model

Heterozygous $Dld^{+/-}$ mice (C57BL/6), deficient in dihydrolipoamide dehydrogenase, were produced as described previously and genotyped using DNA extracted from the tail and a PCR assay (Johnson *et al.* 1997). We examined 12 $Dld^{+/-}$ and 12 littermate wild-type $Dld^{+/+}$ mice at 3–4 months of age. All experiments were carried out in accordance with the National Institute Health Guide for the Care and Use of Laboratory Animals and all procedures were approved by the local institutional animal care and use committee. Mice were housed in a room maintained at 20–22°C on a 12-h light–dark cycle with food and water available *ad libitum*. We administered MPTP to wild-type and $Dld^{+/-}$ mice at a dose of 20 mg/kg i.p. three times at 2-h intervals. Mice were killed 1 week later and the striata dissected.

1-Methyl-4-phenylpyridinium (MPP^+) levels

MPTP (20 mg/kg) was administered intraperitoneally three times at 2-h intervals. Mice were killed 90 min after the last injection. MPP^+ levels were quantified by HPLC with UV detection at 295 nm. Samples were sonicated in 0.1 M perchloric acid and an aliquot of supernatant was injected on to a Brownlee aquapore X 03–224 cation exchange column (Rainin, Woburn, MA, USA). Samples were eluted isocratically with 90% 0.1 mM acetic acid and 75 mM triethylamine HCl, pH 2.3, adjusted with formic acid and 10% acetonitrile.

Malondialdehyde (MDA) assay

MDA levels were measured by HPLC with fluorescence detection in striatal tissue at 18 h after administration of sodium phosphate-buffered saline (PBS) or MPTP (Ferrante *et al.* 1997). Malondialdehyde standard (98% purity) and other chemicals were purchased from Sigma (St Louis, MO, USA). Butylated hydroxytoluene solution was prepared in 95% ethanol to a final concentration of 0.05%. 2-Thiobarbituric acid was dissolved in water on a stirring hot-plate at 50–55°C to a concentration of 42 mM. The MDA standard was prepared with 40% ethanol solution. Standard curves were made with a series of MDA concentrations from 0.001 to 1.0 mM and a blank.

Brain tissues were homogenized in 40% ethanol. Sample derivatization was carried out in 2-mL plastic centrifuge tubes fitted with screw-on caps. To a 50 μL aliquot of sample homogenate or MDA standard, 50 μL butylated hydroxytoluene solution, 400 μL 0.44 M H_3PO_4 solution and 100 μL 2-thiobarbituric acid solution were added. Sample tubes were capped tightly, vortex mixed, then heated for 1 h on a 100°C dry-bath incubator. Following heat derivatization, samples were placed on an iced water bath (0°C) for 5 min to cool. Two hundred and fifty μL of *n*-butanol was subsequently added to each vial for extraction of the MDA–2-thiobarbituric acid complex. Tubes were vortex mixed for 5 min and then centrifuged for 3 min at 10 000 *g* to separate the two phases. Aliquots of 100 μL were removed from the *n*-butanol layer of each sample and placed in HPLC vials for analysis.

PDHC activity in brain tissue

Mice were decapitated and the heads were dropped into liquid N_2 immediately. The brains were removed under liquid nitrogen. The frozen brains were powdered in liquid N_2 and stored in liquid N_2-cooled cryo-vials (Corning Glass Works, Corning, NY, USA). Homogenates (2% by brain weight) were prepared for measurement of total and active forms of PDHC (Ksiezak-Reding *et al.* 1982; Huang *et al.* 1994). To measure the PDHC activity in the active form, the brain powders (2%) were homogenized in buffer without calcium and magnesium (50 mM Tris-HCl, pH 7.2, 1 mM dithiothreitol, 50 μM leupeptin, 0.4% Triton X-100). To measure total PDHC activity, the brain powder (2%) was incubated in the same buffer with the addition of 10 mM $MgCl_2$ and 1 mM $CaCl_2$ at 37°C for 30 min before assay. The total and active forms of PDHC for each brain were assayed in triplicate by monitoring the rate of acetyl-CoA formation as determined by its coupling to the acetylation of *p*-(*p*-aminophenylazo)-benzene sulfonic acid by arylamine *N*-acetyltransferase. PDHC activities were measured for 30 min at 37°C by following the decrease in the absorbence that occurs at 460 nm with the acetylation of *p*-(*p*-aminophenylazo)-benzene sulfonic acid on a spectrophotometric microtiter plate reader (Molecular Devices, Palo Alto, CA, USA). Protein was measured by the Bradford method with the Bio-Rad protein assay (Bio-Rad Laboratories, Hercules, CA, USA). Measurements were done at 595 nm on a spectrophotometric microtiter plate reader (Molecular Devices).

KGDHC activity assay

For assays of KGDHC activity, frozen pulverized tissue (as for PDHC) was prepared as 5% homogenates in 50 mM Tris-HCl pH 7.2, 1 mM dithiothreitol, 50 μM leupeptin 0.2 mM EGTA and 0.4% Triton X-100 (Gibson *et al.* 1988, 1998). KGDHC activity in

each sample was analyzed in triplicate in the presence of saturating concentrations of thiamine pyrophosphate, using a 96-well plate reader. Human postmortem control and brain tissue from patients with HD was obtained from the Harvard Brain Bank (McLean Hospital, Belmont, MA, USA).

Malonate lesions

We examined the effects of malonate-induced striatal lesions in 2.5-month-old $Dld^{+/-}$ mice. The mice were anesthetized with isoflurane and malonate (1.5 μmol in 1.0 μL, pH 7.4) was injected stereotaxically into the left striatum (anterior, 0.5 mm; lateral, 2 mm from bregma; ventral, 3.5 mm from dura). The injections were performed over 2 min using a 10-μL 26-gauge blunt-tipped Hamilton syringe. The needle was left in place for 5 min before being slowly withdrawn. Seven days after the striatal injections animals were killed.

3-NP lesions

Both $Dld^{+/-}$ mice and littermate controls aged 2.5 months were treated with 3-NP for 2 days at a dose of 50 mg/kg i.p. twice daily, followed by 60 mg/kg i.p. twice daily from day 3 to day 9. At 6 h after the last 3-NP injection, mice were killed.

Histological analysis

Mice were anesthetized with sodium pentobarbital and perfused transcardially with 0.1 M PBS, pH 7.4, followed by 4% paraformaldehyde in 0.1 M phosphate buffer (pH 7.4). Brains were removed, postfixed for 2 h in the same fixative, and then placed in 30% sucrose overnight at 4°C. For MPTP-lesioned brains, serial coronal sections (50 μm) were cut through the substantia nigra. Two sets, consisting of eight sections each 100 μm apart, were prepared. One set of sections was used for Nissl staining (cresyl violet). Another set was processed for tyrosine hydroxylase (TH) immunohistochemistry using the avidin–biotin peroxidase technique. Briefly, free-floating sections were pretreated with 3% H_2O_2 in PBS for 30 min. The sections were incubated sequentially in (1) 1% bovine serum albumin (BSA)/0.2% Triton X-100 for 30 min; (2) rabbit anti-TH affinity-purified antibody (Chemicon, Temecula, CA, USA; 1 : 2000 in PBS/0.5% BSA) for 18 h; (3) biotinylated anti-rabbit IgG (Vector Laboratories, Burlingame, CA, USA; 1 : 500 in PBS/0.5% BSA) for 1 h; and (4) avidin–biotin–peroxidase complex (Vector; 1 : 500 in PBS) for 1 h. The immunoreaction was visualized using 3,3′-diaminobenzidine tetrahydrochloride dihydrate with nickel intensification (Vector) as the chromogen. All incubations and rinses were performed with agitation using an orbital shaker at room temperature (37°C). The sections were mounted on to gelatin-coated slides, dehydrated, cleared in xylene and coverslipped. The numbers of Nissl-stained or TH-immunoreactive cells in the substantia nigra pars compacta were counted using the optical fractionator method in the Stereo Investigator (version 4.35) software program (Microbrightfield, Burlington, VT, USA).

Sections from 3-NP- and malonate-lesioned brains were immunostained using an anitibody against the neuronal marker neuron-specific nuclear protein (NeuN). Briefly, sections were pretreated with 0.05 M potassium phosphate-buffered saline (KPBS) containing 1% NaOH and 3% H_2O_2 for 30 min. After rinsing in KPBS three times for 10 min each, the sections were treated with 0.4% Triton X-100 and 1% BSA in KPBS for 30 min. The sections were incubated in NeuN antibody (Chemicon; 1 : 1000 in KPBS/1% BSA/0.4% Triton) for 18 h. After rinsing in KPBS containing 0.25% BSA and 0.02% Triton X-100, the sections were incubated in biotinylated anti-mouse IgG (1 : 200 in KBPS/0.25% BSA/0.02% Triton) for 1 h followed by the avidin–biotin–peroxidase complex (1 : 200) in KPBS for 1 h. The sections were rinsed in 0.05 M KPBS, and the reaction was developed in 0.05% 3,3′-diaminobenzidine tetrahydrochloride dihydrate containing 0.003% H_2O_2 in KBPS. Stereological analysis of lesion volumes was performed using the Cavalieri method in the Stereo Investigator (version 4.35) software program (Microbrightfield). Every other NeuN-stained section was examined.

Mitochondrial respiration

Mouse forebrain mitochondria were isolated according to the method of Rosenthal *et al.* (1987), except that Nagarse protease treatment was omitted and the amount of digitonin was adjusted to the smaller tissue sample (Starkov & Fiskum, 2003). Respiration of isolated mitochondria was measured at 37°C with a commercial Clark-type oxygen electrode (Hansatech Instruments, Kings Lynn, Norfolk, UK). The incubation medium was composed of 125 mM KCl, 10 mM HEPES, pH 7.2, 2 mM $MgCl_2$, 0.4 mg/ml BSA (fatty acid free), 0.8 mM ADP, and a respiratory substrate as indicated in figure legends. Mitochondria were added at 0.5 mg/ml. Membrane potentials of isolated mitochondria were estimated using the fluorescence of safranine O (3 μM), with excitation and emission wavelengths of 495 nm and 586 nm respectively. The incubation medium was as described above. KDGHC activity in mitochondria was measured fluorimetrically. The reaction medium was composed of 50 mM KCl, 10 mM HEPES, pH 7.4, 20 μg/mL alamethicin, 0.3 mM thiamine, 0.01 mM $CaCl_2$, 0.2 mM $MgCl_2$, 5 mM α-ketoglutarate, 1 μM rotenone and 0.2 mM NAD^+. The reaction was started by adding 0.14 mM Coenzyme A (CoASH) to permeabilized mitochondria (0.1–0.25 mg/mL). Reduction of NAD^+ was followed at 460 nm emission after excitation at 346 nm. The scale was calibrated by adding known amounts of freshly prepared NADH.

Succinate dehydrogenase (SDH) activity

SDH (EC 1.3.99.1) was measured spectrophotometrically as described previously (Arrigon and Singer 1962). The reaction medium was composed of 50 mM KCl, 10 mM HEPES, pH 7.4, 20 μg/mL alamethicin, 10 mM succinate, 2 mM KCN, 1 μM rotenone, 50 μM 2,3-dimethoxy-5-methyl-6-decyl-1,4-benzoquinone, 50 μM 2,6-dichlorophenol indophenol and 20 μM EDTA. The reaction was monitored at 600 nm, and the activity was calculated, employing $E_{mM} = 21\ cm^{-1}$ for 2,6-dichlorophenol indophenol.

Statistical analysis

Data are expressed as mean ± SEM. Statistical analysis was performed using one-way ANOVA followed by Newman–Keuls post-hoc test. The Mann–Whitney *U*-test and Student's *t*-test were used to analyze differences in lesion volumes.

Results

We measured KDGHC, total PDHC and active PDHC in cerebral cortex of wild-type and $Dld^{+/-}$ mice ($n = 9$).

KDGHC activity was significantly reduced from 14.0 ± 0.43 mU per mg protein in wild-type mice to 10.11 ± 0.34 mU per mg protein in $Dld^{+/-}$ mice ($p < 0.001$). Similarly, total PDHC activity was significantly reduced from 37.96 ± 1.16 to 30.95 ± 2.61 mU per mg protein in the $Dld^{+/-}$ mice ($p < 0.05$). There was a reduction in active PDHC from 32.3 ± 1.3 to 27.6 ± 2.4 mU per mg protein, but this was not statistically significant ($p = 0.12$). A preliminary study in the putamen of brains from three controls and seven patients with HD showed that KDGHC activity was significantly reduced from 11.5 ± 24 mU per mg protein in controls to 1.6 ± 0.6 mU mg protein in HD postmortem brain tissue ($p < 0.04$).

We carried out studies of MPTP neurotoxicity in $Dld^{+/-}$ mice. We administered MPTP at a dose of 20 mg/kg i.p. three times at 2-h intervals to littermate controls and heterozygous $Dld^{+/-}$ mice. MPTP produced a significantly greater depletion of TH- and Nissl-stained neurons in the $Dld^{+/-}$ mice than in littermate controls (Figs 1 and 2). We

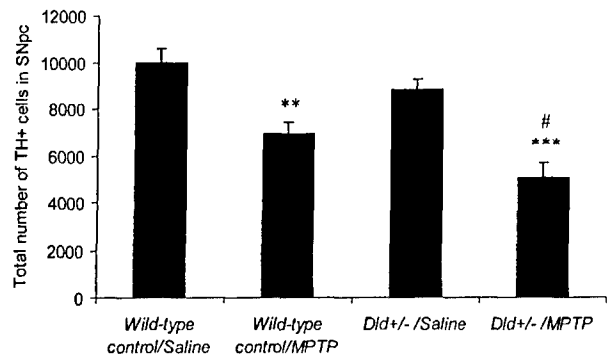

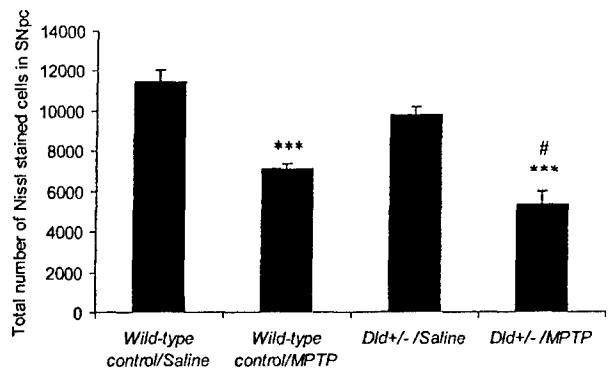

Fig. 1 Stereological (optical fractionator) counts of TH-positive (top) and Nissl-stained neurons (bottom) in the substantia nigra pars compacta (SNpc) of 2-month-old wild-type and $Dld^{+/-}$ mice. MPTP produced a significantly greater depletion of TH-positive and Nissl-stained neurons in the $Dld^{+/-}$ knockout mice than in the wild-type controls. Values are mean ± SEM. $^{**}p < 0.01$ versus wild-type control/saline, $^{***}p < 0.001$ versus respective $Dld^{+/-}$/saline, $\#p < 0.05$ versus wild-type control/MPTP by ANOVA.

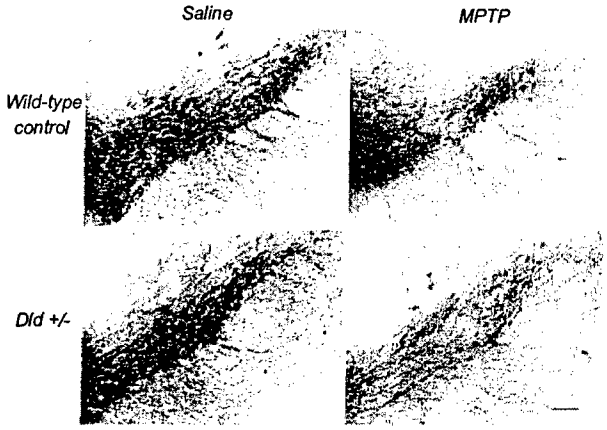

Fig. 2 Photomicrographs of TH-immunoreactive neurons in the substantia nigra pars compacta showing more severe MPTP-induced dopaminergic neuronal loss in $Dld^{+/-}$ mice than in wild-type controls. Scale bar 50 μm.

examined MDA in 6-month-old $Dld^{+/-}$ mice and littermate controls. MDA levels were significantly increased in the striatum of $Dld^{+/-}$ mice and increased further following MPTP administration (Fig. 3). MPP^+ levels were similar in control and $Dld^{+/-}$ mice: 49.7 ± 3.3 ng per mg protein ($n = 12$) versus 49.4 ± 2.7 ng per mg protein ($n = 10$) respectively.

We examined the effects of malonate-induced striatal lesions in $Dld^{+/-}$ mice. Malonate lesion volumes were approximately three-fold larger in the $Dld^{+/-}$ mice than controls (1.9 ± 0.5 vs. 0.7 ± 0.2 mm^3 respectively; $p < 0.05$) (Figs 4 and 5). We also examined 3-NP-induced lesions in the $Dld^{+/-}$ mice and littermate controls (Figs 6 and 7). There were bilateral areas of NeuN-positive cell loss in the striatum of wild-type and $Dld^{+/-}$ mice. The lesion volume in the $Dld^{+/-}$ mice was 3.5 ± 0.6 mm^3 whereas that

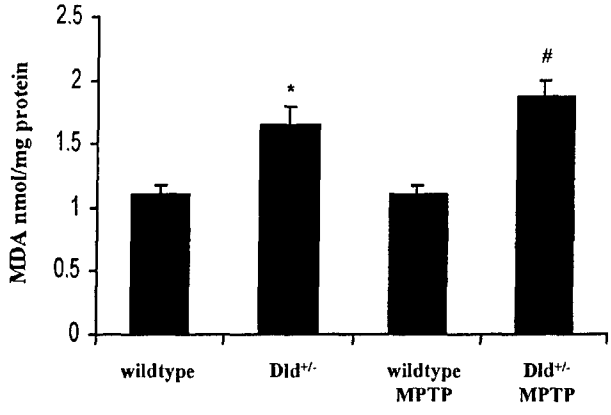

Fig. 3 Striatal MDA levels in $Dld^{+/-}$ mice and littermate controls at 6 months of age at baseline and following administration of MPTP. Values are mean ± SEM. $^{*}p < 0.05$ versus wild-type control, $\#p < 0.001$ versus wild-type control/MPTP by ANOVA.

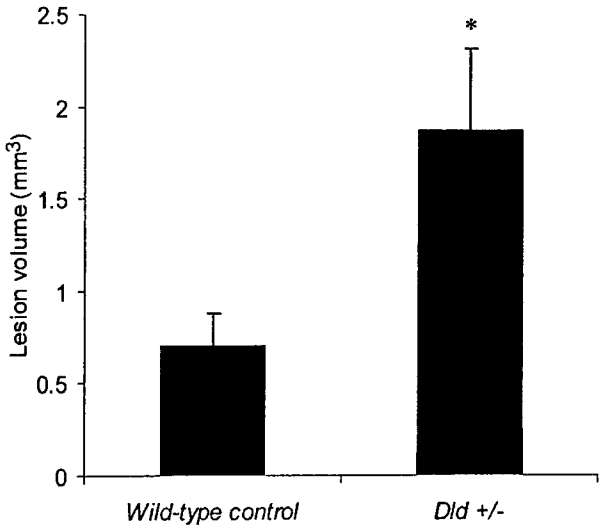

Fig. 4 Lesion volumes (Cavalieri method) in 2.5-month-old wild-type and $Dld^{+/-}$ mice after unilateral striatal malonate injection showing significantly larger lesions in the $Dld^{+/-}$ mice. Values are mean ± SEM. $^{*}p < 0.05$ versus wild-type control by Mann–Whitney *U*-test.

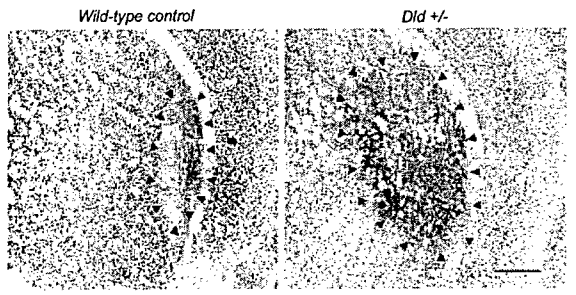

Fig. 5 Photomicrographs of NeuN-immunostained sections through the caudate–putamen of wild-type and $Dld^{+/-}$ mice showing malonate lesions. The lesion in the caudate–putamen (outlined by arrowheads) is larger in the $Dld^{+/-}$ mouse than that in the wild-type mouse. The dark staining at the lesion sites, which is more extensive in the $Dld^{+/-}$ mouse, represents IgG extravasation as detected by anti-mouse IgG, the secondary antibody used for NeuN immunohistochemistry. Scale bar 0.5 mm.

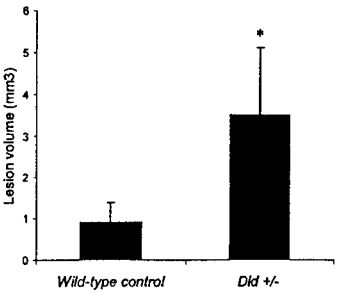

Fig. 6 Lesion volumes (Cavalieri method) of 2.5-month-old wild-type and $Dld^{+/-}$ mice after 3-NP injection, showing significantly larger lesions in the $Dld^{+/-}$ mice. Values are mean ± SEM. $^{*}p < 0.05$ versus wild-type control by Mann–Whitney *U*-test.

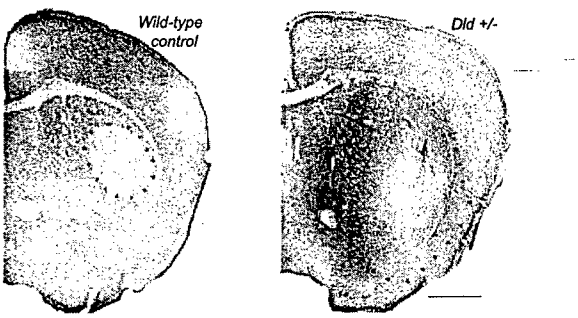

Fig. 7 Photomicrographs of NeuN-immunostained sections through the caudate–putamen of 3-NP treated wild-type and $Dld^{+/-}$ mice. The lesion in the caudate–putamen (outlined by arrowheads) is larger in the $Dld^{+/-}$ mouse than that in the wild-type mouse. The dark staining at the lesion site in the $Dld^{+/-}$ mouse represents IgG extravasation as detected by anti-mouse IgG, the secondary antibody used for NeuN immunohistochemistry. Scale bar 1 mm.

in wild-type mice was 0.9 ± 0.5 mm^3 ($p < 0.05$; $n = 17$ per group).

We examined the effects of 3-NP treatment on bioenergetics of isolated brain mitochondria (Figs 8 and 9). As expected, 3-NP treatment resulted in severe inhibition of SDH (Fig. 8a). However, succinate-supported respiration (Fig. 8c) and the membrane potential (Fig. 8b) were suppressed to a greater extent in mitochondria from $Dld^{+/-}$ mice. Figure 8(b) shows that the membrane potential was lower in $Dld^{+/-}$ mitochondria both in State 3 and following the induction of State 4 by carboxyatractylate, an inhibitor of the ATP/ADP antiporter. The addition of pyruvate to mitochondria oxidizing succinate resulted in an increase in the membrane potentials to almost equal levels in $Dld^{+/-}$ and $Dld^{+/+}$ mitochondria. This increase was sensitive to the complex I inhibitor rotenone. Therefore, the membrane potential was most probably lower in $Dld^{+/-}$ mitochondria because of the lower SDH activity *per se* which was limiting the flux of electrons through the respiratory chain. In accordance with this interpretation, SDH activity in $Dld^{+/-}$ mitochondria was about 50% of that in $Dld^{+/+}$ mitochondria (Fig. 8c).

Figure 9(a) shows that 3-NP treatment also resulted in approximately 30% inhibition of phosphorylating respiration of mitochondria oxidizing pyruvate and malate. However, there were no differences in State 3 respiration rates between mitochondria from $Dld^{+/-}$ mice and their littermates with normal KGDHC activity. State 4 respiration rates were not affected by 3-NP treatment (data not shown). The reasons for inhibition of pyruvate and malate oxidation by 3-NP treatment are not clear. As mentioned above, 3-NP is a selective inhibitor of SDH and fumarase (EC 4.2.1.2), and neither of these enzymes is known to control the rate of State

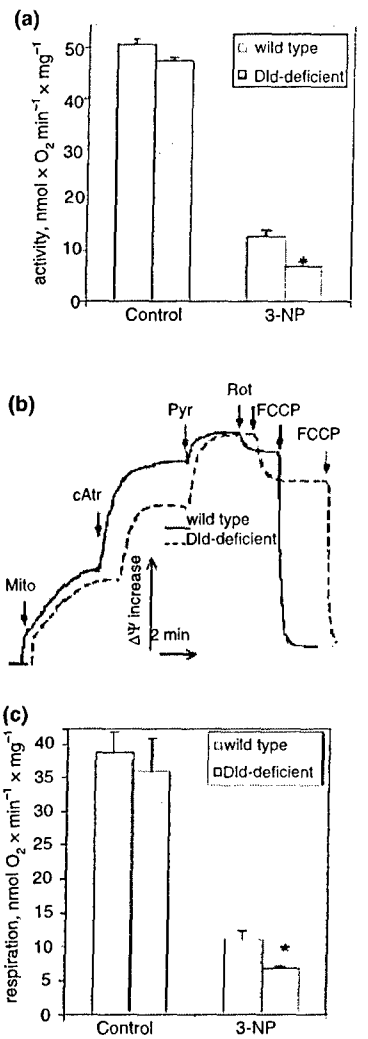

Fig. 8 Effect of *in vivo* 3-NP treatment, State 3 respiration, membrane potential and SDH activity in $Dld^{+/+}$ and $Dld^{+/-}$ mitochondria. (a) SDH activity. (b) Membrane potentials of mitochondria isolated from 3-NP-treated animals. The membrane potential was estimated from fluorescence of safranine O. The incubation medium was supplemented with 10 mM succinate, and 3 μM safranine O was included. Additions: Mito, 0.5 mg/mL mitochondria; cAtr, 4 μM carboxyatractylate; Pyr, 7 mM pyruvate; Rot, 1 μM rotenone; FCCP, 50 nM FCCP. (c) State 3 respiration of mitochondria. Incubation medium (see Materials and methods) was supplemented with 10 mM succinate and 1 μM rotenone. Control, mitochondria from mice not treated with 3-NP ($n = 6$); 3-NP, mitochondria from 3-NP-treated mice ($n = 4$). Values in (a) and (c) are mean ± SEM. There were no differences in State 3 rates (c) and SDH activities (a) between control groups. *$p < 0.05$ versus 3-NP-treated wild-type mice.

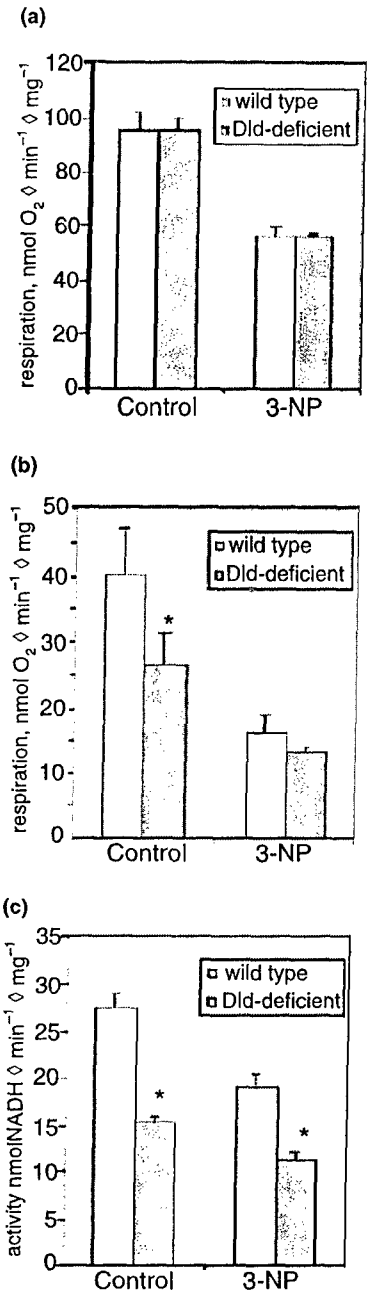

Fig. 9 Inhibition of mitochondrial phosphorylating respiration and KGDHC activity by *in vivo* 3-NP treatment. (a, b) State 3 respiration. Incubation medium and other conditions were as in Fig. 8(c), except that succinate and rotenone were replaced with 7 mM pyruvate and 0.8 mM malate (a) or with 10 mM α-ketoglutarate (b). (c) KGDHC activity. Control, mitochondria from control mice ($n = 7$); 3-NP, mitochondria from 3-NP-treated mice ($n = 4$). Values are mean ± SEM. *Statistically significant difference $p < 0.05$ compared with wild-type controls.

3 respiration supported by pyruvate and malate oxidation. Unexpectedly, 3-NP treatment significantly reduced KGDHC activity. State 3 respiration supported by α-ketoglutarate was suppressed by ~ 60% in wild-type mitochondria and by ~48% in $Dld^{+/-}$ mitochondria (Fig. 9b). In accordance with the respiration data, the activity of KGDHC in mitochondria was also inhibited (Fig. 9c).

Discussion

There is substantial evidence that alterations in α-ketoacid dehydrogenases may play a role in the pathogenesis of neurodegenerative diseases. Strong evidence has accumulated implicating KGDHC deficiency in AD (Gibson *et al.* 1988, 1998; Butterworth *et al.* 1990; Sheu *et al.* 1994). The clinical dementia rating scale is highly correlated with postmortem brain KGDHC activity (Gibson *et al.* 2000). There is also evidence for decreases in KGDHC in the substantia nigra of patients with PD (Mizuno *et al.* 1990, 1995; Gibson *et al.* 2003). Immunostaining for KGDHC declines in many melanized neurons and this reduction correlates with the severity of the degeneration (Mizuno *et al.* 1994). KGDHC is more vulnerable to degeneration than complex II, III and IV as shown by immunostaining. There is evidence for reduced PDHC activity in both AD and HD (Sorbi *et al.* 1983; Butterworth *et al.* 1985).

Although previous studies showed reduced PDHC activity in HD postmortem brain tissue, there have been no reports on measurement of KDGHC activity. We found that KDGHC activity was reduced in the putamen. This may also be a consequence of oxidative damage as we and others found increased oxidative damage in both HD postmortem brain tissue and a transgenic mouse model of HD (Bodganov *et al.* 2001; Browne *et al.* 1999; Perez-Severiano *et al.* 2000; Tabrizi *et al.* 2000). This finding shows that KDGHC activity is reduced in three of the most common neurodegenerative diseases, AD, PD and HD.

Genetic studies also implicate KGDHC in PD and AD. In PD a polymorphism occurs in exon 9 of the *DLST E2* gene of KGDHC (Kobayashi *et al.* 1998). A single nucleotide substitution between G (in allele 1) and A exon 9 (in allele 2) occurs, but it does not change the amino acid code. Frequencies of the genotype that carry the A allele are significantly higher in patients with PD than in controls. These results suggest that a genetic variant of the *E2* gene itself, or in close proximity to the gene, constitutes a risk factor for PD. Polymorphisms in the $Dld^{+/-}$ gene also appear to be a risk factor for AD in caucasians (Sheu *et al.* 1999).

Previous studies showed that MPTP and isoquinoline derivative neurotoxicity was associated with reduced activity of KGDHC (McNaught *et al.* 1995; Joffe *et al.* 1998). The MPTP metabolite MPP^+ inhibits KGDHC (Mizuno *et al.* 1988). It is possible that these effects may be mediated by oxidative stress. Previous work showed that KGDHC is sensitive to a number of oxidants including hydroxynonenal, H_2O_2 and peroxynitrite (Chinopoulos *et al.* 1999; Park *et al.* 1999; Gibson *et al.* 2002). The inactivation by peroxynitrite (Park *et al.* 1999) is particularly interesting as peroxynitrite-mediated neurotoxicity has been strongly implicated in MPTP neurotoxicity (Schulz *et al.* 1995a; Hantraye *et al.* 1996; Przedborski *et al.* 1996). Peroxynitrite may also be involved in PD as shown by increases in 3-nitrotyrosine staining of Lewy bodies in the substantia nigra of patients with PD (Good *et al.* 1998; Giasson *et al.* 2000). KDGHC is also inhibited by oxidized derivatives of dopamine (Shen *et al.* 2000). Exposure of Chinese hamster ovary cells to hyperoxia results in cell death and complete inactivation of KDGHC, whereas KDGHC activity is preserved in cells that are resistant to hyperoxia (Schooner *et al.* 1990, 1991).

In the present experiments we examined whether $Dld^{+/-}$ mice show increased vulnerability to MPTP neurotoxicity. We found that both KGDHC and total PDHC activities were significantly reduced in the cerebral cortex of $Dld^{+/-}$ mice. If a deficiency in KGDHC contributes to PD pathogenesis one would expect these mice to show increased vulnerability to the toxin, which is known to impair mitochondrial function. We found that the $Dld^{+/-}$ mice showed greater loss of TH-stained neurons in the substantia nigra pars compacta. There were no alterations in MPP^+ levels to suggest altered processing or metabolism of MPTP in these mice.

We also examined the effects of malonate lesions in the $Dld^{+/-}$ mice. Malonate is a reversible inhibitor of SDH. We and others showed that intrastriatal injections of malonate produce lesions that in many respects resemble the neuropathology of HD (Beal *et al.* 1993b; Greene *et al.* 1993). The lesions occur by an indirect excitotoxic mechanism as they are blocked by excitatory amino acid antagonists (Beal *et al.* 1993b; Greene *et al.* 1993). The lesions are associated with increases in markers of free radical damage and are attenuated by free radical scavengers (Schulz *et al.* 1995b). This might lead to further inactivation of KGDHC. In the present experiments, we found that striatal lesions produced by malonate were markedly exacerbated in $Dld^{+/-}$ mice. Lesion volumes were approximately three-fold greater than those seen in littermate controls. This is consistent with the possibility that inhibition of the tricarboxylic acid (TCA) cycle at multiple sites may greatly exacerbate bioenergetic defects.

We also examined the effects of 3-NP in $Dld^{+/-}$ mice. 3-NP is a suicide inhibitor of the mitochondrial TCA enzyme SDH (Alston *et al.* 1977; Coles *et al.* 1979) and a reversible inhibitor *in vitro* of fumarase, another TCA enzyme (Porter and Bright 1980). Systemic administration of 3-NP inhibits SDH in the whole brain as well as in the liver and heart (Gould and Gustine 1982; Gould *et al.* 1985), and results in abnormal succinate build-up and inhibition of the mitochondrial TCA cycle (Hassel and Sonnewald 1995).

Systemic administration of 3-NP produces selective lesions in the striatum, which closely mimic the neuropathologic features of HD, as it produces relative sparing of NADPH-diaphorase neurons, a characteristic feature of HD neuropathology (Beal *et al.* 1993a). In baboons, it produces a choreiform movement disorder as well as dystonia (Brouillet *et al.* 1995; Palfi *et al.* 1996). The lesions are attenuated in mice overexpressing Cu/Zn superoxide dismutase (Beal *et al.* 1995). We therefore examined the effects of 3-NP in

$Dld^{+/-}$ mice. $Dld^{+/-}$ mice were significantly more vulnerable to the neurotoxic effects of 3-NP. The lesion volumes in the deficient mice were three- to four-fold larger than those seen in controls.

The *in vivo* treatment with 3-NP induced more pronounced inhibition of SDH activity in brain mitochondria isolated from $Dld^{+/-}$ mice than in mitochondria from $Dld^{+/+}$ mice. Interestingly, KGDHC activity was also severely inhibited. To our knowledge, there are no published reports on inhibition of the purified KGDHC enzyme complex by 3-NP or that 3-NP treatment can inhibit mitochondrial KGDHC activity *in situ* or *in vivo*. Therefore, the mechanism of the inhibition is not clear, although it might be secondary to oxidative damage. However, the KGDHC inhibition may explain the observed decrease in State 3 respiration rates supported by oxidation of pyruvate and malate (Fig. 9), provided that KGDHC exerted significant control over the flux of reducing equivalents in the TCA cycle under our experimental conditions. The data indicate that there may be a direct interaction between SDH and KGDHC *in vivo*, in such a way that an impairment of one of these enzymes results in an increased vulnerability of the other enzyme, consistent with an oxidative stress mechanism. Another interesting possibility relates to the *DLST* gene, which encodes the dihydrolipoamide succinyltansferase component subunit of KGDHC, and was recently shown to possess another important function in regulating mitochondrial energy production. In addition to its full-length product (E2 subunit of KGDHC), this gene encodes truncated mRNA for another protein designated MIRTD, that localizes to mitochondria where it somehow regulates the biogenesis of mitochondrial respiratory chain (Kanamori *et al.* 2003).

In summary, we found that $Dld^{+/-}$ mice show increased vulnerability to MPTP, malonate and 3-NP. These findings provide further evidence that reductions in KGDHC may contribute to the pathogenesis of neurodegenerative diseases.

Acknowledgements

Sharon Melanson, Greta Strong and Connie Boyd are thanked for secretarial assistance. This work was supported by grants from the Department of Defense, National Institute on Aging (NIA) grant AG 14930 and the Parkinson's Disease Foundation.

References

Alston T. A., Mela L. and Bright H. J. (1977) 3-Nitropropionate, the toxic substance of Indigo/era, is a suicide inactivator of succinate dehydrogenase. *Proc. Natl Acad. Sci. USA* **74**, 3767–3771.

Arrigon O. and Singer T. (1962) Limitations of the phenazine methosulfate assay for succinic and related dehydrogenases. *Nature* **193**, 1256–1258.

Beal M. F. (2001) Experimental models of Parkinson's disease. *Nat. Rev. Neurosci.* **2**, 325–334.

Beal M. F., Brouillet E., Jenkins B. G., Ferrante R. J., Kowall N. W., Miller J. M., Storey E., Srivastava R., Rosen B. R. and Hyman B. T. (1993a) Neurochemical and histological characterization of striatal excitotoxic lesions produced by the mitochondrial toxin 3-nitropropionic acid. *J. Neurosci.* **13**, 4181–4192.

Beal M. F., Brouillet E., Jenkins B., Henshaw R., Rosen B. and Hyman B. T. (1993b) Age-dependent striatal excitotoxic lesions produced by the endogenous mitochondrial inhibitor malonate. *J. Neurochem.* **61**, 1147–1150.

Beal M. D., Ferrante R. J., Henshaw R., Matthews R. T., Chan P. H., Kowall N. W., Epstein C. J. and Schulz J. B. (1995) 3-Nitroproprionic acid neurotoxicity is attenuated in copper/zinc superoxide dismutase transgenic mice. *J. Neurochem.* **65**, 919–922.

Bodganov M. B., Andreassen O. A., Dedeoglu A., Ferrante R. J. and Beal M. F. (2001) Increased oxidatve damage to DNA in transgenic mouse model of Huntington's disease. *J. Neurochem.* **79**, 1246–1249.

Brouillet E., Hantraye P., Ferrante R. J., Dolan R., Leroy-Willig A., Kowall N. W. and Beal M. F. (1995) Chronic mitochondrial energy impairment produces selective striatal degeneration and abnormal choreiform movements in primates. *Proc. Natl Acad. Sci. USA* **92**, 7105–7109.

Browne S. E., Ferrante R. J. and Beal M. F. (1999) Oxidative stress in Huntington's disease. *Brain Pathol.* **9**, 147–163.

Butterworth J., Yates C. M. and Reynolds G. P. (1985) Distribution of phosphate-activated glutaminase, succinic dehydrogenase, pyruvate dehydrogenase and gamma-glutamyl transpeptidase in postmortem brain from Huntington's disease and agonal cases. *J. Neurol. Sci.* **67**, 161–171.

Butterworth R. F. and Besnard A. M. (1990) Thiamine-dependent enzyme changes in temporal cortex of patients with Alzheimer's disease. *Metab. Brain Dis.* **5**, 179–184.

Chinopoulos C., Tretter L. and. Adam-Vizi V. (1999) Depolarization of *in situ* mitochondria due to hydrogen peroxide-induced oxidative stress in nerve terminals: inhibition of alpha-ketoglutarate dehydrogenase. *J. Neurochem.* **73**, 220–228.

Coles C. J., Edmondson D. E. and Singer T. P. (1979) Inactivation of succinate dehydrogenase by 3-nitropropionate. *J. Biol. Chem.* **254**, 5161–5167.

Ferrante R. J., Shinobu L. A., Schult Z. J. B., Matthews R. T., Thomas C. E., Kowall N. W., Gurney M. E. and Beal M. F. (1997) Increased 3-nitrotyrosine and oxidative damage in mice with a human copper/zinc superoxide dismutase mutation. *Ann. Neurol.* **42**, 326–334.

Giasson B. I., Duda J. E., Murray I. V., Chen Q., Souza J. M., Hurtig H. I., Ischiropoulos H., Trojanowski J. Q. and Lee V. M. (2000) Oxidative damage linked to neurodegeneration by selective alpha-synuclein nitration in synucleinopathy lesions. *Science* **290**, 985–989.

Gibson G. E., Sheu R. K. F., Blass J. P., Baker A., Carlson K. C. and Harding B. and. Perrino P. (1988) Reduced activities of thiamine-dependent enzymes in the brains and peripheral tissues of patients with Alzheimer's disease. *Arch. Neurol.* **45**, 836–840.

Gibson G. E., Zhang H., Sheu K. F.-R., Bogdanovich N., Lindsay J. G., Lannfelt L., Vestling M. and Cowburn R. F. (1998) Alpha-ketoglutarate dehydrogenease in Alzheimer brain bearing the APP670/671 mutation. *Ann. Neurol.* **44**, 671–681.

Gibson G. E., Park L. C., Sheu K. F., Blass J. P. and Calingasan N. Y. (2000) The alpha-ketoglutarate dehydrogenase complex in neurodegeneration. *Neurochem. Int.* **36**, 97–112.

Gibson G. E., Zhang H., Xu H., Park L. C. and Jeitner T. M. (2002) Oxidative stress increases internal calcium stores and reduces a key mitochondrial enzyme. *Biochim. Biophys. Acta* **1586**, 177–189.

Gibson G. E., Kingsbury A. E., Xu H., Lindsay J. G., Daniel S., Foster O. J. F., Lees A. J. and Blass J. P. (2003) Deficits in a Krebs cycle

enzyme in brains from patients with Parkinson's disease. *Neurochem. Int.* **43**, 129–135.

Good P. F., Hsu A., Werner P., Perl D. P. and Olanow C. W. (1998) Protein nitration in Parkinson's disease. *J. Neuropathol. Exp. Neurol.* **57**, 338–339.

Gould D. H. and Gustine D. L. (1982) Basal ganglia degeneration, myelin alterations, and enzyme inhibition in mice induced by the plant toxin 3-nitropropionic acid. *Neuropathol. Appl. Neurobiol.* **8**, 377–393.

Gould D. H., Wilson M. P. and Hamar D. W. (1985) Brain enzyme and clinical alterations induced in rats and mice by nitroaliphatic toxicants. *Toxicol. Lett.* **27**, 83–89.

Greene J. G., Porter R. H., Eller R. V. and Greenamyre J. T. (1993) Inhibition of succinate dehydrogenase by malonic acid produces an 'excitotoxic' lesion in rat striatum. *J. Neurochem.* **61**, 1151–1154.

Hantraye P., Brouillet E., Ferrante R., Palfi S., Dolan R., Matthews R. T. and Beal M. F. (1996) Inhibition of neuronal nitric oxide synthase prevents MPTP-induced parkinsonism in baboons. *Nat. Med.* **2**, 1017–1021.

Hassel B. and Sonnewald U. (1995) Selective inhibition of the tricarboxylic acid cycle of GABAergic neurons with 3-nitropropionic acid In vivo. *J. Neurochem.* **65**, 1184–1191.

Huang H. M., Toral-Barza L., Sheu K. F. R. and Gibson G. E. (1994) The role of calcium in the regulation of pyruvate dehydrogenase in synaotosomes. *Neurochem. Res.* **19**, 89–95.

Joffe G. T. P., Parks J. K. and Parker W. D. Jr (1998) Secondary inhibition of 2-ketoglutarate dehydrogenase complex by MPTP. *Neuroreport* **9**, 2781–2783.

Johnson M. T., Yang H.-S., Magnuson T. and Patel M. S. (1997) Targeted disruption of the murine dihydrolipoamide dehydrogenase gene (*Dld*) results in perigastrulation lethality. *Proc. Natl Acad. Sci. USA* **94**, 14512–14517.

Kanamori T., Nishimaki K., Asoh S. *et al.* (2003) Truncated product of the bifunctional DLST gene involved in biogenesis of the respiratory chain. *EMBO J.* **22**, 2913–2923.

Kish S. J., Mastrogiacomo F., Guttman M., Furukawa Y., Taanman J. W., Dozic S., Pandolfo M., Lamarche J., DiStefano L. and Chang L. J. (1999) Decreased brain protein levels of cytochrome oxidase subunits in Alzheimer's disease an in hereditary spinocerebellar ataxia disorders: a nonspecific change? *J. Neurochem.* **72**, 700–707.

Kobayashi T., Matsumine H., Matuda S. and Mizuno Y. (1998) Association between the gene encoding the E2 subunit α-ketoglutarate dehydrogenase complex and Parkinson's disease. *Ann. Neurol.* **43**, 120–123.

Ksiezak-Reding H., Blass J. P. and Gibson G. E. (1982) Studies on the pyruvate dehydrogenase complex in brain with the arylamine acetyl-transferase-coupled assay. *J. Neurochem.* **38**, 1627–1636.

McNaught K. S., Altomare C., Cellamare S., Carotti A., Thull U., Carrupt P. A., Testa B., Jenner P. and Marsden C. D. (1995) Inhibition of alpha-ketoglutarate dehydrogenase by isoquinoline derivatives structurally related to 1-methyl-4-phenyl-1,2,3,6-tetrahydropyridine (MPTP). *Neuroreport* **6**, 1105–1108.

Mizuno Y., Sone N., Suzuki K. and Saitoh T. (1988) Studies on the toxicity of 1-methyl-4-phenylpyridinium ion (MPP+) against mitochondria of mouse brain. *J. Neurol. Sci.* **86**, 97–110.

Mizuno Y., Suzuki K. and Ohta S. (1990) Postmortem changes in mitochondrial respiratory enzymes in brain and a preliminary observation in Parkinson's disease. *J. Neurol. Sci.* **96**, 49–57.

Mizuno Y., Matuda S., Yoshino H., Mori H., Hattori N. and Ikebe S.-I. (1994) An immunohistochemical study on α-ketoglutarate dehydrogenase complex in Parkinson's disease. *Ann. Neurol.* **35**, 204–210.

Mizuno Y., Ikebe S., Hattori N., Nakagawa-Hattori Y., Mochizuki H., Tanaka M. and Ozawa T. (1995) Role of mitochondria in the etiology and pathogenesis of Parkinson's disease. *Biochim. Biophys. Acta* **1271**, 265–274.

Palfi S., Ferrante R. J., Brouillet E., Beal M. F., Dolan R., Guyot M. C., Peschanski M. and Hantraye P. (1996) Chronic 3-nitropropionic acid treatment in baboons replicates the cognitive and motor deficits of Huntington's Disease. *J. Neurosci.* **16**, 3019–3025.

Park L. C., Zhang H., Sheu K. F., Calingasan N. Y., Kristal B. S., Lindsay J. G. and Gibson G. E. (1999) Metabolic impairment induces oxidative stress, compromises inflammatory responses, and inactivates a key mitochondrial enzyme in microglia. *J. Neurochem.* **72**, 1948–1958.

Perez-Severiano F., Rios C. and Segovia J. (2000) Striatal oxidative damage parallels the expression of a neurological phenotype in mice transgenic for the mutation of Huntington's disease. *Brain Res.* **862**, 234–237.

Porter D. J. T. and Bright H. J. (1980) 3-Carbanionic substrate analogues bind very tightly to fumarase and aspartase. *J. Biol. Chem.* **255**, 4772–4780.

Przedborski S., Jackon-Lewis V., Yokoyama R., Shibata T., Dawson V. L. and Dawson T. M. (1996) Role of neuronal nitric oxide in 1-methyl-4-phenyl-1,2,3,6-tetrahydropyridine (MPTP)-induced dopaminergic neurotoxicity. *Proc. Natl Acad. Sci. USA* **93**, 4565–4571.

Rosenthal R. E., Hamud F., Fiskum G., Varghese P. J. and Sharpe S. (1987) Cerebral ischemia and reperfusion: prevention of brain mitochondria injury by lidoflazine. *J. Cereb. Blood Flow Metab.* **7**, 752–758.

Schooner W. G., Wanamarta A. H., van der Klei-van Moorsel J. M., Jakobs C. and Joenje H. (1990) Respiratory failure and stimulation of glycolysis in Chinese hamster ovary cells exposed to normobaric hyperoxia. *J. Biol. Chem.* **265**, 1118–1124.

Schooner W. G., Wanamarta A. H., van der Kleivan Moorsel J. M., Jakobs C. and Joenje H. (1991) Characterization of oxygen-resistant Chinese hamster ovary cells. III. Relative resistance of succinate and alpha-ketoglutarate dehydrogenase to hyperoxic inactivation. *Free Radic. Biol. Med.* **10**, 111–118.

Schulz J. B., Henshaw D. R., Matthews R. T. and Beal M. F. (1995a) Coenzyme Q_{10} and nicotinamide and a free radical spin trap protect against MPTP neurotoxicity. *Exp. Neurol.* **132**, 279–283.

Schulz J. B., Henshaw D. R., Siwek D., Jenkins B. G., Ferrante R. J., Cipolloni P. B., Kowall N. W., Rosen B. R. and Beal M. F. (1995b) Involvement of free radicals in excitotoxicity *in vivo*. *J. Neurochem.* **64**, 2239–2247.

Shen X. M., Li H. and Dryhurst G. (2000) Oxidative metabolites of 5-*S*-cysteinyldopamine inhibit the alpha-ketoglutarate dehydrogenase complex: possible relevance to the pathogenesis of Parkinson's disease. *J. Neural Transm.* **107**, 959–978.

Sheu K. F., Brown A. M., Kristal B. S., Kalaria R. N., Lilius L., Lannfelt L. and Blass J. P. (1999) A *DLST* gene associated with reduced risk for Alzheimer's disease. *Neurology* **52**, 1505–1507.

Sheu R.-K. F., Cooper A. J., Koike K., Koike M., Lindsay J. G. and Blass J. P. (1994) Abnormality of the alpha-ketoglutarate dehydrogenase complex in fibroblasts from familial Alzheimer's disease. *Ann. Neurol.* **35**, 312–318.

Sorbi S., Bird E. D. and Blass J. P. (1983) Decreased pyruvate dehydrogenase complex activity in Huntington and Alzheimer brain. *Ann. Neurol.* **13**, 72–78.

Starkov A. A. and Fiskum G. (2003) Regulation of brain mitochondrial H_2O_2 production by membrane potential and NAD(P)H redox state. *J. Neurochem.* **86**, 1101–1107.

Tabrizi S. J., Workman J., Hart P. E., Mangiarini L., Mahal A., Bates G., Cooper J. M. and Schapira A. H. (2000) Mitochondrial dysfunction and free radical damage in the Huntington R6/2 transgenic mouse. *Ann. Neurol.* **47**, 80–86.

APPENDIX 7

Journal of Neurochemistry, 2003, **86**, 267–272 doi:10.1046/j.1471-4159.2003.01868.x

Increased survival and neuroprotective effects of BN82451 in a transgenic mouse model of Huntington's disease

Peter Klivenyi,* Robert J. Ferrante,† Gabrielle Gardian,* Susan Browne,* Pierre-Etienne Chabrier‡ and M. Flint Beal*

**Department of Neurology and Neuroscience, Weill Medical College of Cornell University, New York-Presbyterian Hospital, New York*

†*Geriatric Research Education and Clinical Center, Bedford VA Medical Center, Bedford, MA and Neurology, Pathology and Psychiatry Departments, Boston University School of Medicine, Boston, Massachusetts, USA*

‡*Department of Biochemical Pharmacology, Institute Henri Beaufour, Les Ulis, France*

Abstract

There is substantial evidence that excitotoxicity and oxidative damage may contribute to Huntington's disease (HD) pathogenesis. We examined whether the novel anti-oxidant compound BN82451 exerts neuroprotective effects in the R6/2 transgenic mouse model of HD. Oral administration of BN82451 significantly improved motor performance and improved survival by 15%. Oral administration of BN82451 significantly reduced gross brain atrophy, neuronal atrophy and the number of neuronal intranuclear inclusions at 90 days of age. These findings provide evidence that novel anti-oxidants such as BN82451 may be useful for treating HD.

Keywords: experimental therapeutics, huntington, inflammation, neurodegeneration, oxidative damage, transgenic mice.

J. Neurochem. (2003) **86**, 267–272.

Huntington's disease (HD) is an autosomal dominant progressive neurodegenerative disease that starts in mid life and eventually leads to death. The mean survival after onset is 15–20 years and at present there is no known effective treatment for HD. The mutation that causes the illness is an expanded CAG/polyglutamine repeat stretch that has been postulated to confer its toxic effects by a gain of function. There is accumulating evidence that the polyglutamine expansion causes effects on gene transcription (Cha 2000; Luthi-Carter *et al.* 2000; Wyttenbach *et al.* 2002). These effects may be secondarily linked to energy dysfunction, oxidative damage and excitotoxicity, which are implicated in the pathogenesis of HD. Alternatively, N-terminal fragments of huntingtin may directly impair mitochondrial function (Panov *et al.* 2002).

A breakthrough in HD research was the development of transgenic mouse models. Transgenic mice with exon 1 of the human HD gene with an expanded CAG repeat develop a progressive neurological disorder (Mangiarini *et al.* 1996). These mice (line R6/2) have CAG repeat lengths of 141–157 under the control the human HD promotor. At approximately 6 weeks of age, the R6/2 mice show loss of body weight, and at 9–11 weeks they develop an irregular gait, stuttering stereotypic movements, resting tremors and epileptic seizures. The mice develop progressive weight loss and brain atrophy. Neuronal intranuclear inclusions that are immunopositive for huntingtin and ubiquitin are detected in the striatum at 4.5 weeks.

We and others found that that there is evidence of increased oxidative damage in the R6/2 transgenic mouse model of HD. It was shown that there is increased immunostaining for 3-nitrotyrosine, increased lipid peroxidation and increases in oxidative damage to DNA (Bogdanov *et al.* 2000; Perez-Severiano *et al.* 2000; Tabrizi *et al.* 2000). There is also some evidence that inflammatory mechanisms may contribute to disease pathogenesis (Ona *et al.* 1999; Luthi-Carter *et al.* 2000). In the present studies, we therefore examined whether a novel compound which has both

Received January 27, 2003; revised manuscript received April 14, 2003; accepted April 14, 2003.

Address correspondence and reprint requests to M. Flint Beal, MD, Chairman, Neurology Department, New York Presbyterian Hospital-Weill Medical College of Cornell University, 525 East 68th Street, New York, NY 10021, USA. E-mail: fbeal@med.cornell.edu

Abbreviations used: CBP, CREB binding protein; HD, Huntington's disease.

anti-oxidant and anti-inflammatory properties, BN82451, exerts beneficial effects on survival as well as motor performance and weight loss in the R6/2 transgenic mouse model of HD.

Materials and methods

Animals

Male transgenic HD mice of the R6/2 strain were obtained from Jackson Laboratories (Bar Harbor, ME, USA). Male R6/2 mice were bred locally with females from their background strain (B6CBAFI/J). The offspring were genotyped with a PCR assay on tail DNA. Nine to 10 mice in each group were examined for survival with equal numbers of males and females in each group. All animal experiments were carried out in accordance with the NIH *Guide for the Care and Use of Laboratory animals* and were approved by the local animal care committee.

Treatment

At 30 days of age the mice were fed lab chow diets supplemented with BN82451 at 0.015%, or a standard unsupplemented diet. Assuming an intake of 5 g of lab chow daily, this results in a dose of 30 mg/kg/day.

Behavior and weight assessment

Motor performance was assessed from 30 days of age in the R6/2 experiments (n = 9–10 mice per group) using the rotarod apparatus (Columbus Instruments, Columbus, OH, USA). Mice were tested at 12 r.p.m. Mice were given two trials and better result was recorded. They were weighed at the same time, once a week.

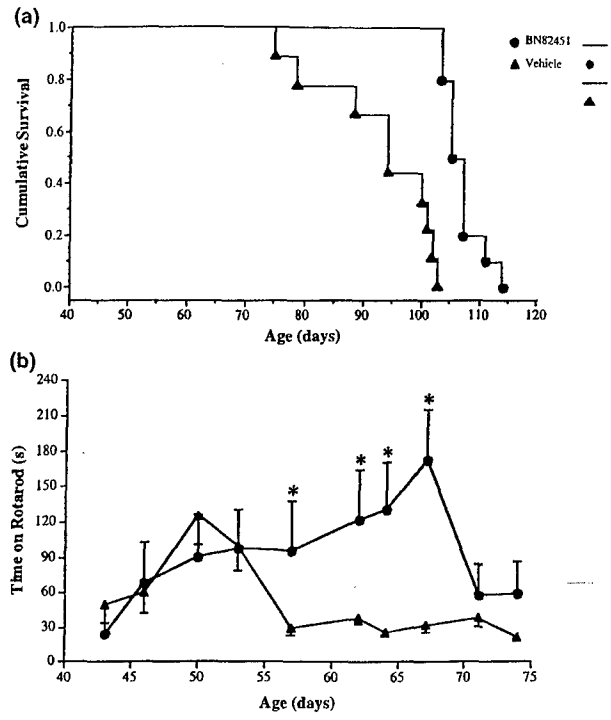

Fig. 1 (a) Cumulative probability of BN82451 on survival in R6/2 transgenic mice, $p < 0.001$ compared with controls. (b) Effects of BN82451 on rotorod performance in R6/2 transgenic mice. The treatment significantly improved motor performance on day 57, 60, 64 and 67 ($^*p < 0.05$).

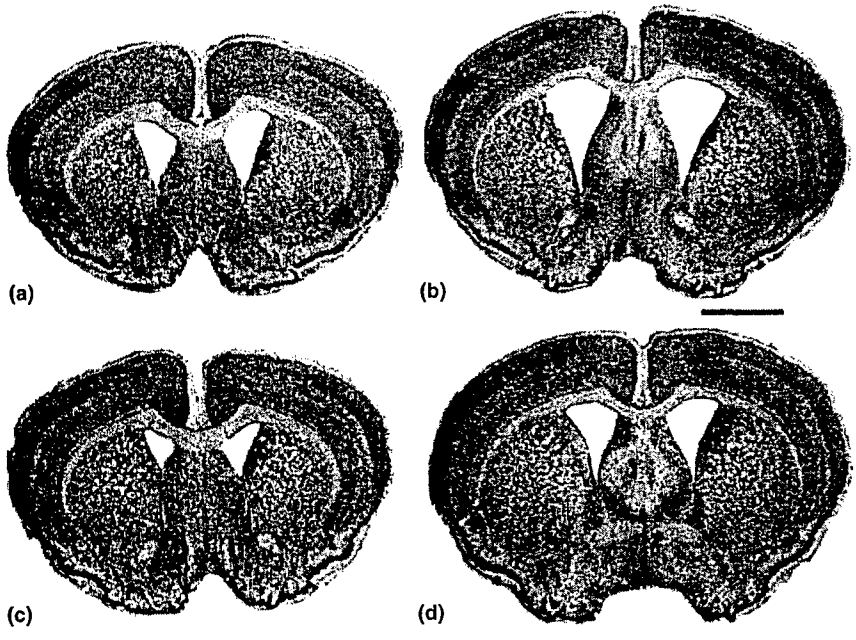

Fig. 2 Effects of BN8541 treatment on gross atrophy and ventricular enlargement in R6/2 mice at 10 weeks of age. Coronal step-sections through the rostral levels of the anterior commissure in untreated R6/2 (b and d) and BN8541-treated R6/2 mice (a and c). There is marked gross atrophy in the untreated R6/2 mouse tissues section with enlarged lateral ventricles. These findings are not as severe in the BN8541-treated mouse. Scale bar (shown in b): 2 mm.

Survival

Mice were observed every morning and late afternoon. The criteria for killing was the point in time at which mice were unable to initiate movement after being gently prodded for 2 min.

Stereology/quantitation

Serial-cut coronal tissue-sections from the rostral segment of the neostriatum at the level of the anterior commissure (interaural 5.34 mm/bregma 1.54 mm to interaural 3.7 mm/bregma −0.10 mm), were used for aggregate analysis. Unbiased stereologic counts of ubiquitin-positive aggregates (≥ 1.0 μm) were obtained from the neostriatum in 10 mice, each from BN82451-treated and unsupplemented diet R6/2 mice at 90 days using Neurolucida Stereo Investigator software (Microbrightfield, Colchester, VT, USA). The total areas of the neostriatum were defined in serial sections in which counting frames were randomly sampled. The dissector counting method was employed in which ubiquitin-positive aggregates were counted in an unbiased selection of serial sections in a defined volume of the neostriatum. Striatal neuron areas were analyzed by microscopic videocapture using a Windows-based image analysis system for area measurement (Optimas, Bioscan Incorporated, Edmonds, WA, USA). The software automatically identifies and measures profiles. Identified cell profiles were manually verified as neurons and exported to Microsoft Excel. Cross-sectional areas were analyzed using Statview.

Statistics

Data are expressed as the mean ± standard error of the mean (SEM). Rotarod and weight data were compared by analysis of variance (ANOVA). Survival data were analyzed by the Kaplan–Meier test.

Results

Oral administration of BN82451 in the diet resulted in significant improvements in the survival of R6/2 mice compared with the survival of mice fed unsupplemented diet (Fig. 1a). The controls deteriorated at 57 days and the treated mice at 72 days of age consistent with a delay in disease onset. The mean survival increased from 92.6 ± 3.5 days to 106.8 ± 1.1 days with BN82451 ($p < 0.001$). Survival was extended by 14 days (15.3%). The treated mice had significantly better motor performance from 57 to 67 days of age than mice fed unsupplemented diets (Fig. 1b). This finding was replicated in another group of control and BN82451-treated mice. The compound did not delay the weight loss, as there were no differences in body weight between the groups (data are not shown). Oral administration of BN82451 attenuated the development of gross atrophy and ventricular enlargement at 10 weeks of age (Fig. 2). At 90 days, striatal volumes: BN82451-treated R6/2 mice: 702 ± 41 mm^3; unsupplemented R6/2 mice: 576 ± 63 mm^3 0.76, $p < 0.01$. At 90 days, ventricular volumes: BN82451-treated R6/2 mice: 212 ± 27 mm^3; unsupplemented R6/2 mice: 120 ± 18 mm^3 0.76, $p < 0.01$. Oral administration of BN82451 also attenuated the development of neuronal atrophy (Fig. 3). Measurements of striatal neuron area at

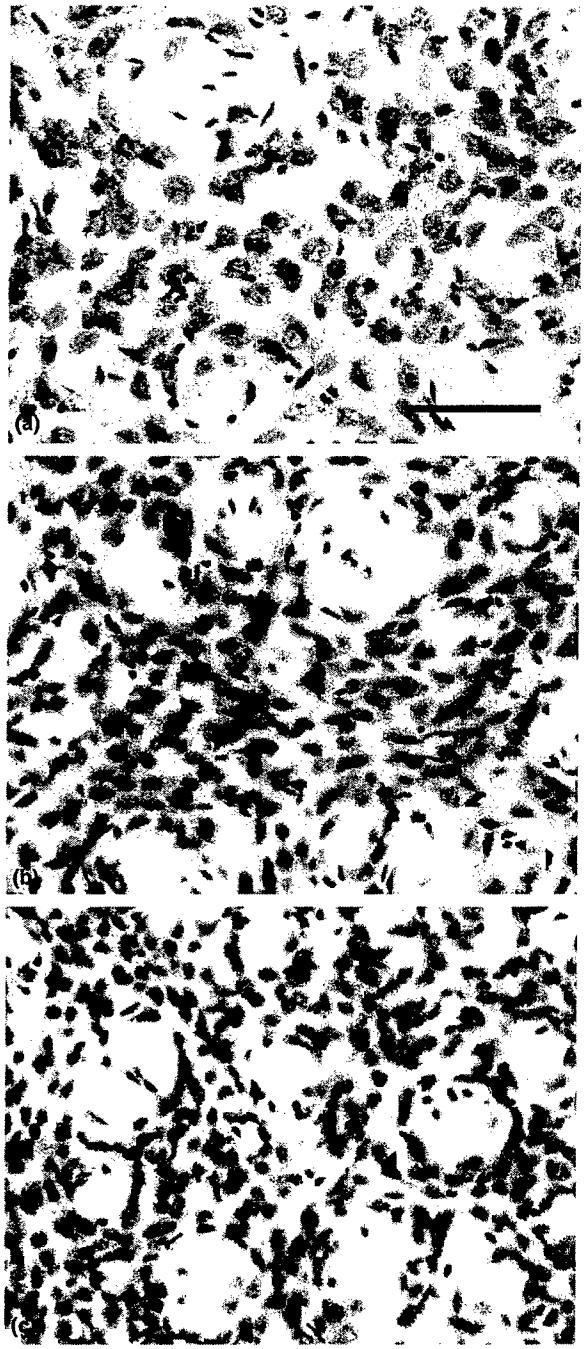

Fig. 3 Nissl-stained tissue sections from the dorso-medial aspect of the neostriatum at the level of the anterior commissure in a littermate wild-type control mouse (a), a BN8541-treated R6/2 mouse (b), and an untreated R6/2 mouse (c) at 10 weeks of age. There is marked neuronal atrophy in the untreated R6/2 mouse, with relative preservation of neuronal size in the BN8541-treated mouse, in comparison with the littermate control. Scale bar (shown in a): 100 μm.

90 days: wild-type littermate control: 114 ± 9.7 μm^2; BN82451-treated R6/2 mice: 79.5 ± 11.1 μm^2; unsupplemented R6/2 mice: 48.1 ± 17.2 μm^2; $p < 0.01$. Lastly,

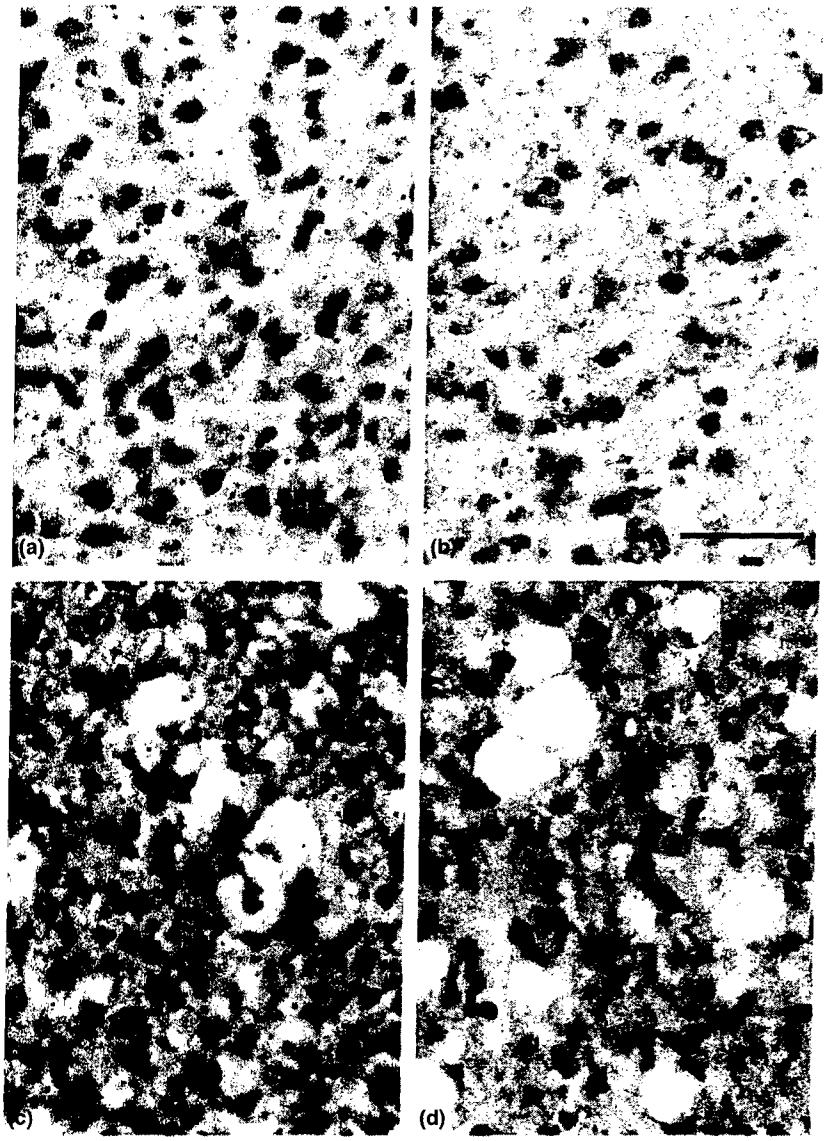

Fig. 4 Ubiquitin-immunostained tissue sections from the neocortex (a and b) and neostriatum (c and d) of untreated (a and c) and BN8541-treated (b and d) R6/2 mice at 10 weeks of age. While there were reduced numbers of ubiquitin-positive inclusions in both the neocortex and neostriatum of BN8541-treated mice, significance was only present in the neostriatum. Scale bar (shown in b): 100 μm.

administration of BN82451 significantly attenuated the numbers of striatal ubiquitin positive inclusions (Fig. 4). The number of aggregates at 90 days: BN82451-treated R6/2 mice: $1.16 \pm 0.43 \times 10^6$; unsupplemented R6/2 mice; $2.72 \pm 0.76 \times 10^6$, $p < 0.01$.

Discussion

The pathogenesis of neuronal degeneration in HD is an area of intense investigation. It has been demonstrated that huntingtin can directly bind to a number of transcription factors. These include the CREB binding protein (CBP) as well as Sp1 and several others (Steffan *et al.* 2000; Nucifora *et al.* 2001; Dunah *et al.* 2002; Li *et al.* 2002). Overexpression of either CBP or Sp1 can rescue cultured cells from the neurotoxicity of mutant huntingtin (Nucifora *et al.* 2001; Dunah *et al.* 2002). The precise mechanisms by which impaired gene transcription lead to cell death in HD, however, remain obscure. There is substantial evidence that both excitotoxicity and oxidative damage contribute to disease pathogenesis (Beal 1995). Transgenic mice with full length huntingtin expressed in a YAC construct show increased vulnerability to striatal excitotoxic lesions (Zeron *et al.* 2002). A secondary consequence of excitotoxicity is oxidative damage (Beal 1995). Expression of mutant huntingtin in neuronal and non-neuronal cells causes increased reactive oxygen species which contributes to cell death (Wyttenbach *et al.* 2002). A number of studies have demonstrated that there is increased oxidative damage in the R6/2 transgenic mouse model of HD. These mice show increased immunostaining for 3-nitrotyrosine, a marker of peroxynitrite-mediated oxidative damage (Tabrizi *et al.*

2000). They also show increased and progressive lipid peroxidation (Perez-Severiano *et al.* 2000). We recently examined concentrations of a marker of oxidative damage to DNA, 8-hydroxy-2-deoxyguanosine (Bogdanov *et al.* 2001). We found increased concentrations of 8-hydroxy-2-deoxyguanosine in the urine, plasma and striatal microdialysates of R6/2 HD mice. There were increased concentrations in isolated brain DNA at 12 and 14 weeks of age, and increased immunostaining in late stages of the illness.

There is also evidence that inflammation may contribute to disease pathogenesis in the R6/2 mice. Gene array studies show that there is increased expression of genes associated with inflammation at both 6 and 12 weeks of age in the R6/2 transgenic HD model (Luthi-Carter *et al.* 2000). There are increased concentrations of interleukin-1β, a pro-inflammatory cytokine (Ona *et al.* 1999). Inhibition of the interleukin-1β converting enzyme by crossing transgenic mice with a dominant-negative inhibitor of this enzyme into the R6/2 mice significantly extends survival (Ona *et al.* 1999). Lastly, minocycline, which is known to inhibit microglial activation, also shows neuroprotective effects in the R6/2 transgenic mice (Chen *et al.* 2000). Microglial activation is a prominent feature of the neuropathology of HD (Singhrao *et al.* 1999; Sapp *et al.* 2001).

In the present study, we therefore studied the effects of a novel compound which is an orally active brain permeable anti-oxidant, that not only acts as an inhibitor of lipid peroxidation but which also has potent anti-inflammatory effects (Chabrier *et al.* 2001). BN82451 has previously been shown to exert neuroprotective effects in animal models in which mitochondrial impairment was produced using malonate or MPTP (Chabrier *et al.* 2001). These models are associated with impaired ATP production as well as oxidative damage. Activated microglia may contribute to neuronal damage in these models, by secreting toxic substances, including free radicals, prostaglandins, inflammatory cytokines and proteolytic enzymes. BN82451 has both anti-oxidant effects, as well as anti-inflammatory activities, and blocking microglial activation and inhibiting cyclooxygenase enzymes following MPTP and malonate administration. *In vitro* BN82451 blocks lipid peroxidation of rat cerebral cortex homogenates with an IC_{50} of ~0.3 μm and it inhibits COX-1 and COX-2 with an IC_{50} of ~0.1 μm.

In the present experiments, we found that BN82451 produced significant improvements in survival and rotarod performance in the R6/2 transgenic mouse model of HD. Surprisingly, there were no effects on loss of body weight, suggesting that delay of weight loss does not necessarily accompany improved survival. It also significantly reduced striatal atrophy, neuronal atrophy and numbers of neuronal intranuclear inclusions. The improvement in survival of 15.3% is equivalent to the effects of co-enzyme Q10, and minocycline, although slightly less than the effects of creatine and cystamine (Chen *et al.* 2000; Ferrante *et al.* 2000; Dedeoglu *et al.* 2002; Ferrante *et al.* 2002). These findings, therefore, provide further evidence that both oxidative damage and inflammation may contribute to disease pathogenesis. They raise the possibility that agents which have anti-oxidative and anti-inflammatory activity may be useful as therapies to slow or halt the progression of neurodegeneration in HD. It is also possible that these agents might be useful in combination with other agents such as creatine, co-enzyme Q10, minocycline, and histone deacetylase inhibitors in producing additive therapeutic benefits for the treatment of HD.

Acknowledgements

Greta Strong and Sharon Melanson are thanked for secretarial assistance. This work was supported by NINDS grant NS39258, The Hereditary Disease Foundation and The Huntington's Disease Society of America.

References

Beal M. F. (1995) Aging, energy and oxidative stress in neurodegenerative diseases. *Ann. Neurol.* **38**, 357–366.

Bogdanov M., Brown R. H., Matson W., Smart R., Hayden D., O'Donnell H., Flint Beal M. and Cudkowicz M. (2000) Increased oxidative damage to DNA in ALS patients. *Free Radic. Biol. Med.* **29**, 652–658.

Bogdanov M. B., Andreassen O. A., Dedeoglu A., Ferrante R. J. and Beal M. F. (2001) Increased oxidative damage to DNA in a transgenic mouse model of Huntington's disease. *J. Neurochem.* **79**, 1–5.

Cha J. H. (2000) Transcriptional dysregulation in Huntington's disease. *Trends Neurosci.* **23**, 387–392.

Chabrier P. E., Roubert V., Harnett J., Cornet S., Delafotte S., Charnet-Roussillot C., Spinnewyn B. and Auguet M. (2001) New neuroprotective agents are potent inhibitors of mitochondrial toxins: *in vivo and in vitro* studies. *Soc. Neurosci. Abstr.* **27**, 530.

Chen M., Ona V. O., Li M., Ferrante R. J., Fink K. B., Zhu S., Bian J., Guo L., Farrell L. A., Hersch S. M., Hobbs W., Vonsattel J. P., Cha J. H. and Friedlander R. M. (2000) Minocycline inhibits caspase-1 and caspase-3 expression and delays mortality in a transgenic mouse model of huntington disease. *Nature Med.* **6**, 797–801.

Dedeoglu A., Jeitner T. M., Matson S. A., Kubilus J. K., Bogdanov M., Kowall N. W., Matson W. R., Cooper A. L., Ratan R. R., Beal M. F., Hersch S. M. and Ferrante R. J. (2002) Therapeutic effects of the transglutaminase inhibitor, cystamine, in a murine model of Huntington's disease. *J. Neurosci.* **22**, 8942–8950.

Dunah A. W., Jeong H., Griffin A., Kim Y. M., Standaert D. G., Hersch S. M., Mouradian M. M., Young A. B., Tanese N. and Krainc D. (2002) Sp1 and TAFII130 transcriptional activity disrupted in early Huntington's disease. *Science* **2**, 2.

Ferrante R. J., Andreassen O. A., Jenkins B. G., Dedeoglu A., Kuemmerle S., Kubilus J. K., Kaddurah-Daouk R., Hersch S. M. and Beal M. F. (2000) Neuroprotective effects of creatine in a transgenic mouse model of Huntington's disease. *J. Neurosci.* **20**, 4389–4397.

Ferrante R. J., Andreassen O. A., Dedeoglu A., Ferrante K. L., Jenkins B. G., Hersch S. M. and Beal M. F. (2002) Therapeutic effects of coenzyme Q10 and remacemide in transgenic mouse models of Huntington's disease. *J. Neurosci.* **22**, 1592–1599.

Li S. H., Cheng A. L., Zhou H., Lam S., Rao M., Li H. and Li X. J. (2002) Interaction of Huntington disease protein with transcriptional activator Sp1. *Mol. Cell Biol.* **22**, 1277–1287.

Luthi-Carter R., Strand A., Peters N. L., Solano S. M., Hollingsworth Z. R., Menon A. S., Frey A. S., Spektor B. S., Penney E. B., Schilling G., Ross C. A., Borchelt D. R., Tapscott S. J., Young A. B., Cha J. H. and Olson J. M. (2000) Decreased expression of striatal signaling genes in a mouse model of Huntington's disease. *Hum. Mol. Genet.* **9**, 1259–1271.

Mangiarini L., Sathasivam K., Seller M., Cozens B., Harper A., Hetherington C., Lawton M., Trottier Y., Lehrach H., Davies S. W. and Bates G. P. (1996) Exon 1 of the *HD* gene with an expanded CAG repeat is sufficient to cause a progressive neurological phenotype in transgenic mice. *Cell* **87**, 493–506.

Nucifora F. C. Jr, Sasaki M., Peters M. F., Huang H., Cooper J. K., Yamada M., Takahashi H., Tsuji S., Troncoso J., Dawson V. L., Dawson T. M. and Ross C. A. (2001) Interference by huntingtin and atrophin-1 with cbp-mediated transcription leading to cellular toxicity. *Science* **291**, 2423–2428.

Ona V. O., Li M., Vonsattel J. P., Andrews L. J., Khan S. Q., Chung W. M., Frey A. S., Menon A. S., Li X. J., Stieg P. E., Yuan J., Penney J. B., Young A. B., Cha J. H. and Friedlander R. M. (1999) Inhibition of caspase-1 slows disease progression in a mouse model of Huntington's disease. *Nature* **399**, 263–267.

Panov A. V., Gutekunst C. A., Leavitt B. R., Hayden M. R., Burke J. R., Strittmatter W. J. and Greenamyre J. T. (2002) Early mitochondrial calcium defects in Huntington's disease are a direct effect of polyglutamines. *Nat. Neurosci.* **1**, 1.

Perez-Severiano F., Rios C. and Segovia J. (2000) Striatal oxidative damage parallels the expression of a neurological phenotype in mice transgenic for the mutation of Huntington's disease. *Brain Res.* **862**, 234–237.

Sapp E., Kegel K. B., Aronin N., Hashikawa T., Uchiyama Y., Tohyama K., Bhide P. G., Vonsattel J. P. and DiFiglia M. (2001) Early and progressive accumulation of reactive microglia in the Huntington disease brain. *J. Neuropathol. Exp. Neurol.* **60**, 161–172.

Singhrao S. K., Neal J. W., Morgan B. P. and Gasque P. (1999) Increased complement biosynthesis by microglia and complement activation on neurons in Huntington's disease. *Exp. Neurol.* **159**, 362–376.

Steffan J. S., Kazantsev A., Spasic-Boskovic O., Greenwald M., Zhu Y. Z., Gohler H., Wanker E. E., Bates G. P., Housman D. E. and Thompson L. M. (2000) The Huntington's disease protein interacts with p53 and CREB-binding protein and represses transcription. *Proc. Natl Acad. Sci. USA* **97**, 6763–6768.

Tabrizi S. J., Workman J., Hart P. E., Mangiarini L., Mahal A., Bates G., Cooper J. M. and Schapira A. H. (2000) Mitochondrial dysfunction and free radical damage in the Huntington R6/2 transgenic mouse. *Ann. Neurol.* **47**, 80–86.

Wyttenbach A., Sauvageot O., Carmichael J., Diaz-Latoud C., Arrigo A. P. and Rubinsztein D. C. (2002) Heat shock protein 27 prevents cellular polyglutamine toxicity and suppresses the increase of reactive oxygen species caused by huntingtin. *Hum. Mol. Genet.* **11**, 1137–1151.

Zeron M. M., Hansson O., Chen N., Wellington C. L., Leavitt B. R., Brundin P., Hayden M. R. and Raymond L. A. (2002) Increased sensitivity to N-methyl-D-aspartate receptor-mediated excitotoxicity in a mouse model of Huntington's disease. *Neuron* **33**, 849–860.

APPENDIX 8

Journal of Neurochemistry, 2003, **85**, 142–150 doi:10.1046/j.1471-4159.2003.01639.x

Iron porphyrin treatment extends survival in a transgenic animal model of amyotrophic lateral sclerosis

Annie S. Wu,* Mahmoud Kiaei,* Norberto Aguirre,* John P. Crow,† Noel Y. Calingasan,* Susan E. Browne* and M. Flint Beal*

**Department of Neurology and Neuroscience, Weill Medical College of Cornell University, New York, USA*

†Departments of Anesthesiology, Pharmacology/Toxicology, and Biochemistry and Molecular Genetics, University of Alabama at Birmingham, Birmingham, Alabama, USA

Abstract

Oxidative damage, produced by mutant Cu/Zn superoxide dismutase (SOD1), may play a role in the pathogenesis of amyotrophic lateral sclerosis (ALS), a devastating motor neuron degenerative disease. A novel approach to antioxidant therapy is the use of metalloporphyrins that catalytically scavenge a wide range of reactive oxygen and reactive nitrogen species. In this study, we examined the therapeutic potential of iron porphyrin (FeTCPP) in the G93A mutant SOD1 transgenic mouse model of ALS. We found that intraperitoneal injection of FeTCPP significantly improved motor function and extended survival in G93A mice. Similar results were seen with a second group of mice wherein treatment with FeTCPP was initiated at the onset of hindlimb weakness—roughly equivalent to the time at which treatment would begin in human patients. FeTCPP-treated mice also showed a significant reduction in levels of malondialdehyde (a marker of lipid peroxidation), in total content of protein carbonyls (a marker of protein oxidation), and increased neuronal survival in the spinal cord. These results therefore provide further evidence of oxidative damage in a mouse model of ALS, and suggest that FeTCPP could be beneficial for the treatment of ALS patients.

Keywords: amyotrophic lateral sclerosis, antioxidant, iron porphyrin, metalloporphyrin, protein carbonyls, Cu/Zn superoxide dismutase.

J. Neurochem. (2003) **85**, 142–150.

Amyotrophic lateral sclerosis (ALS) is an adult-onset, rapidly progressive, neurodegenerative disorder with an unknown etiology. It is characterized by the degeneration of motor neurons in the spinal cord, brainstem and motor cortex. The characteristic physical findings of ALS are the combination of upper motor neuron and lower motor neuron signs that include muscle weakness, atrophy and spasticity. With its inexorable progression, patients usually die within 3–5 years of symptom onset due to secondary aspiration pneumonia or respiratory failure. ALS is most commonly sporadic, with about 10% of cases being inherited as an autosomal dominant familial form.

Since the discovery in 1993 that a mutated form of Cu/Zn superoxide dismutase (SOD1) associates with approximately 20% of cases of familial ALS (Rosen *et al.* 1993), various theories have been postulated about what the gain-of-function caused by the mutant SOD1 could be. One hypothesis centers around the loss of substrate specificity and subsequent aberrant redox activity of the active site copper, resulting in oxidative stress (Cookson and Shaw 1999; Cleveland and Liu 2000). It was proposed that mutations to SOD1 lead to a more open or relaxed active site (Deng *et al.* 1993) that would increase the generation of hydroxyl radicals from hydrogen peroxide (Wiedau-Pazos *et al.* 1996) or peroxynitrite from nitric oxide (Beckman *et al.* 1993). Furthermore, it was shown that several SOD1 mutants have decreased zinc binding affinity (Crow *et al.* 1997) and that, in the absence of zinc, cellular reductants such as ascorbic acid rapidly reduce Cu(II) to the Cu(I) form in the enzyme's

Received October 22, 2002; revised manuscript received December 10, 2002; accepted December 11, 2002.

Address correspondence and reprint requests to M. Flint Beal, Department of Neurology and Neuroscience, Weill Medical College of Cornell University, New York, NY 10021, USA.
E-mail: fbeal@med.cornell.edu

Abbreviations used: ALS, amyotrophic lateral sclerosis; FeTCPP, iron 5,10,15,20-tetrakis-4-carboxyphenyl porphyrin; SOD1, Cu/Zn superoxide dismutase.

active site, which would lead to a net production of superoxide and, in the presence of nitric oxide, production of peroxynitrite (Estevez *et al.* 1999). These possibilities, however, have been questioned by the finding that crossing mutant SOD1 transgenic mice with mice deficient in the copper chaperone protein for SOD (CCS), required for most of the copper loading in SOD, does not alter the disease phenotype (Subramaniam *et al.* 2002). This finding, however, does not rule out aberrant copper incorporation into SOD1 in the absence of the chaperone. Indeed, Subramaniam *et al.* reported that 20–30% of SOD1 activity remained even in the absence of CCS. Moreover, Goto *et al.* (2000) have reported that in the absence of CCS, copper binds abnormally to SOD1, which increases the possibility that it would possess abnormal redox activity.

Although the precise biochemical mechanism whereby SOD1 mutants are pathologic in ALS remains elusive, there is substantial evidence for increased oxidative damage in a transgenic mouse model associated with mutant G93A SOD1 (Ferrante *et al.* 1997a). A novel approach to antioxidant therapy is the use of catalytic antioxidants such as low molecular weight metal-containing porphyrins. Originally developed as SOD1 mimetics, both iron(III) and manganese(III) porphyrins have been shown to catalytically decompose several biological oxidants including superoxide, hydrogen peroxide, lipid peroxyl radicals and peroxynitrite (Patel and Day 1999). Metalloporphyrins are effective at blocking oxidant stress both *in vitro* (Faulkner *et al.* 1994; Benov and Fridovich 1995; Liochev and Fridovich 1995; Batinic-Haberle *et al.* 1998) and *in vivo* (Day and Crapo 1996; Zingarelli *et al.* 1997; Szabo 1998; Cuzzocrea *et al.* 1999). Several manganese (Mn[III]) and iron (Fe[III]) porphyrins have been shown to be excellent peroxynitrite scavengers because they react very rapidly with peroxynitrite (second order rate constants of 10^6–10^7/M/s) and decompose it catalytically (Crow 2000). Manganese porphyrins require exogenous reductants such as ascorbate to reduce Mn(IV) back to Mn(III) to complete the catalytic cycle (Lee *et al.* 1997, 1998; Crow 1999; Ferrer-Sueta *et al.* 1999), whereas iron porphyrins do not require exogenous reductants for the catalytic function. However, because reductants such as ascorbate and glutathione are always present in mammalian tissues, this requirement would not be limiting *in vivo*.

In this study, we evaluated survival, motor function (rotarod) and weight changes, and carried out histological and oxidative damage marker determinations in iron 5,10,15,20-tetrakis-4-carboxyphenyl porphyrin (FeTCPP) (Fig. 1) and vehicle-treated G93A transgenic mice. We also compared treatment regimens wherein FeTCPP administration commenced prior to the onset of weakness (40 days of age) with a second group wherein FeTCPP treatment was initiated on the first day of hindlimb weakness in each

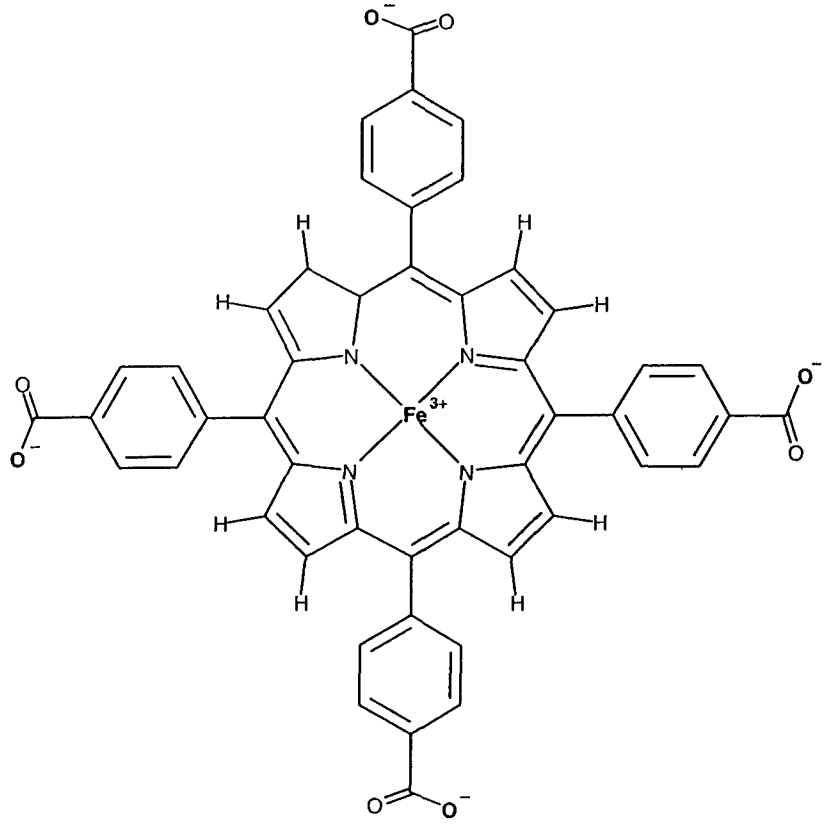

Fig. 1 Structure of FeTCPP.

mouse. The latter regimen is comparable with the earliest time at which drug treatment could begin in human patients.

Materials and methods

Transgenic mice for early (40 days of age) treatment

G93A transgenic familial ALS mice (Gurney *et al.* 1994) were obtained from Jackson Laboratory (Bar Harbor, ME, USA). We maintained the transgenic G93A hemizygotes by mating transgenic males with B6SJLF1/J hybrid females. Transgenic offspring were genotyped by PCR assay of DNA obtained from tail tissue. Twenty-nine G93A transgenic mice were randomly assigned to a treatment or control (vehicle) group. We also included seven N1029 (wild-type SOD1 transgenics instead of G93A SOD1) mice as a control mouse model for G93A transgenic mice in the histological evaluations. All animal experiments were carried out in accordance with the NIH Guide for the Care and Use of Laboratory Animals.

Transgenic mice for late (symptom-onset) treatment

G93A overexpressing mice were initially obtained by breeding transgenic males purchased from Jackson Laboratories with c57b6 females also obtained from Jackson Laboratories Offspring were determined to be transgenic by sampling 2 μL of whole blood from the tail and running SOD activity gels (Beauchamp and Fridovich 1971). Transgenic male offspring from the same litter were used as breeders for the second generation of transgenic mice; all mice used for this study were obtained using this litter-mate breeding strategy. Sixteen G93A transgenic mice were randomly assigned to a FeTCPP-treated ($n = 9$) and untreated control group ($n = 7$). The mean age of onset in the FeTCPP-treated animals was 101.2 ± 1.4 days and in the controls 104.4 ± 2.9 days, which did not significantly differ.

Drug administration

A 1 mg/mL solution of FeTCPP (Porphyrin Products, Inc., Logan, UT, USA) was prepared by dissolving the compound in aqueous NaOH. The solution was made isotonic by addition of 0.9% NaCl and the pH was adjusted to 7.4 with HCl. The final solution was sterile-filtered and the final concentration of FeTCPP was standardized spectrophotometrically ($A_{409nm} = 32\ 400/M/cm$).

Two different treatment regimens were carried out with the transgenic mice: (i) in the early treatment group, 1 mg/kg FeTCPP was administered i.p. once a day beginning at 40 days of age, while 100 μL of PBS (0.15 M potassium phosphate containing 150 mM NaCl, pH 7.4) were administered i.p. to the vehicle group; (ii) in the symptom-onset treatment group, 1 mg/kg of FeTCPP was administered i.p. twice daily following a single 2 mg/kg loading dose beginning on the first day that symptoms appeared in each mouse. Symptom onset was defined as the first day that the mouse displayed abnormal splaying of hindlimbs when lifted by its tail. Hindlimb splaying is a consistent and objective sign that asymmetrical or symmetrical hindlimb weakness and paralysis will follow within 2–3 days.

Survival

The initial sign of disease in G93A transgenic mice is a resting tremor that progresses to gait impairment, asymmetrical or symmetrical paralysis of the hindlimbs, followed by complete paralysis at the end stage. For the early treatment group and the corresponding vehicle group, mice were killed when they were unable to roll over within 20 s after being pushed on their sides and this time point was recorded as the time of death. For the symptom-onset treatment group and its corresponding control group, mice were killed when they displayed any signs of labored breathing or when they were no longer able to eat and drink, as evidenced by significant weight loss in a 24-h period. The untreated control group was treated in an identical manner, except that no injections were given. Upon killing, mice were examined for evidence of peritonitis or any obvious abnormalities related to the i.p. injections. Any mice showing signs of peritonitis or pathology related to injections were excluded from the study. Survival was assessed for all four groups.

Motor function testing (rotarod)

For the early treatment group and its corresponding vehicle group, rotarod performances were assessed twice a week in G93A mice starting at 80 days of age. Mice were trained for 2–3 days to become acquainted with the rotarod apparatus (Columbus instruments, Columbus, OH, USA). The testing began by placing the mice on a rod rotating at 12 rev/min, and the time that the mice stayed on the rod (until falling off or staying a maximum of 5 min) was recorded as a measurement of the competence of their motor function. Three trials were performed and the best result of the three was recorded.

Histological evaluation

Mice were anesthetized and transcardially perfused with 0.9% NaCl. Brains and spinal cords were removed and immediately frozen on solid CO_2. The spinal cords were fixed in 4% paraformaldehyde in 0.1 M phosphate buffer (pH 7.4) for 48 h, and the tissues were cryoprotected in 30% sucrose overnight. Serial transverse sections (50 μm thick) were cut on a cryostat and collected for Nissl staining and immunohistochemistry. Every ninth section through the lumbar spinal cord was immunostained with a rabbit anti-serum against malondialdehyde-modified protein (provided by Dr Craig Thomas, Hoechst Marion Roussel) using a modified avidin-biotin peroxidase technique (Hsu *et al.* 1981). Free-floating sections were pre-treated with 3% H_2O_2 in PBS for 30 min to inactive endogenous peroxidases. All sections were pre-incubated in 1% bovine serum albumin (BSA)/0.2% Triton X-100 in PBS for 30 min on an orbital shaker at room temperature. The sections were incubated in rabbit anti-albumin-modified malondialdehyde (diluted 1 : 1000 in 0.5% BSA/PBS) overnight, followed by biotinylated anti-rabbit IgG (Vector Laboratory, Burlingance, CA, USA) incubation for 1 h (diluted 1 : 200 in 0.5% BSA/PBS). After washing with 0.5% BSA/PBS (3 × 5 min), the sections were incubated in avidin-biotin peroxidase complex (diluted 1 : 200 in PBS) for 1 h. The immunoreaction was visualized using 3,3′-diaminobenzidine tetrahydrochloride dihydrate (DAB) with nickel intensification (Vector) as the chromogen. The sections were mounted onto gelatin-coated slides, dehydrated, cleared in xylene and coverslipped. The specificity of immunostaining was confirmed by pre-incubation of the antibody with antigen and by omission of the primary antibody. The intensity of malondialdehyde immunostaining in the gray and white matter within the lumbar spinal cord was graded blindly using a semi-quantitative scale of weak (+), moderate (+ +) and intense (+ + +).

Sections adjacent to those used for immunocytochemistry were stained with cresyl violet. Every fourth section was analyzed for neuronal volume and number using optical fractionator and nucleator probes of the Stereo Investigator System (Microbrightfield, Colchester, VT, USA). Six tissue sections of the lumbar spinal cord from each mouse were analyzed. All cells were counted from within the ventral horn below a horizontal line across the gray matter through the ventral border of the central canal.

Protein carbonyl measurements

Spinal cords were homogenized in lysis buffer containing 250 mM sucrose, 10 mM $MgCl_2$, 2 mM EDTA pH 6.8, 20 mM HEPES and protease inhibitor (Roche Molecular Biochemicals, Indianapolis, IN, USA). Protein concentration of homogenates was determined using a Bio-Rad (Bio-Rad Laboratories, Hercules, CA, USA) protein detection kit.

Derivatization of the spinal cord homogenates (15 μg of total protein) was performed using the OxyBlot protein oxidation detection kit (Intergen, Purchase, NY, USA) according to the manufacturer's instructions. Then, samples were applied directly to a 4–20% gradient Tris-glycine sodium dodecyl sulfate (SDS) gel (Invitrogen life technolo- gies, Carlsbad, CA, USA) or stored at 4°C for a later use for up to a week.

Electrophoresis was carried out for 90 min at 125 V, and proteins were transferred to a polyvinylidene difluoride (PVDF) membrane for 60 min at 70 V under cold conditions. The membranes were then blocked with 1% BSA/Tris buffered saline Tween 20 (TBST) for 1 h at room temperature on an orbital shaker. The membranes were then incubated with a primary antibody specific to the dinitrophenyl (DNP) moiety of the protein (dilution of 1 : 150 in 1% BSA/TBST) overnight at 4°C on an orbital shaker. The blot was washed with TBST (5 × 10 min) and incubated with secondary antibody (dilution of 1 : 300 in 1% BSA/TBST) for 2 h. Enhanced chemiluminescence (Supersignal; Pierce, Rockford, IL, USA) was used and exposed to X-ray film for 5 min to detect DNP-conjugated protein. Optical densities were analyzed using the Scion Image software for Windows.

HPLC method for FeTCPP in mouse tissue

Mouse tissues (age of onset-treated group, $n = 9$) were homogenized in four volumes of water and sonicated. NaOH was added to a final concentration of 50 mM and an equal volume of ethyl acetate was added and vigorously mixed. After centrifugation, the ethyl acetate layer was removed and the aqueous layer acidified with HCl. An equal volume of tert-butyl methyl ether (tBME) was added, mixed vigorously and separated by centrifugation. The tBME layer was removed and taken to dryness in a vacuum centrifuge. Dried extracts were resuspended in a minimum volume of methanol (MeOH) followed by addition of an equal volume of 100 mM KOH. Resuspended samples were clarified by centrifugation and supernatant fluids injected into the HPLC. FeTCPP standards were prepared and suspended in the same MeOH–KOH solution. Separation was achieved using a 4.6 × 150 mm Waters Sperisorb ODS-II column (Waters, Milford, MA, USA) maintained at 48°C in a column oven. FeTCPP was eluted using a gradient consisting of 0.2% heptafluorobutyric acid in water (buffer A), acetonitrile (buffer B) and MeOH (buffer C). FeTCPP in mouse tissues was identified by its retention time (9.96 min) and by its characteristic UV-visible spectrum using a Shimadzu diode-array detector (Shimadzu, Columbia, MD, USA). FeTCPP was quantified via its absorbance at 400 nm relative to standards of pure FeTCPP. Untreated mouse tissues were spiked with known concentrations of FeTCPP (similar to those found in treated mice) and extracted just as with treated mice samples. The extraction efficiency was determined for brain, spinal cord, kidney and liver and used to calculate concentrations of FeTCPP in the original wet tissues. For the purposes of calculating and expressing tissue concentrations of drug, one microgram of wet tissue was considered to be equal to one microliter.

Statistical analysis

Kaplan-Meier survival analysis and the Logrank (Mantel–Cox) test were used for survival comparisons, repeated measures ANOVA for Rotarod comparisons, ANOVA with Newman-Keuls for neuronal cell count and the unpaired *t*-test for total carbonyl studies. For the symptom-onset study, survival interval data were analyzed by the unpaired *t*-test.

Results

In this study, G93A mice were treated with FeTCPP using two different regimens: (i) the early treatment group, beginning at 40 days of age and dosed once per day and (ii) the symptom-onset treatment group, with twice-daily dosing beginning with a 2× loading dose on the first day that symptoms appeared in each mouse. Each treatment group had its own corresponding control group. Survival was assessed in all four groups. Motor function was assessed by rotarod performance for the early treatment group and its corresponding vehicle group.

FeTCPP tissue levels

A critical issue is whether FeTCPP penetrates the blood–brain barrier to mediate its therapeutic effects. We therefore measured concentrations of FeTCPP in the brain, spinal cord, kidney and liver of the 'age of onset' treatment group of G93A mice (Fig. 2). These results show that FeTCPP does penetrate into the brain and spinal cord and achieves

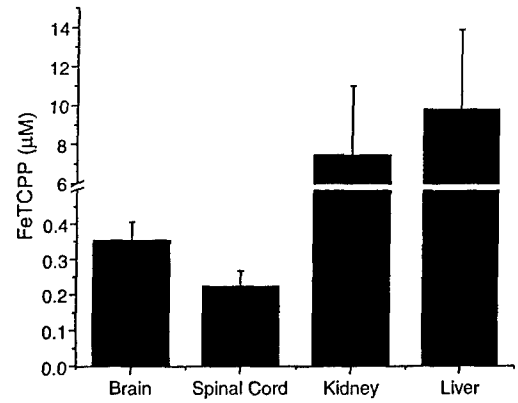

Fig. 2 Mean FeTCPP concentrations (μm) in the 'age of onset' treatment group of G93A mice.

lower μm concentrations. A caveat is that the samples were not perfused. However, we think that blood contamination is unlikely to account for the levels since they were obtained 16–18 h after the last injection, they showed no evidence of blood tingeing and spinal cord contains very little blood.

Survival

In the early treatment group, survival was significantly extended by 7 days with FeTCPP. The mean survivals were 135.6 ± 2.4 days (mean ± SE) for FeTCPP-treated mice, and 128.6 ± 1.7 days for vehicle-treated mice ($n = 19$ per group, $p < 0.02$ by Mantel–Cox rank test) (Fig. 3a).

In the symptom-onset treatment group, the mean survival interval from disease onset to euthanasia was also significantly extended by FeTCPP. The mean survival intervals were 25.8 ± 2.2 days (mean ± SE) for FeTCPP-treated mice ($n = 9$) and 16.7 ± 1.3 days for untreated mice ($n = 7$). This is an overall increase in survival of 9 days ($p < 0.01$ by unpaired *t*-test) (Fig. 3b).

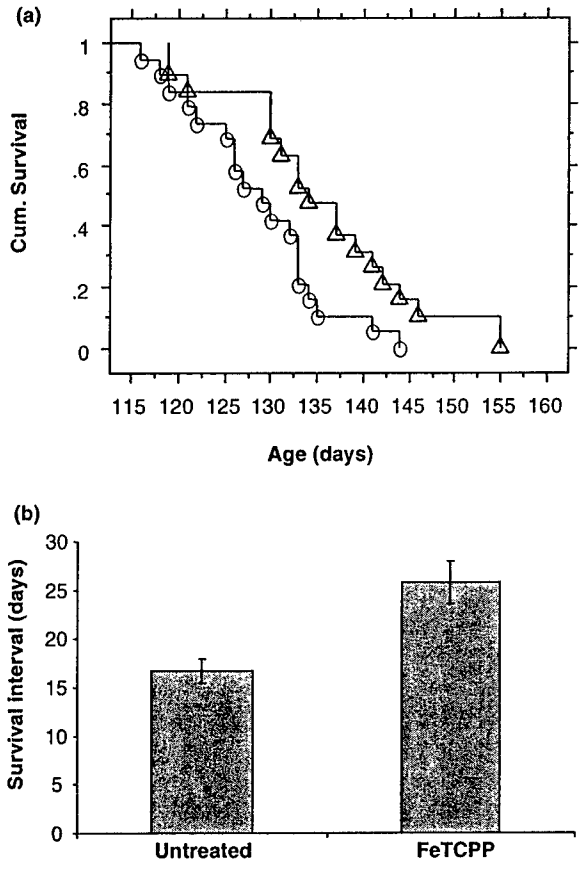

Fig. 3 The effect of FeTCPP treatment on survival in G93A transgenic mice. (a) Cumulative probability of survival for mice treated with either FeTCPP (△) or vehicle (○) beginning at 40 days of age ($n = 19$ per group). There is a significant increase in survival in FeTCPP-treated mice ($p = 0.015$, Mantel–Cox rank test). (b) Survival interval (time from symptom onset to death) for mice treated with FeTCPP or nothing beginning at symptom onset. Survival interval increased from 16.7 ± 1.3 days (mean ± SE) in the untreated group ($n = 7$) to 25.8 ± 2.2 in the FeTCPP-treated group ($n = 9$) ($p = 0.0053$, unpaired *t*-test).

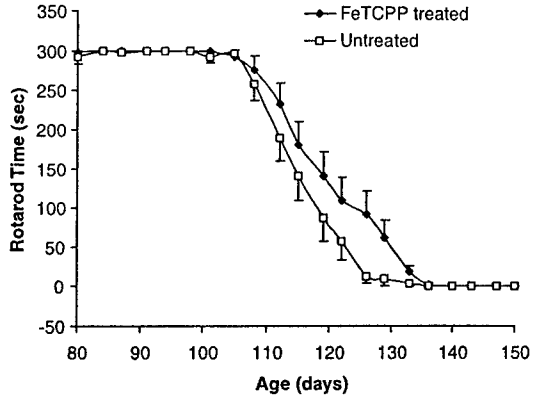

Fig. 4 The effect of FeTCPP treatment on rotarod performance in G93A transgenic mice from 80 days to 150 days of age. There is a significant improved performance in FeTCPP-treated mice ($p = 0.0202$ by repeated measures ANOVA). $n = 19$ per group; □, untreated; ◆, FeTCPP treated.

Motor function (rotarod) and weight

Improved rotarod performance was observed in FeTCPP-treated mice between the ages of 112 and 129 days ($n = 19$/group, $p < 0.03$ by repeated ANOVA measures) (Fig. 4). There was also a trend of attenuated weight loss in the FeTCPP-treated group from the age of 125 days to 140 days compared with the vehicle group (data not shown).

Immunohistological and stereological evaluation

To evaluate whether FeTCPP treatment is efficacious in preventing oxidative damage and neuronal loss within the spinal cord of treated and vehicle G93A mice, equal numbers of females and males were killed by transcardial perfusion at the age of 113 days, and spinal cords were removed ($n = 10$ per group). Four spinal cords from each group were used for immunohistochemistry (Table 1 and Fig. 5) and stereological cell count studies (Table 2), while the remaining spinal cords ($n = 6$ per group) were used to determine indices of oxidative damage (Fig. 6). Immunostaining with malondialdehyde was most robust in neurons of the gray matter, and was more intense in both the gray and white matter of the lumbar spinal cords of the vehicle group, compared with the FeTCPP-treated group (Table 1 and Fig. 5). Malondialdehyde immunostaining from spinal cords of N1029 mice (90 days old, $n = 7$), as a control mouse model for overexpression of the G93A mutant, showed similar intensities to those in the FeTCPP-treated G93A mice (Table 1). The total cell count of neurons in the G93A vehicle group,

Table 1 Relative intensities of malondialdehyde immunoreactivity in the lumbar spinal cord

Animal tag number	Mouse type	Group	Immunostaining intensity
4807	G93A	Vehicle	+++
4802	G93A	Vehicle	+++
4838	G93A	Vehicle	++
4859	G93A	Vehicle	+++
7444	G93A	FeTCPP	+
4885	G93A	FeTCPP	+
4888	G93A	FeTCPP	+
7438	G93A	FeTCPP	++
11121	N1029	Control	+
11123	N1029	Control	+
11117	N1029	Control	+
11115	N1029	Control	+
11124	N1029	Control	+
11116	N1029	Control	+

the G93A FeTCPP-treated group and the N1029 control group were 225.3 ± 30, 318.3 ± 26 and 350.5 ± 16 (mean ± SE), respectively ($n = 4$ per group, Table 2).

Oxidative damage assessment

Oxidative damage was assessed by measuring total protein carbonyls from spinal cords of both untreated and treated groups ($n = 6$ per group) at the age of 113 days. Western blot immunoassay (Fig. 6a) for protein-bound carbonyl groups in spinal cords showed bands from 220 to 21 kDa, with 21 kDa corresponding to the molecular weight of SOD1 subunit under these conditions. Quantification of protein carbonyl content by optical density measurement showed a significant decrease in total protein carbonyls in the treated mice, 138.2 ± 7.0 and 163.5 ± 7.8 (mean of arbitrary unit ± SE) in the FeTCPP-treated and vehicle groups, respectively ($p < 0.05$ by unpaired t-test) (Fig. 6b).

Discussion

These results demonstrate that FeTCPP administration to transgenic G93A ALS mice prior to disease onset increases survival by an average of 7 days. However, it is rarely possible to initiate therapy in humans prior to disease onset because most cases of ALS cannot be predicted. It is therefore encouraging to find that a significant survival effect (9 days) can be obtained even when drug treatment is initiated at the onset of symptoms. FeTCPP was well tolerated at the dose of 1 mg/kg. Some mice showed better improvement than others, which could be caused by different responses to the drug and/or to differences in drug uptake into the CNS. In that regard, we have determined that the pK_a for the four ionizable carboxylic acid groups of FeTCPP is

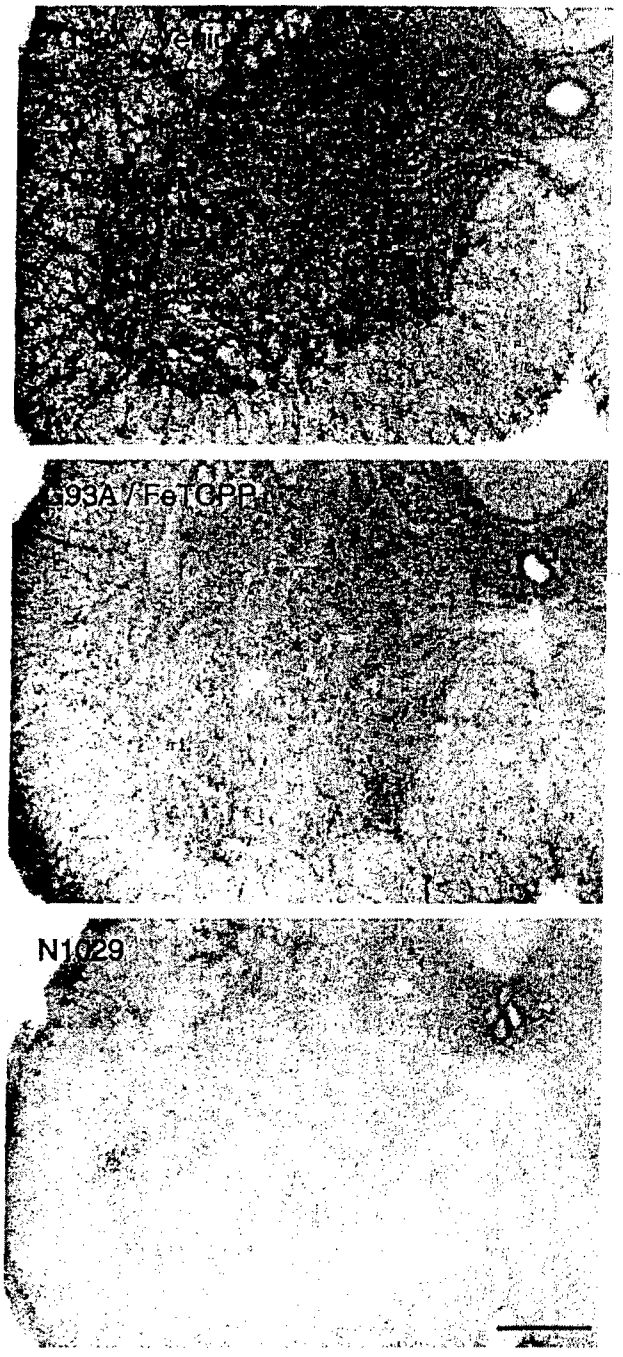

Fig. 5 Malondialdehyde immunostained sections through the ventral horn of the lumbar spinal cord in a G93A/vehicle mouse (top), a G93A/FeTCPP mouse (middle) and a N1029 mouse. A marked reduction of malondialdehyde immunoreactivity occurs in both the gray and white matter of the lumbar spinal cord from the FeTCPP-treated mouse. Scale bar = 200 μm.

6.42. This means that 9% of an administered dose of FeTCPP remains unionized at physiological pH and is therefore much more likely to cross the blood–brain barrier. The unusually high pKa for FeTCPP may help explain why FeTCPP gained

Table 2 Neuronal counts per six 50-μm lumbar spinal cord sections

	Small	Medium	Large	Total
G93A/vehicle mice	142.5 ± 25	74.8 ± 5	8 ± 2	225.3 ± 30*
G93A/FeTCPP mice	205 ± 17	103.8 ± 19	9.5 ± 3	318.3 ± 26#
N1029 mice	188.5 ± 6	136.8 ± 13	25.3 ± 3	350.5 ± 16

Total number and size distribution of neurons per six sections (50-μm thick) through the lumbar spinal cord are expressed as mean ± SEM. *$p < 0.01$ compared with N1029 mice, #$p < 0.05$ compared with G93A/vehicle mice by ANOVA *post-hoc* test.

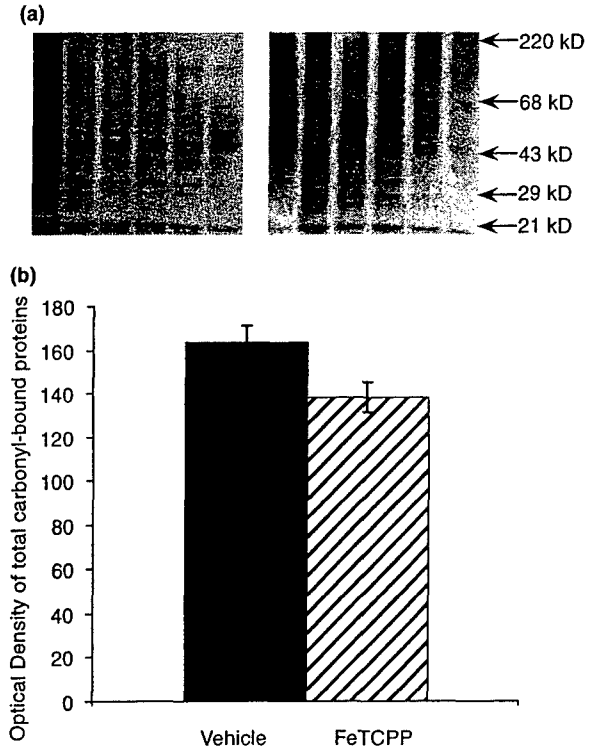

Fig. 6 (a) Western blot immunoassay for protein-bound carbonyl groups in spinal cords from G93A transgenic mice, comparing levels of carbonyl content at the age of 113 days. Total protein (15 μg) from half the spinal cord was treated with dinitrophenylhydrazine (DNPH)-derivatization solution and immunoblotted; proteins were visualized by enhanced chemiluminescence. For each blot, the first three lanes are from the vehicle group and lanes 4, 5 and 6 are from the FeTCPP-treated group. Molecular weights of the proteins are from 220 to 21 kDa, while 21 kDa corresponds to the molecular weight of SOD1. (b) Total protein carbonyl measurements of G93A mice. The optical density of total carbonyl-bound proteins from the vehicle group, indicated by the solid bar, is 163.5 ± 7.8 (mean ± SE). The optical density of total carbonyl-bound proteins from the FeTCPP-treated group, indicated by the shaded bar, is 138.2 ± 7.0 (mean ± SE). There is a significant difference in total carbonyl-bound proteins between the treated mice and the untreated ones ($p = 0.0368$ by unpaired *t*-test).

access to the CNS. We found that FeTCPP did cross the blood–brain barrier and achieved low μm concentrations in the brain and spinal cord.

We saw no indication that early administration of FeTCPP delayed the onset of disease as measured by onset of deficits in rotarod performance. However, we observed that mice in the early FeTCPP treatment group maintained their rotarod performances better than the vehicle group. These results suggest that FeTCPP extended survival in our G93A transgenic mice by slowing the progression of the disease. The fact that early administration showed no benefit on survival over treatment at disease onset suggests that FeTCPP may have its effect after disease onset.

Immunostaining for malondialdehyde of the lumbar region of spinal cords showed more intense immunoreactivity in untreated mice than in FeTCPP-treated mice. Protein carbonyl content, an indicator of protein oxidation, was significantly lower in the FeTCPP-treated group. Neuronal counting in the spinal cords showed a neuroprotective effect exerted by FeTCPP treatment.

Based on previous studies, oxidative damage may play a role in the pathogenesis of ALS (Ferrante *et al.* 1997a; Andrus *et al.* 1998; Bogdanov *et al.* 1998; Hall *et al.* 1998; Liu *et al.* 1998). We found significant increases in concentrations of 3-nitrotyrosine, a marker of peroxynitrite-mediated nitration, in the spinal cord and cerebral cortex of G93A transgenic mice (Ferrante *et al.* 1997b) as well as in the spinal cord of ALS patients (Beal *et al.* 1997). This supports the possibility that iron porphyrins could prevent oxidative damage by acting as catalytic scavengers of peroxynitrite, although other non-oxidant-related drug mechanisms are certainly possible. The above approach was not possible in the current study due to the large amounts of tissue required. In this study, extension of the life span, improved motor performance, reduced malondialdehyde immunostaining and decreased protein oxidation in G93A transgenic mice provide strong evidence that oxidative stress contributes to disease pathogenesis. Other catalytic antioxidants such as EUK-8 and EUK-134 have also been reported to reduce levels of oxidative stress and prolong survival (Jung *et al.* 2001). In another recent study, metalloporphyrin catalytic antioxidants exerted neuroprotective effects against focal ischemic insults by decreasing post-ischemic superoxide-dependent oxidative stress (Mackensen *et al.* 2001).

In addition to the theory that peroxynitrite-mediated nitration may be involved in oxidative damage, another mechanism has been proposed, namely that increased

peroxidase activity of mutant SOD1 oxidizes other cellular constituents via copper-mediated production of hydroxyl radical. Polyamine-modified catalase, an antioxidant enzyme that catalyzes the decomposition of hydrogen peroxide, delayed the onset of the disease and increased survival (Poduslo *et al.* 2000), presumably by eliminating the substrate for peroxidase activity. Other studies support a possible linkage between oxidative injury and excitotoxicity in ALS. For example, riluzole and gabapentin, both putative inhibitors of the glutamatergic system, prolonged survival in G93A transgenic mice (Gurney *et al.* 1996) while carboxyfullerenes, a class of antioxidants that can also block N-methyl-D-aspartate (NMDA) receptor-mediated excitotoxicity, delayed both the onset of symptoms and death (Dugan *et al.* 1997). Minocycline, which has effects both in blocking inflammatory pathways and on release of mitochondrial proteins that trigger apoptosis, is also effective in transgenic mouse models of ALS (Zhu *et al.* 2002). Non-oxidant mechanisms such as protein aggregation (Cleveland and Liu 2000) have also been implicated in motor neuron disease in transgenic mice. One common pathological hallmark in ALS and motor neuron disease in mice is mitochondrial dysfunction (Menzies *et al.* 2002). This observation indirectly supports an oxidative hypothesis, given that mitochondria are a primary source of oxygen radicals even under normal physiological conditions. Our previous study of creatine administration, which increases brain phosphocreatine concentration and may inhibit opening of the mitochondrial transition pore, showed improved motor performance and a 17% extension of life span (Klivenyi *et al.* 1999). Furthermore, it has recently been firmly established that SOD1 is present in mitochondria (Higgins *et al.* 2002; Mattiazzi *et al.* 2002), which was unknown when SOD1 mutations were first identified in familial ALS. Potentially important differences between the cytosolic and mitochondrial pools of SOD1, including how the latter obtains copper and zinc, are largely unexplored. Because abnormalities in mitochondrial morphology and function occur as a prelude to motor neuron death, it is intriguing to speculate that SOD1 within the mitochondria may be the critical pool relevant to ALS. It has also been shown in neuroblastoma cells that the entry of SOD1 into mitochondria depends on demetallation, and that heat-shock proteins (Hsp70, Hsp27 or Hsp25) block the uptake of mutant SOD1 (G37R, G41D or G93A) while having no effect on wild-type SOD1. Therefore, it was proposed that binding heat-shock proteins to mutant SOD1 might make them unavailable for their anti-apoptotic functions and ultimately lead to motor neuron death (Okado-Matsumoto and Fridovich 2002).

Due to the involvement of multiple pathways in ALS, it may be possible to produce more effective neuroprotection and survival effects by therapeutic strategies utilizing combinations of two or more therapeutic agents thought to work by different mechanisms, such as FeTCPP with carboxyfullerene or creatine; these combinations, in theory, should yield greater overall survival.

Acknowledgements

This work was supported by ALS Association and NIA grant AG 12992, and the NINDS division of NIH (grants R29 NS35871 and R01 NS40819 [JPC]). We wish to thank Dr Michael Lin for helpful discussion and Dr Feng Li for western blot technical assistance. We also wish to thank Julie Lynch, CVT (Crow Laboratory), for technical support and extraordinary efforts in caring for partially paralyzed mice.

References

Andrus P. K., Fleck T. J., Gurney M. E. and Hall E. D. (1998) Protein oxidative damage in a transgenic mouse model of familial amyotrophic lateral sclerosis. *J. Neurochem.* **71**, 2041–2048.

Batinic-Haberle I., Benov L., Spasojevic I. and Fridovich I. (1998) The ortho effect makes manganese (III) meso-tetrakis (N-methylpyridinium-2-yl) porphyrin a powerful and potentially useful superoxide dismutase mimic. *J. Biol. Chem.* **273**, 24521–24528.

Beal M. F., Ferrante R. J., Browne S. E., Matthews R. T., Kowall N. W. and Brown R. H. Jr (1997) Increased 3-nitrotyrosine in both sporadic and familial amyotrophic lateral sclerosis. *Ann. Neurol.* **42**, 644–654.

Beauchamp C. and Fridovich I. (1971) Superoxide dismutase: improved assays and an assay applicable to acrylamide gels. *Anal. Biochem.* **44**, 276–287.

Beckman J. S., Carson M., Smith C. D. and Koppenol W. H. (1993) ALS, SOD and peroxynitrite. *Nature* **364**, 584.

Benov L. and Fridovich I. (1995) A superoxide dismutase mimic protects sodA sodB *Escherichia coli* against aerobic heating and stationary-phase death. *Arch. Biochem. Biophys.* **322**, 291–294.

Bogdanov M. B., Ramos L. E., Xu Z. and Beal M. F. (1998) Elevated 'hydroxyl radical' generation in vivo in an animal model of amyotrophic lateral sclerosis. *J. Neurochem.* **71**, 1321–1324.

Cleveland D. W. and Liu J. (2000) Oxidation versus aggregation – how do SOD1 mutants cause ALS? *Nat. Med.* **6**, 1320–1321.

Cookson M. R. and Shaw P. J. (1999) Oxidative stress and motor neurone disease. *Brain Pathol.* **9**, 165–186.

Crow J. P. (1999) Manganese and iron porphyrins catalyze peroxynitrite decomposition and simultaneously increase nitration and oxidant yield: implications for their use as peroxynitrite scavengers in vivo. *Arch. Biochem. Biophys.* **371**, 41–52.

Crow J. P. (2000) Peroxynitrite scavenging by metalloporphyrins and thiolates. *Free Radic. Biol. Med.* **28**, 1487–1494.

Crow J. P., Sampson J. B., Zhuang Y., Thompson J. A. and Beckman J. S. (1997) Decreased zinc affinity of amyotrophic lateral sclerosis-associated superoxide dismutase mutants leads to enhanced catalysis of tyrosine nitration by peroxynitrite. *J. Neurochem.* **69**, 1936–1944.

Cuzzocrea S., Zingarelli B., Costantino G. and Caputi A. P. (1999) Beneficial effects of Mn (III) tetrakis (4-benzoic acid) porphyrin (MnTBAP), a superoxide dismutase mimetic, in carrageenan-induced pleurisy. *Free Radic. Biol. Med.* **26**, 25–33.

Day B. J. and Crapo J. D. (1996) A metalloporphyrin superoxide dismutase mimetic protects against paraquat-induced lung injury in vivo. *Toxicol. Appl. Pharmacol.* **140**, 94–100.

Deng H. X., Hentati A., Tainer J. A., Iqbal Z., Cayabyab A., Hung W. Y., Getzoff E. D., Hu P., Herzfeldt B., Roos R. P. *et al.* (1993)

Amyotrophic lateral sclerosis and structural defects in Cu,Zn superoxide dismutase. *Science* **261**, 1047–1051.

Dugan L. L., Du Turetsky D. M. C., Lobner D., Wheeler M., Almli C. R., Shen C. K., Luh T. Y., Choi D. W. and Lin T. S. (1997) Carboxyfullerenes as neuroprotective agents. *Proc. Natl Acad. Sci. USA* **94**, 9434–9439.

Estevez A. G., Crow J. P., Sampson J. B., Reiter C., Zhuang Y., Richardson G. J., Tarpey M. M., Barbeito L. and Beckman J. S. (1999) Induction of nitric oxide-dependent apoptosis in motor neurons by zinc-deficient superoxide dismutase. *Science* **286**, 2498–2500.

Faulkner K. M., Liochev S. I. and Fridovich I. (1994) Stable Mn (III) porphyrins mimic superoxide dismutase in vitro and substitute for it in vivo. *J. Biol. Chem.* **269**, 23471–23476.

Ferrante R. J., Browne S. E., Shinobu L. A., Bowling A. C., Baik M. J., MacGarvey U., Kowall N. W., Brown R. H. Jr and Beal M. F. (1997a) Evidence of increased oxidative damage in both sporadic and familial amyotrophic lateral sclerosis. *J. Neurochem.* **69**, 2064–2074.

Ferrante R. J., Shinobu L. A., Schulz J. B., Matthews R. T., Thomas C. E., Kowall N. W., Gurney M. E. and Beal M. F. (1997b) Increased 3-nitrotyrosine and oxidative damage in mice with a human copper/zinc superoxide dismutase mutation. *Ann. Neurol.* **42**, 326–334.

Ferrer-Sueta G., Batinic-Haberle I., Spasojevic I., Fridovich I. and Radi R. (1999) Catalytic scavenging of peroxynitrite by isomeric Mn (III) N-methylpyridylporphyrins in the presence of reductants. *Chem. Res. Toxicol.* **12**, 442–449.

Goto J. J., Zhu H., Sanchez R. J., Nersissian A., Gralla E. B., Valentine J. S. and Cabelli D. E. (2000) Loss of in vitro metal ion binding specificity in mutant copper-zinc superoxide dismutases associated with familial amyotrophic lateral sclerosis. *J. Biol. Chem.* **275**, 1007–1014.

Gurney M. E., Pu H., Chiu A. Y., Dal Canto M. C., Polchow C. Y., Alexander D. D., Caliendo J., Hentati A., Kwon Y. W., Deng H. X. *et al.* (1994) Motor neuron degeneration in mice that express a human Cu,Zn superoxide dismutase mutation. *Science* **264**, 1772–1775.

Gurney M. E., Cutting F. B., Zhai P., Doble A., Taylor C. P., Andrus P. K. and Hall E. D. (1996) Benefit of vitamin E, riluzole, and gabapentin in a transgenic model of familial amyotrophic lateral sclerosis. *Ann. Neurol.* **39**, 147–157.

Hall E. D., Andrus P. K., Oostveen J. A., Fleck T. J. and Gurney M. E. (1998) Relationship of oxygen radical-induced lipid peroxidative damage to disease onset and progression in a transgenic model of familial ALS. *J. Neurosci. Res.* **53**, 66–77.

Higgins C. M., Jung C., Ding H. and Xu Z. (2002) Mutant Cu, Zn superoxide dismutase that causes motoneuron degeneration is present in mitochondria in the CNS. *J. Neurosci.* **22**, RC215.

Hsu S. M., Raine L. and Fanger H. (1981) Use of avidin-biotin-peroxidase complex (ABC) in immunoperoxidase techniques: a comparison between ABC and unlabeled antibody (PAP) procedures. *J. Histochem. Cytochem.* **29**, 577–580.

Jung C., Rong Y., Doctrow S., Baudry M., Malfroy B. and Xu Z. (2001) Synthetic superoxide dismutase/catalase mimetics reduce oxidative stress and prolong survival in a mouse amyotrophic lateral sclerosis model. *Neurosci. Lett.* **304**, 157–160.

Klivenyi P., Ferrante R. J., Matthews R. T., Bogdanov M. B., Klein A. M., Andreassen O. A., Mueller G., Wermer M., Kaddurah-Daouk R. and Beal M. F. (1999) Neuroprotective effects of creatine in a transgenic animal model of amyotrophic lateral sclerosis. *Nat. Med.* **5**, 347–350.

Lee J. B., Hunt J. A. and Groves J. T. (1997) Rapid decomposition of peroxynitrite by manganese porphyrin-antioxidant redox couples. *Bioorg. Med. Chem. Lett.* **7**, 2913–2918.

Lee J. B., Hunt J. A. and Groves J. T. (1998) Manganese porphyrins as redox-coupled peroxynitrite reductases. *J. Am. Chem. Soc.* **120**, 6053–6061.

Liochev S. I. and Fridovich I. (1995) A cationic manganic porphyrin inhibits uptake of paraquat by *Escherichia coli*. *Arch. Biochem. Biophys.* **321**, 271–275.

Liu R., Althaus J. S., Ellerbrock B. R., Becker D. A. and Gurney M. E. (1998) Enhanced oxygen radical production in a transgenic mouse model of familial amyotrophic lateral sclerosis. *Ann. Neurol.* **44**, 763–770.

Mackensen G. B., Patel M., Sheng H., Calvi C. L., Batinic-Haberle I., Day B. J., Liang L. P., Fridovich I., Crapo J. D., Pearlstein R. D. *et al.* (2001) Neuroprotection from delayed postischemic administration of a metalloporphyrin catalytic antioxidant. *J. Neurosci.* **21**, 4582–4592.

Mattiazzi M., D'Aurelio M., Gajewski C. D., Martushova K., Kiaei M., Beal M. F. and Manfredi G. (2002) Mutated human SOD1 causes dysfunction of oxidative phosphorylation in mitochondria of transgenic mice. *J. Biol. Chem.* **5**, 5.

Menzies F. M., Ince P. G. and Shaw P. J. (2002) Mitochondrial involvement in amyotrophic lateral sclerosis. *Neurochem. Int.* **40**, 543–551.

Okado-Matsumoto A. and Fridovich I. (2002) Amyotrophic lateral sclerosis: a proposed mechanism. *Proc. Natl Acad. Sci. USA* **11**, 11.

Patel M. and Day B. J. (1999) Metalloporphyrin class of therapeutic catalytic antioxidants. *Trends Pharmacol. Sci.* **20**, 359–364.

Poduslo J. F., Whelan S. L., Curran G. L. and Wengenack T. M. (2000) Therapeutic benefit of polyamine-modified catalase as a scavenger of hydrogen peroxide and nitric oxide in familial amyotrophic lateral sclerosis transgenics. *Ann. Neurol.* **48**, 943–947.

Rosen D. R., Siddique T., Patterson D., Figlewicz D. A., Sapp P., Hentati A., Donaldson D., Goto J., O'Regan J. P., Deng H. X. *et al.* (1993) Mutations in Cu/Zn superoxide dismutase gene are associated with familial amyotrophic lateral sclerosis. *Nature* **362**, 59–62.

Subramaniam J. R., Lyons W. E., Liu J., Bartnikas T. B., Rothstein J., Price D. L., Cleveland D. W., Gitlin J. D. and Wong P. C. (2002) Mutant SOD1 causes motor neuron disease independent of copper chaperone-mediated copper loading. *Nat. Neurosci.* **5**, 301–307.

Szabo C. (1998) Potential role of the peroxynitrate-poly (ADP-ribose) synthetase pathway in a rat model of severe hemorrhagic shock. *Shock* **9**, 341–344.

Wiedau-Pazos M., Goto J. J., Rabizadeh S., Gralla E. B., Roe J. A., Lee M. K., Valentine J. S. and Bredesen D. E. (1996) Altered reactivity of superoxide dismutase in familial amyotrophic lateral sclerosis. *Science* **271**, 515–518.

Zhu S., Stavrovskaya I. G., Drozda M., Kim B. Y., Ona V., Li M., Sarang S., Liu A. S., Hartley D. M., Wu du C. *et al.* (2002) Minocycline inhibits cytochrome c release and delays progression of amyotrophic lateral sclerosis in mice. *Nature* **417**, 74–78.

Zingarelli B., Day B. J., Crapo J. D., Salzman A. L. and Szabo C. (1997) The potential role of peroxynitrite in the vascular contractile and cellular energetic failure in endotoxic shock. *Br. J. Pharmacol.* **120**, 259–267.

APPENDIX 9

TOXIN-INDUCED MITOCHONDRIAL DYSFUNCTION

Susan E. Browne[1] and M. Flint Beal

Department of Neurology and Neuroscience
Weill Medical College of Cornell University
New York, New York 10021

I. Introduction

Mitochondria constitute the cellular powerhouse in the body, providing the bulk of energy generated from aerobic catabolism, and are therefore critical for maintaining cellular function and homeostasis. Within the CNS, where functional activity depends entirely on oxidative glucose metabolism under normal conditions, the mitochondria represent not only a fundamental organelle for neuronal and glial function, but also a target for damage within cells with potentially catastrophic consequences for the cell, organ, and organism.

Mitochondrial dysfunction is well characterized in a number of human disorders, sometimes stemming from inherited or spontaneous mitochondrial or nuclear DNA mutations, from disease related perturbations in

[1]To whom correspondence should be addressed.

0074-7742/02 $35.00

cell homeostasis, or alternatively from direct damage arising from extrinsic sources. Mitochondrial toxins play important roles in the study of mitochondrial function and dysfunction. They not only serve as useful tools for the study of mechanistic pathways involved in mitochondrial damage, consequences on cellular function, and for assays of putative neuroprotective therapies, but in some cases they may also be directly involved in the pathogenesis of mitochondrial disorders in humans. Here we review the mode of action of several well characterized mitochondrial toxins, and, where relevant, contrast their effects with mechanisms of cell death in various degenerative disorders. The majority of known toxins specifically target components of mitochondrial metabolic pathways. Here we have grouped toxic agents in terms of their principal target site within the mitochondria, often reflecting effects on components of the mitochondrial respiratory system. In several cases, however, these agents have multiple sites of action due to their affinity for certain chemical moieties present in multiple mitochondrial proteins, demonstrated by cyanide's propensity for Fe^{3+} containing enzymes which include both complexes II and IV of the electron transport chain.

II. Inhibitors of Mitochondrial Complex I: NADH Ubiquinine Oxidoreductase

A. MPTP/MPP$^+$

1-Methyl-4-phenyl-1,2,3,6-tetrahydropyridine (MPTP) intoxication in humans, nonhuman primates, and rodents induces a motor disorder clinically and pathologically mimicking Parkinson's disease (PD), due to direct actions on mitochondrial function via complex I inhibition (Gerlach and Riederer, 1996; Olanow and Tatton, 1999; Blum *et al.*, 2001). Interestingly, the pathophysiological effects of MPTP only came to light as a result of poor chemistry in the illicit drug trade. In 1978–1982 several heroin addicts in California developed multiple irreversible, L-DOPA-responsive [DOPA: 3-(3,4-dihydroxyphenyl)alanine] PD symptoms as a result of self-administration of a synthetic fentanyl heroin derivative (Davis *et al.*, 1979). The cause was found to be a slight contamination (~3%) with MPTP, a by-product generated accidentally during the synthetic process (Langston *et al.*, 1983).

The toxicity of MPTP is actually conferred by its metabolite 1-methyl-4-phenylpyridinium ion, MPP$^+$, which accumulates in mitochondria selectively within dopaminergic neurons in the CNS. The cascade of cell-damaging events caused by MPP$^+$ appears to be triggered by its potent inhibition of complex I activity, resulting in deficient oxidation of NAD$^+$ substrates,

impaired α-ketoglutarate dehydrogenase activity, and subsequent disruption of the respiratory electron transport chain (Niklas *et al.*, 1985; Mizuno *et al.*, 1989; Sayre, 1989). Reduced oxidative phosphorylation and ATP synthesis ensue, along with disruption of the mitochondrial membrane potential. The finding that MPTP induces a complex I inhibition associated with a PD-like phenotype is in keeping with multiple reports from studies in PD postmortem brain tissue, platelets, and cybrid cell lines that a mitochondrial deficiency of complex I activity underlies the pathogenesis of PD (Parker *et al.*, 1989; Menegon *et al.*, 1998; Swerdlow *et al.*, 1998). The typical symptoms of MPTP/MPP^+ intoxication—rigidity, akinesia, resting tremor, posture, and gait abnormalities—stem from the specific cellular localization of MPP^+'s toxicity within the CNS. The MPTP causes dopamine depletion in the neostriatum due to selective loss of dopaminergic neurons in the substantia nigra that mimics the pathology seen in PD (Burns *et al.*, 1983; Beal, 2001). In primates treated with MPTP, neurons within the substantia nigra *pars compacta* (SN*pc*) and the locus coeruleus are particularly vulnerable, while neurons in the ventral tegmental area (a dopamine nucleus projecting predominantly to the cortex) are relatively resistant. Chronic treatment with low doses of MPTP in monkeys preferentially targets dopaminergic terminals in the putamen, similar to the typical pathology seen in PD brain. In fact, a chronic subacute MPTP dosing regimen in animal models appears to recapitulate the slow evolution of parkinsonian traits seen in humans far better than acute dosing paradigms, inducing uneven striatal dopamine fibre loss and more selective depletion of substantia nigra dopamine neurons in primates (Albanese *et al.*, 1993; Varastet *et al.*, 1994). Another valuable model system in primates involves unilateral internal carotid artery infusion of MPTP to induce a hemiparkinsonian state (Bankiewicz *et al.*, 1986). Typical experimental approaches to evaluate the extent of MPTP toxicity include histologic Nissl staining, biochemical assays of regional content of dopamine and its metabolites 3,4-dihydroxyphenylacetic acid (DOPAC) and homovanillic acid (HVA), and immunocytochemical localization of tyrosine hydroxylase activity (the enzyme that catalyzes the conversion of tyrosine to L-DOPA, the rate-limiting step in dopamine synthesis).

The regional and cellular selectivity of MPTP toxicity is conferred by properties of the agent itself. A highly lipophilic molecule, MPTP readily crosses the blood–brain barrier in humans, primates and mice (but not in rats). Within the CNS it is taken up into glial cells, where it is oxidatively deaminated by monoamine oxidase B (MAO_B), first to the unstable intermediate 1-methyl-4-phenyl-2,3-dihydropyridinium ion ($MPDP^+$), and then to MPP^+ (see Fig. 1). The MPP^+ is a polar molecule, and when released from glial cells it is selectively taken up into dopaminergic neuron terminals and cell bodies via the plasma membrane dopamine transporter for which it

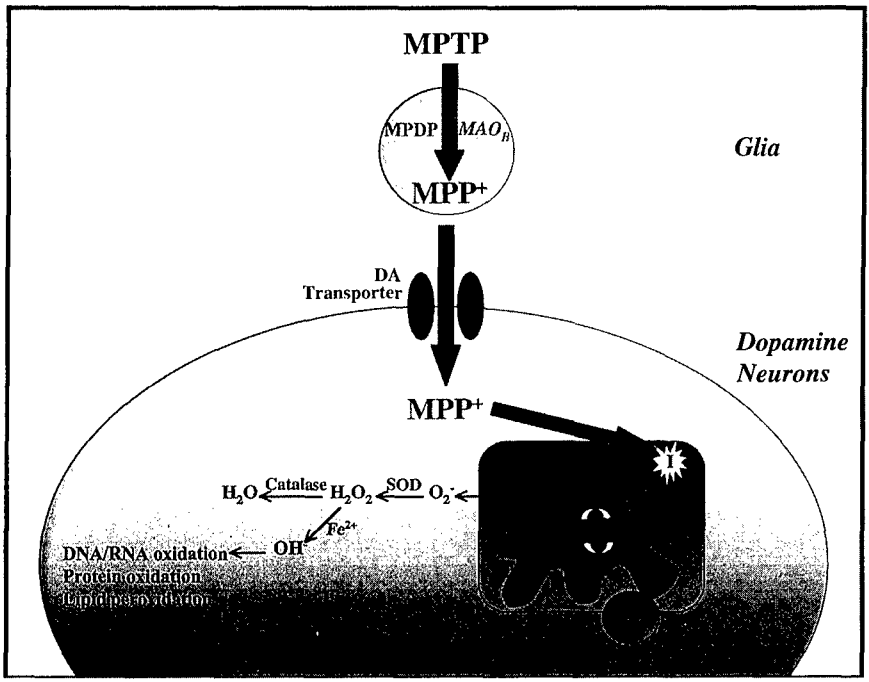

FIG. 1. Dopamine neuron-selective toxicity of MPTP. MPP^+, generated by the catalytic conversion of MPTP in glial cells, is selectively taken up into dopaminergic neurons due to its high affinity for the dopamine transporter. Within cells, MPP^+ is concentrated in mitochondria where it binds to and inhibits activity of complex I ("I"). Increased superoxide radical (O^{2-}), and hydroxyl radical (OH^-) generation may occur as a consequence of the ensuing disruption of the electron transport chain and impaired ATP production. *Abbreviations:* DA, dopamine; MPT, mitochondrial permeability transition; SOD, superoxide dismutase; TCA, tricarboxylic acid cycle.

has high affinity (Irwin and Langston, 1995; Santiago *et al.*, 1996). In neurons, MPP^+ is concentrated within mitochondria via a carrier-independent mechanism, apparently due to its high lipophilicity, where it binds to and irreversibly inhibits complex I at the inner mitochondrial membrane. Both active and passive mechanisms appear to be involved in MPP^+ uptake into mitochondria, but enzyme inhibition appears to depend on steric rather than electrostatic properties of MPP^+, since related isoquinoline derivatives are less potent inhibitors of NADH reductase activity in intact mitochondria (Aiuchi *et al.*, 1995; McNaught *et al.*, 1998). Metabolic inhibition has been shown to precede cell death in *in vitro* assays (Storch *et al.*, 1999). The selective involvement of the dopaminergic system in the motor disorder resulting from MPTP toxicity is reflected by the fact that MPTP-treated primates

show excellent phenotypic responses to treatment with the dopamine precursor L-DOPA, in addition to other dopamine receptor agonists (Treseder *et al.*, 2000; Tahar *et al.*, 2001). Furthermore, lack of the plasma membrane dopamine transporter in knockout mice confers protection against the toxic effects of MPTP (Bezard *et al.*, 1999), as does inhibition of the human dopamine transporter (hDAT), demonstrated using GBR12909 to inhibit dopamine re-uptake in a human embryonic kidney cell line (Storch *et al.*, 1999). The MPP^+ can also be sequestered by the brain vesicular monoamine transporter VMAT2, which uses energy from vesicular proton gradients to pump monoamine neurotransmitters and dopamine neurotoxins from the neuronal cytoplasm into synaptic vesicles. Consequently, VMAT2 function can also affect animals' tolerance to MPP^+. This is demonstrated by the observation that MPTP administration at a dose that reduces tyrosine hydroxylase (TH) immunoreactivity 13% in wild-type mice, was found to decrease SN*pc* TH levels 30% in VMAT2 heterozygous knockout mice (Takahashi *et al.*, 1997).

Indirect evidence that mitochondrial energetic defects underlie MPTP-induced damage comes from findings that pro-energetic agents ameliorate the damaging effects of MPTP, independent of any actions on MPTP metabolism or MPP^+ uptake. One such compound is coenzyme Q_{10}, an essential co-factor for electron transport between complex I and complex III of the electron transport chain, and a potent antioxidant in mitochondria. Coenzyme Q_{10} markedly reduces indices of MPTP damage in aged mice (Beal *et al.*, 1997; Shults *et al.*, 1997; Ebadi *et al.*, 2001). Another pro-energy agent is creatine, which putatively acts by increasing cytosolic energy stores. Creatine treatment results in increased brain levels of the high-energy substrate phosphocreatine, and has also been suggested to modulate toxicity via inhibitory effects on the mitochondrial permeability transition. Chronic oral creatine administration dose dependently protects against MPTP-induced neuronal damage in animal models, with optimal effects at a concentration of 2% creatine in the diet (Matthews *et al.*, 1999). Another protective agent is acetyl-L-carnitine, involved in fatty acid oxidation in mitochondria and responsible for transporting accumulated acyl groups out of mitochondria, which protects against MPTP-induced parkinsonism in primates (Bodis-Wollner *et al.*, 1991). Disruption of mitochondrial energy production also can instigate excitotoxic cascades within cells (Steiner *et al.*, 1997). To explain briefly: reduced ATP generation will disrupt vital ATPase pump activities and reduce the cell membrane potential. If extensive enough, this may facilitate membrane depolarization and activation of glutamate receptor subtypes (notably N-methyl-D-aspartate, NMDA) by normally inert extracellular levels of the excitatory neurotransmitter glutamate (Novelli *et al.*, 1988; Zeevalk and Niklas, 1991). The consequent cellular influx of calcium

may be sufficient to stimulate free radical generation and induce oxidative damage (Albin and Greenamyre, 1992; Beal, 2000). The involvement of this secondary excitotoxic phenomenon in MPTP toxicity is supported by observations that glutamate receptor antagonists, including the NMDA antagonist MK-801, protect against MPTP toxicity in mice (Brouillet and Beal, 1993), while the glutamate release inhibitor riluzole is partially protective in both mice and primates (Boireau *et al.*, 1994; Benazzouz *et al.*, 1995). In addition, the dopamine D2 receptor agonists bromocriptine and pramipexole, which also have antioxidant activity, attenuate MPTP-induced dopamine depletion (Muralikrishnan and Mohanakumar, 1998; Zou *et al.*, 2000).

Increased free radical generation and breakdown in calcium homeostasis also occur following MPTP administration, putatively as a direct consequence of the energetic disturbance induced by MPTP/MPP^+ (although the mitochondrial source of free radical generation has yet to be unequivically proven) (Di Monte *et al.*, 1986; Rossetti *et al.*, 1988; Tipton and Singer, 1993). Mitochondrial MPP^+ accumulation can lead to increased nitric oxide (NO) generation, which may exacerbate cellular damage by reacting with superoxide anion (O^{2-}) to generate the reactive free radical peroxynitrite (Beckman, 1996; Matthews *et al.*, 1997; Przedborski and Jackson-Lewis, 1998). In support of this hypothesis, the involvement of peroxynitrite in MPTP-mediated damage has been demonstrated in both primates and mice by findings of increased 3-nitrotyrosine immunoreactivity following MPTP administration (Schulz *et al.*, 1995a; Pennathur *et al.*, 1999). This observation is reminiscent of similar alterations reported in PD brain (Good *et al.*, 1998). In addition, MPTP toxicity is ameliorated in mice lacking the neuronal isoform of NO synthase (nNOS), or by treatment with nNOS inhibitors (Schulz *et al.*, 1995b; Hantraye *et al.*, 1996; Klivenyi *et al.*, 2000a). Mice that lack the inducible form of NOS (iNOS) also appear to be resistant to the toxin, but protection is confined to dopaminergic neuron cell bodies and not terminals (Liberatore *et al.*, 1999; Dehmer *et al.*, 2000). The importance of oxidative damage to the etiology of MPTP-mediated damage is further exemplified by the demonstration that its toxicity in mouse brain is significantly attenuated when free-radical scavenging enzymes, including Cu/Zn-superoxide dismutase (SOD1) and MnSOD (SOD2), are overexpressed (Przedborski *et al.*, 1992; Klivenyi *et al.*, 1998a). In contrast, mice deficient in certain free-radical scavenging enzymes including glutathione peroxidase, SOD1 and SOD2, show exacerbated MPTP-mediated damage (Wüllner *et al.*, 1996; Andreassen *et al.*, 2001). Further, ebselen, a glutathione peroxidase analogue, prevents both neuronal loss and clinical symptoms produced by MPTP in primates (Moussaoui *et al.*, 2000), and several free-radical spin traps and scavengers including erythropoietin and 17-oestradiol show neuroprotective effects in mice (Matthews *et al.*, 1999; Callier *et al.*,

2000; Genc *et al.,* 2001). An involvement of oxidative damage to DNA is also implied by findings that inhibiting or knocking-out poly-ADP-ribose polymerase (PARP), an enzyme involved in DNA repair that is activated by oxidative damage, significantly attenuates MPTP neurotoxicity in mice (Cosi and Marien, 1998). This is of particular interest since activation of poly-ADP-ribose polymerase could itself be deleterious to cells under conditions of MPTP-induced oxidative stress, since enzyme activation depletes cellular ATP and NAD^+ stores, potentially exacerbating the energetic dysfunction triggered by MPTP. These *in vivo* observations are supported by numerous *in vitro* studies demonstrating increased generation of reactive oxygen species following MPTP administration to cell lines (Kitamura *et al.,* 1998). Interestingly, MPTP administration to striatal synaptosomes has also been reported to reduce cellular levels of the antioxidant glutathione in this preparation (Desole *et al.,* 1993). However, Seyfried and colleagues (2000) demonstrated in PC12 cells that this is a biphasic dose-dependent effect of MPP^+, since low doses (250 μM) markedly increased cellular levels of glutathione (reduced form, GSH) while ten fold higher doses decreased GSH content and increased levels of the oxidized form (GSSG), apparently due to a redox shift in cells that enhanced glutathione oxidation.

Another characteristic of PD is the deposition of Lewy bodies in affected brain regions. These dense fibrillary structures contain proteins including α-synuclein and ubiquitin. Neuronal inclusions containing α-synuclein and ubiquitin, partially resembling Lewy bodies, have been reported in aged primates chronically treated with MPTP (Forno *et al.,* 1986; Kowall *et al.,* 2000), but they do not appear to be a typical feature of MPTP toxicity. However, MPTP does increase α-synuclein expression in both mice and primates (Kowall *et al.,* 2000; Vila *et al.,* 2000), a capability linked with the formation of neuronal inclusions, mitochondrial morphological abnormalities, mitochondrial dysfunction, and increased free-radical production in experiments overexpressing α-synuclein in a hypothalamic neuronal cell line (Hsu *et al.,* 2000). Furthermore, MPTP induces nitration of α-synuclein in mice, reminiscent of the α-synuclein nitration seen in PD brain (Giasson *et al.,* 2000; Przedborski *et al.,* 2001). In addition, expression of mutant α-synuclein in NT2/D1 cells is associated with increased markers of oxidative damage and increased susceptibility to cell death in response to H_2O_2 or MPP^+ exposure (Lee *et al.,* 2001). These findings therefore provide a potential link between the mitochondrial dysfunction and oxidative damage evident following MPTP exposure and the deposition of α-synuclein, which is a typical feature of PD pathology.

In addition to direct mitochondrial toxicity, it should be noted that cellular damage mechanisms originating outside the mitochondria have also been implicated in the etiology of MPTP/MPP^+damage (Khan *et al.,* 1997;

Przedborski and Jackson-Lewis, 1998). Notably, Przedborski and Jackson-Lewis (1998) demonstrated that rho zero cells devoid of an electron transport system are still sensitive to MPP^+ toxicity. Other pathogenic pathways include apoptotic processes, which may involve either mitochondrial and/or extramitochondrial components (reviewed by Nicotra and Parvez, 2000). Interestingly, the MPTP dosing regimen used in experimental models largely dictates whether cells follow apoptotic or necrotic pathways to death. In mice, a subacute dosing regime of MPTP daily over five days was found to induce cell death with terminal deoxynucleotidyl transferase (TUNEL) labeling and chromatin clumping typical of apoptosis (Tatton and Kish, 1997). This is consistent with reports of apoptotic markers in PD brain, including increased caspase-3 and Bax immunoreactivity, TUNEL staining, and chromatin condensation in melanin-containing nigral neurons (Hartmann *et al.*, 2000; Tatton, 2000). Several groups have shown that mice overexpressing Bcl-2 are partially protected against MPTP following an acute dosing paradigm, but to a lesser extent after chronic dosing over five days (Offen *et al.*, 1998; Yang *et al.*, 1998). Similarly, mice with a dominant-negative inhibition of caspase-1 are protected against MPTP, as are mice deficient in the pro-apoptotic protein Bax (Klivenyi *et al.*, 1999; Vila *et al.*, 2001). Further, adenoviral administration of a caspase inhibitor XIAP (X-chromosome-linked inhibitor of apoptosis) protects dopaminergic cell bodies but not terminals, while protection can be extended to the terminals when XIAP is given in combination with the growth factor GDNF (glial cell-derived neurotrophic factor) (Eberhardt *et al.*, 2000). The p53 gene, which regulates growth and programmed cell death, also appears to be involved in the pathway of cell death, since p53 knockout mice are resistant to MPTP-induced death of dopamine neurons (Trimmer *et al.*, 1996). Further, involvement of apoptotic processes is suggested by the activation of C-Jun N-terminal kinase (JNK) by MPTP (Saporito *et al.*, 1999, 2000), and the partial protection against MPTP-induced loss of nigral neurons afforded by the anti-apoptotic agent CGP3466 (Waldmeier *et al.*, 2000). MPP^+ exposure has also been shown to upregulate apoptotic markers in a number of different cell types *in vitro,* inducing increased DNA fragmentation and Bcl-2 expression in human neuroblastoma SH-SY5Y cell lines (Itano and Nomura, 1995; Sheehan *et al.*, 1997). The Bcl-2 overexpression has also been found to attenuate MPP^+-mediated damage in a dopaminergic neuronal cell line (Oh *et al.*, 1995). Other evidence of a role for apoptosis include induction of apoptotic markers in ventral rat mesencephalic-striatal cultures, differentiated PC12 cell lines, cerebellar granule neurons (Mochizuki *et al.*, 1994; Mutoh *et al.*, 1994; Du *et al.*, 1997), and inhibition of $p21^{WAF/Cip1}$-mediated cell proliferation by MPTP (Soldner *et al.*, 1999).

Inflammatory processes are also implicated by observations in both humans and in animal models. Neuropathological studies in three patients

3–16 years after exposure to MPTP showed clustering of microglia around neurons along with active ongoing cell loss in the subatantia nigra (Langston *et al.*, 1999). Similarly, both activated microglia and lymphocytes are evident in mice after MPTP administration, and inhibition of either cyclooxygenase-1 or -2 are markedly neuroprotective (selective inhibition of cyclooxygenase-2 by meloxicam; or both cyclooxygenase-1 and -2 by acetylsalicylic acid) (Kurkowska-Jastrzebska *et al.*, 1999; Teismann and Ferger, 2001). Deficiency in cytoplasmic phospholipase A2 is also protective against MPTP toxicity, putatively due to blockade of production of the substrate for cyclooxygenase-2 (Klivenyi *et al.*, 1998b), as is the anti-inflammatory agent sodium salicylate although this agent also has anti-oxidant effects (Ferger *et al.*, 1999; Mohanakumar *et al.*, 2000).

B. Rotenone

Rotenone is a common component of pesticides that induces mitochondrial toxicity via selective inhibition of the oxidative activity of complex I, and of oxidative free radical production. As might be anticipated given its mode of action, rotenone induces CNS lesions and motor impairments with Parkinsonian features in several *in vivo* models. It is a naturally occurring compound derived from the roots of certain plant species, whose toxic properties have been utilized for many years in farming practices, to regulate fish populations and as an insecticide. Several epidemiological studies have subsequently implicated accidental rotenone exposure as a pathogenetic risk factor in the etiology of PD (Gorrell *et al.*, 1998; Kitada *et al.*, 1998), although studies in animals suggest that its CNS toxicity is extremely low following oral exposure (Betarbet *et al.*, 2000). This observation does not rule out the possibility of susceptibility to environmental exposure, especially when a chronically exposed subject also expresses genetic defects in complex I, or an impaired ability to metabolize xenobiotics (Parker *et al.*, 1989; Menegon *et al.*, 1998; Swerdlow *et al.*, 1998).

Rotenone's toxic action is mediated by steric inhibition of complex I activity after binding at the PSST subunit (Ernster *et al.*, 1963; Horgan *et al.*, 1968; Gutman *et al.*, 1970). This subunit is postulated to play a key role in electron transfer by functionally coupling the iron–sulfur cluster N2 to quinone, and hence metabolic impairment can be induced by blockade of its binding site by rotenone and other inhibitors including piericidin A, pyridaben, and bullatacin (Schuler *et al.*, 1999). Direct stereotaxic injection of rotenone into the substantia nigra in rats lesions dopaminergic neurons in this region (Heikkila *et al.*, 1985). However, *in vivo* studies of rotenone's CNS actions after systemic administration are hindered by the agent's hydrophobicity and insolubility in aqueous solvents. Consequently, recent

studies have turned to a relatively extreme route of administration, employing chronic administration directly into the jugular vein via subcutaneously implanted minipumps. Ferrante and colleagues (1997) demonstrated that intrajugular administration of rotenone to rats (10–18 mg/kg/day for 7–9 days) induced a motor syndrome involving rigidity and akinesia. Histology revealed this was associated with neuronal degeneration and astrogliosis in the striatum and globus pallidus, but found no evidence of cell loss or alterations in tyrosine hydroxylase (TH) immunoreactivity within the substantia nigra, unlike the pattern seen in PD. More recently, Betarbet and colleagues (2000) have further characterized this PD model in rats, again using intrajugular infusions but employing a chronic low dose regimen, and incorporating both histological and biochemical assessments of lesion attributes. Administration of 2–3 mg/kg/day for up to five weeks was found to produce optimal lesion effects. Even using this administration method, the usefulness of this approach as a laboratory model is restricted by the variability of individual rats' susceptibility to the toxin, with only 50% of treated animals developing detectable lesions. In those Lewis rats susceptible to toxicity, however, rotenone induced striatal lesions and a progressive degeneration of nigrostriatal neurons concomitant with a loss of immunoreactivity for tyrosine hydroxylase, the dopamine transporter, and the vesicular monoamine transporter VMAT2 (Betarbet *et al.*, 2000). Furthermore, cytoplasmic α-synuclein- and ubiquitin-positive fibrillary inclusions were observed in nigral neurons of affected rats, similar to Lewy bodies found in PD brain. Intoxicated rats exhibit bradykinesia, postural instability, unsteady gait, and some evidence of tremor. Significantly, the extent of these deficits improved after treatment with the dopamine receptor agonist apomorphine, supporting a dopaminergic selectivity of rotenone's action.

Unlike MPTP toxicity, where the toxin is selectively taken up into the neuronal population which is then targeted for destruction, peripheral rotenone administration results in uniform distribution of the toxin throughout the brain. Yet remarkably, Betarbet and colleagues (2000) reported that in their study rotenone's toxic effects were restricted to dopaminergic neurons within the nigrostriatal system, independent of a requirement for the dopamine transporter (echoing the regional specificity of systemically administered 3-NP, discussed later). This implies that neurons within the SN*pc* are selectively vulnerable to complex I inhibition, and this is consistent with findings of decreased complex I activity in PD postmortem tissue and platelets (Parker *et al.*, 1989; Schapira *et al.*, 1990; Mann *et al.*, 1992). However, Betarbet and colleagues suggest that rotenone's toxicity might be mediated primarily by oxidative damage, since the brain rotenone concentration achieved in their study (20–30 n*M*) was only enough to partially

inhibit complex I, and not high enough to significantly impair oxidative phosphorylation. In addition, several *in vitro* studies have demonstrated that rotenone-mediated complex I inhibition can induce free radical generation, result in damage to proteins and DNA, and chronic exposure may stimulate cytochrome c release from mitochondria (Seaton *et al.,* 1997; Hensley *et al.,* 1998; Sherer *et al.,* 2001).

C. Neurolathyrism

Another CNS motor syndrome involving a mitochondrial component is the spastic paraplegia that occurs as a result of ingestion of certain strains of chick peas found in Europe and India (*Lathyrus sativus* L.). This form of toxicity is also implicated in the etiology of amyotrophic lateral sclerosis and PD dementia of Guam. The toxicity of the chick pea in humans apparently derives from the actions of three excitotoxins identified in these toxic strains—namely amino-β-oxalylaminopropionic acid, amino-oxalylaminobutyric acid, and β-N-oxalylamino-L-alanine (L-BOAA) (Spencer, 1995). Of these, most is understood about the actions of L-BOAA, whose neurodegenerative effects are mediated via actions at AMPA glutamate receptor subtypes, and results in selective inhibition of mitochondrial complex I (Pai and Ravindranath, 1993; Kunig *et al.,* 1994). Toxicity can be prevented by pretreatment with α-amino-3-hydroxy-5-methyl-4-isoxazole (AMPA)/kainate (but not NMDA) glutamate receptor antagonists, including 1,2,3,4,-tetrahydro-6-nitro-2,3-dioxo-benzo(f)quinoxaline-7-sulfonamide disodium (NBQX) and 6-cyano-7-nitroquinoxaline-2,3-dione (CNQX) (Pai and Ravindranath, 1993; Willis *et al.,* 1993; Zeevalk and Nicklas, 1994). *In vitro,* neuron exposure to micromolar concentrations of L-BOAA produces morphologic changes to cell bodies including postsynaptic vacuolization, followed by degeneration (Ross and Spencer, 1987). The involvement of oxidative damage processes in L-BOAA toxicity are suggested by observations that toxicity is reversed by thiol treatment (Sriram *et al.,* 1998). Furthermore, focal administration of putative free radical scavenging agents (including dimethylformamide, DMF; dimethyl sulfoxide, DMSO; dimethylthiourea, DMTU; and mannitol) protected against L-BOAA-induced neurotoxicity induced by intra-hippocampal injections in rats (Willis *et al.,* 1994).

The toxicity of L-BOAA following systemic administration is restricted to specific regions of the CNS, primarily affecting the thoracolumbar spinal cord where myelin loss and eventually axon degeneration occur following anterolateral sclerosis (Spencer *et al.,* 1986, 1987). There is also evidence of amyloid deposition and neurofibrillary tangle formation in Ammon's horn, although a direct link with *Lathyrus* has not been proven (Denny-Brown,

1947). Clinical symptoms vary greatly between patients in onset and priming dose, but are characterized initially by lumbar pain, and weakness with stiffness of the lower extremities (Haque *et al.,* 1996). Weakness is progressive and eventually leg spasticity and clonic seizures occur, leading to gait disturbances. Upper extremities may become involved in severe cases. Muscle atrophy ensues, with sensory deficits, pain, and parasthesias (the latter two lasting one to two weeks). The patient is left with a spastic gait. Interestingly, in both humans and in animal models males have increased risk of developing pathology after exposure to L-BOAA, a circumstance suggested to be due to anti-oxidant properties of female hormones.

III. Inhibitors of Mitochondrial Complex II: Succinate Ubiquinol Oxidoreductase

A. 3-Nitropropionic Acid (3-NP)

The mitochondrial toxin 3-nitropropionic acid (3-NP) irreversibly inhibits the activity of succinate dehydrogenase, a metabolic enzyme that participates in both the tricarboxylic acid (TCA) cycle and in complexes II–III of the electron transport chain. Systemic administration of this agent to humans, nonhuman primates, and rodents results in CNS lesions that selectively target subpopulations of striatal neurons, closely replicating the nature and regional specificity of pathological events seen in Huntington's disease (HD).

The induction of striatal lesions by 3-NP is accompanied by multiple cognitive and motor symptoms, including acute encephalopathies and coma, following initial gastrointestinal disturbances. In fact, 3-NP was first identified following reports of motor disturbances in livestock in the United States that were exposed to fungal-contaminated diet, and observations of symptoms resembling HD with concomitant lesions of the basal ganglia in children in China after ingestion of fungal-contaminated sugar cane. The fungus in question, *Arthrinium,* was subsequently found to contain the 3-nitopropanol metabolite 3-NP (for review, see Ludolph *et al.,* 1991). Of the human cases studied, some comatose patients eventually recovered fully, but most were left with irreversible motor impairments including dystonia, jerky movements, torsion spasms, and facial grimaces. Approximately 10% of affected individuals died. Intoxication generally produces basal ganglia lesions visible by computed tomography (CT) scans, localized principally to the putamen but sometimes extending to the caudate (Ludolph *et al.,* 1991; He *et al.,* 1995). The spatial, pathologic and (to a limited extent) behavioral

features of 3-NP intoxication can be replicated by systemic administration in experimental animals (Gould and Gustine, 1982; Hamilton and Gould, 1987). Hence, this toxin has become a widely used experimental tool to try to model aspects of HD pathology in primates, rats, and mice. However, the extent of lesions and the nature of the pathologic sequelae are minutely dependent on the dosing regimen used, with low-dose chronic treatment paradigms yielding cerebral effects most closely mimicking those seen in HD (for review, see Brouillet *et al.*, 1999). Systemic administration of 3-NP to both rats and primates produces age-dependent striatal lesions that are strikingly similar to those seen in HD (Brouillet *et al.*, 1995, 1998). In primates, chronic 3-NP administration produces selective striatal lesions characterized by a depletion of calbindin neurons with sparing of NADPH-d neurons, and by proliferative changes in the dendrites of spiny neurons. Animals also show both spontaneous and apomorphine-inducible choreiform movement disorders resembling HD (Brouillet *et al.*, 1995). The 3-NP basal ganglia lesions in rats are associated with elevated lactate levels, similar to the increased lactate production seen in HD patients (Jenkins *et al.*, 1993; Matthews *et al.*, 1998). Systemic administration of 3-NP results in increased binding of tritiated MK-801, consistent with activation of NMDA receptors as a secondary consequence of energy depletion (Wullner *et al.*, 1994). Consequently, 3-NP lesions can be prevented by prior removal of glutamatergic excitatory corticostriatal inputs by decortication, by glutamate release inhibitors, and by glutamate receptor antagonists, suggesting that 3-NP toxicity is mediated by secondary excitotoxic mechanisms (Beal, 1994; Schulz *et al.*, 1996a).

Succinate dehydrogenase (SDH) catalyzes the oxidation of succinate to fumarate. Due to its joint roles in the TCA cycle and electron transport chain, it is located on the surface of the inner mitochondrial membrane (Fig. 2). The biochemical mechanism of SDH inhibition by 3-NP has not yet been unequivically proven, but the close similarity in structures of 3-NP ($C_3H_5NO_4$) and succinic acid ($C_4H_6O_4$) may be the key to 3-NP's potency. Currently, two theories predominate. One hypothesis proposes that the dianion form of 3-NP can generate carbanions that preferentially react with the flavin moiety in SDH, forming a covalent adduct that alters the substrate specificity of the enzyme (Alston *et al.*, 1977). Alternatively, Coles and colleagues (1979) suggest that the substrate binding site of SDH is specifically targeted by 3-NP. They demonstrated that the dianion form of 3-NP can bind to SDH, generating nitroacrylate. This nitroacrylate group can then react with and irreversibly bind a thiol group within SDH to block access of succinate to the enzyme. *In vitro* this inhibition of succinate catabolism by 3-NP occurs extremely rapidly (k_{obs} 1.2 min^{-1}), and is dose dependent.

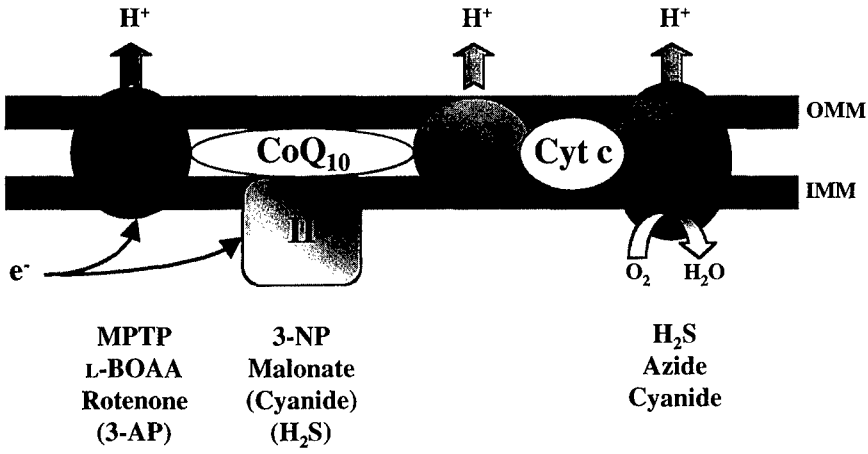

FIG. 2. Sites of metabolic inhibition by mitochondrial toxins. A schematic representation of the enzyme complexes that constitute the electron transport chain, illustrating the principal sites of respiratory disruption by mitochondrial metabolic toxins. Metabolic substrates generated by glycolysis and the TCA cycle donate electrons to complexes I and II, which then transfer electrons to complex III via coenzyme Q_{10} (coQ_{10}). Cytochrome c (cyt c) modulates electron donation on to complex IV. This process promotes the pumping of protons across the inner mitochondrial membrane by complexes I, III, and IV, with the resultant generation of a potential energy gradient. This is converted into stored energy in the high-energy phosphate bond of ATP, by the terminal electron acceptor ATP synthase (not shown). To facilitate this process, complexes I, III, and IV occur in organized supramolecular clusters (respirasomes), situated between the inner and outer mitochondrial membranes (IMM and OMM, respectively). Succinate dehydrogenase (complex II) is located on the surface of the IMM. Disruption of the electon transport chain by direct inhibition of any of the complex subunits may therefore have catastrophic effects on both energy generation, and on the homeostatic regulation of free radical generation during oxidative phosphorylation. *Abbreviations:* 3-AP, 3-acetylpyridine; L-BOAA, β-N-oxalylamino-L-alanine; e^-, electron; H_2S, hydrogen sulphide; MPTP, 1-methyl-4-phenyl-1,2,3,6-tetrahydropyridine; 3-NP, 3-nitropropionic acid.

By inhibiting components of both the TCA cycle and oxidative phosphorylation, 3-NP's toxicity is doubly detrimental to mitochondrial metabolism. The 3-NP impairs both the delivery of NADH from the TCA cycle to complex I of the oxidative phosphorylation pathway, and inhibits the passage of reducing equivalents along the electron transfer chain, thus reducing ATP generation by a two-pronged attack on mitochondrial function. Inhibition of cerebral SDH activity by 3-NP has been demonstrated *in vivo* in a number of studies. Interestingly, the neurodegenerative sequelae of systemic administration of the toxin are largely restricted to the striatum despite a relatively homogeneous distribution of the toxin, resulting in a uniform reduction in SDH activity throughout the brain (Gould and Gustine, 1982; Gould *et al.*, 1985; Brouillet *et al.*, 1998; Browne and Beal, unpublished observations).

This observation appears to once again underscore the vulnerability of striatal neurons to metabolic stress. In fact, 3-NP markedly inhibits SDH activity within 2 h of intraperitoneal administration in rodents, producing 50–70% reductions in SDH activity throughout the brain (Brouillet *et al.*, 1998; Browne and Beal, unpublished observations), consistent with the degree of complex II and III deficiency reported in HD striatum in postmortem studies (Gu *et al.*, 1996; Browne *et al.*, 1997). The energetic component of 3-NP-mediated toxicity is further reflected by observations that the agent found to produce the most profound protection against 3-NP acts by stimulating energy generation within cells. Creatine administration in rats markedly reduces neuronal cell loss induced by 3-NP, as well as attenuating increases in cerebral lactate levels and decreases in levels of high-energy phosphate compounds (including ATP) seen in the striata of 3-NP-treated rats (Matthews *et al.*, 1998).

The 3-NP toxicity in animals is also associated with increased oxidative damage in the CNS. Hydroxyl (OH^-) free radical production is elevated in the striatum following systemic 3-NP administration, as are levels of the DNA damage marker 8-hydroxy-deoxyguanosine (OH^8dG) and 3-nitrotyrosine (a marker for peroxynitrite-mediated oxidative damage) (Schulz *et al.*, 1996b). Findings that 3-NP-induced lesions and concomitant increases in oxidative damage markers are markedly attenuated in mice overexpressing the superoxide free radical scavenger Cu/Zn superoxide dismutase (SOD1) imply that oxidative free radicals contribute to lesion formation (Beal *et al.*, 1995). Furthermore, 3-NP striatal lesions are attenuated by free radical spin traps and nitric oxide synthase (NOS) inhibitors (Schulz *et al.*, 1995c). In addition, lack of the free radical scavenging enzyme glutathione peroxidase (GSHPx) in knockout mice exacerbates striatal damage and 3-nitrotyrosine elevations casued by systemic administration of 3-NP (Klivenyi *et al.*, 2000b). These results indicate that a knockout of GSHPx may be adequately compensated under normal conditions, but following toxin-induced mitochondrial dysfunction GSHPx plays an important role in detoxifying oxygen radicals.

B. Malonate

Malonate is another selective inhibitor of succinate dehydrogenase activity that induces motor impairment following intrastriatal administration in rodents. Lesion pathology reveals neuronal selectivity similar to the pattern of neuronal vulnerability in HD brain. In contrast to 3-NP toxicity, systemic administration of this agent is ineffective as it is unable to cross the blood–brain barrier. However malonate is still a useful tool for modeling

the effects of complex II inhibition *in vitro* and *in vivo*. Intrastriatal injection of malonate produces age-dependent striatal lesions that can be significantly attenuated by treatment with the NMDA receptor antagonist MK-801. Further indirect evidence that energetic defects contribute to malonate-induced neurodegeneration come from observations that pro-energy compounds protect against cell death. Coenzyme Q_{10} (CoQ_{10}), a co-factor for electron transfer during oxidative phosphorylation in the mitochondria and a potent antioxidant, attenuates malonate neurotoxicity in animal models (Beal *et al.*, 1994; Schulz *et al.*, 1996b). Interestingly, oral administration of CoQ_{10} has also been shown to ameliorate elevated lactate levels seen in the cerebral cortex of HD patients (Koroshetz *et al.*, 1997). Coenzyme Q_{10} is reported to also improve symptoms in some other mitochondrial-associated disorders including MELAS (mitochondrial myopathy, encephalopathy, lactic acidosis, and stroke-like episodes) and Kearns-Sayre syndrome, where it additionally reduces CSF and serum lactate and pyruvate levels, and enhances mitochondrial enzyme activities in platelets (Bresolin *et al.*, 1988; Ihara *et al.*, 1989). In addition, oral supplementation with either creatine or cyclocreatine produced significant protection against malonate lesions, and ameliorated malonate-induced increases in hydroxyl radical generation (Matthews *et al.*, 1998). The magnitude of protection against malonate toxicity, in terms of lesion volume, was exacerbated by combining nicotinamide with creatine treatment (Malcon *et al.*, 2000).

Malonate-induced increases in conversion of salicylate to 2,3- and 2,5-dihydroxybenzoic acid, an index of hydroxyl radical generation, were greater in GSHPx knockout mice than in wild-type control animals, suggesting an involvement of oxidative damage mechanisms in malonate toxicity (Klivenyi *et al.*, 2000b). This is supported by findings that impaired nitric oxide (NO) generation in mice lacking the gene for the neuronal isoform of NOS (nNOS) reduced the volume of malonate lesions (Schulz *et al.*, 1996b). Further, elevated 3-nitrotyrosine concentrations are reported after intrastriatal malonate injection, and malonate lesions are attenuated by free radical spin traps and nitric oxide synthase (NOS) inhibitors. Hence there is substantial evidence that NO-mediated oxidative damage is involved in cell death processes following energetic disruption induced by both 3-NP and malonate.

IV. Inhibitors of Mitochondrial Complex IV: Cytochrome *c* Oxidase

A. Cyanide

Cyanide is an extremely potent neurotoxin principally targeting complex IV of the electron transport chain, although its actions within

the mitochondria are not limited to this site. Ingestion of an average dose of only 200 mg of potassium cyanide by humans proves fatal. Although most cyanide-related deaths in the United States result from homicide or suicide attempts, intoxication may also occur from accidental exposure to cyanide compounds used in industrial processes, cyanide gas from burning certain compounds including polyurethanes, nitrocellulose, and wool, or *in vivo* biotransformation of cyanogenic compounds including nitriles (Albin, 2000). Cassava and some fruit stones (for example, apricot and peach) contain cyanogenic compounds, and sodium nitroprusside treatment can lead to cyanide generation *in vivo*.

Cyanide inhibits ferric ion (Fe^{3+}) containing enzymes, including cytochrome oxidase (a vital component of complex IV), succinate dehydrogenase, and mitochondrial and cytoplasmic SOD. Hence its actions are principally inhibition of mitochondrial aerobic metabolism and increased free radical generation. The CNS is particularly vulnerable to the toxic effects of cyanide, putatively because of its high metabolic rate and dependence on oxidative phosphorylation to supply functional energy demands. Death is caused by respiratory arrest thought to result from paralysis of brain-stem neurons that control respiratory muscles. Initial symptoms are headache, delirium, seizures, agitation, and swift onset of coma, and fatality often occurs within minutes of exposure. In the few survivors of cyanide exposure, motor neurologic symptoms appear days or weeks after dosing. The principle symptoms are parkinsonism and dystonia, with the possibility of dysarthria, ataxia, and eye movement abnormalities (Uitti *et al.*, 1985; Borgohain *et al.*, 1995; Rosenow *et al.*, 1995). Lesions occur in the putamen and globus pallidus, while magnetic resonance (MR) studies also reveal changes in the cortex, cerebellum, subthalamus, and substantia nigra (Uitti *et al.*, 1985). Positron emission tomography (PET) studies have also shown presynaptic dopaminergic terminal loss after cyanide exposure. Treatment paradigms are limited, but include thiosulfate administration to induce cyanide conversion to thiocyanate, administration of nitrites to promote methemoglobin formation (which has a high affinity for cyanide and thus draws it from the tissues), and respiratory support.

B. Hydrogen Sulfide

Hydrogen sulfide is an environmental toxin that is thought to induce its toxic effects in a similar manner to cyanide by inhibiting Fe^{3+} containing enzymes, particularly cytochrome oxidase in complex IV (Tvedt *et al.*, 1991; Snyder *et al.*, 1995; Kerns and Kirk, 1998). In contrast to cyanide, its effects are generally reversible. Acute symptoms include vertigo, seizures, delirium, coma, and respiratory paralysis, thought to arise from inhibition

of brain-stem neurons modulating respiratory mechanics. Again, the CNS is particularly vulnerable to the toxic effects of hydrogen sulfide, and putaminal and pallidal degeneration may occur in severe cases.

C. Sodium Azide

Sodium azide (NaN_3) is another compound selectively toxic to mitochondria that targets Fe^{3+} containing proteins, in particular cytochrome oxidase (see Fig. 2). Azide exposure induces striatal-specific degeneration in animal models following systemic administration (Hicks, 1950a; Köryney, 1963; Miyoshi, 1968; Shibasaki, 1969). Observations in rats (following a dosing regimen of 3 mg/kg NaN_3 i.p., four times per day for four days) reported initial slight motor effects, typically sluggishness, followed a few days later by the rapid onset of marked motor abnormalities including akinesis and paretic gait, with forelimb tremor (Miyoshi, 1967). Animals generally survived but showed sustained gait abnormalities despite dosing cessation. After this treatment paradigm distinct bilateral striatal necrosis was evident, with variable involvement of other brain regions including the globus pallidus in some animals, and occasional degeneration in the cerebral cortex and demyelination of the optic tract. Systemic toxicity was also evident, affecting lung and heart muscle predominantly. Other studies also show axon damage in the corpus callosum (Hicks, 1950a,b; Köryney, 1963). Systemic NaN_3 administration produces reductions in cytochrome oxidase activity diffusely throughout the brain, including both the striatum and regions spared by damage (such as cerebral cortex, cerebellum, and choroid plexus), again underscoring the peculiar sensitivity of striatal neurons to impaired energy metabolism *in vivo*.

V. Manganese

Chronic manganese exposure induces a movement disorder characterized by bradykinesia and rigidity. Onset is slow but insidious, with several subjects experiencing severe psychiatric symptoms before onset of an akinetic-rigid parkinsonian state. Manganese toxicity was first observed in manganese ore miners, millworkers, and smelter workers in 1837 (Couper, 1837), but also results from accidental exposure to or ingestion of potassium permanganate, fungicides, and gasoline additives containing manganese (Albin, 2000).

The symptom phenotype of manganese toxicity results from the fact that systemically administered manganese accumulates within the CNS in

the basal ganglia—in particular, in the globus pallidus, caudate, and putamen (Newland *et al.,* 1989). The exact mechanism of manganese toxicity is still ill-defined, but the fact that within cells manganese accumulates in mitochondria suggests that mitochondrial dysfunction plays an intrinsic role. One hypothesis is that manganese increases oxidative damage due to catecholamine oxidation (Sloot *et al.,* 1994). More recently, manganese has been shown to stimulate astrocytic and microglial NOS production *in vitro,* potentially increasing nitric oxide production leading to free radical damage (Spranger *et al.,* 1998; Chang and Liu, 1999). Further, manganese has been shown to directly inhibit mitochondrial oxidative phosphorylation, inhibiting activity of the TCA cycle enzyme aconitase, located in the mitochondrial matrix (Zheng *et al.,* 1998). Zheng and colleagues suggest that a potential mechanism of enzyme impairment might be by the substitution of manganese for iron in enzymes that require iron as a co-factor. The involvement of manganese in mitochondrial dysfunction is supported by PET studies that demonstrate reductions in cerebral glucose utilization rates in a number of subjects with mild manganese toxicity (Wolters *et al.,* 1989).

Calne *et al.* (1994) describe a movement disorder closely resembling idiopathic PD following chronic manganese exposure, with early signs of gait disturbances and dysarthria. Sufferers may show axial and extremity dystonia and a postural tremor, but resting tremor does not occur. Dementia and cerebellar dysfunction may also occur. Symptoms can still progress after discontinued exposure to manganese, and manganese clears only very slowly from mitochondria and the brain (Huang *et al.,* 1998; Pal and Calne, 1999). It has been suggested that this progressive feature of the disorder might reflect a vicious cycle of oxidative damage as a result of mitochondrial impairment, leading to mitochondrial DNA damage and perpetuated mitochondrial dysfunction (Brouillet *et al.,* 1993; Desole *et al.,* 1997). Although clinical symptoms of manganese toxicity partially resemble Parkinsonism, the pathological alterations are very different. In the few manganese-exposure victims studied, neuronal degeneration and reactive gliosis were prevalent in the globus pallidus, particularly in the internal segment, and to a lesser extent in the striatum and substantia nigra *pars reticulata,* SN*r* (Yamada *et al.,* 1986). This pathology contrasts with the primary loss of dopaminergic neurons within the SN*pc* in PD. Animal models of manganese exposure, in nonhuman primates and rodents, mimic this pattern of pallidal and SN*r* vulnerability, and show some degeneration within the subthalamic nucleus (Pentschew *et al.,* 1962; Brouillet *et al.,* 1993; Olanow *et al.,* 1996). Dopamine depletion has been demonstrated in experimental animals after direct intrastriatal or intranigral manganese injection in primates and in rats (Lista *et al.,* 1986; Newland *et al.,* 1989; Daniels and Abarca, 1991), and after chronic systemic exposure in rabbits and squirrel monkeys (Neff *et al.,* 1969; Mustafa and Chandra, 1971). Manganese application also has been shown

to decrease dopamine release in striatal slice preparations (Daniels *et al.*, 1981). Moreover, a study in rat striatal tissue slices reported that manganese exposure reduced dopamine biosynthesis by inhibiting tyrosine hydroxylase activity (Hirata *et al.*, 2001). This effect was associated with increased lactate production in the slices, suggesting abnormal aerobic metabolism following manganese exposure. In contrast, fluorodopa PET imaging studies showing that the dopaminergic nigrostriatal pathway remains intact in manganese exposure patients, and observations that dopaminergic treatment is ineffective in the disorder, argue against an involvement of the dopaminergic system in the toxicity phenotype (Calne *et al.*, 1994; Lu *et al.*, 1994).

VI. 3-Acetylpyridine

Another neurotoxin that selectively targets mitochondrial components is the nicotinamide antagonist 3-acetylpyridine (3-AP). Systemic administration of 3-AP in animals induces selective degeneration of the inferior olivary nucleus and cerebellum, resulting in a motor disorder resembling olivopontocerebellar atrophy in humans (Deutsch *et al.*, 1989). Toxicity is mediated via incorporation of 3-AP into nicotinamide nucleotides within the cell, resulting in inhibition of both NADH and NADPH-dependent enzymes (Herken, 1968). Consequently, hydrogen ion transfer between enzymes and substrates using NADH and NADPH as co-factors is impaired, potentially leading to dysfunction of both the TCA cycle and the electron transport chain within mitochondria. Dehydrogenase enzymes are particularly affected, including the mitochondrial enzymes lactate dehydrogenase, α-ketoglutarate dehydrogenase, malate dehydrogenase, isocitrate dehydrogenase, and glutathione reductase. Cytosolic glycolytic enzymes may also be vulnerable, including glucose-6-phosphate dehydrogenase. Thus, 3-AP toxicity results in energy depletion, as has been demonstrated by findings of reduced ATP levels following systemic 3-AP administration (Sethy *et al.*, 1996), and after intrastriatal 3-AP injections in rats (Schulz *et al.*, 1994). Findings that intrastriatal 3-AP injections did not induce acute lactate generation are consistent with a putative impairment of lactate dehydrogenase activity by 3-AP. However, the involvement of metabolic inhibition in 3-AP-mediated toxicity is supported by the observation that enhancing glycolytic ATP production by preadministration of fructose-1,6-biphosphate partially attenuated 3-AP lesions (Schulz *et al.*, 1994). The 3-AP toxicity, both *in vitro* and *in vivo*, is antagonized by nicotinamide (Desclin and Escubi, 1974; Weller *et al.*, 1992).

Consistent with the involvement of a secondary excitotoxic mechanism resulting from impaired mitochondrial energy metabolism, cell loss following stereotactic injections of 3-AP into both striatum and hippocampus can be attenuated by competitive and noncompetitive NMDA receptor antagonists, including 2-amino-5-phosphonovaleric acid (APV), LY274614, and MK-801 (Armanini *et al.*, 1990; Schulz *et al.*, 1994). Schulz and colleagues (1994) went on to show that the glutamate release inhibitor lamotrigine also reduced lesion volume after intrastriatal 3-AP injection, and noted that the pattern of cell vulnerability following 3-AP resembles that following excitotoxic lesions induced by NMDA. Both lesion paradigms show relative sparing of NADPH-diaphorase-positive neurons that contain NOS within the striatum (Beal *et al.*, 1991). However, MK-801 did not protect cultured cerebellar granule cells against 3-AP toxicity, whereas nicotinamide was protective in this *in vitro* model (Weller *et al.*, 1992).

The 3-AP also induces increased oxidative stress, as shown by reports that striatal injection of 3-AP increased hydroxyl (OH^-) radical generation, and that administration of the spin trap N-*tert*-butyl-α-(2-sulphophenyl)-nitrone (S-PBN) markedly reduced striatal lesion volume (Schulz *et al.*, 1995c). In fact, spin traps were found to be more effective against 3-AP lesions than against other mitochondrial toxins. This phenomenon is potentially due to 3-AP's propensity to deplete NADPH, since NADPH is necessary for glutathione reductase-mediated regeneration of the free-radical scavenger glutathione (GSH) from its oxidized form (GSSG). In addition, pyrrolopyramidine antioxidants including U-104067F markedly attenuate the reduction in cerebellar ATP production induced by systemic 3-AP administration in rats, and restore motor impairments (Sethy *et al.*, 1996). This effect is putatively due to inhibition of OH^--mediated lipid peroxidation. Dopaminergic agonists and $GABA_A$ receptor partial agonists have also been reported to protect against 3-AP-mediated cerebellar ATP depletions and loss of inferior olivary neurons (Sethy *et al.*, 1997a,b).

Systemic administration of 3-AP primarily targets the climbing fiber projection from the inferior olivary nucleus that innervates cerebellar purkinje cells (Desclin and Escubi, 1974; Balaban, 1985; Sethy *et al.*, 1996). Other areas affected include the SN*pc*, hippocampal formation, diagonal band of Broca horizontal limb, dorsal motor nucleus of the vagus, interpeduncular nucleus, nucleus ambiguus, hypolassal nucleus, and supraoptic and paraventricular nuclei. Although 3-AP does not cause degeneration of the basis pontis, the neurotoxin induces motor impairment closely resembling OPCA with a phenotype including ataxia, forelimb tremor, hyperkinesia, and tonic cramps (Herken, 1968). Concomitant depletion of dopamine levels and TH immunoreactivity in rat striatum, and of nigral TH immunoreactivity in mice, led to the proposal that 3-AP toxicity may model OPCA

with Parkinsonism, or multiple system atrophy (Deutsch *et al.*, 1989; Takada and Kono, 1993). As with the majority of mitochondrial toxins, the reason for the regional selectivity of 3-AP toxicity is unclear. However, selective vulnerability may be explained by regional impairments or mutations in one or more NAD(P)-dependent oxidoreductases. One of the enzymes particularly susceptible to 3-AP is glutamate dehydrogenase (GDH). Inhibition of GDH activity by 3-AP could lead to increased extracellular glutamate levels, and thus increase the risk of excitotoxic injury. Overall, observations to date strongly imply that both secondary excitotoxicity and free-radical mediated cellular damage play roles in 3-AP-mediated toxicity, concomitant to impaired mitochondrial energy metabolism.

VII. Myopathies and Myotoxic Agents

A number of mitochondrial toxins are also implicated in toxin-induced myopathies. Some antiviral nucleoside drugs used in HIV therapy including zalcitabine (ddI) and didanosine (ddC) produce axonal neuropathies, thought to be caused by disrupted mitochondrial function (Jay *et al.*, 1994; Pedrol *et al.*, 1996; Benbrick *et al.*, 1997). Thallium toxicity also interferes with mitochondrial oxidative activity, and both nucleoside therapy and thallium intoxication are associated with painful peripheral neuropathies. Zidovudine (AZT), a thymidine analogue also used in HIV treatment, produces a different sequelae of myotoxic events, but still mitochondrial dysfunction is involved. Zidovudine inhibits reverse transcriptase and mitochondrial DNA polymerase, hence blocking DNA replication and leading to depletion of mitochondrial DNA (Semino-Mora *et al.*, 1994). Mitochondrial DNA levels in patients have been reported to be reduced reversibly by up to 78% following treatment doses of AZT, inducing impaired mitochondrial protein synthesis (Love and Miller, 1993). In addition, AZT produces partial cytochrome c oxidase deficiency, reducing mitochondrial energy production. Accumulations of mitochondria are visible in muscle biopsies, where "ragged-red fibers" and mitochondrial proliferation are seen. There is also evidence of increased lipid and reduced carnitine levels in affected fibers, which respond to carnitine therapy. Myalgia generally occurs 6–11 months after commencing AZT treatment, and gradually dissipates on cessation of treatment.

Muscle's primary energy source when at rest or during mild exercise (provided blood supply is adequate) is lipid metabolism utilizing cytoplasmic long-chain fatty acids (LCFAs). This process employs L-carnitine to

transport these LCFAs across the inner mitochondrial membrane and into the mitochondrial matrix. The reversible binding of the LCFAs to carnitine to form acylcarnitine esters is catalyzed by carnitine palmitoyl transferase. Within the matrix, β oxidation of the acylcarnitine esters yields acetylcoenzyme A (acetyl-coA) and high-energy molecules including ATP, along with the reduced forms of flavin adenine dinucleotide ($FADH_2$) and nicotinamide adenine dinucleotide (NADH) which can take part in the electron trasport chain. Acetyl-coA enters the TCA cycle in the matrix to yield further ATP, NADH, and $FADH_2$. Myopathy can be produced by the inhibition of this pathway—for example, by agents that induce carnitine deficiency, leading to impaired energy production in the muscle. Such agents include the medication valproic acid, which can also partially inhibit β oxidation. Valproate toxicity is characterized by increased intracellular lipid levels, abnormal mitochondrial morphology, and a mild myopathy (Melegh and Trombitas, 1997). Other agents affecting carnitine function to induce mitochondrial toxicity include pivampicillin, which inhibits absorption of dietary carnitine (Love and Miller, 1993), and chloramphenicol, which inhibits protein synthesis and induces myogenic abnormalities in animal models (Korohoda *et al.*, 1993).

VIII. Discussion: What Determines the Regional and Cellular Specificity of Mitochondrial Toxins?

Agents that disrupt the mitochondrial electron transport chain have a propensity to induce selective neuronal damage within the CNS, often targeting the basal ganglia. In some instances the reason for regional selectivity of a given substance is well understood. For example, in the case of MPTP it is the affinity of the dopamine reuptake transporter that localizes the toxic moiety, MPP^+, to dopaminergic nerve terminals in the SN*pc*, resulting in selective neuronal degeneration in the nigrostriatal pathway. In the cases of other toxins, the cause of the regional vulnerability is less clear. 3-NP, for example, when administered systemically in various animal species, induces neuronal damage primarily in the basal ganglia, despite a universal and more or less equal distribution throughout the CNS. In this case, its regional selectivity may be related more to the susceptibility of basal ganglia neurons than to metabolic inhibition. Complex II and III activity is equally impaired throughout the brains of rodents and primates following systemic 3-NP administration, but striatal neurons are preferentially damaged. Potential explanations for this phenomenon include the suggestion

that striatal neurons have a high energy demand and may be less capable of buffering energetic stress than neurons in other brain regions. The striatum also receives a profound excitatory glutamatergic innervation from cortical regions, increasing the probability of excitotoxic processes being invoked in times of metabolic compromise. These suppositions are supported by observations that other metabolic toxins including cyanide and azide also selectively target striatal neurons, despite widespread complex IV inhibition throughout the CNS, and observations that NMDA receptor antagonist treatment or decortication protect striatal neurons against toxin-induced damage. Further, other hypoxic conditions also preferentially target the striatum, including insulin hypoglycemia, carbon disulfide, and malononitrile toxicity (disregarding ischemic lesions that are dependent on vascular zones for lesion localization) (Hicks, 1950a,b; Kristian *et al.*, 1995; Huang *et al.*, 1996; Hageman *et al.*, 1999). The underlying reasons for the metabolic vulnerability of certain neuronal populations within the brain, however, have yet to be elucidated.

One potentially important factor in the phenomenon of neuronal vulnerability is the role that differences in mitochondrial composition may play. For instance, rotenone binding to complex I differs between brain regions, suggesting variability in complex I subunit composition (Higgins and Greenamyre, 1996). It is also known that the relative expression levels of different isoforms of complex IV subunits vary between CNS regions. Other factors likely to be important in differential vulnerability are numbers and types of glutamate receptors, calcium binding proteins, presence of nitric oxide synthase, and levels of antioxidant enzymes. For instance, levels of the mitochondrial free radical scavenger MnSOD are particularly high in striatal NADPH-diaphorase-positive neurons, which show relative resistance to mitochondrial toxins including 3-NP and 3-AP (Inagaki *et al.*, 1991; Gonzalez-Zulueta *et al.*, 1998).

In conclusion, mitochondrial toxin models provide a wealth of information on the contributions of different functional components of mitochondria to overall cell and system function, and mechanisms of dysfunction in degenerative disorders. They have also given new insight into potential therapeutic approaches in models of several neurodegenerative diseases. In particular, a number of studies in mitochondrial toxin models suggest that CoQ_{10} and creatine may be useful for the treatment of PD, HD, and Friedrich's ataxia (Lodi *et al.*, 2001; Tarnapolsky and Beal, 2001). Consequently, findings of neuroprotection in toxin model systems have been extrapolated to transgenic mouse models of HD (Ferrante *et al.*, 2000; Andreassen *et al.*, 2001), and candidate therapeutic agents originally identified using mitochondrial toxin models are beginning to reach clinical trials for human degenerative diseases.

References

Aiuchi, T., Matsunaga, M., Syo, M., and Nakaya, K. (1996). The relation between respiratory inhibition and uptake of 1-methyl-isoquinoline (MIQ+) in mitochondria. *Neurochem. Int.* **28,** 319–323.

Albanese, A., Granata, R., Gregori, B., Piccardi, M. P., Colosimo, C., and Tonali, P. (1993). Chronic administration of 1-methyl-4-phenyl-1,2,3,6-tetrahydropyridine to monkeys: Behavioural, morphological and biochemical correlates. *Neuroscience* **55,** 823–832.

Albin, R. L. (2000). Basal ganglia neurotoxins. *Neurol. Clin.* **18,** 665–680.

Albin, R. L., and Greenamyre, J. T. (1992). Alternative excitotoxic hypotheses. *Neurology* **42,** 733–738.

Alston, T. A., Mela, L., and Bright, H. J. (1977). 3-Nitropropionate, the toxic substance of indigofera, is a suicide inactivator of succinate dehydrogenase. *Proc. Natl. Acad. Sci. USA* **74,** 3767–3771.

Andreassen, O. A., Ferrante, R. J., Dedeoglu, A., Albers, D. W., Klivenyi, P., Carlson, E. J., Epstein, C. J., and Beal, M. F. (2001). Mice with a partial deficiency of manganese superoxide dismutase show increased vulnerability to the mitochondrial toxins malonate, 3-nitropropionic acid, and MPTP. *Exp. Neurol.* **167,** 189–195.

Armanini, M. P., Hutchins, C., Stein, B. A., and Sapolsky, R. M. (1990). Glucocorticoid endangerment of hippocampal neurons is NMDA-receptor dependent. *Brain Res.* **532,** 7–12.

Balaban, C. D. (1985). Central neurotoxic effects of intraperitoneally administered 3-acetylpyridine, harmaline and niacinamide in Sprague-Dawley and Long-Evans rats: A critical review of central 3-acetylpyridine neurotoxicity. *Brain Res.* **356,** 21–42.

Bankiewicz, K. S., Oldfield, E. H., Chiueh, C. C., Doppman, J. L., Jacobowitz, D. M., and Kopin, I. J. (1986). Hemiparkinsonism in monkeys after unilateral internal carotid artery infusion of 1-methyl-4-phenyl-1,2,3,6-tetrahydropyridine (MPTP). *Life Sci.* **39,** 7–16.

Beal, M. F. (1994). Huntington's disease, energy, and excitotoxicity. *Neurobiol. Aging* **15,** 275–276.

Beal, M. F. (2000). Energetics in the pathogenesis of neurodegenerative diseases. *Trends Neurosci.* **23,** 294–300.

Beal, M. F. (2001). Experimental models of Parkinson's disease. *Nat. Rev. Neurosci.* **2,** 325–334.

Beal, M. F., Ferrante, R. J., Swartz, K. J., and Kowall, N. W. (1991). Chronic quinolinic acid lesions in rats closely resemble Huntington's disease. *J. Neurosci.* **11,** 1649–1659.

Beal, M. F., Henshaw, D. R., Jenkins, B. G., Rosen, B. R., and Schulz, J. B. (1994). Coenzyme Q_{10} and nicotinamide block striatal lesions produced by the mitochondrial toxin malonate. *Ann. Neurol.* **36,** 882–888.

Beal, M. F., Ferrante, R. J., Henshaw, R., Matthews, R. T., Chan, P. H., Kowall, N. W., Epstein, C. J., and Schulz, J. B. (1995). 3-Nitropropionic acid neurotoxicity is attenuated in copper/zinc superoxide dismutase transgenic mice. *J. Neurochem.* **65,** 919–922.

Beal, M. F., Matthews, R., Tieleman, A., and Schults, C. W. (1997). Coenzyme Q_{10} attenuates the MPTP induced loss of striatal dopamine and dopaminergic axons in aged mice. *Brain Res.* **783,** 109–114.

Beckman, J. S. (1996). Oxidative damage and tyrosine nitration from peroxynitrite. *Chem. Res. Toxicol.* **9,** 836–844.

Benazzouz, A., Boraud, T., Dubedat, P., Boireau, A., Stutzmann, J. M., and Gross, C. (1995). Riluzole prevents MPTP-induced parkinsonism in the rhesus monkey: A pilot study. *Eur. J. Pharmacol.* **284,** 299–307.

Benbrik, E., Chariot, P., Bonavaud, S., Ammi-Said, M., Frisdal, E., Rey, C., Gherardi, R., and Barlovatz-Meimon, G. (1997). Cellular and mitochondrial toxicity of zidovudine (AZT), didanosine (ddI) and zalcitabine (ddC) on cultured human muscle cells. *J. Neurol. Sci.* **149,** 19–25.

Betarbet, R., Sherer, T. B., MacKenzie, G., Garcia-Osuna, M., Panov, A. V., and Greenamyre, J. T. (2000). Chronic systemic pesticide exposure reproduces features of Parkinson's disease. *Nature Neurosci.* **3,** 1301–1306.

Bezard, E., Gross, C. E., Fournier, M. C., Dovero, S., Bloch, B., and Jaber, M. (1999). Absence of MPTP-induced neuronal death in mice lacking the dopamine transporter. *Exp. Neurol.* **155,** 268–273.

Bindhoff, L. A., Birch-Machin, M., Cartlidge, N. E., Parker, W. D., Jr., and Turnbull, D. M. (1989). Mitochondrial function in Parkinson's disease. *Lancet* **2,** 49.

Blum, D., Torch, S., Lambeng, N., Nissou, M., Benabid, A. L., Sadoul, R., and Verna, J. M. (2001). Molecular pathways involved in the neurotoxicity of 6-OHDA, dopamine and MPTP: Contribution to the apoptotic theory in Parkinson's disease. *Prog. Neurobiol.* **65,** 135–172.

Bodis-Wollner, I., Chung, E., Ghilardi, M. F., Glover, A., Onofrj, M., Pasik, P., and Samson, Y. (1991). Acetyl-levo-carnitine protects against MPTP-induced parkinsonism in primates. *J. Neural. Transm. Park. Dis. Dement. Sect.* **3,** 63–72.

Boireau, A., Dubedat, P., Bordier, F., Peny, C., Miquet, J. M., Durand, G., Meunier, M., and Doble, A. (1994). Riluzole and experimental parkinsonism: Antagonism of MPTP-induced decrease in central dopamine levels in mice. *Neuroreport* **5,** 2657–2660.

Borgohain, R., Singh, A. K., Radhakrishna H., Rao V. C., and Mohandas, S. (1995). Delayed onset generalized dystonia after cyanide poisoning. *Clin. Neurol. Neurosurg.* **97,** 213.

Bresolin, N., Bet, L., Binda, A., Moggio, M., Comi, G., Nador, F., Ferrante, C., Carenzi, A., and Scarlato, G. (1988). Clinical and biochemical correlations in mitochondrial myopathies treated with coenzyme Q_{10}. *Neurology* **38,** 892–899.

Brouillet, E., and Beal, M. F. (1993). NMDA antagonists partially protect against MPTP induced neurotoxicity in mice. *Neuroreport* **4,** 387–390.

Brouillet, E. P., Shinobu, L, McGarvey, U., Hochberg, F., and Beal, M. F. (1993). Manganese injection into the rat striatum produces excitotoxic lesions by impairing energy metabolism. *Exp. Neurol.* **120,** 89.

Brouillet, E., Hantraye, P., Ferrante, R. J., Dolan, R., Leroy-Willig, A., Kowall, N. W., and Beal, M. F. (1995). Chronic mitochondrial energy impairment produces selective striatal degeneration and abnormal choreiform movements in primates. *Proc. Natl. Acad. Sci. USA* **92,** 7105–7109.

Brouillet, E., Guyot, M. C., Mittoux, V., Altairac, S., Condé, F., Palfi, S., and Hantraye, P. (1998). Partial inhibition of brain succinate deshydrogenase by 3-nitropropionic acid is sufficient to initiate striatal degeneration in rat. *J. Neurochem.* **70,** 794–805.

Brouillet, E., Conde, F., Beal, M. F., and Hantraye, P. (1999). Replicating Huntington's disease phenotype in experimental animals. *Prog. Neurobiol.* **59,** 427–468.

Browne, S. E., Bowling, A. C., McGarvey, U., Baik, M. J., Berger, S. C., Muqit, M. K., Bird, E. D., and Beal, M. F. (1997). Oxidative damage and metabolic dysfunction in Huntington's disease: Selective vulnerability of the basal ganglia. *Ann. Neurol.* **41,** 646–653.

Burns, R. S., Chiueh, C. C., Markey, S. P., Ebert, M. H., Jacobowitz, D. M., and Kopin, I. J. (1983). A primate model of parkinsonism: Selective destruction of dopaminergic neurons in the pars compacta of the substantia nigra by N-methyl-4-phenyl-1,2,3,6-tetrahydropyridine. *Proc. Natl. Acad. Sci. USA* **80,** 4546–4550.

Callier, S., Morissette, M., Grandbois, M., and Di Paolo, T. (2000). Stereospecific prevention by 17-estradiol of MPTP-induced dopamine depletion in mice. *Synapse* **37,** 245–251.

Calne, D. B., Langston, J. W., Martin, W. R., Stoessl, A. J., Ruth, T. J., Adam, M. J., Pate, B. D., and Schulzer, M. (1985). Positron emission tomography after MPTP: Observations relating to the cause of Parkinson's disease. *Nature* **317,** 246.

Calne, D. B., Chu, N. S., Huang, C. C., Lu, C. S., and Olanow, W. (1994). Manganism and idiopathic parkinsonism: Similarities and differences. *Neurology* **44,** 1583–1586.

Chang, J. Y., and Liu, L.-Z. (1999). Manganese potentiates nitric oxide production by microglia. *Mol. Brain Res.* **68,** 22.

Coles, C. J., Edmonson, D. E., and Singer, T. P. (1979). Inactivation of succinate dehydrogenase by 3-nitropropionate. *J. Biol. Chem.* **255,** 4772–4780.

Cosi, C., and Marien, M. (1998). Decreases in mouse brain NAD+ and ATP induced by 1-methyl-4-phenyl-1,2,3,6-tetrahydropyridine (MPTP): Prevention by the poly(ADP-ribose) polymerase inhibitor, benzamide. *Brain Res.* **809,** 58–67.

Couper, J. (1837). On the effects of black oxide of magnesium when inhaled into the lungs. *Br. Ann. Med. Pharmacol.* **1,** 41.

Daniels, A. J., and Abarca, J. (1991). Effect of intranigral Mn^{2+}, on striatal and nigral synthesis and levels of dopamine and cofactor. *Neurotoxicol. Teratol.* **13,** 483.

Daniels, A. J., Gysling, K., and Abarca, J. (1981). Uptake and release of manganese by rat striatal slices. *Biochem. Pharmacol.* **30,** 1833–1837.

Davis, G. C., Williams, A. C., Markey, S. P., Ebert, M. H., Caine, E. D., Reichert, C. M., and Kopin, I. J. (1979). Chronic Parkinsonism secondary to intravenous injection of meperidine analogues. *Psychiatre Res.* **1,** 249–254.

Dehmer, T., Lindenau, J., Haid, S., Dichgans, J., and Schulz, J. B. (2000). Deficiency of inducible nitric oxide synthase protects against MPTP toxicity in vivo. *J. Neurochem.* **74,** 2213–2216.

Denny-Brown, D. (1947). Neurological conditions resulting from prolonged and severe dietary restrictions. *Medicine* **26,** 41–48.

Desclin, J. C., and Escubi, J. (1974). Effects of 3-acetylpyridine on the central nervous system of the rat, as demonstrated by silver methods. *Brain Res.* **77,** 349–364.

Desole, M. S., Esposito, G., Fresu, L., Migheli, R., Enrico, P., Miele, M., De Natale, G., and Miele, E. (1993). Correlation between 1-methyl-4-phenylpyridinium ion (MPP+) levels, ascorbic acid oxidation and glutathione levels in the striatal synaptosomes of the 1-methyl-4-phenyl-1,2,3,6-tetrahydropyridine (MPTP)-treated rat. *Neurosci. Lett.* **161,** 121–123.

Desole, M. S., Sciola, L., Delogu, M. R., Sircana, S., Migheli, R., and Miele, E. (1997). Role of oxidative stress in the manganese and 1-methyl-4-(2′-ethylphenyl)-1,2,3,6-tetrahydropyridine-induced apoptosis in PC12 cells. *Neurochem. Int.* **31,** 169–176.

Deutsch, A. Y., Rosin, D. L., Goldstein, M., and Roth, R. H. (1989). 3-Acetylpyridine-induced degeneration of the nigrostriatal dopamine system: An animal model of olivopontocerebellar atrophy-associated parkinsonism. *Exp. Neurol.* **105,** 1–9.

Di Monte, D., Jewell, S. A., Ekstrom, G., Sandy, M. S., and Smith, M. T. (1986). MPTP and MPP+ cause rapid ATP depletion in isolated hepatocytes. *Biochem. Biophys. Res. Comm.* **137,** 310–315.

Du, Y., Dodel, R. C., Bales, K. R., Jemmersom, R., Hamilton-Byrd, E., and Paul, S. M. (1997). Involvement of a caspase-3-like cysteine protease in 1-methyl-4-phenylpyridinium-mediated apoptosis of cultured cerebellar granule neurons. *J. Neurochem.* **69,** 1382–1388.

Ebadi, M., Govitrapong, P., Sharma, S., Muralikrishnan, D., Shavali, S., Pellett, L., Schafer, R., Albano, C., and Eken, J. (2001). Ubiquinone (coenzyme q10) and mitochondria in oxidative stress of parkinson's disease. *Biol. Signals Recept.* **10,** 224–253.

Eberhardt, O., Coelln, R. V., Kugler, S., Lindenau, J., Rathke-Hartlieb, S., Gerhardt, E., Haid, S., Isenmann, S., Gravel, C., Srinivasan, A., Bahr, M., Weller, M., Dichgans, J., and Schulz, J. B. (2000). Protection by synergistic effects of adenovirus-mediated X-chromosome-linked

inhibitor of apoptosis and glial cell line-derived neurotrophic factor gene transfer in the 1-methyl-4-phenyl-1,2,3,6-tetrahydropyridine model of Parkinson's disease. *J. Neurosci.* **20,** 9126–9134.

Ernster, L., Dallner, G., and Azzone, G. F. (1963). Differential effects of rotenone and amytal on mitochondrial electron and energy transfer. *J. Biol. Chem.* **238,** 1124–1131.

Ferger, B., Teismann, P., Earl, C. D., Kuschinsky, K., and Oertel, W. H. (1999). Salicylate protects against MPTP-induced impairments in dopaminergic neurotransmission at the striatal and nigral level in mice. *Naunyn Schmiedebergs Arch. Pharmacol.* **360,** 256–261.

Ferrante, R. J., Schulz, J. B., Kowall, N. W., and Beal, M. F. (1997). Systemic administration of rotenone produces selective damage in the striatum and globus pallidus, but not in the substantia nigra. *Brain Res.* **753,** 157–162.

Ferrante, R. J., Andreassen, O. A., Jenkins, B. G., Dedeoglu, A., Kuemmerle, S., Kubilus, J. K., Kaddurah-Daouk, R., Hersch, S. M., and Beal, M. F. (2000). Neuroprotective effects of creatine in a transgenic mouse model of Huntington's disease. *J. Neurosci.* **20,** 4389–4397.

Forno, L. S., Langston, J. W., DeLanney, L. E., Irwin, I., and Ricaurte, G. A. (1986). Locus ceruleus lesions and eosinophilic inclusions in MPTP-treated monkeys. *Ann. Neurol.* **20,** 449–455.

Genc, S., Kuralay, F., Genc, K., Akhisaroglu, M., Fadiloglu, S., Yorukoglu, K., Fadiloglu, M., and Gure, A. (2001). Erythropoietin exerts neuroprotection in 1-methyl-4-phenyl-1,2,3,6-tetrahydropyridine-treated C57/BL mice via increasing nitric oxide production. *Neurosci. Lett.* **298,** 139–141.

Gerlach, M., and Riederer, P. (1996). Animal models of Parkinson's disease: An empirical comparison with the phenomenology of the disease in man. *J. Neural Transm.* **103,** 987–1041.

Giasson, B. I., Duda, J. E., Murray, I. V., Chen, Q., Souza, J. M., Hurtig, H. I., Ischiropoulos, H., Trojanowski, J. Q., and Lee, V. M. (2000). Oxidative damage linked to neurodegeneration by selective alpha-synuclein nitration in synucleinopathy lesions. *Science* **290,** 985–989.

Gonzalez-Zulueta, M., Ensz, L. M., Mukhina, G., Lebovitz, R. M., Zwacka, R. M., Engelhardt, J. F., Oberley, L. W., Dawson, V. L., and Dawson, T. M. (1998). Manganese superoxide dismutase protects nNOS neurons from NMDA and nitric oxide-mediated neurotoxicity. *J. Neurosci.* **18,** 2040–2055.

Good, P. F., Hsu, A., Werner, P., Perl, D. P., and Olanow, C. W. (1998). Protein nitration in Parkinson's disease. *J. Neuropathol. Exp. Neurol.* **57,** 338–339.

Gorell, J. M., Johnson, C. C., Rybicki, B. A., Peterson, E. L., and Richardson, R. J. (1998). The risk of Parkinson's disease with exposure to pesticides, farming, well water, and rural living. *Neurology* **50,** 1346–1350.

Gould, D. H., and Gustine, D. L. (1982). Basal ganglia degeneration, myelin alterations, enzyme inhibition induced in ice by the plant toxin 3-nitropropionic acid. *Neuropathol. Appl. Neurobiol.* **8,** 377–393.

Gould, H., Wilson, M. P., and Hamar, D. W. (1985). Brain enzyme and clinical alterations induced in rats and mice by nitroaliphatic toxicants. *Tox. Lett.* **27,** 83–89.

Gu, M., Gash, M. T., Mann, V. M., Javoy-Agid, F., Cooper, J. M., and Shapira, A. H. (1996). Mitochondrial defect in Huntington's disease caudate nucleus. *Ann. Neurol.* **39,** 385–389.

Gutman, M., Singer, T. P., and Casida, J. E. (1970). Studies on the respiratory chain-linked reduced nicotinamide adenine dinucleotide dehydrogenase. XVII. Reaction sites of piericidin A and rotenone. *J. Biol. Chem.* **245,** 1992–1997.

Hageman, G., van der Hoek, J., van Hout, M., van der Laan, G., Steur, E.J., de Bruin, W., and Herholz, K. (1999). Parkinsonism, pyramidal signs, polyneuropathy, and cognitive decline after long-term occupational solvent exposure. *J. Neurol.* **246,** 198–206.

Hamilton, B. F., and Gould, D. H. (1987). Nature and distribution of brain lesions in rats intoxicated with 3-nitropropionic acid: A type of hypoxic (energy deficient) brain damage. *Acta Neuropathol. (Berlin)* **72,** 286–297.

Hantraye, P., Brouillet, E., Ferrante, R., Palfi, S., Dolan, R., Matthews, R. T., and Beal, M. F. (1996). Inhibition of neuronal nitric oxide synthase prevents MPTP-induced parkinsonism in baboons. *Nature Med.* **2,** 1017–1021.

Haque, A., Hossain, M., Wouters, G., and Lambein, F. (1996). Epidemiological study of lathyrism in northwestern districts of Bangladesh. *Neuroepidemiology* **15,** 83–91.

Hartmann, A., Hunot, S., Michel, P. P., Muriel, M. P., Vyas, S., Faucheux, B. A., Mouatt-Prigent, A., Turmel, H., Srinivasan, A., Ruberg, M., Evan, G. I., Agid, Y., and Hirsch, E. C. (2000). Caspase-3: A vulnerability factor and final effector in apoptotic death of dopaminergic neurons in Parkinson's disease. *Proc. Natl. Acad. Sci. USA* **97,** 2875–2880.

He, F., Zhang, S., Qian, F., and Zhang, C. (1995). Delayed dystonia with striatal CT lucencies induced by a mycotoxin (3-nitropropionic acid). *Neurology* **45,** 2178–2183.

Heikkila, R. E., Nicklas, W. J., Vyas, I., and Duvoisin, R. C. (1985). Dopaminergic toxicity of rotenone and the 1-methyl-4-phenylpyridinium ion after their stereotaxic administration to rats: Implication for the mechanism of 1-methyl-4-phenyl-1,2,3,6-tetrahydropyridine toxicity. *Neurosci. Lett.* **62,** 389–394.

Hensley, K., Pye, Q. N., Maidt, M. L., Stewart, C. A., Robinson, K. A., Jaffrey, F., and Floyd, R. A. (1998). Interaction of alpha-phenyl-N-tert-butyl nitrone and alternative electron acceptors with complex I indicates a substrate reduction site upstream from the rotenone binding site. *J. Neurochem.* **71,** 2549–2557.

Herken, H. (1968). Functional disorders of the brain induced by synthesis of nucleotides containing 3-acetylpyridine. *Z. Klin. Chem. Klin. Biochem.* **6,** 357–367.

Hicks, S. P. (1950a). Brain metabolism in vivo I. *Arch. Pathol.* **49,** 111–137.

Hicks, S. P. (1950b). Brain metabolism in vivo II. *Arch. Pathol.* **50,** 545–561.

Higgins, D. S., Jr., and Greenamyre, J. T. (1996). [^{3}H] Dihydrorotenone binding to NADH: Ubiquinone reductase (complex I) of the electron transport chain: an autoradiographic study. *J. Neurosci.* **16,** 3807–3816.

Hirata, Y., Kiuchi, K., and Nagatsu, T. (2001). Manganese mimics the action of 1-methyl-4-phenylpyridinium ion, a dopaminergic neurotoxin, in rat striatal tissue slices. *Neurosci. Lett.* **311,** 53–56.

Horgan, D. J., Singer, T. P., and Casida, J. E. (1968). Studies on the respiratory chain-linked reduced nicotinamide adenine dinucleotide dehydrogenase: 13. Binding sites of rotenone, piericidin A, and amytal in the respiratory chain. *J. Biol. Chem.* **243,** 834–843.

Hsu, L. J., Sagara, Y., Arroyo, A., Rockenstein, E., Sisk, A., Mallory, M., Wong, J., Takenouchi, T., Hashimoto, M., and Masliah, E. (2000). α-Synuclein promotes mitochondrial deficit and oxidative stress. *Am. J. Pathol.* **157,** 401–410.

Huang, C. C., Chu, C. C., Chen, R. S., Lin, S. K., and Shih, T. S. (1996). Chronic carbon disulfide encephalopathy. *Eur. Neurol.* **36,** 364–368.

Huang, C. C., Chu, N. S., Lu, C. S., Chen, R. S., and Calne, D. B. (1998). Long-term progression in chronic manganism: Ten years of follow-up. *Neurology* **50,** 698–700.

Ihara, Y., Namba, R., Kuroda, S., Sato, T., and Shirabe, T. (1989). Mitochondrial encephalomyopathy (MELAS): Pathological study and successful therapy with coenzyme Q_{10} and idebenone. *J. Neurol. Sci.* **90,** 263–271.

Inagaki, S., Takagi, H., Suzuki, K., Akai, F., and Taniguchi, N. (1991). Intense immunoreactivity for Mn-superoxide dismutase (Mn-SOD) in cholinergic and non-cholinergic neurons in the rat basal forebrain. *Brain Res.* **541,** 354–357.

Irwin, I., and Langston, J. W. (1995). The selective accumulation of MPP+ in the substantia nigra: A key to neurotoxicity? *Life Sci.* **36,** 207–212.

Itano, Y., and Nomura, Y. (1995). 1-Methyl-4-phenylpyridinium ion (MPP+) causes DNA fragmentation and increases the Bcl-2 expression in human neuroblastoma, SH-SY5Y cells through different mechanisms. *Brain Res.* **704,** 240–245.

Jay, C., Ropka, M., and Dalakas, M. (1994). The drugs 2,3-dideoxyinosine (ddI) and 2,3-dideoxycytidine (ddC) are safe alternatives in people with AIDS with zidovudine-induced myopathy. *J. AIDS* **7,** 630–631.

Jenkins, B. G., Koroshetz, W., Beal, M. F., and Rosen, B. (1993). Evidence for an energy metabolism defect in Huntington's disease using localized proton spectroscopy. *Neurology* **43,** 2689–2695.

Kerns, W. P., and Kirk, M. A. (1998). Cyanide and hydrogen sulfide. *In "Goldfrank's Toxicologic Emergencies,"* 6th ed., p. 1567.

Khan, U., Filiano, B., King, M. P., and Przedborski, S. (1997). Is Parkinson's disease (PD) an extra-mitochondrial disorder? *Neurology* **48,** A201.

Kitada, T., Asakawa, S., Hattori, N., Matsumine, H., Yamamura, Y., Minoshima, S., Yokochi, M., Mizuno, Y., and Shimizu, N. (1998). Mutations in the parkin gene cause autosomal recessive juvenile parkinsonism. *Nature* **392,** 605–608.

Kitamura, Y., Kosaka, T., Kakimura, J. I., Matsuoka, Y., Kohno, Y., Nomura, Y., and Taniguchi, T. (1998). Protective effects of the antiparkinsonian drugs talipexole and pramipexole against 1-methyl-4-phenylpyridinium-induced apoptotic death in human neuroblastoma SH-SY5Y cells. *Mol. Pharmacol.* **54,** 1046–1054.

Klivenyi, P. St., Clair, D., Wermer, M., Yen, H. C., Oberley, T., Yang, L., and Beal, M. F. (1998a). Manganese superoxide dismutase overexpression attenuates MPTP toxicity. *Neurobiol. Dis.* **5,** 253–258.

Klivenyi, P., Beal, M. F., Ferrante, R. J., Andreassen, O. A., Wermer, M., Chin, M. R., and Bonventre, J. V. (1998b). Mice deficient in group IV cytosolic phospholipase A2 are resistant to MPTP neurotoxicity. *J. Neurochem.* **71,** 2634–2637.

Klivenyi, P., Ferrante, R. J., Matthews, R. T., Bogdanov, M. B., Klein, A. M., Andreassen, O. A., Mueller, G., Wermer, M., Kaddurah-Daouk, R., and Beal, M. F. (1999). Neuroprotective effects of creatine in a transgenic animal model of amyotrophic lateral sclerosis. *Nature Med.* **5,** 347–350.

Klivenyi, P., Andreassen, O. A., Ferrante, R. J., Lancelot, E., Reif, D., and Beal, M. F. (2000a). Inhibition of neuronal nitric oxide synthase protects against MPTP toxicity. *Neuroreport* **11,** 1265–1268.

Klivenyi, P., Andreassen, O. A., Ferrante, R. J., Dedeoglu, A., Mueller, G., Lancelot, E., Bogdanov, M., Andersen, J. K., Jiang, D., and Beal, M. F. (2000b). Mice deficient in cellular glutathione peroxidase show increased vulnerability to malonate, 3-nitropropionic acid, and 1-methyl-4-phenyl-1,2,5,6-tetrahydropyridine. *J. Neurosci.* **20,** 1–7.

Környey, S. (1963). Patterns of CNS vulnerability in CO, cyanide and other poisoning. *In* "Selective vulnerability of the brain in hypoxaemia" (J. P. Schadé and W. H. McMenemey, eds.), pp. 165–176. Oxford, Blackwell.

Korohoda, W., Pietrzkowski, Z., and Reiss, K. (1993). Chloramphenicol, an inhibitor of mitochondrial protein synthesis, inhibits myoblast fusion and myotube differentiation. *Folia Histochem. Cytobiol.* **31,** 9–13.

Koroshetz, W. J., Jenkins, B. G., Rosen, B. R., and Beal, M. F. (1997). Energy metabolism defects in Huntington's disease and possible therapy with coenzyme Q_{10}. *Ann. Neurol.* **41,** 160–165.

Kowall, N. W., Hantraye, P., Brouillet, E., Beal, M. F., McKee, A. C., and Ferrante, R. J. (2000). MPTP induces alpha-synuclein aggregation in the substantia nigra of baboons. *Neuroreport* **11,** 211–213.

Kristian, T., Gido, G., and Siesjo, B. K. (1995). The influence of acidosis on hypoglycemic brain damage. *J. Cereb. Blood Flow Metab.* **15,** 78–87.

Kunig, G., Hartmann, J., Niedermeyer, B., Deckert, J., Ransmayr, G., Heinsen, H., Beckmann, H., and Riederer, P. (1994). Excitotoxins L-beta-oxalyl-amino-alanine (L-BOAA) and 3,4,6-trihydroxyphenylalanine (6-OH-DOPA) inhibit [3H] alpha-amino-3-hydroxy-5-methyl-4-isoxazole-propionic acid (AMPA) binding in human hippocampus. *Neurosci. Lett.* **169,** 219–222.

Kurkowska-Jastrzebska, I., Wronska, A., Kohutnicka, M., Czlonkowski, A., and Czlonkowska, A. (1999). The inflammatory reaction following 1-methyl-4-phenyl-1,2,3,6-tetrahydropyridine intoxication in mouse. *Exp. Neurol.* **156,** 50–61.

Langston, J. W., Ballard, P., Tetrud, J. W., and Irwin, I. (1983). Chronic Parkinsonism in human due to a product of meperidine-analog synthesis. *Science* **219,** 979–980.

Langston, J. W., Forno, L. S., Tetrud, J., Reeves, A. G., Kaplan, J. A., and Karluk, D. (1999). Evidence of active nerve cell degeneration in the substantia nigra of humans years after 1-methyl-4-phenyl-1,2,3,6-tetrahydropyridine exposure. *Ann. Neurol.* **46,** 598–605.

Lee, M., Hyun, D. H., Halliwell, B., and Jenner, P. (2001). Effect of the overexpression of wild-type or mutant α-synuclein on cell susceptibility to insult. *J. Neurochem.* **76,** 998–1009.

Liberatore, G. T., Jackson-Lewis, V., Vukosavic, S., Mandir, A. S., Vila, M., McAuliffe, W. G., Dawson, V. L., Dawson, T. M., and Przedborski, S. (1999). Inducible nitric oxide synthase stimulates dopaminergic neurodegeneration in the MPTP model of Parkinson disease. *Nature Med.* **5,** 1403–1409.

Lista, A., Abarca, J., Ramos, C., and Daniels, A. J. (1986). Rat striatal dopamine and tetrahydrobiopterin content following an intrastriatal injection of manganese chloride. *Life Sci.* **38,** 2121–2127.

Lodi, R., Hart, P. E., Rajagopalan, B., Taylor, D. J., Crilley, J. G., Bradley, J. L., Blamire, A. M., Manners, D., Styles, P., Schapira, A. H., and Cooper, J. M. (2001). Antioxidant treatment improves in vivo cardiac and skeletal muscle bioenergetics in patients with Friedreich's ataxia. *Ann. Neurol.* **49,** 590–596.

Love, L. A., and Miller, F. W. (1993). Noninfectious environmental agents associated with myopathies. *Curr. Opin. Rheumatol.* **5,** 712–718.

Lu, C. S., Huang, C. C., Chu, N. S., and Calne, D. B. (1994). Levodopa failure in chronic manganism. *Neurology* **44,** 1600.

Ludolph, A. C., He, F., Spencer, P. S., Hammerstad, J., and Sabri, M. (1991). 3-Nitroproprionic acid-exogenous animal neurotoxin and possible human striatal toxin. *Can. J. Neurol. Sci.* **18,** 492–498.

Malcon, C., Kaddurah-Daouk, R., and Beal, M. F. (2000). Neuroprotective effects of creatine administration against NMDA and malonate toxicity. *Brain Res.* **860,** 195–198.

Mann, V. M., Cooper, J. M., Krige, D., Daniel, S. E., Schapira, A. H., and Marsden, C. D. (1992). Brain, skeletal-muscle and platelet homogenate mitochondrial function in Parkinson's disease. *Brain* **115,** 333–342.

Matthews, R. T., Beal, M. F., Fallon, J., Fedorchak, K., Huang, P. L., Fishman, M. C., and Hyman, B. T. (1997). MPP+ induced substantia nigra degeneration is attenuated in nNOS knockout mice. *Neurobiol. Dis.* **4,** 114–121.

Matthews, R. T., Yang, L., Jenkins, B. G., Ferrante, R. J., Rosen, B. R., Kaddurah-Daouk, R., and Beal, M. F. (1998). Neuroprotective effects of creatine and cyclocreatine in animal models of Huntington's disease. *J. Neurosci.* **18,** 156–163.

Matthews, R. T., Klivenyi, P., Mueller, G., Yang, L., Wermer, M., Thomas, C. E., and Beal, M. F. (1999). Novel free radical spin traps protect against malonate and MPTP neurotoxicity. *Exp. Neurol.* **157,** 120–126.

McNaught, K. S., Carrupt, P. A., Altomare, C., Cellamare, S., Carotti, A., Testa, B., Jenner, P., and Marsden, C. D. (1998). Isoquinoline derivatives as endogenous neurotoxins in the aetiology of Parkinson's disease. *Biochem. Pharmacol.* **56,** 921–933.

Melegh, B., and Trombitas, K. (1997). Valproate treatment induces lipid globule accumulation with ultrastructural abnormalities of mitochondria in skeletal muscle. *Neuropediatrics* **28,** 257–261.

Menegon, A., Board, P. G., Blackburn, A. C., Mellick, G. D., and Le Couteur, D. G. (1998). Parkinson's disease, pesticides, and glutathione transferase polymorphisms. *Lancet* **352,** 1344–1346.

Miyoshi, K. (1967). Experimental striatal necrosis induced by sodium azide. A contribution to the problem of selective vulnerability and histochemical studies of enzymatic activity. *Acta Neuropathol.* (Berl). **9,** 199–216.

Mizuno, Y., Ohta, S., Tanaka, M., Takamiya, S., Suzuki, K., Sato, T., Oya, H., Ozawa, T., and Kagawa, Y. (1989). Deficiencies in complex I subunits of the respiratory chain in Parkinson's disease. *Biochem. Biophys. Res. Commun.* **163,** 1450–1455.

Mochizuki, H., Nakamura, N., Nishi, K., and Mizuno, Y. (1994). Apoptosis is induced by 1-methyl-4-phenylpyridinium ion (MPP+) in ventral mesencephalic-striatal co-colture in rat. *Neurosci. Lett.* **170,** 191–194.

Mohanakumar, K. P., Muralikrishnan, D., and Thomas, B. (2000). Neuroprotection by sodium salicylate against 1-methyl-4-phenyl-1,2,3,6-tetrahydropyridine-induced neurotoxicity. *Brain Res.* **864,** 281–290.

Moussaoui, S., Obinu, M. C., Daniel, N., Reibaud, M., Blanchard, V., and Imperato, A. (2000). The antioxidant ebselen prevents neurotoxicity and clinical symptoms in a primate model of Parkinson's disease. *Exp. Neurol.* **166,** 235–245.

Muralikrishnan, D., and Mohanakumar, K. P. (1998). Neuroprotection by bromocriptine against 1-methyl-4-phenyl-1,2,3,6-tetrahydropyridine-induced neurotoxicity in mice. *FASEB J.* **12,** 905–912.

Mustafa, S. J., and Chandra, S. V. (1971). Levels of 5-hydroxytryptamine, dopamine and norepinephrine in whole brain of rabbits in chronic manganese toxicity. *J. Neurochem.* **18,** 931–933.

Mutoh, T., Tokuda, A., Marini, A. M., and Fujiki, N. (1994). 1-Methyl-4-phenylpyridinium kills differentiated PC12 cells with a concomitant change in protein phosphorylation. *Brain Res.* **661,** 51–55.

Neff, N. H., Barrett, R. E., and Costa, E. (1969). Selective depletion of caudate nucleus dopamine and serotonin during chronic manganese dioxide administration to squirrel monkeys. *Experientia* **25,** 1140–1141.

Newland, M. C., Ceckler, T. L., Kordower, J. H., and Weiss, B. (1989). Visualizing manganese in the primate basal ganglia with magnetic resonance imaging. *Exp. Neurol.* **106,** 251.

Nicklas, W. J., Vyas, I., and Heikkila, R. E. (1985). Inhibition of NADH-linked oxidation in brain mitochondria by 1-methyl-4-phenyl-pyridine, a metabolite of the neurotoxin, 1-methyl-4-phenyl-1,2,5,6-tetrahydropyridine. *Life Sci.* **36,** 2503–2508.

Nicotra, A., and Parvez, S. H. (2000). Cell death induced by MPTP, a substrate for monoamine oxidase B. *Toxicology* **153,** 157–166.

Novelli, A., Reilly, J. A., Lysko, P. G., and Henneberry, R. C. (1988). Glutamate becomes neurotoxic via the N-methyl-D-aspartate receptor when intracellular energy levels are reduced. *Brain Res.* **451,** 205–212.

Offen, D., Beart, P. M., Cheung, N. S., Pascoe, C. J., Hochman, A., Gorodin, S., Melamed, E., Bernard, R., and Bernard, O. (1998). Transgenic mice expressing human Bcl-2 in their neurons are resistant to 6-hydroxydopamine and 1-methyl-4-phenyl-1,2,3,6-tetrahydropyridine neurotoxicity. *Proc. Natl. Acad. Sci. USA* **95,** 5789–5794.

Oh, Y. J., Wong, S. C., Moffat, M., and O'Malley, K. L. (1995). Overexpression of Bcl-2 attenuates MPP+ but not 6-ODHA, induced cell death in a dopaminergic neuronal cell line. *Neurobiol. Dis.* **2,** 157–167.

Olanow, C. W., and Tatton, W. G. (1999). Etiology and pathogenesis of Parkinson's disease. *Ann. Rev. Neurosci.* **22,** 123–144.

Olanow, C. W., Good, P. F., Shinotoh, H., Hewitt, K. A., Vingerhoets, F., Snow, B. J., Beal, M. F., Calne, D. B., and Perl, D. P. (1996). Manganese intoxication in the rhesus monkey: A clinical, imaging, pathologic, and biochemical study. *Neurology* **46,** 492.

Pai, K. S., and Ravindranath, V. (1993). L-BOAA induces selective inhibition of brain mitochondrial enzyme, NADH-dehydrogenase. *Brain Res.* **621,** 215–221.

Pal, P. K., Samii, A., and Calne, D. B. (1999). Manganese neurotoxicity: A review of clinical features, imaging and pathology. *Neurotoxicology* **20,** 227–238.

Parker, W. D., Jr., Boyson, S. J., and Parks, J. K. (1989). Abnormalities of the electron transport chain in idiopathic Parkinson's disease. *Ann. Neurol.* **26,** 719–723.

Pedrol, E., Masanes, F., Fernandez-Sola, J., Cofan, M., Casademont, J., Grau, J. M., and Urbano-Marquez, A. (1996). Lack of muscle toxicity with didanosine (ddI): Clinical and experimental studies. *J. Neurol. Sci.* **138,** 42–48.

Pennathur, S., Jackson-Lewis, V., Przedborski, S., and Heinecke, J. W. (1999). Mass spectrometric quantification of 3-nitrotyrosine, ortho-tyrosine, and o,o′-dityrosine in brain tissue of 1-methyl-4-phenyl-1,2,3,6-tetrahydropyridine-treated mice, a model of oxidative stress in Parkinson's disease. *J. Biol. Chem.* **274,** 34621–34628.

Pentschew, A., Ebner, F. F., and Kovatch, R. M. (1962). Experimental manganese encephalopathy in monkeys: A preliminary report. *J. Neuropathol. Exp. Neurol.* **22,** 488.

Przedborski, S., and Jackson-Lewis, V. (1998). Mechanisms of MPTP toxicity. *Mov. Disord.* **13,** 35–38.

Przedborski, S., Kostic, V., Jackson-Lewis, V., Naini, A. B., Simonetti, S., Fahn, S., Carlson, E., Epstein, C. J., and Cadet, J. L. (1992). Transgenic mice with increased Cu/Zn-superoxide dismutase activity are resistant to N-methyl-4-phenyl-1,2,3,6-tetrahydropyridine-induced neurotoxicity. *J. Neurosci.* **12,** 1658–1667.

Przedborski, S., Chen, Q., Vila, M., Giasson, B. I., Djaldatti, R., Vukosavic, S., Souza, J. M., Jackson-Lewis, V. V., Lee, V. M., and Ischiropoulos, H. (2001). Oxidative post-translational modifications of α-synuclein in the 1-methyl-4-phenyl-1,2,3,6-tetrahydropyridine (MPTP) mouse model of Parkinson's disease. *J. Neurochem.* **76,** 637–640.

Rosenow, F., Herholz, K., Lanfermann, H., Weuthen, G., Ebner, R., Kessler, J., Ghaemi, M., and Heiss, W. D. (1995). Neurological sequelae of cyanide intoxication: The patterns of clinical, magnetic resonance imaging, and positron emission tomography findings. *Ann. Neurol.* **38,** 825.

Ross, S. M., and Spencer, P. S. (1987). Specific antagonism of behavioral action of "uncommon" amino acids linked to motor-system diseases. *Synapse* **1,** 248–253.

Rossetti, Z. L., Sotgiu, A., Sharp, D. E., Hadjiconstantinou, M., and Neff, N. H. (1988). 1-Methyl-4-phenyl-1,2,3,6-tetrahydropyridine (MPTP) and free radicals in vitro. *Biochem. Pharmacol.* **37,** 4573–4574.

Santiago, M., Machado, A., and Cano, J. (1996). Nigral and striatal comparative study of the neurotoxic action of 1-methyl-4-phenylpyridinium ion: Involvement of dopamine uptake system. *J. Neurochem.* **66,** 1182–1190.

Saporito, M. S., Brown, E. M., Miller, M. S., and Carswell, S. (1999). CEP-1347/KT-7515, an inhibitor of c-jun N-terminal kinase activation, attenuates the 1-methyl-4-phenyl tetrahydropyridine-mediated loss of nigrostriatal dopaminergic neurons in vivo. *J. Pharmacol. Exp. Ther.* **288,** 421–427.

Saporito, M. S., Thomas, B. A., and Scott, R. W. (2000). MPTP activates c-Jun NH(2)-terminal kinase (JNK) and its upstream regulatory kinase MKK4 in nigrostriatal neurons in vivo. *J. Neurochem.* **75,** 1200–1208.

Sayre, L. M. (1989). Biochemical mechanism of action of the dopaminergic neurotoxin 1-methyl-4-phenyl-1,2,3,6-tetrahydropyridine (MPTP). *Toxicol. Lett.* **48,** 121–149.

Schapira, A. H., Cooper, J. M., Dexter, D., Clark, J. B., Jenner, P., and Marsden, C. D. (1990). Mitochondrial complex I deficiency in Parkinson's disease. *J. Neurochem.* **54,** 823–827.

Schuler, F., Yano, T., Di Bernardo, S., Yagi, T., Yankovskaya, V., Singer, T. P., and Casida, J. E. (1999). NADH-quinone oxidoreductase: PSST subunit couples electron transfer from iron-sulfur cluster N2 to quinone. *Proc. Natl. Acad. Sci. USA* **96,** 4149–4153.

Schulz, J. B., Henshaw, D. R., Jenkins, B. G., Ferrante, R. J., Kowall, N. W., Rosen, B. R., and Beal, M. F. (1994). 3-Acetylpyridine produces age-dependent excitotoxic lesions in rat striatum. *J. Cereb. Blood Flow Metab.* **14,** 1024–1029.

Schulz, J. B., Henshaw, D. R., Matthews, R. T., and Beal, M. F. (1995a). Coenzyme Q10 and nicotinamide and a free radical spin trap protect against MPTP neurotoxicity. *Exp. Neurol.* **132,** 279–283.

Schulz, J. B., Matthews, R. T., Muqit, M. M. K., Browne, S. E., and Beal, M. F. (1995b). Inhibition of neuronal nitric oxide synthase by 7-nitroindazole protects against MPTP-induced neurotoxicity in mice. *J. Neurochem.* **64,** 936–939.

Schulz, J. B., Henshaw, D. R., Siwek, D., Jenkins, B. G., Ferrante, R. J., Cipolloni, P. B., Kowall, N. W., Rosen, B. R., and Beal, M. F. (1995c). Involvement of free radicals in excitotoxicity in vivo. *J. Neurochem.* **64,** 2239–2247.

Schulz, J. B., Matthews, R. T., Henshaw, D. R., and Beal, M. F. (1996a). Neuroprotective strategies for treatment of lesions produced by mitochondrial toxins: Implications for neurodegenerative diseases. *Neuroscience* **71,** 1043–1048.

Schulz, J. B., Henshaw, D. R., MacGarvey, U., and Beal, M. F. (1996b). Involvement of oxidative stress in 3-nitropropionic acid neurotoxicity. *Neurochem. Intl.* **29,** 167–171.

Seaton, T. A., Cooper, J. M., and Schapira, A. H. (1997). Free radical scavengers protect dopaminergic cell lines from apoptosis induced by complex I inhibitors. *Brain Res.* **777,** 110–118.

Semino-Mora, M., Leon-Monzon, M., and Dalakas, M. (1994). The effect of L-carnitine on the AZT-induced destruction of human myotubes. Part II: Treatment with L-carnitine improves the AZT-induced changes and prevents further destruction. *Lab. Invest.* **71,** 773–781.

Sethy, V. H., Wu, H., Oostveen, J. A., and Hall, E. D. (1996). Neuroprotective effects of the pyrrolopyrimidine U-104067F in 3-acetylpyridine-treated rats. *Exp. Neurol.* **140,** 79–83.

Sethy, V. H., Wu, H., Oostveen, J. A., and Hall, E. D. (1997a). Neuroprotective effects of the GABA(A) receptor partial agonist U-101017 in 3-acetylpyridine-treated rats. *Neurosci. Lett.* **228,** 45–49.

Sethy, V. H., Wu, H., Oostveen, J. A., and Hall, E. D. (1997b). Neuroprotective effects of the dopamine agonists pramipexole and bromocriptine in 3-acetylpyridine-treated rats. *Brain Res.* **754,** 181–186.

Seyfried, J., Soldner, F., Kunz, W. S., Schulz, J. B., Klockgether, T., Kovar, K. A., and Wüllner, U. (2000). Effect of 1-methyl-4-phenylpyridinium on glutathione in rat pheochromocytoma PC 12 cells. *Neurochem. Int.* **36,** 489–497.

Sheehan, J. P., Palmer, P. E., Helm, G. A., and Tuttle, J. B. (1997). MPP+ induced apoptotic cell death in SH-SY5Y neuroblastoma cells: An electron microscope study. *J. Neurosci. Res.* **48,** 226–237.

Sherer, T. B., Trimmer, P. A., Borland, K., Parks, J. K., Bennett, J. P., Jr., and Tuttle, J. B. (2001). Chronic reduction in complex I function alters calcium signaling in SH-SY5Y neuroblastoma cells. *Brain Res.* **891,** 94–105.

Shibasaki, H. (1969). Electron microscope study of the rat brain with experimental sodium azide intoxication. *Acta Neuropathol* (Berl). **14,** 185–193.

Shults, C. W., Haas, R. H., Passov, D., and Beal, M. F. (1997). Coenzyme Q10 is reduced in mitochondria from parkinsonian patients. *Ann. Neurol.* **42,** 261–264.

Sloot, W. N., van der Sluijs-Gelling, A. J., and Gramsberger, J. B. P. (1994). Selective lesions by manganese and extensive damage by iron after injection in rat striatum or hippocampus. *J. Neurochem.* **62,** 205.

Snyder, J. W., Safir, E. R., and Summerville, G. P. (1995). Occupational fatality and persistent neurological sequelae after mass exposure to hydrogen sulfide. *Am. J. Emerg. Med.* **13,** 199.

Soldner, F., Weller, M., Haid, S., Beinroth, S., Miller, S. W., Wüllner, U., Davis, R. E., Dichgans, J., Klockgether, T., and Schulz, J. B. (1999). MPP+ inhibits proliferation of PC12 cells by a p21WAF1/Cip1-dependent pathway and induces cell death in cells lacking p21WAF1/Cip1. *Exp. Cell Res.* **250,** 75–85.

Spencer, P. S. (1995). Lathyrism. *In* "Handbook of Clinical Neurology" (P. J. Vinken and G. W. Bruyn, eds.), pp. 1–20. Elsevier, Amsterdam.

Spencer, P. S., Roy, D. N., Ludolph, A., Hugon, J., Dwivedi, M. P., and Schaumburg, H. H. (1986). Lathyrism: Evidence for role of the neuroexcitatory aminoacid BOAA. *Lancet* **2,** 1066–1067.

Spencer, P. S., Nunn, P. B., Hugon, J., Ludolph, A. C., Ross, S. M., Roy, D. N., and Robertson, R. C. (1987). Guam amyotrophic lateral sclerosis-parkinsonism-dementia linked to a plant excitant neurotoxin. *Science* **237,** 517–522.

Spranger, M., Schwab, S., Desiderato, S., Bonmann, E., Krieger, D., and Fandrey, J. (1998). Manganese augments nitric oxide synthesis in murine astrocytes: A new pathogenetic mechanism in manganism? *Exp. Neurol.* **149,** 277.

Sriram, K., Shankar, S. K., Boyd, M. R., and Ravindranath, V. (1998). Thiol oxidation and loss of mitochondrial complex 1 precede excitatory amino acid-mediated neurodegeneration. *J. Neurosci.* **18,** 10287–10296.

Steiner, J. P., Hamilton, G. S., Ross, D. T., Valentine, H. L., Guo, H., Connolly, M. A., Liang, S., Ramsey, C., Li, J. H., Huang, W., Howorth, P., Soni, R., Fuller, M., Sauer, H., Nowotnik, A. C., and Suzdak, P. D. (1997). Neurotrophic immunophilin ligands stimulate structural and functional recovery in neurodegenerative animal models. *Proc. Natl Acad. Sci. USA* **94,** 2019–2024.

Storch, A., Ludolph, A. C., and Schwarz, J. (1999). HEK-293 cells expressing the human dopamine transporter are susceptible to low concentrations of 1-methyl-4-phenylpyridine (MPP+) via impairment of energy metabolism. *Neurochem. Int.* **35,** 393–403.

Swerdlow, R. H., Parks, J. K., Davis, J. N., 2nd, Cassarino, D. S., Trimmer, P. A., Currie, L. J., Dougherty, J., Bridges, W. S., Bennett, J. P., Jr., Wooten, G. F., and Parker, W. D. (1998). Matrilineal inheritance of complex I dysfunction in a multigenerational Parkinson's disease family. *Ann. Neurol.* **44,** 873–881.

Tahar, A. H., Ekesbo, A., Gregoire, L., Bangassoro, E., Svensson, K. A., Tedroff, J., and Bedard, P. J. (2001). Effects of acute and repeated treatment with a novel dopamine D2 receptor ligand on L-DOPA-induced dyskinesias in MPTP monkeys. *Eur. J. Pharmacol.* **412,** 247–254.

Takada, M., and Kono, T. (1993). 3-Acetylpyridine neurotoxicity to the nigrostriatal dopamine system in mice. *Neurosci. Lett.* **161,** 211–214.

Takahashi, N., Miner, L. L., Sora, I., Ujike, H., Revay, R. S., Kostic, V., Jackson-Lewis, V., Przedborski, S., and Uhl, G. R. (1997). VMAT2 knockout mice: heterozygotes display reduced amphetamine-conditioned reward, enhanced amphetamine locomotion, and enhanced MPTP toxicity. *Proc. Natl. Acad. Sci. USA* **94,** 9938–9943.

Tarnopolsky, M. A., and Beal, M. F. (2001). Potential for creatine and other therapies targeting cellular energy dysfunction in neurological disorders. *Ann. Neurol.* **49,** 561–574.

Tatton, N. A. (2000). Increased caspase 3 and Bax immunoreactivity accompany nuclear GAPDH translocation and neuronal apoptosis in Parkinson's disease. *Exp. Neurol.* **166,** 29–43.

Tatton, N. A., and Kish, S. J. (1997). In situ detection of apoptotic nuclei in the substantia nigra compacta of 1-methyl-4-phenyl-1,2,3,6-tetrahydropyridine-treated mice using terminal deoxynucleotidyl transferase labelling and acridine orange staining. *Neuroscience* **77,** 1037–1048.

Teismann, P., and Ferger, B. (2001). Inhibition of the cyclooxygenase isoenzymes COX-1 and COX-2 provide neuroprotection in the MPTP-mouse model of Parkinson's disease. *Synapse* **39,** 167–174.

Tipton, K. F., and Singer, T. P. (1993). Advances in our understanding of the mechanisms of the neurotoxicity of MPTP and related compounds. *J. Neurochem.* **61,** 1191–1206.

Treseder, S. A., Smith, L. A., and Jenner, P. (2000). Endogenous dopaminergic tone and dopamine agonist action. *Mov. Disord.* **15,** 804–812.

Trimmer, P. A., Smith, T. S., Jung, A. B., and Bennett, J. P. Jr. (1996). Dopamine neurons from transgenic mice with a knockout of the p53 gene resist MPTP neurotoxicity. *Neurodegeneration* **5,** 233–239.

Tvedt, B., Skyberg, K., Aaserud, O., Hobbesland, A., and Mathiesen, T. (1991). Brain damage caused by hydrogen sulfide: A follow-up study of six patients. *Am. J. Indust. Med.* **20,** 91.

Uitti, R. J., Rajput, A. H., Ashenhurst, E. M., and Rozdilsky, B. (1985). Cyanide-induced parkinsonism: A clinicopathologic report. *Neurology* **35,** 921.

Varastet, M., Riche, D., Maziere, M., and Hantraye, P. (1994). Chronic MPTP treatment reproduces in baboons the differential vulnerability of mesencephalic dopaminergic neurons observed in Parkinson's disease. *Neuroscience* **63,** 47–56.

Vila, M., Vukosavic, S., Jackson-Lewis, V., Neystat, M., Jakowec, M., and Przedborski, S. (2000). α-Synuclein upregulation in substantia nigra dopaminergic neurons following administration of the parkinsonian toxin MPTP. *J. Neurochem.* **74,** 721–729.

Vila, M., Jackson-Lewis, V., Vukosavic, S., Djaldetti, R., Liberatore, G., Offen, D., Korsmeyer, S. J., and Przedborski, S. (2001). Bax ablation prevents dopaminergic neurodegeneration in the 1-methyl-4-phenyl-1,2,3,6-tetrahydropyridine mouse model of Parkinson's disease. *Proc. Natl. Acad. Sci. USA* **98,** 2837–2842.

Waldmeier, P. C., Spooren, W. P., and Hengerer, B. (2000). CGP 3466 protects dopaminergic neurons in lesion models of Parkinson's disease. *Naunyn Schmiedebergs Arch. Pharmacol.* **362,** 526–537.

Weller, M., Marini, A. M., and Paul, S. M. (1992). Niacinamide blocks 3-acetylpyridine toxicity of cerebellar granule cells in vitro. *Brain Res.* **594,** 160–164.

Wieland, S., Kreider, M. S., McGonigle, P., and Lucki, I. (1990). Destruction of the nucleus raphe obscurus and potentiation of serotonin-mediated behaviors following administration of the neurotoxin 3-acetylpyridine. *Brain Res.* **520,** 291–302.

Willis, C. L., Meldrum, B. S., Nunn, P. B., Anderton, B. H., and Leigh, P. N. (1993). Neuronal damage induced by beta-N-oxalylamino-L-alanine, in the rat hippocampus, can be prevented by a non-NMDA antagonist, 2,3-dihydroxy-6-nitro-7-sulfamoylbenzo(F)quinoxaline. *Brain Res.* **627,** 55–62.

Willis, C. L., Meldrum, B. S., Nunn, P. B., Anderton, B. H., and Leigh, P. N. (1994). Neuroprotective effect of free radical scavengers on beta-N-oxalylamino-L-alanine (BOAA)-induced neuronal damage in rat hippocampus. *Neurosci. Lett.* **182,** 159–162.

Wolters, E. C., Huang, C. C., Clark, C., Peppard, R. F., Okada, J., Chu, N. S., Adam, M. J., Ruth, T. J., Li, D., and Calne, D. B. (1989). Positron emission tomography in manganese intoxication. *Ann. Neurol.* **26,** 647.

Wüllner, U., Young, A., Penney, J., and Beal, M. F. (1994). 3-Nitropropionic acid toxicity in the striatum. *J. Neurochem.* **63,** 1772–1781.

Wüllner, U., Loschmann, P. A., Schulz, J. B., Schmid, A., Dringen, R., Eblen, F., Turski, L., and Klockgether, T. (1996). Glutathione depletion potentiates MPTP and MPP+ toxicity in nigral dopaminergic neurones. *Neuroreport* **7,** 921–923.

Yamada, M., Ohno, S., Okayasu, I., Okeda, R., Hatakeyama, S., Watanabe, H., Ushio, K., and Tsukagoshi, H. (1986). Chronic manganese poisoning: A neuropathological study with determination of manganese distribution in the brain. *Acta Neuropathol. (Berlin)* **70,** 273.

Yang, L., Matthews, R. T., Schulz, J. B., Klockgether, T., Liao, A. W., Martinou, J. C., Penney, J. B., Jr., Hyman, B. T., and Beal, M. F. (1998). 1-Methyl-4-phenyl-1,2,3,6-tetrahydropyride neurotoxicity is attenuated in mice overexpressing Bcl-2. *J. Neurosci.* **18,** 8145–8152.

Zedda, M., Acone, F., Panu, R., Farina, V., Sanna, L., and Palmieri, G. (1996). Neurotoxic effects of 3-acetylpyridine (3-AP) in the hamster (mesocricetus auratus). *Ital. J. Anat. Embryol.* **101,** 57–66.

Zeevalk, G. D., and Nicklas, W. J. (1991). Mechanisms underlying initiation of excitotoxicity associated with metabolic inhibition. *J. Pharm. Exp. Ther.* **257,** 870–878.

Zeevalk, G. D., and Nicklas, W. J. (1994). Nitric oxide in retina: Relation to excitatory amino acids and excitotoxicity. *Exp. Eye Res.* **58,** 343–350.

Zheng, W., Ren, S., and Graziano, J. H. (1998). Manganese inhibits mitochondrial aconitase, a mechanism of manganese neurotoxicity. *Brain Res.* **799,** 334.

Zou, L., Xu, J., Jankovic, J., He, Y., Appel, S. H., and Le, W. (2000). Pramipexole inhibits lipid peroxidation and reduces injury in the substantia nigra induced by the dopaminergic neurotoxin 1-methyl-4-phenyl-1,2,3,6-tetrahydropyridine in C57BL/6 mice. *Neurosci. Lett.* **281,** 167–170.

Neurobiology of Disease **11,** 410–424 (2002)
doi:10.1006/nbdi.2002.0562

Huntington's Disease of the Endocrine Pancreas: Insulin Deficiency and Diabetes Mellitus due to Impaired Insulin Gene Expression

Ole A. Andreassen,[*] Alpaslan Dedeoglu,[*,†] Violeta Stanojevic,[‡,§] Duncan B. Hughes,[¶] Susan E. Browne,[¶] Colin A. Leech,[‡,§] Robert J. Ferrante,[†] Joel F. Habener,[‡,§] M. Flint Beal,[*,¶] and Melissa K. Thomas[‡,‖,1]

[*]*Neurochemistry Laboratory,* [‡]*Laboratory of Molecular Endocrinology, and* [‖]*Diabetes Unit, Massachusetts General Hospital,* [§]*Howard Hughes Medical Institute and Harvard Medical School, Boston, Massachusetts 02114;* [†]*Geriatric Research Education and Clinical Center, Bedford VA Medical Center, Bedford, Massachusetts 01730, and Boston University School of Medicine, Boston, Massachusetts 02118; and* [¶]*Neurology Department, New York Hospital–Cornell Medical Center, New York, New York 10021*

Received April 22, 2002; revised September 25, 2002; accepted for publication October 3, 2002

In a transgenic mouse model of the neurodegenerative disorder Huntington's disease (HD), age-dependent neurologic defects are accompanied by progressive alterations in glucose tolerance that culminate in the development of diabetes mellitus and insulin deficiency. Pancreatic islets from HD transgenic mice express reduced levels of the pancreatic islet hormones insulin, somatostatin, and glucagon and exhibit intrinsic defects in insulin production. Intranuclear inclusions accumulate with aging in transgenic pancreatic islets, concomitant with the decline in glucose tolerance. HD transgenic mice develop an age-dependent reduction of insulin mRNA expression and diminished expression of key regulators of insulin gene transcription, including the pancreatic homeoprotein PDX-1, E2A proteins, and the coactivators CBP and p300. Disrupted expression of a subset of transcription factors in pancreatic β cells by a polyglutamine expansion tract in the huntingtin protein selectively impairs insulin gene expression to result in insulin deficiency and diabetes. Selective dysregulation of gene expression in triplet repeat disorders provides a mechanism for pleiotropic cellular dysfunction that restricts the toxicity of ubiquitously expressed proteins to highly specialized subpopulations of cells.

INTRODUCTION

Neurodegeneration with aging occurs in a large number of diseases, including Huntington's disease, spinal and bulbar muscular atrophy, spinocerebellar ataxias, and dentatorubropallidoluysian atrophy, as a result of the incorporation of polyglutamine segments encoded by trinucleotide CAG repeats within targeted proteins (Martin, 1999). The mechanisms of neuronal degeneration in these disorders are unknown, but likely involve gain or loss of the normal functions of the mutant proteins, abnormal protein–protein interactions, toxicity from the accumulation of polyglutamine-containing intranuclear inclusions, and aberrant protein processing through the ubiquitin/proteasome pathway (Ferrigno and Silver, 2000; Martin, 1999). Huntington's disease (HD), an autosomal dominant neurodegenerative disease characterized by a severe movement disorder, cognitive impairment, and early death, results from an expanded polyglutamine repeat in the amino terminus of huntingtin, a widely

[1] To whom correspondence should be addressed at Laboratory of Molecular Endocrinology and Diabetes Unit, Massachusetts General Hospital, Wellman 340, 50 Blossom Street, Boston, MA 02114. Fax: (617) 726-6954. E-mail: mthomas1@partners.org.

0969-9961/03 $35.00

expressed protein of unknown function (The Huntington's Disease Collaborative Research Group, 1993). Excitotoxic mechanisms, mitochondrial energy impairment, oxidative damage, and apoptosis also are implicated in the pathogenesis of HD (Beal, 2000; Browne *et al.*, 1999).

Polyglutamine tracts independently contribute to cellular toxicity. The numbers of CAG repeats correlate with both age of onset and severity of disease in polyglutamine expansion disorders (Young, 1998). Long polyglutamine tracts promote cell injury (Nagai *et al.*, 1999; Senut *et al.*, 2000), the formation of intranuclear aggregates (Onodera *et al.*, 1997; Preisinger *et al.*, 1999), and the sequestration of glutamine-rich proteins (Kazantsev *et al.*, 1999; Preisinger *et al.*, 1999). Altered patterns of gene expression are observed in cellular and animal models of CAG repeat disorders (Cha *et al.*, 1998; Li *et al.*, 1999; Lin *et al.*, 2000; Luthi-Carter *et al.*, 2000) in which polyglutamine tracts in mutant proteins can mediate direct interaction with nuclear proteins, including coactivators and corepressors (Boutell *et al.*, 1999; Hsiao *et al.*, 1999; Kegel *et al.*, 2002; Nucifora *et al.*, 2001; Steffan *et al.*, 2001; Stenoien *et al.*, 1999; Waragai *et al.*, 1999).

Diabetes mellitus, a disorder with increasing prevalence of epidemic proportions, results from a failure of the β cells within the islets of Langerhans of the endocrine pancreas to produce insulin in sufficient amounts to maintain normal blood glucose levels. Normal regulation of insulin gene transcription is of central importance in the maintenance of glucose homeostasis. Multiple forms of heritable diabetes, including maturity-onset diabetes of the young (MODY) and type 2 diabetes, are associated with mutations in transcription factors that regulate the expression of the insulin gene (Fajans *et al.*, 2001; Hani *et al.*, 1999; Macfarlane *et al.*, 1999; Stoffers *et al.*, 1997a). Patients with HD have an increased prevalence of diabetes and have pathological glucose tolerance tests (Farrer, 1985; Podolsky and Leopold, 1977). The etiology of this diabetes is unknown. HD transgenic mice develop hyperglycemia (Hurlbert *et al.*, 1999; Jenkins *et al.*, 2000), providing an experimental model system for studies of diabetes mellitus and HD. Here we report that HD transgenic mice develop intranuclear inclusions in the pancreatic β cells that produce insulin. The accumulation of intranuclear inclusions is temporally associated with selective impaired expression of transcriptional regulatory proteins essential for glucose-responsive insulin gene expression and with progressive reductions in insulin mRNA expression that culminate in the development of diabetes.

METHODS

HD Transgenic Mice

Male R6/2 transgenic mice (Mangiarini *et al.*, 1996) [B6CBA-TgN (HD exon1) 62Gpb: The Jackson Laboratory, Bar Harbor, ME] were bred with female B6CBA mice (The Jackson Laboratory). All studies were conducted in accordance with the NIH *Guide for the Care and Use of Laboratory Animals* with approval from the local institutional animal care and use committee.

Glucose, Insulin, and Glycated Hemoglobin Measurements

Plasma glucose levels were assessed with a One Touch Basic Glucose Monitoring System glucometer (Lifescan Inc., Milpitas, CA) and validated by semiautomatic glucose oxidase enzyme assays. Random glucose levels were obtained in mice with free access to chow, and fasting glucose levels were obtained after 6–7 h of fasting. For glucose tolerance testing, animals were fasted for 6–7 h prior to intraperitoneal injection of 1.5 g glucose/kg body wt and tail vein blood samples were collected 0, 30, and 60 min following glucose administration. For insulin administration intermediate-acting purified pork insulin (Lente Iletin II, Lilly, Indianapolis, IN) was administered by intraperitoneal injection. Tail vein blood samples were collected at the indicated times for glucose measurements.

Plasma insulin levels were determined in duplicate using a rat insulin ELISA kit normalized with mouse insulin standards (Crystal Chem., Inc., Chicago, IL). Pancreatic islets were isolated from 12-week-old HD or nontransgenic littermate control mice using standard methods and manually separated from digested exocrine tissue as visualized by stereomicroscopy (Lacy and Kostianovsky, 1967). Islets of comparable size were incubated in multiwell culture dishes with 25 islets per well in modified RPMI medium at 37°C. After 90- to 120-min preincubation period, culture medium was replaced and aliquots of medium were removed for insulin radioimmunoassays (Linco Research, Inc., St. Charles, MO) following an additional 1- or 24-h incubation period.

Glycated hemoglobin levels were measured from whole blood samples with a Glyc-Affin Ghb kit (Isolab, Inc.). *P* values were determined with Student's *t* test (Microsoft Excel, Microsoft Corporation, Redmond, WA).

Immunohistochemistry

Pancreatic tissues from R6/2 transgenic and nontransgenic littermate control mice were embedded in Tissue-Tek O.C.T. compound (Sakura Finetek, Torrance, CA) and frozen on dry ice or embedded in paraffin, and fixed and processed as described (Thomas *et al.*, 1999). Primary antisera included guinea pig anti-insulin (Linco Research, Inc.), rabbit polyclonal anti-somatostatin (Dako Corp., Carpinteria, CA), rabbit polyclonal anti-proglucagon, rabbit polyclonal anti-PDX-1 (Stoffers *et al.*, 2000), rabbit polyclonal anti-CBP (A-22), rabbit polyclonal anti-p300 (C-20), rabbit polyclonal anti-E2A (V-18), and goat polyclonal anti-huntingtin (N-18) (Santa Cruz Biotechnology, Inc., Santa Cruz, CA). Immunostaining was developed with biotinylated secondary antisera and avidin–horseradish peroxidase complex kits (Vectastain ABC System, Vector Laboratories, Burlingame, CA) or with donkey anti-goat IgG Cy3 and donkey anti-guinea pig IgG Cy2 (Jackson ImmunoResearch, West Grove, PA). Rabbit polyclonal antiserum directed against the first 256 amino acids of the human huntingtin protein (EM48) was used to stain intranuclear inclusions as described (Kuemmerle *et al.*, 1999). Images were captured with an Optronics TEC-470 camera (Optronics Engineering, Goleta, CA) or a SPOT-RT color camera (Diagnostic Instruments, Inc., Sterling Heights, MI) and a Nikon epifluorescence microscope interfaced with a Macintosh computer and processed with IP Lab Spectrum (Signal Analytics Corp., Vienna, VA) and Adobe Photoshop (Adobe Systems Incorporated, San Jose, CA) software.

Northern Blots

Total pancreatic RNA was prepared with Qiagen RNeasy columns (Qiagen Inc., Valencia, CA), by modifying the manufacturer's protocol to include 1 M β-mercaptoethanol during tissue homogenization. RNA was separated on 1% agarose gels and visualized with ethidium bromide prior to blotting on nylon membranes (Hybond-N+, Amersham Pharmacia Biotech, Inc., Piscataway, NJ). Insulin transcripts were probed with a ^{32}P-radiolabeled 231-nucleotide fragment of rat insulin cDNA as described (Thomas *et al.*, 2000). Corresponding autoradiograms were scanned with a Computing Densitometer (Molecular Dynamics, Sunnyvale, CA) and band intensities were calculated using ImageQuant software (Molecular Dynamics).

Western Blots

Total pancreatic or pancreatic islet protein extracts were prepared in an SDS lysis buffer (Stoffers *et al.*, 2000). Equal amounts of protein as determined with a MicroBCA kit (Pierce, Rockford, IL) were separated by SDS–polyacrylamide gel electrophoresis, electroblotted on Immobilon PVDF (Millipore, Bedford, MA) membranes, subjected to Western blotting with rabbit polyclonal anti-PDX-1, rabbit polyclonal anti-Creb, rabbit polyclonal anti-glucagon-like peptide-1 (GLP-1) receptor, rabbit polyclonal anti-Stat-3 (K-15), rabbit polyclonal anti-CEBP-β (C-19), goat polyclonal anti-Smad 2/3 (N-19), rabbit polyclonal anti-actin (H-300) (Santa Cruz Biotechnology), or mouse monoclonal anti-p300 (RW 128) antiserum (Upstate Biotechnology, Lake Placid, NY), and developed with species-specific secondary antiserum and enhanced chemiluminescence (Amersham Life Sciences, Arlington Heights, IL) (Thomas *et al.*, 2001b). In some experiments blots were sequentially probed with antiserum, developed with enhanced chemiluminescence, washed, and reprobed with additional antiserum.

Intracellular Calcium Measurements

Pancreatic islets were isolated from HD transgenic or nontransgenic littermate control mice according to standard methods (Lacy and Kostianovsky, 1967) and dispersed with trypsin. Single-cell suspensions were plated on concanavalin A-coated coverslips and cultured in modified RPMI medium. Cells were loaded with fura-2 acetoxymethyl ester, bathed in a solution containing 138 mM NaCl, 5.6 mM KCl, 2.6 mM $CaCl_2$, 1.2 mM $MgCl_2$, 10 mM Hepes, pH 7.4, and 5.6 mM glucose, and incubated at 32°C. Intracellular calcium levels were measured with an IonOptix fluorescence ratio imaging system (Leech and Habener, 1997).

RESULTS

Huntington's Disease Transgenic Mice Develop Progressive Defects in Glucose Tolerance with Aging

The HD (R6/2) transgenic mice express an expansion tract of 145–150 CAG repeats within a transcript encoding a portion of the human huntingtin protein. This established mouse model develops a rapidly progressive postnatal neurologic phenotype reminiscent of HD in humans that begins at about 8 weeks of age

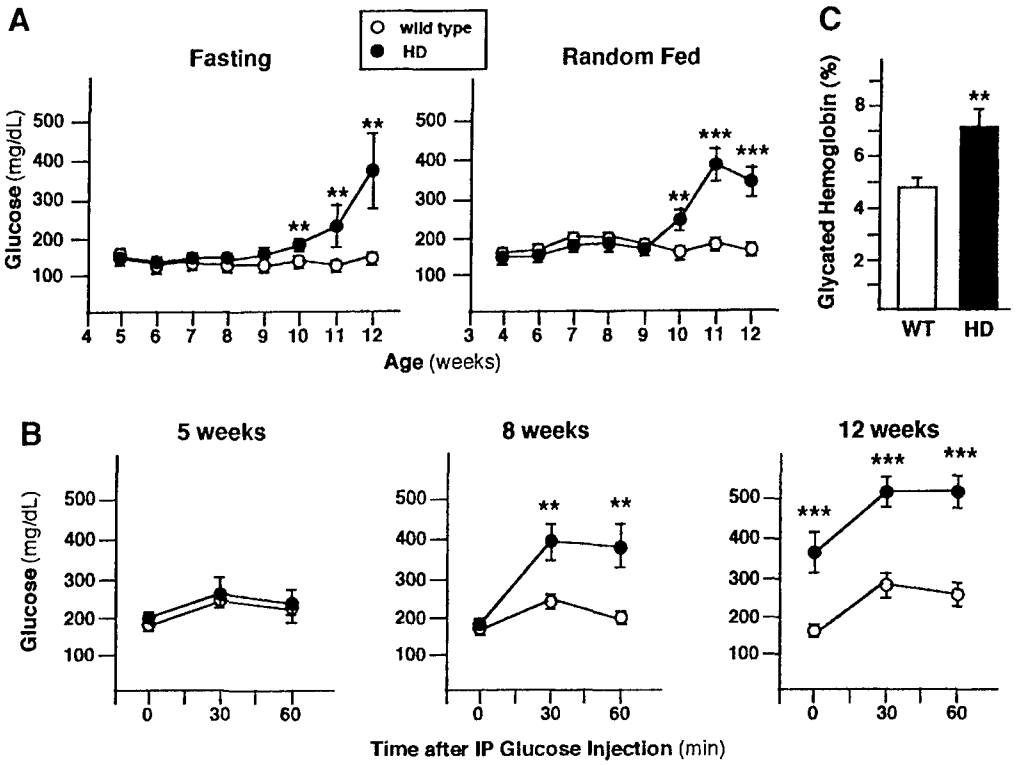

FIG. 1. Progressive development of diabetes mellitus in HD transgenic mice. (A) Fasting and random-fed glucose levels rise with aging in HD transgenic mice. Fasting (left) and random (ad lib)-fed (right) glucose levels were measured from R6/2 HD transgenic (HD, solid circles) and nontransgenic littermate control (wild type, open circles) mice at the ages indicated. Data are presented as means ± SEM (n = 6–12 per group; $^{**}P < 0.01$, $^{***}P < 0.001$). (B) Glucose tolerance declines with aging in HD transgenic mice. Intraperitoneal glucose tolerance tests were conducted on R6/2 HD transgenic (HD, solid circles) and nontransgenic littermate control (wild type, open circles) mice at 5, 8, and 12 weeks of age, as indicated. Data are presented as means ± SEM (n = 8–10 per group; $^{**}P < 0.01$, $^{***}P < 0.001$). (C) Glycated hemoglobin levels are elevated in 12-week-old HD transgenic mice. Glycated hemoglobin levels were measured in 12-week-old R6/2 HD transgenic (HD) and nontransgenic littermate control (WT) mice. Data are presented as means ± SEM (n = 8–10 per group; $^{**}P < 0.01$).

and culminates in death by 14 weeks of age (Mangiarini *et al.*, 1996). The phenotype also includes the appearance of neuronal intranuclear inclusions similar to those described in human patients with HD (Davies *et al.*, 1999). To assess metabolic function in HD transgenic mice glucose levels were measured at regular intervals between 4 and 12 weeks of age. Fasting and random-fed serum glucose levels were similar in HD transgenic and nontransgenic littermate control mice for the first 9 weeks of life (Fig. 1A). By 10 weeks of age HD transgenic animals had significantly higher serum glucose levels than nontransgenic littermate controls, and both fasting and random-fed glucose levels continued to rise with age.

The course of the metabolic dysfunction of HD transgenic mice is more clearly demonstrated by intraperitoneal glucose tolerance testing (Fig. 1B). At 5 weeks of age glucose tolerance tests of HD transgenic mice and their nontransgenic littermate controls were indistinguishable. By 8 weeks of age HD transgenic and nontransgenic littermate control mice had comparable fasting glucose levels, but the transgenic mice had impaired glucose tolerance. At 12 weeks of age HD transgenic mice had diabetes mellitus with fasting hyperglycemia and markedly abnormal glucose tolerance. The HD diabetic phenotype also was apparent in measurements of glycated hemoglobin levels, a method that reflects the average serum glucose levels over the 2 to 3 weeks prior to testing and hence is unaffected by acute central nervous system input during sample collection. Glycated hemoglobin levels of 8-week-old HD transgenic mice were not significantly higher than those of nontransgenic littermate controls, but 12-week-old HD transgenic mice had elevated glycated hemoglobin levels typical of diabetes (Fig. 1C).

Insulin Production Is Reduced in Huntington's Disease Transgenic Mice

Metabolic dysfunction that worsens with aging from impaired glucose tolerance to diabetes mellitus often is observed in the progression of Type 2 diabetes in humans. Adult-onset diabetes frequently is characterized by insulin resistance of target tissues with compensatory hyperinsulinemia. In our analyses the HD transgenic mice with diabetes had no demonstrable hyperinsulinemia. Fasting serum insulin levels from 12-week-old HD transgenic mice were approximately threefold lower than those from nontransgenic littermate control mice (Fig. 2A). The insulin levels were remarkably low in HD transgenic mice when considered in the context of the accompanying hyperglycemia. No significant differences in fasting serum insulin levels were observed between HD transgenic mice and nontransgenic littermate control mice at 7 or 9 weeks of age before the development of diabetes.

Pancreatic β Cells from Huntington's Disease Transgenic Mice with Diabetes Have an Intrinsic Defect in Insulin Production

The reduction in serum insulin levels of HD transgenic mice with diabetes suggested that insulin production from the β cells of the islets of Langerhans of the endocrine pancreas might be impaired. To test for intrinsic β-cell defects independent of central nervous system dysfunction, pancreatic islets from 12-week old diabetic HD transgenic mice and nontransgenic littermate controls were isolated and cultured. One-hour *ex vivo* insulin secretion was reduced by two-thirds in islets derived from HD transgenic mice relative to those derived from nontransgenic littermate control mice (Fig. 2B). Insulin secretion also was measured from the islets in culture over a longer period of 24 h to control for prior short-term depletion of insulin stores in the HD diabetic mice. This extended culture period was selected to allow time for recovery from hyperglycemia and for replenishing of intracellular insulin content. After 24 h in culture the islets derived from HD diabetic mice had a more severe defect in insulin secretion relative to islets derived from nontransgenic littermate controls, with a 10-fold reduction in insulin secretion after 24 h as compared with a 3-fold reduction after the first hour of culture. These results implied that the decreased insulin secretion from pancreatic islets of HD transgenic mice was secondary to diminished insulin production. Consistent with hyperglycemia secondary to insulin deficiency,

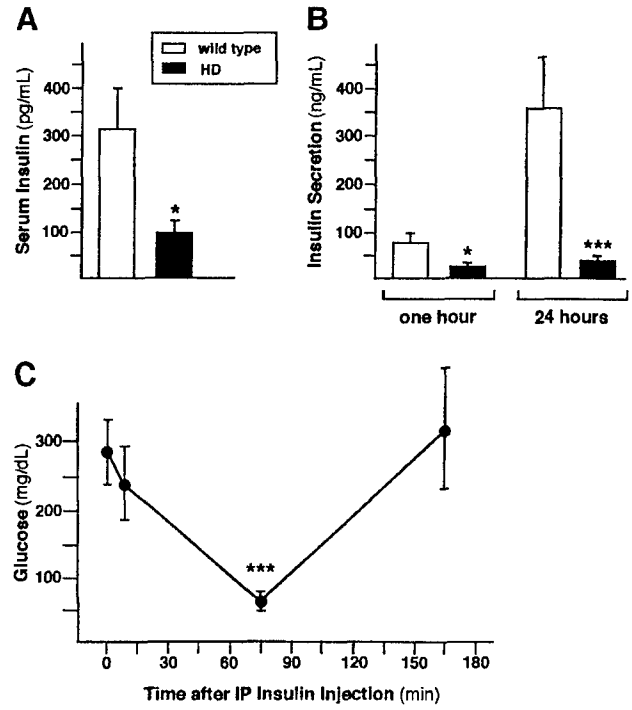

FIG. 2. Insulin production is diminished in diabetic HD transgenic mice. (A) Serum insulin levels are reduced in 12-week-old HD transgenic mice. Fasting serum insulin levels were measured in 12-week-old R6/2 HD transgenic (HD, solid bar) and nontransgenic littermate control (wild type, open bar) mice. Data are presented as means ± SEM (n = 8–11 per group; $^*P < 0.05$). (B) Pancreatic islets derived from HD transgenic mice have intrinsic defects in insulin production. Pancreatic islets were isolated and cultured *ex vivo* from 12-week-old R6/2 HD transgenic (HD, solid bars) and nontransgenic littermate control (wild type, open bars) mice. Insulin secretion was measured by radioimmunoassay in duplicate from aliquots of culture medium from groups of 25 islets, at 1 and 24 hours, as indicated. Data are presented as means ± SEM (n = 6 mice per group; n = 7–8 islet pools per group; $^*P < 0.05$, $^{***}P < 0.001$). (C) Insulin administration reduces glucose levels in HD transgenic mice with diabetes. Intermediate-acting insulin (0.2 U) was administered by intraperitoneal injection into 11-week-old (approx 20 g) R6/2 HD transgenic mice. Glucose levels were measured at 0, 10, 75, and 165 min as indicated. Data are presented as means ± SEM (n = 5; $^{***}P <$ 0.001 as compared with time 0).

the administration of intermediate-acting insulin transiently reduced blood glucose levels in the HD transgenic mice with diabetes (Fig. 2C).

To further characterize the defective pancreatic islet function observed in the HD transgenic animals, pancreatic histology was analyzed. In 12-week-old HD animals the gross architecture, size, and distribution of the pancreatic islets were normal. No evidence of islet inflammation, infiltration, or destruction was found to suggest a pattern resembling Type 1 diabetes.

The nuclear morphology of pancreatic islet cells from HD transgenic mice consisted largely of minimally condensed euchromatin, a nuclear pattern consistent with active transcription (Fig. 3A). Increased cytoplasmic heterogeneity was observed in HD pancreatic islets as compared with control islets. Pancreatic islets from 12-week-old HD transgenic mice expressed lower levels of the islet hormones insulin, glucagon, and somatostatin as compared with nontransgenic littermate controls (Fig. 3B).

Huntington's Disease Transgenic Mice Develop Intranuclear Inclusions in Pancreatic Islets with Aging

Pancreatic sections from HD transgenic animals at 6, 9, and 12 weeks of age were immunostained for intranuclear inclusions with antiserum directed against the human huntingtin protein to determine whether the mechanism of pancreatic islet dysfunction might be related to that of affected neurons in HD transgenic mice (Fig. 4A). Intranuclear inclusions were present in the pancreas and more prominent in the pancreatic islets than in the exocrine tissue. Polyglutamine inclusions in HD transgenic mice are found outside the central nervous system in a variety of postmitotic cells (Sathasivam *et al.*, 1999). The inclusions in the endocrine pancreas accumulated with aging in a pattern reminiscent of that seen in neurons. At 6 weeks of age very few intranuclear inclusions were observed in pancreatic islets. The density of intranuclear aggregates increased at 9 weeks of age, and by 12 weeks of age the islets and the insulin-expressing pancreatic β cells of HD mice had a substantial number of intranuclear inclusions (Figs. 4A, 4B). Although intranuclear inclusions were not detected in all of the insulin-producing cells, the time course of the accumulation of intranuclear aggregates in pancreatic islets was remarkably concordant with the observed metabolic abnormalities and suggested a correlation between the density of intranuclear inclusions and the severity of pancreatic β-cell dysfunction.

Insulin Gene Expression Is Progressively Impaired with Aging in Huntington's Disease Transgenic Mice

The analysis of pancreatic islet function *ex vivo* implied that β-cell insulin production was defective. To assess insulin gene expression we isolated total pancreatic RNA from HD transgenic mice and nontransgenic littermate controls at 8 and 12 weeks of age. On Northern blots the HD transgenic mice had markedly diminished insulin mRNA levels as compared with controls (Figs. 5A, 5B). A twofold reduction in insulin

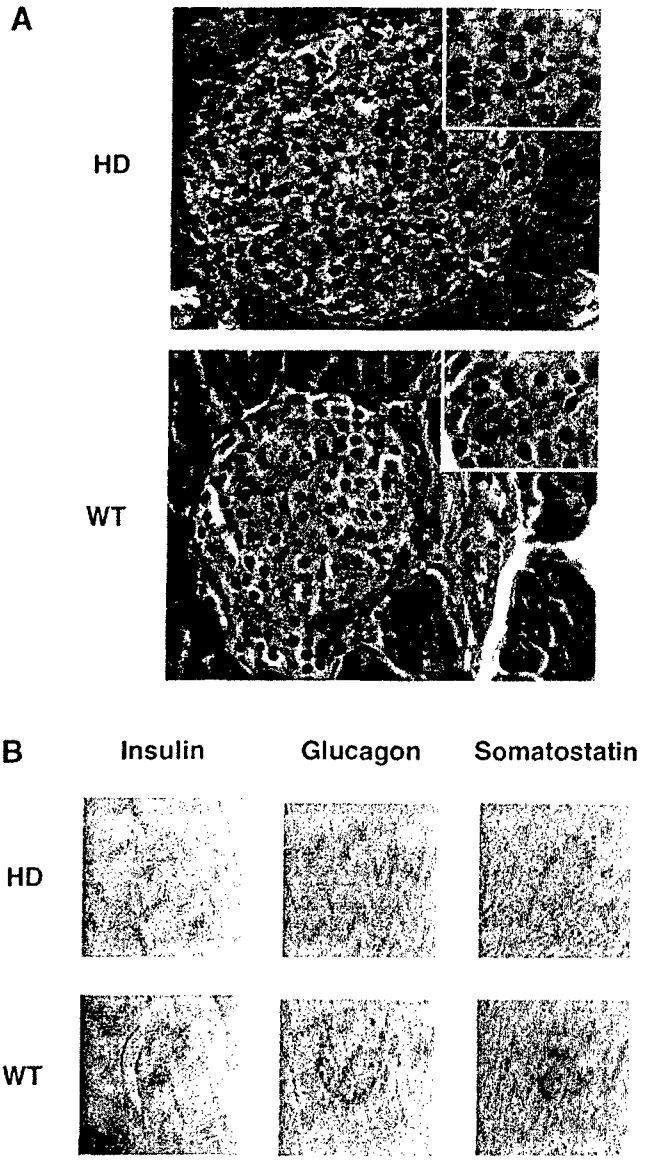

FIG. 3. Pancreatic islets in HD transgenic mice have distinct nuclear morphology and reduced islet hormone expression. (A) Hematoxylin and eosin staining of pancreas sections derived from an HD transgenic mouse with diabetes (HD) and a nontransgenic control mouse (WT). Representative images (400X and 1000X (inset) magnification) of pancreatic islets from paraffin-embedded pancreas sections are shown. (B) Reduced insulin, glucagon, and somatostatin expression in diabetic HD transgenic mice. Pancreas sections from 12-week-old R6/2 HD transgenic (HD) and nontransgenic littermate control (WT) mice were immmunostained with antisera directed against insulin, somatostatin, or proglucagon, as indicated. Representative images of pancreatic islets are shown.

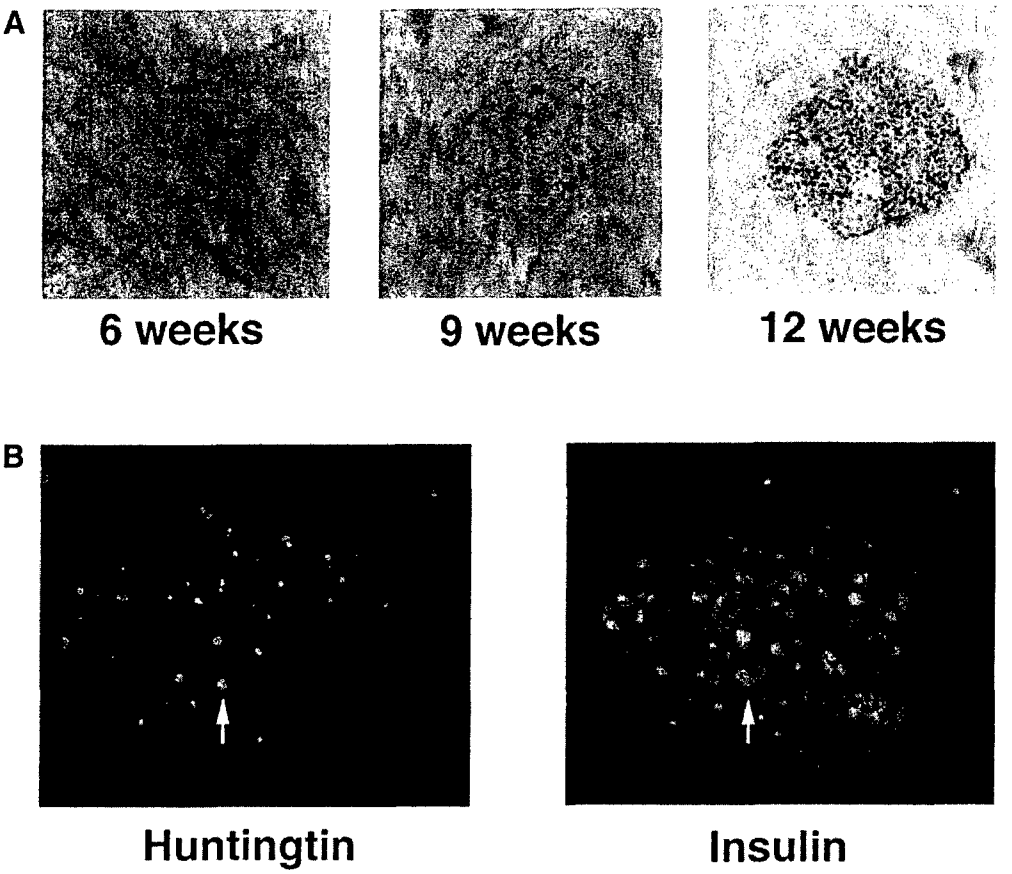

FIG. 4. Pancreatic islets in HD transgenic mice progressively develop intranuclear inclusions. (A) Intranuclear inclusions accumulate in pancreatic islets of HD transgenic mice with aging. Pancreas sections from 6-, 9-, and 12-week-old R6/2 HD transgenic mice (as indicated) were immunostained for intranuclear inclusions with anti-huntingtin (EM 48) antiserum. Representative images of pancreatic islets demonstrating the time-dependent increase in density of punctate intranuclear inclusions within islets are shown. (B) Intranuclear inclusions are present in insulin-expressing cells in pancreatic islets of HD transgenic mice. Images are shown of dual immunofluorescence immunostaining of a pancreatic islet from a 12-week old R6/2 transgenic mouse pancreas with anti-huntingtin (N-18) antiserum (left) and anti-insulin antiserum (right). Arrows indicate a representative pancreatic β cell with coexpression of huntingtin and insulin.

gene expression was observed at 8 weeks of age that correlated with the metabolic phenotype of impaired glucose tolerance but preceded the elevation in fasting serum glucose levels, the decline in serum insulin levels, and the development of diabetes in the HD transgenic mice. Less than 20% of control insulin mRNA expression was detected in pancreatic tissue from 12-week-old HD transgenic mice with diabetes. As HD transgenic mice continued to age, after insulin gene expression was more severely reduced, the capacity of the pancreatic β cells to maintain adequate insulin production was exceeded and the mice developed fasting hyperglycemia.

Notably 8-week-old HD transgenic mice had normal fasting serum glucose levels in the setting of reduced insulin gene expression. Maintenance of fasting glucose levels requires adequate glucose disposal following nutrient ingestion via both insulin secretion by pancreatic β cells and insulin signaling in peripheral tissues. β-Cell function is likely the more important of the two factors in determining glucose disposal in humans at risk for the development of diabetes (Jensen *et al.*, 2002). Elevated basal intracellular calcium levels in pancreatic β cells are associated with reductions in nutrient-induced insulin secretion, deterioration of cellular function, and acceleration of cellular death (Wang *et al.*, 1999; Conroy *et al.*, 2002; Grill and Bjorklund, 2001). In a transgenic mouse model of the polyglutamine expansion disease spinocerebellar ataxia 1 (SCA1) mRNA expression levels of two regulators of intracellular calcium stores, IP3R1 and SERCA2, decline before the development of a neuro-

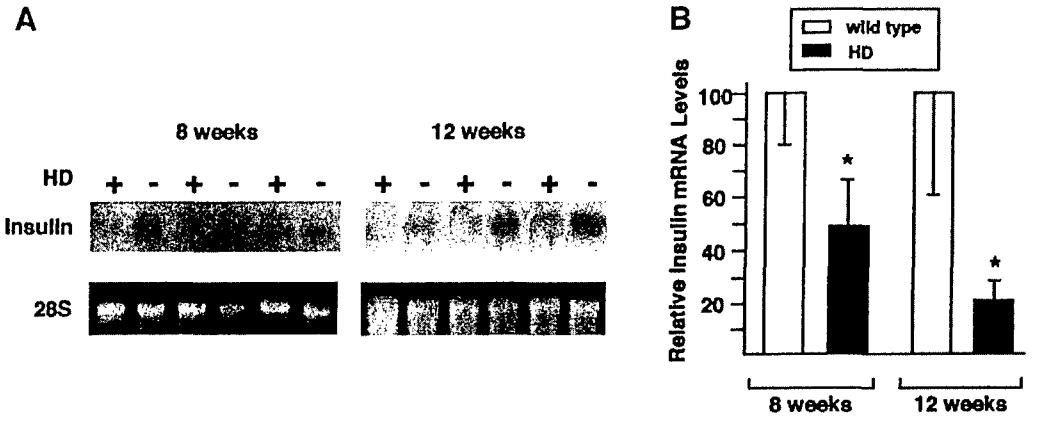

FIG. 5. Expression of insulin mRNA declines with aging in HD transgenic mice. (A) Insulin mRNA expression is progressively reduced in HD transgenic mice. Total pancreatic RNA was isolated from 8- and 12-week-old R6/2 HD transgenic (+) and nontransgenic littermate control (−) mice as indicated and analyzed by Northern blotting (15 μg per lane) with radiolabeled insulin cDNA probe (insulin) (n = 3 mice per age and genotype group). Photographs of the corresponding ethidium bromide-stained agarose gels showing levels of 28 S ribosomal RNA (28S) are shown as loading controls. (B) Relative insulin mRNA expression in HD transgenic and nontransgenic littermate controls at 8 and 12 weeks of age. Levels of insulin mRNA expression were calculated by scanning densitometry of autoradiograms shown in Fig. 4A. The average level of insulin mRNA expression for nontransgenic littermate control (−) mice was set at 100% and compared with the average level of insulin mRNA expression for HD transgenic mice at each time point (n = 3 per age and genotype group).

logic phenotype (Lin *et al.*, 2000), but the basic electrophysiologic properties of transgenic Purkinje cells are qualitatively similar to those of wild-type neurons (Inoue *et al.*, 2001). In the HD transgenic mice early defects in intracellular calcium levels in pancreatic islet cells were not demonstrable. At 8 weeks of age intracellular calcium levels were not significantly different between islet cells isolated from HD transgenic mice and those from nontransgenic littermate control mice (46.9 ± 6.0 nM vs 40.2 ± 4.4 nM; n = 40, P = 0.37).

Expression of Pancreatic Islet Transcription Factors Is Selectively Impaired in Huntington's Disease Transgenic Mice

In addition to impaired expression of insulin mRNA, protein expression patterns of key regulators of glucose-mediated insulin gene transcription were altered in HD pancreatic islets. In pancreas sections from 12-week-old HD transgenic mice expression levels of glucose-responsive insulin gene regulators PDX-1 and E2A (German *et al.*, 1992; Peers *et al.*, 1994) and the transcriptional coactivators CBP and p300 (Qiu *et al.*, 1998; Sharma *et al.*, 1999) were impaired relative to nontransgenic littermate control mice (Fig. 6). Expression of the coactivator CBP was modestly reduced in HD transgenic mouse islets, with expression in a smaller proportion of islet cells at a lower level. The reduction of the expression of the coactivator p300 was more striking with very little residual islet staining in the islets of HD transgenic mice. Expression levels of the pancreatic regulator PDX-1 also were reduced in HD transgenic mice, with variation in the extent of expression among islets, reduced cytoplasmic staining within islet cells, and central areas of islets entirely lacking PDX-1 expression. The change in pattern of expression of the transcriptional regulators of the E2A family was more subtle, with a reduction in cytoplasmic staining within islets of HD transgenic mice leaving a residual punctate nuclear expression pattern.

Similar to the early deficits observed in insulin gene expression, reductions in PDX-1 protein levels preceded the development of diabetes mellitus in HD transgenic mice. PDX-1 is a transcription factor essential for both glucose-responsive insulin gene transcription and the development of the pancreas (Stoffers *et al.*, 1997b). Heterozygosity for inactivating or missense mutations in *pdx-1* confers a predisposition to the development of diabetes mellitus in humans (Hani *et al.*, 1999; Macfarlane *et al.*, 1999; Stoffers *et al.*, 1997a), and small changes in PDX-1 expression levels can have major metabolic consequences (Thomas *et al.*, 2001a). Decreased expression of PDX-1 was evident on Western blots of total pancreatic and pancreatic islet extracts derived from HD transgenic mice relative to nontransgenic littermate controls at both 9 and 12

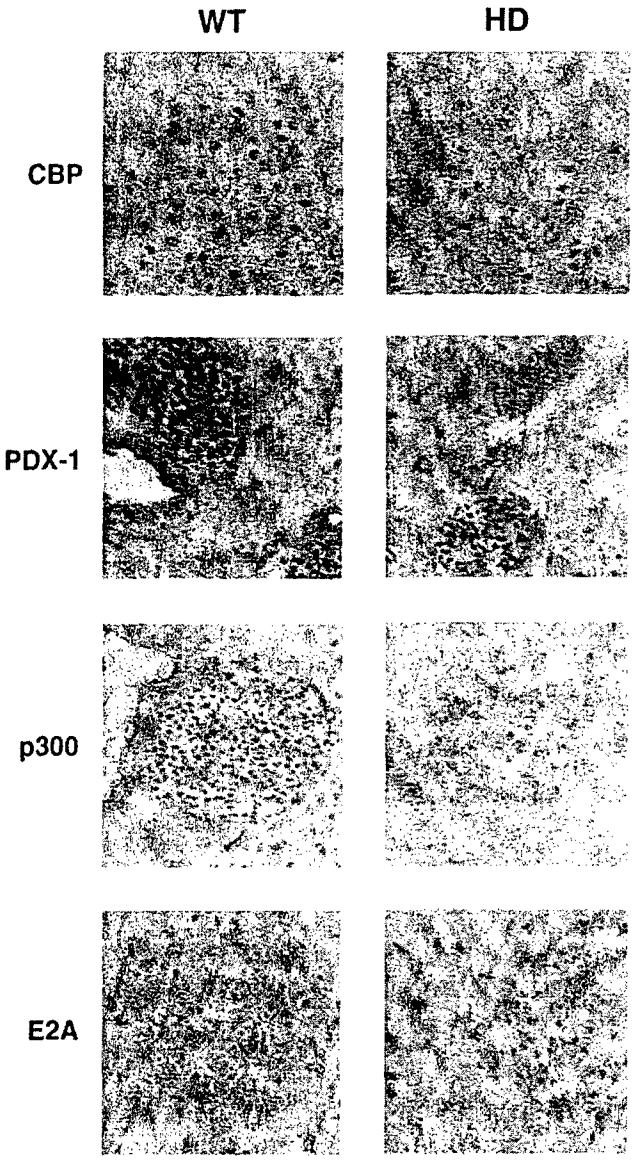

FIG. 6. Expression patterns of insulin gene regulators CBP, PDX-1, p300, and E2A are altered in diabetic HD transgenic mice. Pancreas sections from 12-week-old R6/2 HD transgenic (HD) and nontransgenic littermate control (WT) mice were immunostained for CBP, PDX-1, p300, and E2A as indicated. Representative images of pancreatic islets are shown.

weeks of age (Figs. 7A, 7B). The reduction in PDX-1 expression was the result of a selective not a universal process. The expression patterns of the transcription factors Stat-3, Smads-2/3, CEBP-β, CREB, and the glucagon-like peptide-1 (GLP-1) receptor were distinct from that of PDX-1 in pancreatic extracts from 9- and 12-week-old HD transgenic and nontransgenic littermate control mice (Fig. 7A). The selectivity of the reductions of PDX-1 and p300 expression within the pancreatic islets of HD transgenic mice was confirmed

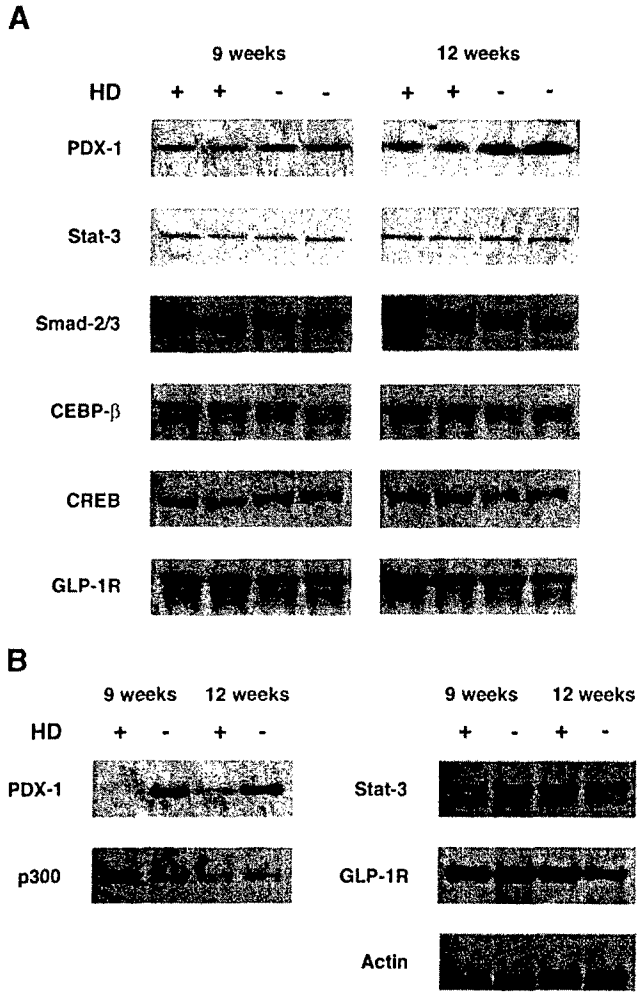

FIG. 7. Pancreatic islet expression levels of the insulin gene activators PDX-1 and p300 are selectively reduced in HD transgenic mice. (A) PDX-1 expression levels are reduced in total pancreas extracts. Whole pancreatic extracts derived from 9- and 12-week-old HD transgenic (+) and nontransgenic littermate control (−) mice were subjected to Western blotting with anti-PDX-1, anti-Stat-3, anti-Smad-2/3, anti-CEBP-β, anti-Creb, or anti GLP-1 receptor antiserum as indicated (n = 2 mice per age and genotype group). Analysis of blots by scanning densitometry indicated that pancreatic PDX-1 protein levels were reduced by 30% in 9-week-old and by 30–70% in 12-week-old HD transgenic mice. (B) PDX-1 and p300 expression levels are reduced in pancreatic islet extracts from HD transgenic mice. Extracts derived from pancreatic islets isolated and pooled from 9- and 12-week-old HD transgenic (+) and nontransgenic control (−) mice were subjected to Western blotting with anti-PDX-1, anti-p300, anti-Stat-3, anti-GLP-1 receptor, or anti-actin antiserum as indicated. Analysis of blots by scanning densitometry indicated that islet PDX-1 protein levels were reduced by 80–95% and islet p300 protein levels were reduced by 35–60% in HD transgenic mice. Representative images are shown.

on Western blots of pancreatic islet extracts by the different expression patterns observed for Stat-3, actin, and the GLP-1 receptor (Fig. 7B).

DISCUSSION

This analysis of the mechanism by which HD transgenic mice develop diabetes demonstrates a functional relationship between impaired gene expression due to a polyglutamine expansion tract and a physiologic dysfunction. In the age-dependent progression of HD transgenic mice from normal glucose tolerance to a phenotype of diabetes, decreased levels of pancreatic insulin mRNA precede the development of diabetes mellitus. Diminished levels of insulin gene expression in HD transgenic mice are found in the context of the accumulation of intranuclear inclusions and of altered expression patterns of a subset of protein regulators of insulin gene transcription within the pancreatic islets. It is interesting to note that defects in insulin gene expression were apparent before the development of diabetes in the HD transgenic mice, analogous to a mouse model of SCA1 in which expression patterns of selected cerebellar mRNA transcripts changed before the onset of neurologic symptoms (Lin *et al.*, 2000).

Defects in insulin production in HD transgenic mice develop in parallel with the accumulation of intranuclear inclusions in the endocrine pancreas. The accumulation of intranuclear inclusions in affected cells may be the result of aberrant protein processing by the proteasome, as ubiquitin and other proteasome protein components are found with mutant polyglutamine proteins in nuclear aggregates (Martin, 1999). The potential of intranuclear inclusions to contribute to cellular toxicity is controversial (Perutz and Windle, 2001).

It is somewhat surprising that pancreatic endocrine cells and neural cells are susceptible to cellular dysfunction in HD while other cells are unaffected by expression of the mutant huntingtin protein (Freiman and Tijan, 2002). Pancreatic islet cells share extraordinarily similar protein expression patterns with cells in the central nervous system (Le Douarin, 1988; Scharfmann, 1997; Schwartz *et al.*, 2000). Both neurons and pancreatic β cells finely regulate secretory processes and are electrically excitable cells. Despite these similar properties, pancreatic neuroendocrine cells are not derived from the neural crest during embryonic development (Le Douarin, 1988). However, embryonic or adult-derived stem/progenitor cells that express the neural stem cell marker nestin are capable of *in vitro* differentiation toward either neuronal or pancreatic β-cell lineages (Zulewski *et al.*, 2001, Lumelsky *et al.*, 2001).

The cell-specific repertoire of transcription factor expression is likely an important determining factor in susceptibility to polyglutamine-mediated cellular dysfunction. Polyglutamine extension tracts interact with and sequester other glutamine-rich proteins (Kazantsev *et al.*, 1999; Preisinger *et al.*, 1999), possibly by folding into β sheets or compact random coils (Starikov *et al.*, 1999). Transcriptional regulatory proteins are susceptible to such interactions because they often employ glutamine-rich stretches as transcriptional activation and dimerization domains (Courey, 1988; Freiman and Tijan, 2002; Su *et al.*, 1991). Altered conformations of mutant proteins with polyglutamine tracts also promote new protein–protein interactions (Ferrigno and Silver, 2000; Nucifora *et al.*, 2001). Thus polyglutamine expansions in proteins are able to alter cellular gene expression patterns by promoting interactions of transcription factors with repressors, disrupting interactions with activators, and unbalancing the stoichiometry of multiprotein transcriptional activation complexes. Homopolymeric glutamine tracts are sufficient to confer transcriptional activation or repression properties to fusion proteins, depending on the cellular context and the gene reporter (Gerber *et al.*, 1994; Grierson *et al.*, 1999; Irvine *et al.*, 2000; Steffan *et al.*, 2000), probably because the polyglutamine tracts in mutant proteins mediate direct interaction with nuclear proteins (Hsiao *et al.*, 1999; Irvine *et al.*, 2000; Waragai *et al.*, 1999).

Transcriptional coactivators and corepressors, such as CBP, SRC-1, and N-CoR, associate with polyglutamine nuclear protein aggregates in transfected cells (Boutell *et al.*, 1999; Kazantsev *et al.*, 1999; Nucifora *et al.*, 2001; Stenoien *et al.*, 1999). Neuronal intranuclear inclusions in HD transgenic mice sequester CBP (Nucifora *et al.*, 2001; Steffan *et al.*, 2000), and CBP is incorporated into intranuclear inclusions in human patients and in a transgenic mouse model of the CAG repeat expansion disorder spinal and bulbar muscular atrophy (McCampbell *et al.*, 2000). Other nuclear factors, such as the glucocorticoid receptor, have the capacity to regulate the nuclear localization and aggregation of polyglutamine-expanded proteins (Diamond *et al.*, 2000). Interactions of proteins encoding polyglutamine tracts with regulators of gene transcription are implicated in the pathogenesis of triplet

repeat disorders as illustrated by the identification of transcriptional cofactors sin3a, rpde, and CtBP as genetic modifiers of the SCA1 phenotype in *Drosophila* (Fernandez-Funez *et al.*, 2000).

The altered patterns of transcription factor expression in the pancreatic islets of HD transgenic mice could result from multiple mechanisms. Direct sequestration of transcriptional regulators by polyglutamine tracts and accelerated transcription factor degradation are likely explanations. In some contexts, huntingtin represses transcription by inhibiting the acetyltransferase activity of the coactivators CBP, p300 and p/CAF or by interacting with corepressors such as NCOR and CtBP (Boutell *et al.*, 1999; Kegel *et al.*, 2002). Mutant huntingtin also may interfere with the coupling of transcription factors to the basal transcription machinery (Dunah *et al.*, 2002). Alterations in mRNA stability also may conceivably regulate gene expression in HD. In the *Drosophila* SCA1 model, RNA-binding proteins are genetic modifiers of the SCA1 phenotype (Fernandez-Funez *et al.*, 2000).

Mutations in pancreatic islet cell transcription factors are associated with diabetes mellitus in humans. Five of the six MODY syndromes are linked to mutations in transcription factors that are direct or indirect regulators of the insulin gene (Fajans *et al.*, 2001). In particular, a heterozygous inactivating mutation in the insulin gene activator *pdx-1* is linked to MODY4 and heterozygous missense mutations in *pdx-1* confer a predisposition to the development of Type 2 (adult-onset) diabetes (Hani *et al.*, 1999; Macfarlane *et al.*, 1999; Stoffers *et al.*, 1997a). Heterozygous disruption of *pdx-1* in mice results in impaired glucose tolerance and reductions in PDX-1 expression in mice after the pancreas has developed result in diabetes mellitus (Ahlgren *et al.*, 1998; Dutta *et al.*, 1998; Thomas *et al.*, 2001a). In this respect, the observed reduction of PDX-1 expression alone in HD transgenic mice likely is sufficient to explain defects in insulin gene expression and the phenotype of diabetes mellitus. The severity of the phenotype is compounded by altered E2A, CBP, and p300 expression patterns. E2A transcription factors and the coactivators CBP and p300 also are important regulators of insulin gene transcription in pancreatic β cells (German *et al.*, 1992; Peers *et al.*, 1994; Qiu *et al.*, 1998; Sharma *et al.*, 1999). The decreased expression of the islet hormones glucagon and somatostatin in HD transgenic mice is interesting in this context because both E2A proteins and p300 activate the glucagon promoter (Dumonteil *et al.*, 1998; Hussain and Habener, 1999) and PDX-1 activates the somatostatin promoter (Leonard *et al.*, 1993; Miller *et al.*, 1994). In contrast to the absence of observed defects in p300 expression or function in the HD central nervous system (Zuccato *et al.*, 2001), expression levels of p300 were reduced markedly in pancreatic islets of HD transgenic mice. p300 interacts with multiple transcription factors in pancreatic β cells, including E2A, Beta-2/neuroD, and PDX-1 (Qiu *et al.*, 1998, 2002), and thereby contributes substantially to the stability of the multiprotein enhanceasome that governs the activation and glucose responsiveness of the insulin promoter. The susceptibility of the insulin gene to the expression of a polyglutamine expansion tract protein may reflect endogenous insulin gene regulation by glutamine-rich transcription factors. It is conceivable that altered expression of other regulators of transcription also contribute to the defective β-cell gene expression in HD transgenic mice.

Defects in insulin gene expression and pancreatic PDX-1 expression preceded the development of diabetes and were apparent at 9 weeks of age when the HD transgenic mice had normal fasting glucose levels but impaired glucose tolerance. These findings are harbingers of β-cell dysfunction and impending diabetes in the prediabetic state. Whether the underlying mechanism involves inherited mutations in MODY syndromes or sequestration and degradation of essential transcription factors in HD, decreased insulin gene expression may be a common final pathway in the development of diabetes.

As in neuronal cellular toxicity in HD, the severity of the diabetes phenotype is inversely related to the number of polyglutamine repeats fused to the huntingtin protein. In a HD transgenic mouse model with 82 CAG repeats, the age of onset and extent of hyperglycemia are delayed relative to the HD transgenic mice with 145–150 CAG repeats. In contrast, HD transgenic mice with only 18 CAG repeats do not develop hyperglycemia (Andreassen *et al.*, 2001). Phenotypic changes outside the central nervous system in response to polyglutamine tract expansions are observed in other diseases. For example, in the setting of a polyglutamine tract expansion within the androgen receptor in spinal and bulbar muscular atrophy, shorter CAG repeat tracts are associated with an increased risk of benign prostatic hyperplasia while longer stretches of CAG repeats confer androgen insensitivity (Giovannucci *et al.*, 1999).

Comodifying genes are likely to exacerbate or ameliorate the susceptibility for metabolic dysfunction in transgenic mouse models of HD. In our colony of R6/2 HD transgenic mice, full penetrance of the diabetes phenotype is observed by 12 weeks of age, sim-

ilar to the prevalence of diabetes observed in independent studies (Hickey *et al.*, 2002). However, other investigators have observed that despite full penetrance of impaired glucose tolerance in R6/2 HD transgenic mice at 9 weeks of age, only 25% of the mice progress to hyperglycemia and diabetes by 12 weeks of age (Luesse *et al.*, 2001). These observed differences in penetrance of the diabetes phenotype probably reflect differences in the expression of comodifier genes. Similar differences are commonly reported in distinct colonies of inbred genetically modified mouse models. Other studies of the R6/2 HD mice at 8–10 weeks of age do not detect significant increases in random-fed glucose levels or reductions in random-fed insulin levels (Fain *et al.*, 2001). These data are consistent with our findings that significant increases in fasting or fed glucose levels are not observed before 10 weeks of age and significant reductions in serum insulin levels are detected only in HD mice with diabetes.

Additional studies are needed to determine whether similar β-cell dysfunction occurs in humans with HD. An increased prevalence of diabetes mellitus has been reported in humans with HD and with other triplet repeat disorders (Farrer, 1985; Podolsky and Leopold, 1977). However, metabolic phenotypes have not been assessed rigorously or observed over time in a large enough cohort of individuals with HD to adequately characterize pancreatic β-cell function. Because individuals with HD have a markedly shortened life span, the intermediate phenotype of impaired glucose tolerance may be more prevalent than currently recognized. Diabetes mellitus is common in other triplet repeat disorders including Friedreich's ataxia (GAA repeat) and myotonic dystrophy (CTG repeat). In both of these diseases the diabetic phenotype is associated with hyperinsulinemia and insulin resistance (Finocchiaro *et al.*, 1988; Krentz *et al.*, 1992) and additional analyses of pancreatic β-cell function in these disorders would be of interest.

Characterization of the endocrine pancreatic phenotype in response to the expression of the mutant huntingtin protein illustrates the important potential of polyglutamine expansion tracts to selectively disrupt gene expression and alter cellular function. Selective dysregulation of gene expression in neurons, in a manner analogous to that in pancreatic β cells, likely contributes to neuronal dysfunction and degeneration in triplet repeat disorders and provides a mechanism for the restricted toxicity of ubiquitously expressed mutant proteins to highly specialized subpopulations of cells.

ACKNOWLEDGMENTS

We appreciate the expert technical assistance of M. Castonguay, O. Devon, K. McManus, H. Hermann, and V. Kaur. We thank D. Nathan and the hemoglobin A1C clinical laboratory at Massachusetts General Hospital for assistance with glycated hemoglobin assays. We appreciate the assistance of D. Hufnagel and K. MacDonald in the preparation of the manuscript. This work was supported by grants from the National Institutes of Health [NS31579, AG12292 (M.F.B.), DK55365 (J.F.H.), DK02476 (M.K.T.)], the Hereditary Disease Foundation (M.F.B.), the Huntington Disease Society of America (M.F.B.), the Norwegian Research Council (O.A.A.), and the U.S. Veteran's Administration (R.J.F.). J.F.H. is an Investigator with the Howard Hughes Medical Institute.

REFERENCES

Ahlgren, U., Jonsson, J., Jonsson, L., Simu, K., & Edlund, H. (1998) Beta-cell-specific inactivation of the mouse *IPF1/PDX1* gene results in loss of the beta-cell phenotype and maturity onset diabetes. *Genes Dev.* **12**, 1763–1768.

Andreassen, O. A., Dedeoglu, A., Ferrante, R. J., Jenkins, B. G., Ferrante, K. L., Thomas, M., Friedlich, A., Browne, S. E., Schilling, G., Borchelt, D. R., Hersch, S. M., Ross, C. A., & Beal, M. F. (2001) Creatine increases survival and delays motor symptoms in a transgenic animal model of Huntington's disease. *Neurobiol. Dis.* **8**, 479–491.

Beal, M. F. (2000) Energetics in the pathogenesis of neurodegenerative diseases. *Trends Neurosci.* **23**, 298–304.

Boutell, J. M., Thomas, P., Neal, J. W., Weston, V. J., Duce, J., Harper, P. S., & Jones, A. L. (1999) Aberrant interactions of transcriptional repressor proteins with the Huntington's disease gene product, huntingtin. *Hum. Mol. Genet.* **8**, 1647–1655.

Browne, S. E., Ferrante, R. J., & Beal, M. F. (1999) Oxidative stress in Huntington's disease. *Brain Pathol.* **9**, 147–163.

Cha, J. H. (2000) Transcriptional dysregulation in Huntington's disease. *Trends Neurosci.* **23**, 387–392.

Cha, J. H., Kosinski, C. M., Kerner, J. A., Alsdorf, S. A., Mangiarini, L., Davies, S. W., Penney, J. B., Bates, G. P., & Young, A. B. (1998) Altered brain neurotransmitter receptors in transgenic mice expressing a portion of an abnormal human Huntington's disease gene. *Proc. Natl. Acad. Sci. USA* **95**, 6480–6485.

Conroy, S. J., Green, I., Dixon, G., Byrne, P. M., Nolan, J., Abdel-Wahab, Y. H., McClenaghan, N., Flatt, P. R., & Newsholme, P. (2002) Evidence for a sustained increase in clonal beta-cell basal intracellular Ca^{2+} levels after incubation in the presence of newly diagnosed Type-1 diabetic patient sera: Possible role in serum-induced inhibition of insulin secretion. *J. Endocrinol.* **173**, 53–62.

Courey, A. J. (1988) Analysis of Sp1 in vivo reveals multiple transcriptional domains, including a novel glutamine-rich activation motif. *Cell* **55**, 887–898.

Davies, S. W., Turmaine, M., Cozens, B. A., Raza, A. S., Mahal, A., Mangiarini, L., & Bates, G. P. (1999) From neuronal inclusions to neurodegeneration: Neuropathological investigation of a transgenic mouse model of Huntington's disease. *Philos. Trans. R. Soc. London Ser. B.* **354**, 981–989.

Diamond, M. I., Robinson, M. R., & Yamamoto, K. R. (2000) Regulation of expanded polyglutamine protein aggregation and nuclear localization by the glucocorticoid receptor. *Proc. Natl. Acad. Sci. USA* **97**, 657–661.

Dumonteil, E., Laser, B., Constant, I., & Philippe, J. (1998) Differential regulation of the glucagon and insulin I gene promoters by the basic helix-loop-helix transcription factors E47 and Beta2. *J. Biol. Chem.* **273**, 19945–19954.

Dunah, A. W., Jeong, H., Griffin, A., Kim, Y. M., Standaert, D. G., Hersch, S. M., Mouradian, M. M., Young, A. B., Tanese, N., & Krainc, D. (2002) Sp1 and TAFII130 transcriptional activity disrupted in early Huntington's disease. *Science* **296**, 2238–2243.

Dutta, S., Bonner-Weir, S., Montminy, M., & Wright, C. (1998) Regulatory factor linked to late-onset diabetes? *Nature* **392**, 560.

Fain, J. N., Del Mar, N. A., Meade, C. A., Reiner, A., & Goldowitz, D. (2001) Abnormalities in the functioning of adipocytes from R6/2 mice that are transgenic for the Huntington's disease mutation. *Hum. Mol. Genet.* **10**, 145–152.

Fajans, S. S., Bell, G. I., & Polonsky, K. S. (2001) Molecular mechanisms and clinical pathophysiology of maturity-onset diabetes of the young. *N. Engl. J. Med.* **345**, 971–980.

Farrer, L. A. (1985) Diabetes mellitus in Huntington disease. *Clin. Genet.* **27**, 62–67.

Fernandez-Funez, P., Nino-Rosales, M. L., de Gouyon, B., She, W. C., Luchak, J. M., Martinez, P., Turiegano, E., Benito, J., Capovilla, M., Skinner, P. J., McCall, A., Canal, I., Orr, H. T., Zoghbi, H. Y., & Botas, J. (2000) Identification of genes that modify ataxin-1-induced neurodegeneration. *Nature* **408**, 101–106.

Ferrigno, P., & Silver, P. A. (2000) Polyglutamine expansions: Proteolysis, chaperones, and the dangers of promiscuity. *Neuron* **26**, 9–12.

Finocchiaro, G., Baio, G., Micossi, P., Pozza, G., & di Donato, S. (1988) Glucose metabolism alterations in Friedreich's ataxia. *Neurology* **38**, 1292–1296.

Freiman, R. N., & Tijian, R. (2002) A glutamine-rich trail leads to transcription factors. *Science* **296**, 2149–2150.

Gerber, H. P., Seipel, K., Georgiev, O., Hofferer, M., Hug, M., Rusconi, S., & Schaffner, W. (1994) Transcriptional activation modulated by homopolymeric glutamine and proline stretches. *Science* **263**, 808–811.

German, M. S., Wang, J., Chadwick, R. B., & Rutter, W. J. (1992) Synergistic activation of the insulin gene by a LIM-homeodomain protein and a basic helix-loop-helix protein: Building a functional insulin minienhancer complex. *Genes Dev.* **6**, 2165–2176.

Giovannucci, E., Platz, E. A., Stampfer, M. J., Chan, A., Krithivas, K., Kawachi, I., Willett, W. C., & Kantoff, P. W. (1999) The CAG repeat within the androgen receptor gene and benign prostatic hyperplasia. *Urology* **53**, 121–125.

Grierson, A. J., Mootoosamy, R. C., & Miller, C. C. (1999) Polyglutamine repeat length influences human androgen receptor/c-Jun mediated transcription. *Neurosci. Lett.* **277**, 9–12.

Grill, V., & Bjorklund, A. (2001) Overstimulation and beta-cell function. *Diabetes* **50**, S122–S124.

Hani, E. H., Stoffers, D. A., Chevre, J. C., Durand, E., Stanojevic, V., Dina, C., Habener, J. F., & Froguel, P. (1999) Defective mutations in the insulin promoter factor-1 (IPF-1) gene in late-onset type 2 diabetes mellitus. *J. Clin. Invest.* **104**, R41–R48.

Hickey, M. A., Reynolds, G. P., & Morton, J. A. (2002) The role of dopamine in motor symptoms in the R6/2 transgenic mouse model of Huntington's disease. *J. Neurochem.* **81**, 46–59.

Hsiao, P. W., Lin, D. L., Nakao, R., & Chang, C. (1999) The linkage of Kennedy's neuron disease to ARA24, the first identified androgen receptor polyglutamine region-associated coactivator. *J. Biol. Chem.* **274**, 20229–20234.

The Huntington's Disease Collaborative Research Group (1993) A novel gene containing a trinucleotide repeat that is expanded and unstable on Huntington's disease chromosomes. *Cell* **72**, 971–983.

Hurlbert, M. S., Zhou, W., Wasmeier, C., Kaddis, F. G., Hutton, J. C., & Freed, C. R. (1999) Mice transgenic for an expanded CAG repeat in the Huntington's disease gene develop diabetes. *Diabetes* **48**, 649–651.

Hussain, M. A., & Habener, J. F. (1999) Glucagon gene transcription activation mediated by synergistic interactions of pax-6 and cdx-2 with the p300 co-activator. *J. Biol. Chem.* **274**, 28950–28957.

Inoue, T., Lin, X., Kohlmeier, K. A., Orr, H. T., Zoghbi, H. Y., & Ross, W. N. (2001) Calcium dynamics and electrophysiological properties of cerebellar Purkinje cells in SCA1 transgenic mice. *J. Neurophysiol.* **85**, 1750–1760.

Irvine, R. A., Ma, H., Yu, M. C., Ross, R. K., Stallcup, M. R., & Coetzee, G. A. (2000) Inhibition of p160-mediated coactivation with increasing androgen receptor polyglutamine length. *Hum. Mol. Genet.* **9**, 267–274.

Jenkins, B. G., Klivenyi, P., Kustermann, E., Andreassen, O. A., Ferrante, R. J., Rosen, B. R., & Beal, M. F. (2000) Nonlinear decrease over time in *N*-acetyl aspartate levels in the absence of neuronal loss and increases in glutamine and glucose in transgenic Huntington's disease mice. *J. Neurochem.* **74**, 2108–2119.

Jensen, C. C., Cnop, M., Hull, R. L., Fujimoto, W. Y., Kahn, S. E., & the American Diabetes Association GENNID Study Group (2002) β-Cell function is a major contributor to oral glucose tolerance in high-risk relatives of four ethnic groups in the U.S. *Diabetes* **51**, 2170–2178.

Kazantsev, A., Preisinger, E., Dranovsky, A., Goldgaber, D., & Housman, D. (1999) Insoluble detergent-resistant aggregates form between pathological and nonpathological lengths of polyglutamine in mammalian cells. *Proc. Natl. Acad. Sci. USA* **96**, 11404–11409.

Kegel, K. B., Meloni, A. R., Yi, Y., Kim, Y. J., Doyle, E., Cuiffo, B. G., Sapp, E., Wang, Y., Qin, Z. H., Chen, J. D., Nevins, J. R., Aronin, N., & DiFiglia, M. (2002) Huntingtin is present in the nucleus, interacts with the transcriptional corepressor C-terminal binding protein, and represses transcription. *J. Biol. Chem.* **277**, 7466–7476.

Krentz, A. J., Clark, P. M., Cox, L., Williams, A. C., & Nattrass, M. (1992) Hyperproinsulinaemia in patients with myotonic dystrophy. *Diabetologia* **35**, 1170–1172.

Kuemmerle, S., Gutekunst, C. A., Klein, A. M., Li, X. J., Li, S. H., Beal, M. F., Hersch, S. M., & Ferrante, R. J. (1999) Huntington aggregates may not predict neuronal death in Huntington's disease. *Ann. Neurol.* **46**, 842–849.

Lacy, P. E., & Kostianovsky, M. (1967) Method for the isolation of intact islets of Langerhans from the rat pancreas. *Diabetes* **16**, 35–39.

Le Douarin, N. M. (1988) On the origin of pancreatic endocrine cells. *Cell* **53**, 169–171.

Leech, C. A., & Habener, J. F. (1997) Insulinotropic glucagon-like peptide-1-mediated activation of non-selective cation currents in insulinoma cells is mimicked by maitotoxin. *J. Biol. Chem.* **272**, 17987–17993.

Leonard, J., Peers, B., Johnson, T., Ferreri, K., Lee, S., & Montminy, M. R. (1993) Characterization of somatostatin transactivating factor-1, a novel homeobox factor that stimulates somatostatin expression in pancreatic islet cells. *Mol. Endocrinol.* **7**, 1275–1283.

Li, S. H., Cheng, A. L., Li, H., & Li, X. J. (1999) Cellular defects and altered gene expression in PC12 cells stably expressing mutant huntingtin. *J. Neurosci.* **19**, 5159–5172.

Lin, X., Antalffy, B., Kang, D., Orr, H. T., & Zoghbi, H. Y. (2000) Polyglutamine expansion down-regulates specific neuronal genes before pathologic changes in SCA1. *Nat. Neurosci.* **3**, 157–163.

Luesse, H. G., Schiefer, J., Spruenken, A., Puls, C., Block, R., & Kosinski, C. M. (2001) Evaluation of R6/2 HD transgenic mice for therapeutic studies in Huntington's disease: Behavioral testing and impact of diabetes mellitus. *Behav. Brain Res.* **126**, 185–195.

Lumelsky, N., Blondel, O., Laeng, P., Velasco, I. Ravin, R., & McKay, R. (2001) Differentiation of embryonic stem cells to insulin-secreting structures similar to pancreatic islets. *Science* **292**, 1389–1394.

Luthi-Carter, R., Strand, A., Peters, N. L., Solano, S. M., Hollingsworth, Z. R., Menon, A. S., Frey, A. S., Spektor, B. S., Penney, E. B., Schilling, G., Ross, C. A., Borchelt, D. R., Tapscott, S. J., Young, A. B., Cha, J. H., & Olson, J. M. (2000) Decreased expression of striatal signaling genes in a mouse model of Huntington's disease. *Hum. Molec. Genet.* **9**, 1259–1271.

Macfarlane, W. M., Frayling, T. M., Ellard, S., Evans, J. C., Allen, L. I., Bulman, M. P., Ayres, S., Shepherd, M., Clark, P., Millward, A., Demaine, A., Wilkin, T., Docherty, K., & Hattersley, A. T. (1999) Missense mutations in the insulin promoter factor-1 gene predispose to type 2 diabetes. *J. Clin. Invest.* **104**, R33–R39.

Mangiarini, L., Sathasivam, K., Seller, M., Cozens, B., Harper, A., Hetherington, C., Lawton, M., Trottier, Y., Lehrach, H., Davies, S. W., & Bates, G. P. (1996) Exon 1 of the HD gene with an expanded CAG repeat is sufficient to cause a progressive neurological phenotype in transgenic mice. *Cell* **87**, 493–506.

Martin, J. B. (1999) Molecular basis of the neurodegenerative disorders. *N. Engl. J. Med.* **340**, 1970–1980.

McCampbell, A., Taylor, J. P., Taye, A. A., Robitschek, J., Li, M., Walcott, J., Merry, D., Chai, Y., Paulson, H., Sobue, G., & Fischbeck, K. H. (2000) CREB-binding protein sequestration by expanded polyglutamine. *Hum. Mol. Genet.* **9**, 2197–2202.

Miller, C. P., McGehee, R. E., & Habener, J. F. (1994) IDX-1: A new homeodomain transcription factor expressed in rat pancreatic islets and duodenum that transactivates the somatostatin gene. *EMBO J.* **13**, 1145–1156.

Nagai, Y., Onodera, O., Strittmatter, W. J., & Burke, J. R. (1999) Polyglutamine domain proteins with expanded repeats bind neurofilament, altering the neurofilament network. *Ann. NY Acad. Sci.* **893**, 192–202.

Nucifora, F. C., Sasaki, M., Peters, M. F., Huang, H., Cooper, J. K., Yamada, M., Takahashi, H., Tsuji, S., Troncoso, J., Dawson, V. L., Dawson, T. M., & Ross, C. A. (2001) Interference by huntingtin and atrophin-1 with CBP-mediated transcription leading to cellular toxicity. *Science* **291**, 2423–2428.

Onodera, O., Burke, J. R., Miller, S. E., Hester, S., Tsuji, S., Roses, A. D., & Strittmatter, W. J. (1997) Oligomerization of expanded-polyglutamine domain fluorescent fusion proteins in cultured mammalian cells. *Biochem. Biophys. Res. Commun.* **238**, 599–605.

Peers, B., Leonard, J., Sharma, S., Teitelman, G., & Montminy, M. R. (1994) Insulin expression in pancreatic islet cells relies on cooperative interactions between the helix loop helix factor E47 and the homeobox factor STF-1. *Mol. Endo. Crinol.* **8**, 1798–1806.

Perutz, M. F., & Windle, A. H. (2001) Cause of neural death in neurodegenerative diseases attributable to expansion of glutamine repeats. *Nature* **412**, 143–144.

Podolsky, S., & Leopold, N. A. (1977) Abnormal glucose tolerance and arginine tolerance tests in Huntington's disease. *Gerontology* **23**, 55–63.

Preisinger, E., Jordan, B. M., Kazantsev, A. & Housman, D. (1999) Evidence for a recruitment and sequestration mechanism in Huntington's disease. *Philos. Trans. R. Soc. London Ser. B* **354**, 1029–1034.

Qiu, Y., Guo, M., Huang, S., & Stein, R. (2002) Insulin gene transcription is mediated by interactions between the p300 coactivator and PDX-1, BETA2, and E47. *Mol. Cell. Biol.* **22**, 412–420.

Qiu, Y., Sharma, A., & Stein, R. (1998) p300 mediates transcriptional stimulation by the basic helix–loop–helix activators of the insulin gene. *Mol. Cell. Biol.* **18**, 2957–2964.

Sathasivam, K., Hobbs, C., Turmaine, M., Mangiarini, L., Mahal, A., Bertaux, F., Wanker, E. E., Doherty, P., Davies, S. W., & Bates, G. P. (1999) Formation of polyglutamine inclusions in non-CNS tissue. *Hum. Mol. Genet.* **8**, 813–822.

Scharfmann, R. (1997) Neurotrophin and neurotrophin receptors in islet cells. *Horm. Metab. Res.* **29**, 294–296.

Schwartz, P. T., Perez-Villamil, B., Rivera, A., Moratalla, R., & Vallejo, M. (2000) Pancreatic homeodomain transcription factor IDX1/IPF1 expressed in developing brain regulates somatostatin gene transcription in embryonic neural cells. *J. Biol. Chem.* **275**, 19106–19114.

Senut, M. C., Suhr, S. T., Kaspar, B., & Gage, F. H. (2000) Intraneuronal aggregate formation and cell death after viral expression of expanded polyglutamine tracts in the adult rat brain. *J. Neurosci.* **20**, 219–229.

Sharma, A., Moore, M., Marcora, E., Lee, J. E., Qiu, Y., Samaras, S., & Stein, R. (1999) The NeuroD1/BETA2 sequences essential for insulin gene transcription colocalize with those necessary for neurogenesis and p300/CREB binding protein binding. *Mol. Cell. Biol.* **19**, 704–713.

Starikov, E. B., Lehrach, H., & Wanker, E. E. (1999) Folding of oligoglutamines: A theoretical approach based upon thermodynamics and molecular mechanics. *J. Biomol. Struct. Dyn.* **17**, 409–427.

Steffan, J. S., Kazantsev, A., Spasic-Boskovic, O., Greenwald, M., Zhu, Y. Z., Gohler, H., Wanker, E. E., Bates, G. P., Housman, D. E., & Thompson, L. M. (2000) The Huntington's disease protein interacts with p53 and CREB-binding protein and represses transcription. *Proc. Natl. Acad. Sci. USA* **97**, 6763–6768.

Steffan, J. S., Bodai, L., Pallos, J., Poelman, M., McCampbell, A., Apostol, B. L., Kazantsev, A., Schmidt, E., Zhu, Y. Z., Greenwald, M., Kurokawa, R., Housman, D. E., Jackson, G. R., Marsh, J. L., & Thompson, L. M. (2001) Histone deacetylase inhibitors arrest polyglutamine-dependent neurodegeneration in *Drosophila*. *Nature* **413**, 739–743.

Stenoien, D. L., Cummings, C. J., Adams, H. P., Mancini, M. G., Patel, K., DeMartino, G. N., Marcelli, M., Weigel, N. L., & Mancini, M. A. (1999) Polyglutamine-expanded androgen receptors form aggregates that sequester heat shock proteins, proteasome components and SRC-1, and are suppressed by the HDJ-2 chaperone. *Hum. Mol. Genet.* **8**, 731–741.

Stoffers, D. A., Ferrer, J., Clarke, W. L., & Habener, J. F. (1997a) Early-onset type-II diabetes mellitus (MODY4) linked to *IPF-1*. *Nat. Genet.* **17**, 138–139.

Stoffers, D. A., Kieffer, T. J., Hussain, M. A., Drucker, D. J., Bonner-Weir, S., Habener, J. F., & Egan, J. M. (2000) Insulinotropic glucagon-like peptide 1 agonists stimulate expression of homeodomain protein IDX-1 and increase islet size in mouse pancreas. *Diabetes* **49**, 741–748.

Stoffers, D. A., Thomas, M. K., & Habener, J. F. (1997b) Homeodo-

main protein IDX-1: A master regulator of pancreas development and insulin gene expression. *Trends Endocrinol. Metab.* **8**, 145–151.

Su, W., Jackson, S., Tijan, R., & Echols, H. (1991) DNA looping between sites for transcriptional activation: Self-association of DNA-bound Sp1. *Genes Dev.* **5**, 820–826.

Thomas, M. K., Devon, O. N., Lee, J. H., Peter, A., Schlosser, D. A., Tenser, M. S., & Habener, J. F. (2001a) Development of diabetes mellitus in aging transgenic mice following suppression of pancreatic homeoprotein IDX-1. *J. Clin. Invest.* **108**, 319–329.

Thomas, M. K., Lee, J. H., Rastalsky, N., & Habener, J. F. (2001b) Hedgehog signaling regulation of homeodomain protein IDX-1 expression in pancreatic β-cells. *Endocrinology* **142**, 1033–1040.

Thomas, M. K., Rastalsky, N., Lee, J., & Habener, J. F. (2000) Hedgehog signaling regulates insulin production by pancreatic β-cells. *Diabetes* **49**, 2039–2047.

Thomas, M. K., Yao, K. M., Tenser, M. S., Wong, G. G., & Habener, J. F. (1999) Bridge-1, a novel PDZ-domain coactivator of E2A-mediated regulation of insulin gene transcription. *Mol. Cell. Biol.* **19**, 8492–8404.

Wang, L., Bhattacharjee, A., Zuo, Z., Hu, F., Honkanen, R. E., Berggren, P. O., & Li, M. (1999) A low voltage-activated Ca^{2+} current mediates cytokine-induced pancreatic beta-cell death. *Endocrinology* **140**, 1200–1204.

Waragai, M., Lammers, C. H., Takeuchi, S., Imafuku, I., Udagawa, Y., Kanazawa, I., Kawabata, M., Mouradian, M. M., & Okazawa, H. (1999) PQBP-1, a novel polyglutamine tract-binding protein, inhibits transcription activation by Brn-2 and affects cell survival. *Hum. Mol. Genet.* **8**, 977–987.

Young, A. B. (1998) Huntington's disease and other trinucleotide repeat disorders. In: *Molecular Neurology* (J. B. Martin, Ed.), Scientific American, New York.

Zuccato, C., Ciammola, A., Rigamonti, D., Leavitt, B. R., Goffredo, D., Conti, L., MacDonald, M. E., Friedlander, R. M., Silani, V., Hayden, M. R., Timmusk, T., Sipione, S., & Cattaneo, E. (2001) Loss of huntington-mediated BDNF gene transcription in Huntington's disease. *Science* **293**, 493–498.

Zulewski, H., Abraham, E. J., Gerlach, M. J., Daniel, P. B., Moritz, W., Muller, B., Vallejo, M., Thomas, M. K., & Habener, J. F. (2001) Multipotential nestin-positive stem cells isolated from adult pancreatic islets differentiate *ex vivo* into pancreatic endocrine, exocrine, and hepatic phenotypes. *Diabetes* **50**, 521–533.

Brain Pathology 9: 147-163(1999)

APPENDIX 11

SYMPOSIUM: Oxidative Stress in Neurological Disease

Oxidative Stress in Huntington's Disease

Susan E. Browne[1], Robert J. Ferrante[2], M. Flint Beal[1,3]

[1] Department of Neurology, Massachusetts General Hospital and Harvard Medical School, Boston MA
[2] Bedford VA Medical Center, Bedford MA, and Departments of Neurology, Pathology, and Psychiatry, Boston University School of Medicine, Boston, MA
[3] Department of Neurology, New York Hospital and Cornell University Medical College, New York NY.

It has been five years since the elucidation of the genetic mutation underlying the pathogenesis of Huntington's disease (HD) (97), however the precise mechanism of the selective neuronal death it propagates still remains an enigma. Several different etiological processes may play roles, and strong evidence from studies in both humans and animal models suggests the involvement of energy metabolism dysfunction, excitotoxic processes, and oxidative stress. Importantly, the recent development of transgenic mouse models of HD led to the identification of neuronal intranuclear inclusion bodies in affected brain regions in both mouse models and in HD brain, consisting of protein aggregates containing fragments of mutant huntingtin protein. These observations opened new avenues of investigation into possible huntingtin protein interactions and their putative pathogenetic sequelae. Amongst these studies, findings of elevated levels of oxdative damage products such as malondialdehyde, 8-hydroxydeoxyguanosine, 3-nitrotyrosine and heme oxygenase in areas of degeneration in HD brain, and of increased free radical production in animal models, indicate the involvement of oxidative stress either as a causative event, or as a secondary constituent of the cell death cascade in the disease. Here we review the evidence for oxidative damage and potential mechanisms of neuronal death in HD.

Corresponding author:
Susan E. Browne, Ph.D., Neurology Research, Warren 408, Massachusetts General Hospital, Fruit Street, Boston, MA 02114; Tel.: (617) 726-8463; Fax: (617) 724-1480
E-mail: browne@helix.mgh.harvard.edu

Introduction

The late onset and progressive development of the behavioural abnormalities, cognitive impairment and involuntary choreiform movements which characterize Huntington's disease (HD) are the physical manifestations of a mutation in a gene on chromosome 4 encoding so-called "huntingtin" protein. The first clinical symptoms of HD are generally psychiatric abnormalities, most commonly depression and mood disturbances, which typically present in the fourth or fifth decade of life. Involuntary choreiform movements and dementia develop over the next 15-20 years, and death generally results from complications of immobility. This autosomal dominantly inherited degenerative disorder is characterized neuropathologically by bilateral striatal atrophy with marked neuronal loss and astrogliosis within the caudate and putamen. Within the striatum, spiny projection neurons containing the inhibitory neurotransmitter γ-aminobutyric acid (GABA) are particularly vulnerable to degeneration in HD, whilst large cholinergic interneurons and aspiny interneurons containing nicotinamide adenine dinucleotide phosphate diaphorase (NADPH-d), somatostatin and neuropeptide Y appear to be relatively spared (46, 39, 81, 82). Less severe neuropathological changes also occur in other brain regions, notably cerebral cortex, at more advanced stages of the disease.

Despite identification of the genetic abnormality in HD (97), resulting in expression of an expanded polyglutamine tract in huntingtin protein, the definitive role of mutant huntingtin in neuronal degeneration remains unclear. As discussed below, the insidious progression of motor and behavioural disturbances in HD reflect the selective pattern of cell loss in the brain, and the specific neurotransmitter pathways affected. The reason for the preferential vulnerability of striatal neurons is also unknown at present, and cannot be simply explained in terms of the distribution of abnormal huntingtin since the gene mutation is expressed throughout the body. However, experimental evidence suggests that the

pathogenesis of cell death in HD is linked to a gain of function of mutant huntingtin, and involves energetic defects, oxidative damage and excitotoxic processes. In this review we summarize the current understanding of neuropathological events in HD brain and discuss putative pathogenetic mechanisms, with particular emphasis on the role of oxidative damage in cell death. We will address three broad themes: 1) Neuropathological changes in HD; 2) Functional alterations in HD brain; and 3) Potential mechanisms linking functional alterations with their pathological sequelae in HD.

Neuropathological Changes in HD

Gross Neuropathological Features of HD. Motor dysfunction in HD results from the disruption of basal ganglia-thalamocortical pathways regulating movement control. The primary site of neuronal loss and atrophy in HD brain is in the caudate-putamen, although in many cases atrophy also occurs in a number of non-striatal regions, including cerebral cortex, thalamus, globus pallidus (GP), cerebellum and white matter tracts (31, 99). The typical neuropathological features of HD have recently been thoroughly and definitively outlined in a review by Vonsattel and DiFiglia (100), and therefore will be addressed only briefly here. In summary, the typical pattern of striatal cell loss in HD occurs gradually along a topographically well defined pathway (31, 99). Neurodegeneration in both the caudate and putamen follows a caudo-rostral progression, with a preferential dorsal to ventral gradient. Thus, at end stage cell loss is maximal in the tail of the caudate nucleus, less severe in the body, and least in the head of the caudate, although in severe cases neuronal populations are devastated throughout the neostriatum (100). Fibrillary astrogliosis follows the path of cell loss in striatum, however reac-

Figure 1. Immunocytochemical localization of lipofuscin in cortical pyramidal neurons and striatal neurons, but lack of colocalization with NADPH-diaphorase staining, in HD brain. Plates are frontal cortex (Brodmann area 8) and caudate nucleus sections single- and double-stained for SMI-32 (neuro-filament), acid phosphatase (lipofuscin), and NADPH-diaphorase (NADPH-d). **A**) Low power view of the cortex immunocytochemically stained with SMI-32 antisera. Note the pyramidal distribution of SMI-32 labeling, predominantly in laminae 2, 3 and 5. **B**) Low power view of the same cortical region as in A, staining acid phosphatase activity (lipofuscin). The staining distribution pattern is equivalent to SMI-32 labeling. **C**) High power photomicrograph of a cortical section double-stained for SMI-32 and acid phosphatase activity, demonstrating colocalization of SMI-32 labeling with punctate acid phosphatase (lipofuscin) within the same pyramidal neuron. **D**) Photomicrograph of a neocortex section double-stained for acid phosphatase and NADPH-diaphorase. There is little or no phosphatase activity within the NADPH-diaphorase positive neuron. **E**) Photomicrograph of a striatal section double-stained for acid phosphatase and NADPH-diaphorase. As in D, there is little or no colocalization of the endproducts. However, **F**) acid phophatase can be identified in a small population of NADPH-d neurons within the striatum, although it is less pronounced than in surrounding non-NADPH-d neurons.

tive gliosis does not accompany the chronic cell loss seen elsewhere in the brain, and no inflammatory response is involved (73).

On the basis of the progressive involvement of striatal regions, Vonsattel developed guidelines for grading HD patients based on gross and microscopic measures of neuropathological severity, determined in three standardized coronal brain sections including the striatum (99). Grades range from 0 to 4 with increasing severity and extent of striatal involvement. Briefly, Grade 0 cases are generally indistinguishable from normal brains on gross examination, but exhibit 30-40% neuronal loss in the head of the caudate, with no visible signs of reactive gliosis. In contrast, in Grade 4 the striatum is severely atrophic with loss of more than 95% of neurons and markedly increased oligodendrocytic density. Cell loss in the nucleus accumbens is evident in approximately 50% of Grade 4 cases. The majority of HD cases (approximately 80%) are Grades 3 or 4 at time of death (100). The grade of striatal pathology appears to correlate closely with the involvement of other cerebral regions. Non-striatal regions are largely unaffected in grades 1 and 2, whilst atrophy and neuronal loss are evident in the GP, cortex, and to a lesser extent thalamus, subthalamic nucleus, substantia nigra, white matter and cerebellum in Grade 3 and 4 cases (17, 92, 100). Cerebellar atrophy is particularly prevalent in cases of juvenile onset HD.

Surviving neostriatal neurons generally appear morphologically normal, but may be reduced in size and contain elevated levels of the oxidative damage marker lipofuscin. However Vonsattel has described a sub-population of neurons scattered largely between the zones of atrophic and healthy cells, referred to as "neostriatal dark neurons" (NDN) because of their relatively intense staining with Luxol-fast-blue and haematoxylin and eosin. These cells have characteristically scalloped membranes, granulation of the cytoplasm and condensation of nuclear chromatin, and some can be labeled by TdT-mediated dUTP-biotin nick end-labelling (TUNEL), suggesting that they may be undergoing apoptosis (100).

Clinical Correlates of Neuronal Loss. *Striatal Neuronal Populations in HD.* The striatal cell type most susceptible to degeneration in HD is the medium spiny projection neuron (81, 82, 99). Spiny neurons constitute 80% of striatal neurons, and are the principal input and output neurons of the striatum. Spiny neurons may be classified as small-, medium- or large-sized, but all contain the inhibitory neurotransmitter γ-aminobutyric acid

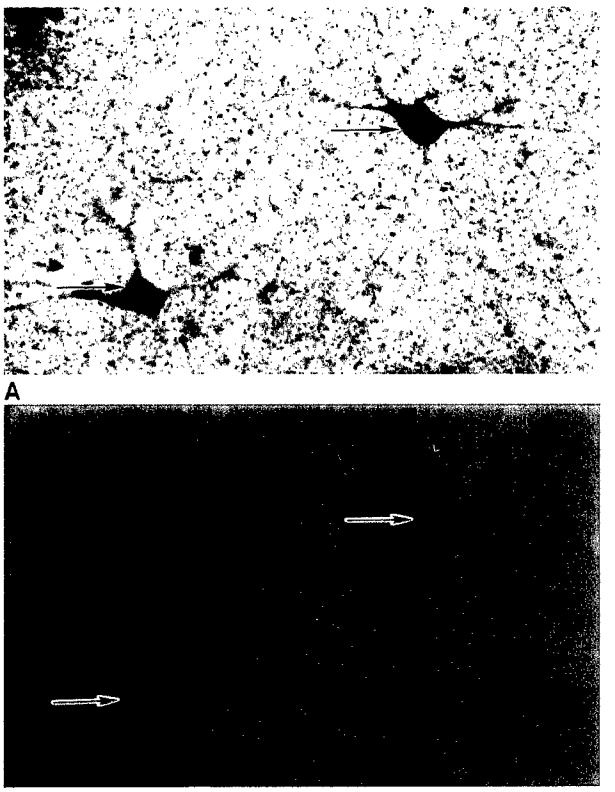

Figure 2. Photomicrographs of a double-stained tissue section from human HD caudate nucleus using NADPH-diaphorase enzyme histochemistry (**A**) and immunofluorescence for acid phosphatase activity (lipofuscin) (**B**). Two NADPH-diaphorase neurons are identified by arrows in A. The same area of the section was photographed in B for acid phosphatase activity. Bright red identifies lipofuscin within neurons. There is little or no colocalization of lipofuscin within NADPH-diaphorase neurons.

(GABA). Subsets of spiny neurons also contain enkephalin (ENK), substance-P (SP), dynorphin or calbindin. The other major class of striatal neuron are aspiny interneurons. Nicotinamide adenine dinucleotide phosphate diaphorase (NADPH-d), neuropeptide Y (NPY), somatostatin (SS) and nitric oxide synthase (NOS) typically colocalize in medium-sized aspiny neurons, and some contain cholecystokinin (CCK) or the calcium binding protein parvalbumin. The large aspiny neurons contain acetylcholine. In HD striatum, spiny projection neurons containing SP or ENK are involved earliest and most severely, whereas aspiny interneurons and the larger cholinergic interneurons are relatively spared (9, 40). There is also some hierarchy in vulnerability of different spiny neuron subsets, ENK-positive neurons projecting to the external segment of the globus pallidus (GPe) degenerating prior to SP-containing neu-

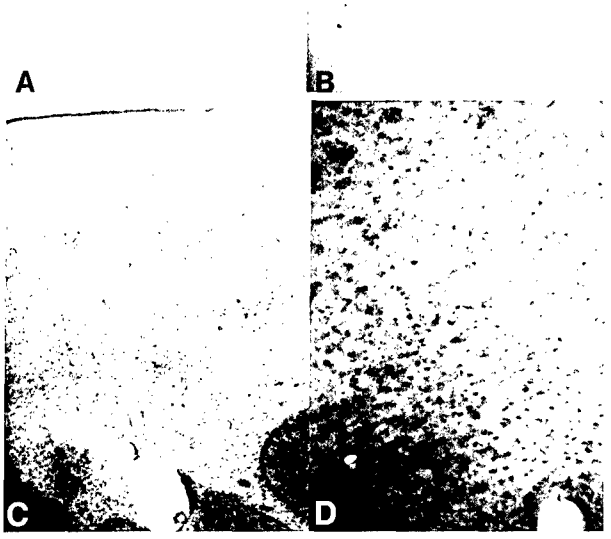

Figure 3. In situ end labeling (ISEL) detection of DNA fragmentation in normal control (**A**, **B**) and HD caudate (**C**, **D**), at low and higher power, respectively. ISEL staining is significantly greater in HD than in control striatal neurons. Note that ISEL is distributed predominantly within the cytoplasm with little or no labeling within the nucleus, implying more severe involvement of mitochondrial than nuclear DNA.

rons projecting to the internal segment (GPi) (81, 82, 84). Golgi staining shows that spiny neurons are also susceptible to morphological changes in HD, including recurving of the dendrites, altered shape and size of the spines, and increased density of spines.

Motor Dysfunction in HD. The clinical symptoms of HD reflect the pattern and extent of neuronal loss within different components of the basal ganglia-thalamocortical circuit. The neostriatum (caudate nucleus and putamen) receives excitatory glutamatergic inputs from the entire neocortex, the first step in the anatomical loop responsible for the initiation and execution of movement. Processed signals are transmitted via basal ganglia output nuclei (the internal segment of the globus pallidus, GPi; the substantia nigra pars reticulata, SNr; and ventral pallidum) to the thalamus, which in turn sends excitatory projections to areas of the frontal cortex associated with motor planning and execution (2, 4, 47). The GABAergic basal ganglia output projections to the thalamus maintain a tonic inhibition of their target nuclei, which is modulated by two opposing pathways (direct and indirect) which integrate the input and output compartments within the basal ganglia. It is an imbalance in the relative contributions of these two regulatory pathways which triggers, and dictates the nature of, the motor dysfunction in HD.

In the direct (monosynaptic) pathway, striatal efferents containing GABA and SP (GABA/SP) project directly to the internal segment of the globus pallidus (GPi). Activation of this pathway results in disinhibition of thalamic activity. In contrast, the indirect pathway consists of a polysynaptic projection between the striatum and GPi. In the first step of the indirect pathway, striatal efferents containing GABA and enkephalin (GABA/ENK) project to the external segment of the globus pallidus (GPe) which then sends purely GABAergic projections to the subthalamic nucleus. The efferent projection to the basal ganglia output nuclei (SNr and GPi) from the subthalamic nucleus is excitatory, most likely glutamatergic. The GPe projection generally exerts a tonic inhibition on the subthalamic nucleus, and activation of the GABA/ENK striatal efferents tends to suppress the activation of GPe neurons, resulting in disinhibiton of the subthalamic nucleus and hence an increase in the excitatory innervation of the basal ganglia output nuclei. This leads to an increased inhibitory input to the target thalamic nuclei. Consequently the thalamic innervation of the cortex is differentially modulated depending on the basal ganglia pathway activated (2, 4). Disruption of these pathways in HD leads to motor dysfunction. In HD there is preferential loss of the GABA/ENK neurons comprising the indirect pathway. The resulting "disinhibition" of the thalamus is manifest by the development of involuntary choreic movements. In contrast, it is proposed that the rigid akinetic state seen in some HD patients results from the additional loss of striatal GABA/SP efferents projecting directly to the GPi (1). There is also recent evidence that the dyskinesia seen in HD patients is influenced by imbalances between neuronal activities within the basal ganglia internal and external pallidal segments, as well as between segments (68).

Neurotransmitter Factors Influencing Cell Vulnerability in the HD Striatum. Several factors including cell localization, afferent and efferent projections, and neurochemical content appear to influence cell fate in HD. It has been proposed that the variable rates of cell death within the striatum and the selective neuronal

vulnerability in HD may reflect the neuronal distribution of glutamate receptor subtypes. The spiny neurons most vulnerable to degeneration contain mainly N-methyl-D-aspartate (NMDA) glutamate receptor subtypes (predominantly NMDAR-1 and NMDAR-2B) which are implicated as mediators of excitotoxic cell death in numerous pathological situations (27). Furthermore, an early and preferential loss of NMDA receptors in HD has been demonstrated (103). In contrast, the relatively preserved aspiny interneurons are rich in GluR-1 AMPA ionotropic glutamate receptor subtypes. Striatal spiny neurons also contain high densities of mGlu5 (group 1) and mGlu3 (group II) metabotropic glutamate receptor subtypes, which modulate excitatory synaptic transmission via activation of G-proteins in cell membranes. Group I mGluR subtypes have been proposed to be involved in neurotoxic processes, whereas group II subtypes are protective. Dopaminergic (DA) transmission also appears to influence cell vulnerability in the striatum. Striatal spiny neurons contain D1 receptors in the direct pathway, and D2 receptors in the indirect pathway. D1 and especially D2 receptors are markedly reduced in asymptomatic HD mutation carriers, suggesting that loss of DA innnervation contributes to the pathophysiology of HD (101).

NADPH-d-containing aspiny interneurons are relatively resistant to degeneration in HD. This has been postulated to reflect the type of glutamatergic receptors they express, and to be associated with their co-localization with NOS. NOS-containing neurons in the striatum are historically resistant to acute excitotoxic insults putatively mediated by nitric oxide (NO), including ischemic insults, leading to the proposition that the capacity to generate NO confers some degree of protection on this cell type (57, 98). A recent report suggests that this resistance to NO toxicity may be related to antioxidant properties of these cells, since cultured NO-resistant neurons were found to contain elevated levels of the mitochondrial superoxide radical scavenging enzyme manganese superoxide dismutase (MnSOD) (45). Furthermore, presence of MnSOD was found to be critical for the resistance of these nNOS-positive cultured neurons to NO- and NMDA-mediated toxicity. The involvement of excitotoxic processes is inferred by observations that intrastriatal injections of the endogenous NMDA receptor agonist quinolinic acid induce preferential loss of medium spiny neurons but spare NADPH-d neurons, whilst injection of the non-NMDA receptor agonists kainate or quisqualate result in loss of both spiny and NADPH-d positive aspiny neurons (8, 57). In contrast, s-4-carboxy-3-hydroxyphenylglycine (a group II mGluR agonist and a group I mGluR antagonist) is protective against quinolinic acid lesions (75). However, the extreme striatal atrophy and neuronal loss seen in Grade 4 HD patients suggests that ultimately all cell types are susceptible to cell death in HD.

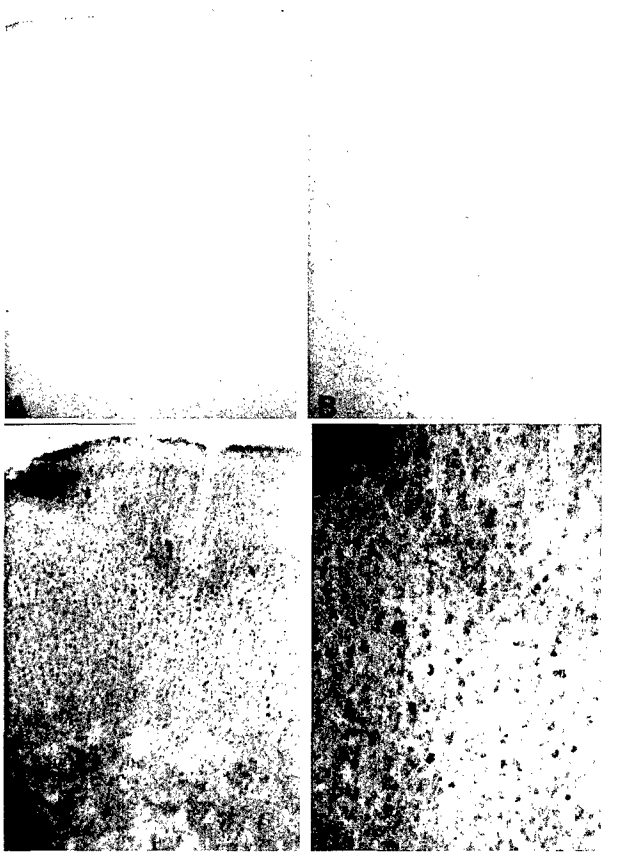

Figure 4. In situ end labeling (ISEL) detection of DNA fragmentation in normal control (**A**, **B**) and HD cortex (**C**, **D**), at low and higher power, respectively. The amount of label is markedly increased in HD cortex, relative to age-matched control levels.

Mutant Huntingtin Protein and the HD Brain. The genetic defect in HD is an expansion of an unstable CAG repeat encoding polyglutamines at the 5' end of a gene on chromosome 4, termed "interesting transcript 15" (IT15) (97). cDNA analysis reveals a predicted 348 kD gene product containing 3144 amino acids, termed "huntingtin" protein. In unaffected individuals the IT15 trinucleotide repeat typically contains 11-34 CAGs. Expansion to 35-39 CAG repeats in one or both alleles confers the likelihood of developing HD, whilst individuals with greater than 39 CAG repeats in either allele will develop the disease. The trinucleotide repeat is polymorphic and undergoes alterations during meiosis,

generally fluctuating by ± 1-5 repeats per transmission, although larger increases can occur following paternal transmission (83). At present the physiological functions of both normal and mutant huntingtin are unknown. However it is known that several features of the HD phenotype are influenced by CAG repeat length in the mutant gene. Most individuals develop the first symptoms of HD in adulthood, although age of onset of the disease is inversely correlated with size of the CAG repeat expansion, and a small proportion of cases have a juvenile onset associated with large CAG repeat lengths (5, 36). CAG repeat length has also been correlated with neuropathological severity, although this observation is controversial since grade of disease at time of death is dependent on a number of factors also influenced by repeat length, including age of onset and disease duration (43).

The elucidation of a pathogenic function for mutant huntingtin is currently the subject of intense research activity, but to date little is known about its potential roles in cell death processes, and distribution studies give little insight into the regional selectivity of cell loss in the disease. Studies in huntingtin "knock-out" mice suggest that the mutation results in the gain of a novel function, since murine *HD* homologue null mice die *in utero*, whilst heterozygous knock-out mice show little or no pathology (37). In addition, mice expressing abnormally low levels of murine huntingtin exhibit developmental abnormalities (102). Observations that antibodies to expanded polyglutamine stretches can discriminate between normal and mutant forms of huntingtin imply that the gene defect causes a conformational change in the protein (96). Findings that huntingtin protein is widely expressed throughout the body, showing no apparent selectivity for cerebral regions targeted by the disease process, suggest that another property of basal ganglia neurons confers vulnerability to degeneration in HD (62, 90). However, immunohistochemical studies have recently revealed a heterogeneous distribution of huntingtin immunoreactivity within the striatum which may underly cell susceptibility (39). Ferrante and colleagues (39) report huntingtin immunoreactivity located primarily within the matrix compartment, whereas little or no immunoreactivity was seen in the patch compartment. Double labeling techniques

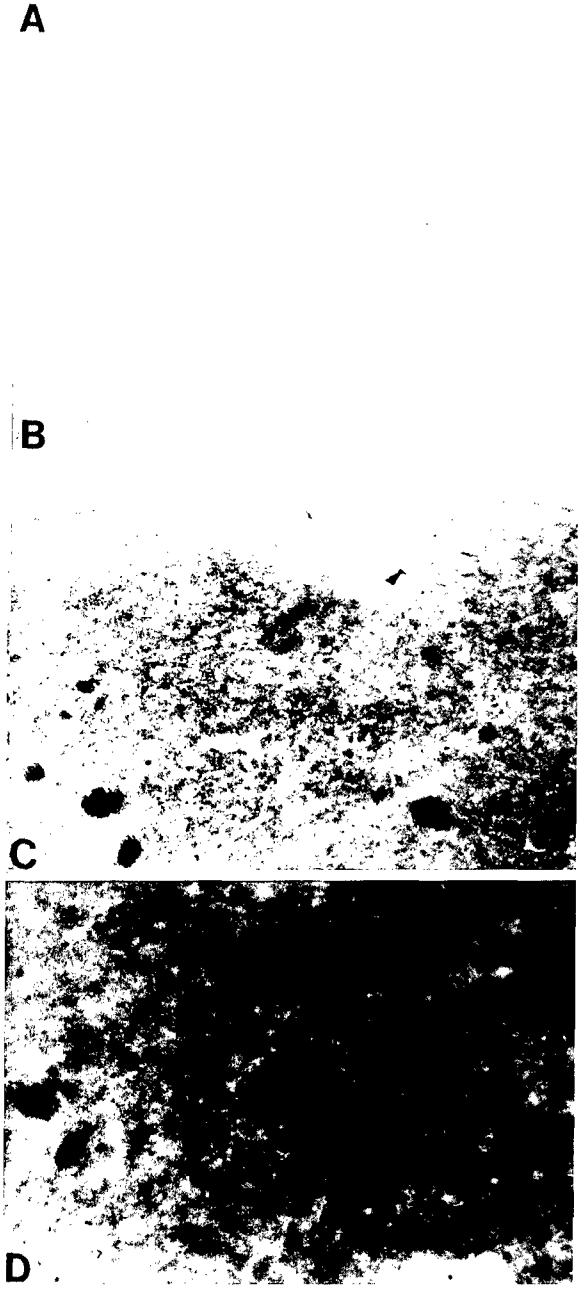

Figure 5. 3-Nitrotyrosine (3-NT) immunoreactivity, a marker for protein nitration, is increased in HD caudate. Relative to levels of immunoreactivity in normal caudate nucleus (**A**, **B**), there is a marked increase in immunohistochemical expression of 3-NT in HD striatum, predominantly localized to neuronal and neuropil elements.

revealed higher levels of huntingtin expression in medium spiny neurons and colocalization with calbindin, in contrast to little or no colocalization between huntingtin and NADPH-d or NOS neurons.

In neurons, huntingtin protein has a cytoplasmic distribution in perikarya, axons, dendrites and some nerve terminals. Potential roles in intracellular trafficking and synaptic function have been proposed on the basis of subcellular fractionation studies which indicated an association of huntingtin with synaptic vesicles and microtubules (32, 50). Huntingtin protein has also recently been identified in neuronal nuclei. N-terminal fragments of huntingtin have been found in ubiquinated protein aggregates deposited in neuronal nuclei (neuronal intranuclear inclusions, NII) and in dystrophic neurites (cytoplasmic inclusions, CI). These protein aggregates have been identified in both HD brain, and in the brains of transgenic mice expressing a fragment of human mutant huntingtin (30, 33). The mechanism of inclusion formation is unclear at present, but Perutz and colleagues (79) have suggested that the expanded polyglutamine stretches in mutant huntingtin facilitate the formation of β-pleated sheets held together by hydrogen bonds between amide groups. The CAG repeat length appears to be critical for aggregate formation, and Scherzinger and colleagues (86) demonstrated the formation of insoluble high molecular weight protein aggregates following proteolytic cleavage of a GST-huntingtin fusion protein containing 51 glutamine residues. However no protein aggregation occurred when polyglutamine repeat stretches were reduced to 20 or 30. Similar intranuclear inclusions have also been reported in other CAG repeat disorders including spinocerebellar ataxia type 3 (78). It is yet to be determined whether these huntingtin protein aggregates are directly involved in processes of cellular dysfunction, or whether deposition is secondary to another pathogenetic process.

Functional Alterations in HD Brain

Energy Metabolism is Selectively Disrupted in Brain Regions Targeted in HD. *Human Studies.* Despite identification of the HD mutation gene product, it is still not known how the gene defect results in selective cell death. One hypothesis is that the gain of function associated with expanded polyglutamine repeats leads either directly or indirectly to a defect in mitochondrial energy metabolism. As discussed later, mitochondrial defects may result from oxidative damage to cellular elements, or alternatively may induce oxidative stress via increased free radical production.

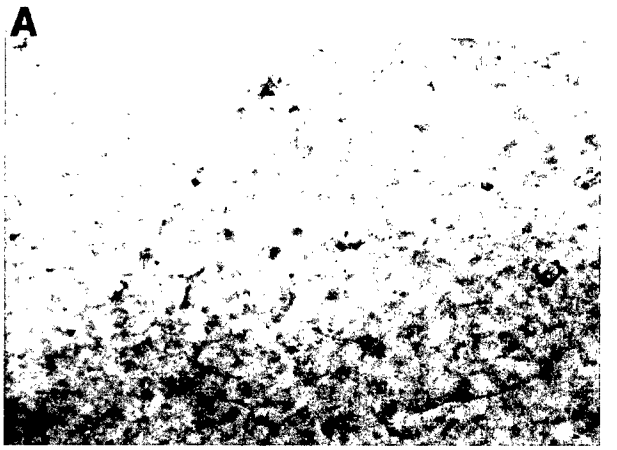

Figure 6. Malondialdehyde immunoreactivity, detecting lipid peroxidation, is increased in HD caudate nucleus (**B**), relative to levels in normal control caudate nucleus (**A**), and is evident in neuronal, astrocytic and vascular tissue elements.

Mitochondrial abnormalities in HD were first identified in ultrastructural studies of cortical biopsies from juvenile and adult onset HD cases (44). A metabolic defect in HD is also implicated by observations of insidious weight loss in HD patients despite a sustained caloric intake (77). The bulk of evidence comes from positron emission tomography (PET) studies and biochemical studies in post-mortem brain which show selective metabolic defects in brain regions targeted by the disease.

Glucose metabolism is markedly reduced in the basal ganglia and cerebral cortex of symptomatic HD patients (23, 60, 61, 70). Moreover, findings in PET studies that rates of striatal glucose utilization are reduced prior to the bulk of tissue loss in HD, and in asymptomatic subjects at risk of developing the disease provide compelling evidence that energetic defects play a causative role in the disease process (23, 60, 70). Cortical hypometabolism is also seen in patients suffering psychological disturbances and mood changes, before the onset of motor symptoms (61). Nuclear magnetic resonance (NMR) imaging studies also demonstrate meta-

bolic abnormalities in HD brain, suggestive of enhanced glycolytic activity to compensate for impaired oxidative phophorylation (55, 58). Elevated lactate concentrations were found in the occipital cortex and basal ganglia of symptomatic HD patients, but were not altered in asymptomatic or at risk patients (55, 56). The degree of increased lactate production correlated well with the duration of the disease, implying that normal energy metabolism is progressively impaired by the disease process. Interestingly, increased lactate production in HD brain can be ameliorated by treatment with the metabolic co-factor and antioxidant coenzyme Q_{10} (58).

Biochemical studies in HD post-mortem tissue show selective dysfunction of components of the oxidative phosphorylation pathway and Krebs' cycle in brain regions targeted in the disorder. Activities of succinate dehydrogenase and cytochrome oxidase (components of complexes II-III and IV of the electron transport chain, respectively) are markedly reduced in advanced grade HD caudate and putamen, but are unaltered in other brain regions (22, 25, 49). Brennan and colleagues (18) have also reported decreased cytochrome aa_3 levels in HD caudate, whereas cytochome b and cc1 levels do not change in the disease. Reduced pyruvate dehydrogenase activity has been reported in the basal ganglia and hippocampus in HD, while polarographic studies show decreased oxygen consumption in HD striatum, relative to levels in age-matched controls (25).

Animal Models of HD: Mitochondrial Toxins. A role for mitochondrial energy metabolism dysfunction in the pathogenesis of neuronal degeneration in HD is further supported by observations, in both humans and in experimental animals, that the basal ganglia neurons are particularly vulnerable to mitochondrial toxins such as the complex II inhibitors 3-nitropropionic acid (3-NP) and malonate; aminooxyacetic acid (AOAA) and MPTP (complex I); potassium cyanide and sodium azide (complex IV) (7, 10, 13, 20, 48, 65). Ingestion of 3-NP, an irreversible inhibitor of succinate dehydrogenase (complex II), produces selective basal ganglia lesions and delayed dystonia in humans (65). Systemic administration of 3-NP to both rats and primates produces age-dependent striatal lesions which are strikingly similar to

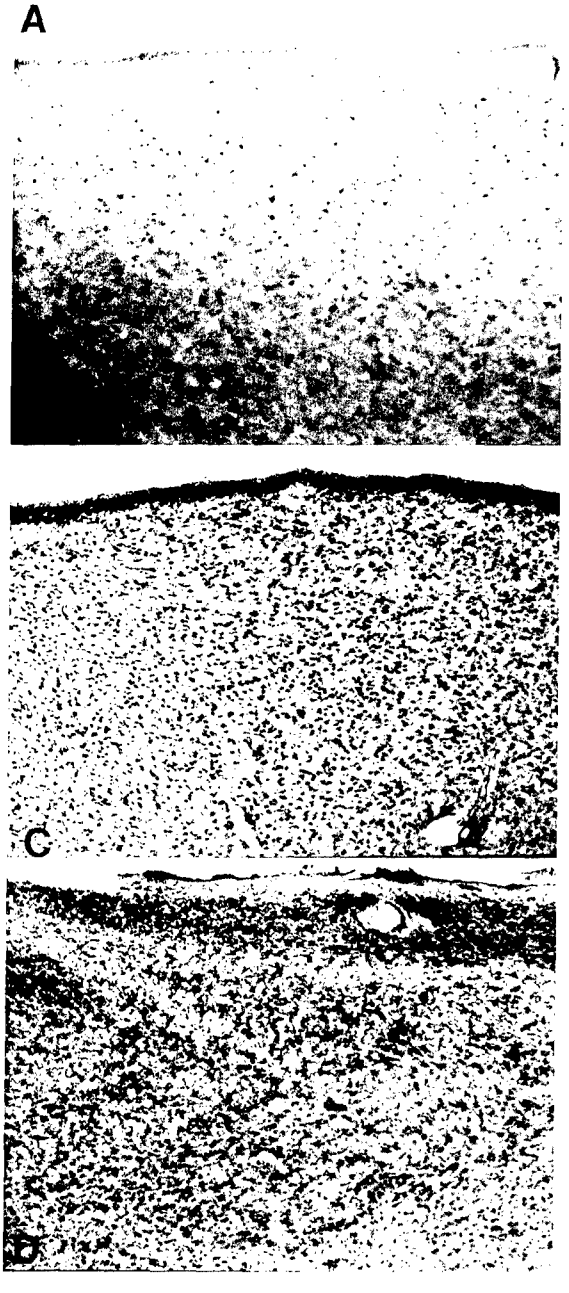

Figure 7. 8-Hydroxy-deoxyguanosine (8-OHdG) expression, a marker of DNA oxidation, is significantly increased in HD striatum, and levels of expression in cells and neuropil increase with severity of the disease. In comparison to immunoreactivity in normal caudate nucleus (**A**), 8-OHdG expression is moderately increased in low garde HD (**B**, Vonsattel Grade 1), and to a greater extent in moderate (**C**, Grade 2) and severe (**D**, Grade 4) HD. Less cellular staining in **D** may reflect greater neuronal loss.

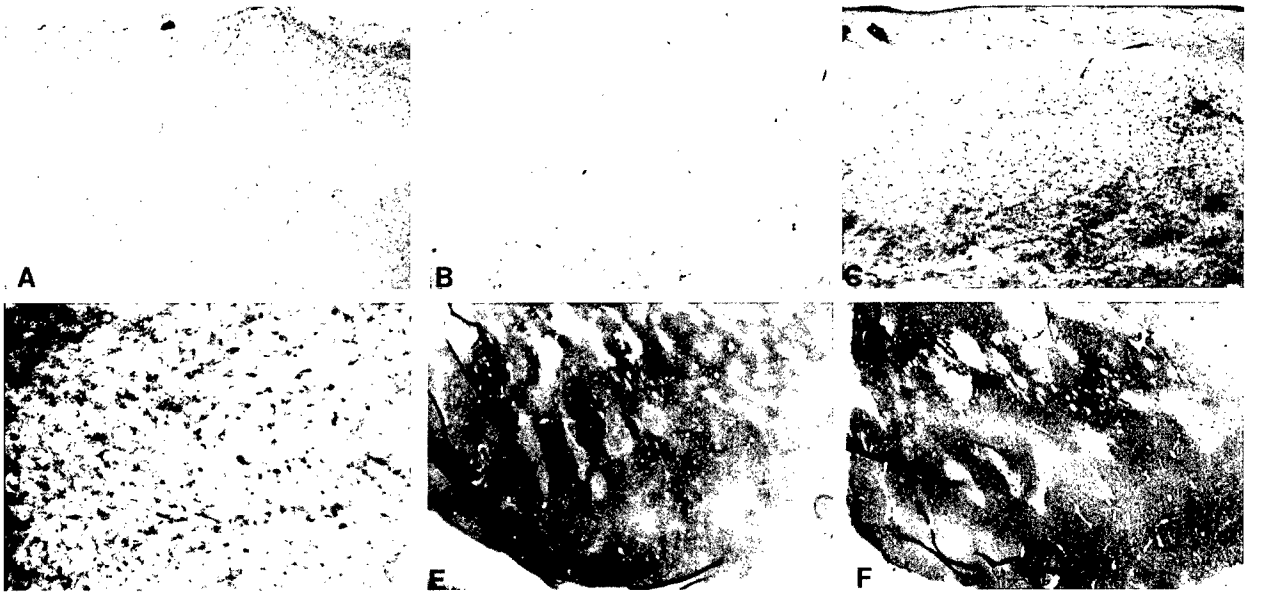

Figure 8. Heme oxygenase 1 (HO1), a marker for inducible oxidative stress, is increased in HD striatum. Relative to levels in normal caudate nucleus (**A**, **B**), there is a marked increase in HO1 immunoreactivity in HD caudate (**C**, **D**) associated with cellular and vascular tissue elements. Topographic heterogeneity of of HO1 immunoreactivity was observed within the HD caudate. Areas of greatest HO1 immunoreactivity (**E**) conformed to the matrix compartment , as shown in a contiguous striatal section stained for calbindin-Dk28 immunoreactivity (**F**). Arrows identify comparable patches of low activity.

those seen in HD (20, 21). In primates, chronic 3-NP administration produces selective striatal lesions which spare NADPH-d neurons, and induce proliferative changes in the dendrites of spiny neurons. Animals also show both spontaneous and apomorphine-inducible movement disorders resembling HD (21). 3-NP basal ganglia lesions in rats are associated with elevated lactate levels, similar to the increased lactate production seen in HD patients (20). 3-NP lesion formation in rats can be blocked by removal of glutamatergic excitatory striatal inputs by decortication, by glutamate release inhibitors, and by glutmate receptor antagonists, suggesting that 3-NP toxicity is mediated by secondary excitotoxic mechanisms (7, 89).

Increased Energy Metabolism is Neuroprotective in HD and Animal Models of HD. Further indirect evidence that energetic defects contribute to neurodegenerative processes in HD is provided by evidence that agents which enhance energy production in the brain exert neuroprotective effects. Preliminary studies in rodent mitochondrial toxin models, and NMR measurements of lactate production in man, suggest that coenzyme Q_{10} and creatine are neuroprotective, putatively via enhancing cerebral energy metabolism (58, 69). A number of agents which may improve mitochondrial function have been suggested as potential therapeutic strategies. These include vitamins that are coenzymes of respiratory enzymes, such as thiamine, riboflavin or biotin, or agents which serve as supplementary electron donors and acceptors, such as vitamins C, K_3 and coenzyme Q_{10} (CoQ_{10}). Coenzyme Q_{10} also has potent antioxidant effects. To date CoQ_{10} has been investigated most thoroughly, and oral administration improves symptoms in some mitochondrial-associated disorders including MELAS (mitochondrial myopathy, encephalopathy, lactic acidosis and stroke-like episodes) and Kearns-Sayre syndrome patients (reducing CSF and serum lactate and pyruvate levels, and enhancing mitochondrial enzyme activities in platelets) (19, 52). We recently showed that oral administration of CoQ_{10} over 1-2 months significantly ameliorated elevated lactate levels seen in the cortex of HD patients, an effect which was reversible on withdrawal of CoQ_{10} (58). Furthermore, CoQ_{10} attenuates neurotoxicity induced by the mitochondrial toxins MPTP and malonate in animal models (13, 89).

An alternative strategy is to increase brain energy stores of the high energy compound phosphocreatine (PCr) by creatine administration. Creatine is phosphorylated by mitochondrial creatine kinase. PCr then essentially shuttles energy in the form of a high-energy phosphate bond from the mitochondria to cell regions where it is required. ATP is regenerated in the cytoplasm where it is used in many different functions including maintenance of the membrane potential by the Na^+/K^+-ATPase

pump, and for Ca^{2+} buffering by Ca^{2+}-ATPase (51). It is hypothesized that PCr may be neuroprotective during periods of energetic compromise by providing an alternative energy source to ATP. This hypothesis is supported by observations that PCr levels are reduced prior to any ATP loss during depletion of energy stores in ischemic conditions. We recently showed that oral creatine administration in rats attenuates neurotoxicity induced by the succinate dehydrogenase inhibitor 3-NP (69). In addition, increases in cerebral lactate levels and decreases in levels of high energy phosphate compounds seen in the striata of 3-NP treated rats were attenuated by pre-treatment with creatine.

Evidence of Oxidative Damage In HD. *Human Studies.* Abnormal increases in levels of a number of markers for oxidative damage have been reported in HD brain. These include increased incidence of DNA strand breaks, exacerbated lipofuscin accumulation, and increased immunohistochemical staining of oxidative damage products in HD striatum and cortex (see Figures 1-8) (41, 44, 94).

A number of studies indicate increased peroxidative damage in HD. These include evidence that HD skin fibroblasts show increased vulnerability to glutamate toxicity which can be attenuated by antioxidant treatment (71), and findings of enhanced lipofuscin deposition in HD brain (94). Lipofuscin is a fluorophore produced by the reaction of amino compounds with secondary aldehydic products of oxidative free radical-induced oxidation of macromolecules, in particular lipid peroxidation. It accumulates in lysosomes in post-mitotic cells such as neurons and cardiac myocytes, and is commonly known as "age pigment" since its accumulation increases with age (95). The rate and extent of lipofuscin deposition in cells also increases under conditions of increased oxidative stress and metabolic rate (74, 91). As shown in Figures 1 and 2, both striatal and cortical neurons in HD brain contain higher levels of lipofuscin than age-matched controls. In addition, the extent of lipofuscin accumulation increases with the neuropathological severity of the disease. These results suggest increased lipid peroxidative damage in affected brain regions in HD.

Free radical-induced oxidative damage to DNA can induce DNA strand breaks (34). A number of studies show evidence of increased DNA strand breaks in HD striatal neurons, and have suggested the involvement of both apoptotic and necrotic mechanisms of cell death (26, 80). Moreover, a recent study demonstrates that the degree of DNA fragmentation in HD striatum is positively correlated with the length of the polyglutamine expansion in huntingtin (26). Using *in situ* end labelling techniques (ISEL), we found marked increases in DNA fragmentation in HD striatal and cortical neurons, relative to levels in the corresponding regions of age-matched controls (Figures 3 and 4). Furthermore, it appears that mitochondrial DNA (mtDNA) is more susceptible than nuclear DNA (nDNA) to fragmentation, since little or no ISEL labeling was detected within cell nuclei.

Oxidative damage can also induce excessive oxidation of DNA bases, such as deoxyguanosine (to produce 8-hydroxy-deoxyguanosine; 8-OHdG) (42). We found significant increases in levels of 8-OHdG in nDNA in the caudate of Grade 4 HD cases, using HPLC detection methods in post-mortem tissue (22). No alterations in nDNA 8-OHdG content were seen in brain regions affected to a lesser extent in HD, including frontal and parietal cortices and cerebellum, in the same subject population.

Using immunohistochemical markers to examine oxidative damage to a number of cellular macromolecules, we found abnormal elevations in oxidative damage to lipid, protein and DNA in HD cortex and striatum (Figures 5-8; 41). In control brains, we found that immunoreactive staining for 3-nitrotyrosine (3-NT; a marker for peroxynitrite-mediated protein nitration), malondialdehyde (MDA; marker for oxidative damage to lipids), 8-OHdG (DNA oxidative damage product) and heme oxygenase (HO; formed during oxidative stress) was weak, evident only in scattered cortical and striatal neurons, with enhanced staining in the striatal matrix zone. The extent and intensity of immunoreactivity were enhanced in HD brain, and patterns of staining seen in cases of different grades mirrored the pattern of progressive cell loss throughout the brain. In low grade HD cases, 3-NT, MDA, 8-OHdG and HO all showed greater immunoreactivity in dorsal versus caudal striatum, and the extent of immunoreactivity increased through the striatum with increasing grade of disease. In grades 3 and 4 striatal immunoreactivity was reduced, consistent with the severe striatal cell loss at end stage

Animal Studies. Oxidative damage is also implicated in the pathogenesis of striatal lesion formation induced by the mitochondrial toxins malonate and 3-NP, which inhibit succinate dehydrogenase and produce striatal lesions resembling HD (88, 89). Intrastriatal injection of either agent in rats increased the rate of hydroxyl free radical production in the striatum, as detected by microdialysis measurement of 2,3- and 2,5-dihydroxybenzoic

acid levels, generated by the reaction of hydroxyl radicals with salicylate. Increased 8-OHdG levels in striatum were also detected following systemic 3-NP administration, and elevated 3-nitrotyrosine concentrations were seen after either systemic 3-NP administration, or intrastriatal malonate injection. Lesion volumes and associated increases in oxidative damage markers induced by 3-NP were markedly attenuated in mice overexpressing the superoxide free radical scavenger Cu/Zn superoxide dismutase (Cu/Zn-SOD), suggesting the involvement of oxidative free radical damage in lesion formation (14). Furthermore, malonate and 3-NP striatal lesions were attenuated by free radical spin traps and nitric oxide synthase (NOS) inhibitors (89). Inhibition of nitric oxide (NO) generation in mice lacking the gene for the neuronal isoform of NOS (nNOS), also resulted in reduced volume of malonate lesions. Results support the involvement of nitric oxide-mediated oxidative damage in cell death processes following energetic disruption in these models (89).

Putative Mechanisms of Cell Death in HD: Mitochondrial Damage, Oxidants and Excitotoxicity.

Mitochondrial Dysfunction and Excitotoxicity. What are the common pathways linking the huntingtin mutation with bioenergetic defects, oxidative damage and cell loss in HD? The definitive answer is currently unknown, but one hypothesis is that bioenergetic defects could lead to neuronal death via so-called secondary excitotoxicity (3, 6). Energetic defects might occur as a primary event in HD, or as a consequence of oxidative damage to cellular elements. Reduced ATP production due to impaired mitochondrial energy metabolism can result in partial cell depolarization, by making neurons more vulnerable to endogenous levels of glutamate (15, 28). The concomitant increase in Ca^{2+} influx into neurons may trigger further free radical production, exacerbating damage to cellular elements. This hypothesis is supported by findings that normally ambient levels of excitatory amino acids become toxic in the presence of oxidative phosphorylation inhibitors, sodium-potassium pump inhibitors, or potassium-induced partial cell membrane depolarization (76, 104). Further, excitatory amino acid antagonists such as MK-801 can ameliorate cerebral lesions induced by mitochondrial toxins including AOAA, malonate, 3-NP and 3-acetylpyridine, 3-AP (10, 48, 65, 87). Excitotoxic mechanisms have been implicated in the mechanism of cell death in HD largely on the basis of observations of NMDA glutamate receptor distribution within striatal cell populations, and findings that excitotoxic striatal lesions in animal models closely resemble those seen in HD brain (6, 8).

Impaired activity of components of the energy metabolism pathways including pyruvate dehydrogenase and succinate dehydrogenase have been reported in HD, as discussed previously. Direct impairment of the mitochondrial oxidative phosphorylation pathway, or reduced substrate trafficking into this pathway as a result of disruption of glycolysis or the Krebs cycle, will result in reduced ATP production by mitochondria. The bulk of ATP production within cells takes place within the mitochondrial electron transport chain. It is comprised of five protein complexes: NADH ubiquinone oxidoreductase (complex I), succinate ubiquinol oxidoreductase (II), ubiquinol cytochrome c oxidoreductase (III), and cytochrome c oxidase (IV) which act in series to oxidize NADH and $FADH_2$, generated in the mitochondrial matrix by the Krebs cycle, via electron transfer, ultimately to oxygen. Electron movement involves pumping of protons across the inner mitochondrial membrane, producing an electrochemical gradient which complex V (ATP synthase) utilizes as an energy source for the high-energy bonds in ATP. Optimal metabolic activity is dependent on the efficiency of electron movement along the electron transport chain and its coupling to oxidative phosphorylation, and processes which disrupt electron transfer may potentially impair mitochondrial energy metabolism.

Reduced ATP production can result in cell death via disruption of energy-dependent processes (6). ATP is essential to fuel ionic pumps which generate and maintain ionic and voltage gradients across neuronal membranes, including Na^+/K^+-ATPase pumps which control the restoration of the resting membrane potential after depolarization, and ATPases which regulate intracellular levels of Ca^{2+}. Impaired Na^+/K^+-ATPase pump activity will inhibit membrane repolarization, resulting in prolonged or inappropriate opening of voltage-dependent ion channels. If severe enough, this partial membrane depolarization may facilitate activation of NMDA receptors by endogenous levels of glutamate, by alleviating the voltage-dependent Mg^{2+} blockade of NMDA receptor channels. The resultant excessive inward flux of Na^+ and Ca^{2+} ions can set in motion neurotoxic cascades. Ca^{2+} influx into neurons is implicated as a trigger for increased free radical production via NO-mediated mechanisms, and associated oxidative damage to cellular elements including proteases, lipases and endonucleases, ultimately leading to cell death. The cascade may become self-perpetuating, high cytosolic Ca^{2+} levels inducing Ca^{2+} uptake by mitochondria, leading to irre-

versible mitochondrial damage which is exacerbated by the actions of Ca^{2+}-activated phospholipases. Increased intracellular Na+ levels will decrease the activity of the Na^{+}/Ca^{2+} antiport system, which would normally extrude Ca^{2+} from the cell. In addition, reduced ATP levels will impair ATP-dependent extrusion and storage of Ca^{2+}, further increasing intracellular concentrations of free Ca^{2+}.

Oxidative Damage and Energetic Dysfunction. It is presently unclear whether mitochondrial dysfunction is a direct consequence of the huntingtin mutation in HD, or occurs as a secondary event. However, recent evidence suggests that mitochondrial energy metabolism dysfunction may result from excessive oxidative damage to DNA or other neuronal macromolecules, as a consequence of increased free radical and oxidant generation. Free radicals including superoxide ($O_2^{\bullet-}$) and hydroxyl radicals ($HO^{\bullet}$) are constantly produced as by-products of aerobic metabolism, but production increases under circumstances of electron transport chain inhibition or molecular defects (35, 38). Elevated Ca^{2+} influx induced by excitotoxic processes leads to sequestering of Ca^{2+} in mitochondria, which in turn increases free radical generation by the mitochondria. Increased generation of hydroxyl and carbon-centered radicals by mitochondria in response to Ca^{2+} concentrations similar to those induced by neuronal exposure to excitotoxins has been demonstrated *in vitro* (38). Redox sensitive dyes, including dihydrorhodamine, have also shown glutamate-induced increases in mitochondrial Ca^{2+} content and free radical generation *in vitro* (35). Incresed nitric oxide (NO) production in response to elevated Ca^{2+}/calmodulin-mediated activation of NOS, may also result in increased peroxynitrite ($ONOO^-$) formation. $ONOO^-$, produced by the reaction of NO with superoxide radical, may then react with Cu/Zn-SOD to form nitronium ion, which nitrates tyrosine residues in proteins (53). An alternative pathway for NO/$ONOO^-$-mediated toxicity is via peroxidative DNA damage leading to activation of poly(ADP-ribose) synthetase (PARP). PARP is a nuclear enzyme invoved in DNA repair, but excessive PARP activation can exhaust cellular energy supplies, inducing cell death cascades due to energetic dysfunction (105).

Free radicals can induce oxidative damage to cell macromolecules including DNA, proteins and lipids by a number of different mechanisms, including DNA strand breaks or formation of DNA adducts such as 8-OHdG, protein carbonylation, or by lipid peroxidation (42, 67, 93). Potential functional consequences include perturbations of DNA transcription and translation, protein synthesis, enzyme activities and membrane fluidity. Mitochondria are thought to be particularly vulnerable to oxidative injury since most intracellular free radicals are generated by the mitochondrial electron transport chain. MtDNA is extremely susceptible due to its localization in the mitochondrial matrix, lack of protective histones, and limited repair mechanisms (64). Thus any increase in free radical production, or impaired activity of a regulatory enzyme such as Cu/Zn-SOD or glutathione peroxidase, could reduce the functional capacity of the oxidative phosphorylation pathway. In addition, the slow, progressive nature of neuronal injury in chronic neurodegenerative disorders may be explained by cycling of free radicals and mitochondrial dysfunction. Further evidence supporting a role for oxidative damage in HD is that the energetic defects seen in HD brain are similar to those induced in cell culture by peroxynitrite, which preferentially inhibits complex II-III and (to a lesser extent) complex IV activity in the electron transport chain (16).

Pathological Interactions of Mutant Huntingtin Protein? A number of possible cellular interactions of mutant huntingtin have been proposed. These include suggestions that expanded glutamine repeats may allow protein-protein interactions, or that polyglutamines may be a substrate for transglutaminase (29, 79). The principal candidate protein interactors are huntingtin-associated protein-1 (HAP-1) and glyceraldehyde 3-phosphate dehydrogenase (GAPDH) (24, 63). HAP-1 is found only in brain but does not show a preferential striatal distribution. GAPDH is a critical glycolytic enzyme, leading to suggestions that an interaction with huntingtin may result in impaired metabolic function. The potential for huntingtin to deleteriously affect GAPDH function is supported by a recent report that both GAPDH and α-ketoglutarate dehydrogenase are inactivated by fusion proteins containing polyglutamine stretches of pathological length, in reactions catalyzed by transglutaminase (29). However, the glycolytic function of GAPDH appears to remain intact in HD, as a recent study failed to detect any differences in levels of cytosolic GAPDH activity between HD grade 4 and age-matched control brain tissue (22).

There is a great deal of debate concerning whether NII deposition plays a causative role in the pathogenesis of cell death in HD. Interestingly, a recent study reports that in HD cortex and striatum inclusion deposition does not mirror the pattern of cell death in the disease (59). NII and CI are seen in NADPH-d neurons spared in the

disease, but are not found in acetylcholinesterase- and choline acetyltransferase-positive interneurons, suggesting that NII formation is not critical for cell death mechanisms. Furthermore, although expression of human mutant huntingtin in transgenic mouse models of HD is associated with the development of movement disorders and deposition of huntingtin aggregates reminiscent of HD, no murine model reported to date exhibits the selective neuronal death which characterizes HD (30, 66, 102). There is *in vitro* evidence that expanded CAG repeats can induce huntingtin aggregation and cell death in transfected cerebellar granule cell cultures (72). In addition, transfection of a human mutant huntingtin fragment into *Drosophila* eye cells induced CAG repeat-dependent photoreceptor degeneration and death, putatively via apoptotic mechanisms (54). However, Saudou and colleagues (85) recently reported cell-selective neurodegeneration resembling apoptotic cell death in cultured striatal (but not hippocampal) neurons transfected with a human mutant huntingtin fragment, independent of the presence of intranuclear inclusions, suggesting that NII deposition may reflect a protective mechanism within cells. This proposition is supported by observations that suppression of NII deposition led to increased cell death in this neuronal population.

Although neither full length huntingtin or huntingtin fragments have yet been found in mitochondria, an effect on mitochondrial function cannot be ruled out. For instance, huntingtin may play a role in mitochondrial trafficking, or alternatively NII may influence nuclear transcription and thus affect the expression of nuclear-encoded proteins including subunits of mitochondrial complex II. The latter is of particular note since complex II activity is impaired in affected brain areas in HD.

Conclusions

Multiple lines of evidence indicate that oxidative stress and energetic defects may play roles in the etiology of selective neuronal death in HD. To date it has been impossible to determine whether bioenergetic dysfunction or oxidative damage are causative factors in the disease process, or merely occur secondarily to neuronal loss in HD. Furthermore, although the genetic mutation responsible for the phenotype in HD is known and its protein product identified, the mechanism whereby abnormal huntingtin protein leads to region-specific cell death is unknown. The recent development of transgenic mouse models of HD has provided a valuable opportunity to elucidate the pathologic sequence of events culminating in disease phenotype and cell death associated with the HD gene mutation, which is impossible to determine from end-stage post-mortem tissue.

Several transgenic mouse models of HD have recently been developed. Of these the best characterized to date are R6/2 mice, developed by inserting a transgene containing an N-terminal fragment of human mutant huntingtin carrying CAG repeat expansions of 145-150 units (66). Mice exhibit a rapidly progressing neurological phenotype, with onset at approximately 2 months of age and lifespan of up to 17 weeks. They develop a movement disorder involving resting tremor, shuddering, stereotypic grooming behaviour, and epileptic seizures, and lose body weight from 8 weeks of age. Brain weight is reduced approximately 20% at 12 weeks, relative to normal littermate controls. Neuronal intranuclear inclusions (NII) of the transgene protein are evident by 3-4 weeks of age (30). It is anticipated that the investigation of oxidative stress markers in this and other transgenic mouse models of HD will soon provide vital insight into the etiologic role of oxidative damage in mechanisms of neuronal death in HD.

Acknowledgements

This work was supported in part by NIH grant NS35255 (RJF), by the Huntington's Disease Society of America (SEB), and by NS16367 (Huntington's Disease Center Without Walls, MFB).

References

1. Albin RL, Reiner A, Anderson KD, Penney JB, Young AB (1990) Striatal and nigral neuron subpopulations in rigid Huntington's disease: Implications for the functional anatomy of chorea and rigidity-akinesia. *Ann Neurol* 27: 357-365
2. Albin RL, Young AB, Penney JB (1989) The functional anatomy of basal ganglia disorders. *Trends Neurosci* 12: 366-375
3. Albin RL, Greenamyre JT (1992) Alternative excitotoxic hypotheses. *Neurology* 42: 733-738
4. Alexander GE, Crutcher MD (1990) Functional architecture of basal ganglia circuits: neural substrates of parallel processing. *Trends Neurosci* 13: 266-271
5. Andrew SE, Goldberg YP, Kremer B, Telenius H, Theilmann J, Adam S, Starr E, Squitieri F, Lin B, Kalchman MA et al. (1993) The relationship between trinucleotide (CAG) repeat length and clinical features of Huntington's disease. *Nat Genet* 4: 398-403
6. Beal MF. (1992) Does impairment of energy metabolism result in excitotoxic neuronal death in neurodegenerative illness? *Ann Neurol* 31: 119-130
7. Beal MF (1994) Neurochemistry and toxin models in Huntington's disease. *Curr Op Neurol* 7: 542-547

8. Beal MF, Kowall NW, Ellison DW, Mazurek MF, Swartz KJ, Martin JB (1986) Replication of the neurochemical characteristics of Huntington's disease by quinolinic acid. *Nature* 321: 168-171
9. Beal MF, Ellison DW, Mazurek MF, Swartz KJ, Malloy JR, Bird ED, Martin JB (1988) A detailed examination of substance P in pathologically graded cases of Huntington's disease. *J Neurol Sci* 84: 51-61
10. Beal MF, Swartz KJ, Hyman BT, Storey E. Finn SF and Koroshetz W. (1991b) Aminooxyacetic acid results in excitotoxin lesions by a novel indirect mechanism. *J Neurochem* 57: 1068-1073
11. Beal MF, Brouillet E, Jenkins BG, Ferrante RJ, Kowall NW, Miller JM, Storey E, Srivastava R, Rosen BR, Hymen BT (1993a) Neurochemical and histologic characterization of excitotoxic lesions produced by mitochondrial toxin 3-nitropropionic acid. *J Neurosci* 13: 4181-4192
12. Beal MF, Hyman BT and Koroshetz W. (1993b) Do defects in mitochondrial energy metabolism underlie the pathology of neurodegenerative diseases? *Trends Neurosci* 16: 125-131
13. Beal MF, Henshaw DR, Jenkins BG, Rosen BR, Schulz JB. (1994) Coenzyme Q10 and nicotinamide block striatal lesions produced by the mitochondrial toxin malonate. *Ann Neurol* 36: 882-888
14. Beal MF, Ferrante RJ, Henshaw R, Matthews RT, Chan PH, Kowall NW, Epstein CJ, Schulz JB (1995) 3-Nitropropionic acid neurotoxicity is attenuated in copper/zinc superoxide dismutase transgenic mice. *J Neurochem* 65: 919-922
15. Blaustein MP (1988) Calcium transport and buffering in neurons. *Trends Neurosci* 11: 438-443
16. Bolanos JP, Heales SJR, Land JM, Clark, JB (1995) Effect of peroxynitrite on the mitochondrial respiratory chain: Differential susceptibility of neurones and astrocytes in primary culture. *J Neurochem* 64: 1965-1972
17. Braak H, Braak E (1992) Allocortical involvement in Huntington's disease. *Neuropathol App Neurobiol* 18: 539-547
18. Brennan WA, Bird ED, Aprille JR. (1985) Regional mitochondrial respiratory activity in Huntington's disease brain. *J Neurochem* 44: 1948-1950
19. Bresolin N, Bet L, Binda A, Moggio M, Comi G, Nador F, Ferrante C, Carenzi A, Scarlato G (1988) Clinical and biochemical correlations in mitochondrial myopathies treated with coenzyme Q10. *Neurology* 38: 892-899
20. Brouillet EP, Jekins BG, Hyman BT, Ferrante, RJ, Kowall NW, Srivastava R, Samanta-Roy D, Rosen BR, Beal MF (1993) Age-dependent vulnerability of the striatum to the mitochondrial toxin 3-nitropropionic acid. *J Neurochem* 60: 356-359
21. Brouillet E, Hantraye P, Ferrante RJ, Dolan R, Leroy-Willig A, Kowall NW, Beal MF (1995) Chronic mitochondrial energy impairment produces selective striatal degeneration and abnormal choreiform movements in primates. *Proc Natl Acad Sci USA* 92: 7105-7109
22. Browne SE, Bowling AC, MacGarvey U, Baik MJ, Berger SC, Muqit MMK, Bird ED, Beal MF (1997) Oxidative damage and metabolic dysfunction in Huntington's Disease: Selective vulnerability of the basal ganglia. *Annals Neurol* 41: 646-653
23. Browne SE, Beal MF (1994) Oxidative damage and mitochondrial dysfunction in neuro-degenerative diseases. *Biochem Soc Trans* 22: 1002-1006
24. Burke JR, Enghild JJ, Martin ME, Jou Y-S, Myers RM, Roses AD, Vance VM, Strittmatter WJ (1996) Huntingtin and DRPLA proteins selectively interact with the enzyme GAPDH. *Nature Med* 2: 347-350
25. Butterworth J, Yates CM, Reynolds GP (1985) Distribution of phosphate-activated glutaminase, succinic dehydrogenase, pyruvate dehydrogenase, and α-glutamyl transpeptidase in post-mortem brain from Huntington's disease and agonal cases. *J Neurol Sci* 67: 161-171
26. Butterworth NJ, Williams L, Bullock JY, Love DR, Faull RLM, Dragunow M. (1998) Trinucleotide (CAG) repeat length is positively correlated with the degree of DNA fragmentation in Huntington's disease striatum. *Neurosci* 87: 49-53
27. Calabresi P, Centonze D, Pisani A, Sancesario G, Gubellini P, Marfia GA, Bernardi G (1998) Striatal spiny neurons and cholinergic interneurons express differential ionotropic glutamatergic responses and vulnerability: implications for ischemia and Huntington's disease. *Ann Neurol* 43: 586-597
28. Choi DW (1988) Calcium-mediated neurotoxicity: relationship to specific channel types and role in ischemic damage. *Trends Neurosci* 11: 465-469
29. Cooper AJL, Sheu K-FR, Burke JR, Onodera O, Strittmatter WJ, Roses AD, Blass JP. (1997) Transglutaminase-catalyzed inactivation of glyceraldehyde 3-phosphate dehydrogenase and a-ketoglutarate dehydrogenase complex by polyglutamine domains of pathological length. *Proc Natl Acad Sci USA*. 94: 12604-12609
30. Davies SW, Turmaine M, Cozens B, DiFiglia M, Sharp A, Ross CA, Scherzinger E, Wanker EE, Mangiarini L, Bates G. (1997) Formation of neuronal intranuclear inclusions (NII) underlies the neurological dysfunction in mice transgenic for the HD mutation. *Cell* 90: 537-548.
31. de la Monte SM, Vonsattel JP, Richardson Jr EP (1988) Morphometric demonstration of atrophic changes in the cerebral cortex, white matter, and neostriatum in Huntington's disease. *J Neuropath Exp Neurol* 47: 516-525
32. DiFiglia M, Sapp E, Chase K, Schwarz C, Meloni A, Young C, Martin E, Vonsattel J-P, Carraway R, Reeves SA, Boyce FM, Aronin N (1995) Huntingtin is a cytoplasmic protein associated with vesicles in human and rat brain neurons. *Neuron* 14: 1075-1081
33. DiFiglia M, Sapp E, Chase KO, Davies SW, Bates GP, Vonsattel J-P, Aronin N. (1997) Aggregation of huntingtin in neuronal intranuclear inclusions and dystrophic neurites in brain. *Science* 277: 1990-1993

34. Driggers WJ, Holmquist GP, LeDoux SP, Wilson GL (1997) Mapping frequencies of endogenous oxidative damage and the kinetic response to oxidative stress in a region of rat mtDNA. *Nucleic Acids Res* 25: 4362-9

35. Dugan LL, Sensi SL, Canzoniero LM, Handran SD, Rothman SM, Lin TS, Goldberg MP, Choi DW (1995) Mitochondrial production of reactive oxygen species in cortical neurons following exposure to N-methyl-D-aspartate. *J Neurosci* 15: 6377-6388

36. Duyao M, Ambrose C, Myers R, Novelletto A, Persichetti F, Frontali M, Folstein S, Ross C, Franz M, Abbott M, et al (1993) Trinucleotide repeat length instability and age of onset in Huntington's disease. *Nat Genet* 4: 387-92

37. Duyao MP, Auerbach AB, Persichetti F, Barnes GT, McNeil SM, Ge P, Vonsattel J-P, Gusella JF, Joyner AL, MacDonald ME (1995) Inactivation of the mouse Huntington's disease gene homolog (*Hdh*). *Science* 269: 407-410

38. Dykens JA (1994) Isolated cerebral and cerebellar mitochondria produce free radicals when exposed to elevated Ca^{2+} and Na^{+}: implications for neurodegeneration. *J Neurochem* 63: 584-91

39. Ferrante RJ, Gutekunst C-A, Persichetti F, McNeil SM, Kowall NW, Gusella JF, MacDonald ME, Beal MF, Hersch SM (1997) Heterogeneous topographic and cellular distribution of huntingtin expression in the normal human neostriatum. *J Neurosci* 17: 3052-3063

40. Ferrante RJ, Kowall NW, Beal MF, Martin JB, Bird ED, Richardson EP (1987) Morphologic and histochemical characteristics of a spared subset of striatal neurons in Huntington's disease. *J Neuropath Exp Neurol* 46: 12-27

41. Ferrante RJ, Kowall NW, Hersch SM, Brown rh, Beal MF (1996) Immunohistochemical localization of markers of oxidative injury in Huntington's disease. *Soc Neurosci* 22: 92.5

42. Fraga CG, Shigenaga MK, Park J-W, Degan P, Ames BN (1990) Oxidative damage to DNA during aging: 8-hydroxy-2'-deoxyguanosine in rat organ DNA and urine. *Proc Natl Acad Sci USA* 87: 4533-4537

43. Furtado S, Suchowersky O, Rewcastle B, Graham L, Klimek ML, Garber A. (1996) Relationship between trinucleotide repeats and neuropathological changes in Huntington's disease. *Ann Neurol* 39: 132-136

44. Goebel HH, Heipertz R, Scholz W, Iqbal K, Tellez-Nagel I. (1978) Juvenile Huntington chorea: clinical, ultrastructural, and biochemical studies. *Neurology* 28: 23-31

45. Gonzalez-Zulueta M, Ensz LM, Mukhina G, Lebovitz RM, Zwacka RM, Engelhardt JF, Oberley LW, Dawson VL, Dawson TM. (1998) Manganese superoxide dismutase protects nNOS neurons from NMDA and nitric oxide-mediated neurotoxicity. *J Neurosci* 18: 2040-2055

46. Graveland GA, Williams RS, DiFiglia M (1985) Evidence for degenerative and regenerative changes in neostriatal spiny neurons in Huntington's disease. *Science* 227: 770-773 n

47. Graybiel AM, Aosaki T, Flaherty AW, Kimura M (1994) The basal ganglia and adaptive motor control. *Science* 265: 1826-1831

48. Greene JG, Porter RH, Eller RV, Greenamyre JT (1993) Inhibition of succinate dehydrogenase by malonic acid produces an "excitotoxic" lesion in rat striatum. *J Neurochem* 61: 1151-1154

49. Gu M, Gash MT, Mann VM, Javoy-Agid F, Cooper JM, Schapira AHV (1996) Mitochondrial defect in Huntington's disease caudate nucleus. *Ann Neurol* 39: 385-389

50. Gutekunst C-A, Levey AI, Heilman CJ, Whaley WL, Yi H, Nash NR, Rees HD, Madden JJ, Hersch SM (1995) Identification and localization of huntingtin in brain and human lympho-blastoid cell lines with anti-fusion protein antibodies. *Proc Natl Acad Sci USA* 92: 8710-8714

51. Hemmer W, Wallimann T. (1993) Functional aspects of creatine kinase in brain. *Dev Neurosci* 15: 249-260

52. Ihara Y, Namba R, Kuroda S, Sato T, Shirabe T (1989) Mitochondrial encephalomyopathy (MELAS): pathological study and successful therapy withcoenzyme Q10 and idebenone. *J Neurol Sci* 90: 263-271

53. Ischiropoulos H, Zhu L, Chen J, Tsai M, Martin JC, Smith CD, Beckman JS (1992) Peroxynitrite-mediated tyrosine nitration catalyzed by superoxide dismutase. *Arch Biochem Biophys* 298: 431-7

54. Jackson GR, Salecker I, Schulze KL, Dong X, Yao X, Arnheim N, Faber P, MacDonald ME, Zipursky SL (1998) Age- and polyglutamine length-dependent degeneration of drosophila photoreceptor neurons induced by human huntingtin transgenes. *Soc Neurosci* 24: 205.2

55. Jenkins BG, Koroshetz W, Beal MF, Rosen B (1993) Evidence for an energy metabolism defect in Huntington's disease using localized proton spectroscopy. *Neurology* 43: 2689-2695

56. Jenkins BG, Rosas HD, Chen Y-CI, Makabe T, Myers R, MacDonald M, Rosen BR, Beal MF, Koroshetz WJ (1998) 1H-NMR spectroscopy studies of Huntington's disease. *Neurology* 50: 1357-1365

57. Koh J-Y, Peters S, Choi DW (1986) Neurons containing NADPH-diaphorase are selectively resistant to quinolinate toxicity. *Science* 234: 73-76

58. Koroshetz WJ, Jenkins BG, Rosen BR, Beal MF (1997) Energy metabolism defects in Huntington's disease and possible therapy with coenzyme Q_{10}. *Ann Neurol* 41: 160-165

59. Kuemmerle S, Klein AM, Gutekunst C-A, Li X-J, Li S-H, Hersch SM, Ferrante R (1998) Distribution of huntingtin aggregation in spared and vulnerable neurons in Huntington's disease. *Soc Neurosci* 24: 380.14

60. Kuhl DE, Markham CH, Metter EJ, Riege WH, Phelps ME, Mazziotta JC (1985) Local cerebral glucose utilization in symptomatic and presymptomatic Huntington's disease. *Research Publications - Association for Research in Nervous and Mental Disease* 63: 199-209

61. Kuwert T, Lange HW, Langer K-J, Herzog H, Aulich A, Feinendegen LE (1990) Cortical and subcortical glucose consumption measured by PET in patients with Huntington's disease. *Brain* 113: 1405-1423

62. Landwehrmeyer GB, McNeil SM, Dure LS, Ge P, Aizawa H, Huang Q, Ambrose CM, Duyao MP, Bird ED, Bonilla E, de Young M, Avila-Gonzales AJ, Wexler NS, DiFiglia M, Gusella JF, MacDonald ME, Penney JB, Young AB and Vonsattel J-P (1995) Huntington's disease gene: Regional and cellular expression in brain of normal and affected individuals. *Ann Neurol* 37: 218-230

63. Li X-J, Li S-H, Sharp AH, Nucifora FC Jr., Schilling G, Lanahan A, Worley P, Snyder SH, Ross CA (1995) Huntingtin-associated protein enriched in brain with implicatins for pathology. *Nature* 378: 398-402

64. Linnane AW, Marzuki S, Ozawa T, Tanaka M (1989) Mitochondrial DNA mutations as an important contributor to ageing and degenerative diseases. *Lancet* 1(8639): 642-645

65. Ludolph AC, He F, Spencer PS, Hammerstad J, Sabri M. (1990) 3-nitropropionic acid: exogenous animal neurotoxin and possible human striatal toxin. *Can. J. Neurol. Sci.* 18: 492-498

66. Mangiarini L, Sathasivam K, Seller M, Cozens B, Harper A, Hetherington C, Lawton M, Trottier Y, Lehrach H, Davies SW, Bates G (1996) Exon 1 of the HD gene with an expanded CAG repeat is sufficient to cause a progressive neurological phenotype in transgenic mice. *Cell* 87: 493-506

67. Marnett LJ, Buck J, Tuttle MA, Basu AK, Bull AW (1985) Distribution and oxidation of malondialdehyde in mice. *Prostaglandins* 30: 241-254

68. Matsumara M, Tremblay L, Richard H, Filion M (1995) Activity of pallidal neurons in the monkey during dyskinesia induced by injection of bicuculline in the external pallidum. *Neurosci* 65: 59-70

69. Matthews RT, Yang L, Jenkins BJ, Ferrante RJ, Rosen BR, Kaddurah-Daouk R, Beal MF (1998) Neuroprotective effects of creatine and cyclocreatine in animal models of Huntington's disease. *J Neurosci* 18: 156-163

70. Mazziotta JC, Phelps ME, Pahl JJ, Huang SC, Baxter LR, Riege WH, Hoffman JM, Kuhl DE, Lanto AB, Wapenski JA, Markham CH (1987) Reduced cerebral glucose metabolism in asymptomatic patients at risk for Huntington's disease. *New Eng J Med* 316: 357-362

71. May PC, Gray PN (1985) The mechanism of glutamate-induced degeneration of cultured Huntington's disease and control fibroblasts. *J Neurol Sci* 70: 101-112

72. Moulder KL, Onodera O, Burke J, Strittmatter WJ, Johnson Jr EM (1998) Polyglutamine containing proteins produce length-dependent aggregation and death in cultured cerebellar granule cells. *Soc Neurosci* 24: 379.5

73. Myers RH, Vonsattel JP, Paskevich PA, Kiely DK, Stevens TJ, Cupples LA, Richardson EP Jr, Bird ED (1991) Decreased neuronal and increased oligodendroglial densities in Huntington's disease caudate nucleus. *J Neuropathol Exp Neurol.* 50: 729-742

74. Nakano M, Gotoh S (1992) Accumulation of cardiac lipofuscin depends on metabolic rate of mammals. *J Gerontol* 47: B126-129

75. Nicoletti F, Bruno V, Copani A, Casabona G, Knopfel T (1996) Metabotropic glutamate receptors: A new target for the therapy of neurodegenerative disorders? *Trends Neurosci* 19: 267-271

76. Novelli A, Reilly JA, Lysko PG, Henneberry RC (1988) Glutamate becomes neurotoxic via the N-methyl-D-aspartate receptor when intracellular energy levels are reduced. *Brain Res* 451: 205-212

77. O'Brien CF, Miller C, Goldblatt D, Welle S, Forbes G, Lipinski B, Panzik J, Peck R, Plumb S, Oakes D, Kurlan R, Shoulson I (1990) Extraneural metabolism in early Huntington's disease. *Ann Neurol* 28: 300-301

78. Paulson HL, Perez MK, Trottier Y, Trojanowski JQ, Subramony SH, Das SS, Vig P, Mandel JL, Fischbeck KH, Pittman RN (1997) Intranuclear inclusions of expanded polyglutamine protein in spinocerebellar ataxia type 3. *Neuron* 19: 333-344

79. Perutz M, Johnson T, Suzuki M, Finch JT (1994) Glutamine repeats as polar zippers: Their possible role in inherited neurodegenerative diseases. *Proc Natl Acad Sci USA* 91: 5355-5358

80. Portera-Cailliau C, Hedreen JC, Price DL, Koliatsos VE (1995) Evidence for apoptotic cell death in Huntington disease and excitotoxic animal models. J Neurosci 15: 3775-3787

81. Reiner A, Albin RL, Anderson KD, D'Amato CJ, Penney JB, Young AB (1988) Differential loss of striatal projection neurons in Huntington disease. *Proc Natl Acad Sci USA* 85: 5733-5737

82. Richfield EK, Maguire-Zeiss KA, Cox C, Gilmore J, Voorn P (1995) Reduced expression of preproenkephalin in striatal neurons from Huntington's disease patients. *Ann Neurol* 37: 335-343

83. Ross CA (1995) When more is less: pathogenesis of glutamine repeat neurodegenerative diseases. *Neuron* 15:493-6

84. Sapp E, Ge P, Aizawa H, Bird E, Penney J, Young AB, Vonsattel JP, DiFiglia M (1995) Evidence for a preferential loss of enkephalin immunoreactivity in the external globus pallidus in low grade Huntington's disease using high resolution image analysis. *Neurosci* 64: 397-404

85. Saudou F, Finkbeiner S, Devys D, Greenberg ME (1998) Huntingtin acts in the nucleus to induce apoptosis but death does not correlate with the formation of intranuclear inclusions. *Cell* 95: 55-66

86. Scherzinger E, Kurz R, Turmaine M, Mangiarini L, Hollenbach B, Hasenbank R, BatesGP, Davies SW, Lehrach H, Wanker EE (1997) Huntingtin-encoded polyglutamine expansions form amyloid-like aggregates in vitro and in vivo. *Cell* 90: 549-558

87. Schulz JB, Henshaw DR, Jenkins BG, Ferrante RJ, Kowall NW, Rosen BR and Beal MF (1994) 3-Acetylpyridine produces age-dependent excitotoxic lesions in rat striatum. *J Cereb Blood Flow Metab* 14: 1024-1029

88. Schulz JB, Henshaw DR, MacGarvey U and Beal MF. (1996a) Involvement of oxidative stress in 3-nitropropionic acid neurotoxicity. *Neurochem Intl* 29: 167-171

89. Schulz JB, Matthews RT, Henshaw DR, Beal MF (1996b) Neuroprotective strategies for treatment of lesions produced by mitochondrial toxins: implications for neurodegenerative diseases. *Neurosci* 71: 1043-1048

90. Sharp NH, Loev SJ, Schilling G, Li S-H, Li X-J, Bao J, Wagster MV, Kotzuk JA, Steiner JP, Lo A, Hedreen J, Sisodia S, Snyder SH, Dawson TM, Ryugo DK, Ross CA (1995) Widespread expression of the Huntington's disease gene (IT-15) protein product. *Neuron* 14: 1065-1074

91. Sohal RS, Marzabadi MR, Galaris D, Brunk UT (1989) Effect of ambient oxygen concentration on lipofuscin accumulation in cultured rat heart myocytes—a novel in vitro model of lipofuscinogenesis. *Free Radic Biol Med* 6: 23-30

92. Sotrel A, Paskevich PA, Kiely DK, Bird ED, Willimas RS, Myers RH (1991) Morphometric analysis of the prefrontal cortex in Huntington's disease. *Neurology* 41: 1117-1123

93. Stadtman ER (1992) Protein oxidation and aging. *Science* 257: 1220-1224

94. Tellez-Nagel I, Johnson AB, Terry RD (1995) Studies on brain biopsies of patients with Huntington's chorea. *J Neuropathol Exp Neurol* 33: 308-332

95. Terman A, Brunk UT (1998) Lipofuscin: mechanisms of formation and increase with age. *APMIS* 106: 265-276

96. Trottier Y, Devys D, Imbert G, Saudou F, An I, Lutz Y, Weber C, Agid Y, Hirsch EC, Mandel JL (1995) Cellular localization of the Huntington's disease protein and discrimination of the normal and mutated form. *Nat Genet* 10: 104-110

97. The Huntington's Disease Collaborative Research Group (1993) A novel gene containing a trinucleotide repeat that is expanded and unstable on Huntington's disease chromosome. *Cell* 72: 971-983

98. Uemera Y, Kowall NW, Beal MF (1990) Relative sparing of NADPH-diaphorase-somatostatin-neuropeptide Y neurons in ischemic gerbil striatum. *Ann Neurol* 27: 620-625

99. Vonsattel J-P, Myers RH, Stevens TJ, Ferrante RJ, Bird ED, Richardson EP (1985) Neuropathological classification of Huntington's disease. *J Neuropath Exp Neurol* 44: 559-577

100. Vonsattel JPG, DiFiglia M (1998) Huntington Disease. *J Neuropathol Exp Neurol* 57: 369-384

101. Weeks RA, Harding AE, Brooks DJ (1996) Striatal D1 and D2 dopamine receptor loss in asymptomatic mutation carriers of Huntington's disease. *Ann Neurol* 40: 49-54

102. White JK, Auerbach W, Duyao MP, Vonsattel J-P, Gusella JF, Joyner AL, MacDonald ME (1997) Huntingtin function is required for mouse brain development and is not impaired by the Huntington's disease CAG expansion mutation. *Nat Genet* 17: 404-410

103. Young AB, Greenamyre JT, Hollingsworth Z, Albin R, D'Amato C, Shoulson I, Penney JB (1988) NMDA receptor losses in putamen from patients with Huntington's disease. *Science* 241: 981-3

104. Zeevalk GD, Nicklas WJ (1991) Mechanisms underlying initiation of excitotoxicity associated with metabolic inhibition. *J Pharm Exp Ther* 257: 870-878

105. Zhang J, Dawson VL, Dawson TM, Snyder SH (1994) Nitric oxide activation of poly(ADP-ribose) synthetase in neurotoxicity. *Science* 263: 687-689

In: ***Manual of Neuropsychiatric Disorders.*** **F Tarazi and J Schetz, Eds.**
Humana Press. **(2005) 63-86.**

HUNTINGTON'S DISEASE

Susan E. Browne, Ph.D.

Dept. of Neurology and Neuroscience,
Weill Medical College of Cornell University, New York, NY USA.

Susan E. Browne, Ph.D.,
Department of Neurology and Neuroscience,
Weill Medical College of Cornell University,
525 East 68th Street, A-502,
New York,
NY 10021, USA.
Tel: (212) 746-4672
Fax: (212) 746-8276
E-mail: sub2001@med.cornell.edu

SUMMARY

Huntington's disease (HD) is an autosomal dominantly inherited, fatal neurodegenerative disorder, named for the author of the first definitive report of the condition in 1872, George Huntington. It is characterized by the progressive development of involuntary choreiform movements, although neuropsychiatric symptoms are sometimes the earliest and often the most devastating features of HD. These include detrimental emotional disturbances, behavioral and personality changes, and cognitive impairment. Gross pathological changes are restricted to the brain. Degeneration of specific basal ganglia neurons is a hallmark of HD, but dysfunction in multiple CNS pathways contributes to the motor and neuropsychiatric phenotype. HD is caused by an abnormal expansion of a trinucleotide repeat in the huntingtin gene. It is a relatively rare disease with highest prevalence rates of 5-10 per 100,000 found in Europe and the USA, while incidence is extremely low in Japan and Africa. The typical duration of disease before premature death is 15-20 years. Age of onset is associated with the size of the trinucleotide expansion and is generally in adulthood, although approximately 10% of cases have juvenile onset. There are currently no effective treatments for the disease.

KEY WORDS

Huntington's disease, Trinucleotide, Polyglutamine, Neurodegeneration, Striatum, Movement Disorder.

1. BRAIN PATHWAYS AFFECTED IN HD.

The motor and behavioral disturbances in HD result from alterations in specific neurotransmitter systems and degeneration of selective neuronal subpopulations in the brain. The principal neuropathological feature of HD is progressive caudal to rostral degeneration of the neostriatum (caudate and putamen) (1). A post-mortem grading system classifies patients according to the extent of neuropathological severity at death, grades ranging from 0 to 4 with increasing severity and extent of

striatal involvement. Grade 0 brains show 30-40% neuronal loss in the head of the caudate, with no visible gliosis. In Grade 4 brains the striatum is severely atrophic with neuronal depletion exceeding 95%, gliosis is extensive, and 50% of cases show cell loss in the nucleus accumbens. Most HD patients reach Grade 3 or 4 by the time of death, by which stage neuronal degeneration is evident in several non-striatal regions including the globus pallidus (GP) and cerebral cortex, and to a lesser extent in thalamus, subthalamic nucleus, substantia nigra, white matter and cerebellum. Cerebellar atrophy is particularly prevalent in juvenile onset HD.

Striatal medium spiny projection neurons are most vulnerable to degeneration in HD. Positron emission tomography (PET) has demonstrated that the first clinical symptoms of the disease correlate with loss of 30-40% of striatal dopamine D1 and D2 receptors, which are localized on the medium spiny neurons (2). These constitute 80% of all striatal neurons and are the principal input and output neurons of the striatum. They utilize the inhibitory neurotransmitter γ-aminobutyric acid (GABA), and subsets additionally contain either enkephalin (ENK), substance-P (SP), dynorphin or calbindin. Aspiny interneurons containing nicotinamide adenine dinucleotide phosphate diaphorase (NADPH-d), neuropeptide Y (NPY), somatostatin (SS) and nitric oxide synthase (NOS) are relatively spared in HD, but are eventually affected by the disease process. Striatal spiny projection neurons containing SP or ENK degenerate earliest in the disease, ENK-positive neurons projecting to the external segment of the globus pallidus (GPe) degenerating prior to SP-containing neurons that project to the internal segment (GPi). Neuronal degeneration eventually affects other brain regions and dysfunction within the cerebral cortex and limbic sub-cortical circuitry is thought to underlie the mood and personality changes prevalent in many HD patients (3).

1.1 *Neuropathologic Basis of Motor Dysfunction*

The uncontrolled, hyperkinetic choreic movements typical of HD result from the disruption of basal ganglia-thalamocortical pathways that regulate movements (4). Signals to stimulate initiation and execution of movements originate in the cerebral cortex in response to sensory afferent input. Excitatory glutamatergic efferents from the cortex innervate the neostriatum, which sends projections to other basal ganglia nuclei where signals are processed. Basal ganglia output nuclei (GPi, GPe, the substantia nigra pars reticulata (SNr), and ventral pallidum) then transmit "sorted" impulses to appropriate thalamic nuclei. From the thalamus, excitatory projections are sent back to topographically organized motor output areas of the frontal cortex to initiate execution of the appropriate motor response. The type of movement initiated thus depends on the combination of neostriatal neuron pathways activated, their downstream routing to the thalamus, and the resultant cortical activation (as discussed in Chapter 1). An imbalance in the relative contributions of the two regulatory basal ganglia pathways ("direct" mediated by GABA and SP, "indirect" mediated by GABA and ENK) triggers the motor dysfunction in HD and dictates its phenotype. In HD there is preferential loss of the GABA/ENK neurons comprising the indirect pathway. Disinhibition of the thalamus and increased excitation of cortical motor output regions result (Figure 1), manifest in HD patients by the development of involuntary, unregulated choreic movements. The late onset of rigidity and akinesia in some HD patients is thought to be due to disruption of the direct motor pathway following additional loss of striatal GABA/SP neurons. The predominance of bradykinesia in juvenile onset HD results from simultaneous loss of SP and ENK neurons.

1.2 *Neuropathologic Basis of Psychiatric Symptoms*

A number of psychiatric disorders are prevalent in HD, often occurring before motor symptoms. While neuropathologic pathways underlying these traits specifically in the context of HD are not well documented, these syndromes generally involve anatomical and neurotransmitter pathways that are

disrupted by HD pathology. Common psychiatric syndromes including depression, apathy, mania, and cognition changes in HD generally involve dysfunction in the cerebral cortex and the sub-cortical limbic system.

Loss of cerebral cortex neurons is well documented in HD brain. At disease end-stage more than half the neurons in layer VI of frontal cortex that project to thalamus, claustrum and other cortical regions are lost, and in excess of 70% of cortico-striatal projection neurons in layer V (1). Positron emission tomography (PET) studies of cerebral glucose metabolism in presymptomatic and at risk patients indicate cortical dysfunction prior to disease manifestation in many patients (3). In particular, reduced cerebral metabolism in the prefrontal cortex of symptomatic and presymptomatic patients, and at-risk individuals, correlates with depression and increased suicide risk. Apathy is also associated with frontal lobe dysfunction. Bipolar disorder and mania are associated with alterations in neurotransmitter systems affected by HD pathology, including glutamatergic transmission in the cerebral cortex and striatum, and GABAergic transmission in cortex and hippocampus. Dysfunction and damage to neurons in the cerebral cortex and striatum, and subsequent dysfunction within synaptic projections from these regions to limbic structures including cingulate cortex and hippocampus are therefore likely to contribute to several of the emotional disturbances identified in HD.

2. GENETIC BACKGROUND

2.1 ***The HD Gene Mutation:*** HD is caused by a mutation in a gene on chromosome 4p16.3 termed "*huntingtin*" (*HD*; formally *IT15*, "interesting transcript 15") (5). The mutation is an expansion of an unstable CAG repeat region in exon 1 of *HD* that is manifest as an expanded polyglutamine (Q_n) stretch in the 348 kDa protein product "huntingtin" (Htt). The polyQ stretch is associated with a proline (P)-rich domain. Wildtype *HD* in unaffected individuals contains 11-34 CAGs. Repeat lengths of 35-39

CAGs in one allele are variably penetrant, conferring the possibility of developing HD late in life, while the disease shows complete penetrance when triplet repeats exceed 39.

HD, generally a monozygotic trait, is considered a true dominant disorder with full penetrance since carriers with greater than 39 CAG repeats will develop the disease during a normal lifespan (6). Homozygosity does not alter either age of onset, duration, or severity. Another disease trait is anticipation, whereby age of onset in an individual precedes that in their affected parent. Trinucleotide repeats of 27 or more are polymorphic and undergo alterations during meiosis, fluctuating by ± 1-5 repeats per transmission with a bias towards expansion. Instability in spermatogenesis typically yields the largest expansions, meaning that anticipation is more pronounced following paternal inheritance. This characteristic contributes to the appearance of "sporadic" HD cases estimated to constitute about 8% of HD patients. Non-penetrant but unstable repeats (27-35 CAGs) may expand to penetrant length during transmission, or expand due to novel mutations. Other factors contributing to apparent sporadic onset include lack of knowledge of a family history of HD, for example due to adoption, no parental contact, or presymptomatic death or misdiagnosis of the affected parent.

Several features of the HD phenotype are influenced by CAG repeat length. Age of onset is inversely correlated with CAG expansion size, and especially long repeats (>55) confer juvenile onset. The most common repeat lengths of 42-50 generally correspond to symptom onset in the fourth and fifth decades, although the large variances in onset ages mean that repeat sizes in this range are often not accurate predictors for the age of symptom appearance. Disease severity, extent of neuropathological degeneration, and degree of DNA damage are all positively correlated with triplet repeat length. In contrast, rates of functional decline do not correspond with mutation size. It therefore seems likely that aspects of the disease process are influenced by extrinsic factors such as stochastic, environmental or genetic modifiers. Genomic studies in HD families have revealed a number of genetic loci that may influence disease course including genes encoding ubiquitination enzymes (such as *UCHL1* which

encodes ubiquitin carboxyl-terminal hydrolase L1), the glutamate GluR6 kainate receptor subunit, and apolipoprotein E (6, 7).

Polymerase chain reaction (PCR)-based assays to quantify CAG repeat lengths are now available for confirmatory diagnostic testing, predictive testing in at-risk individuals, and pre-natal testing in known mutation carriers (for review see 8). Linkage-based exclusion testing is offered to pregnant at-risk women who choose not to know their own gene status (termination is only an option if gene linkage analysis implies the fetus shows the same 50% genetic risk as the mother). Pre-implantation testing of *in vitro* fertilized (IVF) embryos is also available. Genetic testing is an emotive subject and testing procedures are closely governed by International guidelines. Genetic counseling is a pre-requisite for participants. Current testing approaches are not 100% reliable, but identify CAG repeat number to within 1 or 2 triplets. Potential problems include interpretation of disease risk when CAG repeat lengths in the mutable or at-risk lengths are detected, which provide no accurate determination of the probability of disease onset or the risk of transmission to a child.

2.2 ***Htt Protein:*** Huntingtin (htt) protein was unknown until identification of the HD gene mutation in 1993, and the endogenous functions of both wildtype and mutant huntingtin have still to be definitively elucidated (6).

a) *Wildtype Htt:* A role in developmental apoptosis is suggested by observations that (i) mice entirely lacking the murine *HD* homologue gene *Hdh* die *in utero,* but heterozygous knock-out mice show little or no pathology, and (ii) abnormally low levels of huntingtin expression are associated with developmental abnormalities. Huntingtin protein is ubiquitously expressed throughout the body. At the sub-cellular level it is present in multiple compartments with a largely cytoplasmic distribution in perikarya, axons, dendrites and some nerve terminals. The protein contains a nuclear export signal domain and at any given time approximately 5% of the protein is found in the nucleus, suggesting that

huntingtin shuttles between the nucleus and the cytoplasm. Reports of colocalization with synaptic vesicles and microtubules infer an involvement in trafficking, and possibly RNA biogenesis or signaling (see 9, 10, and section 3).

Htt is a large protein that takes on multiple conformations within cells, putatively due to multiple HEAT domains throughout the protein (~40 amino acid sequence repeats, named for the first four disease-related proteins this motif was identified in: htt, elongation factor 3, regulatory A subunit of protein phosphatase 2A, and TOR1). HEAT repeats form hydrophobic α helices that can generate elongated superhelices. Htt binding with other proteins is facilitated by several protein components, including the HEAT superhelices, htt amino terminal, and the polyglutamine/proline tract.

b) *Mutant Htt:* Mutant htt's toxicity is due to the gain of a novel function, rather than loss of wild-type huntingtin function, since (i) mice homozygous for the mutant gene still develop normally, and (ii) expression of a single allele of mutant huntingtin is sufficient to rescue *Hdh*-null mice from death *in utero* (6). Mutant htt is also expressed ubiquitously throughout the body and its distribution shows no apparent selectivity for cerebral regions targeted by the disease process, suggesting that another property of neurons within these regions confers vulnerability to htt toxicity.

Htt contains multiple cleavage sites and proteolytic processing of htt appears to be a normal physiological event (11, 12). Studies suggest that polyQ-induced toxicity is exacerbated in protein fragments, and is inversely correlated with fragmant length. Therefore cleavage of mutant htt to generate N-terminal htt fragments encompassing the expanded polyQ region may contribute to htt toxicity. Htt fragments are most abundant in cortical projection neurons, suggesting that accumulation of mutant htt fragments contributes to cortico-striatal dysfunction in HD pathogenesis.

N-terminal fragments of mutant htt eventually form ubiquitinated sodium dodecyl sulphate (SDS)-resistant protein aggregates in neuronal nuclei (neuronal intranuclear inclusions, NII) and in dystrophic

neurites (cytoplasmic inclusions, CI). Aggregates have been identified in HD brain and in the brains of transgenic mice expressing mutant htt, but are not restricted to CNS cells. Aggregate deposition patterns differ between CNS and somatic cells. In skeletal muscle cells, for example, aggregates are found solely within nuclei, whereas in the brain the bulk of aggregates are neuritic. The mechanism of inclusion formation is not yet known, but CAG repeat length is critical for aggregate formation and mutant polyglutamine stretches lend themselves to the formation of ß-pleated sheets held together by hydrogen bonds between amide groups.

3. CELLULAR AND MOLECULAR TARGETS OF THE DISEASE

How the *HD* gene defect leads to progressive, selective neurodegeneration remains a tantalizing question. *In vivo* imaging and analysis of post-mortem human tissue, *in vitro* studies and animal models expressing mutant htt have identified a number of cellular components and pathways that involve wildtype htt interactions, or are altered during mutant htt-mediated toxicity, discussed below and summarized in Table 1. The htt-mediated event triggering toxicity remains elusive.

3.1 Abnormal protein/protein interactions

One hypothesis of neurotoxicity in HD is that mutant htt influences cellular functions via interactions with proteins that are either novel, or modify the effects of wildtype htt binding (reviewed in 9). Htt contains several binding sites for protein interactions:

a) *The polyglutamine/proline (Q/P)-rich domain* binds with proteins with Src homology region 3 (SH3) or tryptophan (WW) residues. These include protein kinase C and casein kinase substrate 1 (PACSIN1) and SH3GL3/endophilin3 involved in endocytosis, the transcription factor p53, and the synaptic scaffold protein PSD-95. other interactors include the multifunctional enzyme glyceraldehyde 3-phosphate dehydrogenase (GAPDH), the calcium sensor protein calmodulin, and pro-apoptotic caspase-3.

b) *HEAT domains* bind with several proteins, including the transcription factor NFκB, and contribute to binding with htt-associated protein (HAP) 1, and htt-interacting proteins (HIP) 1 and 14 (HYP-H) involved in intraneuronal trafficking and endocytosis.

c) *The amino terminal region* (including the polyQ region) binds to molecules involved in endocytosis (e.g. α-adaptin C/HYP-J) and several transcription regulators including cAMP response element binding protein (CREB) binding protein (CBP), specificity protein 1 (Sp1), TATA-binding protein-associated factor (TAFII-130), and Sin3a. Other interactors include components of signal transduction pathways including Cdc42-interacting protein 4 (CIP4), Akt/PKB, and Ras GTPase activating protein (RasGAP). The functional consequences of some of these interactions are reviewed below.

Findings of increased transglutaminase (TGase) activity in HD caudate and in transgenic mouse models imply that the gene mutation increases the extent of htt/protein interactions. TGases catalyze the covalent linkage of Q residues with lysine (K) and polyamines in other proteins. The concentration of glutamyl-lysine crosslinks is also elevated in HD brain and CSF, and crosslinks are found in htt positive aggregates. TGase-mediated htt-protein interactions appear to contribute to htt-mediated toxicity, since knocking out the TGase-2 gene delayed neuronal damage in HD transgenic mice (13).

3.2 Endocytosis pathways

Endocytosis is the process whereby the cell membrane invaginates to form membrane-bound vesicles containing substances previously bound at the cell surface. A number of proteins that interact with htt modulate steps in the endocytosis process, and thus mutant htt may deleteriously affect this pathway (reviewed in 9). An early stage in vesicle generation is the formation of pits in the cell membrane that are lined with the structural protein clathrin, via clathrin's interaction with adaptor protein-2 (AP2) which binds to membrane phopholipids. A number of htt-interactor proteins may modify the formation of clathrin-coated pits and vesicles. HIP1 can interact with clathrin, and both

HIP1 and htt directly interact with the AP-2 α-adaptin subunit. HIP1 and HIP12 influence vesicle budding and actin-mediated transport. PACSIN1 has roles in actin polymerization and phosphoinositide turnover, and is thought to contribute to vesicle detachment. Another htt interactor, SH3GL3 (endophilin 3), appears to affect membrane curvature, invagination and vesicle scission. Htt also binds to HIP14 (HYP-H), which has sequence similarity with a yeast endocytotic protein, Ark1p. Since HIP14 localizes to the Golgi apparatus and cytoplasmic vesicles in cell lines, it has been proposed to act as a perinuclear endocytosis regulator. Thus wildtype htt may serve regulatory roles in clathrin-mediated endocytosis, and mutations in htt could deleteriously modify clathrin binding to membranes, vesicle budding and actin-mediated vesicle transport.

3.3 Intraneuronal trafficking

Mutant htt-induced defects in axonal trafficking were first proposed on the basis that distribution of htt aggregates within neuropil seemed to correlate with neurodegeneration more closely than nuclear deposition, in HD patients and "knock-in: mouse models. In addition, htt is enriched in membranous cell fractions, shows affinity for cytoskeletal and vesicular components. More compelling evidence for a role of wildtype htt in trafficking is provided by a recent study demonstrating that reduced expression of htt in Drosophilae induces abnormal accumulations of cellular organelles in larval neurons, termed axonal blockages, and concomitant disruption of axonal transport. Another study demonstrated that mutant polyQ expansions in truncated htt and androgen receptor (AR) proteins impair intergraded and retrograde fast axonal transport in squid giant axons. Increased polyQ repeat length exacerbates this defect (reviewed in 10).

3.4 Transcriptional regulation

Huntingtin protein can bind to and functionally alter the activity of several transcription factors, co-activators and repressors (for review see 14).

a) *Transcription factors:* Mutant htt exon 1 interacts with both p53 and CREB binding protein (CBP) and represses transcription of the p53-regulated promoters $p21^{WAF/CIP1}$ and MDR1. CBP colocalizes with htt aggregates in HD mouse models, cell culture preparations, and in human HD post-mortem brain tissue. PolyQ toxicity *in vitro* can be blocked by overexpression of CBP.

b) *Transcriptional activators:* Htt binds to the transcriptional activator Sp1 that recruits the transcription factor TAFIID to DNA. It also binds the co-activator TAFII-130. Since TAFII-130 interacts directly with Sp1, it has been proposed that htt may form a support to facilitate transcription activation.

c) *Transcriptional repression:* Htt also interacts with repressor machinery, including the complex containing N-CoR and Sin3A that represses transcription induced by some ligand-activated nuclear receptors (e.g. retinoic acid receptors). N-CoR links DNA binding proteins to histone deacetylases, and interacts directly with transcription factors through TFIIB. Several genes regulated by NcoR-Sin3A-mediatred transcription (9, 14). Further, mSin3 also colocalizes with htt and CBP in protein aggregates.

The mechanism underlying mutant htt's effects on gene transcription is currently unclear. It was initially suggested that reduced transcriptional activity of some factors (e.g. CBP and TAFII-130) might result from sequestration into htt-containing aggregates. Sequestration now seems unlikely to be the primary step in HD pathogenesis since transcriptional changes precede aggregate formation in several experimental models. An alternative hypothesis is that a deficiency in cAMP underlies decreases in CRE-mediated gene transcription. ATP-dependent cAMP generation is reduced in HD CSF, cerebral cortex, and lymphoblastoid cell lines, while the adenylate cyclase stimulator forskolin attenuates mutant htt-induced toxicity in cell lines. Reduced cortical and striatal levels of cAMP also precede alterations in PKA/CREB signaling, nuclear aggregate formation, and neuronal death in a mouse model of HD (15).

Changes in cAMP-mediated transcription will have downstream effects on many cell components. There is substantial evidence of defects in brain derived neurotrophic factor (BDNF) function, a cell survival protein regulated by CREB, in HD. BDNF protein and mRNA levels are markedly reduced in the fronto-parietal cortex of symptomatic patients. Reduced BDNF gene transcription and protein levels are also evident in cerebral cortex and striatum of multiple mouse models expressing mutant htt (15). In contrast, mice expressing human wildtype huntingtin show increased levels of BDNF. It has therefore been hypothesized that the selective vulnerability of striatal neurons may result from loss of neurotrophic support by BDNF, since the striatal pool of BDNF arises from cortical projection neurons.

3.5 Postsynaptic signaling

Htt binds to postsynaptic density-95 (PSD-95), a member of the membrane-associated guanylate kinase (MAGUK) protein family that is involved in organization of the post-synaptic density. PSD-95 binds to kainite and N-methyl-D-aspartate (NMDA) glutamate receptor subtypes, as well as to cytoplasmic signaling molecules including SynGAP (synaptic GTPase-activating protein). SynGAP also modulates excitatory synapses via down-regulation of GTPase Ras. PSD-95 further influences dendritic spine morphology via effects on Rac1 signalling involved in actin cytoskeleton remodeling. Htt binding to CIP4 and FIP-2 may also affect dendritic spine morphology (reviewed in 9).

3.6 Apoptotic cascades

One putative function of wildtype htt is regulation of apoptosis during development, and it has been suggested that striatal htt protects neurons from pro-apoptotic pathways, possibly through inhibition of the cytochrome C (cyt C)-dependent procaspase-9 pathway. The htt interactor HIP1 induces caspase-3-dependent cell death, but co-expression of htt abrogates this toxicity in cell lines. Mutant expansion of the htt polyQ tract reduces the ability of htt to bind HIP1, suggesting a possible

pathway for increased apoptotic damage in HD. Free HIP1 can associate with HIP1 protein interactor (Hippi) to induce procaspase-8 cleavage and apoptosis *in vitro* (16). It has also been proposed that htt acts as a survival factor in the phosphoinositide 3-kinase (PI3K)-Akt pathway, as it is a substrate for Akt. This pathway stimulates the expression of survival genes including Bcl-xL and brain-derived neurotrophic factor (BDNF), and represses death genes including BAX and Bcl-2.

3.7 Mitochondria and energy metabolism pathways

Energy metabolism is impaired in affected brain regions of HD patients (reviewed in 17). Reduced ATP generation can be detrimental to cells in a number of ways, including direct reduction of functional activity within cells, increasing free radical generation, and increasing neuronal vulnerability to excitotoxic damage. Thus energetic defects are postulated to be important contributors to HD pathogenesis.

The most prominent metabolic alteration in HD patients is profound weight loss, even when caloric intake is maintained. In the CNS, impairments in energy metabolism have been found in brain regions targeted by the disease. Glucose uptake is reduced in the caudate, putamen and cerebral cortex prior to the bulk of tissue loss in symptomatic patients, and pre-symptomatically in approximately 50% of gene-positive mutation carriers. Cerebral levels of lactate are abnormally elevated in affected basal ganglia and cerebral cortex of HD patients. This abnormality can be ameliorated by treatment with the metabolic co-factor coenzyme Q_{10} (18). Biochemical studies in HD post-mortem tissue have revealed selective dysfunction of components of the mitochondrial tricarboxylic acid (TCA) cycle and electron transport chain (ETC) in affected brain regions, in particular succinate dehydrogenase in complex II and the TCA cycle, complex IV, and aconitase. Further indirect evidence that energetic defects contribute to neurodegeneration in HD is provided by findings that creatine and coenzyme Q_{10} are protective in

animal models of HD, putatively via enhancing the efficiency of energy production and delivery in neurons.

Involvement of mitochondrial damage in HD is supported by observations of degenerating mitochondria in mutant mouse models of HD, in some cases concomitant with symptom onset. Htt staining in degenerated mitochondria in symptomatic mice suggests that mutant htt may interact directly with neuronal mitochondria (19). Another HD mouse line (N171-82Q) shows evidence of apoptotic cell death in the striatum and cerebral cortex associated with mitochondrial cytochrome C release and caspase 9 activation in the striatum and cerebral cortex. *In vitro* studies show that mutant htt can alter mitochondrial function by influencing mitochondrial calcium handling (see Browne and Beal, 2004). Pathogenic polyglutamine constructs have also been shown to decrease mitochondrial membrane potential and to increase mitochondrial vulnerability to Ca^{2+}-induced depolarization.

3.8 Excitotoxic processes

Mutant htt expression induces alterations in several components of the glutamate neurotransmitter system in affected brain regions that may render cells vulnerable to glutamate-mediated excitotoxic damage (reviewed in 17). The considerable glutamatergic innervation of the neostriatum from the cerebral cortex is postulated to exacerbate the risk of excitotoxic damage to striatal neurons.

Studies of glutamate receptor subtypes in postmortem tissue from late-stage and presymptomatic HD patients show that NMDA receptors are selectively depleted in HD striatum. Findings suggest that NMDA receptor-bearing neurons are preferentially vulnerable to degeneration, and that excitotoxic stress may occur early in the disease course. In animal models, striatal lesions induced by excitotoxins (glutamate receptor agonists) in rodents and primates closely resemble those seen in HD brain. The NMDA receptor agonist quinolinic acid produces neuronal-specific lesions typical of HD, with relative sparing of NADPH-diaphorase and parvalbumin-positive neurons. NMDA receptor-mediated lesions in

primates are associated with an apomorphine-inducible movement disorder resembling the choreic movements in HD. Some genetic models of HD (discussed further in section 4) also show age-dependent declines in glutamate receptor densities in striatum and cerebral cortex, and increased vulnerability to excitotoxic damage.

Excitotoxic damage may also occur in circumstances when extracellular glutamate levels are normal but energy metabolism is impaired, by so-called "secondary excitotoxicity" (20). Reduced ATP production disrupts energy-dependent processes within neurons, including the maintenance of pumps regulating ionic and voltage gradients across cell membranes. Impaired Na^+/K^+-ATPase activities at the cell membrane may cause prolonged or inappropriate opening of voltage-dependent ion channels leading to partial depolarization. If depolarization is severe enough, normally inert extracellular levels of glutamate can trigger NMDA receptor activation resulting in Ca^{2+} influx, nitric oxide synthase (NOS) activation and free radical production. Secondary excitotoxicity is responsive to blockade by NMDA receptor antagonists and glutamate release inhibitors.

3.9 Htt and Oxidative Damage

Mutant htt expression is linked with oxidative damage to multiple cellular components in HD, including proteins, DNA and phospholipids (reviewed in 21). Studies in HD post-mortem brain show increased levels of DNA strand breaks, DNA oxidative damage products such as 8-hydroxydeoxyguanosine (OH^8dG), 3-nitrotyrosine (a marker for peroxynitrite-mediated protein nitration), malondialdehyde (marker for oxidative damage to lipids), lipofuscin accumulation (a marker of lipid peroxidation), and heme oxygenase (formed during oxidative stress) in HD striatum and cortex. Findings that oxidative damage to DNA and lipids is increased after symptom onset in mouse models of HD suggest that it is a downstream consequence of htt-induced damage. Glutamate agonists, Ca^{2+} influx,

and nitric oxide can stimulate free radical generation, and therefore oxidative damage in HD may result from excitotoxic damage or energy impairments.

3.10 Huntington Aggregates in Pathogenesis

Intracellular htt-containing protein aggregates are a hallmark of HD. In some experimental models, including *Drosophila* photoreceptors, mutant htt's toxicity is associated with the presence of neuronal aggregates (neuronal intranuclear inclusions, "NII"). Thus it has been proposed that htt-positive aggregates could be detrimental to cells by sequestering other critical cell proteins and macromolecules, by preventing htt from performing its normal function, or by disrupting vital processes such as proteosome pathways. However, this hypothesis is countered by observations that aggregates are found throughout the body of HD patients and deposition patterns do not mirror cell death in post-mortem tissue. In addition, several studies in cell lines have shown that human mutant htt can induce cell-selective neurodegeneration independent of the presence of NII, while suppression of NII formation can increase htt-mediated toxicity, suggesting that aggregate deposition may be part of a protective mechanism within cells (see 17). Transgenic and knock-in mouse models (discussed in Section 6) further support the argument that NII are not a pre-requisite for toxicity in HD models, since there is no direct link between the timing and distribution of NII deposition and cell damage or dysfunction in the majority of models. Aggregates may, therefore, be the result of an intrinsic mechanism to remove toxic htt from the cell milieu, or alternatively be an inert side effect of the propensity for htt to self-aggregate.

4. ANIMAL MODELS

The existing approaches for modeling Huntington's disease in animals utilize knowledge of the genetic basis of the disease and neurochemical facets of its etiology (largely the involvement of the glutamate neurotransmitter system and energetic defects). Three categories predominate: models

recapitulating specific neurotransmitter pathway lesions using either 1) excitotoxic or 2) mitochondrial toxins in rodents and non-human primates, and 3) models expressing the HD gene defect.

4.1 Excitotoxins

Excitotoxic striatal lesions in rodents and primates closely resemble those seen in HD brain (17). Intrastriatal injection of the NMDA agonist quinolinic acid induces striatal neurodegeneration of medium spiny projection neurons, but spares NADPH-diaphorase and parvalbumin-positive neurons. In primates, NMDA receptor-mediated striatal lesions result in an apomorphine inducible movement disorder resembling that seen in HD patients. This phenomenon appears to be NMDA receptor-specific, since degeneration induced by AMPA and kainate receptor agonists does not target the same neuronal populations.

Expression of the HD gene mutation also confers some susceptibility to excitotoxic damage, but reports to date suggest that the context in which the mutant gene is expressed influences vulnerability. For example, striatal NMDA receptor-mediated quinolinic acid lesions are exacerbated in a full-length htt mouse model (YAC-72Q mice), possibly associated with expression of the NMDA receptor NR2B subunit in this model. In contrast, another transgenic mouse model expressing an N-terminal fragment of mutant huntingtin (N171-82Q) showed no preferential susceptibility to quinolinic acid lesions, while expression of a shorter gene fragment with longer CAG repeats (in R6/2 and R6/1 mice) conferred resistance to quinolinic acid, malonate, NMDA and 3-NP toxicity. Hypotheses to explain the differences between models include reduced synaptic activity in resistant lines, or differential vulnerabilities of background mouse strains. In contrast, R6/2 striatal and cortical neurons show increased susceptibility to NMDA *ex vivo*. The fact that the glutamate release inhibitor riluzole prolongs survival in R6/2 mice reinforces suggestions of an excitotoxic component of pathogenesis in this model.

4.2 Mitochondrial Toxins: 3-Nitropropionic Acid (3-NP) and Malonate

Mitochondrial defects are implicated in HD by findings of reduced glucose metabolism and mitochondrial succinate dehydrogenase (SDH) activity in the caudate and putamen of symptomatic patients. SDH, located on the matrix surface of the inner mitochondrial membrane, catalyzes the oxidation of succinate to fumarate in both the tricarboxylic acid (TCA) cycle and complex II of the electron transport chain (ETC). Impaired SDH activity therefore decreases substrate delivery from the TCA cycle to complex I of the ETC and impairs electron transfer, ultimately reducing ATP generation. Some of the clinical and pathological characteristics of HD are replicated by inhibiting striatal SDH activity with 3-nitropropionic acid (3-NP) and malonate (reviewed in 17).

3-Nitropropionic Acid (3-NP): Systemic administration of 3-NP causes selective degeneration of striatal medium spiny neurons and motor abnormalities resembling HD. 3-NP's utility as a HD mimetic was discovered by chance, when a group of children in China developed motor disturbances and dystonia associated with discrete basal ganglia lesions after eating sugar cane contaminated with the fungus *Arthrinium.* The toxic moiety was found to be the 3-nitopropanol metabolite 3-NP (22). 3-NP toxicity in humans induces gait abnormalities, multiple cognitive symptoms including acute encephalopathies and coma, and may be fatal. Systemic administration of 3-NP to both rats and primates produces age-dependent striatal lesions that are strikingly similar to those seen in HD. For example, striatal 3-NP lesions in non-human primates show sparing of NADPH-d neurons and proliferative changes in the dendrites of spiny neurons. Animals also develop both spontaneous and apomorphine-inducible movement disorders. The extent of basal ganglia lesions induced in animals are minutely dependent on the dosing regimen used, with chronic low dose paradigms inducing cerebral pathology most closely mimicking HD.

Malonate: Malonate is another selective inhibitor of SDH activity that induces motor impairments following intrastriatal administration in rodents. Since malonate does not cross the blood brain barrier

systemic administration is ineffective, but it remains a useful tool for modeling the effects of complex II inhibition *in vitro* and *in vivo*.

Selective Toxicity of Mitochondrial Toxins: The striatum is discretely targeted by 3-NP toxicity despite uniform distribution of 3-NP throughout the brain and uniform depression of SDH activity following systemic administration. It has been suggested that this susceptibility of striatal neurons to metabolic stress might contribute to their selective vulnerability in HD, supported by findings that improving energy generation within neurons (by creatine or coenzyme Q_{10} administration) protects against 3-NP toxicity. 3-NP administration also causes activation of NMDA receptors, and lesions can be prevented by prior removal of glutamatergic excitatory cortico-striatal inputs by decortication, by glutamate release inhibitors, and by glutamate receptor antagonists, suggesting that 3-NP toxicity is mediated by excitotoxic mechanisms secondary to metabolic defects (23). NMDA receptor antagonists also abrogate malonate toxicity. 3-NP and malonate lesions induce oxidative damage, resulting in increased hydroxyl radical generation, DNA and protein damage. Free radical scavengers and nitric oxide synthase inhibitors attenuate lesions (21).

4.3 Genetic Models of HD.

One of the major drawbacks of relying on human tissue to determine disease mechanism in progressive neurodegenerative disorders is the inability to adequately map early events in the disease process. The development of animal models expressing the HD gene mutation has been invaluable in circumventing many of these issues. A number of model organisms have been utilized, including *C. elegans* and drosophila which are particularly useful for rapid, high-throughput screening applications, and HD-mutant rodent models which allow multi-system evaluation of potential disease pathways.

Mutant mouse lines are the most thoroughly characterized HD genetic models currently available (reviewed in 17, 24; summarized in Table 2). Several different mutants have been generated that vary

in the technique used to incorporate the gene mutation into the mouse genome. As a result phenotypes vary between mouse lines depending on the nature of the mutation incorporated (full length human *HD,* a fragment of human *HD*, or precise "knock-in" of a polyglutamine repeat into the murine *HD* homologue *Hdh*), CAG repeat length, copy number of the mutant gene, promoter-dependent cellular specificity of expression, expression levels, and background strains of the mice. The utilities of these different types of mouse models can be divided into three broad categories:

4.3.1 Mice expressing N-terminal exon-1 fragments of the human *huntingtin* gene *(HD)* containing CAG expansions (plus both alleles of murine wildtype *huntingtin, Hdh*).

Typical characteristics of "fragment" mouse models are short life spans, and relatively rapid onset of phenotype that includes reductions in body weight and brain weight, htt aggregate formation, and neuronal atrophy. R6/2 mice expressing ~150 CAGs were the first mutant HD mice developed, and are therefore the best characterized to date (25). Mice have extremely short lifespan (~13-17 weeks), and develop NII (~3-4 weeks); gait abnormalities, rotarod impairments, glucose intolerance, body weight loss, brain weight loss, diabetes, striatal atrophy and ventricular enlargement (6-10 weeks); and cerebral neurotransmitter receptor alterations including depletions of metabotropic glutamate and dopamine receptors (~12 weeks). N171-82Q mice express a longer fragment of human htt exon 1 with a shorter polyQ repeat (82Q). As a result phenotype onset is later and progression slower than R6/2s, but mice develop a behavioral phenotype more closely reminiscent of HD. Weight loss, gait abnormalities, impaired motor performance, systemic glucose intolerance and NII deposition are evident by 3-4 months of age, before premature death at 4-6 months (26). There is little evidence of overt neuronal loss in R6/2 mice, but degeneration of organelles including mitochondria has been reported in symptomatic mice (19). End-stage N171-82Q mice show evidence of apoptotic cell death in striatum and cortex.

Another genetic HD modeling strategy uses an inducible tetracycline-responsive gene system to turn on expression of an *HD* gene fragment postnatally (27). Gene expression in this context induced a

progressive phenotype of intranuclear and cytoplasmic inclusion formation, striatal atrophy and astrocytosis, hind-limb clasping and rotarod motor impairments, and receptor changes in the striatum. Some of these changes partially reverse or resolve following transgene turn-off, including aggregate load, receptor fluctuations, and motor performance. These observations suggest that appropriate HD treatments may still be beneficial when applied after symptom onset.

4.3.2 Mice expressing the full-length human *HD* gene (and murine *Hdh*).

"Full length" mouse models show behavioral phenotypes and selective neuronal degeneration more closely resembling HD than fragment models, but onset and progression is slower. YAC128 mice express full length *HD* using the human promoter, with expression levels ~75% of endogenous (28). Mice show early hyperkinetic movements, followed by impaired motor function, reduced brain weight, cortical and striatal atrophy, neuronal atrophy and striatal cell loss (affecting primarily medium spiny neurons), and late deposition of htt aggregates. These full length mutant mice live normal life spans.

4.3.3 Mice with pathogenic CAG repeats inserted into murine *Hdh*.

"Knock-in" mice generated by inserting mutant CAG expansions into the murine *HD* homologue *Hdh* represent the most accurate models for mutant htt expression. In general these models develop pathologic phenotypes most closely resembling HD, but behavioral phenotypes are less severe and slower progressing than human full length and fragment *HD* models. Mice have normal life spans. Several knock-in models have been generated of which the Hdh^{Q92} and Hdh^{Q111} mice are the best characterized (29). Mice show nuclear localization of htt selectively in striatal medium spiny neurons, eventual htt aggregate formation, and striatal-specific cell loss around 24 months of age in Hdh^{Q111} mice. Increased CAG repeat length is associated with acceleration of neuronal intranuclear inclusion

(NII) formation and cell death. Other knock-in models show overt behavioral abnormalities including hypoactivity, hindlimb clasping, and gait abnormalities (see 24).

In summary, while all mutant HD models exhibit some features of the human disorder, invariably involving htt aggregate formation, few develop the cardinal signs of striatal neuronal degeneration. Neurodegeneration seems to depend ultimately on the context in which the HD mutation is expressed. Some generalities can be drawn from a survey of existing mouse lines. Firstly, mice require longer CAG repeats than humans to elicit pathogenic events, putatively due to their relatively short life spans. Secondly, onset is accelerated when gene fragments are expressed, and both age of onset and survival decrease with shorter fragments. In contrast, expression of longer fragments or full-length huntingtin is associated with neuronal death patterns more closely resembling human HD pathology. Age of phenotype onset, aggregate formation, and cell death are all slower in full-length models (including knock-in mice), compared with fragment models. Within each of these subsets, longer CAG repeats accelerate all phenotypes.

5. CLINICAL PHENOTYPES

A diagnosis of Huntington's disease is based largely on the development of the hallmark choreic movement disorder, and is aided by a positive family history. Genetic testing to detect the abnormal CAG repeat may now be used to confirm suspected HD. Approximately one third of HD cases initially present with emotional disturbances and neuropsychiatric conditions, however, which can lead to misdiagnosis. In the absence of a family history, a correct diagnosis in these cases may be difficult until the movement disorder presents.

The clinical phenotype of HD includes a primary movement disorder, emotional disturbances and cognitive decline. The heterogeneous clinical presentations of HD and treatment paradigms are extensively reviewed by Rosenblatt and colleagues (30).

5.1 ***HD Movement Disorder.*** The earliest motor abnormalities in HD typically affect the *eye.* Initiation of eye movement is delayed, the speed of saccades declines, patients show impaired ability to suppress blinks when saccades are initiated, and pursuit movements become jerky. *Choreic body movements* gradually develop, and are the most noticeable feature of HD. The earliest changes are subtle and are often suppressible at first. These include clumsiness, variable stride length, a propensity to fidget, restlessness, and the appearance of fragmentary or exaggerated facial expressions or gestures. As the movement disorder becomes more profound and disabling patients develop a choreic "dancing" or "drunken" gait. Patients are unable to suppress involuntary movements involving many muscle groups, principally affecting the limbs and trunk generating irregular jerking and writhing movements, and often face, mouth and tongue. As a result HD patients show an increasing frequency of falls and muscle movements controlling respiration may become irregular. *Motor impersistence* develops, typified by incomplete chewing (increasing the risk of choking and aspiration), inconsistent driving speed, and a tendency to drop objects. *Dystonia and bradykinesia* become prominent later in the disease. Voluntary movements and postural reflexes slow, and patients lose facial expression. As a result dysphagia, dysarthria, aspiration, reduced dexterity and coordination, and balance problems are common occurrences in HD.

5.2 ***Emotional Disturbances.*** Mood and behavioral disorders are often the most disruptive features of HD not only for patients, but also their families and other relationships. Emotional changes precede the appearance of overt motor symptoms in approximately one third of patients, and an increased risk of

suicide has been identified in pre-symptomatic HD patients. While the appearance of emotional disturbances is quite variable between individuals they may include depression (with concomitant social withdrawal and suicide risk), increased impulsivity, obsessive-compulsive behavior, increased anxiety and irritability, or psychosis. Overt changes in personality are also common, including the development of uncharacteristically rude behavior and impatience, violent outbursts, changes in sexual behavior, and errors in social judgement.

5.3 ***Cognitive Decline.*** As the disease progresses, symptoms of cognitive decline become prevalent. Patients become easily distractible and the speed of their intellectual maneuvers decreases. Visual-spatial abilities become impaired, often manifest as a decreased awareness of their environment and the relationship of their body to objects, and a tendency to get lost. Executive function is impaired, affecting attention, decision-making, planning and organization abilities, and initiation and sequencing of actions. Decline in short term memory and learning skills are also prevalent. Cognitive changes in HD are considered "sub-cortical" in origin, since they generally lack cortical-associated symptoms such as aphasia, agnosia and amnesia typical of Alzheimer's type dementia.

5.4 ***Juvenile and Late Onset HD.*** Consistent with the pathological differences between adult and juvenile onset forms, juvenile HD shows phenotypic variations. Chorea is much less prominent, and bradykinesia is overt and occurs early (the so-called Westphal variant). Juvenile patients also typically show tremor, rigidity, and dystonia. Myoclonic jerks and seizures may occur. Behavioral problems are often manifest as attention deficit, poor impulse control, inappropriate behavior, and failure at school. Late onset HD may present purely as chorea.

6. CURRENT AND PROTOTYPICAL TREATMENTS

6.1 Current Treatments. There are no therapeutic approaches to prevent the neuronal degeneration in HD available at present (agents in clinical trial are discussed below). Approaches currently used treat the symptoms rather than the disease. The multiple neurological and psychological components of HD mean that medications used to treat these symptoms often have side effects that compound other features of the disease. Wherever possible, therefore, non-pharmacologic techniques are applied first, and if pharmacologic agents are necessary the lowest effective doses are used. HD is associated with reduced energy metabolism, weight loss and associated loss of strength. Therefore nutrition is important and patients should be maintained on high calorie diets, with supplements if necessary. Swallowing is often impaired and easy to swallow food should be chosen. An eating environment designed to reduce distractions and improve food access (e.g. using adapted utensils) is also beneficial. Pharmacologic and non-pharmacologic approaches are discussed in detail in "A Physician's Guide to the Management of Huntington's Disease" (30).

6.1.1 ***Movement Disorder:*** While the appearance of involuntary choreic movements is typically the most overt feature of HD, it is often the least troublesome symptom for patients and therefore often needs no treatment. If chorea is severe and distressful, standard antiphsychotics such as the neuroleptics haloperidol or fluphenazine may be used to suppress movements. Possible side effects include sedation, parkinsonism, and dystonia, of which the latter two can be addressed by using less potent antiphsychotics (e.g. clozapine or quetiapine; 31). Benzodiazepines including clonazepam and diazepam, or dopamine-depleting agents (e.g. reserpine and tetrabenazine) may have some beneficial effects. The impaired initiation and control of voluntary movements have greater impacts on functional ability in HD, but no effective pharmacologic agents are available. Physical, occupational, speech and swallowing therapies can delay decline of these functions. Bradykinesia, dystonia and spasticity may develop late in the disease. Antiparkinsonism drugs such as levodopa/carbidopa and amantadine can be

used to treat bradykinesia, but are associated with delirium and tolerance. Benzodiazepines may relieve stiffness, although increased bradykineisa is a potential side effect. Myoclonus may respond to clonazepam or divalproex sodium, although it is often not debilitating enough to warrant treatment. Divalproex sodium is also used to treat myoclonic epilepsy or seizures that occur in approximately 30% of juvenile HD patients.

6.1.2 ***Emotional Changes:*** Many of the symptoms of mood disturbances and personality changes can be improved by conventional pharmacologic approaches. Antidepressants are commonly used, and do not generally affect motor deficits. Selective serotonin re-uptake inhibitors (SSRIs) (including fluoxetine, sertraline, paroxetine and fluvoxamine) are usually the class chosen since have less severe side effects and less chance of overdose. Tricyclic antidepressants are avoided if possible, especially in impulsive or suicidal patients, due to their adverse cardiovascular effects and relatively high risk of toxicity in overdose, although they may be used for acute treatment if depression is unresponsive to SSRIs (e.g. Nortryptaline). Psychotherapy can be beneficial, and in refractive or severe cases electroconvulsive therapy has been used (30). Concomitant presentation of hallucinations, delusions or severe agitation can be treated with antipsychotic medications. Standard antipsychotics should be administered at low doses to avoid the detrimental side effects of parkinsonism, rigidity or sedation. If chorea is not an overt problem in psychotic patients, newer agents that are less sedative and display low or no parkinsonian side effects (e.g. quetiapine or aripiprazole) may be beneficial (31).

A small cohort of HD patients develops mania, and some may develop bipolar disorder (alternating between depression, mania, and normal mood). Mood stabilizers such as lithium are useful in these cases. Impulsivity can also be treated with mood stabilizers (e.g. carbamazepine, gabapentin, divalproex sodium and valproic acid). SSRIs or the tricyclic antidepressant clomipramine are typically used to treat obsessive-compulsive behavior. Commonly used anti-anxiety agents include SSRI's and

benzodizaepines. Mood stabilizers, SSRIs and antipsychotic agents are often useful to treat irritability. One prevalent behavioral affect of HD is a change in sexual behavior. If inappropriate sexual activity is a problem, agents that reduce libido as a side effect such as propranolol or fluoxetine may be useful.

6.1.3 ***Cognitive Changes:*** No pharmacologic interventions are currently available. Non-pharmacologic approaches include compensating for poor organizational skills by instigating daily routines, prompting patients to initiate activity, and behavioral approaches to deal with impulsivity and temper outbursts.

6.2 Prototypical Treatments.

Mutant htt interactions and animal models of the disease have revealed several targets for pharmacological interventions aimed at preventing or arresting the progression of neurodegeneration in HD. A number of agents induced moderate beneficial effects in animal models, including agents that improve energy metabolism, modulate glutamate receptor activation, inhibit free radical-mediated oxidative damage, modulate dopamine and cannabinoid neurotransmission, and prevent caspase activation. The most promising agents identified to date are being assessed in clinical trials in the HD population.

Coenzyme Q_{10} and Creatine improve aspects of HD phenotype putatively via enhancing cerebral energy metabolism (see 17). Oral administration of CoQ_{10} ameliorated elevated lactate levels seen in the cortex of HD patients, an effect that was reversible on withdrawal of the agent (18). CoQ_{10} attenuated neurotoxicity induced by the mitochondrial toxins MPTP and malonate in animal models, and increased survival and delayed symptom onset in genetic mouse models of HD. These findings led to CoQ_{10} being tested in a 30-month clinical trial in early-stage HD patients, both alone and in combination with the weak NMDA receptor antagonist remacemide (32). Although this multi-arm trial did not detect a

significant ameliorative effect of CoQ_{10}, it did demonstrate a trend towards a protective effect with treatment slowing the decline in "total functional capacity" of HD patients by 13%. Whilst findings were not immediately conclusive, results are encouraging and further studies of different doses are planned.

An alternative strategy to enhance cerebral energy metabolism is to increase brain energy stores of the high-energy compound phosphocreatine (PCr) via systemic creatine administration. Oral creatine treatment successfully attenuated neurotoxicity induced by 3-NP in rats, ameliorating increases in striatal lactate levels and decreases in energy metabolites including ATP induced by the toxin (see 17). Furthermore, oral creatine administration delayed disease onset in HD mouse models, and protected against purkinje cell loss in a transgenic mouse model of another polyglutamine repeat disease, SCA1. As a result of these promising effects, creatine's efficacy in HD is currently being assessed in clinical trials.

Riluzole is a glutamate release inhibitor that has been shown to abrogate damage in models of excitotoxic damage, and of HD and other neurodegenerative disorders. The effects of riluzole on components of the Unified HD Rating Scale (UHDRS) were recently assessed in an eight-week 2-dose study in 63 HD patients (33). The higher dose tested (200mg/kg/day) significantly reduced the progression of chorea over this period, but had no effects on motor, cognition, behavioral, or functional components of the UHDRS.

The modified tetracycline antibiotic **minocycline** is currently in initial clinical trials as an HD therapeutic. This agent has been shown to inhibit htt aggregation, caspase 3 activation, and calpain cleavage. It has been reported to be protective in some animal models of focal and global cerebral ischemia, mitochondrial toxicity, and neurodegenerative disorders including HD and amyotrophic lateral sclerosis (ALS). However beneficial effects are not universal, and a number of recent studies report no effects or even detrimental

effects of this agent, suggesting its reported beneficial effects may be associated with a small dosing window. The potential utility of this agent in HD therapy is controversial.

A number of other therapeutic approaches are being actively explored for HD, including stem cell transplantation, viral vector delivery of neurotrophic hormones, gene therapy approaches, and genetic technology designed to silence mutant HD gene expression. As a result, Huntington's disease is currently at the forefront of therapeutic design in neurodegenerative disorders, and the current high volume of HD-related research implies that ameliorative treatments may be available in the near future.

7. TERMINOLOGY

Anticipation	Age of disease onset decreases in successive generations, due to mutation instability.
Atrophy	A wasting or decrease in size of a body organ, tissue, or part, owing to disease, injury, or lack of use.
Apoptosis	Programmed cell death (or "cell suicide") induced by intracellular signals in response to variety of stimuli. Apoptosis may occur in development, or due to disease, or age. Cell death occurs in a controlled fashion, requires energy, and generally occurs without inflammatory responses.
Autosomal dominant	A dominant trait (expressed even if represented in only one of two alleles) in a non-sex determining chromosome.
Chorea	Irregular, sustained jerking or writhing movements involving multiple muscle groups.
Dysarthria	Difficulty with the physical production of speech.

Dysphagia Difficulty in swallowing.

Dystonia A neurologic movement disorder characterized by sustained muscle contractions, usually producing twisting and repetitive movements or abnormal postures or positions.

Monozygotic Trait resulting from expression of a gene carried on only one of a pair of chromosome alleles.

Mutation A random change in a gene or chromosome resulting in a new trait or characteristic that can be inherited.

Myoclonus Sudden brief jerking movements involving discrete groups of muscles.

Oxidative damage Detrimental events in cells induced by altering the function or bioavailability of molecules by oxidization, for example by interaction with free radicals.

Polyglutamine (polyQ) Repetitive sequence of glutamine amino acid moieties.

Transcription The first step in converting genetic instructions encoded in DNA. The genetic code in DNA is transferred to messenger RNA molecules that carry the code to protein-generating machinery.

BIBLIOGRAPHY

1. Vonsattel JPG, DiFiglia M. Huntington Disease. J Neuropathol Exp Neurol 1998; 57:369-384.
2. Backman L, Farde L. Dopamine and cognitive functioning: brain imaging findings in Huntington's disease and normal aging. Scand J Psychol 2001; 42:287-296.

3. Mayberg HS, Starkstein SE, Peyser CE, Brandt J, Dannals RF, Folstein SE. Paralimbic frontal lobe hypometabolism in depression associated with Huntington's disease. Neurology 1992; 42:1791-1797.
4. Albin RL, Young AB, Penney JB. The functional anatomy of basal ganglia disorders. Trends Neurosci 1989; 12:366-375.
5. The Huntington's Disease Collaborative Research Group. A novel gene containing a trinucleotide repeat that is expanded and unstable on Huntington's disease chromosome. Cell 1993; 72:971-983.
6. MacDonald ME, Gines S, Gusella JF, Wheeler VC. Huntington's disease. Neuromolecular Med 2003; 42:7-20.
7. Kehoe P, Krawczak M, Harper PS, Owen MJ, Jones AL. Age of onset in Huntington disease: sex specific influence of apolipoprotein E genotype and normal CAG repeat length. J Med Genet 1999; 36:108-111.
8. Margolis RL, Ross CA. Diagnosis of Huntington disease. Clin Chem 2003; 49:1726-1732.
9. Harjes P, Wanker EE. The hunt for huntingtin function: interaction partners tell many different stories. Trends Biochem Sci 2003; 28:425-433.
10. Feany MB, La Spada AR. Polyglutamines stop traffic: axonal transport as a common target in neurodegenerative diseases. Neuron 2003; 40:1-2.
11. DiFiglia M. Huntingtin fragments that aggregate go their separate ways. Mol Cell 2002; 10:224-225.
12. Wellington CL, Ellerby LM, Gutekunst CA, Rogers D, Warby S, Graham RK, Loubser O, van Raamsdonk J, Singaraja R, Yang YZ, Gafni J, Bredesen D, Hersch SM, Leavitt BR, Roy S, Nicholson DW, Hayden MR. Caspase cleavage of mutant huntingtin precedes neurodegeneration in Huntington's disease. J Neurosci 2003; 22:7862-7872.

13. Mastroberardino PG, Iannicola C, Nardacci R, Bernassola F, De Laurenzi V, Melino G, Moreno S, Pavone F, Oliverio S, Fesus L, Piacentini M. 'Tissue' transglutaminase ablation reduces neuronal death and prolongs survival in a mouse model of Huntington's disease. Cell Death Differ 2002; 9:873-880.
14. Sugars KL, Rubinsztein DC. Transcriptional abnormalities in Huntington disease. Trends Genet 2003; 19:233-238.
15. Gines S, Seong IS, Fossale E, Ivanova E, Trettel F, Gusella JF, Wheeler VC, Persichetti F, MacDonald ME. Specific progressive cAMP reduction implicates energy deficit in presymptomatic Huntington's disease knock-in mice. Hum Mol Genet 2003; 12:497-508.
16. Gervais FG, Singaraja R, Xanthoudakis S, Gutekunst CA, Leavitt BR, Metzler M, Hackam AS, Tam J, Vaillancourt JP, Houtzager V, Rasper DM, Roy S, Hayden MR, Nicholson DW. Recruitment and activation of caspase-8 by the Huntingtin-interacting protein Hip-1 and a novel partner Hippi. Nat Cell Biol 2002; 4:95-105.
17. Browne SE, Beal MF. The energetics of HD. Neurochem Res 2004; 29:531-546.
18. Koroshetz WJ, Jenkins BG, Rosen BR and Beal MF. Energy metabolism defects in Huntington's disease and possible therapy with coenzyme Q_{10}. Ann. Neurol 1997; 41:160-165.
19. Yu Z-X, Li S-H, Evans J, Pillarisetti A, Li H, Li X-J. Mutant huntingtin causes context-dependent neurodegeneration in mice with Huntington's Disease. J Neurosci 2003; 23:2193-2202.
20. Albin RL, Greenamyre JT. Alternative excitotoxic hypotheses. Neurology 1992; 42:733-738.
21. Browne SE, Ferrante RJ, Beal MF. Oxidative stress in Huntington's disease. Brain Pathol 1999; 9:147-163.
22. Ludolph AC, He F, Spencer PS, Hammerstad J, Sabri M. 3-nitropropionic acid: exogenous animal neurotoxin and possible human striatal toxin. Can J Neurol Sci 1990; 18:492-498.
23. Beal MF. Huntington's disease, energy, and excitotoxicity. Neurobiol Aging 1994;15:275-276.

24. Hickey MA, Chesselet MF. The use of transgenic and knock-in mice to study Huntington's disease. Cytogenet Genome Res. 2003; 100:276-286.

25. Mangiarini L, Sathasivam K, Seller M, Cozens B, Harper A, Hetherington C, Lawton M, Trottier Y, Lehrach H, Davies SW and Bates G. Exon 1 of the HD gene with an expanded CAG repeat is sufficient to cause a progressive neurological phenotype in transgenic mice. Cell 1996; 87:493-506.

26. Schilling G, Becher MW, Sharp AH, Jinnah HA, Duan K, Kotzuk JA, Slunt HH, Ratovitski T, Cooper JK, Jenkins NA, Copeland NG, Price DL, Ross CA, Borchelt DR. Intranuclear inclusions and neuritic aggregates in transgenic mice expressing a mutant N-terminal fragment of huntingtin. Hum Mol Genet 1999; 8:397-407.

27. Yamamoto A, Lucas JJ, Hen R. Reversal of neuropathology and motor dysfunction in a conditional model of Huntington's disease. Cell 2000;101:57-66.

28. Slow EJ, van Raamsdonk J, Rogers D, Coleman SH, Graham RK, Deng Y, Oh R, Bissada N, Hossain SM, Yang YZ, Li XJ, Simpson EM, Gutekunst CA, Leavitt BR, Hayden MR. Selective striatal neuronal loss in a YAC128 mouse model of Huntington disease. Hum Mol Genet 2003; 12:1555-1567.

29. Wheeler VC, Gutekunst CA, Vrbanac V, Lebel LA, Schilling G, Hersch S, Friedlander RM, Gusella JF, Vonsattel JP, Borchelt DR, MacDonald ME. Early phenotypes that presage late-onset neurodegenerative disease allow testing of modifiers in Hdh CAG knock-in mice. Hum Mol Genet 2002 15;11:633-640.

30. Rosenblatt A, Ranen NG, Nance MA, Paulsen, JS. A Physician's Guide to the Management of Huntington's Disease. Huntington's Disease Society of America 1999.

31. Tarsy D, Baldessarini RJ, Tarazi FI. Effects of newer antipsychotics on extrapyramidal function. CNS Drugs 2002; 16:23-45.

32. Huntington Study Group. A randomized, placebo-controlled trial of coenzyme Q10 and remacemide in Huntington's disease. Neurology 2001; 57:375-376.
33. Huntington Study Group. Dosage effects of riluzole in Huntington's disease: a multicenter placebo-controlled study. Neurology 2003; 61:1551-1556.

FIGURE LEGEND

Figure 1: Modulation of the "Indirect" Basal Ganglia Pathway Controlling Movement in HD. A representative diagram showing the major neurotransmitter systems involved in the indirect basal ganglia output pathways. Under normal circumstances (left), activation of the indirect pathway increases the inhibitory input to thalamic nuclei, resulting in reduced excitatory output to the cortex. Choreic movements in HD are thought to result from decreased activity of the indirect pathway due to loss of GABA/Enk neurons projecting from the striatum to GPe, reducing the tonic inhibition of the thalamo-cortical projection (4). *Abbreviations:* CTX, cerebral cortex; GPe, Globus pallidus, external segment; GPi, Globus pallidus, internal segment; Thal, Thalamus; SNR, substantia nigra *pars reticulata*; STN, Subthalamic nucleus; Stri, Striatum. "X" represents pathways inhibited by presynaptic inhibitory input, or in the case of GABA/ENK Stri-GPe projection in HD, by neuronal loss.

Table 1: Synopsis of wildtype and mutant htts' interactions with cellular and molecular targets.

Process Altered	**Htt Target**	**Effect**
Protein/Protein Interactions	Multiple, described below, plus calmodulin, GAPDH.	Potential to modify or abrogate activity of bound protein. Many covalent interactions are catalyzed by transglutaminases, forming glutamyl-lysine crosslinks.
Endocytosis	HIP-1, HIP-12, HIP-14, AP-2αadaptin, PACSIN1, SH3GL3.	Htt modulates clathrin-mediated vesicle formation and endocytosis. Mutant htt may disrupt vesicle formation and transport.
Intracellular Trafficking	HAP-1.	PolyQ increases axonal blockages
Gene Transcription	CBP, p53. Sp1, TAFII-130. N-CoR, Sin3A.	Mutant htt affects transcription factors, transcriptional activators and co-activators, and transcription repressor activities.
Postsynaptic Signalling	PSD-95. CIP4, FIP-2.	Htt influences organization of the post-synaptic density, including glutamate receptor subtypes, and dendrite morphology.
Apoptosis	HIP1. Caspase 3.	Htt binding to HIP1 prevents HIP-induced caspase-dependent cell death cascades. PolyQ expansion reduces htt's binding to HIP1.
Energy Metabolism	Mitochondrial enzymes (TCA cycle and respiratory chain)	Mitochondrial damage, reduced energy production, increased risk of excitotoxicity.
Glutamatergic Signalling	NMDA receptor-bearing neurons.	Brain regions receiving glutamatergic innervation at risk of excitotoxic damage.
Oxidative Damage	Mutant htt-mediated cascades induce free radical generation.	Oxidative damage to proteins, DNA, and phospholipids.
Htt Aggregation	Mutant-length polyQ expansions lead to htt self-aggregation.	Deposition of ubiquitinated htt-positive protein aggregates, that may sequester or bind other proteins, and may disrupt proteosomal processing.

Table 2: Animal models of Huntington's disease [17].

Approach	Model	HD-like Phenotypes	Atypical Phenotypes
Excitotoxic Lesions	Intrastriatal injections of NMDA receptor agonists (quinolinic acid, kynurenic acid) in non-human primates, rats, mice.	Striatal neurodegeneration. Medium spiny neurons targeted. Apomorphine-inducible movement disorder in primates.	Rapidly progressing, acute phenotypes. Toxins are not region-specific, and intrastriatal placement is required.
Mitochondrial Toxins	SDH / Complex II inhibition by systemic administration of 3-NP; Intrastriatal injection of malonate. Primates, rats, mice.	Striatal neurodegeneration. Medium spiny neurons targeted. Often fatal. 3-NP's effects are striatal-specific. Induce motor disturbances and dystonia. Disrupt energy metabolism and induce oxidative damage.	Rapidly progressing, acute phenotypes (but can be titered for more chronic effects).
Gene Constructs	**Mouse Lines**		
Fragment, human htt.	R6/2 (144Q), R6/1 (115Q) N171-82Q (82Q) HD100 (100Q)	Weight loss, movement disorder, htt aggregates, atrophy of cortex and striatum, neurotransmitter receptor changes, transcriptional dysregulation, reduced life span.	Little or no overt striatal cell death. Diabetes or glucose intolerance. Disease onset very rapid. Peripheral toxicity.
Full length, human htt.	YAC (72Q & 128Q) HD89 (89Q)	Weight loss, movement disorder, htt aggregates, transcriptional dysregulation, atrophy of cortex and striatum, some cell death. Symptoms develop slowly.	Normal life span.
Inducible, human htt.	Tet-off (94Q)	Movement disorder, htt aggregates, atrophy of cortex and striatum, neurotransmitter receptor changes. (Many symptoms reversible on gene turn-off).	Normal life span. Symptom-onset rapid after gene turn-on.
CAG insertion, murine htt.	*HdhQ111* (111Q) *Hdh-150Q* (150Q) *Hdh4/6* Knock-in (80Q) HD/*Hdh* Chimera (80Q)	Selective cell death and atrophy of cortex and striatum observed in some models, htt aggregates. Subtle behavioral changes. Symptoms develop slowly.	Normal life span. No overt movement disorder.

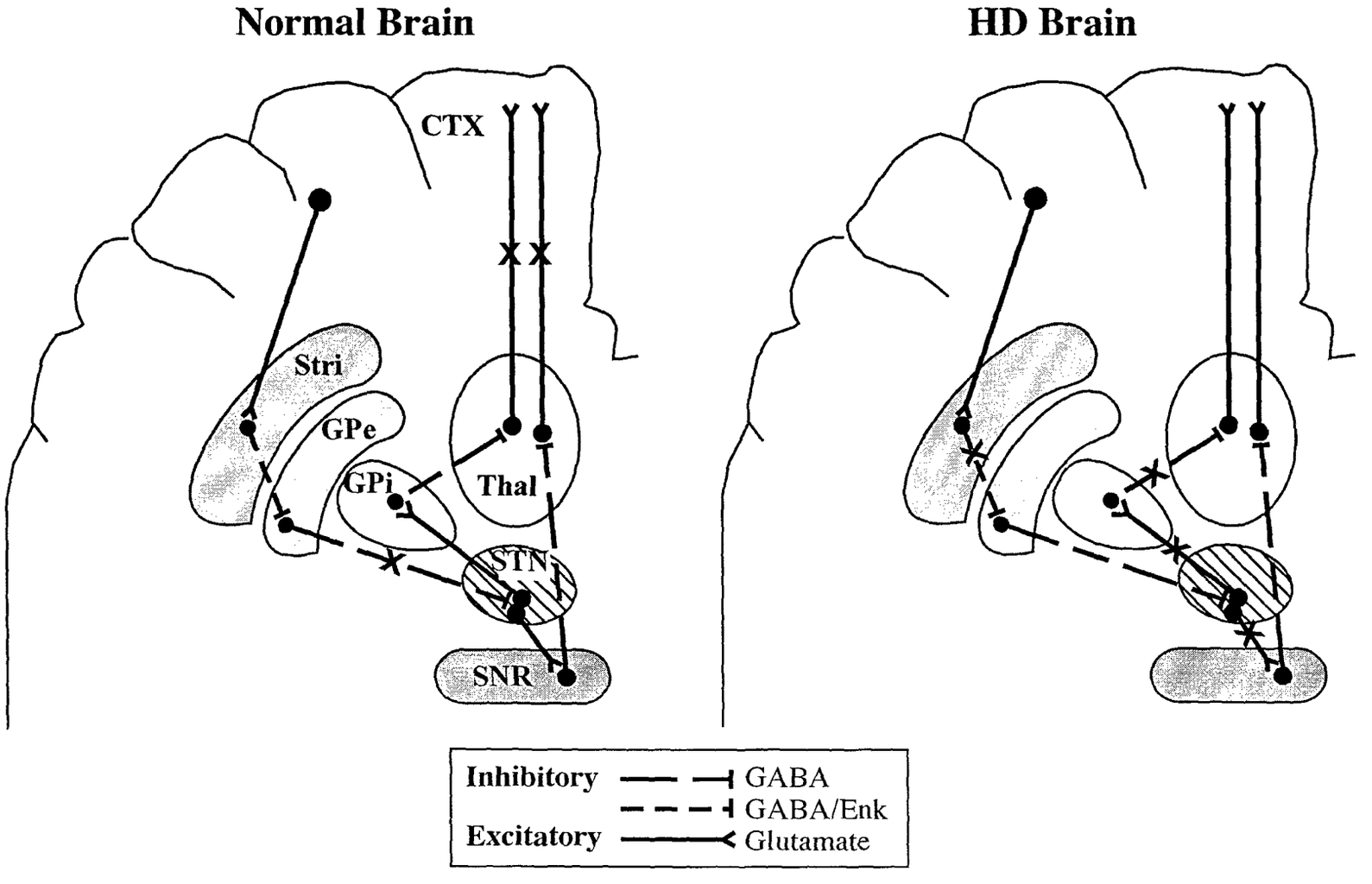
Normal Brain
HD Brain
CTX
Stri
GPe
GPi
Thal
STN
SNR
Inhibitory
GABA
GABA/Enk
Excitatory
Glutamate

APPENDIX 13

Susan E. Browne and M. Flint Beal

49

Huntington's Disease

Huntington's disease is one of several devastating neurodegenerative diseases, including amyotrophic lateral sclerosis and Alzheimer's disease (AD), which are characterized by late onset in adult life. Their debilitating symptoms include cognitive dysfunction, behavioral changes and mood disturbances, and movement disorders, and in the cases of amyotrophic lateral sclerosis and Huntington's disease paralysis and death can occur. As the mean age of the population increases, so does the frequency of occurrence of these disorders. Symptoms are associated with region-specific loss of neurons within the central nervous system (CNS), but to date the mechanism of this selective neuronal death remains unknown. Several different etiological processes may play roles, and strong evidence from studies in humans and in animal models suggests the involvement of energy metabolism dysfunction, excitotoxic processes, and oxidative stress. The recent development of transgenic mouse models expressing the human Huntington's disease mutation has provided novel opportunities to determine the chronological order of events underlying the selective neuronal death seen in the disease, which have hitherto been impossible to determine in humans.

I. Introduction

Over a century elapsed between the first description of the Huntington's disease phenotype by George Huntington in 1872 and the discovery of the genetic defect underlying the disease in 1993 (Huntington's Disease Collaborative Research Group, 1993). A physician in Long Island, New York, the familial inheritance of the disease was well known to Huntington from the family histories passed down to him by his grandfather and father. Huntington's disease is now known to be an autosomal dominantly inherited neurodegenerative disorder characterized by the adult onset and progressive development of behavioral abnormalities, cognitive impairment, and involuntary choreiform movements, with a typical duration of 15–20 years. The genetic abnormality in Huntington's disease is a CAG repeat expansion in a gene encoding a 350 kDa protein of unknown function, termed "huntingtin" (Huntington's Disease Collaborative Research Group, 1993). It is thought to be a true dominant disorder since homozygous patients do not seem to differ from heterozygote carriers in either age of onset, duration, or severity of the disease (Durr *et al.*, 1999). Despite its identification, the definitive role of mutant huntingtin in neuronal degeneration remains unknown. As discussed below, the insidious progression of motor and behavioral disturbances in Huntington's disease reflects the selective pattern of cell loss in the brain and the specific neurotransmitter pathways affected. The reason for the preferential vulnerability of striatal neurons in Huntington's disease is still enigmatic, and cannot be simply explained in terms of the distribution of abnormal huntingtin since the gene mutation is expressed throughout the body. However, experimental evidence suggests that the pathogenesis of cell death in Huntington's disease is linked to a gain of function of mutant huntingtin. In addition, studies in both human Huntington's disease brain and transgenic mouse model of Huntington's disease have identified widespread neuronal intranuclear and cytoplasmic aggregations of mutant huntingtin that may be linked to the disease process. In the following review we have collated the experimental information available to date to give insight into the link between the Huntington's disease gene mutation and selective neuronal dysfunction and death in this disease.

II. Neuropathological Features and Motor Dysfunction in Huntington's Disease

A. Pathological Changes in Huntington's Disease Brain

The typical neuropathological features of Huntington's disease are progressive caudal to rostral degeneration of the caudate-putamen (Vonsattel and DiFiglia, 1998). Patients are graded at postmortem according to the extent of gross and microscopic measures of neuropathological severity, grades ranging from 0 to 4 with increasing severity and extent of striatal involvement (Vonsattel *et al.*, 1985). Briefly, grade 0 brains exhibit 30–40% neuronal loss in the head of the caudate, with no visible signs of reactive gliosis. In contrast, in grade 4 more than 95% of striatal neurons are lost, the striatum is severely atrophic with marked gliosis, and about 50% of end-stage

cases show cell loss in the nucleus accumbens. Most Huntington's disease cases reach grade 3 or 4 by the time of death, by which stage nonstriatal regions are also involved, in particular the globus pallidus, cortex, and, to a lesser extent, thalamus, subthalamic nucleus, substantia nigra, white matter, and cerebellum (Sotrel *et al.*, 1991; Braak and Braak, 1992; Vonsattel and DiFiglia, 1998). Fibrillary astrogliosis occurs in the striatum, but has not been reported in other affected areas, and no inflammatory responses are involved (Myers *et al.*, 1991). In cases of juvenile onset Huntington's disease cerebellar atrophy is particularly prevalent.

The striatal cells most susceptible to degeneration in Huntington's disease are medium spiny projection neurons (Beal, 1994a). Spiny neurons, which constitute 80% of striatal neurons, are the principal input and output neurons of the striatum. All contain the inhibitory neurotransmitter γ-aminobutyric acid (GABA), while subsets also contain enkephalin (ENK), Substance P (SP), dynorphin, or calbindin. The other major class of striatal neurons are aspiny interneurons. Nicotinamide adenine dinucleotide phosphate diaphorase (NADPH-d), neuropeptide Y (NPY), somatostatin, and nitric oxide synthase (NOS) typically colocalize in medium-sized aspiny neurons, and some also contain cholecystokinin or the calcium-binding protein parvalbumin. In Huntington's disease striatum, spiny projection neurons containing SP or ENK degenerate earliest in the course of the disease, whereas aspiny interneurons and the larger cholinergic interneurons are relatively spared (Ferrante *et al.*, 1987; Beal *et al.*, 1988). There is also some hierarchy in the vulnerability of different spiny neuron subpopulations; ENK-immunoreactive neurons projecting to the external segment of the globus pallidus (GPe) degenerate prior to SP-containing neurons projecting to the internal segment (GPi) (Reiner *et al.*, 1988; Richfield *et al.*, 1995; Sapp *et al.*, 1995). Spiny neurons also undergo morphological changes in the course of the disease process in Huntington's disease, including recurving of the dendrites, altered shape and size of the spines, and increased density of spines.

Surviving neostriatal neurons are generally morphologically normal, although some are reduced in size and contain elevated levels of the oxidative damage marker lipofuscin. A subpopulation of "neostriatal dark neurons" has also been described by Vonsattel *et al.* (1985), scattered between the zones of atrophic and healthy cells. Interestingly, markers of apoptotic cell death have been detected in these neostriatal dark neurons (for example, granulation of the cytoplasm and condensation of nuclear chromatin and labeling by TdT-mediated dUTP-biotin nick end-labelling [TUNEL]; Vonsattel and DiFiglia, 1998).

B. Motor Dysfunction

The motor defects typical of Huntington's disease result from the disruption of basal ganglia-thalamocortical pathways which regulate movement control. The neostriatum (caudate nucleus and putamen) receives excitatory glutamatergic inputs from the entire neocortex, the first step in the anatomical loop responsible for the initiation and execution of movement. Processed signals are transmitted via basal ganglia output nuclei (GPi, the substantia nigra pars reticulata, SNr, and ventral pallidum) to the thalamus, which in turn sends excitatory projections to areas of the frontal cortex associated with motor planning and execution (Albin *et al.*, 1989; Alexander and Crutcher, 1990; Graybiel *et al.*, 1994). The GABAergic basal ganglia output projections to the thalamus maintain a tonic inhibition of their target nuclei, which is modulated by two opposing pathways (direct and indirect) which integrate the input and output compartments within the basal ganglia (Fig. 49.1). It is an imbalance in the relative contributions of these two regulatory pathways that triggers, and dictates the nature of, the motor dysfunction in Huntington's disease. In the direct (monosynaptic) pathway, activation of striatal efferents containing GABA and SP projecting directly to the GPi results in disinhibition of thalamic activity. In contrast, in the indirect (polysynaptic) pathway striatal efferents containing GABA and enkephalin project to the GPe which sends purely GABAergic projections to the subthalamic nucleus. From here, excitatory efferents (probably glutamatergic) project to the basal ganglia output nuclei (SNr and GPi). The GPe projection generally exerts a tonic inhibition on the subthalamic nucleus. Activation of GABA/ENKergic striatal efferents tends to suppress activation of GPe neurons, causing disinhibiton of the subthalamic nucleus and hence an increase in the excitatory innervation of the basal ganglia output nuclei. This leads to an increased inhibitory input to the target thalamic nuclei. Thus, cortical function is differentially modulated depending on which basal ganglia pathway, and therefore which thalamocortical pathway, is activated (Albin *et al.*, 1989; Alexander and Crutcher, 1990). In Huntington's disease there is preferential loss of the GABA/ENK-containing neurons comprising the indirect pathway. "Disinhibition" of the thalamus results, which is manifest in Huntington's disease patients by the development of involuntary choreic movements. The later onset of a rigid akinetic state in some Huntington's disease patients is thought to result from the additional loss of striatal GABA/SP-containing efferents projecting directly to the GPi (Albin *et al.*, 1990).

III. Mutant Huntingtin Protein in Huntington's Disease

The genetic defect in Huntington's disease is an expansion of an unstable CAG repeat encoding polyglutamines (Q_n) at the 5′ end of a gene on chromosome 4, *IT15* ("interesting transcript 15"), now termed *huntingtin (HD)* (Huntington's Disease Collaborative Research Group, 1993). Similar trinucleotide mutations in different genes are responsible for at least seven other neurodegenerative disorders: the spinocerebellar ataxias (SCA1, SCA2, SCA3 [Machado-Joseph disease], SCA6, and SCA7), dentatorubral-pallidoluysian atrophy, and spinal bulbar muscular atrophy (Ross, 1995; Zoghbi, 1997). While the genes affected in these disorders have now been identified, only in spinal bulbar muscular atrophy is the function of the affected protein known (androgen receptor). All the glutamine repeat diseases involve neuronal loss and gliosis. However, while gene expression is widespread throughout the body, cell death occurs in specific regions of the brain and spinal cord. How these genetic defects lead to progressive, selective neurodegeneration, remains elusive. The gene product in Huntington's disease, huntingtin protein, is a 348 kDa protein containing 3144 amino acids. Normal, unaffected indi-

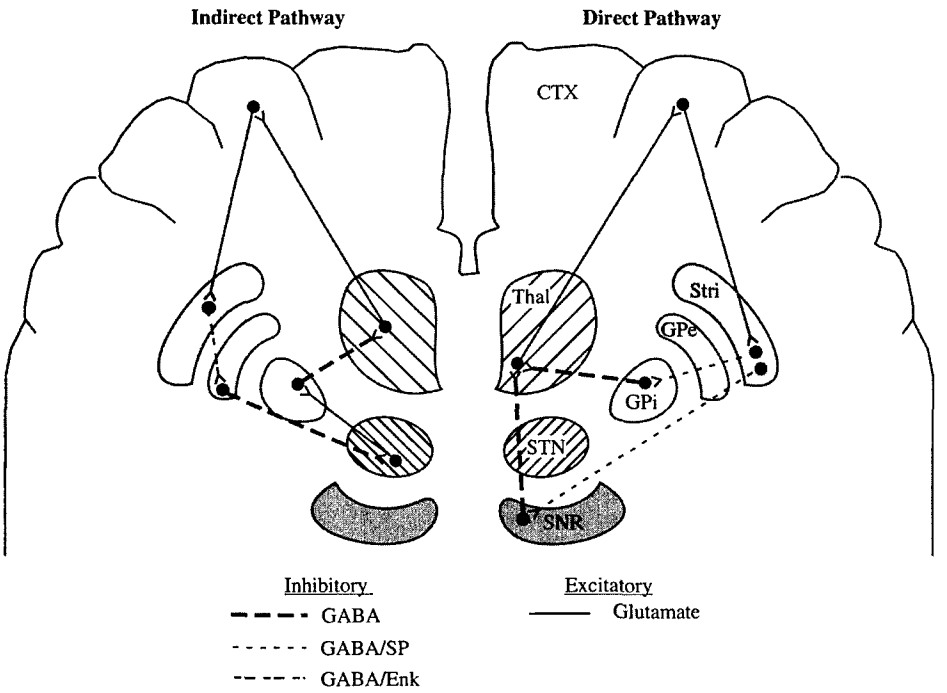

FIG. 49.1. Corticofugal pathways controlling movement. A representative diagram showing the major neurotransmitter systems involved in the direct (right) and indirect (left) basal ganglia output pathways. Activation of the indirect pathway increases the inhibitory input to thalamic nuclei, resulting in reduced excitatory output to the cortex. In contrast, activation of GABA/SP-containing striatal efferents in the direct pathway results in inhibition of the GPi and SNR projection to the thalamus, effectively releasing the thalamus from pallidal inhibition. As a result, the excitatory output to the cortex increases. Choreic movements in Huntington's disease are thought to result from reduced activity of the indirect pathway, due to loss of GABA/Enkephalinergic neurons (Albin *et al.*, 1989; Andrews and Brooks, 1998). CTX, cerebral cortex; GPe, globus pallidus, external segment; GPi, globus pallidus, internal segment; Thal, Thalamus; SNR, substantia nigra pars reticulata; STN, subthalamic nucleus; Stri, striatum.

viduals typically have trinucleotide repeats of 11–34 CAGs. Expansion to 34–39 CAG repeats in one or both alleles confers the possibility of developing Huntington's disease, while the disease is inescapable when CAG repeats in either allele exceed 39. The trinucleotide repeat is polymorphic and undergoes alterations during meiosis, generally fluctuating by ± 1–5 repeats per transmission, although larger increases can occur following paternal transmission (Ross, 1995). The physiological functions of both normal and mutant huntingtin have not yet been determined, although several features of the Huntington's disease phenotype are known to be influenced by CAG repeat length, such as age of onset of the disease (Andrew *et al.*, 1993; Duyao *et al.*, 1993; MacDonald *et al.*, 1999) and the extent of DNA fragmentation in Huntington's disease striatal neurons (Butterworth *et al.*, 1998). CAG repeat length has also been correlated with neuropathological severity, although this observation is controversial since the grade of disease at time of death is dependent on a number of factors also influenced by repeat length, including age of onset and disease duration (Furtado *et al.*, 1996; Sieradzan and Mann, 1998).

Distribution studies give little insight into the involvement of mutant huntingtin in the regional selectivity of cell loss in the disease, since huntingtin protein is ubiquitously expressed throughout the body. The fact that its distribution shows no apparent selectivity for cerebral regions targeted by the disease process suggests that another property of basal ganglia neurons confers vulnerability to degeneration in Huntington's disease (Strong *et al.*, 1993; Sharp *et al.*, 1995). However, recent immunohistochemical studies suggest that huntingtin may be differentially distributed at the cellular level within the striatum. Ferrante *et al.* (1997) reported that within the striatum huntingtin immunoreactivity is heterogeneous, the patch compartment showing low levels or no immunoreactivity in neurons and neuropil, while levels are relatively higher in the matrix. Double labeling techniques revealed higher levels of huntingtin expression in medium spiny neurons and colocalization with calbindin, in contrast to little or no colocaliztion of huntingtin with NADPH-d or NOS neurons, suggesting that there is some correlation between huntingtin's cellular location and cell vulnerability. A more recent study (Fusco *et al.*, 1999) supports Ferrante and colleagues' observations that huntingtin protein load varies within the striatal population of medium-sized neurons and is not consistently found in all medium spiny projection neurons. Taken with their observations that large striatal cholinergic interneurons which are relatively spared in the disease contain high levels of huntingtin, Fusco and colleagues suggest that the huntingtin mutation is not directly toxic to cells.

At the neuronal level, huntingtin protein is widely expressed throughout cells, with a largely cytoplasmic distribution in perikarya, axons, dendrites, and some nerve terminals, and protein fragments have been identified in neuronal nuclei. Subcellular fractionation studies revealed an association of

huntingtin with synaptic vesicles (DiFiglia *et al.*, 1995), while another report suggests association with the microtubules (Gutekunst *et al.*, 1995), implicating potential roles in intracellular trafficking and synaptic function. N-terminal fragments of huntingtin form ubiquinated protein aggregates in neuronal nuclei (neuronal intranuclear inclusions) and in dystrophic neurites (cytoplasmic inclusions). These protein aggregates have been identified in both Huntington's disease brain and in the brains of transgenic mice expressing a fragment of human mutant huntingtin (Davies *et al.*, 1997; DiFiglia *et al.*, 1997; Reddy *et al.*, 1998; Hodgson *et al.*, 1999). The mechanism of inclusion formation has not yet been detrmined, but Perutz and colleagues (1994) suggest that the expanded polyglutamine stretches in mutant huntingtin lend themselves to the formation of β-pleated sheets held together by hydrogen bonds between amide groups. CAG repeat length appears to be critical for aggregate formation (Scherzinger *et al.*, 1997). Similar intranuclear inclusions also occur in other CAG repeat disorders including spinocerebellar ataxia type 3 (Paulson *et al.*, 1997) and in transgenic mice expressing merely an expanded CAG repeat (Ordway *et al.*, 1997), suggesting that nuclear inclusions are a common product of trinucleotide expansions irrespective of the affected gene.

The toxic function associated with mutated huntingtin appears to be due to gain of a novel function, rather than loss of wild-type huntingtin function, since murine *HD* homolog-null mice die *in utero* while heterozygous knock-out mice show little or no pathology (Duyao *et al.*, 1995). Further, Huntington's disease knock-out mice are completely rescued by crossing into knock-in Hdh^{Q50} mice with a mutant polyglutamine expansion (48 CAGs), while mice expressing abnormally low levels of murine huntingtin exhibit developmental abnormalities (White *et al.*, 1997). Putative mechanisms of huntingtin dysfunction include altered cellular interactions. These include suggestions that expanded glutamine repeats may allow protein–protein interactions or that polyglutamines might be substrates for transglutaminases (Perutz *et al.*, 1994; Cooper *et al.*, 1997b). The principal candidates for protein interactors are huntingtin-associated protein-1 (HAP-1) and glyceraldehyde 3-phosphate dehydrogenase (GAPDH) (Li *et al.*, 1995; Burke *et al.*, 1996). Others include calmodulin, caspase-3, α-adaptin, cystathionine β-synthase, and huntingtin interacting protein (HIP-1) (see Aronin *et al.*, 1999). Interestingly, in the case of calmodulin the polyglutamine expansion seems to increase huntingtin's affinity (Bao *et al.*, 1996). A potential role for HAP-1 in the pathogenesis of Huntington's disease has largely been discounted on the basis of reports that although it is found only in brain it does not show a preferential striatal distribution, and that HAP-1 does not interact with the mutant stretch in huntingtin (Bertaux *et al.*, 1998). GAPDH is a critical glycolytic enzyme, which led to intriguing proposals that an interaction with mutant huntingtin might impair metabolic function. Arguing against this idea, we found that the glycolytic function of GAPDH is not altered in postmortem Huntington's disease brain tissue (Browne *et al.*, 1997). However, a recent study in fibroblast preparations showed that GAPDH's glycolytic activity is less responsive to metabolic stress in Huntington's disease patients than in fibroblasts from control subjects and unaffected Huntington's disease family members (Cooper *et al.*, 1998). GAPDH also has a number of other functions within the cell which might be altered by an interaction with huntingtin. These include a role as a uracil DNA glycosylase in DNA repair, and binding to a number of proteins including DNA, RNA, ATP, actin, tubulin, amyloid precursor protein, and calcyclin. GAPDH expression is very susceptible to metabolic stress, and a glycolytically inactive form of the enzyme found in the nucleus has been implicated in apoptotic mechanisms in neurons and somatic cells (Saunders *et al.*, 1997; Sawa *et al.*, 1997). The potential for huntingtin to deleteriously affect GAPDH function is supported by a report that both GAPDH and α-ketoglutarate dehydrogenase are inactivated by fusion proteins containing polyglutamine stretches of pathological length, in reactions catalyzed by transglutaminase (Cooper *et al.*, 1997a). Tissue transglutaminases (tTGase) are also implicated in the pathogenesis of trinucleotide repeat disorders including Huntington's disease due to another functional role within neurons and astrocytes, catalyzing Ca^{2+}-dependent cross-linking of glutamine residues with lysine and polyamines in other proteins (Aeschlimann and Paulsson, 1994; Kahlem *et al.*, 1996; Lorand, 1996; Cooper *et al.*, 1997a,b, 1999).

IV. Huntingtin Aggregates: Toxic, Protective, or Inert?

A great deal of debate surrounds the issue of whether neuronal intranuclear inclusion deposition plays a causative role in the pathogenesis of cell death in Huntington's disease, or is merely a secondary event. There is conflicting evidence about the role of neuronal intranuclear inclusions, although at present the weight of opinion seems to favor a lack of involvement, or even a neuroprotective role. The original thesis that nuclear localization of huntingtin aggregates was essential for pathogenic processes came from observations in the R6/2 transgenic mouse line, that neuronal intranuclear inclusion deposition preceded symptoms and pathology in the mouse phenotype (Mangiarini *et al.*, 1996; Davies *et al.*, 1997). Expanded CAG repeats have also been shown to induce huntingtin aggregation and cell death in transfected cerebellar granule cell cultures (Moulder *et al.*, 1998). In addition, transfection of a human mutant huntingtin fragment into *Drosophila* eye cells induced CAG repeat-dependent photoreceptor degeneration and death, putatively via apoptotic mechanisms (Jackson *et al.*, 1998).

The case against a pathogenic role of neuronal intranuclear inclusions is steadily growing. In Huntington's disease postmortem brain, neuronal intranuclear inclusion deposition in the cortex and striatum does not mirror the pattern of cell death in the disease (Ferrante *et al.*, 1997; Fusco *et al.*, 1999). Neuronal intranuclear inclusions and cytoplasmic inclusions are seen in NADPH-d neurons spared in the disease, but are not found in acetylcholinesterase- and choline acetyltransferase-positive interneurons, suggesting that neuronal intranuclear inclusion formation is not critical for cell death mechanisms. Also, in the majority of Huntington's disease patients huntingtin aggregates are most commonly found in neurites, with the exception of 5–10% of patients with juvenile onset of disease in whom neuronal intranuclear inclusions are prevalent in the cortex and striatum (Aronin *et al.*, 1999). In addition, Sawa

et al. (1999) demonstrated in cultured Huntington's disease and control lymphoblasts that stress-induced depolarization is much greater in Huntington's disease mitochondria than in mitochondria from controls, in the absence of any neuronal intranuclear inclusion deposition—suggesting that neuronal intranuclear inclusions are not necessary for cellular dysfunction. They went on to demonstrate that this mitochondrial dysfunction is linked to apoptotic cell death. Furthermore, Saudou and colleagues (1998) recently reported cell-selective neurodegeneration resembling apoptotic cell death in cultured striatal (but not hippocampal) neurons transfected with a human mutant huntingtin fragment, independent of the presence of intranuclear inclusions. Observations that suppression of neuronal intranuclear inclusion deposition resulted in increased cell death in this neuronal population led to the proposal that neuronal intranuclear inclusion deposition may reflect a protective mechanism within cells.

Another study in cultured mouse clonal striatal neurons supports the argument that nuclear aggregates are unnecessary for the cell death mechanism to be activated in Huntington's disease. Kim *et al.* (1999) demonstrated that transfecting mouse clonal cells with either full-length or truncated huntingtin containing mutant CAG repeat lengths induced the formation of both nuclear and cytosolic inclusions, whereas huntingtin with wild-type CAG repeats remained within the cytoplasm. Nuclear inclusions consisted largely of N-terminal cleaved fragments of huntingtin, while cytoplasmic inclusions contained both fragments and intact proteins. Apoptotic features were present in both wild-type and mutant huntingtin transfected cells, but were exacerbated in mutant cells. Findings that inhibiting caspase activity with Z-VAD-FMK increased cell survival, but had no effect on either neuronal intranuclear inclusion or cytoplasmic inclusion number, imply that neuronal death is independent of aggregate formation in this model. This hypothesis was supported by observations that another caspase inhibitor, Z-DEVD-FMK, reduced neuronal intranuclear inclusion and cytoplasmic inclusion number but had no effect on cell survival. The authors also demonstrated that only mutant, and not wild-type, huntingtin underwent cleavage to form N-terminal fragments, which suggests that the polyglutamine domain confers some propensity for cleavage by caspases (Kim *et al.*, 1999). In another study, nuclear import and export sequences were inserted into huntingtin fragments in 293T cultured cells to alter their normal distribution within the cells (Hackam *et al.*, 1999). Results show that toxicity of mutant huntingtin is unaffected by the intracellular location of huntingtin aggregates. Although neither full-length huntingtin or huntingtin fragments have yet been found in mitochondria, an effect on mitochondrial function cannot be ruled out. For instance, huntingtin may play a role in mitochondrial trafficking, or alternatively neuronal intranuclear inclusions may influence nuclear transcription and thus affect the expression of nuclear-encoded proteins including subunits of mitochondrial complex II. The latter is of particular note since complex II activity is impaired in affected brain areas in Huntington's disease.

Transgenic and knock-in mouse models (discussed in section VI) further support the argument that neuronal intranuclear inclusions are not needed for cell toxicity in Huntington's disease models. Although neuronal intranuclear inclusion deposition precedes behavioral symptoms and neurotransmitter changes in R6/2 mice, there is no direct link between the distribution of neuronal intranuclear inclusion deposition and patterns of cell death or dysfunction in several other mutant Huntington's disease mouse models (Reddy *et al.*, 1998; Hodgson *et al.*, 1999; Levine *et al.*, 1999). In addition, R6/2 transgenic mice also develop neuronal inclusions in many postmitotic peripheral tissues from about 6 weeks of age, including both skeletal and cardiac muscle, kidney, liver, pancreas, and adrenal glands (Sathasivam *et al.*, 1999). Peripheral aggregate formation seems to coincide with tissue atrophy, but there is no direct evidence of cell death. It is of interest, therefore, that unlike the brain where the bulk of aggregtes are neuritic, inclusions in skeletal muscle cells are found solely within nuclei. There is also increasing evidence from transgenic mouse models that the mechanism of neuronal death in other polyglutamine repeat disorders is independent of nuclear aggregation of the mutant protein. Lin *et al.* (2000) report that polyglutamine expansion in ataxin-1 causes the downregulation of several neuronal genes involved in signal transduction and calcium homeostasis in SCA-1 mice expressing the transgene. More interestingly, these changes precede any pathological changes in the mice by at least 3 weeks (pathology is evident at 6 weeks). Mutant ataxin-1 also forms intranuclear inclusions in cerebellar Purkinje cells of SCA-1 mice, and in humans, by aggregating with proteosomes and ubiquitin (Cummings *et al.*, 1998). However, these inclusions do not appear to be pathogenic, since decreasing the frequency of nuclear inclusion formation (by treating with E6-AP ubiquitin ligase) actually exacerbated the rate and extent of pathology in SCA-1 mice (Cummings *et al.*, 1999).

V. Putative Mechanisms of Cell Death

The main question still confounding researchers is how the huntingtin mutation results in selective neuronal cell loss in Huntington's disease. The definitive answer is still elusive, but several hypotheses exist.

A. Bioenergetic Defects

One hypothesis is that the gain of function associated with expanded polyglutamine repeats leads either directly or indirectly to a defect in energy metabolism, potentially via secondary excitotoxicity (Albin and Greenamyre, 1992; Beal, 1994b). Reduced ATP production due to impaired energy metabolism can lead to partial cell depolarization by making neurons more vulnerable to endogenous levels of glutamate. The concomitant increase in Ca^{2+} influx into neurons may trigger further free radical production, exacerbating damage to cellular elements. This hypothesis is supported by findings that normally ambient levels of excitatory amino acids become toxic in the presence of oxidative phosphorylation inhibitors, sodium–potassium pump inhibitors, or potassium-induced partial cell membrane depolarization. Further, excitatory amino acid antagonists such as MK-801 can ameliorate cerebral lesions induced by mitochondrial toxins such as 3-nitropropionic acid (3-NP), 3-acetylpyridine (3-AP), aminooxyactic acid (AOAA), 1-methyl-4-phenylpyridinium (MPP^+), and malo-

nate (Storey *et al.*, 1992; Beal, 1996; Schulz *et al.*, 1996b). The principal indicator of an energetic involvement in the disease process is the observation of insidious weight loss in Huntington's disease patients despite a sustained caloric intake (O'Brien *et al.*, 1990). Subsequently, positron emission tomography (PET) and biochemical studies in postmortem brain have shown selective metabolic defects in brain regions targeted by the disease, and mitochondrial abnormalities in Huntington's disease have been identified in ultrastructural studies of cortical biopsies from juvenile and adult-onset Huntington's disease cases (Goebel *et al.*, 1978).

PET studies show marked reductions in glucose metabolism in the basal ganglia and cerebral cortex of symptomatic Huntington's disease patients (Kuhl *et al.*, 1985; Kuwert *et al.*, 1990; Andrews and Brooks, 1998). Caudate hypometabolism in symptomatic patients has been shown to correlate with clinical test scores for bradykinesia, rigidity, dementia, and functional capacity, while the extent of putaminal hypometabolism correlates with chorea and eye-movement dysfunction, and thalamic hypermetabolism correlates with dystonia scales (Young *et al.*, 1986; Berent *et al.*, 1988; Kuwert *et al.*, 1990). Cortical hypometabolism is also seen in patients suffering psychological disturbances and mood changes, before the onset of motor symptoms (Kuwert *et al.*, 1990). More convincing evidence of a causative role for energetic defects comes from observations of striatal hypometabolism prior to the bulk of tissue loss, and in asymptomatic subjects at risk of developing the disease (Grafton *et al*, 1992; Kuwert *et al.*, 1993; Antonini *et al.*, 1996). Approximately 50% of gene-positive mutation carriers exhibit metabolic defects years before the onset of clinical symptoms (Antonini *et al.*, 1996). PET techniques have also demonstrated that the first clinical symptoms of the disease correlate with loss of 30–40% of striatal dopamine D1 and D2 receptors, which are localized on the GABAergic medium spiny projection neurons in the striatum (Andrews *et al.*, 1997; Hussey *et al.*, 1998). More evidence of metabolic dysfunction in Huntington's disease comes from proton nuclear magnetic resonance (^{1}H NMR) imaging studies which show increased lactate production in the basal ganglia and occipital cortex of Huntington's disease patients (Jenkins *et al.*, 1993, 1998). Notably, these lactate defects can be ameliorated by treatment with the metabolic cofactor coenzyme Q_{10} (Koroshetz *et al.*, 1997).

Biochemical studies in Huntington's disease postmortem tissue have revealed selective dysfunction of components of the oxidative phosphorylation pathway and the tricarboxylic acid (TCA) cycle in brain regions targeted in the disorder. Activities of complexes II-III and IV are markedly reduced in advanced grade Huntington's disease caudate and putamen, while enzyme activities are unaltered in other brain regions (Gu *et al.*, 1996; Browne *et al.*, 1997). Complex I activity is also reported to be impaired in muscle from Huntington's disease patients, but has not been shown to be affected in brain (Parker *et al.*, 1990; Browne *et al.*, 1997; Arenas *et al.*, 1998). Pyruvate dehydrogenase activity is decreased in Huntington's disease basal ganglia and hippocampus, while polarographic studies show that striatal oxygen consumption in Huntington's disease patients is lower than in age-matched controls (Butterworth *et al.*, 1985). The most profound enzyme defect seen in Huntington's disease to date is the dramatic reduction in activity of the TCA cycle enzyme aconitase in affected brain regions and muscle (> 70%; Tabrizi *et al.*, 1999). In addition, mitochondrial toxins, which inhibit succinate dehydrogenase in the TCA cycle and complex II (3-nitropropionic acid and malonate), induce selective striatal lesions in rodents and primates which closely resemble those seen in Huntington's disease (Beal *et al.*, 1993, 1994; Wullner *et al.*, 1994; Schulz *et al.*, 1996a,b). Mitochondrial abnormalities and metabolic defects are also features of other trinucleotide repeat disorders, including SCA1, SCA2, and SCA3, leading to the proposal that energetic dysfunction may play a common role in these disorders, and is directly linked to the polyglutamine defect (Matthew *et al.*, 1993; Mastrogiacomo and Kish, 1994; Mastrogiacomo *et al.*, 1994; Matsuishi *et al.*, 1996).

Further indirect evidence that energetic defects contribute to neurodegenerative processes in Huntington's disease is provided by findings that agents which enhance energy production in the brain exert neuroprotective effects. Preliminary studies in rodent mitochondrial toxin models, and NMR measurements of lactate production in man, suggest that coenzyme Q_{10} and creatine are neuroprotective, putatively via enhancing cerebral energy metabolism (Koroshetz *et al.*, 1997; Matthews *et al.*, 1998). Coenzyme Q_{10} also has potent antioxidant effects. Oral administration of coenzyme Q_{10} improves symptoms in some other mitochondrial-associated disorders including MELAS (mitochondrial myopathy, encephalopathy, lactic acidosis, and stroke-like episodes) and Kearns-Sayre syndrome (reducing cerebrospinal fluid, serum lactate and pyruvate levels, and enhancing mitochondrial enzyme activities in platelets) (Bresolin *et al.*, 1988; Ihara *et al.*, 1989). We recently showed that oral administration of coenzyme Q_{10} ameliorated elevated lactate levels seen in the cortex of Huntington's disease patients, an effect which was reversible on withdrawal of coenzyme Q_{10} (Koroshetz *et al.*, 1997). Furthermore, coenyme Q_{10} attenuates neurotoxicity induced by the mitochondrial toxins MPTP and malonate in animal models (Beal *et al.*, 1994; Schulz *et al.*, 1996b). An alternative strategy is to increase brain energy stores of the high-energy compound phosphocreatine by creatine administration. We recently showed that oral creatine administration in rats attenuates neurotoxicity induced by the succinate dehydrogenase inhibitor 3-NP (Matthews *et al.*, 1998). In addition, increases in cerebral lactate levels and decreases in levels of high-energy phosphate compounds seen in the striata of 3-NP treated rats were attenuated by pretreatment with creatine.

B. Oxidative Damage

Oxidative damage can affect cell viability directly, via oxidation of DNA and other neuronal macromolecules, or indirectly, for example by impairing mitochondrial energy metabolism (Schulz *et al.*, 1996b; Browne *et al.*, 1999a). Evidence for oxidative damage in Huntington's disease is steadily accumulating. Findings include increased incidence of DNA strand breaks, exacerbated lipofuscin accumulation (a marker of lipid peroxidation), elevated DNA oxidative damage products such as 8-hydroxydeoxyguanosine (OH8dG), and increased immunohistochemical staining of oxidative damage products in Huntington's disease striatum and cortex, including staining for 3-nitrotyrosine (a marker for peroxynitrite-

mediated protein nitration), malondialdehyde (marker for oxidative damage to lipids), heme oxygenase (formed during oxidative stress), and OH8dG (Goebel *et al.*, 1978; Tellez-Nagel *et al.*, 1995; Ferrante *et al.*, 1996; Browne *et al.*, 1997, 1999a).

A potential mechanism of mitochondrial dysfunction is via increased generation of free radicals and oxidants. Free radicals including superoxide ($O_2^{\cdot-}$) and hydroxyl radicals ($HO^{\cdot}$) are constantly produced as by-products of aerobic metabolism, but production increases under circumstances of electron transport chain inhibition or molecular defects (Schapira *et al.*, 1992). These agents can induce oxidative damage to cell macromolecules including DNA, proteins, and lipids by a number of different mechanisms, including DNA strand breaks or formation of DNA adducts (e.g., OH8dG), protein carbonylation, or lipid peroxidation. Potential functional consequences include perturbations in DNA transcription and translation, protein synthesis, enzyme activities, and membrane fluidity. Mitochondria are thought to be particularly vulnerable to oxidative injury since most intracellular free radicals are generated by the mitochondrial electron transport chain. Mitochondrial DNA is extremely susceptible due to its localization in the mitochondrial matrix, lack of protective histones, and limited repair mechanisms (Linnane *et al.*, 1989). Thus any increase in free radical production, for example due to impaired activity of a regulatory enzyme such as Cu/Zn SOD or glutathione peroxidase, could reduce the functional capacity of the respiratory transport chain. In addition, the tricarboxylic acid cycle enzyme aconitase, which is severely affected in Huntington's disease, is a prime target for free radical-mediated oxidative damage. The slow, progressive nature of neuronal injury in neurodegenerative disorders may be explained by cycling of free radicals and mitochondrial dysfunction. We have previously found increased levels of oxidative markers in both Huntington's disease and aminotrophic lateral sclerosis. Nuclear DNA OH8dG levels are significantly elevated in Huntington's disease caudate relative to controls (Browne *et al.*, 1997, 1999a). Further evidence supporting a role for oxidative damage in Huntington's disease is that the energetic defects seen in Huntington's disease brain are similar to those induced in cell culture by peroxynitrite, which preferentially inhibits complex II-III and (to a lesser extent) complex IV activity in the electron transport chain (Bolanos *et al.*, 1995).

VI. State of the Art Approaches: Animal Models Provide Insights into Disease Etiology

A. Mitochondrial Toxin Models

A role for mitochondrial energy metabolism dysfunction in the pathogenesis of neuronal degeneration in Huntington's disease is further supported by observations, in both humans and in experimental animals, that the basal ganglia neurons are particularly vulnerable to mitochondrial toxins. These include the complex II inhibitors 3-NP and malonate, AOAA (complex I), potassium cyanide, and sodium azide (complex IV) (Browne and Beal, 1994). Ingestion of 3-NP, an irreversible inhibitor of succinate dehydrogenase (complex II), produces selective basal ganglia lesions and delayed dystonia in humans (Ludolph *et al.*, 1990). Systemic administration of 3-NP to both rats and primates produces age-dependent striatal lesions which are strikingly similar to those seen in Huntington's disease (Brouillet *et al.*, 1993, 1995). In primates, chronic 3-NP administration produces selective striatal lesions which spare NADPH-d neurons, and induce proliferative changes in the dendrites of spiny neurons. Animals also show both spontaneous and apomorphine-inducible movement disorders resembling Huntington's disease (Brouillet *et al.*, 1995). 3-NP basal ganglia lesions in rats are associated with elevated lactate levels, similar to the increased lactate production seen in Huntington's disease patients (Jenkins *et al.*, 1993). 3-NP lesions can be prevented by prior removal of glutamatergic excitatory corticostriatal inputs by decortication, by glutamate release inhibitors, and by glutmate receptor antagonists, suggesting that 3-NP toxicity is mediated by secondary excitotoxic mechanisms (Beal, 1994a; Schulz *et al.*, 1996b).

Intrastriatal injection of either malonate or 3-NP in rats is also associated with increased oxidative damage. We found that the rate of hydroxyl free radical production is elevated in the striatum, as detected by microdialysis (Schulz *et al.*, 1996a). Increased OH^8dG levels in striatum are also detected following systemic 3-NP administration, and elevated 3-nitrotyrosine concentrations are reported after either systemic 3-NP or intrastriatal malonate injection. Further, the finding that 3-NP-induced lesions and concomitant increases in oxidative damage markers were markedly attenuated in mice overexpressing the superoxide free radical scavenger Cu/Zn superoxide dismutase (SOD1) implies that oxidative free radicals contribute to lesion formation (Beal *et al.*, 1995). Furthermore, malonate and 3-NP striatal lesions were attenuated by free radical spin traps and NOS inhibitors. Inhibition of nitric oxide (NO) generation in mice lacking the gene for the neuronal isoform of NOS (nNOS) also resulted in reduced volume of malonate lesions (Schulz *et al.*, 1996b). Hence there is substantial evidence that nitric oxide-mediated oxidative damage is involved in cell death processes following energetic disruption in these models.

B. Transgenic Mouse Models of Huntington's Disease

One of the major drawbacks of relying on human tissue for asessment of neurological disease progression is the inability to adequately map early events in the disease etiology. Substantial evidence of a causative role in the disorder would be provided by evidence of occurrence prior to symptoms and pathology in models of Huntington's disease. Over the past few years, the development of methodology to generate transgenic mouse lines expressing the physiological phenotypes associated with human gene mutations has provided much needed *in vivo* models to circumvent many of these issues. A number of different groups have developed several different transgenic and "knock-in" mouse models of Huntington's disease, which vary in terms of the transgene incorporation technique employed. As a result, mouse phenotypes vary between lines, the features manifested by the animals depending on the nature of the transgene incorporated (i.e., full-length human mutant huntingtin, or a huntingtin *HD* gene fragment incorporating the mutant region in exon 1, or merely an expansion

inserted into the murine *HD* homolog *Hdh*); CAG repeat length; copy number of the mutant gene incorporated; promoter used, and hence cellular specificity of expression; background strains; and expression levels of the mutant gene. The different mouse lines reported to date are discussed below and listed in Table 49.1, which compares the salient features of each of the models.

1. Transgenic Mice Expressing Full-Length Human Mutant Huntingtin

The *HD89* and YAC72 mice discussed below represent two of the most useful transgenic mouse lines developed to date. Their utility is encumbent on the fact that disease-length huntingtin mutations are expressed in the context of the human

TABLE 49.1 Characteristics of Transgenic and Knock-in Mouse Models Expressing the Huntington Disease Mutation

Mutant mouse lines	Background strain	Promoter	Insert	CAG repeat	Symptom onset (weeks)	NII onset (weeks)	Neuronal loss (at end stage)	Life span (weeks)
HD[a]								
HD16 (Wt)	FVB/N	CMV	Full-length	16+/− (A–E)	None	None	None	Normal
HD48			*HD* cDNA,	48 +/− (B,D)	8	12	Stri, CTX >	29–31
HD89			2–22 copies	48 +/− (C)	25	Stri, CTX,	Thal, Hip	29–31
				89 +/− (A–C)	8	Thal, Hip,	(Not 48C)	29–31
				48B +/+	0–8	CBL		21–23
				89A +/+	0–8			21–23
YAC[b]								
YAC18 (Wt)	FVB/N	Constitutive	Full-length	18	None	None	None	Normal
YAC46			*HD* DNA,	46	42	None	None	N/D
YAC72			1–2 copies	72 (2511 line)	26	None	Stri[j]	N/D
Hdh Knock-in[c]								
Hdh^{Q7} (Wt)	C57B16/J	Murine	Full length	7	None	None	None	Normal
Hdh^{Q50}		endogenous	mouse *Hdh*,	48	None	None	None	Normal
Hdh^{Q92}			CAG insert	90	16	60	None	Normal
Hdh^{Q111}				109		16	None	Normal
CAG Knock-in[d]								
CAG 71	C57B16/J	Constitutive	Mouse *Hdh*	71	12	None	None	N/D
CAG 94			−100 bp,	94	8	None	None	N/D
			CAG insert					
Hdh4/6 Knock-in[e]								
Hdh 6/Q72	RF8	Constitutive	Full length	72	12	None	None	N/D
Hdh 4/Q80	JM-1		mouse *Hdh*,	80	12	None	None	N/D
			CAG insert					
N171[f]								
N171-18Q (Wt)	C57B16/C3	Mouse prion	N-terminal	18	None	None	None	Normal
N171-44Q		protein	truncated	44	None	None	None	Normal
N171-82Q			*HD* cDNA,	82	14	21–26	Some; CTX,	21–26
			171 aa				Stri, Hip, CBL	
L63[g]								
L63-46	SJL/B6	Rat NSE	N-terminal	46	12+	N/D	None	N/D
L63-100			fragment,	100	12	CTX, Stri	Stri	N/D
			epitope tag					
R6[h]								
Hdex6 (Wt)	C57B16/CBA	Constitutive	1.9-kb *HD*	18	None	None	None	Normal
Hdex27 (Wt)			DNA	18	None	None	None	Normal
R6/0			fragment	142	None	None	None	Normal
R6/1				113	16–20	Yes	Atrophy/loss?	
R6/2				144	8	3.5	Atrophy/loss?	17–25
R6/5				128–156 +/+	36	Yes	Atrophy/loss?	
				128–156 +/−	None	None	None	Normal
Tet-Off[i]								
		CamKII	Full length		Tet-on	Yes, reversible	Atrophy/loss?	N/D
			mouse *Hdh*,					
			CAG insert					

Note. The models listed reflect those reported by February 2000. CBL, cerebellum; CTX, neocortex; Hip, hippocampus; N/D, not determined to date; NII, neuronal intranuclear inclusions; Stri, striatum; Tet, tetracyclin; Thal, thalamus; wks, weeks of age; Wt, wild type.
[j]Evident in striatal medium spiny neurons by 52 weeks of age.

full-length gene inserted into the mouse genome, rather than just a gene fragment. In contrast to some other putative Huntington's disease models (such as the *Hdh* knock-in mice and R6/2 mice), animals develop region-specific neuronal degeneration over their life span, which provides a suitable context for measuring the efficacy of potential neuroprotective agents.

a. HD48 *and* HD89 *Mice.* Tagle and colleagues generated mice expressing 16 (wild type), 48, and 89 glutamines from full-length human huntingtin cDNA constructs. Using the human promoter, huntingtin expression is widespread throughout the brain and periphery. In these mice, copy number of the gene incorporated varied from two to six in mutant CAG lines. Both 48 and 89 CAG repeat mice showed motor deficits from an early age, developing foot clasping and stereotypic hyperkinetic activity, followed by hypokinesis and locomotor deterioration. Mice die prematurely (24–32 weeks). By about 24 weeks of age marked neuronal cell loss and astrogliosis is evident in the striata of both *HD48* and *HD89* mice, but few neuronal intranuclear inclusions occur. The lack of a distinct correlation between CAG repeat number and disease progression is thought to be associated with the levels of expression in each of the mouse lines, which vary from approximately endogenous levels in 89/89 mice to fivefold higher in 48/48 mice (Reddy *et al.*, 1998).

b. YAC HD T*g* *Mice.* Hodgson *et al.* (1999) used yeast artificial chromosome (YAC) technology to generate transgenic mice expressing normal (YAC18: 18 glutamines) and mutant huntingtin (YAC46 and 72: 46 and 72 glutamines, respectively). Mutations are expressed in the context of full-length huntingtin protein. By 12 months of age YAC72 mice have a selective degeneration of medium spiny neurons in the lateral striatum (similar to the selective cell death seen in Huntington's disease patients). Neurodegeneration seems to require nuclear translocation of N-terminal huntingtin fragments, but not neuronal intranuclear inclusion formation. Both YAC46 and YAC72 develop progressive electrophysiological abnormalities at approximately 7 months of age that precede nuclear translocation of huntingtin and cell death. Behavioral changes are manifest in YAC72 mice at 7 months of age.

2. "Knock-in" Mice Expressing Full-Length Huntingtin

"Knock-in" mice arguably represent an excellent model system for investigating the effects of the huntingtin mutation, since the mutation is expressed in the context of the full-length murine huntingtin analog, *Hdh*. Hence, the system uses the endogenous promoter to produce protein at normal murine expression levels, so any differences between animals may be attributed to different polyglutamine repeat lengths. In reality their utility is confounded to some extent by the fact that they do not develop overt, quantifiable, neurodegenerative, or behavioral changes over the animals' life spans. However, as discussed below, there is some evidence of cellular dysfunction associated with the CAG expansion in these models which may be useful as testable parameters for investigating disease mechanisms.

The reason for the lack of neuropathological features of Huntington's disease in these models is thought to result from the combination of low expression levels of the gene and the short life span of mice. In support of this hypothesis, HD48 mice, which do show selective cell death, neuronal intranuclear inclusion, cytoplasmic inclusion formation, and motor disturbances, express up to 5 × wild-type endogenous levels of full-length huntingtin protein (Reddy *et al.*, 1998). However, in the knock-in lines only endogenous murine levels of huntingtin are expressed. Also, the CAG repeat number required to confer toxicity in mice seems to be longer than in humans, perhaps reflecting the short life span of the animals.

a. H*dh knock-in* *Mice.* White *et al.* (1997) developed a mouse model of Huntington's disease by extending the polyglutamine tract of the murine homolog (*Hdh*) of the human huntingtin gene (*HD*). CAG repeats from an *HD* chromosome were inserted into the appropriate position in *Hdh* exon 1, altering the mouse *HD* homolog to encode huntingtin protein with 50, 92, or 111 glutamine residues, instead of the 7 normally found in the mouse protein. The transgene has the endogenous promoter, and mice express wild-type levels of huntingtin protein. Mice homozygous for mutant huntingtin do not exhibit any behavioral symptomatology up to 18 months of age. However, recent observations have shown CAG length-dependent translocation of huntingtin protein from cytosol to the nucleus, and eventual neuronal intranuclear inclusion formation in Hdh^{Q92} and Hdh^{Q111} mice (Wheeler *et al.*, 2000). Although there is no evidence of selective cellular pathology in any of these mouse lines yet, we have found that cerebral glucose metabolism and mitochondrial enzyme activities are impaired in Hdh^{Q92} mice at 4 months of age (Browne *et al.*, 1999b, and unpublished observations). This corresponds with a time point preceding neuronal intranuclear inclusion formation in these mice, and may be indicative of early bioenergetic changes associated with the huntingtin mutation (Fig. 49.2, see color insert).

b. CAG71 *and* CAG94 *Mice.* Similar to the technique in *Hdh* mice, the endogenous murine *Hdh* gene was modified by replacing a portion of mouse exon 1 and the adjacent intron with a human sequence containing an expanded CAG repeat region (71 or 94) from a juvenile Huntington's disease lymphoblastoid cell line (Levine *et al.*, 1999). Although no overt cell loss has been reported to date in this model, there is evidence of neuronal dysfunction in CAG94 knock-ins, which showed an increased sensitivity of cortical and striatal cells to *N*-methyl-D-aspartate (NMDA) receptor activation. In contrast, mice expressing fewer glutamines (94) CAG71 knock-ins were less affected than CAG94 knock-ins, showing NMDA responses similar to littermate controls. No cerebral neuronal intranuclear inclusions have been detected in either mouse line.

c. H*dh*4/Q80 *and* H*dh*6/Q72 *Mice.* Another knock-in Huntington's disease model was generated by Shelbourne and colleagues (1999). They inserted an expanded CAG repeat (72–80) into the murine *Hdh* by homologous recombination and generated two heterozygous knock-in lines, *Hdh4/Q80* and *Hdh6/Q72*. These mice do not develop any neuropathological abnormalities at the cellular level by 17 months of age, but do exhibit a 10–15% reduction in brain size, which is evident by 4 months of age. Neuronal intranuclear inclusions have not been

seen in either line to date, but mice do display an abnormal behavioral phenotype, in the form of chronically increased aggressive behavior toward other mice from about 3 months of age, which is more prevalent in males than in females. There is also evidence of reduced long-term potentiation in hippocampal neurons (Usdin *et al.*, 1999), which the authors suggest reflects the cognitive impairments seen at an early stage in Huntington's disease.

3. Transgenic Mice Expressing Human Mutant Huntingtin Fragments

a. N171 HD *Mice.* N171 transgenic mice express a truncated portion of Huntington's disease cDNA, consisting of 171 amino acids from the N-terminal, with an expanded glutamine repeat of 44 or 82 (N171-44Q and N171-82Q). Wild-type N171-18Q express 18 glutamines (Schilling *et al.*, 1999). N171-82Q mice display a phenotype of uncoordination, ataxia, and weight loss with onset at approximately 3–4 months, and die prematurely at about 6 months of age. On pathologic examination brains show neuronal intranuclear inclusions when labeled with antibodies to ubiquitin or the N-terminal of huntingtin protein and evidence of neuronal degeneration in the striatum.

b. L63 HD *Mice.* The L63 mouse line express a FLAG–huntingtin cDNA fusion protein consisting of the first 3221 huntingtin bases from the N-terminal, with 46 or 100 glutamines (Laforet *et al.*, 1998). Motor defects and approximately 20% loss of striatal neuron occur in most mice with 100 CAGs by 6 months of age. Low levels of neuronal intranuclear inclusions are also seen in striatum by 6 months (Laforet *et al.*, 1998; Aronin *et al.*, 1999).

c. R6 HD *Mice.* The R6 mouse lines were the first Huntington's disease transgenic mice developed and are therefore the best characterized to date. Importantly, it was the development of this model which led to the identification of neuronal intranuclear inclusion formation in the disease paradigm. The R6 mouse lines are transgenic for a fragment of the human *HD* gene, containing 1 kb of the *HD* promoter region and exon 1 containing the abnormal CAG repeat expansion and 262 bp of intron 1 (Mangiarini *et al.*, 1996). The R6/2 line expressing 144 CAGs is the most studied to date, since these animals develop a rapidly progressing neurological phenotype reminiscent of Huntington's disease, before dying prematurely at 17–22 weeks of age. The first motor symptoms occur at about 8 weeks of age, but are preceded by neuronal intranuclear inclusion deposition throughout the brain by 3.5 weeks of age (although it may occur even earlier) (Davies *et al.*, 1997). The motor disorder includes abnormal gait, a resting tremor, abrupt shuddering movements, and stereotypic grooming. However, some features of the disease phenotype do not bear much resemblance to the human disease, including the propensity for seizures in these animals, the lack of overt striatal-specific cell death, and the development of diabetes (Mangiarini *et al.*, 1996; Davies *et al.*, 1997; Hughes *et al.*, 1999; Hurlbert *et al.*, 1999; Sathasivam *et al.*, 1999). Neurotransmitter and receptor abnormalities also occur in R6/2 mice, including dopamine D1 and D2 receptor loss by 8 weeks of age, and alterations in levels of the glutamatergic mGluR1, mGluR2, mGluR3, and mGluR5 metabotropic receptors by 12 weeks of age (Cha *et al.*, 1998). Further, *in situ* studies revealed that D1 and mGluR receptor mRNA is abnormal by as early as 4 weeks of age, preceding the onset of symptoms in these animals. However, contrary to the picture in Huntington's disease brain, GABAergic and NMDA receptor binding levels are not altered in these animals, although AMPA and kainate receptors show some downregulation (Cha *et al.*, 1998). Similarly, neurotransmitter changes do not bear close resemblance to the pattern seen in Huntington's disease. For instance, Reynolds *et al.* (1999) report that striatal GABA levels are unaltered in symptomatic 12-week-old mice, although a slight decrease was observed in the cerebellum. Further, levels of serotonin and 5-hydroxyindoleacetic acid (5-HIAA) are reduced in all brain regions of R6/2 mice, while noradrenaline is decreased in the hippocampus. In contrast, dopamine levels in the striatum are reduced in aged animals, consistent with changes seen in Huntington's disease brain.

As discussed earlier, metabolic defects prior to disease onset are also typical of Huntington's disease. In the R6/2 mouse line, Tabrizi *et al.* (2000) reported that complex II-III and aconitase activities are impaired in the brains of 12-week-old R6/2 Huntington's disease transgenic mouse brains, but these alterations do not precede the onset of the behavioral phenotype and neuronal intranuclear inclusion deposition (S. E. Browne and M. F. Beal, unpublished observations). However, at 12 weeks of age R6/2 mice show an increased vulnerability to metabolic stress, as demonstrated by increased free radical generation and lesion size in response to a 3-NP toxic insult (Bogdanov *et al.*, 1998). Further, we have recently found that treatment of R6/2 mice with creatine, administered in feed from the time of weaning, significantly increases survival and delays brain atrophy, striatal neuron atrophy, and the formation of nuclear inclusions (Ferrante *et al.*, 2000). In addition, prevention of huntingtin cleavage by caspase inhibitors has recently been shown to delay phenotype onset and animal death in this mouse model (Ona *et al.*, 1999).

4. "Inducible" Transgenic Mice Transiently Expressing Mutant Huntingtin

Perhaps the most exciting development in the past few years is the generation of a reversible Huntington's disease mouse model, which incorporates a "tet off" system to modulate expression of the huntingtin gene mutation (Yamamoto *et al.*, 2000). The expression promoter is α-CamKII, which facilitates high levels of expression in the forebrain. Mutant gene expression is under the regulation of a tetracyclin binding sequence, bi-TetO, linked to galactosidase, and then to exon 1 of mutant huntingtin containing an expanded CAG repeat. Tetracyclin binding switches huntingtin transcription off. Yamamoto and colleagues raised mice up to 18 weeks of age in the absence of tetracyclin. Animals developed a severe, progressive motor phenotype, characterized by tremor and foot clasping. Galactosidase staining showed that mutant huntingtin was widely expressed throughout the forebrain in homozygous gene-positive mice, as well as the striatum, hippocampus, hypothalamus, septum, and neocortex. No immunoreactivity was detectable in heterozygote mice. The animals also developed neuronal intra-

nuclear inclusions in all gal-positive regions, but neuronal intranuclear inclusion deposition was limited to brain regions where mutant huntingtin was expressed. Mice went on to develop striatal atrophy, gliosis, and reduced D1 and D2 receptor binding densities in the striatum, indicative of GABAergic cell loss or dysfunction. Most interestingly, all of these parameters of neuronal dysfunction could be reversed, to some extent, by effectively switching expression of the transgene off by treating the animals with the tetracycline analog doxycycline. Animals treated for 4 months showed a marked reduction in the number of neuronal intranuclear inclusions in the striatum and neocortex and partial recovery of striatal atrophy and D1 and D2 binding levels, suggesting that there may be a therapeutic window for disease treatment in postsymptomatic patients. This breakthrough development opens up a plethora of opportunities to observe the consequences of manipulating huntingtin gene expression and to test potential therapeutic strategies.

VII. Conclusions

Although the pathogenic mechanism in Huntington's disease does not seem to be directly linked to the formation of intranuclear huntingtin inclusions, there is an association between the cell death process and CAG repeat length in mutant huntingtin. This is well demonstrated by the observation that incorporation of an expanded CAG repeat stretch (146 CAGs) into a murine gene normally lacking CAG repeats, the hypoxanthine phosphoribosyltransferase gene (*hprt*), resulted in a mouse phenotype reminiscent of other human CAG repeat disorders (JO1 mice, Ordway *et al.*, 1997). Mice develop a progressive neurological phenotype consisting of a late-onset resting tremor, ataxia, decreased open field motor activity, propensity to fall from the rotarod, foot clasping, some incidence of seizures, and premature death at approximately 42–53 weeks of age. CAG length-dependence of these traits was verified by the observations that mice expressing 70 CAG repeats in the *hprt* gene did not develop a behavioral phenotype by 35 weeks of age, whereas the first behavioral symptoms are evident by 12 weeks in JO1 mice (Ordway *et al.*, 1997). A great deal of conjecture now surrounds the question of whether translocation of huntingtin protein into the nucleus, with or without aggregate formation, is an essential step in the pathogenic process in Huntington's disease. Several groups have suggested that huntingtin translocation into the nucleus precedes cell pathology (Saudou *et al.*, 1998; Hackam *et al.*, 1999; Hodgson *et al.*, 1999; Wheeler *et al.*, 1999). Interestingly, in another polyglutamine disease ataxin-1 movement into the nucleus has been shown to be a prerequisite for pathogenesis, and has been associated with gene downregulation in SCA-1 transgenic mice (Lin *et al.*, 2000).

Whereas the definitive pathway underlying cell death in Huntington's disease is yet to be determined, the development and characterization of transgenic and knock-in mouse models of the disorder can only help achieve this goal. In the meantime, it is heartening that initial studies of metabolic enhancers and caspase inhibitors are showing some degree of efficacy in delaying disease onset and extending survival in animal models of the disease.

References

Aeschlimann, D., and Paulsson, M. (1994). Transglutaminases: Protein cross-linking enzymes in tissues and body fluids. *Thromb. Haemostasis* **71**, 402–415.

Albin, R. L., and Greenamyre, J. T. (1992). Alternative excitotoxic hypotheses. *Neurology* **42**, 733–738.

Albin, R. L., Young, A. B., and Penney, J. B. (1989). The functional anatomy of basal ganglia disorders. *Trends Neurosci.* **12**, 366–375.

Albin, R. L., Reiner, A., Anderson, K. D., Penney, J. B., and Young, A. B. (1990). Striatal and nigral neuron subpopulations in rigid Huntington's disease: Implications for the functional anatomy of chorea and rigidity-akinesia. *Ann. Neurol.* **27**, 357–365.

Alexander, G. E., and Crutcher, M. D. (1990). Functional architecture of basal ganglia circuits: Neural substrates of parallel processing. *Trends Neurosci.* **13**, 266–271.

Andrew, S. E., Goldberg, Y. P., Kremer, B., Telenius, H., Theilmann, J., Adam, S., Starr, E., Squitieri, F., Lin, B., Kalchman, M. A. *et al.* (1993). The relationship between trinucleotide (CAG) repeat length and clinical features of Huntington's disease. *Nat. Genet.* **4**, 398–403.

Andrews, T. C., and Brooks, D. J. (1998). Advances in the understanding of early Huntington's disease using the functional imaging techniques of PET and SPET. *Mol. Med. Today* **4**, 532–539.

Andrews, T. C., Weeks, R. A., and Brooks, D. J. (1997). [^{11}C]Raclopride and [^{11}C]SCH 23390 PET and the unified Huntington's disease rating scale can be used to monitor disease progression in asymptomatic Huntington's disease gene carriers. *Soc. Neurosci. Abstr.* **23**, 1912.

Antonini, A., Leenders, K. L., Spiegel, R., Meier, D., Vontobel, P., Weigell-Weber, M., Sanchez-Pernaute, R., de Yebenez, J. G., Boesiger, P., Weindl, A., and Maguire, R. P. (1996). Striatal glucose metabolism and dopamine D2 receptor binding in asymptomatic gene carriers and patients. *Brain* **119**, 2085–2095.

Arenas, J., Campos, Y., Ribacoba, R., Martin, M. A., Rubio, J. C., Ablanedo, P., and Cabello, A. (1998). Complex I defect in muscle from patients with Huntington's disease. *Ann. Neurol.* **43**, 397–400.

Aronin, N., Kim, M., Laforet, G., and DiFiglia, M. (1999). Are there multiple pathways in the pathogenesis of Huntington's disease? *Philos. Trans. R. Soc. London* **354**, 995–1003.

Bao, J., Sharp, A. H., Wagster, M. V., Becher, M., Schilling, G., Ross, C. A., Dawson, V. L., and Dawson, T. M. (1996). Expansion of polyglutamine repeat in huntingtin leads to abnormal protein interactions involving calmodulin. *Proc. Natl. Acad. Sci. U.S A.* **93**, 5037–5042.

Beal, M. F. (1994a). Huntington's disease, energy, and excitotoxicity. *Neurobiol. Aging.* **15**, 275–276.

Beal, M. F. (1994b). Neurochemistry and toxin models in Huntington's disease. *Curr. Opin. Neurol.* **7**, 542–547.

Beal, M. F. (1996). Mitochondria, free radicals, and neurodegeneration. *Curr. Opin. Neurobiol.* **6**, 661–666.

Beal, M. F., Ellison, D. W., Mazurek, M. F., Swartz, K. J., Malloy, J. R., Bird, E. D., and Martin, J. B. (1988). A detailed examination of substance P in pathologically graded cases of Huntington's disease. *J. Neurol. Sci.* **84**, 51–61.

Beal, M. F., Brouillet, E., Jenkins, B. G., Ferrante, R. J., Kowall, N. W., Miller, J. M., Storey, E., Srivastava, R., Rosen, B. R., and Hyman, B. T. (1993). Neurochemical and histologic characterization of excitotoxic lesions produced by mitochondrial toxin 3-nitropropionic acid. *J. Neurosci.* **13**, 4181–4192.

Beal, M, F., Henshaw, D, R., Jenkins, B. G., Rosen, B. R., and Schulz, J. B. (1994). Coenzyme Q_{10} and nicotinamide block striatal lesions produced by the mitochondrial toxin malonate. *Ann. Neurol.* **36**, 882–888.

Beal, M. F., Ferrante, R. J., Henshaw, R., Matthews, R. T., Chan, P. H., Kowall, N. W., Epstein, C. J., and Schulz, J. B. (1995). 3-Nitropropionic acid neurotoxicity is attenuated in copper/zinc superoxide dismutase transgenic mice. *J. Neurochem.* **65**, 919–922.

Berent, S., Giordani, B., Lehtinen, S., Markel, D., Penney, J. B., Buchtel, H. A., Starosta-Rubinstein, S., Hichwa, R., and Young, A. B. (1988). Positron emission tomographic scan investigations of Huntington's disease: Cerebral metabolic correlates. *Ann. Neurol.* **23**, 541–546.

Bertaux, F., Sharp, A. H., Ross, C. A., Lehrach, H., Bates, G. P., and Wanker, E. (1998). HAP1-huntingtin interactions do not contribute to the molecular pathology in Huntington's disease transgenic mice. *FEBS Lett.* **426**, 229–232.

Bogdanov, M. B., Ferrante, R. J., Kuemmerle, S., Klivenyi, P., and Beal, M. F. (1998). Increased vulnerability to 3-nitropropionic acid in an animal model of Huntington's disease. *J. Neurochem.* **71**, 2642–2644.

Bolanos, J. P., Heales, S. J. R., Land, J. M., and Clark, J. B. (1995). Effect of peroxynitrite on the mitochondrial respiratory chain: Differential susceptibility of neurones and astrocytes in primary culture. *J. Neurochem.* **64**, 1965–1972.

Braak, H., and Braak, E. (1992). Allocortical involvement in Huntington's disease. *Neuropathol. Appl. Neurobiol.* **18**, 539–547.

Bresolin, N., Bet, L., Binda, A., Moggio, M., Comi, G., Nador, F., Ferrante, C., Carenzi, A., and Scarlato, G. (1988). Clinical and biochemical correlations in mitochondrial myopathies treated with coenzyme Q_{10}. *Neurology* **38**, 892–899.

Brouillet, E. P., Jekins, B. G., Hyman, B. T., Ferrante, R. J., Kowall, N. W., Srivastava, R., Samanta-Roy, D., Rosen, B. R., and Beal, M. F. (1993). Age-dependent vulnerability of the striatum to the mitochondrial toxin 3-nitropropionic acid. *J. Neurochem.* **60**, 356–359.

Brouillet, E., Hantraye, P., Ferrante, R. J., Dolan, R., Leroy-Willig, A., Kowall, N. W., and Beal, M. F. (1995). Chronic mitochondrial energy impairment produces selective striatal degeneration and abnormal choreiform movements in primates. *Proc. Natl. Acad. Sci. U.S. A.* **92**, 7105–7109.

Browne, S. E., and Beal, M. F. (1994). Oxidative damage and mitochondrial dysfunction in neurodegenerative diseases. *Biochem. Soc. Trans.* **22**, 1002–1006.

Browne, S. E., Bowling, A. C., MacGarvey, U., Baik, M. J., Berger, S. C., Muqit, M. M. K., Bird, E. D., and Beal, M. F. (1997). Oxidative damage and metabolic dysfunction in Huntington's disease: Selective vulnerability of the basal ganglia. *Ann. Neurol.* **41**, 646–653.

Browne, S. E., Ferrante, R. J., and Beal, M. F. (1999a). Oxidative stress in Huntington's disease. *Brain Pathol.* **9**, 147–163.

Browne, S. E., Wheeler, V., White, J. K., Fuller, S. W., MacDonald, M., and Beal, M. F. (1999b). Dose-dependent alterations in local cerebral glucose use associated with the huntingtin mutation in *Hdh* CAG knock-in transgenic mice. *Soc. Neurosci. Abstr.* **25**, 218.11.

Burke, J. R., Enghild, J. J., Martin, M. E., Jou, Y.-S., Myers, R. M., Roses, A. D., Vance, V. M., and Strittmatter, W. J. (1996). Huntingtin and DRPLA proteins selectively interact with the enzyme GAPDH. *Nat. Med.* **2**, 347–350.

Butterworth, J., Yates, C. M., and Reynolds, G. P. (1985). Distribution of phosphate-activated glutaminase, succinic dehydrogenase, pyruvate dehydrogenase, and γ-glutamyl transpeptidase in post-mortem brain from Huntington's disease and agonal cases. *J. Neurol. Sci.* **67**, 161–171.

Butterworth, N. J., Williams, L., Bullock, J. Y., Love, D. R., Faull, R. L., and Dragunow, M. (1998). Trinucleotide (CAG) repeat length is positively correlated with the degree of DNA fragmentation in Huntington's disease striatum. *Neuroscience* **87**, 49–53.

Cha, J. H., Kosinski, C. M., Kerner, J. A., Alsdorf, S. A., Mangiarini, L., Davies, S. W., Penney, J. B., Bates, G. P., and Young, A. B. (1998). Altered brain neurotransmitter receptors in transgenic mice expressing a portion of an abnormal human Huntington disease gene. *Proc. Natl. Acad. Sci. U. S. A.* **95**, 6480–6485.

Cooper, A. J. L., Sheu, K.-F. R., Burke, J. R., Onodera, O., Strittmatter, W. J., Roses, A. D., and Blass, J. P. (1997a). Transglutaminase-catalyzed inactivation of glyceraldehyde 3-phosphate dehydrogenase and α-ketoglutarate dehydrogenase complex by polyglutamine domains of pathological length. *Proc. Natl. Acad. Sci. U. S. A.* **94**, 12604–12609.

Cooper, A. J., Sheu, K. -F. R., Burke, J.R., Onodera, O., Strittmatter, W. J., Roses, A. D., and Blass, J. P. (1997b). Polyglutamine domains are substrates of tissue transglutaminase: Does transglutaminase play a role in expanded CAG/poly-Q neurodegenerative diseases? *J. Neurochem.* **69**, 431–434.

Cooper, A. J., Sheu, K. F., Burke, J. R., Strittmatter, W. J., and Blass, J. P. (1998). Glyceraldehyde 3-phosphate dehydrogenase abnormality in metabolically stressed Huntington disease fibroblasts. *Dev. Neurosci.* **20**, 462–468.

Cooper, A. J., Sheu, K. F., Burke, J. R., Strittmatter, W. J., Gentile, V., Peluso, G., and Blass, J. P. (1999). Pathogenesis of inclusion bodies in (CAG)n/Qn-expansion diseases with special reference to the role of tissue transglutaminase and to selective vulnerability. *J. Neurochem.* **72**, 889–899.

Cummings, C. J., Mancini, M. A., Antalffy, B., DeFranco, D. B., Orr, H. T., and Zoghbi, H. Y. (1998). Chaperone suppression of aggregation and altered subcellular proteasome localization imply protein misfolding in SCA1. *Nat. Genet.* **19**, 148–154.

Cummings, C. J., Reinstein, E., Sun, Y., Antalffy, B., Jiang, Y., Ciechanover, A., Orr, H. T., Beaudet, A. L., and Zoghbi, H. Y. (1999). Mutation of the E6-AP ubiquitin ligase reduces nuclear inclusion frequency while accelerating polyglutamine-induced pathology in SCA1 mice. *Neuron* **24**, 879–892.

Davies, S. W., Turmaine, M., Cozens, B., DiFiglia, M., Sharp, A., Ross, C. A., Scherzinger, E., Wanker, E. E., Mangiarini, L., and Bates, G. (1997). Formation of neuronal intranuclear inclusions (NII) underlies the neurological dysfunction in mice transgenic for the HD mutation. *Cell (Cambridge, Mass.)* **90**, 537–548.

DiFiglia, M., Sapp, E., Chase, K., Schwarz, C., Meloni, A., Young, C., Martin, E., Vonsattel, J. -P., Carraway, R., Reeves, S. A., Boyce, F. M., and Aronin, N. (1995). Huntingtin is a cytoplasmic protein associated with vesicles in human and rat brain neurons. *Neuron* **14**, 1075–1081.

DiFiglia, M., Sapp, E., Chase, K. O., Davies, S. W., Bates, G. P., Vonsattel, J. -P., and Aronin, N. (1997). Aggregation of huntingtin in neuronal intranuclear inclusions and dystrophic neurites in brain. *Science* **277**, 1990–1993.

Durr, A., Hahn-Barma, V., Brice, A., Pecheux, C., Dode, C., and Feingold, J. (1999). Homozygosity in Huntington's disease. *J. Med. Genet.* **36**, 172–173.

Duyao, M., Ambrose, C., Myers, R., Novelletto, A., Persichetti, F., Frontali, M., Folstein, S., Ross, C., Franz, M., Abbott, M. *et al.* (1993). Trinucleotide repeat length instability and age of onset in Huntington's disease. *Nat. Genet.* **4**, 387–392.

Duyao, M. P., Auerbach, A. B., Persichetti, F., Barnes, G. T., McNeil, S. M., Ge, P., Vonsattel, J.-P., Gusella, J. F., Joyner, A. L., and MacDonald, M. E. (1995). Inactivation of the mouse Huntington's disease gene homolog *Hdh*. *Science* **269**, 407–410.

Ferrante, R. J., Kowall, N. W., Beal, M. F., Martin, J. B., Bird, E. D., and Richardson, E. P. (1987). Morphologic and histochemical characteristics of a spared subset of striatal neurons in Huntington's disease. *J. Neuropathol. Exp. Neurol.* **46**, 12–27.

Ferrante, R. J., Kowall, N. W., Hersch, S. M., Brown, R. H., and Beal, M. F. (1996). Immunohistochemical localization of markers of oxidative injury in Huntington's disease. *Soc. Neurosci. Abstr.* **22**, 92.5.

Ferrante, R. J., Gutekunst, C. A., Persichetti, F., McNeil, S. M., Kowall, N. W., Gusella, J. F., MacDonald, M. E., Beal, M. F., and Hersch, S. M. (1997). Heterogeneous topographic and cellular distribution of huntingtin expression in the normal human neostriatum. *J. Neurosci.* **17**, 3052–3063.

Ferrante, R. J., Andreassen, O. A., Dedeoglu, A., Kuemmerle, S., Kubilus, J. K., Kaddurah-Daouk, R., Hersch, S. M., and Beal, M. F. (2000). Neuroprotective effects of creatine in a transgenic mouse model of Huntington's disease. *J. Neurosci.* (in press).

Furtado, S., Suchowersky, O., Rewcastle, B., Graham, L., Klimek, M. L., and Garber, A. (1996). Relationship between trinucleotide repeats and neuropathological changes in Huntington's disease. *Ann. Neurol.* **39**, 132–136.

Fusco, F. R., Chen, Q., Lamoreaux, W. J., Figueredo-Cardenas, G., Jiao, Y., Coffman, J. A., Surmeier, D. J., Honig, M. G., Carlock, L. R., and Reiner, A. (1999). Cellular localization of huntingtin in striatal and cortical neurons in rats: Lack of correlation with neuronal vulnerability in Huntington's disease. *J. Neurosci.* **19**, 1189–1202.

Goebel, H. H., Heipertz, R., Scholz, W., Iqbal, K., and Tellez-Nagel, I. (1978). Juvenile Huntington chorea: Clinical, ultrastructural, and biochemical studies. *Neurology* **28**, 23–31.

Grafton, S. T., Mazziotta, J. C., Pahl, J. J., St. George-Hyslop, P., Haines, J. L., Gusella, J., Hoffman, J. M., Baxter, L. R., and Phelps, M. E. (1992). Serial changes of cerebral glucose metabolism and caudate size in persons at risk for Huntington's disease. *Arch. Neurol. (Chicago)* **49**, 1161–1167.

Graybiel, A. M., Aosaki, T., Flaherty, A. W., and Kimura, M. (1994). The basal ganglia and adaptive motor control. *Science* **265**, 1826–1831.

Gu, M., Gash, M. T., Mann, V. M., Javoy-Agid, F., Cooper, J. M., and Schapira, A. H. V. (1996). Mitochondrial defect in Huntington's disease caudate nucleus. *Ann. Neurol.* **39**, 385–389.

Gutekunst, C.-A., Levey, A. I., Heilman, C. J., Whaley, W. L., Yi, H., Nash, N. R., Rees, H. D., Madden, J. J., and Hersch, S. M. (1995). Identification and localization of huntingtin in brain and human lymphoblastoid cell lines with anti-fusion protein antibodies. *Proc. Natl. Acad. Sci. U. S. A.* **92**, 8710–8714.

Hackam, A. S., Singaraja, R., Zhang, T., Gan, L., and Hayden, M. R. (1999). In vitro evidence for both the nucleus and cytoplasm as subcellular sites of pathogenesis in Huntington's disease. *Hum. Mol. Genet.* **8**, 25–33.

Hodgson, J. G., Agopyan, N., Gutekunst, C. -A., Leavitt, B. R., LePiane, F., Singaraja, R., Smith, D. J., Bissada, N., McCutcheon, K., Nasir, J., Jamot, L., Li, X. -J., Rosemond, E., Roder, J. C., Phillips, A. G., Rubin, E. M., Hersch, S. M., and Hayden, M. R. (1999). A YAC mouse model for Huntington's disease with full-length mutant huntingtin, cytoplasmic toxicity, and selective striatal neurodegeneration. *Neuron* **23**, 1–20.

Hughes, D. B., Thomas, M., Dedeoglu, A., Browne, S. E., Ferrante, R. J., Andreassen, O. A., and Beal, M. F. (1999). Hyperglycemia in a transgenic animal model of Huntington's disease. *Soc. Neurosci. Abstr.* **25**, 237.14.

Hurlbert, M. S., Zhou, W., Wasmeier, C., Kaddis, F. G., Hutton, J. C., and Freed, C. R. (1999). Mice transgenic for an expanded CAG repeat in the Huntington's disease gene develop diabetes. *Diabetes* **48**, 649–651.

Hussey, D., Stewart, D., Houle, S., and Guttman, M. (1998). [^{11}C]Raclopride striatal binding potential as a measure of Huntington's disease pregression: Implications for prospective neuroprotective studies. *J. Nucl. Med.* **39**, 209.

Huntington's Disease Collaborative Research Group. (1993). A novel gene containing a trinucleotide repeat that is expanded and unstable on Huntington's disease chromosome. *Cell (Cambridge, Mass.* **72**, 971–983.

Ihara, Y., Namba, R., Kuroda, S., Sato, T., and Shirabe, T. (1989). Mitochondrial encephalomyopathy (MELAS): Pathological study and successful therapy withcoenzyme Q_{10} and idebenone. *J. Neurol. Sci.* **90**, 263–271.

Jackson, G. R., Salecker, I., Schulze, K. L., Dong, X., Yao, X., Arnheim, N., Faber, P., MacDonald, M. E., and Zipursky, S. L. (1998). Age- and polyglutamine length-dependent degeneration of *Drosophila* photoreceptor neurons induced by human huntingtin transgenes. *Soc. Neurosci. Abstr.* **24**, 205.2.

Jenkins, B. G., Koroshetz, W., Beal, M. F., and Rosen, B. (1993). Evidence for an energy metabolism defect in Huntington's disease using localized proton spectroscopy. *Neurology* **43**, 2689–2695.

Jenkins, B. G., Rosas, H. D., Chen, Y. C., Makabe, T., Myers, R., MacDonald, M., Rosen, B. R., Beal, M. F., and Koroshetz, W. J. (1998). ^{1}H NMR spectroscopy studies of Huntington's disease: Correlations with CAG repeat numbers. *Neurology* **50**, 1357–1365.

Kahlem, P., Terré, C., Green, H., and Djian, P. (1996). Peptides containing glutamine repeats as substrates for transglutaminase-catalyzed cross-linking: Relevance to diseases of the nervous system. *Proc. Natl. Acad. Sci. U. S. A.* **93**, 14580–14585.

Kim, M., Lee, H. S., LaForet, G., McIntyre, C., Martin, E. J., Chang, P., Kim, T. W., Williams, M., Reddy, P. H., Tagle, D., Boyce, F. M., Won, L., Heller, A., Aronin, N., and DiFiglia, M. (1999). Mutant huntingtin expression in clonal striatal cells: Dissociation of inclusion formation and neuronal survival by caspase inhibition. *J. Neurosci.* **19**, 964–973.

Koroshetz, W. J., Jenkins, B. G., Rosen, B. R., and Beal, M. F. (1997). Energy metabolism defects in Huntington's disease and possible therapy with coenzyme Q_{10}. *Ann. Neurol.* **41**, 160–165.

Kuhl, D. E., Markham, C. H., Metter, E. J., Riege, W. H., Phelps, M. E., and Mazziotta, J. C. (1985). Local cerebral glucose utilization in symptomatic and presymptomatic Huntington's disease. *Res. Publ. Assoc. Res. Nerv. Ment. Dis.* **63**, 199–209.

Kuwert, T., Lange, H. W., Langer, K.-J., Herzog, H., Aulich, A., and Feinendegen, L. E. (1990). Cortical and subcortical glucose consumption measured by PET in patients with Huntington's disease. *Brain* **113**, 1405–1423.

Kuwert, T., Lange, H. W., Boecker, H., Titz, H., Herzog, H., Aulich, A., Wang, B. C., Nayak, U., and Feinendegen, L. E. (1993). Striatal glucose consumption in chorea-free subjects at risk of Huntington's disease. *J. Neurol.* **241**, 31–36.

Laforet, G. A., Lee, H. S., Cadigan, B., Chang, P., Chase, K. O., Sapp, E., Martin, E. M., McIntyre, C., Williams, M., Reddy, P. H., Tagle, D., Stein, J. S., Boyce, F. M., DiFiglia, M., and Aronin, N. (1998). Development and chracterization of a novel transgenic model of Huntington's disease which recapitulates features of the human illness. *Soc. Neurosci. Abstr.* **24**, 380.8

Levine, M. S., Klapstein, G. J., Koppel, A., Gruen, E., Cepeda, C., Vargas, M. E., Jokel, E. S., Carpenter, E. M., Zanjani, H., Hurst, R. S., Efstratiadis, A., Zeitlin, S., and Chesselet, M. F. (1999). Enhanced sensitivity to N-methyl-D-aspartate receptor activation in transgenic and knockin mouse models of Huntington's disease. *J. Neurosci. Res.* **58**, 515–532.

Li, X.-J., Li, S. -H., Sharp, A. H., Nucifora, F. C., Jr., Schilling, G., Lanahan, A., Worley, P., Snyder, S. H., and Ross, C. A. (1995). Huntingtin-associated protein enriched in brain with implicatins for pathology. *Nature (London)* **378**, 398–402.

Lin, X., Antalffy, B., Kang, D., Orr, H. T., and Zoghbi, H. Y. (2000). Polyglutamine expansion down-regulates specific neuronal genes before pathologic changes in SCA1. *Nat. Neurosci.* **3**, 157–163.

Linnane, A. W., Marzuki, S., Ozawa, T., and Tanaka, M. (1989). Mitochondrial DNA mutations as an important contributor to ageing and degenerative diseases. *Lancet* **1**, 642–645.

Lorand, L. (1996). Neurodegenerative diseases and transglutaminase. *Proc. Natl. Acad. Sci. U. S. A.* **93**, 14310–14313.

Ludolph, A. C., He, F., Spencer, P. S., Hammerstad, J., and Sabri, M. (1990). 3-nitropropionic acid: Exogenous animal neurotoxin and possible human striatal toxin. *Can. J. Neurol. Sci.* **18**, 492–498.

MacDonald, M. E., Vonsattel, J. -P., Shrinidhi, J., Couropmitree, N. N., Cupples, L. A., Bird, E. D., Gusella, J. F., and Myers, R. H. (1999). Evidence for the GluR6 gene associated with younger onset age of Huntington's disease. *Neurology* **53**, 1330–1332.

Mangiarini, L., Sathasivam, K., Seller, M., Cozens, B., Harper, A., Hetherington, C., Lawton, M., Trottier, Y., Lehrach, H., Davies, S. W., and Bates, G. (1996). Exon 1 of the HD gene with an expanded CAG repeat is sufficient to cause a progressive neurological phenotype in transgenic mice. *Cell (Cambridge, Mass.)* **87**, 493–506.

Mastrogiacomo, F., and Kish, S. J. (1994). Cerebellar_-ketoglutarase dehydrogenase activity is reduced in spinocerebellar ataxia type 1. *Ann. Neurol.* **35**, 624–626.

Mastrogiacomo, F., LaMarche, J., Dozic, S., Lindsay, G., Bettendorff, L., Robitaille, Y., Schut, L., and Kish, S. J. (1994). Immunoreactive levels of α-ketoglutarase dehydrogenase subunits in Friedreich's ataxia and spinocerebellar ataxia type 1. *Neurodegeneration* **5**, 27–33.

Matsuishi, T., Sakai, T., Naito, E., Nagamitsu, S., Kuroda, Y., Iwashita, H., and Kato, H. (1996). Elevated cerebrospinal fluid lactate/pyruvate ratio in Machado-Joseph disease. *Acta Neurol. Scand.* **93**, 72–75.

Matthew, E., Nordahl, T., Schut, L., King, A. C., and Cohen, R. (1993). Metabolic and cognitive changes in hereditary ataxia. *J. Neurol. Sci.* **119**, 134–140.

Matthews, R. T., Yang, L., Jenkins, B. J., Ferrante, R. J., Rosen, B. R., Kaddurah-Daouk, R., and Beal, M. F. (1998). Neuroprotective effects of creatine and cyclocreatine in animal models of Huntington's disease. *J. Neurosci.* **18**, 156–163.

Moulder, K. L., Onodera, O., Burke, J., Strittmatter, W. J., and Johnson, E. M., Jr. (1998). Polyglutamine containing proteins produce length-dependent aggregation and death in cultured cerebellar granule cells. *Soc. Neurosci. Abstr.* **24**, 379.5.

Myers, R. H., Vonsattel, J. P., Paskevich, P. A., Kiely, D. K., Stevens, T. J., Cupples, L. A., Richardson, E. P., Jr., and Bird, E. D. (1991). Decreased neuronal and increased oligodendroglial densities in Huntington's disease caudate nucleus. *J. Neuropathol. Exp. Neurol.* **50**, 729–742.

O'Brien, C. F., Miller, C., Goldblatt, D., Welle, S., Forbes, G., Lipinski, B., Panzik, J., Peck, R., Plumb, S., Oakes, D., Kurlan, R., and Shoulson, I. (1990). Extraneural metabolism in early Huntington's disease. *Ann. Neurol.* **28**, 300–301.

Ona, V. O., Li, M., Vonsattel, J. P., Andrews, L. J., Khan, S. Q., Chung, W. M., Frey, A. S., Menon, A. S., Li, X. J., Stieg, P. E., Yuan, J., Penney, J. B., Young, A. B., Cha, J. H., and Friedlander, R. M. (1999). Inhibition of caspase-1 slows disease progression in a mouse model of Huntington's disease. *Nature (London)* **399**, 263–267.

Ordway, J. M., Tallaksen-Greene, S., Gutekunst, C. A., Bernstein, E. M., Cearley, J. A., Wiener, H. W., Dure, L. S., 4th, Lindsey, R., Hersch, S. M., Jope, R. S., Albin, R. L., and Detloff, P. J. (1997). Ectopically expressed CAG repeats cause intranuclear inclusions and a progressive late onset neurological phenotype in the mouse. *Cell (Cambridge, Mass.)* **91**, 753–763.

Parker, W. D., J. r., Boyson, S. J., Luder, A. S., and Parks, J. K. (1990). Evidence for a defect in NADH: Ubiquinone oxidoreductase (complex I) in Huntington's disease. *Neurology* **40**, 1231–1234.

Paulson, H. L., Perez, M. K., Trottier, Y., Trojanowski, J. Q., Subramony, S. H., Das, S. S., Vig, P., Mandel, J. L., Fischbeck, K. H., and Pittman, R. N. (1997). Intranuclear inclusions of expanded polyglutamine protein in spinocerebellar ataxia type 3. *Neuron* **19**, 333–344.

Perutz, M., Johnson, T., Suzuki, M., and Finch, J. T. (1994). Glutamine repeats as polar zippers: Their possible role in inherited neurodegenerative diseases. *Proc. Natl. Acad. Sci. U. S. A.* **91**, 5355–5358.

Reddy, P. H., Williams, M., Charles, V., Garrett, L., Pike-Buchanan, L., Whetsell, W. O., Jr., Miller, G., and Tagle, D. A. (1998). Behavioural abnormalities and selective neuronal loss in HD transgenic mice expressing mutated full-length HD cDNA. *Nat. Genet.* **20**, 198–202.

Reiner, A., Albin, R. L., Anderson, K. D., D'Amato, C. J., Penney, J. B., and Young, A. B. (1988). Differential loss of striatal projection neurons in Huntington disease. *Proc. Natl. Acad. Sci. U. S. A.* **85**, 5733–5737.

Reynolds, G. P., Dalton, C. F., Tillery, C. L., Mangiarini, L., Davies, S. W., Bates, G. P. (1999). Brain neurotransmitter deficits in mice transgenic for the Huntington's disease mutation. *J. Neurochem.* **72**, 1773–1776.

Richfield, E. K., Maguire-Zeiss, K. A., Cox, C., Gilmore, J., and Voorn, P. (1995). Reduced expression of preproenkephalin in striatal neurons from Huntington's disease patients. *Ann. Neurol.* **37**, 335–343.

Ross, C. A. (1995). When less is more: Pathogenesis in glutamine repeat neurodegenerative diseases. *Neuron* **15**, 493–496.

Sapp, E., Ge, P., Aizawa, H., Bird, E., Penney, J., Young, A. B., Vonsattel, J. P., and DiFiglia, M. (1995). Evidence for a preferential loss of enkephalin immunoreactivity in the external globus pallidus in low grade Huntington's disease using high resolution image analysis. *Neuroscience* **64**, 397–404.

Sathasivam, K., Hobbs, C., Turmaine, M., Mangiarini, L., Mahal, A., Bertaux, F., Wanker, E. E., Doherty, P., Davies, S. W., and Bates, G. P. (1999). Formation of polyglutamine inclusions in non-CNS tissue. *Hum. Mol. Genet.* **8**, 813–822.

Saudou, F., Finkbeiner, S., Devys, D., and Greenberg, M. E. (1998). Huntingtin acts in the nucleus to induce apoptosis but death does not correlate with the formation of intranuclear inclusions. *Cell (Cambridge, Mass.)* **95**, 55–66.

Saunders, P. A., Chalecka-Franaszek, E., and Chuang, D. M. (1997). Subcellular distribution of glyceraldehyde-3-phosphate dehydrogenase in cerebellar granule cells undergoing cytosine arabinoside-induced apoptosis. *J. Neurochem.* **69**, 1820–1828.

Sawa, A., Khan, A. A., Hester, L. D., and Snyder, S. H. (1997). Glyceraldehyde-3-phosphate dehydrogenase: Nuclear translocation participates in neuronal and nonneuronal cell death. *Proc. Natl. Acad. Sci. U. S. A.* **94**, 11669–11674.

Sawa, A., Wiegand, G. W., Cooper, J., Margolis, R., Sharp, A. H., Lawler, J. F., Greenamyre, J. T., Snyder, S. H., and Ross, C. A. (1999). Increased apoptosis of Huntington disease lymphoblasts associated with repeat length-dependent mitochondrial depolarization. *Nature Med.* **5**, 1194–1198.

Schapira, A. H. V., Mann, V. M., Cooper, J. M., Krige, D., Jenner, P. J., and Marsden, C. D. (1992). *Ann. Neurol.* **32**, S116–S124.

Scherzinger, E., Kurz, R., Turmaine, M., Mangiarini, L., Hollenbach, B., Hasenbank, R., Bates, G. P., Davies, S. W., Lehrach, H., and Wanker, E. E. (1997). Huntingtin-encoded polyglutamine expansions form amyloid-like aggregates in vitro and in vivo. *Cell (Cambridge, Mass.)* **90**, 549–558.

Schilling, G., Bacher, M. W., Sharp, A. H., Jinnah, H. A., Duyao, K., Kotzuk, J. A., Slunt, H. H., Ratovitski, T., Cooper, J. A., Jenkins, N. A. *et al.* (1999). Intranuclear inclusions and neuritic aggregates in transgenic mice expressing a mutant N-terminal fragment of huntingtin. *Hum. Mol. Genet.* **8**, 397–407.

Schulz, J. B., Henshaw, D. R., MacGarvey, U., and Beal, M. F., (1996a). Involvement of oxidative stress in 3-nitropropionic acid neurotoxicity. *Neurochem. Int.* **29**, 167–171.

Schulz, J. B., Matthews, R. T., Henshaw, D. R., and Beal, M. F. (1996b). Neuroprotective strategies for treatment of lesions produced by mitochondrial toxins: Implications for neurodegenerative diseases. *Neurosci.* **71**, 1043–1048.

Sharp, N. H., Loev, S. J., Schilling, G., Li, S.-H., Li, X.-J., Bao, J., Wagster, M. V., Kotzuk, J. A., Steiner, J. P., Lo, A., Hedreen, J., Sisodia, S., Snyder, S. H., Dawson, T. M., Ryugo, D. K., and Ross, C. A. (1995). Widespread expression of the Huntington's disease gene (IT-15) protein product. *Neuron* **14**, 1065–1074.

Shelbourne, P. F., Killeen, N., Hevner, R. F., Johnston, H. M., Tecott, L., Lewandoski, M., Ennis, M., Ramirez, L., Li, Z., Iannicola, C., Littman, D. R., and Myers, R. M. (1999). A Huntington's disease CAG expansion at the murine Hdh locus is unstable and associated with behavioural abnormalities in mice. *Hum. Mol. Genet.* **8**, 763–774.

Sieradzan, K. A., and Mann, D. M. (1998). On the pathological progression of Huntington's disease. *Ann. Neurol.* **44**, 148–149.

Sotrel, A., Paskevich, P. A., Kiely, D. K., Bird, E. D., Willimas, R. S., and Myers, R. H. (1991). Morphometric analysis of the prefrontal cortex in Huntington's disease. *Neurology* **41**, 1117–1123.

Storey, E., Hyman, B. T., Jenkins, B. T., Brouillet, E., Miller, J. M., Rosen, B. R., and Beal, M. F. (1992). MPP^+ produces excitotoxic lesions in rat striatum due to impairment of oxidative metabolism. *J. Neurochem.* **58**, 1975–1978.

Strong, T. V., Tagle, D. A., Valdes, J. M., Elmer, L. W., Boehm, K., Swaroop, M., Kaatz, K. W., Collins, F. S., and Albin, R. L. (1993). Widespread expression of the human and rat Huntington's disease gene in brain and nonneural tissues. *Nat Genet.* **5**, 259–265.

Tabrizi, S. J., Cleeter, M. W., Xuereb, J., Taanman, J. W., Cooper, J. M., and Schapira, A. H. (1999). Biochemical abnormalities and excitotoxicity in Huntington's disease brain. *Ann. Neurol.* **45**, 25–32.

Tabrizi, S. J., Workman, J., Hart, P. E., Mangiarini, L., Mahal, A., Bates, G., Cooper, J. M., and Schapira, A. H. (2000). Mitochondrial dysfunction and free radical damage in the Huntington R6/2 transgenic mouse. *Ann. Neurol.* **47**, 80–86.

Tellez-Nagel, I., Johnson, A. B., and Terry, R. D. (1995). Studies on brain biopsies of patients with Huntington's chorea. *J. Neuropathol. Exp. Neurol.* **33**, 308–332.

Usdin, M. T., Shelbourne, P. F., Myers, R. M., and Madison, D. V. (1999). Impaired synaptic plasticity in mice carrying the Huntington's disease mutation. *Hum. Mol. Genet.* **8**, 839–846.

Vonsattel, J.-P., Myers, R. H., Stevens, T. J., Ferrante, R. J., Bird, E. D., and Richardson, E. P. (1985). Neuropathological classification of Huntington's disease. *J. Neuropathol. Exp. Neurol.* **44**, 559–577.

Vonsattel, J. P. G., and DiFiglia, M. (1998). Huntington disease. *J. Neuropathol. Exp. Neurol.* **57**, 369–384.

Wheeler, V. C., White, J. K., Gutekunst, C. A., Vrbanac, V., Weaver, M., Li, X. J., Li, S. H., Yi, H., Vonsattel, J. P., Gusella, J. F., Hersch, S., Auerbach, W., Joyner, A. L. and MacDonald, M. E. (2000). Long glutamine tracts cause nuclear localization of a novel form of huntingtin in medium spiny striatal neurons in HdhQ92 and HdhQ111 knock-in-mice. *Hum. Mol. Genet.* **9**, 503–513.

White, J. K., Auerbach, W., Duyao, M. P., Vonsattel, J.-P., Gusella, J. F., Joyner, A. L., and MacDonald, M. E. (1997). Huntingtin function is required for mouse brain development and is not impaired by the Huntington's disease CAG expansion mutation. *Nat. Genet.* **17**, 404–410.

Wullner, U., Young, A. B., Penney, J. B., and Beal, M. F. (1994). 3-Nitropropionic acid toxicity in the striatum. *J. Neurochem.* **63**, 1772–1781.

Yamamoto, A., Lucas, J. J., Hen, R. (2000). Reversal of nuropathology and motor dysfunction in a conditional model of Huntington's disease. *Cell* **101**, 57–66.

Young, A. B., Penney, J. B., Starosta-Rubinstein, S., Markel, D. S., Berent, S., Giordani, B., Ehrenkaufer, R., Jewett, D., and Hichwa, R. (1986). PET scan investigations of Huntington's disease: Cerebral metabolic correlates of neurological features and functional decline. *Ann. Neurol.* **20**, 296–303.

Zoghbi, H. Y. (1997). CAG repeats in SCA6. Anticipating new clues. *Neurology* **49**, 1196–1199.

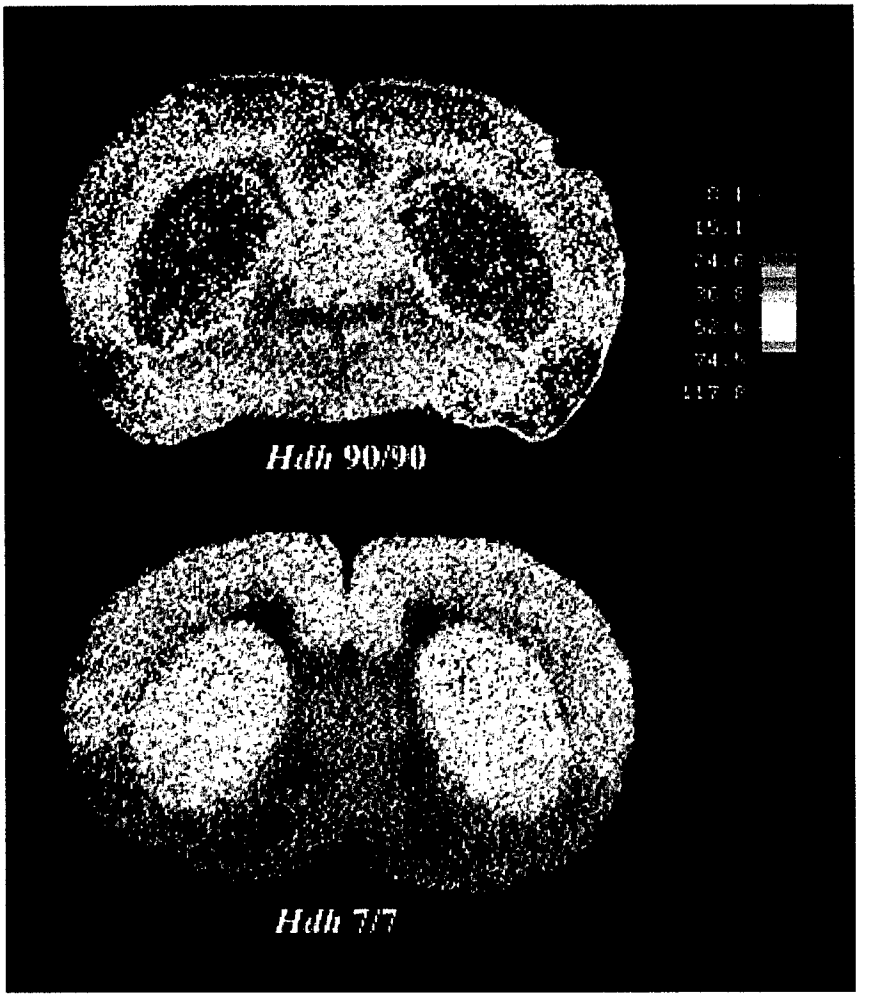

FIG. 49.2 Cerebral glucose use is increased prior to pathological changes in *Hdh* knock-in mice. These representative images are color coded to show local rates of cerebral glucose utilization in the forebrain of *Hdh* knock-in mice at 4 months of age, at the level of the striatum. The color bar illustrates the coding for glucose use (μmol/100 g/min). Glucose use is markedly increased in most forebrain regions of mice expressing 92 glutamines in mutant huntingtin (*Hdh* 90/90, top image) compared to levels in wild-type mice expressing 7 glutamines in huntingtin (*Hdh* 7/7; lower image). These changes in HDH^{Q92} mice precede any behavioral changes, and the formation of neuronal intranuclear inclusions, suggesting that the gene mutation may induce energetic abnormalities at an early stage of the associated disorder (Browne *et al.*, 1999b).

FIG. 63.2 Pseudo-color-enhanced photomicrographs of [^{125}I]IGF-1 binding in hippocampus (H) and layers II/III and V/VI of cortex of 10- (left), 19- (center), and 30-month-old (right) rats. Red indicates the highest level of binding. Data indicate a decline in type 1 IGF receptors in brain with age.